



Journal of
Clinical Medicine

Characterization and Clinical Management of Dilated Cardiomyopathy

Edited by

Marco Merlo

Printed Edition of the Special Issue Published in
Journal of Clinical Medicine

Characterization and Clinical Management of Dilated Cardiomyopathy

Characterization and Clinical Management of Dilated Cardiomyopathy

Editor

Marco Merlo

MDPI • Basel • Beijing • Wuhan • Barcelona • Belgrade • Manchester • Tokyo • Cluj • Tianjin



Editor

Marco Merlo
Cardiovascular Department,
Azienda Sanitaria Universitaria
Giuliano Isontina (ASUGI),
University of Trieste,
Italy

Editorial Office

MDPI
St. Alban-Anlage 66
4052 Basel, Switzerland

This is a reprint of articles from the Special Issue published online in the open access journal *Journal of Clinical Medicine* (ISSN 2077-0383) (available at: https://www.mdpi.com/journal/jcm/special_issues/dilated_cardiac).

For citation purposes, cite each article independently as indicated on the article page online and as indicated below:

LastName, A.A.; LastName, B.B.; LastName, C.C. Article Title. <i>Journal Name</i> Year , <i>Volume Number</i> , Page Range.
--

ISBN 978-3-03943-761-0 (Hbk)

ISBN 978-3-03943-762-7 (PDF)

© 2020 by the authors. Articles in this book are Open Access and distributed under the Creative Commons Attribution (CC BY) license, which allows users to download, copy and build upon published articles, as long as the author and publisher are properly credited, which ensures maximum dissemination and a wider impact of our publications.

The book as a whole is distributed by MDPI under the terms and conditions of the Creative Commons license CC BY-NC-ND.

Contents

About the Editor vii

Marco Merlo, Antonio Cannatà and Gianfranco Sinagra
Dilated Cardiomyopathy: A Paradigm of Revolution in Medicine
Reprinted from: *J. Clin. Med.* 2020, 9, 3385, doi:10.3390/jcm9113385 1

Antonio Cannata, Paolo Manca, Vincenzo Nuzzi, Caterina Gregorio, Jessica Artico, Piero Gentile, Carola Pio Loco, Federica Ramani, Giulia Barbati, Marco Merlo and Gianfranco Sinagra
Sex-Specific Prognostic Implications in Dilated Cardiomyopathy after Left Ventricular Reverse Remodeling
Reprinted from: *J. Clin. Med.* 2020, 9, 2426, doi:10.3390/jcm9082426 5

Giulia Stronati, Federico Guerra, Alessia Urbinati, Giuseppe Ciliberti, Laura Cipolletta and Alessandro Capucci
Tachycardiomyopathy in Patients without Underlying Structural Heart Disease
Reprinted from: *J. Clin. Med.* 2019, 8, 1411, doi:10.3390/jcm8091411 17

Bianca Olivia Cojan-Minzat, Alexandru Zlibut, Ioana Danuta Muresan, Carmen Cionca, Dalma Horvat, Eva Kiss, Radu Revnic, Mira Florea, Razvan Ciortea and Lucia Agoston-Coldea
Left Ventricular Geometry and Replacement Fibrosis Detected by cMRI Are Associated with Major Adverse Cardiovascular Events in Nonischemic Dilated Cardiomyopathy
Reprinted from: *J. Clin. Med.* 2020, 9, 1997, doi:10.3390/jcm9061997 31

Miloš Kubánek, Tereza Schimerová, Lenka Piherová, Andreas Brodehl, Alice Krebsová, Sandra Ratnavadivel, Caroline Stanasiuk, Hana Hansíková, Jiří Zeman, Tomáš Paleček, Josef Houšťek, Zdeněk Drahotá, Hana Nůšková, Jana Mikešová, Josef Zámečník, Milan Macek Jr., Petr Ridzoň, Jana Malusková, Viktor Stránecký, Vojtěch Melenovský, Hendrik Milting and Stanislav Kmoch
Desminopathy: Novel Desmin Variants, a New Cardiac Phenotype, and Further Evidence for Secondary Mitochondrial Dysfunction
Reprinted from: *J. Clin. Med.* 2020, 9, 937, doi:10.3390/jcm9040937 47

Weng-Tein Gi, Jan Haas, Farbod Sedaghat-Hamedani, Elham Kayvanpour, Rewati Tappu, David Hermann Lehmann, Omid Shirvani Samani, Michael Wisdom, Andreas Keller, Hugo A. Katus and Benjamin Meder
Epigenetic Regulation of Alternative mRNA Splicing in Dilated Cardiomyopathy
Reprinted from: *J. Clin. Med.* 2020, 9, 1499, doi:10.3390/jcm9051499 67

Przemyslaw Chmielewski, Ewa Michalak, Ilona Kowalik, Maria Franaszczyk, Malgorzata Sobieszczanska-Malek, Grazyna Truszkowska, Malgorzata Stepien-Wojno, Elzbieta Katarzyna Biernacka, Bogna Foss-Nieradko, Michal Lewandowski, Artur Oreziak, Maria Bilinska, Mariusz Kusmierczyk, Frédérique Tesson, Jacek Grzybowski, Tomasz Zielinski, Rafal Ploski and Zofia T. Bilinska
Can Circulating Cardiac Biomarkers Be Helpful in the Assessment of LMNA Mutation Carriers?
Reprinted from: *J. Clin. Med.* 2020, 9, 1443, doi:10.3390/jcm9051443 85

Rebeca Lorca, María Martín, Isaac Pascual, Aurora Astudillo, Beatriz Díaz Molina, Helena Cigarrán, Elías Cuesta-Llavona, Pablo Avanzas, José Julián Rodríguez Reguero, Eliecer Coto, César Morís and Juan Gómez Characterization of Left Ventricular Non-Compaction Cardiomyopathy Reprinted from: <i>J. Clin. Med.</i> 2020 , <i>9</i> , 2524, doi:10.3390/jcm9082524	101
Keiichi Hirono, Yukiko Hata, Nariaki Miyao, Mako Okabe, Shinya Takarada, Hideyuki Nakaoka, Keihiro Ibuki, Sayaka Ozawa, Naoki Yoshimura, Naoki Nishida, Fukiko Ichida and LVNC study collaborators Left Ventricular Noncompaction and Congenital Heart Disease Increases the Risk of Congestive Heart Failure Reprinted from: <i>J. Clin. Med.</i> 2020 , <i>9</i> , 785, doi:10.3390/jcm9030785	117
Ibadete Bytyçi, Gani Bajraktari, Per Lindqvist and Michael Y. Henein Improved Left Atrial Function in CRT Responders: A Systematic Review and Meta-Analysis Reprinted from: <i>J. Clin. Med.</i> 2020 , <i>9</i> , 298, doi:10.3390/jcm9020298	133
Charles Tharp, Luisa Mestroni and Matthew Taylor Modifications of Titin Contribute to the Progression of Cardiomyopathy and Represent a Therapeutic Target for Treatment of Heart Failure Reprinted from: <i>J. Clin. Med.</i> 2020 , <i>9</i> , 2770, doi:10.3390/jcm9092770	147
Michelle L. Law, Houda Cohen, Ashley A. Martin, Addeli Bez Batti Angulski and Joseph M. Metzger Dysregulation of Calcium Handling in Duchenne Muscular Dystrophy-Associated Dilated Cardiomyopathy: Mechanisms and Experimental Therapeutic Strategies Reprinted from: <i>J. Clin. Med.</i> 2020 , <i>9</i> , 520, doi:10.3390/jcm9020520	165
Rachele Adorisio, Erica Mencarelli, Nicoletta Cantarutti, Camilla Calvieri, Liliana Amato, Marianna Cicenia, Massimo Silveti, Adele D'Amico, Maria Grandinetti, Fabrizio Drago and Antonio Amodeo Duchenne Dilated Cardiomyopathy: Cardiac Management from Prevention to Advanced Cardiovascular Therapies Reprinted from: <i>J. Clin. Med.</i> 2020 , <i>9</i> , 3186, doi:10.3390/jcm9103186	197
Babken Asatryan Cardiac Sodium Channel Dysfunction and Dilated Cardiomyopathy: A Contemporary Reappraisal of Pathophysiological Concepts Reprinted from: <i>J. Clin. Med.</i> 2019 , <i>8</i> , 1029, doi:10.3390/jcm8071029	215

About the Editor

Marco Merlo is associate professor of Cardiology at University of Trieste. From the beginning of his career in 2008, he has shown continuous interest in the research on heart failure and cardiomyopathies, with a specific focus on dilated cardiomyopathy, arrhythmogenic cardiomyopathy, and myocarditis. He is author and coauthor of more than 150 peer-review publications in the more important journals of Cardiology and Medicine and several chapters of books. His research is particularly focused on natural history, genotype–phenotype correlation, prognostic stratification of dilated cardiomyopathy and myocarditis.



Editorial

Dilated Cardiomyopathy: A Paradigm of Revolution in Medicine

Marco Merlo ^{1,*}, Antonio Cannata ^{1,2} and Gianfranco Sinagra ¹

¹ Cardiovascular Department, Azienda Sanitaria Universitaria Giuliano Isontina (ASUGI), University of Trieste, 34100 Trieste, Italy; anto.cannata@gmail.com (A.C.); gianfranco.sinagra@asugi.sanita.fvg.it (G.S.)

² James Black Centre, School of Cardiovascular Medicine and Sciences, King's College London British Heart Foundation Centre of Excellence, 125 Coldharbour Lane, London SE5 9NU, UK

* Correspondence: marco.merlo79@gmail.com; Tel.: +39-040-399-4477; Fax: +39-040-399-4878

Received: 16 October 2020; Accepted: 20 October 2020; Published: 22 October 2020

Dilated Cardiomyopathy (DCM) has a straightforward and apparently “simple” definition: a heart muscle disease characterized by left ventricular (LV) or biventricular dilation and systolic dysfunction in the absence of either pressure or volume overload or coronary artery disease sufficient enough to explain the dysfunction [1]. DCM currently carries a relatively benign outcome, significantly improved with respect to the past decades. Contemporary analysis shows the survival/free from heart transplant rate beyond 85% at 10-year follow-up [2]. Nevertheless, the knowledge regarding pathophysiology, aetiology, diagnostic workup and prognostic stratification of DCM is rapidly and progressively evolving, reflecting the clinical management of the disease that remains extremely challenging in daily practice [3]. Indeed, DCM patients are often relatively young at the time of diagnosis (between their 30s and 50s) with a low-co-morbidity profile, and their current diagnostic workup and risk stratification is characterized by several pitfalls (particularly regarding the arrhythmic risk). Consequently, a not-negligible proportion of DCM patients still experience an unfavourable prognosis, particularly in the short-term [2].

One of the reasons behind this complicated scenario is the heterogeneous aetiology of the disease. DCM is an “umbrella” term describing the final common pathway of different pathogenic processes and gene–environment interactions. More commonly than once believed, DCM recognizes a complex genetic background, far from being a monogenic disease, with multiple unknown epigenetic interactions. On the other side, it might be the result of possible extrinsic triggers (i.e., tachyarrhythmias, hypertension, alcohol, chemotherapy, inflammation), which, once removed, promote a reverse remodelling. Therefore, the term “idiopathic” DCM is progressively vanishing, and investigations on the complex interaction between environmental factors and genetic background are increasing. Future research in this perspective is likely to result in better prognostic stratification and ultimately targeted therapy [4].

Noteworthy, thorough phenotyping (through modern imaging techniques such as speckle tracking echocardiography or tissue characterization by cardiac magnetic resonance) and genotyping of DCM patients represent the basis for their optimal clinical management. Furthermore, compelling evidence shows that DCM is not exclusively a cardiological disease, requiring a multidisciplinary team (including geneticist, neurologist, radiologist and other specialists) for accurate management. Therefore, a novel approach to DCM patients, including comprehensive evaluation, should be promoted to tailor therapeutic strategies in the era of precision medicine.

Starting from these concepts, the idea of this Special Issue is to explore the DCM universe providing updated knowledge on pathophysiology, future directions of the research on DCM and practical guidelines useful for clinical management of DCM patients.

A series of focused reviews, meta-analyses and original articles are reported in this Special Issue with the precise aim of providing a deep insight into crucial gaps of knowledge in DCM. In particular, it extensively discusses the pathophysiology, mechanisms underlying the disease and the interaction

between genetic background, molecular pathways and environmental triggers, as the basis for future targeted therapies [5–7]. The knowledge of precise genetic pathogenesis and molecular mechanisms causing DCM has stimulated the research towards new treatments targeting gene expression [8,9]. Shifting from symptomatic treatments to targeted therapy on specific disease mechanisms represents the new mindset from slowing disease progression to disease reversal. Furthermore, some articles present in this Special Issue explore the genetic background of DCM, such as mutations in *DES*, *LMN* and *TTN*, remarking once again the current cultural revolution in this field of medicine. In the future, we might indeed abandon the current general definition of DCM, switching towards specific diseases such as Desminopathy, Laminopathy or Titinopathy and so on, each of them with specific diagnostic workup, prognostic stratification and therapeutic strategies [10–12]. Importantly, the need of a multidisciplinary network involving different specialists clearly emerges in specific and challenging diseases, such as Duchenne-related DCM in order to improve the global clinical management of those challenging patients [13]. Finally, the prognostic stratification of DCM has been further explored, focusing on (1) the identification of specific subgroups of DCM without a structural myocardial disease, such as the tachycardia-induced cardiomyopathy [14]; (2) the application of gender medicine to DCM clinical management [15]; (3) the usefulness of tissue characterization by cardiac magnetic resonance in the multi-parametric approach of DCM patients [16] and (4) the role of the left atrium, other than just the left ventricle, as a therapeutic target of pharmacological and non-pharmacological treatments in DCM [17]. Finally, a section is dedicated to the characterization of left ventricular non-compaction that is frequently encountered in clinical practice in overlap with the DCM phenotype [16,18]. The definition of left ventricular non-compaction as a specific cardiomyopathy or, more likely, as a specific trait of genetic cardiomyopathy is debated, and it still represents a gap in knowledge in clinical management, particularly for the first phases of the disease.

Far from providing the absolute truth, this Special Issue is intended to help physicians (not only cardiologists) in their everyday clinical practice to deal with patients affected by DCM in a multifaceted, multidisciplinary and individualized approach.

Author Contributions: M.M.: conceptualization, drafting the manuscript, final approval; A.C.: drafting the manuscript; critical revisions; final approval. G.S.: critical revision; supervision; final approval. All authors have read and agreed to the published version of the manuscript.

Funding: This research received no external funding.

Conflicts of Interest: The authors declare no conflict of interest

References

1. Elliott, P.M.; Andersson, B.; Arbustini, E.; Bilinska, Z.; Cecchi, F.; Charron, P.; Dubourg, O.; Kühl, U.; Maisch, B.; McKenna, W.J.; et al. Classification of the cardiomyopathies: A position statement from the European Society of Cardiology Working Group on Myocardial and Pericardial Diseases. *Eur. Heart J.* **2008**, *29*, 270–276. [[CrossRef](#)] [[PubMed](#)]
2. Merlo, M.; Cannatà, A.; Loco, C.P.; Stolfo, D.; Barbati, G.; Artico, J.; Gentile, P.; De Paris, V.; Ramani, F.; Zecchin, M.; et al. Contemporary survival trends and aetiological characterization in non-ischaemic dilated cardiomyopathy. *Eur. J. Heart Fail.* **2020**. [[CrossRef](#)] [[PubMed](#)]
3. Merlo, M.; Cannatà, A.; Gobbo, M.; Stolfo, D.; Elliott, P.M.; Sinagra, G. Evolving concepts in dilated cardiomyopathy. *Eur. J. Heart Fail.* **2018**, *20*, 228–239. [[CrossRef](#)] [[PubMed](#)]
4. Sinagra, G.; Elliott, P.M.; Merlo, M. Dilated cardiomyopathy: So many cardiomyopathies! *Eur. Heart J.* **2019**, *ehz908*. [[CrossRef](#)] [[PubMed](#)]
5. Law, M.L.; Cohen, H.; Martin, A.A.; Angulski, A.B.B.; Metzger, J.M. Dysregulation of Calcium Handling in Duchenne Muscular Dystrophy-Associated Dilated Cardiomyopathy: Mechanisms and Experimental Therapeutic Strategies. *J. Clin. Med.* **2020**, *9*, 520. [[CrossRef](#)] [[PubMed](#)]
6. Asatryan, B. Cardiac Sodium Channel Dysfunction and Dilated Cardiomyopathy: A Contemporary Reappraisal of Pathophysiological Concepts. *J. Clin. Med.* **2019**, *8*, 1029. [[CrossRef](#)] [[PubMed](#)]

7. Gi, W.-T.; Haas, J.; Sedaghat-Hamedani, F.; Kayvanpour, E.; Tappu, R.; Lehmann, D.H.; Shirvani Samani, O.; Wisdom, M.; Keller, A.; Katus, H.A.; et al. Epigenetic Regulation of Alternative mRNA Splicing in Dilated Cardiomyopathy. *J. Clin. Med.* **2020**, *9*, 1499. [[CrossRef](#)] [[PubMed](#)]
8. Repetti, G.G.; Toepfer, C.N.; Seidman, J.G.; Seidman, C.E. Novel Therapies for Prevention and Early Treatment of Cardiomyopathies. *Circ. Res.* **2019**, *124*, 1536–1550. [[CrossRef](#)] [[PubMed](#)]
9. Muchir, A.; Wu, W.; Choi, J.C.; Iwata, S.; Morrow, J.; Homma, S.; Worman, H.J. Abnormal p38 mitogen-activated protein kinase signaling in dilated cardiomyopathy caused by lamin A/C gene mutation. *Hum. Mol. Genet.* **2012**, *21*, 4325–4333. [[CrossRef](#)] [[PubMed](#)]
10. Kubánek, M.; Schimerová, T.; Piherová, L.; Brodehl, A.; Krebsová, A.; Ratnavadivel, S.; Stanasiuk, C.; Hansíková, H.; Zeman, J.; Paleček, T.; et al. Desminopathy: Novel Desmin Variants, a New Cardiac Phenotype, and Further Evidence for Secondary Mitochondrial Dysfunction. *J. Clin. Med.* **2020**, *9*, 937. [[CrossRef](#)] [[PubMed](#)]
11. Chmielewski, P.; Michalak, E.; Kowalik, I.; Franaszczyk, M.; Sobieszczanska-Malek, M.; Truszkowska, G.; Stepien-Wojno, M.; Biernacka, E.K.; Foss-Nieradko, B.; Lewandowski, M.; et al. Can Circulating Cardiac Biomarkers Be Helpful in the Assessment of LMNA Mutation Carriers? *J. Clin. Med.* **2020**, *9*, 1443. [[CrossRef](#)] [[PubMed](#)]
12. Tharp, C.; Mestroni, L.; Taylor, M. Modifications of Titin Contribute to the Progression of Cardiomyopathy and Represent a Therapeutic Target for Treatment of Heart Failure. *J. Clin. Med.* **2020**, *9*, 2770. [[CrossRef](#)] [[PubMed](#)]
13. Stronati, G.; Guerra, F.; Urbinati, A.; Ciliberti, G.; Cipolletta, L.; Capucci, A. Tachycardiomyopathy in Patients without Underlying Structural Heart Disease. *J. Clin. Med.* **2019**, *8*, 1411. [[CrossRef](#)] [[PubMed](#)]
14. Adorasio, R.; Mencarelli, E.; Cantarutti, N.; Calvieri, C.; Amato, L.; Cicienia, M.; Silvetti, M.; D'Amico, A.; Grandinetti, M.; Drago, F.; et al. Duchenne Dilated Cardiomyopathy: Cardiac Management from Prevention to Advanced Cardiovascular Therapies. *J. Clin. Med.* **2020**, *9*, 3186. [[CrossRef](#)] [[PubMed](#)]
15. Cannata, A.; Manca, P.; Nuzzi, V.; Gregorio, C.; Artico, J.; Gentile, P.; Pio Loco, C.; Ramani, F.; Barbati, G.; Merlo, M.; et al. Sex-Specific Prognostic Implications in Dilated Cardiomyopathy After Left Ventricular Reverse Remodeling. *J. Clin. Med.* **2020**, *9*, 2426. [[CrossRef](#)] [[PubMed](#)]
16. Cojan-Minzat, B.O.; Zlibut, A.; Muresan, I.D.; Cionca, C.; Horvat, D.; Kiss, E.; Revnic, R.; Florea, M.; Ciortea, R.; Agoston-Coldea, L. Left Ventricular Geometry and Replacement Fibrosis Detected by cMRI Are Associated with Major Adverse Cardiovascular Events in Nonischemic Dilated Cardiomyopathy. *J. Clin. Med.* **2020**, *9*, 1997. [[CrossRef](#)] [[PubMed](#)]
17. Bytyçi, I.; Bajraktari, G.; Lindqvist, P.; Henein, M.Y. Improved Left Atrial Function in CRT Responders: A Systematic Review and Meta-Analysis. *J. Clin. Med.* **2020**, *9*, 298. [[CrossRef](#)] [[PubMed](#)]
18. Hirono, K.; Hata, Y.; Miyao, N.; Okabe, M.; Takarada, S.; Nakaoka, H.; Ibuki, K.; Ozawa, S.; Yoshimura, N.; Nishida, N.; et al. Left Ventricular Noncompaction and Congenital Heart Disease Increases the Risk of Congestive Heart Failure. *J. Clin. Med.* **2020**, *9*, 785. [[CrossRef](#)] [[PubMed](#)]

Publisher's Note: MDPI stays neutral with regard to jurisdictional claims in published maps and institutional affiliations.



© 2020 by the authors. Licensee MDPI, Basel, Switzerland. This article is an open access article distributed under the terms and conditions of the Creative Commons Attribution (CC BY) license (<http://creativecommons.org/licenses/by/4.0/>).

Article

Sex-Specific Prognostic Implications in Dilated Cardiomyopathy after Left Ventricular Reverse Remodeling

Antonio Cannata ^{1,2,†}, Paolo Manca ^{1,†}, Vincenzo Nuzzi ¹, Caterina Gregorio ³, Jessica Artico ¹, Piero Gentile ¹, Carola Pio Loco ¹, Federica Ramani ¹, Giulia Barbati ³, Marco Merlo ^{1,*} and Gianfranco Sinagra ¹

- ¹ Cardiovascular Department, Azienda Sanitaria Universitaria Giuliano Isontina (ASUGI), University of Trieste, 34100 Trieste, Italy; anto.cannata@gmail.com (A.C.); paolo.manca91@yahoo.it (P.M.); vincenzo_nuzzi@libero.it (V.N.); jessica.artico@hotmail.it (J.A.); pierogentile.87@gmail.com (P.G.); carola.pioloco@gmail.com (C.P.L.); fedis84it@yahoo.it (F.R.); gianfranco.sinagra@asuits.sanita.fvg.it (G.S.)
 - ² Department of Cardiovascular Sciences, Faculty of Life Sciences & Medicine, King's College London, London SE5 9NU, UK
 - ³ Biostatistics Unit, University of Trieste, 34100 Trieste, Italy; caterina.gregorio@outlook.com (C.G.); gbarbati@units.it (G.B.)
- * Correspondence: marco.merlo79@gmail.com; Tel.: +39-04-0399-4477; Fax: +39-04-0399-4878
† These authors equally contributed as first author.

Received: 2 July 2020; Accepted: 27 July 2020; Published: 29 July 2020

Abstract: Background. Women affected by Dilated Cardiomyopathy (DCM) experience better outcomes compared to men. Whether a more pronounced Left Ventricular Reverse Remodelling (LVRR) might explain this is still unknown. Aim. We investigated the relationship between LVRR and sex and its long-term outcomes. Methods. A cohort of 605 DCM patients with available follow-up data was consecutively enrolled. LVRR was defined, at 24-month follow-up evaluation, as an increase in left ventricular ejection fraction (LVEF) $\geq 10\%$ or a LVEF $> 50\%$ and a decrease $\geq 10\%$ in indexed left ventricular end-diastolic diameter (LVEDDi) or an LVEDDi ≤ 33 mm/m². Outcome measures were a composite of all-cause mortality/heart transplantation (HTx) or ventricular assist device (VAD) and a composite of Sudden Cardiac Death (SCD) or Major Ventricular Arrhythmias (MVA). Results. 181 patients (30%) experienced LVRR. The cumulative incidence of LVRR at 24-months evaluation was comparable between sexes (33% vs. 29%; $p = 0.26$). During a median follow-up of 149 months, women experiencing LVRR had the lowest rate of main outcome measure (global $p = 0.03$) with a 71% relative risk reduction compared to men with LVRR, without significant difference between women without LVRR and males. A trend towards the same results was found regarding SCD/MVA (global $p = 0.06$). Applying a multi-state model, male sex emerged as an independent adverse prognostic factor even after LVRR completion. Conclusions. Although the rate of LVRR was comparable between sexes, females experiencing LVRR showed the best outcomes in the long term follow up compared to males and females without LVRR. Further studies are advocated to explain this difference in outcomes between sexes.

Keywords: sex differences; dilated cardiomyopathy; left ventricular reverse remodelling; long-term outcomes

1. Introduction

Dilated cardiomyopathy (DCM) is a heterogeneous primary muscle disease predominantly affecting men, with a male to female ratio 3:1. The prognosis of DCM has dramatically improved over

the last decades [1–3] and the occurrence of left ventricular reverse remodelling (LVRR) under optimal medical treatment has been shown as one of the main prognostic drivers [1,4,5].

Female sex has recently emerged as an important outcome modifier in DCM patients, being independently associated with more favourable long-term outcomes and with a lower incidence of cardiovascular events in comparison to the male counterpart [6–8]. However, little is known regarding the mechanism underlying this important sex-specific effect. So far, none of the available reports have evaluated whether this difference could be partially explained by a different response to treatment and a more frequent occurrence of LVRR in women.

The aim of the present study was to investigate the rates of LVRR in males and females, and the prognostic impact of the relationship between LVRR and sex in a well-selected large cohort of real-world DCM patients with a long-term follow-up.

2. Methods

2.1. Study Population

All DCM patients consecutively enrolled in the Heart Muscle Disease Registry of Trieste between 1 January 1990 and 31 December 2015 and, with available data at 24-month follow up, were retrospectively analysed.

DCM was defined as an impairment of the Left Ventricular Ejection Fraction (LVEF) to < 50% and a left ventricular dilation in the absence of: a history of significant hypertension, obstruction > 50% of a major coronary artery branch, excessive alcohol intake, chemotherapy, an advanced systemic disease affecting short-term prognosis, pericardial diseases, congenital heart diseases, pulmonary, persistent supraventricular tachyarrhythmias, and active myocarditis [1,6].

The presence of a significant coronary artery obstruction was carefully excluded by a coronary artery angiography or, in case of a low likelihood of coronary artery disease, by coronary computed tomography scan.

All patients were on optimal medical treatment, receiving the highest tolerated doses of angiotensin-converting enzyme inhibitors or angiotensin receptor blockers and beta-blockers unless contraindicated [9]. Furthermore, implanted cardioverter defibrillators (ICDs) and cardiac resynchronization therapy (CRT) have been systematically introduced respectively since 1998 and 2005, according to international guidelines [10].

A structured outpatient follow-up, comprehensive of clinical evaluation, a 12-lead ECG, and two-dimensional echocardiography were performed at regularly scheduled time points until 24 months from enrolment (i.e., first evaluation at our Department) and then yearly or every other year afterwards according to specific clinical needs.

The institutional ethics board approved the study. The investigation complied with the Declaration of Helsinki.

2.2. Echocardiographic Evaluation

Left Ventricular (LV) dimensions and function were assessed according to international guidelines [11]. In particular, LV volumes and LVEF were calculated by Simpson's biplane method, and all volumes were indexed according to body surface area. LV dilation based on LV end-diastolic volume was considered mild, moderate, or severe according to international guideline sex-specific reference values [11–13]. The LV filling pattern was classified as a restrictive filling pattern in the presence of E-wave deceleration time < 120 ms or E-wave/A-wave > 2 associated with E-wave deceleration time < 150 ms. Right ventricular dysfunction was defined as a right ventricle fractional area change (RVFAC) < 35%. Mitral regurgitation (MR) was considered significant only if moderate to severe.

2.3. LVRR Definition and Study Outcome Measures

LVRR was defined as an increase in the LVEF $\geq 10\%$ (or LVEF $> 50\%$) associated with a decrease $\geq 10\%$ in indexed left ventricular end-diastolic diameter (LVEDDI) or (LVEDDI ≤ 33 mm/m²) at 24-month follow-up after enrolment, as previously described [5].

The main outcome measure was considered a composite of all-cause mortality, heart transplantation (HTx), and ventricular assist device (VAD) as destination therapy. A composite of sudden cardiac death (SCD) or major ventricular arrhythmias (MVA) was considered as the secondary outcome measure.

Specifically, MVA was defined as sustained ventricular tachycardia, ventricular fibrillation/flutter, or appropriate intervention of an ICD. SCD was defined as a death occurred within 1 h from the symptom's onset, or as a death occurred during sleep in clinically stable patients with New York Heart Association (NYHA) class I–III.

To evaluate the association with the study outcome measures, the population was stratified into four groups, based on sex and the occurrence of LVRR.

Outcomes were investigated directly from the patient during the follow-up visit, medical records from the referral hospital or by telephone interview with the patient, relatives, or the general practitioner.

2.4. Statistical Analysis

Variables were expressed as mean and standard deviation, median and interquartile range (IQR), or counts and percentage, as appropriate. Comparisons between groups were made by the analysis of variance (ANOVA) test on continuous variables using the Brown-Forsythe statistic when the assumption of equal variances did not hold, or the nonparametric Mann-Whitney test when necessary; the chi-square test or the Fisher's exact test were calculated for discrete variables.

Survival curves for the composite outcome measure of all-cause mortality/HTx/VAD were estimated and compared between groups by means of the Log-rank test. Cumulative incidence curves for the composite outcome measure of SCD/MVA were estimated and compared taking into account competing risks of death from other causes, and the appropriate statistical test suitable for competing risks was performed [14]. To investigate the impact of sex and LVRR on the outcomes, cause-specific multivariable Cox models were estimated from a list of candidate prognostic variables obtained from the univariable analyses (i.e., those with a p -value ≤ 0.1). For this analysis, the follow-up started after 24 months from enrolment, when the LVRR is considered to be completed [5]. Moreover, to further evaluate the relationship between sex and LVRR, a Markov illness-death model with all-cause mortality/HTx/VAD as absorbing state and the risk of LVRR as an intermediate state was estimated. The model consists of three discrete health states (i.e., alive without LVRR; alive with LVRR; dead or HTx or VAD) and a transition probability matrix (P) is calculated between states (see Supplementary Figure S1 for schematic representation). Specifically, a multi-state model fitting a Cox-type regression for each transition was used to estimate transition-specific hazard ratio (HR) for Sex. In this case, the follow-up started at the time of enrolment and this model was adjusted for a list of candidate variables significantly different at the univariable analysis of the multi-state model. The IBM-SPSS (New York, NY, USA) statistical software version 19 was used for descriptive analyses; the software R (R Foundation for Statistical Computing, Vienna, Austria. <https://www.r-project.org/>) was used for the cumulative incidence curves estimation (library "cmprsk"), to test the proportional hazards assumption for the Cox model and for the multi-state model (packages "ggplot2", "survival" and "mstate") [15].

3. Results

A total cohort of 605 consecutive DCM patients with available data at a median follow-up of 24 (IQR 20–26) months was analysed (Figure 1). The main characteristics of the population at 24-month follow-up evaluation are summarized in Table 1. Patients were predominantly males (73% $n = 440$), and males were slightly younger than females (47 ± 15 vs. 51 ± 14 years respectively, $p = 0.007$). Females

had a higher incidence of left bundle branch block (LBBB) compared to their male counterparts (34% vs. 25%, respectively, $p = 0.02$). All patients received optimal medical treatment, without differences between sexes.

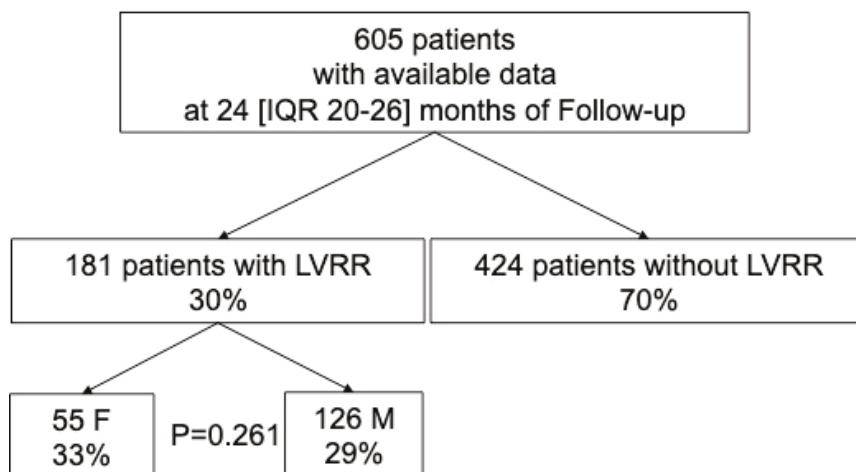


Figure 1. Diagram of study population. Legend. F: Females; LVRR: Left Ventricular Reverse Remodelling; M: Males.

subsection Left Ventricular Reverse Remodeling

Overall, 30% of patients experienced a LVRR ($n = 181$), without significant differences between sexes: the cumulative incidence of LVRR at the 24 months evaluation was 33% in women vs. 29% in men ($p = 0.26$) (Figure 1). Indeed, the probability of undergoing LVRR was similar between men and women (Hazard Ratio for male sex [HR] 0.81, 95% Confidence Intervals [CI] 0.53–1.22, $p = 0.31$). Interestingly, at the 24-months evaluation, despite a comparable LVEF ($40 \pm 12\%$ in women vs. $41 \pm 11\%$ in men, $p = 0.32$), women had a higher incidence of moderate to severe sex-specific LV dilation compared to men (59% vs. 28% respectively, $p \leq 0.001$).

3.1. Outcomes

Overall, starting from the 24-months evaluation, the outcomes of women were more favourable compared to men (Figure 2). During a median follow-up of 149 (IQR 90–232) months, 189 patients (31%) experienced the main outcome measure (44 males with LVRR, 35%; 105 males without LVRR, 34%; 10 females with LVRR, 18%; and 30 females without LVRR, 27%; global log-rank $p = 0.03$) and 128 patients (21%) the secondary outcome measure (36 males with LVRR, 29%; 76 males without LVRR, 24%; 6 females with LVRR, 11%; 24 females without LVRR, 22%; global $p = 0.06$). The cumulative incidence at 10 years of follow-up of specific components of the outcome measure is reported in Table 2. Women experiencing LVRR had the lowest incidence of all-cause mortality/HTx/VAD at 10 years of follow-up compared to the other groups, with an absolute risk reduction of 12% and a relative risk reduction of 71% of the main outcome measure compared to men with LVRR ($p = 0.04$). Interestingly, women without LVRR at 24 months showed a similar incidence of adverse outcomes as males (Figure 2). Noteworthy, the cumulative incidence of arrhythmic events followed the same trend, being lower in women with LVRR than in the other subgroups ($p = 0.06$) with an absolute risk reduction of 6% and a relative risk reduction of 60% of the arrhythmic outcome measure at 10 years of follow-up compared to men with LVRR ($p = 0.02$) (Figure 2).

Table 1. Characteristics of the Population at 24-month evaluation.

<i>n</i>	Total Cohort		<i>p</i> -Value
	605 Patients		
	Female 165	Male 440	
Age, (mean ± SD)	51 ± 14	47 ± 15	0.007
SBP, (mean ± SD)	123 ± 18	127 ± 50	0.39
NYHA III/IV, <i>n</i> (%)	20 (13%)	34 (8%)	0.11
Familial History of DCM, <i>n</i> (%)	37 (23%)	109 (26%)	0.45
Sinus Rhythm, <i>n</i> (%)	138 (90%)	348 (86%)	0.19
LBBB, <i>n</i> (%)	52 (34%)	101 (25%)	0.02
QRS Length, (mean ± SD)	116 ± 35	115 ± 35	0.69
LVEDDI, mm/m ² (mean ± SD)	34 ± 5	31 ± 5	<0.001
LVEDVI, mL/m ² (mean ± SD)	78 ± 31	81 ± 32	0.42
Normal Volumes *, <i>n</i> (%)	50 (32%)	223 (53%)	0.001
Mild Dilatation *, <i>n</i> (%)	13 (8%)	80 (19%)	
Moderate Dilatation *, <i>n</i> (%)	37 (24%)	30 (7%)	
Severe Dilatation *, <i>n</i> (%)	55 (35%)	89 (21%)	<0.001
Moderate-Severe Dilatation, <i>n</i> (%)	92 (59%)	119 (28%)	
LVEF %, (mean ± SD)	40 ± 12	41 ± 11	0.50
RFP, <i>n</i> (%)	12 (11%)	28 (9%)	0.57
RV Dysfunction, <i>n</i> (%)	9 (8%)	39 (11%)	0.29
ACE-I/ARBs, <i>n</i> (%)	122 (82%)	343 (85%)	0.51
β-blockers, <i>n</i> (%)	135 (85%)	368 (87%)	0.41
MRAs, <i>n</i> (%)	22 (14%)	57 (14%)	0.89
ICD during follow-up, <i>n</i> (%)	39 (24%)	140 (32%)	0.06
CRT during follow-up, <i>n</i> (%)	19 (12%)	59 (13%)	0.59

* Gender specific volumes (LVEDV/BSA): Normal volumes Females: < 61 mL/m². Males: < 74 mL/m²; Mild dilatation Females: 62–70 mL/m². Males: 75–89 mL/m²; Moderate Dilatation Females: 71–80 mL/m². Males: 90–100 mL/m²; Severe Dilatation Females: > 80 mL/m². Males: > 100 mL/m². [10] Legend: ACE-I: Angiotensin Converting Enzyme-Inhibitors; ARBs: Angiotensin Receptor Blockers; BSA: Body Surface Area; CRT: Cardiac Resynchronization Therapy; ICD: Implantable Cardioverter Defibrillator; LBBB: Left Bundle Branch Block; LVEDDI: Left Ventricular End Diastolic Diameter Indexed; LVEDVI: Left Ventricular End Diastolic Volume Indexed; LVEF: Left Ventricular Ejection Fraction; MRAs: Mineralocorticoid Receptor Antagonists; NYHA: New York Heart Association; RFP: Restrictive filling pattern; RV: Right ventricular; SBP: Systolic Blood Pressure.

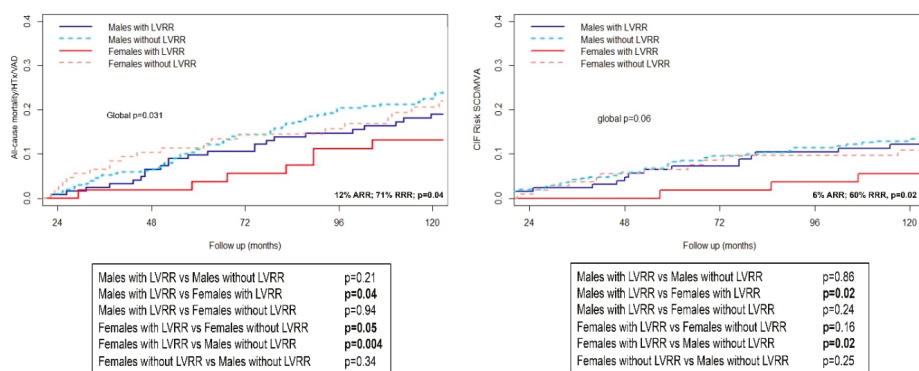


Figure 2. Kaplan-Meier curves for the incidence of All-cause mortality/HTx/VAD (Left Panel) and cumulative incidence function for SCD/MVA (Right Panel) according to LVRR and sex. Legend. HTx: Heart Transplantation; LVRR: Left Ventricular Reverse Remodelling; VAD: Ventricular Assist Device. MVA: Major Ventricular Arrhythmias; SCD Sudden Cardiac Death.

Table 2. Cumulative incidence of events at 10 years of follow-up (starting from the 24 months evaluation) according to sex and LVRR.

	Male with LVRR	Male without LVRR	Females with LVRR	Females without LVRR
Median follow-up, months (IQR)	187 (122–269)	136 (80–202)	199 (123–278)	135 (72–222)
All-cause mortality/HTx/VAD	0.17	0.18	0.05	0.18
CV death/HTx/VAD	0.11	0.13	0.04	0.15
Death for pump failure	0	0.04	0.04	0.2
Heart Transplantation	0.05	0.05	0	0.10
VAD	0.007	0.003	0	0
SCD	0.06	0.03	0	0.04
SCD/MVA	0.10	0.12	0.04	0.12

Legend: CV: cardiovascular; HTx: Heart Transplantation; MVA: major ventricular arrhythmias; SCD: Sudden Cardiac Death; VAD: Ventricular assist device.

3.2. Multi-State Model Analysis

After adjustment for the different variables at the 24 months evaluation (i.e., Age, NYHA class, Sinus Rhythm, Severe LV Dilation, LVEF, Restrictive Filling Pattern, Right Ventricular Dysfunction, and medical therapy) male sex emerged as an independent risk factor of adverse outcomes (HR 1.86, 95% CI 1.07–3.82, $p = 0.02$). To further investigate the relationship between sex and the prognostic role of LVRR over time, a multistate model was built considering LVRR as an intermediate state, with the follow up starting from the baseline. The multi-state model highlights how the occurrence of LVRR over time was strongly associated with better outcomes (HR 0.01, 95% CI 0.001–0.04, $p < 0.001$) and male sex emerged as a strong prognostic factor in patients who experienced LVRR (HR 2.81, 95% CI 1.03–7.64, $p = 0.04$), whereas the impact of sex was diluted in patients without LVRR. Indeed, men with LVRR had a significantly higher probability of experiencing adverse outcomes over time ($p = 0.04$), whereas sex differences were blunted in those without LVRR over time ($p = 0.52$) (Figure 3).

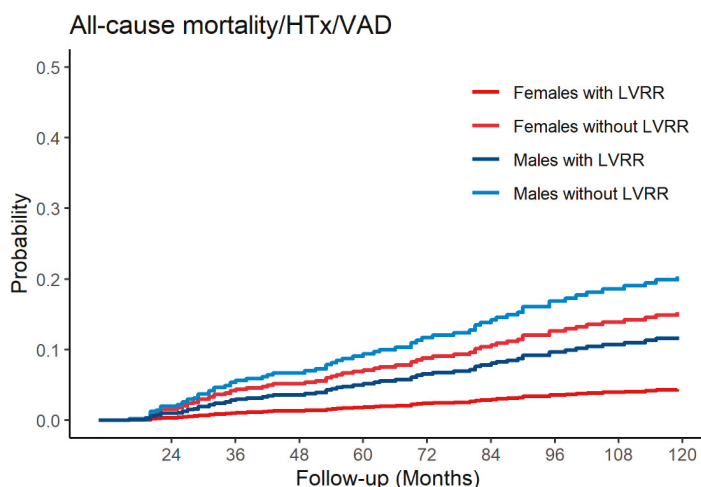


Figure 3. Adjusted Cumulative Incidence estimated from the multi-state model of All-cause mortality/HTx/VAD according to sex in patients with LVRR and without LVRR: Left Ventricular Re. Legend. HTx: Heart Transplantation; VAD: Ventricular Assist Device.

4. Discussion

Female sex has emerged as an important outcome modifier in different cardiovascular scenarios. In patients with DCM, previous reports highlighted the protective role of female sex towards adverse outcomes over the long-term follow-up [6–8,16,17]. However, besides speculative hypotheses and observational analyses, there is no evidence so far investigating the possible mechanisms underlying this prognostic difference between sexes. Although one possible explanation might dwell in a different sex-specific response to medical treatment and, therefore, a different rate of LVRR with subsequent prognostic implications [5], evidence of that is still unavailable. To date, this is the first study addressing the interaction between sex and LVRR as potential outcome modifier in a large population of well-characterized DCM patients with available follow-up data.

The LVRR is a complex process that usually starts with the introduction of medical therapy and takes up to 24 months to complete [1]. Although several factors have been associated with the occurrence of LVRR over time [5], so far, little is known about the influence of sex on the rate of LVRR. Similarly to previous reports [5], in our population approximately 30% of patients experienced LVRR at 24 months of follow-up and the occurrence of LVRR was strongly associated with better prognosis (HR 0.01, 95% CI 0.001–0.04, $p < 0.001$). Interestingly and unexpectedly, the rate of LVRR was comparable between man and women (Figure 1). Noteworthy, among patients experiencing LVRR, females had an overall better prognosis compared to males during a very long-term follow-up; conversely a comparable prognosis between males and females without LVRR was found. To evaluate the prognostic impact of sex over time, we used a multi-state model considering the occurrence of LVRR as an intermediate state. The LVRR was confirmed as a long-term prognostic predictor and the female sex was strongly associated with better outcomes predominantly in patients experiencing LVRR whereas its prognostic implications were diluted in those not experiencing LVRR (Figure 3).

Despite the optimization of medical and device therapy, at 24-months reevaluation women still showed a more advanced phenotype of the disease, characterized by larger LV diameters and a higher incidence of moderate to severe sex-specific dilation, which might partially justify the comparable outcomes in patients without LVRR (Table 1). Despite the more advanced phenotype of DCM observed at 24-month reevaluation, women had overall better long-term outcomes than men. This was probably driven by the excellent long-term outcome showed by women experiencing LVRR, compared to

either men with LVRR or patients without LVRR regardless of their sex (Figure 2). Indeed, women experiencing LVRR showed a 71% relative risk reduction of experiencing a composite adverse outcome of all-cause mortality/HTx/VAD compared to men with LVRR. Similar trends were found for arrhythmic events (Figure 2).

In the era of precision medicine, these findings might have important clinical implications, opening new possible scenarios in patients' management. In fact, different treatment strategies might be employed between sexes experiencing LVRR or not over time. Our results highlight an independent prognostic role of female sex, especially after the LVRR is achieved, and opens up novel scenarios to investigate the mechanism underlying this prognostic advantage of women besides response to treatment.

Women and DCM, a Fairy Tale?

The mechanisms behind a prognostic benefit of female sex are still largely unknown. Indeed, in large clinical trials, women showed a variable response to medical treatment whereas the benefit in men was clear-cut [18]. Furthermore, large registry analysis, probably due to the short-term observation provided, failed to demonstrate a prognostic advantage of female sex in heart failure (HF) patients [19]. Our results provide novel prognostic insights into sex differences in patients with DCM. In the present analysis, we demonstrated that, despite previous hypotheses, there is no difference in response to standard heart failure treatment between sexes, with a similar rate of LVRR over time. However, despite the comparable rate of LVRR, male sex was confirmed as an important independent adverse prognostic factor in those patients (Figure 4). This finding suggests that the reason for this prognostic benefit in women might dwell in some intrinsic factors specifically related to the female sex. Furthermore, potential and yet unknown protective mechanisms might be present in female patients with DCM helping either to control the occurrence or to suppress life-threatening arrhythmic events, highlighting the protective role of female sex also in this setting. Whether different social or cultural behaviours associated with hormonal status or genetic background might have a role in this is still largely unknown and deserves further study [18,20–23].

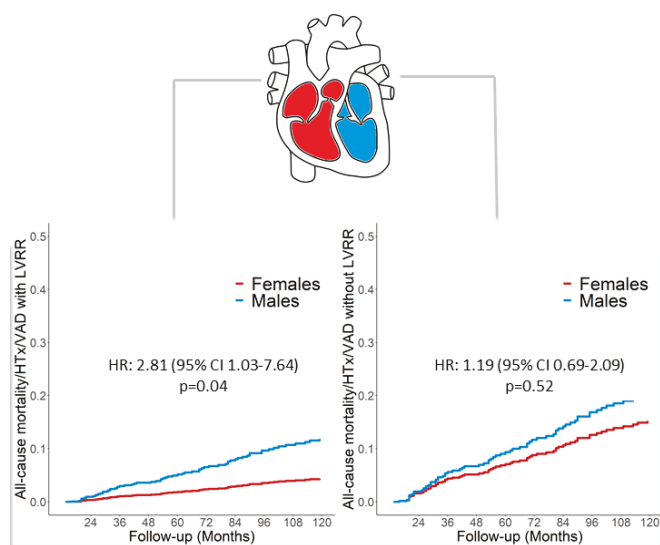


Figure 4. Central Illustration Schematic representation of the main results of the study. The rate of LVRR is comparable between sexes; however, male sex is an independent adverse prognostic factor regardless of the occurrence of LVRR. Legend: Legend. HTx: Heart Transplantation; LVRR: Left Ventricular Reverse Remodelling; VAD: Ventricular Assist Device.

5. Limitations

This retrospective analysis has been conducted in patients with DCM consecutively enrolled in a tertiary referral centre. Therefore, these results might be not genuinely representative of the entire DCM spectrum and should be applied only to patients with similar characteristics. A possible selection bias imposed by the long enrolment period has been imposed by the relatively low event rate. However, guideline-directed medical treatment has been provided to all patients regardless of the date of enrolment, partially overcoming this limitation. Data on cardiac magnetic resonance, biomarkers and genetics were not available for all patients. Similarly, evaluation of the potential sex-specific effect of device therapy requires larger multicentre analysis. Therefore, limiting the investigation of these specific subgroups might introduce a significant bias in the population analysed. Lastly, sex-specific analyses on the occurrence of arrhythmic events are needed to provide more in-depth characterization of these patients. Further research is needed to confirm these data in larger multicentric populations, focusing on advanced imaging analysis and novel biomarkers or genetic status aiming to provide novel insights in this field.

6. Conclusions

In this large and well-selected cohort of patients affected by DCM, the rate of LVRR was similar between males and females. However, females achieving LVRR experienced a more favourable long-term prognosis and male sex has been confirmed as independently associated to adverse prognosis even after the LVRR is achieved. A precise characterization of DCM, including genetic background, will be essential to explain this difference in outcomes between men and women in the future.

Supplementary Materials: The following are available online at <http://www.mdpi.com/2077-0383/9/8/2426/s1>, Figure S1: The model consists of three discrete health states (i.e., alive without LVRR; alive with LVRR; dead or HTx or VAD) and a transition probability matrix (P) is calculated between states.

Author Contributions: Conceptualization, A.C., P.M., V.N. and M.M.; methodology, A.C., P.M., V.N., C.G., J.A., P.G., G.B., M.M.; software, A.C., C.G., G.B.; validation, A.C., P.M., V.N., C.G., J.A., P.G., C.P.L., G.B., M.M.; formal analysis, A.C., P.M., C.G., G.B.; investigation, A.C., M.M., G.S.; resources, M.M., G.S.; data curation, A.C., C.P.L., F.R., M.M.; writing-original draft preparation, A.C., P.M., M.M.; writing-review & editing, A.C., P.M., V.N., C.G., J.A., P.G., C.P.L., G.B., M.M.; visualization, C.G.; supervision, M.M., G.S. All authors have read and agreed to the published version of the manuscript.

Funding: This research received no external funding.

Acknowledgments: We would like to thank Fondazione CRTrieste, Fondazione CariGO, Fincantieri and all the healthcare professionals for the continuous support to the clinical management of patients affected by cardiomyopathies, followed in Heart Failure Outpatient Clinic of Trieste, and their families.

Conflicts of Interest: The authors declare no conflict of interest.

References

1. Merlo, M.; Cannata, A.; Gobbo, M.; Stolfo, D.; Elliott, P.M.; Sinagra, G. Evolving concepts in dilated cardiomyopathy. *Eur. J. Heart Fail.* **2017**, *20*, 228–239. [[CrossRef](#)]
2. Merlo, M.; Pivetta, A.; Pinamonti, B.; Merlo, M.; Pivetta, A.; Pinamonti, B.; Stolfo, D.; Zecchin, M.; Barbati, G.; Lenarda, A.D.; et al. Long-term prognostic impact of therapeutic strategies in patients with idiopathic dilated cardiomyopathy: Changing mortality over the last 30 years. *Eur. J. Heart Fail.* **2014**, *16*, 317–324. [[CrossRef](#)] [[PubMed](#)]
3. Merlo, M.; Cannata, A.; Vitagliano, A.; Zambon, E.; Lardieri, G.; Sinagra, G. Clinical management of dilated cardiomyopathy: Current knowledge and future perspectives. *Expert Rev. Cardiovasc. Ther.* **2016**, *14*, 137–340. [[CrossRef](#)]

4. Tayal, U.; Wage, R.; Newsome, S.; Manivarmane, R.; Izgi, C.; Muthumala, A.; Dungu, J.N.; Assomull, R.; Hatipoglu, S.; Halliday, B.P.; et al. Predictors of left ventricular remodelling in patients with dilated cardiomyopathy—a cardiovascular magnetic resonance study. *Eur. J. Heart Fail.* **2020**. [[CrossRef](#)] [[PubMed](#)]
5. Merlo, M.; Pyxaras, S.A.; Pinamonti, B.; Barbati, G.; Di Lenarda, A.; Sinagra, G. Prevalence and prognostic significance of left ventricular reverse remodeling in dilated cardiomyopathy receiving tailored medical treatment. *J. Am. Coll. Cardiol.* **2011**, *57*, 1468–1476. [[CrossRef](#)] [[PubMed](#)]
6. Cannatà, A.; Fabris, E.; Merlo, M. Sex differences in the long-term prognosis of dilated cardiomyopathy. *Can. J. Cardiol.* **2019**, *36*, 37–44. [[CrossRef](#)]
7. Halliday, B.P.; Gulati, A.; Ali, A.; Simon, N.; Amrit, L.; Upasana, T.; Vassilios, S.V.; Monika, A.; Cemil, I.; Kaushiga, K.; et al. Sex- and age-based differences in the natural history and outcome of dilated cardiomyopathy. *Eur. J. Heart Fail.* **2018**, *20*, 1392–1400. [[CrossRef](#)]
8. De Bellis, A.; De Angelis, G.; Fabris, E.; Cannata, A.; Merlo, M.; Sinagra, G. Gender-related differences in heart failure: Beyond the “one-size-fits-all” paradigm. *Heart Fail. Rev.* **2020**, *25*, 245–255. [[CrossRef](#)]
9. Ponikowski, P.; Voors, A.A.; Anker, S.D.; Héctor, B.; John, G.F.C.; Andrew, J.S.C.; Volkmar, F.; José, R.; Veli-Pekka, H.; Ewa, A.J.; et al. 2016 ESC Guidelines for the diagnosis and treatment of acute and chronic heart failure: The Task Force for the diagnosis and treatment of acute and chronic heart failure of the European Society of Cardiology (ESC) Developed with the special contribution of the Heart Failure Association (HFA) of the ESC. *Eur. Heart J.* **2016**, *37*, 2129–2200.
10. Brignole, M.; Auricchio, A.; Baron-Esquivias, G. 2013 ESC Guidelines on cardiac pacing and cardiac resynchronization therapy: The Task Force on cardiac pacing and resynchronization therapy of the European Society of Cardiology (ESC). Developed in collaboration with the European Heart Rhythm Association (EHRA). *Eur. Heart J.* **2013**, *34*, 2281–2329.
11. Lang, R.M.; Badano, L.P.; Mor-Avi, V.; Pierre, B.; Giuseppe, B.; Ole, B.; John, C.; Jean-Claude, D.; Victoria, D.; Perry, M.E.; et al. Recommendations for cardiac chamber quantification by echocardiography in adults: An update from the American society of echocardiography and the european association of cardiovascular imaging. *J. Am. Soc. Echocardiogr.* **2015**, *28*, 1–39. [[CrossRef](#)]
12. Kajimoto, K.; Sato, N. Investigators of the acute decompensated heart failure syndromes, r. sex differences in New York heart association functional classification and survival in acute heart failure patients with preserved or reduced ejection fraction. *Can. J. Cardiol.* **2020**, *36*, 30–36. [[CrossRef](#)] [[PubMed](#)]
13. Kajimoto, K.; Minami, Y.; Otsubo, S.; Sato, N.; Investigators of the Acute Decompensated Heart Failure Syndromes, R. Sex differences in left ventricular cavity dilation and outcomes in acute heart failure patients with left ventricular systolic dysfunction. *Can. J. Cardiol.* **2018**, *34*, 477–484. [[CrossRef](#)] [[PubMed](#)]
14. Gray, R.J. A class of k-sample tests for comparing the cumulative incidence of a competing risk. *Ann. Statist.* **1988**, *16*, 1141–1154. [[CrossRef](#)]
15. Therneau, T.M.; Grambsch, P.M. Proportional hazards tests and diagnostics based on weighted residuals. *Biometrika* **1994**, *81*, 515–526.
16. Meyer, S.; van der Meer, P.; van Tintelen, J.P.; van den Berg, M.P. Sex differences in cardiomyopathies. *Eur. J. Heart Fail.* **2014**, *16*, 238–247. [[CrossRef](#)]
17. Mosca, L.; Barrett-Connor, E.; Wenger, N.K. Sex/gender differences in cardiovascular disease prevention: What a difference a decade makes. *Circulation* **2011**, *124*, 2145–2154. [[CrossRef](#)]
18. Lam, C.S.P.; Arnott, C.; Beale, A.L. Sex differences in heart failure. *Eur. Heart J.* **2019**, *40*, 3859–3868. [[CrossRef](#)]
19. Lainscak, M.; Milinkovic, I.; Polovina, M. Sex and age related differences in the management and outcomes of chronic heart failure: An analysis of patients from the ESC HFA EORP Heart Failure Long-Term Registry. *Eur. J. Heart Fail.* **2020**, *22*, 92–102. [[CrossRef](#)]
20. Boheler, K.R.; Volkova, M.; Morrell, C.; Rahul, G.; Yi, Z.; Kenneth, M.; Anne-Marie, S.; Edward, G.L. Sex- and age-dependent human transcriptome variability: Implications for chronic heart failure. *Proc. Natl. Acad. Sci. USA* **2003**, *100*, 2754–2759. [[CrossRef](#)]
21. Kaneda, R.; Takada, S.; Yamashita, Y. Genome-wide histone methylation profile for heart failure. *Genes Cells* **2009**, *14*, 69–77. [[CrossRef](#)] [[PubMed](#)]

22. Feridooni, H.A.; Dibb, K.M.; Howlett, S.E. How cardiomyocyte excitation, calcium release and contraction become altered with age. *J. Mol. Cell Cardiol.* **2015**, *83*, 62–72. [[CrossRef](#)] [[PubMed](#)]
23. Cannata, A.; Camparini, L.; Sinagra, G.; Giacca, M.; Loffredo, F.S. Pathways for salvage and protection of the heart under stress: Novel routes for cardiac rejuvenation. *Cardiovasc. Res.* **2016**, *111*, 142–153. [[CrossRef](#)] [[PubMed](#)]



© 2020 by the authors. Licensee MDPI, Basel, Switzerland. This article is an open access article distributed under the terms and conditions of the Creative Commons Attribution (CC BY) license (<http://creativecommons.org/licenses/by/4.0/>).

Article

Tachycardiomyopathy in Patients without Underlying Structural Heart Disease

Giulia Stronati [†], Federico Guerra ^{*,†}, Alessia Urbinati, Giuseppe Ciliberti, Laura Cipolletta and Alessandro Capucci

Cardiology and Arrhythmology Clinic, Marche Polytechnic University, University Hospital "Umberto I-Lancisi-Salesi", 60126 Ancona, Italy

* Correspondence: f.guerra@staff.univpm.it; Tel.: +39-0715-965-693

[†] Contributed equally to the manuscript.

Received: 31 July 2019; Accepted: 5 September 2019; Published: 8 September 2019

Abstract: Tachycardiomyopathy (TCM) is an underestimated cause of reversible left ventricle dysfunction. The aim of this study was to identify the predictors of recurrence and incidence of major cardiovascular events in TCM patients without underlying structural heart disease (pure TCM). The prospective, observational study enrolled all consecutive pure TCM patients. The diagnosis was suspected in patients admitted for heart failure (HF) with a reduced ejection fraction and concomitant persistent arrhythmia. Pure TCM was confirmed after the clinical and echocardiographic recovery during follow-up. From 107 pure TCM patients (9% of all HF admission, the median follow-up 22.6 months), 17 recurred, 51 were hospitalized for cardiovascular reasons, two suffered from thromboembolic events and one died. The diagnosis of obstructive sleep apnoea syndrome (OSAS, hazard ratio (HR) 5.44), brain natriuretic peptide on admission (HR 1.01 for each pg/mL) and the heart rate at discharge (HR 1.05 for each bpm) were all independent predictors of TCM recurrence. The left ventricular ejection fraction at discharge (HR 0.96 for each%) and the heart rate at discharge (HR 1.02 for each bpm) resulted as independent predictors of cardiovascular-related hospitalization. Pure TCM is more common than previously thought and associated with a good long-term survival but recurrences and hospitalizations are frequent. Reversing OSAS and controlling the heart rate could prevent TCM-related complications.

Keywords: arrhythmias; atrial fibrillation; cardiomyopathy; heart failure; supraventricular arrhythmia; systolic dysfunction; tachycardiomyopathy; ventricular arrhythmia

1. Introduction

Tachycardiomyopathy (TCM) is an important cause of dysfunction of the left ventricle [1]. It is defined as an arrhythmia induced cardiomyopathy in which the impairment of the left ventricle is secondary to rapid and/or asynchronous, irregular myocardial contraction and is partially or completely reversible after treatment of the triggering arrhythmia [2]. Both atrial and ventricular arrhythmias, as well as the premature atrial or ventricular complexes have been noted to cause TCM [1] and no specific heart rate cut-off at which the condition develops has been identified [3].

The first descriptions of TCM were collected by Phillips and Levine in 1949. In their milestone paper, they hypothesized that patients with long-lasting atrial fibrillation could develop heart failure without any other evidence of structural heart disease, and such heart failure could completely disappear after the restoration of the sinus rhythm [4]. TCM is nowadays classified as a non-familial cause of dilated cardiomyopathy, although doubts have been cast on the inclusion of such a disease among those conditions directly affecting the structure and/or function of the heart [5].

TCM is estimated to be under-recognized [3] and the incidence and prevalence of the condition are currently unknown. The mechanisms of TCM and pathways responsible in individual patients

are not fully understood [2,6], however it is hypothesised that subclinical ischaemia, abnormalities in energy metabolism, and an overload of calcium and oxidative stress play a role in the pathogenesis of the condition [1]. To this day, two categories of the disease have been described: Arrhythmia-induced TCM, where the arrhythmia is the sole reason for the dysfunction, and arrhythmia-mediated TCM, where the arrhythmia can exacerbate or worsen heart failure (HF) or an underlying heart disease [1]. The former can also be referred to as “pure” TCM and the latter as “impure” TCM [7,8].

The diagnosis of TCM is retrospective and based on the evidence of recovery after appropriate treatment. In fact, although, an arrhythmia is present with a concomitant left ventricular ejection fraction (LVEF) impairment, a cause-effect relationship is not always ascertainable [2]. There is very little data regarding the recurrences and adverse events in patients with TCM in the current available literature.

The aim of this study was to identify the possible predictors of recurrence and long-term morbidity and mortality of pure TCM.

2. Materials and Methods

2.1. Study Population

This is a prospective, observational study taking into account all patients admitted for acute HF with reduced ejection fraction from January 2012 to the end June 2018 in the Cardiology and Arrhythmology Clinic of the University Hospital “Ospedali Riuniti” of Ancona, Italy, and presenting with evidence of atrial or ventricular arrhythmias on admission.

The potential triggering arrhythmias considered were: Atrial fibrillation (AF), atrial flutter, supraventricular tachycardia, ventricular tachycardia and premature atrial and ventricular complexes. More specifically, this study considered significant > 20000 premature ventricular complexes per day, according to the current available literature [8].

The selection process is detailed in Figure 1 and consisted of two main phases. The first phase started with the hospitalization and aimed at detecting all potential patients with pure TCM. In order to assess the real weight of TCM in clinical practice, the patients with arrhythmia-mediated (impure) TCM were excluded, ruling out all structural or functional heart diseases. Ischemic heart disease was defined as a previous history of revascularization, or evidence of significant coronary obstruction at coronary angiography performed during hospitalization. The patients with non-significant coronary atherosclerosis and no clinical instrumental signs of ischemia were not excluded. Valvular heart disease was defined as a previous history of aortic or mitral replacement or the repair, evidence of severe aortic or mitral regurgitation, severe aortic stenosis, or moderate or severe mitral stenosis. Congenital heart diseases, cardiac amyloidosis, hypertrophic cardiomyopathy, myocarditis, non-compaction cardiomyopathy, post-partum cardiomyopathy, arrhythmogenic right ventricular dysplasia, Fabry’s disease and alcoholic cardiomyopathy were defined according to the current standards. The non-invasive and invasive diagnostic procedures, such as coronary angiography or cardiac magnetic resonance, were performed according to clinical suspicion in all eligible patients. All patients were treated for HF and underwent rhythm or rate control strategies according to the current guidelines [9–12]. After discharge, the second phase of the selection process started and aimed at confirming pure TCM out of all potential patients (Figure 1). All the patients with suspected TCM were followed-up in the heart failure outpatient clinic at one month and three months after discharge, and twice a year from then on. The patients presenting an improvement of at least one New York Heart Association (NYHA) class and the recovery of at least five points of the left ventricular ejection fraction (LVEF) during the follow-up were diagnosed with arrhythmia-induced (pure) TCM and included in the analysis (Figure 1) [1,13].

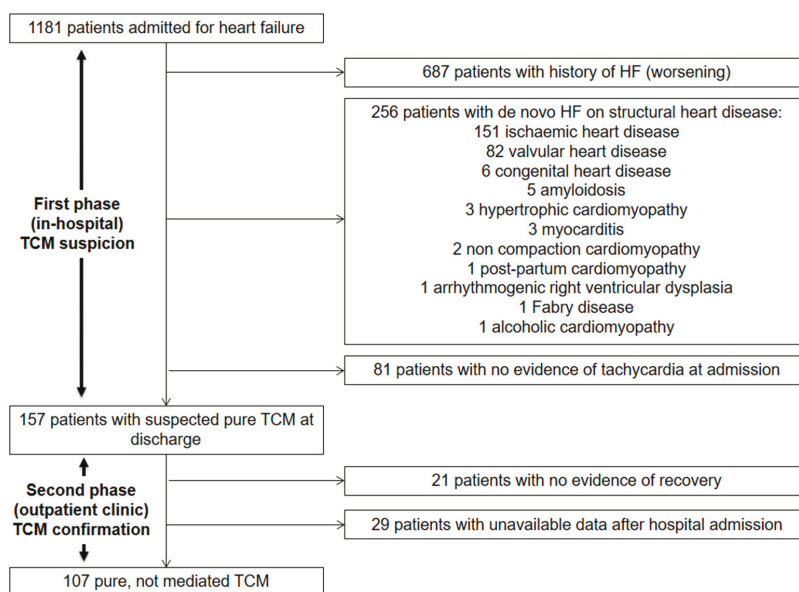


Figure 1. Selection process.

The study was conducted according to institutional guidelines, national legal requirements, European standards and the revised Declaration of Helsinki. Being an observational study, a formal approval of the ethics committee was not sought. All patients provided prior written informed consent for anonymous collection and publication of their clinical data. The present report complies with the STROBE initiative (Table S1) [14].

2.2. Endpoints

The primary endpoint was the recurrence of TCM, defined as a new episode of acute HF with reduced ejection fraction along with the evidence of atrial or ventricular arrhythmia, occurring after complete clinical (no HF symptoms) and echocardiographic (LVEF \geq 50%) recovery of the original episode.

The secondary endpoints were: Death from all causes, major adverse cardiovascular events (defined as non-fatal stroke, non-fatal myocardial infarction and cardiovascular death), and cardiovascular hospitalizations. Cardiovascular hospitalizations were defined as any hospitalization longer than 12 h for one or more of the following reasons: Acute coronary syndrome, unstable angina, HF, atrial or ventricular arrhythmia, valvular heart disease, infective endocarditis, myocarditis, pericarditis, aortic disease, pulmonary embolism, stroke/transient ischemic attack, syncope, cardiovascular-related elective and urgent procedures and complications of such procedures.

2.3. Data Collection

Two expert physicians were responsible for the prospective data collecting regarding the patients' demographics, risk factors, medical history and treatment. Continuous 12-lead ECG monitoring (Mortara Rangoni, Arezzo, Italy) was used to assess the heart rate during hospitalization and underlying arrhythmias. The blood samples for brain natriuretic peptide (BNP) and troponin I were collected on admission and at discharge. Echocardiographic examinations were performed with a monoplane ultrasound probe 4 MHz (M4S) of Vivid 7 Pro (GE Medical Systems, Milwaukee). The digital loops were captured, recording at least three consecutive beats, and analysed off-line using a dedicated software

(EchoPAC 13.0; GE Medical Systems, Milwaukee) according to the most recent recommendations. A complete echocardiogram was performed on admission, at discharge, at a 3-month follow-up. Serial echocardiograms were then performed at least every 6 months until complete recovery of LVEF. The echocardiographic loops were obtained with the patient supine and in the left lateral decubitus at the end of a normal breath, minimizing the depth in order to optimize the frame rate (40–80 fps). LVEF was calculated by the Simpson biplane method. All echo exams were reviewed by two authors (G.S. and F.G.), who were responsible for the off-line analysis and collected all measurements blinded to the recurrence or other clinical endpoints. The inter-operator coefficient of variations for LVEF was 3.2% and the intra-operator coefficient of variation was 2.4%.

To allow for the comparability of drug regimens across the patients taking many different medications, a treatment intensity score (TIS) was calculated. As previously reported, [15] the recorded daily dose taken by the patient was divided by the maximum recommended daily dose to obtain a proportional dose for that medication, called intensity. The maximum recommended daily doses were set by the European and American guidelines [9–12].

2.4. Statistical Analysis

All continuous variables were checked for normality through the Kolmogorov-Smirnov test. The normally-distributed variables were described by the mean and standard deviation and compared by analysis of variance. The not-normally-distributed variables were described as the median and 1st–3rd IQR and compared by non-parametric tests. The categorical variables were described as the absolute and relative values, and compared by chi-square test or Fisher exact test, as appropriate.

The Kaplan-Meier analysis was used in order to assess the time free from primary and secondary endpoints. The association between the individual variables and the risk of TCM recurrence and cardiovascular hospitalization was investigated by using univariate Cox proportional hazards models. The variables that showed an association with each endpoint with a significance level < 0.1 on univariate analyses were entered into the multivariable Cox proportional hazards model. The independent risk factors for each endpoint were then presented as hazard ratios (HRs) and 95% confidence intervals (CIs).

The linearity assumption of the relationship between the independent continuous risk factors and the outcome of interest was represented using restricted cubic splines with three knots located to the 10th, 50th, and 90th percentiles according to the Harrell rule, and assessed by the Wald test for linearity.

SPSS 22.0 for Windows (SPSS Inc., Chicago, IL, USA) and R (R Foundation for Statistical Computing, Vienna, Austria) were used for statistical analysis. The values of $p < 0.05$ (two-tailed) were considered as statistically significant.

3. Results

The population included 107 patients (68 males, mean age 66.7 ± 14.5 years). The patients' characteristics are summarized in Table 1. The median follow-up was 22.6 months (1st–3rd quartile 10.0–40.0 months). The median hospitalization time (i.e., the first phase of the selection process) was 7 days (1st–3rd quartile 4–11 days). The median time to TCM diagnosis confirmation (i.e., the second phase of the selection process) was 72 days (1st–3rd quartile 48–130 days). Eighty-three patients (77.6%) were diagnosed with atrial fibrillation (AF) as underlying arrhythmia, and 16 (15.0%) with atrial flutter. Other triggering arrhythmias included non-sustained ventricular tachycardia (4, 3.7%), paroxysmal supraventricular tachycardia (1, 0.9%) and premature ventricular contractions (PVCs) (3, 2.8%).

Table 1. Baseline characteristics, also divided by the incidence of tachycardiomyopathy recurrence and cardiovascular-related hospitalization.

Variable	Total Population (n = 107)	No Recurrence (n = 90)	Recurrence (n = 17)	p Value	No CV Hospitalization (n = 56)	CV Hospitalization (n = 51)	p Value
Male gender	68 (64%)	58 (64%)	10 (59%)	0.659	32 (57%)	36 (71%)	0.149
Age (years)	66.7 ± 14.5	66.9 ± 15.1	66.0 ± 11.3	0.816	68.8 ± 15.4	64.4 ± 13.2	0.117
BMI (Kg/m ²)	28.6 ± 5.3	28.5 ± 5.3	29.1 ± 5.3	0.692	28.4 ± 5.7	28.7 ± 5.0	0.655
Hypertension	68 (64%)	57 (63%)	11 (65%)	0.911	39 (67%)	29 (57%)	0.170
Diabetes	14 (13%)	14 (15%)	0 (0%)	0.081	7 (12%)	7 (14%)	0.851
Dyslipidaemia	36 (34%)	29 (32%)	7 (41%)	0.474	19 (34%)	17 (33%)	0.948
CKD	22 (21%)	20 (22%)	2 (12%)	0.328	12 (21%)	10 (20%)	0.816
COPD	12 (11%)	11 (12%)	1 (6%)	0.447	9 (16%)	3 (6%)	0.095
OSAS	6 (6%)	2 (2%)	4 (24%)	0.006	1 (2%)	5 (10%)	0.100
Hyperthyroidism	6 (6%)	5 (5%)	1 (6%)	0.273	5 (9%)	1 (2%)	0.118
Hypothyroidism	7 (7%)	4 (4%)	3 (17%)	0.043	3 (5%)	4 (8%)	0.707
AF as trigger	83 (77%)	67 (74%)	16 (94%)	0.075	43 (77%)	40 (78%)	0.838
On admission:							
NYHA class II	18 (17%)	15 (17%)	3 (18%)		9 (16%)	9 (18%)	
NYHA class III	62 (58%)	51 (57%)	11 (65%)	0.730	33 (59%)	29 (60%)	0.970
NYHA class IV	27 (25%)	24 (27%)	3 (17%)		14 (25%)	13 (25%)	
Heart rate (bpm)	126.5 ± 28.9	127.0 ± 30.8	124.2 ± 17.5	0.714	127.2 ± 23.1	125.9 ± 34.2	0.818
BNP (pg/mL)	575 (312–786)	541 (293–771)	781 (655–1247)	0.012	547 (364–765)	624 (270–851)	0.413
Troponin I (ng/mL)	0.02 (0.01–0.06)	0.02 (0.01–0.06)	0.03 (0.01–0.07)	0.694	0.02 (0.01–0.06)	0.03 (0.01–0.08)	0.146
LVEF (%)	32.9 ± 9.7	32.9 ± 9.4	32.6 ± 8.7	0.918	34.2 ± 7.9	31.4 ± 10.4	0.129
iLAV (mL/m ²)	50.15 ± 14.5	48.2 ± 14.0	58.7 ± 13.9	0.037	49.5 ± 11.8	51.0 ± 17.5	0.717
At discharge:							
Heart rate (bpm)	71.0 ± 15.0	69.5 ± 14.8	78.2 ± 14.4	0.029	68.4 ± 13.5	73.9 ± 16.2	0.067
BNP (pg/mL)	257 (124–511)	244 (123–429)	307 (169–670)	0.141	165 (89–252)	354 (249–551)	0.02
Troponin I (ng/mL)	0.03 (0.01–0.04)	0.05 (0.01–0.06)	0.02 (0.01–0.04)	0.99	0.02 (0.01–0.05)	0.03 (0.02–0.03)	0.99
LVEF (%)	41.0 ± 11.8	41.8 ± 12.1	36.0 ± 8.8	0.179	43.5 ± 9.8	37.5 ± 13.6	0.047
NYHA class I	27 (26%)	24 (27%)	3 (17%)		16 (29%)	11 (22%)	
NYHA class II	74 (70%)	61 (69%)	13 (76%)	0.655	39 (67%)	35 (71%)	0.431
NYHA class III	4 (4%)	3 (3%)	1 (6%)		1 (2%)	3 (6%)	

AF: atrial fibrillation; BMI: body mass index; BNP: brain natriuretic peptide; CKD: chronic kidney disease; COPD: chronic obstructive pulmonary disease; CV: cardiovascular; iLAV: indexed left atrial volume; LVEF: left ventricular ejection fraction; NYHA: New York Heart Association; OSAS: obstructive sleep apnoea.

During the follow-up, 17 patients experienced at least one recurrence (15.8% of all patients) and 51 were hospitalized for cardiovascular reasons (47.7%). Among the major adverse cardiovascular events, two patients suffered from thromboembolic events (1.8%) and one died from cardiovascular causes (0.9%). No non-fatal myocardial infarctions were reported. The annual incidence of recurrence was 8.4% per year, 0.9% per year for thromboembolic events and 0.4% per year for cardiovascular mortality.

The only death occurred in a 58-year old male, one year and three months after recovery of both NYHA class and LVEF. The patient had no evidence of progression to any kind of structural heart disease and died suddenly after an out-of-hospital cardiac arrest due to idiopathic ventricular fibrillation. One transient ischemic attack and one non-fatal stroke occurred in two different patients after 3 and 832 days, respectively. The treatment strategies at discharge are described in Table 2.

Table 2. Treatment strategies at discharge.

Variable	Total Population (n = 107)	Mean TIS *
ACE-Inhibitors	59 (55%)	0.40 ± 0.26
ARBs	34 (32%)	0.46 ± 0.36
Beta-blockers	98 (92%)	0.54 ± 0.24
MRA	86 (80%)	0.50 ± 0.24
Loop diuretics	92 (86%)	49.73 ± 36.55 **
Ivabradine	2 (2%)	0.50
Flecainide	4 (4%)	0.50
Amiodarone	57 (53%)	0.97 ± 0.09
Digoxin	11 (10%)	0.45 ± 0.22
CCBs	12 (11%)	0.75 ± 0.23
Pharmacological cardioversion	11 (10%)	
Electrical cardioversion	68 (64%)	
Catheter ablation	18 (17%)	
Successful rhythm control	67 (63%)	
WCD	10 (9%)	

* The mean therapeutic index was calculated only in those patients who were administered the drug at least until discharge. ** For loop diuretics we considered the total dose per day as equivalents of furosemide. ACE-I: angiotensin converting enzyme inhibitor; ARB: angiotensin II receptor blocker; CCB: calcium-channel blocker; MRA: mineralocorticoid receptor antagonist; WCD: wearable cardioverter-defibrillator.

3.1. Tachycardiomyopathy Recurrences

Out of the 17 patients experiencing recurrences, seven had multiple recurrences, with six patients experiencing two recurrences and one experiencing four. The arrhythmic disorder underlying TCM recurrences was AF in 15 cases (88%) and atrial flutter in two cases (12%).

The majority of recurrences occurred between the fifth and the sixth year after the first diagnosis as seen in Figure 2.

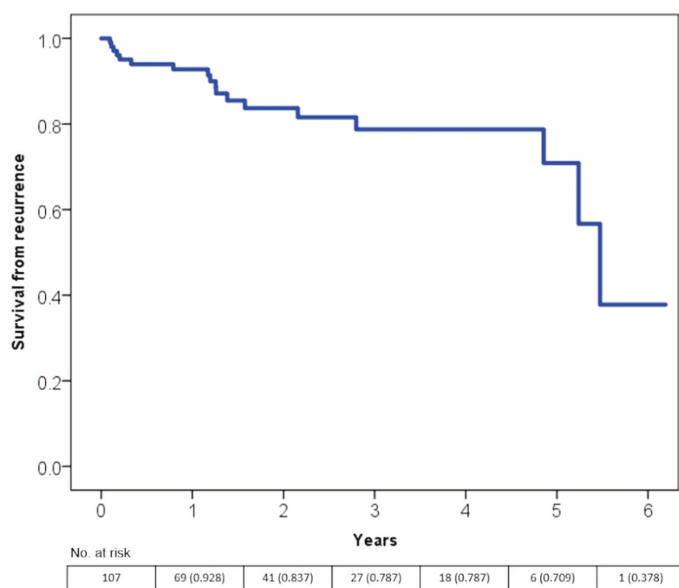


Figure 2. Time free from tachycardiomyopathy recurrence according to the Kaplan-Meier curves.s.

The multivariate Cox regression analysis showed that presence of obstructive sleep apnoea syndrome (OSAS), BNP on admission and the heart rate at discharge were all independent predictors of TCM recurrence (Table 3).

Table 3. Multivariable Cox-proportional hazard model for tachycardiomyopathy recurrence.

Variable	HR	95% CI Lower Bound	95% CI Upper Bound	p Value
OSAS	5.88	1.38	17.29	0.045
BNP at admission (for each pg/mL)	1.01	1.01	1.03	0.014
Heart rate at discharge (for each bpm)	1.05	1.01	1.10	0.029

The univariate model included: The male gender, age, body mass index, hypertension, diabetes, dyslipidaemia, chronic kidney disease, chronic obstructive pulmonary disease, OSAS, hyperthyroidism, hypothyroidism, type of arrhythmia, NYHA class on admission and at discharge, heart rate on admission and at discharge, BNP on admission and at discharge, Troponin I on admission and at discharge, LVEF on admission and at discharge, iLAV, rate or rhythm control (dummy variable) and pharmacological treatment at discharge (with each drug class from Table 2 considered as a separate variable). The complete model is detailed in Table S2.

BNP: brain natriuretic peptide; CI: confidence interval; iLAV: indexed left atrial volume; LVEF: left ventricular ejection fraction; NYHA: New York Heart Association; OSAS: obstructive sleep apnoea.

According to the spline curves, the heart rate at discharge and the risk of TCM recurrence had a linear association (Figure S1a,b, *sp* for linearity < 0.001). The mean values for both the heart rate and LVEF throughout the index event, the follow-up and at the time of recurrence are shown in Figure 3a,b. Consistently with other statistical models, the heart rate at discharge and during follow-up is significantly higher in patients experiencing a recurrence when compared with the patients with no recurrence. Furthermore, all patients showed a LVEF ≥50% at a 1-year follow-up.

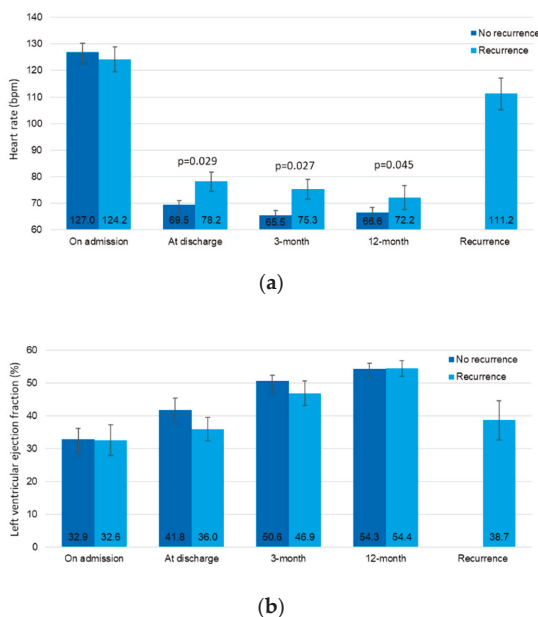


Figure 3. The mean values of the heart rate (a) and left ventricular ejection fraction (b) during follow-up, according to the presence or absence of future recurrences.

Comparing TIS for each drug class considered in Table 2 showed no differences between patients with and without recurrences (all $p > 0.05$).

From the 17 patients experiencing recurrences, 13 were under a rhythm-control strategy and four were under a rate-control strategy. Twelve patients underwent catheter ablation of AF and two underwent ablation of atrial flutter. The patients undergoing catheter ablation of atrial flutter experienced no further TCM recurrences, while five patients presented a second TCM recurrence after the procedure. Three patients with AF refused consent to catheter ablation and were therefore shifted to a rate-control strategy, with one patient experiencing no further recurrences, one experiencing a second recurrence and another patient experiencing three more recurrences over the follow-up.

3.2. Cardiovascular Hospitalizations

From the 51 patients hospitalized for cardiovascular reasons during the follow-up, 15 were hospitalized more than once.

More than 40% of all cardiovascular-related hospitalizations occurred within the first year after the first diagnosis (Figure 4).

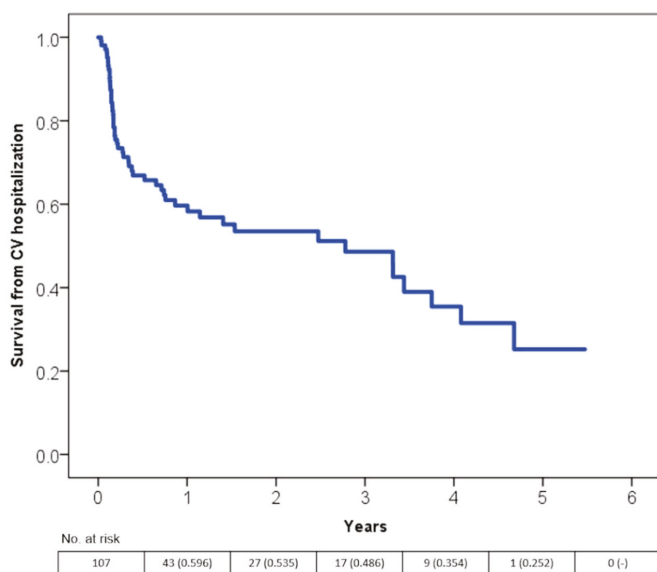


Figure 4. Time free from hospitalization for cardiovascular reasons according to the Kaplan-Meier curves.

EF at discharge and the heart rate at discharge resulted as independent predictors of cardiovascular-related hospitalization according to the multivariate Cox regression model (Table 4 and Figure S1c,d).

Table 4. Multivariable Cox-proportional hazard model for cardiovascular hospitalization.

Variable	HR	95% CI Lower Bound	95% CI Lower Bound	p Value
LVEF at discharge (for each%)	0.96	0.93	0.99	0.020
Heart rate at discharge (for each bpm)	1.02	1.01	1.04	0.032

The univariate model included: The male gender, age, body mass index, hypertension, diabetes, dyslipidaemia, chronic kidney disease, chronic obstructive pulmonary disease, OSAS, hyperthyroidism, hypothyroidism, type of arrhythmia, NYHA class on admission and at discharge, heart rate on admission and at discharge, BNP on admission and at discharge, Troponin I on admission and at discharge, LVEF on admission and at discharge, iLAV, rate or rhythm control (dummy variable) and pharmacological treatment at discharge (with each drug class from Table 2 considered as a separate variable). The complete model is detailed in Supplementary Table S3.

BNP: brain natriuretic peptide; CI: confidence interval; iLAV: indexed left atrial volume; LVEF: left ventricular ejection fraction; NYHA: New York Heart Association; OSAS: obstructive sleep apnoea.

Comparing TIS for each drug class considered in Table 2 showed no differences between the patients with and without cardiovascular hospitalizations (all $p > 0.05$).

4. Discussion

The main message of the present study is that, while TCM is associated with an overall good prognosis, TCM patients do recur over a long-time follow-up.

This represents an outstanding difference between HF patients and pure TCM patients as the former is known to be a progressive, worsening condition commonly culminating in the patient's exitus. Although under-recognized, this study shows that almost 10% of all hospitalizations for acute HF meet the diagnostic criteria for TCM. Therefore, early recognition of the possible triggering

arrhythmia is of paramount importance as it can lead to treatment strategies which can favour patient recovery. A clinical suspicion of TCM should arise in all patients presenting with new and quickly worsening symptoms of HF, a low overall cardiovascular risk profile and the recent evidence of high-rate arrhythmia. In these cases, a prompt reduction of the heart rate (either through rate control drugs or restoration of sinus rhythm) should be performed as soon as possible, and possibly even while the diagnostic workup for the exclusion of structural heart disease is still in progress. A cardioversion attempt should be made (when feasible) in order to prevent further deterioration of the systolic function and catheter ablation should be taken into serious consideration [10]. Moreover, in these patients, a sleep study and polysomnography should be performed as soon as possible, even during the hospital stay, as potentially able to unmask OSAS.

The rate of TCM recurrence is higher between the fifth and the sixth year after diagnosis. It can only be speculated that this could be due to the natural progressive reduction of the patients' adherence to treatment over time.

Our multivariate analysis found three major independent predictors of TCM recurrence. The most important was a concomitant diagnosis of OSAS, which increased the risk of recurrence 5-fold. It was hypothesized that this could be related to the fact that OSAS can alter the physiological parasympathetic modulation of the heart during sleep leading to sympathetic excitation and favouring ventricular and atrial ectopic beats [16,17]. Moreover, OSAS has been described to be an independent risk factor for AF and has been shown to decrease the success rate of antiarrhythmic drugs, electrical cardioversion and catheter ablation [18], potentially leading to TCM recurrence. Despite the lack of information regarding the actual adherence to non-invasive ventilation, it is noted that half of the patients with OSAS and TCM recurrence were not treated with continuous positive airway pressure at all. Therefore, it appears important to educate patients affected by OSAS on the importance of non-invasive ventilation while offering the best treatment strategy in order to improve long-term compliance.

Another striking result that warrants discussion is that the heart rate at discharge is associated with an increased risk of TCM recurrence. More precisely, for each increased beat per minute, the risk of recurrence increases by 5%. Moreover, this association proved to be linear, at least within the ranges of the heart rate seen in our population, and holds true independently of the rhythm at discharge, the treatment strategy and the class of medications used. To make an example, a patient with a lenient rate control strategy (110 bpm) has a 2.5-fold risk of TCM recurrence when compared to the same patient undergoing a strict rate control strategy (80 bpm). This is in contrast to the known evidence that both the heart rate targets are considered similarly effective in preventing adverse events in patients with AF [19]. The reasons for such a striking difference can be found in the different pathophysiological mechanisms. In the RACE II trial, AF patients with severe HF or with recent decompensation were excluded, thus leaving only patients without HF or with stable mild symptoms for at least three months [20]. In this setting, it has already been demonstrated that the actual benefit from the heart rate reduction and sinus rhythm restoration could be counterbalanced by the increased likelihood of adverse effects due to anti-arrhythmic drugs [21] and, therefore, pushing too hard on heart rate reduction could produce no further clinical benefits. On the other hand, it is well known that the heart rate is a risk factor in patients with HF, even when the sinus rhythm is present. Dysfunctional myocardium is energetically depleted and myocardial exerted force is negatively associated with the rate of contraction [22]. In an HF setting, such as the one of TCM occurrence, reducing the heart rate improves contractility, extends coronary diastolic filling time, reduces energy expenditure and improves cardiac output [23]. Moreover, the benefits of a reduced heart rate are consistent over the years, due to the positive modifications of the extracellular matrix and myocytes properties [24], resulting in a reduced risk of cardiovascular events and HF recurrences over a long follow-up. Regarding BNP, a small study already demonstrated that a NT-proBNP drop after four weeks was able to identify TCM with a sensitivity of 84% and a specificity of 95% [25]. In our population, this study found that BNP during the acute phase is an independent predictor of recurrences. This adds evidence to the notion that the patients with pure TCM may benefit from a continuation of HF treatment even after

normalization of LVEF in order to prevent recurrences, even if the usefulness, duration and safety of HF treatment in TCM still represent an unexplored grey area.

Although recent reviews and small case series [1,26,27] have hypothesized the TCM recurrences may be characterized by a more severe onset of the condition, our prospective study on a larger population, actually showed that the recurrences are characterized by a higher LVEF and a reduced heart rate. This could be related to the rate-control strategy and to the continuation of HF treatment after discharge. In our population, 15 out of 17 patients had AF as the trigger of TCM recurrence. Therefore, it is feasible to hypothesize that the progressive nature of AF could contribute to the risk of TCM recurrence. Furthermore, when compared to other supraventricular arrhythmias, such as atrial flutter or atrioventricular node re-entry tachycardia, currently available pharmacological and non-pharmacological rhythm control strategies for AF are surely less effective in obtaining an optimal and long-lasting restoration of the sinus rhythm [10].

Regarding major clinical events, there were a few and potentially unrelated to the combination between HF and tachyarrhythmia. Finally, in terms of cardiovascular related hospitalizations, almost half of this study's population was re-hospitalized, even though by definition, none had structural heart disease. Most hospitalizations occurred during the first year after the event and were related to rhythm control procedures, such as elective cardioversions and catheter ablations. Moreover, 16 hospitalizations were due to the recurrence of TCM. The heart rate at discharge confirmed its predicting value along with the LVEF at discharge. Similar to the fact that heart rate reduction has been demonstrated to be beneficial in HF [23], our data confirm the role of the rate control in the pathophysiology of this peculiar, reversible form of systolic dysfunction. This strengthens the message that, in pure TCM, the lower the heart rate at discharge, the better the long-term prognosis.

Limitations

This paper shares all the limitations characterizing all prospective observational studies. In addition, this study's population was relatively small, and the low sample size made subgroup analyses unfeasible. Nonetheless, current available literature relies on case series and, to our knowledge, this is the largest dataset on pure TCM taken into account so far.

The cut-off used to define pure TCM (improvement of at least one NYHA class and > 5% EF) could seem rather small, but unfortunately, there is no consensus on any cut-off for TCM. Although surely arbitrary, the authors chose this cut-off because it was thought that, after ruling out all causes of structural heart disease, a patient undergoing a clinical and echographic improvement could be considered as having TCM, being the arrhythmia the only remaining and plausible cause of his/her condition. A higher cut-off, as the one proposed by Jeong and colleagues [13], could have ruled out many TCM that just had not time to recover completely because of arrhythmic recurrence, without offering alternative explanations behind the first decompensation. Moreover, according to Table 3, all the patients reached a LVEF of 50% or more after one year, making the authors quite confident that the population was correctly selected.

Furthermore, HF treatment could be considered as a potential confounder in the association between the heart rate and EF improvement/worsening. However, the heart rate was a predictor of the recurrence independently of any kind of pharmacological treatment at discharge (Table 3). As the criteria for TCM recurrence are the same as for the first event, it can be hypothesized that, in the patients, the heart rate is what matters and the association with LVEF worsening could be considered as independent of HF treatment. Of course, subsequent modification or intensification of the HF therapy over time could have modified the strength of such an association, but there is no means to assess that as it would be a daunting task to properly include all treatment changes in the statistical models.

5. Conclusions

In conclusion, TCM is an under-diagnosed entity, affecting nearly one out of ten patients admitted for HF. Pure TCM (i.e., without underlying structural heart disease) is associated with a good long-term

survival. Nonetheless, recurrences are frequent and can occur after many years. The treatment aimed at reversing OSAS and lowering the heart rate after the acute event could prevent these recurrences and their related hospitalizations.

Supplementary Materials: The following are available online at <http://www.mdpi.com/2077-0383/8/9/1411/s1>, Figure S1a: splines curve detailing the association between heart rate at discharge and the risk or TCM, Figure S1b: splines curve detailing the association between BNP on admission and the risk or TCM, Figure S1c: splines curve detailing the association between heart rate at discharge and the risk of cardiovascular hospitalization, Figure S1d: splines curve detailing the association between LVEF at discharge and the risk of cardiovascular hospitalization, Table S1: STROBE Statement—checklist of items that should be included in reports of observational studies, Table S2: univariable and multivariable Cox-proportional hazard model for tachycardiomyopathy recurrence, Table S3: univariable and multivariable Cox-proportional hazard model for cardiovascular hospitalization.

Author Contributions: Conceptualization, G.S. and F.G.; methodology, G.S. and F.G.; formal analysis, G.S. and F.G.; investigation, G.S., F.G., G.C., and A.U.; data curation, G.S., F.G. and L.C.; writing—original draft preparation, G.S. and F.G.; writing—review & editing, all; supervision, A.C.; funding acquisition, F.G.

Funding: This research was funded by Marche Polytechnic University (FFARB 2017).

Acknowledgments: The authors would like to thank Mary Elizabeth Orme for the linguistic support and editing assistance.

Conflicts of Interest: The authors declare no conflict of interest.

References

1. Martin, C.A.; Lambiase, P.D. Pathophysiology, diagnosis and treatment of tachycardiomyopathy. *Heart* **2017**, *103*, 1543–1552. [[CrossRef](#)] [[PubMed](#)]
2. Simantirakis, E.N.; Koutalas, E.P.; Vardas, P.E. Arrhythmia-induced cardiomyopathies: The riddle of the chicken and the egg still unanswered? *Europace* **2012**, *14*, 466–473. [[CrossRef](#)] [[PubMed](#)]
3. Gopinathannair, R.; Etheridge, S.P.; Marchlinski, F.E.; Spinale, F.G.; Lakkireddy, D.; Olshansky, B. Arrhythmia-Induced Cardiomyopathies. *J. Am. Coll. Cardiol.* **2015**, *66*, 1714–1728. [[CrossRef](#)] [[PubMed](#)]
4. Phillips, E.; Levine, S.A. Auricular fibrillation without other evidence of heart disease. *Am. J. Med.* **1949**, *7*, 478–489. [[CrossRef](#)]
5. Santangeli, P.; Marzo, F.; Camporeale, A.; Bellocchi, F.; Crea, F.; Pieroni, M. What do tachycardiomyopathy belong to? *Eur. Heart J.* **2008**, *29*, 1073–1074. [[CrossRef](#)] [[PubMed](#)]
6. Merlo, M.; Cannatà, A.; Gobbo, M.; Stolfo, D.; Elliott, P.M.; Sinagra, G. Evolving concepts in dilated cardiomyopathy. *Eur. J. Heart Fail.* **2018**, *20*, 228–239. [[CrossRef](#)] [[PubMed](#)]
7. Fenelon, G.; Wijns, W.; Andries, E.; Brugada, P. Tachycardiomyopathy: Mechanisms and clinical implications. *Pacing Clin. Electrophysiol.* **1996**, *19*, 95–106. [[CrossRef](#)] [[PubMed](#)]
8. Della Rocca, D.G.; Santini, L.; Forleo, G.B.; Sanniti, A.; Del Prete, A.; Lavalle, C.; Di Biase, L.; Natale, A.; Romeo, F. Novel perspectives on arrhythmia-induced cardiomyopathy: Pathophysiology, clinical manifestations and an update on invasive management strategies. *Cardiol. Rev.* **2015**, *23*, 135–141. [[CrossRef](#)]
9. Ponikowski, P.; Voors, A.A.; Anker, S.D.; Bueno, H.; Cleland, J.G.F.; Coats, A.J.S.; Falk, V.; González-Juanatey, J.R.; Harjola, V.-P.; Jankowska, E.A.; et al. 2016 ESC Guidelines for the diagnosis and treatment of acute and chronic heart failure. *Eur. Heart J.* **2016**, *37*, 2129–2200. [[CrossRef](#)]
10. Kirchhof, P.; Benussi, S.; Kotecha, D.; Ahlsson, A.; Atar, D.; Casadei, B.; Castella, M.; Diener, H.-C.; Heidbuchel, H.; Hendriks, J.; et al. 2016 ESC Guidelines for the management of atrial fibrillation developed in collaboration with EACTS: The Task Force for the management of atrial fibrillation of the European Society of Cardiology (ESC) Developed with the special contribution of the Europea. *Eur. Heart J.* **2016**, *37*, 2893–2962. [[CrossRef](#)]
11. Yancy, C.W.; Jessup, M.; Bozkurt, B.; Butler, J.; Casey, D.E.; Colvin, M.M.; Drazner, M.H.; Filippatos, G.S.; Fonarow, G.C.; Givertz, M.M.; et al. 2017 ACC/AHA/HFSA Focused Update of the 2013 ACCF/AHA Guideline for the Management of Heart Failure. *J. Am. Coll. Cardiol.* **2017**, *70*, 776–803. [[CrossRef](#)] [[PubMed](#)]
12. January, C.T.; Wann, L.S.; Calkins, H.; Chen, L.Y.; Cigarroa, J.E.; Cleveland, J.C.; Ellinor, P.T.; Ezekowitz, M.D.; Field, M.E.; Furie, K.L.; et al. 2019 AHA/ACC/HRS Focused Update of the 2014 AHA/ACC/HRS Guideline for the Management of Patients With Atrial Fibrillation. *J. Am. Coll. Cardiol.* **2019**, *140*, e125–e151.

13. Jeong, Y.-H.; Choi, K.-J.; Song, J.-M.; Hwang, E.-S.; Park, K.-M.; Nam, G.-B.; Kim, J.-J.; Kim, Y.-H. Diagnostic Approach and Treatment Strategy in Tachycardia-induced Cardiomyopathy. *Clin. Cardiol.* **2008**, *31*, 172–178. [[CrossRef](#)] [[PubMed](#)]
14. Von Elm, E.; Altman, D.G.; Egger, M.; Pocock, S.J.; Gøtzsche, P.C.; Vandenbroucke, J.P. The Strengthening the Reporting of Observational Studies in Epidemiology (STROBE) statement: Guidelines for reporting observational studies. *PLoS Med.* **2007**, *4*, 1623–1627. [[CrossRef](#)] [[PubMed](#)]
15. Sarzani, R.; Guerra, F.; Mancinelli, L.; Buglioni, A.; Franchi, E.; Dessi-Fulgheri, P. Plasma Aldosterone Is Increased in Class 2 and 3 Obese Essential Hypertensive Patients Despite Drug Treatment. *Am. J. Hypertens.* **2012**, *25*, 818–826. [[CrossRef](#)] [[PubMed](#)]
16. Leung, R.S.T. Sleep-Disordered Breathing: Autonomic Mechanisms and Arrhythmias. *Prog. Cardiovasc. Dis.* **2009**, *51*, 324–338. [[CrossRef](#)] [[PubMed](#)]
17. Schlatzer, C.; Schwarz, E.I.; Sievi, N.A.; Clarenbach, C.F.; Gaisl, T.; Haegeli, L.M.; Duru, F.; Stradling, J.R.; Kohler, M. Intrathoracic pressure swings induced by simulated obstructive sleep apnoea promote arrhythmias in paroxysmal atrial fibrillation. *Europace* **2016**, *18*, 64–70. [[CrossRef](#)]
18. Goudis, C.A.; Ketikoglou, D.G. Obstructive sleep and atrial fibrillation: Pathophysiological mechanisms and therapeutic implications. *Int. J. Cardiol.* **2017**, *230*, 293–300. [[CrossRef](#)]
19. Van Gelder, I.C.; Groenveld, H.F.; Crijns, H.J.G.M.; Tuininga, Y.S.; Tijssen, J.G.P.; Alings, A.M.; Hillege, H.L.; Bergsma-Kadijk, J.A.; Cornel, J.H.; Kamp, O.; et al. Lenient versus Strict Rate Control in Patients with Atrial Fibrillation. *N. Engl. J. Med.* **2010**, *362*, 1363–1373. [[CrossRef](#)]
20. Van Gelder, I.C.; Van Veldhuisen, D.J.; Crijns, H.J.G.M.; Tuininga, Y.S.; Tijssen, J.G.P.; Alings, A.M.; Bosker, H.A.; Cornel, J.H.; Kamp, O.; Veeger, N.J.G.M.; et al. RAte Control Efficacy in permanent atrial fibrillation: A comparison between lenient versus strict rate control in patients with and without heart failure. Background, aims, and design of RACE II. *Am. Heart J.* **2006**, *152*, 420–426. [[CrossRef](#)]
21. Steinberg, J.S.; Sadaniantz, A.; Kron, J.; Krahn, A.; Denny, D.M.; Daubert, J.; Campbell, W.B.; Havranek, E.; Murray, K.; Olshansky, B.; et al. Analysis of Cause-Specific Mortality in the Atrial Fibrillation Follow-up Investigation of Rhythm Management (AFFIRM) Study. *Circulation* **2004**, *109*, 1973–1980. [[CrossRef](#)] [[PubMed](#)]
22. Colin, P.; Ghaleh, B.; Monnet, X.; Hittinger, L.; Berdeaux, A. Effect of Graded Heart Rate Reduction with Ivabradine on Myocardial Oxygen Consumption and Diastolic Time in Exercising Dogs. *J. Pharmacol. Exp. Ther.* **2004**, *308*, 236–240. [[CrossRef](#)] [[PubMed](#)]
23. Swedberg, K.; Komajda, M.; Böhm, M.; Borer, J.S.; Ford, I.; Dubost-Brama, A.; Lerebours, G.; Tavazzi, L.; SHIFT Investigators. Ivabradine and outcomes in chronic heart failure (SHIFT): A randomised placebo-controlled study. *Lancet* **2010**, *376*, 875–885. [[CrossRef](#)]
24. Mulder, P.; Barbier, S.; Chagraoui, A.; Richard, V.; Henry, J.P.; Lallemand, F.; Renet, S.; Lerebours, G.; Mahlberg-Gaudin, F.; Thuillez, C. Long-Term Heart Rate Reduction Induced by the Selective If Current Inhibitor Ivabradine Improves Left Ventricular Function and Intrinsic Myocardial Structure in Congestive Heart Failure. *Circulation* **2004**, *109*, 1674–1679. [[CrossRef](#)] [[PubMed](#)]
25. Nia, A.M.; Gassanov, N.; Dahlem, K.M.; Caglayan, E.; Hellmich, M.; Erdmann, E.; Er, F. Diagnostic accuracy of NT-proBNP ratio (BNP-R) for early diagnosis of tachycardia-mediated cardiomyopathy: A pilot study. *Clin. Res. Cardiol.* **2011**, *100*, 887–896. [[CrossRef](#)]
26. Nerheim, P.; Birger-Botkin, S.; Piracha, L.; Olshansky, B. Heart Failure and Sudden Death in Patients With Tachycardia-Induced Cardiomyopathy and Recurrent Tachycardia. *Circulation* **2004**, *110*, 247–252. [[CrossRef](#)] [[PubMed](#)]
27. Watanabe, H.; Okamura, K.; Chinushi, M.; Furushima, H.; Tanabe, Y.; Kodama, M.; Aizawa, Y. Clinical characteristics, treatment, and outcome of tachycardia induced cardiomyopathy. *Int. Heart J.* **2008**, *49*, 39–47. [[CrossRef](#)]



Article

Left Ventricular Geometry and Replacement Fibrosis Detected by cMRI Are Associated with Major Adverse Cardiovascular Events in Nonischemic Dilated Cardiomyopathy

Bianca Olivia Cojan-Minzat^{1,2}, Alexandru Zlibut¹, Ioana Danuta Muresan¹, Carmen Cionca³, Dalma Horvat¹, Eva Kiss¹, Radu Revnic², Mira Florea², Razvan Ciortea^{1,4} and Lucia Agoston-Coldea^{1,3,5,*}

- ¹ Department of Internal Medicine, Iuliu Hatieganu University of Medicine and Pharmacy, 400006 Cluj-Napoca, Romania; cojanminzat.bianca@yahoo.com (B.O.C.-M.); alex.zlibut@yahoo.com (A.Z.); ioanamuresandanuta@yahoo.com (I.D.M.); hdalma92@yahoo.com (D.H.); kiss.eva24@yahoo.com (E.K.); r_ciortea@yahoo.com (R.C.)
 - ² Department of Family Medicine, Iuliu Hatieganu University of Medicine and Pharmacy, 400001 Cluj-Napoca, Romania; radu_revnic@yahoo.com (R.R.); mira_florea@yahoo.com (M.F.)
 - ³ Department of Radiology, Affidea Hiperdia Diagnostic Imaging Center, 400015 Cluj-Napoca, Romania; carmen.cionca@yahoo.com
 - ⁴ Department of Obstetrics and Gynecology, Emergency County Hospital, 400124 Cluj-Napoca, Romania
 - ⁵ 2nd Department of Internal Medicine, Emergency County Hospital, 400006 Cluj-Napoca, Romania
- * Correspondence: luciacoldea@yahoo.com; Tel.: +402-6459-1942; Fax: +402-6459-9817

Received: 7 May 2020; Accepted: 22 June 2020; Published: 25 June 2020

Abstract: To investigate the relationship between left ventricular (LV) long-axis strain (LAS) and LV sphericity index (LVSI) and outcomes in patients with nonischemic dilated cardiomyopathy (NIDCM) and myocardial replacement fibrosis confirmed by late gadolinium enhancement (LGE) using cardiac magnetic resonance imaging (cMRI), we conducted a prospective study on 178 patients (48 ± 14.4 years; 25.2% women) with first NIDCM diagnosis. The evaluation protocol included ECG monitoring, echocardiography and cMRI. LAS and LVSI were cMRI-determined. Major adverse cardiovascular events (MACEs) were defined as a composite outcome including heart failure (HF), ventricular arrhythmias (VAs) and sudden cardiac death (SCD). After a median follow-up of 17 months, patients with LGE+ had increased risk of MACEs. Kaplan-Meier curves showed significantly higher rate of MACEs in patients with LGE+ ($p < 0.001$), increased LVSI ($p < 0.01$) and decreased LAS ($p < 0.001$). In Cox analysis, LAS (HR = 1.32, 95%CI (1.54–9.14), $p = 0.001$), LVSI [HR = 1.17, 95%CI (1.45–7.19), $p < 0.01$] and LGE+ (HR = 1.77, 95%CI (2.79–12.51), $p < 0.0001$) were independent predictors for MACEs. In a 4-point risk scoring system based on LV ejection fraction (LVEF) $< 30\%$, LGE+, LAS $> -7.8\%$ and LVSI $> 0.48\%$, patients with 3 and 4 points had a significantly higher risk for MACEs. LAS and LVSI are independent predictors of MACEs and provide incremental value beyond LVEF and LGE+ in patients with NIDCM and myocardial fibrosis.

Keywords: nonischemic dilated cardiomyopathy; cardiac magnetic resonance imaging; late gadolinium enhancement; long axis strain; left ventricle sphericity index; major adverse cardiovascular events

1. Introduction

Nonischemic dilated cardiomyopathy (NIDCM) is the most common primary myocardial disease, being characterized by left ventricular (LV) enlargement and global systolic LV function impairment in the absence of ischemic heart disease (IHD), hypertension or valve disease [1]. Due to its significant

increased mortality [2] and sudden cardiac death (SCD) risk [3], NIDCM represents an important global healthcare burden. Nowadays, the development of more effective methods of assessing NIDCM severity and the risk of major adverse cardiovascular events (MACEs) remains a topic of great interest for current research.

While current guidelines recommend echocardiography as the first line of investigation in patients with NIDCM [4,5], it cannot evaluate the structural myocardial impairment [6]. Myocardial replacement fibrosis is part of the cardiac remodelling process, being responsible for heart failure (HF), ventricular arrhythmia (VA) and SCD. It is encountered in one-third of NIDCM patients, being detected using cardiac magnetic resonance imaging (cMRI) with late gadolinium enhancement (LGE) [7–10]. T1 mapping imaging is a state-of-the-art cMRI technique that is able to characterize extracellular volume fraction and it has been validated by comparative studies with the histopathological examination in NIDCM [11,12]. LV long-axis strain (LAS) determined by cMRI is an efficient and reliable method for quantifying global LV longitudinal function and it has an important prognostic value in patients with NIDCM [13,14]. Last but not least, cMRI-determined LV sphericity index (LVSI) is a parameter that predicts MACEs in NIDCM and it can be used in the assessment of LGE presence and LGE mass [15,16].

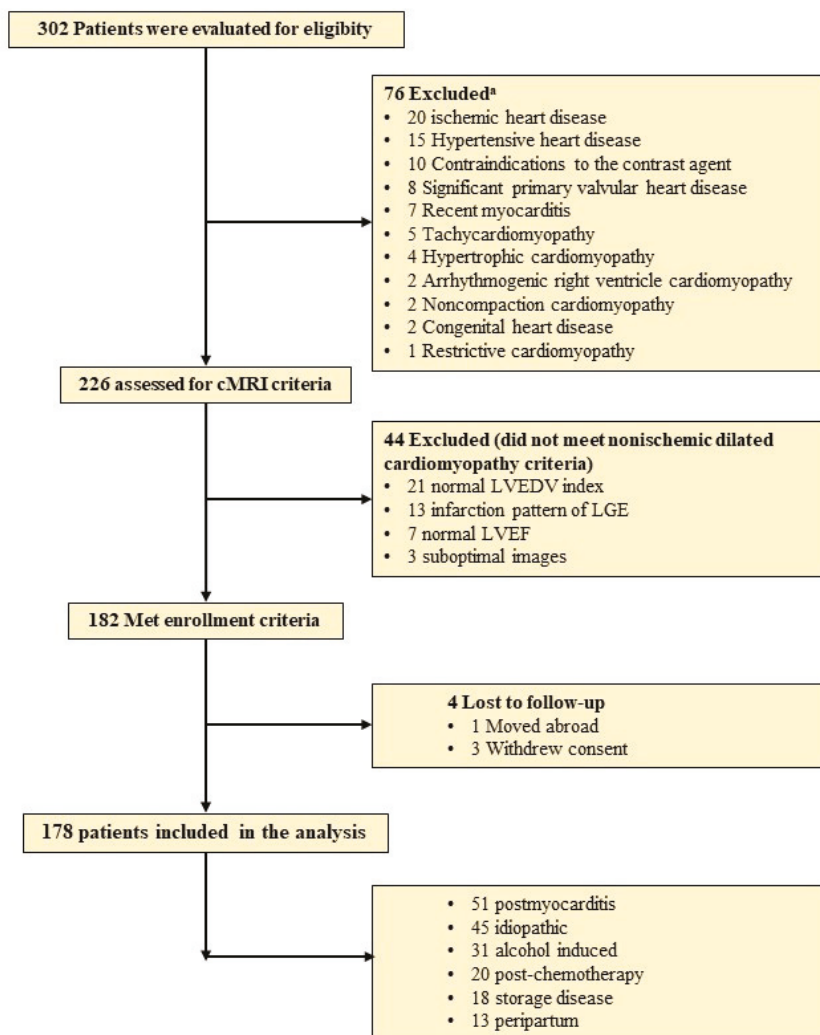
The aim of this study was to investigate the relationship between cardiac remodelling process and MACEs, and if it increases outcome prediction beyond LGE, in patients with NIDCM.

2. Methods

2.1. Study Population

We conducted a prospective study on 302 consecutive patients with first NIDCM diagnosis, which were examined in the 2th Department of Internal Medicine of the Iuliu Hatieganu University of Medicine and Pharmacy from October 2017 to November 2019. The inclusion criteria were [1]: (1) impaired global LV function with a LV ejection fraction (LVEF) $\leq 45\%$; (2) LV chamber dilation with an indexed LV end-diastolic volume (LVEDV) ≥ 97 mL/m²; both cMRI-determined. The exclusion criteria are represented by (1) IHD, other cardiomyopathies, significant valvular and congenital heart disease (CHD, CVD); (2) contraindications to cMRI (incompatible metallic devices, significant chronic renal disease with estimated glomerular filtration rate < 30 mL/min/1.73 m², or claustrophobia); (3) refusal to participate in the study (Figure 1). IHD was excluded by coronarography in 72 patients (41%), stress imaging studies in 64 patients (36%) and the remaining 42 patients (23%) had no history of angina, 1 or 0 risk factors for IHD and stress ECG test and computed tomography coronary angiography with Agatston calcium scoring were also negative.

We recorded demographic data including age, gender, height, weight, medical history, cardiovascular symptoms (dyspnoea, syncope, palpitations), and current medication; biomarkers and 12-lead ECG. 24-h Holter monitoring, transthoracic echocardiography and cMRI were performed. The current research was approved by the Ethics Committee of the Iuliu Hatieganu University of Medicine and Pharmacy, Cluj-Napoca—decision number 280/26.07.2018. The study was conducted in accordance with the principles of the Declaration of Helsinki. All patients were informed about the investigation protocol and signed a written consent form.



*coronary artery disease was defined as >50% angiographical stenosis in any epicardial coronary artery. Primary valvular disease was defined as moderate or higher valvular stenosis or regurgitation, with the exception of the functional ones. Functional mitral regurgitation was defined as mitral regurgitation secondary to left ventricular remodeling resulting in failure of leaflet coadaptation, in the setting of normal mitral valve anatomy, on echocardiography and cardiovascular magnetic resonance imaging.

Figure 1. Flow chart detailing the identification of the study cohort. Abbreviations: cMRI, cardiac magnetic resonance imaging; LGE, late gadolinium enhancement; LVEDV, left ventricular end diastolic volume; LVEF, left ventricular ejection fraction.

2.2. cMRI

All cMRI images were ECG-gated and were acquired during apnoea with a 1.5 T magnetic resonance (MR) scanner (Magnetom Symphony, Siemens Medical Solutions, Erlanger, Germany).

A standard scanning protocol that was in accordance with current international guidelines was used [17]. The acquisition of fast imaging employing steady-state free precession (SSFP) sequences was performed to detect ventricular function and mass in the conventional cardiac short-axis and long-axis planes (including two-chamber, three-chamber, and four-chamber), to enclose both ventricles from base to apex. SSFP sequence parameters were as follows: repetition time (TR) 3.6 ms; echo time (TE) 1.8 ms; flip angle 60°; slice thickness 6 mm; field of view 360 mm; image matrix of 192 × 192 pixels; voxel size 1.9 × 1.9 × 6 mm; 25–40 ms temporal resolution reconstructed to 25 cardiac phases. LGE imaging was performed to detect focal myocardial scars acquired 10 min after intravenous administration of 0.2 mmol/kg gadoteric acid (Clariscan, GH Healthcare AS, Oslo, Norway) in long- and short axis-views, using a segmented inversion-recovery gradient-echo sequence. LGE imaging sequence parameters were presented by: TR 4.8 ms, TE 1.3 ms, and inversion time 200 to 300 ms. Inversion time was adjusted to optimize nulling of apparently normal myocardium. Brachial blood pressure was monitored during cMRI-SSFP acquisitions.

Image analysis: All images were evaluated by two experienced observers, blinded to all clinical data. LVEDV and LV end-systolic volume (LVESV), LVEF and end-diastolic LV mass (LVM) were measured on short-axis cine-SSFP images. Epicardial and endocardial borders were traced semi-automatically at end-diastole and end-systole using specialized software (Syngo.Via VB20A_HF04, Argus, Siemens Medical Solutions). The maximum left atrium (LA) and right atrium (RA) volumes were measured in all patients from the four-chamber view. All volumes were indexed to body surface area. Tricuspid annular plane systolic excursion (TAPSE) was measured from the mid-four-chamber cardiac view to assess right ventricular (RV) longitudinal motion. LV longitudinal function was assessed by LAS, defined as the difference in mitral annular displacement at end-systole vs. end-diastole, and expressed as a percentage [13]. LVSI was calculated by dividing LVEDV to the volume of a sphere whose LV length (L) is measured at end-diastole: $LVSI = LVEDV / (\pi/6 \times L^3)$ [15] (Figure 2).

The presence and distribution of LGE in the LV were assessed from short-axis images, using the 17-segments model, as recommended by the American Heart Association [18], and were quantified using a signal intensity threshold of >5SD above a remote reference for normal myocardium. Due to the fact that the LGE quantification with the threshold of 5SD demonstrated the best agreement with visual assessment and best reproducibility among different technique thresholds, we used a threshold of 5SD above the signal intensity of normal myocardium [19,20]. LGE's distribution was characterized as mid-wall, subepicardial, focal or diffuse. The assessment of LGE mass in the LV was automatically quantified from short-axis LGE images using cardiac dedicated software (cvi42, Circle Cardiovascular Imaging Inc., Calgary, CA). The extent of LGE was expressed by gram (g) and also as percentage of LVM. According to the cMRI, the studied population was divided into two groups, namely: patients without LGE (LGE-) and patients with LGE (LGE+).

2.3. Follow-Up of Clinical Outcomes

The clinical follow-up was obtained by completing a questionnaire either on hospital visits, telephone house-calls, or both, aiming at delineating the occurrence of the clinical outcomes, which corresponded to the first event occurring in each patient among the following MACEs: death or aborted death from cardiac cause, sustained ventricular tachyarrhythmia (beats with ventricular origin that lasts >30 s and has a rate greater than >100 beats/min), and HF requiring hospitalization defined accordingly to current international guidelines [4,5]. Hospitalisation due to non-cardiac causes was not counted as event. Survival analysis was performed for the clinical outcomes. The median follow-up was 17 months and maximum follow-up reached 29 months.

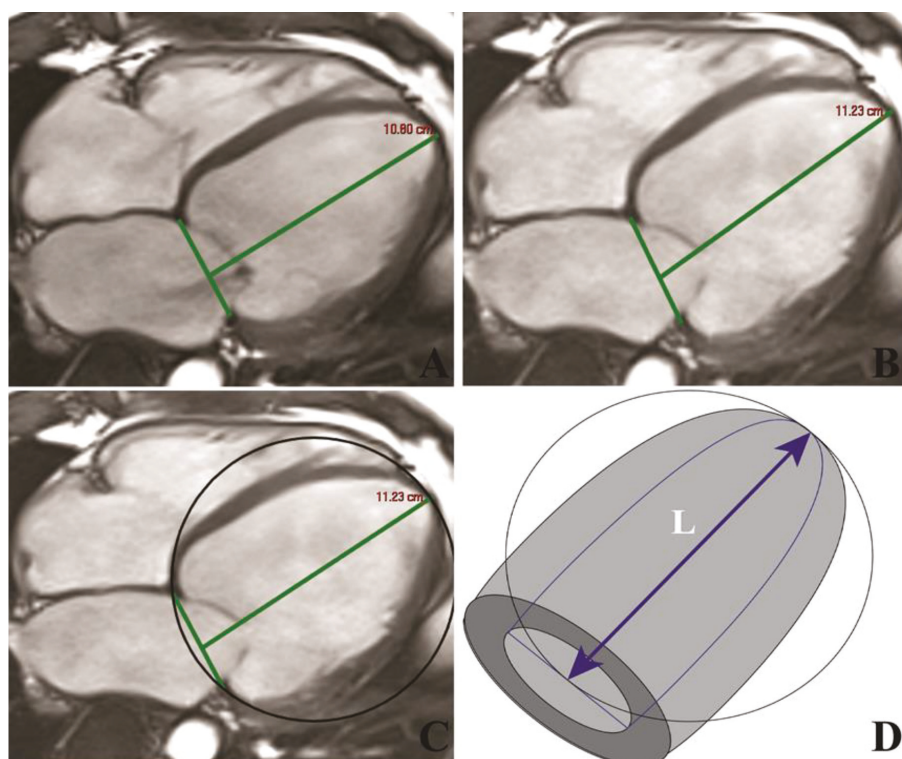


Figure 2. Representative image illustrating the technique for assessment of LAS (A,B) and LVSI (C,D) in a patient with severe NIDCM in end-diastole and end-systole, respectively. Abbreviations: LAS, left ventricular long axis strain; LVSI, left ventricular sphericity index; NIDCM, non-ischemic dilated cardiomyopathy.

2.4. Statistical Analysis

All data were tested for normality using the Kolmogorov-Smirnov test. Data were presented as median, mean \pm standard deviation (SD) or percentage. Baseline characteristics among those with and without LGE patients with clinical outcomes were compared by Chi-square χ^2 test or Fischer exact test as appropriate (categorical data) and Wilcoxon signed rank test (continuous data). The hazard ratio (HR) for the prediction of events was calculated using a Cox regression model. For each outcome, we considered all of the significant variables in the univariate analysis and sought the best overall multivariate models for the composite end-point, by stepwise-forward selection, with a probability to enter set at $p < 0.05$ and to remove the effect of regression at $p < 0.05$. Event-free survival was generated by the Kaplan–Meier method and statistical significance was determined by the log-rank test. Multivariate analysis was performed by constructing a multiple logistic regression model, including the HR (95%CI) calculation. Cohen’s Kappa inter- and intra-observer coefficient calculation was performed. Retrospective test power calculation and prospective sample size were estimated, with type I and type II variation according to sample size. The statistical analysis was performed using the MedCalc (Version 19.1.7, MedCalc Software, Ostend, Belgium).

3. Results

3.1. Baseline Characteristics

A total of 178 patients (48 ± 14.4 years old, 74.7% male) met the enrolment criteria (Figure 1). They were divided in two groups according to LGE+ and LGE− (n = 64, 36% vs. n = 114, 64%). The baseline characteristics are presented in Table 1.

Table 1. Baseline characteristics of patients in study.

	All Patients n = 178	LGE− n = 114	LGE+ n = 64	p-Value
Clinical characteristics				
- Age, mean (SD), years	48 (14.4)	47 (15.0)	45 (13.4)	NS
- Male gender, n (%)	133 (74.7)	83 (72.8)	50 (78.1)	NS
- Body-mass index, kg/m ²	27.4 (4.8)	27.3 (4.4)	27.5 (5.7)	NS
- Heart rate, mean (SD), bpm	73 (16.0)	71 (14.3)	76 (18.3)	<0.05
- Systolic blood pressure, mean (SD), mmHg	133 (18.9)	134 (18.4)	130 (19.5)	NS
- Hypertension, n (%)	98 (55.1)	69 (60.5)	29 (45.5)	<0.05
- Diabetes mellitus, n (%)	58 (32.5)	41 (35.9)	17 (26.5)	NS
- Dyslipidemia, n (%)	104 (58.4)	67 (58.8)	37 (57.8)	NS
- Smoking, n (%)	58 (32.5)	39 (34.2)	19 (29.6)	NS
- NYHA functional class I/II/III, n	29/59/27	19/39/19	10/20/8	<0.05
Electrocardiogram				
- Atrial fibrillation, n (%)	26 (14.6)	18 (15.7)	8 (12.5)	NS
- Left bundle branch block, n (%)	15 (8.4)	10 (8.7)	5 (7.8)	NS
- Right bundle branch block, n (%)	17 (9.5)	12 (10.5)	5 (7.8)	NS
- Significant Q waves, n (%)	21 (11.8)	14 (12.3)	7 (10.9)	NS
Medications				
- Beta-blockers, n (%)	142 (79.7)	91 (79.8)	51 (79.6)	NS
- ACEIs or ARBs, n (%)	130 (73.0)	84 (73.6)	46 (71.8)	NS
- Calcium channel blockers, n (%)	28 (15.7)	18 (15.7)	10 (15.6)	NS
- Statins, n (%)	105 (58.9)	67 (58.7)	38 (59.3)	NS
- Antiplatelet therapy, n (%)	68 (38.2)	44 (38.5)	25 (37.5)	NS
- Diuretics, n (%)	111 (62.3)	70 (61.4)	41 (64.0)	NS
- Digitalis, n (%)	13 (7.3)	8 (7.0)	5 (7.8)	NS
Biomarker levels				
- NT-proBNP, median (IQR), pg/mL	2639.5 (378–11,960)	2600 (378–9893)	2679 (570–11,960)	NS
- eGFR, mean (SD), ml/min/1.73 m ²	87.1 (21.2)	87.7 (20.4)	86.1 (22.6)	NS
Echocardiography				
- E/E' ratio, mean (SD)	9.27 (2.5)	8.2 (2.4)	12.3 (2.6)	<0.001
- DT, mean (SD), ms	217 (56.7)	215 (53.4)	221 (63.1)	NS
- sPAP, mean (SD), mmHg	30.8 (12.0)	30.1 (12.5)	32.2 (11.0)	NS
Cardiovascular magnetic resonance				
- LVEDV index, mean (SD), mL/m ²	132.3 (34.5)	124.8 (30.2)	145.5 (37.8)	<0.001
- LVESV index, mean (SD), mL/m ²	87.5 (34.4)	78.6 (29.6)	103.5 (36.8)	<0.001
- LVM index, mean (SD), g/m ²	86.7 (20.6)	83.7 (19.6)	92.0 (21.6)	<0.01
- LVEF, mean (SD), %	35.0 (9.3)	37.8 (7.7)	29.9 (9.7)	<0.001
- LAV index, mean (SD), mL/m ²	55.8 (21.3)	53.1 (20.4)	60.6 (22.2)	<0.05
- LAS, mean (SD), %	−9.6 (5.3)	−10.7 (5.4)	−7.8 (4.6)	<0.001
- LVSI, mean (SD)	0.40 (0.12)	0.38 (0.11)	0.43 (0.13)	<0.001
- TAPSE, mean (SD), mm	18.6 (5.2)	19.5 (5.3)	16.9 (4.7)	0.001
- RVEDV index, mean (SD), mL/m ²	53.4 (21.2)	52.7 (19.2)	54.7 (24.4)	NS
- RVESV index, mean (SD), mL/m ²	29.0 (15.5)	27.2 (11.9)	32.2 (20.0)	<0.01
- RVEF, mean (SD), %	46.8 (9.55)	49.0 (8.7)	42.8 (9.7)	<0.01
- LV-LGE mass median (IQR), g			30.5 (1–88)	
- LV-LGE mass/LVM, median (IQR), %			17.2 (0.6–54)	

Abbreviations: ACEI, angiotensin converting enzyme inhibitor; ARB, angiotensin receptor blocker; DT, early diastolic filling deceleration time; E, peak mitral flow velocity; E', early diastolic peak myocardial velocity; eGFR, estimated glomerular filtration rate; IQR, interquartile range; LAS, left ventricular longitudinal-axis strain; LAV, left atrial volume; LGE, left ventricular late gadolinium enhancement; LVEDV, left ventricular end-diastolic volume; LVEF, left ventricular ejection fraction; LVESV, left ventricular end-systolic volume; LVM, left ventricular mass; LVSI, left ventricular sphericity index; n, number of patients; NT-proBNP, N-terminal pro-Brain Natriuretic Peptide; NYHA, New York Heart Association; RVEDV, right ventricular end-diastolic volume; RVEF, right ventricular ejection fraction; RVESV, right ventricular end-systolic volume; SD, standard deviation; sPAP, systolic pulmonary artery pressure; TAPSE, tricuspid annular plane systolic excursion. Data are reported as mean (standard deviation) or median (IQR) or n (%).

At admission, 54 (30.3%) presented with dyspnoea, 28 (15.7%) with palpitations and 18 (10.1%) had history of syncope. LGE+ patients had significantly increased LV end-diastolic filling pressures (E/E' ratio; $p < 0.001$) and many more of these had LVEF $< 30\%$ ($n = 46$, 71.8%). The LGE+ group presented with increased LVM index $\geq 92 \text{ g/m}^2$ ($p = 0.01$), LVEDV $\geq 145.5 \text{ mL/m}^2$ ($p < 0.001$), LVSI ≥ 0.43 ($p < 0.001$) and reduced LAS $< -7.8\%$ ($p < 0.001$).

3.2. Reproducibility of cMRI Measurements

cMRI measurements were repeatedly performed on the same set of images, acquired from all patients in the study group. Regarding LVEF, LAS, LVSI and the assessment of LGE+, the intra- and inter-observer reproducibility were excellent. The inter-observer kappa coefficients of agreement were 0.91 for LVEF, 0.97 for LAS, 0.93 for LVSI and 0.88 for LGE+, while the intra-observer kappa coefficients of agreement were 0.98 for LVEF, 0.98 for LAS, 0.92 for LVSI and 0.90 for LGE+ (Table 2).

Table 2. Reproducibility inter and intra-reader agreement of cMRI measurements.

Parameters	Coefficient Kappa	95% Confidence Interval	Standard Error
Inter-observer			
LVEF	0.91	0.872 to 0.941	0.026
LAS	0.97	0.909 to 0.989	0.012
LGE	0.88	0.771 to 0.939	0.066
LVSI	0.93	0.856 to 0.952	0.029
Intra-observer			
LVEF	0.98	0.977 to 0.992	0.009
LAS	0.98	0.967 to 0.991	0.004
LGE	0.90	0.835 to 0.948	0.023
LVSI	0.92	0.871 to 0.928	0.032

Abbreviations: LAS, left ventricular longitudinal-axis strain; LGE, left ventricular late gadolinium enhancement; LVEF, left ventricular ejection fraction; LVSI, left ventricular sphericity index.

3.3. Survival Analysis

Initial cMRI evaluation was performed. During a median follow-up of 17 months (IQR 1 to 29 months), 31 patients (17.4%) experienced MACEs: VA ($n = 14$), HF requiring hospitalization ($n = 11$), and SCD ($n = 6$). The patients with VA were majority males, had increased LVESV (mean 107,533 mL, $p < 0.001$), decreased LVEF (28,429%, $p < 0.0001$), increased LGE mass (24,5 g, $p < 0.0001$) and LVSI (0.46, $p < 0.001$). Of them, ten received ICD therapy and 4 were ablated due to implantable cardioverter defibrillator therapy refusal, the last had a mean LVEF around 30%, two of them had NIDCM post-myocarditis and two were idiopathic NIDCM. The incidence of MACEs was significantly higher in the LGE+ group vs. the LGE- group ($n = 21$, 67.7% vs. $n = 10$, 33.4%). The Kaplan-Meier curves for event-free survival showed a significantly higher rate of MACEs in patients with LGE+ (HR = 4.02; 95%CI (1.91–8.45), $p < 0.001$), high LVSI (HR = 3.23; 95%CI (1.59–6.53), $p < 0.01$) and decreased LAS (HR = 3.94; 95%CI (1.93–8.03), $p < 0.001$) (Figure 3).

3.4. Univariate and Multivariate Cox Analysis

Among the evaluated parameters, in univariate analysis and multivariate Cox regression analysis, only four remained independent predictors for MACEs, namely LGE+ (HR = 1.77, 95%CI (2.79 to 12.51), $p < 0.0001$), reduced LAS (HR = 1.32, 95%CI (1.54 to 9.14), $p < 0.001$) and increased LVSI (HR = 1.17, 95%CI (1.45 to 7.19), $p < 0.001$) and LGE mass (HR = 1.43, 95%CI (1.01–6.12), $p < 0.001$) (Table 3).

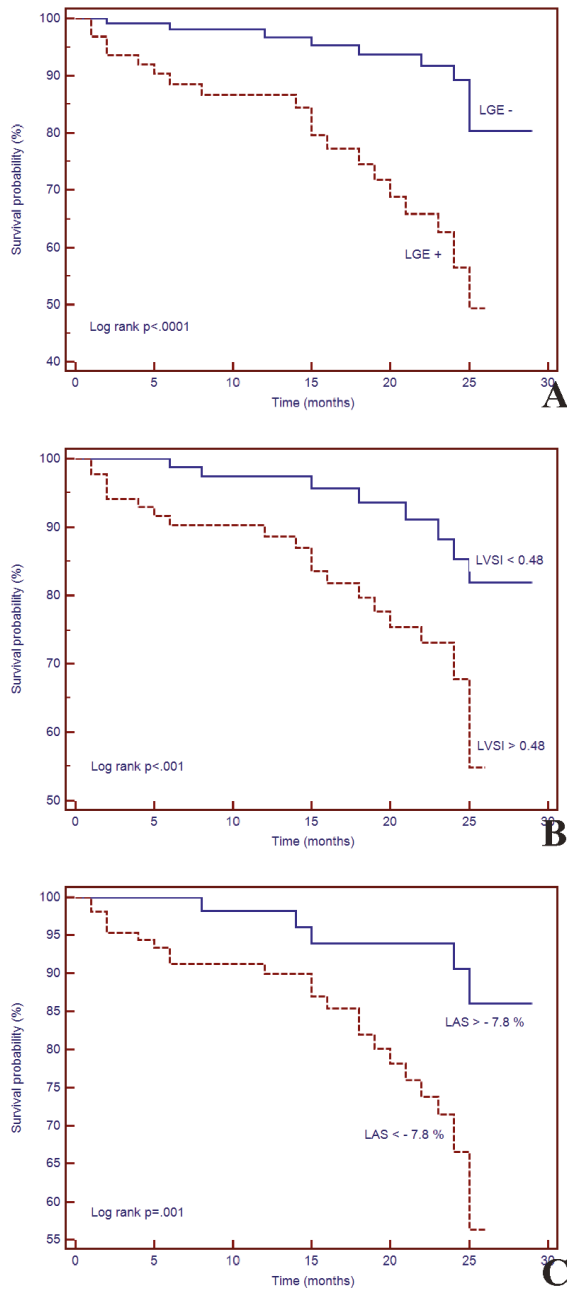


Figure 3. Kaplan–Meier curves for event-free survival for (A) LGE+, (B) LAS, (C) LVSI. Abbreviations: LAS, long axis strain; LGE, left ventricular late gadolinium enhancement; LVSI, left ventricular sphericity index.

Table 3. Univariable and multivariable Cox analysis testing between studied parameters and MACEs.

	No Events <i>n</i> = 147	Events <i>n</i> = 31	Univariable Analysis			Multivariable Analysis		
			Unadjusted HR (95% CI)	<i>p</i> Value	Adjusted HR (95% CI)	<i>p</i> Value		
Age, years	48 (13.8)	48 (17.5)	1.00 (0.98–1.03)	NS				
Male gender, <i>n</i> , %	111 (75.5)	22 (37.9)	1.14 (0.53–2.48)	NS				
Body-mass index, kg/m ²	27.7 (4.8)	25.8 (4.5)	0.94 (0.87–1.01)	NS				
Systolic blood pressure	134 (19.2)	130 (17.4)	0.99 (0.97–1.01)	NS				
NT-proBNP, pg/mL	2564 (378–11960)	2834 (834–9892)	1.00 (0.99–1.01)	NS				
eGFR, mL/min/1.73 m ²	86.3 (20.1)	91.0 (25.9)	1.01 (0.97–1.03)	NS				
LVEDV index, mL/m ²	131.4 (35.6)	136.6 (32.7)	1.01 (0.99–1.01)	NS				
LVESV index, mL/m ²	86.4 (34.5)	93.1 (33.8)	1.05 (0.98–1.07)	NS				
LVM index, g/m ²	87.0 (20.7)	85.2 (20.8)	0.99 (0.97–1.01)	NS				
LVEF, %	35.5 (9.2)	32.4 (9.4)	0.97 (0.93–1.01)	NS				
LAV index, mL/m ²	54.7 (21.7)	61.3 (18.6)	1.01 (1.00–1.03)	NS				
LGE+	43 (29.2)	21 (67.7)	4.03 (1.90–8.52)	<0.0001	1.77 (2.79–12.51)	<0.0001	<0.0001	
LGE mass, g	11.3 (10.6)	28.8 (19.3)	1.23 (1.90–4.52)	<0.0001	1.43 (1.01–6.12)	<0.0001	<0.0001	
LAS, %	−10.0 (5.6)	−7.8 (3.6)	1.19 (1.01–2.18)	<0.001	1.32 (1.54–9.14)	<0.001	0.001	
LVSI, %	0.38 (0.11)	0.48 (0.13)	2.13 (1.05–8.11)	<0.001	1.17 (1.14–7.19)	<0.001	<0.01	
E/E' ratio	9.1 (2.3)	15.7 (4.8)	1.08 (0.95–1.22)	<0.05	1.02 (0.92–1.01)	NS	NS	
TAPSE, mm	18.8 (5.2)	17.4 (5.4)	0.77 (0.70–0.84)	NS				
RVEDV index, mL/m ²	53.3 (19.7)	53.8 (27.6)	1.00 (0.98–1.02)	NS				
RVESV index, mL/m ²	28.2 (13.5)	32.4 (13.9)	1.02 (1.00–1.04)	NS				
RVEF, %	47.5 (9.3)	43.4 (10.2)	0.84 (0.79–0.88)	NS				

Abbreviations: E, peak mitral flow velocity; E', early diastolic peak myocardial velocity; eGFR, estimated glomerular filtration rate; IQR, interquartile range; LAS, left ventricular longitudinal-axis strain; LAV, left atrial volume; LGE, left ventricular late gadolinium enhancement; LVEDV, left ventricular end-diastolic volume; LVEF, left ventricular ejection fraction; LVESV, left ventricular end-systolic volume; LVM, left ventricular mass; LVSI, left ventricular spherical index; *n*, number of patients; NT-proBNP, N-terminal pro-Brain Natriuretic Peptide; RVEDV, right ventricular end-diastolic volume; RVEF, right ventricular ejection fraction; RVESV, right ventricular end-systolic volume; TAPSE, tricuspid annular plane systolic excursion.

3.5. Incremental Predictive Value of cMRI-Based LV Geometry and Strain for Outcomes

Sequential Cox proportional-hazards models yielded significantly increased predictive power the combined outcome of MACEs when both LVSI and LAS were used in addition to LVEF and LGE+ (Chi-square = 24.52, $p < 0.0001$) (Figure 4). However, LAS did not provide incremental predictive power when used alone, in addition to LVEF and LGE+.

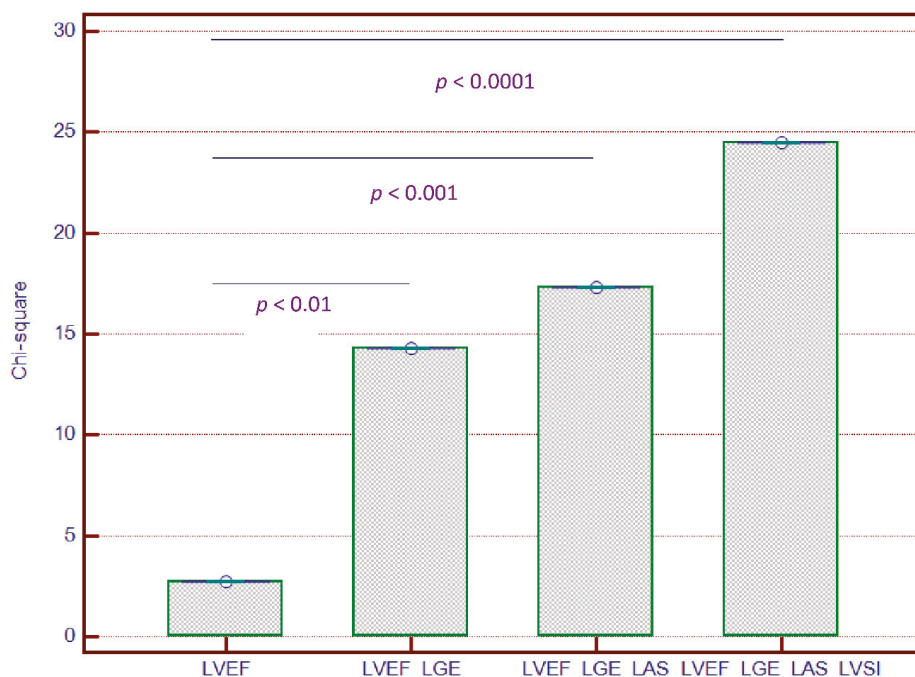


Figure 4. Incremental predictive value of LVSI and LAS added to LVEF and to LGE for outcome in patients with NIDCM. Abbreviations: LAS, left ventricular long axis strain; LGE, left ventricular late gadolinium enhancement; LVSI, left ventricular sphericity index; NIDCM, nonischemic dilated cardiomyopathy.

3.6. Risk Stratification Scoring System

The embedment of LVSI and LAS to LVEF and LGE allowed us to create a risk stratification score, using the following criteria: LVEF < 30%, LGE+, LVSI > 0.48 and LAS < -7.8%. These cut-off values were best correlated with outcome in our studied group. We created a scoring system and Kaplan–Meier curves based on the four parameters (Chi-square = 56.53, $p < 0.0001$) (Figure 5). We observed that patients with 3–4 points had significantly higher rates of MACEs during the follow-up period than others.

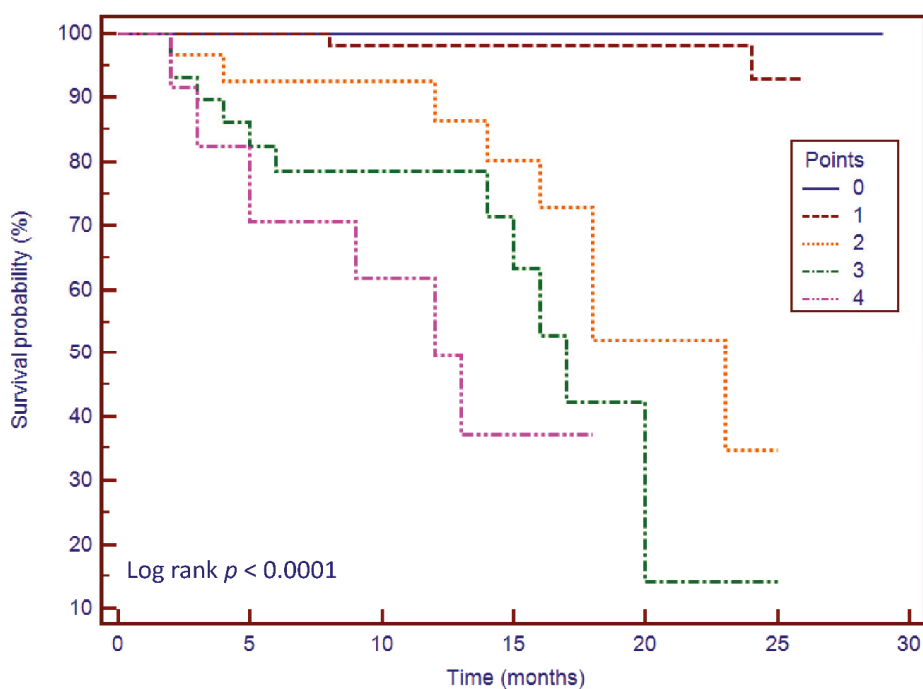


Figure 5. Kaplan-Meier curves for the risk stratification score. The scoring system ranges from 0 to 4 points: 1 point for each of the following LVEF < 30%, LGE+, LAS > -7.8% and LVSI > 0.48. Abbreviations: LAS, left ventricular long axis strain; LGE, left ventricular late gadolinium enhancement; LVSI, left ventricular sphericity index.

4. Discussion

This prospective study is the first to evaluate the association between cMRI-based LV geometry and strain and outcome, in a significant, well-diagnosed NIDCM cohort. LAS and LVSI were independent predictors of MACEs in patients with NIDCM and myocardial replacement fibrosis. These findings were independent of LVEF and other established prognostic factors in a multivariable analysis. We also demonstrated that the addition of both LAS and LVSI to LVEF and LGE was superior for the prediction of MACEs over those based only on LVEF and LGE. The incidence of MACEs was higher in those with myocardial replacement fibrosis and altered LV geometry and strain, therefore representing a group who may require more aggressive therapy and rigorous follow-up.

NIDCM is typically associated with LV mid-wall replacement fibrosis, which worsens its prognosis [21,22]. Furthermore, Lehrke et al. have shown that NIDCM can be confirmed by cMRI-determined LV midwall fibrosis [23]. In our study, the incidence of LGE in NIDCM was similar with other studies [8,24] and, in addition, we demonstrated that LGE was an independent predictor of MACEs. Similarly, in patients with NIDCM, Gulati et al. showed that the presence of mid-wall LGE was an independent predictor for outcome and improved risk stratification beyond LVEF [9]. Furthermore, several studies have confirmed that the presence LGE is independently associated with all-cause mortality, SCD and aborted SCD [25,26].

In our study, we confirmed the role of LVSI in predicting MACEs with a cut-off value of >0.43 ($p < 0.001$), similar with other published data. In patients with NIDCM, LVSI was initially evaluated in 2- and 3-dimensional echocardiography-based studies, which demonstrated that it was an independent predictor of MACEs, having a significant long-term prognostic impact [15,27].

Furthermore, in cMRI-based studies, it has been confirmed that LVSI is inversely correlated with LVEF in patients with NIDCM [28,29], while in a multi-ethnic study conducted on healthy subjects, lowest LVSI was an independent predictor for CHD, CVD and HF at 10-year follow-up and the highest LVSI was correlated with increased incidence of HF and atrial fibrillation [30]. Moreover, in a small study, LVSI was an independent predictor for correct ICD therapy [31]. Thereby, LVSI could become an important prediction parameter in this category of patients.

Furthermore, we demonstrated that LAS, a myocardial strain parameter, was an independent predictor for outcome in patients with NIDCM. cMRI-based myocardial strain has proved its utility in early diagnosing and predicting various cardiac diseases. In patients with myocardial infarction, Gjesdal et al. showed that LAS was progressively reduced in larger mitral insufficiency and was associated with the infarction mass [32], while Schuster et al. identified that the assessment of LAS provided incremental prognostic value for cardiovascular risk [33]. In a multi-ethnic study, LAS was also associated with LVEF and MACEs [34]. In a study conducted on patients with aortic stenosis, our research team identified that LAS was an independent predictor of outcome and provided incremental value beyond LVEF and LGE [35]. Lastly, in patients with NIDCM, a single study identified that LAS was an independent predictor for SCD, aborted SCD, heart transplantation and HF hospitalization [36].

The role of LVEF and LGE as independent predictors of MACEs in patients with NIDCM has been confirmed by recently published data. To our knowledge, only two studies have approached our goals, namely Kano et al. identified that the addition of LVSI to LGE significantly increased prognosis of MACEs [37], while Riffel et al. demonstrated that the addition of LAS to LGE provides incremental value for outcome prediction in patients with NIDCM [36]. Our investigation is the first to demonstrate that the combined addition of both LVSI and LAS to LVEF and LGE significantly increased the predictive power of outcome, thus conferring an incremental predictive value.

Based on these four parameters, we were able to create a risk stratification scoring system. Hitherto, a single study created a similar scoring system based on LAS, LVEF and LGE+ which provided significant predictive value [36]. We demonstrated that the addition of one point for each of these parameters (LVEF < 30%, LGE+, LAS > -7.8% and LVSI > 0.48) is highly correlated with MACEs. In patients without these risk features (score = 0), no MACEs were observed during follow-up. Thereby, we propose a combined risk score consisting of LVEF, LGE, LVSI and LAS in order to improved risk stratification.

Study limitations: Firstly, we conducted a single centre study. Secondly, we were unable to acquire T1 mapping sequences, and therefore extracellular volume and diffuse myocardial fibrosis could not be quantified. Additionally, the follow-up was, relatively speaking, not very long.

5. Conclusions

cMRI parameters of geometry and longitudinal strain, namely LVSI and LAS, are independently associated with increased risk of MACEs in NIDCM patients with myocardial replacement fibrosis confirmed by cMRI-LGE. For the first time, we demonstrate that the combined usage of LVSI and LAS provide incremental value beyond the assessment of LVEF and LGE in outcome prediction. These findings have potential therapeutic implications regarding the management of patients with NIDCM.

Author Contributions: B.O.C.-M. and L.A.-C. conception and design of the study; L.A.C.-acquisition, analysis and interpretation of data; statistical methods and interpretation of results; project administration. A.Z., I.D.M., C.C., D.H., E.K., R.R., R.C., and M.F.-acquisition, analysis and interpretation of data; critical revision of the manuscript for intellectual content. B.O.C.-M., A.Z. and L.A.-C. drafting of the manuscript. All authors granted final approval of the manuscript submitted. All authors have read and agreed to the published version of the manuscript.

Funding: This research received no external funding.

Acknowledgments: This work was supported by internal institutional doctoral fellowship from the Iuliu Hatieganu University of Medicine and Pharmacy of Cluj-Napoca.

Conflicts of Interest: The authors declare no conflict of interest.

References

1. Pinto, Y.M.; Elliott, P.M.; Arbustini, E.; Adler, Y.; Anastasakis, A.; Böhm, M.; Duboc, D.; Gimeno, J.; de Groote, P.; Imazio, M.; et al. Proposal for a Revised Definition of Dilated Cardiomyopathy, Hypokinetic Non-Dilated Cardiomyopathy, and Its Implications for Clinical Practice: A Position Statement of the ESC Working Group on Myocardial and Pericardial Diseases. *Eur. Heart J.* **2016**, *37*, 1850–1858. [[CrossRef](#)] [[PubMed](#)]
2. Felker, G.M.; Thompson, R.E.; Hare, J.M.; Hruban, R.H.; Clemetson, D.E.; Howard, D.L.; Baughman, K.L.; Kasper, E.K. Underlying Causes and Long-Term Survival in Patients with Initially Unexplained Cardiomyopathy. *N. Engl. J. Med.* **2000**, *342*, 1077–1084. [[CrossRef](#)] [[PubMed](#)]
3. Kadish, A.; Dyer, A.; Daubert, J.P.; Quigg, R.; Estes, N.A.M.; Anderson, K.P.; Calkins, H.; Hoch, D.; Goldberger, J.; Shalaby, A.; et al. Prophylactic Defibrillator Implantation in Patients with Nonischemic Dilated Cardiomyopathy. *N. Engl. J. Med.* **2004**, *350*, 2151–2158. [[CrossRef](#)] [[PubMed](#)]
4. Ponikowski, P.; Voors, A.A.; Anker, S.D.; Bueno, H.; Cleland, J.G.F.; Coats, A.J.S.; Falk, V.; González-Juanatey, J.R.; Harjola, V.-P.; Jankowska, E.A.; et al. 2016 ESC Guidelines for the Diagnosis and Treatment of Acute and Chronic Heart Failure. *Eur. Heart J.* **2016**, *37*, 2129–2200. [[CrossRef](#)]
5. Al-Khatib, S.M.; Stevenson, W.G.; Ackerman, M.J.; Bryant, W.J.; Callans, D.J.; Curtis, A.B.; Deal, B.J.; Dickfeld, T.; Field, M.E.; Fonarow, G.C.; et al. 2017 AHA/ACC/HRS Guideline for Management of Patients With Ventricular Arrhythmias and the Prevention of Sudden Cardiac Death. *J. Am. Coll. Cardiol.* **2018**, *72*, e91–e220. [[CrossRef](#)]
6. Buxton, A.E.; Ellison, K.E.; Lorvidhaya, P.; Ziv, O. Left Ventricular Ejection Fraction for Sudden Death Risk Stratification and Guiding Implantable Cardioverter-Defibrillators Implantation. *J. Cardiovasc. Pharmacol.* **2010**, *55*, 450–455.
7. Iles, L.M.; Ellims, A.H.; Llewellyn, H.; Hare, J.L.; Kaye, D.M.; McLean, C.A.; Taylor, A.J. Histological Validation of Cardiac Magnetic Resonance Analysis of Regional and Diffuse Interstitial Myocardial Fibrosis. *Eur. Heart J. Cardiovasc. Imaging* **2015**, *16*, 14–22. [[CrossRef](#)]
8. Halliday, B.P.; Gulati, A.; Ali, A.; Guha, K.; Newsome, S.; Arzanauskaite, M.; Vassiliou, V.S.; Lota, A.; Izgi, C.; Tayal, U.; et al. Association Between Midwall Late Gadolinium Enhancement and Sudden Cardiac Death in Patients With Dilated Cardiomyopathy and Mild and Moderate Left Ventricular Systolic Dysfunction. *Circulation* **2017**, *135*, 2106–2115. [[CrossRef](#)]
9. Gulati, A.; Jabbour, A.; Ismail, T.F.; Guha, K.; Khwaja, J.; Raza, S.; Morarji, K.; Brown, T.D.H.; Ismail, N.A.; Dweck, M.R.; et al. Association of Fibrosis With Mortality and Sudden Cardiac Death in Patients with Nonischemic Dilated Cardiomyopathy. *JAMA* **2013**, *309*, 896. [[CrossRef](#)]
10. Di Marco, A.; Anguera, I.; Schmitt, M.; Klem, I.; Neilan, T.G.; White, J.A.; Sramko, M.; Masci, P.G.; Barison, A.; McKenna, P.; et al. Late Gadolinium Enhancement and the Risk for Ventricular Arrhythmias or Sudden Death in Dilated Cardiomyopathy. *JACC Heart Fail.* **2017**, *5*, 28–38. [[CrossRef](#)]
11. Yancy, C.W.; Jessup, M.; Bozkurt, B.; Butler, J.; Casey, D.E.; Drazner, M.H.; Fonarow, G.C.; Geraci, S.A.; Horwich, T.; Januzzi, J.L.; et al. 2013 ACCF/AHA Guideline for the Management of Heart Failure. *J. Am. Coll. Cardiol.* **2013**, *62*, e147–e239. [[CrossRef](#)] [[PubMed](#)]
12. Coelho-Filho, O.R.; Mongeon, F.-P.; Mitchell, R.; Moreno, H.; Nadruz, W.; Kwong, R.; Jerosch-Herold, M. Role of Transcytolemmal Water-Exchange in Magnetic Resonance Measurements of Diffuse Myocardial Fibrosis in Hypertensive Heart Disease. *Circ. Cardiovasc. Imaging* **2013**, *6*, 134–141. [[CrossRef](#)] [[PubMed](#)]
13. Arenja, N.; Andre, F.; Riffel, J.H.; aus dem Siepen, F.; Heigenbart, U.; Schönland, S.; Kristen, A.V.; Katus, H.A.; Buss, S.J. Prognostic Value of Novel Imaging Parameters Derived from Standard Cardiovascular Magnetic Resonance in High Risk Patients with Systemic Light Chain Amyloidosis. *J. Cardiovasc. Magn. Reson.* **2019**, *21*, 53. [[CrossRef](#)]
14. Tsadok, Y.; Friedman, Z.; Haluska, B.A.; Hoffmann, R.; Adam, D. Myocardial Strain Assessment by Cine Cardiac Magnetic Resonance Imaging Using Non-Rigid Registration. *Magn. Reson. Imaging* **2016**, *34*, 381–390. [[CrossRef](#)] [[PubMed](#)]
15. Liang, Y.; Li, W.; Zeng, R.; Sun, J.; Wan, K.; Xu, Y.; Cao, Y.; Zhang, Q.; Han, Y.; Chen, Y. Left Ventricular Spherical Index Is an Independent Predictor for Clinical Outcomes in Patients With Nonischemic Dilated Cardiomyopathy. *JACC Cardiovasc. Imaging* **2019**, *12*, 1578–1580. [[CrossRef](#)]

16. Muthalaly, R.G.; Kwong, R.Y.; John, R.M.; van der Geest, R.J.; Tao, Q.; Schaeffer, B.; Tanigawa, S.; Nakamura, T.; Kaneko, K.; Tedrow, U.B.; et al. Left Ventricular Entropy Is a Novel Predictor of Arrhythmic Events in Patients With Dilated Cardiomyopathy Receiving Defibrillators for Primary Prevention. *JACC Cardiovasc. Imaging* **2019**, *12*, 1177–1184. [[CrossRef](#)]
17. Kramer, C.M.; Barkhausen, J.; Flamm, S.D.; Kim, R.J.; Nagel, E. Standardized Cardiovascular Magnetic Resonance (CMR) Protocols 2013 Update. *J. Cardiovasc. Magn. Reson.* **2013**, *15*, 91. [[CrossRef](#)]
18. Cerqueira, M.D.; Weissman, N.J.; Dilsizian, V.; Jacobs, A.K.; Kaul, S.; Laskey, W.K.; Pennell, D.J.; Rumberger, J.A.; Ryan, T.; Verani, M.S. Standardized Myocardial Segmentation and Nomenclature for Tomographic Imaging of the Heart. *Circulation* **2002**, *105*, 539–542. [[CrossRef](#)]
19. Bondarenko, O.; Beek, A.; Hofman, M.; Kühl, H.; Twisk, J.; van Dockum, W.; Visser, C.; van Rossum, A. Standardizing the Definition of Hyperenhancement in the Quantitative Assessment of Infarct Size and Myocardial Viability Using Delayed Contrast-Enhanced CMR. *J. Cardiovasc. Magn. Reson.* **2005**, *7*, 481–485. [[CrossRef](#)]
20. Gao, P.; Yee, R.; Gula, L.; Krahn, A.D.; Skanes, A.; Leong-Sit, P.; Klein, G.J.; Stirrat, J.; Fine, N.; Pallaveshi, L.; et al. Prediction of Arrhythmic Events in Ischemic and Dilated Cardiomyopathy Patients Referred for Implantable Cardiac Defibrillator. *Circ. Cardiovasc. Imaging* **2012**, *5*, 448–456. [[CrossRef](#)]
21. Piek, A.; de Boer, R.A.; Silljé, H.H.W. The Fibrosis-Cell Death Axis in Heart Failure. *Heart Fail. Rev.* **2016**, *21*, 199–211. [[CrossRef](#)] [[PubMed](#)]
22. Doltra, A.; Amundsen, B.; Gebker, R.; Fleck, E.; Kelle, S. Emerging Concepts for Myocardial Late Gadolinium Enhancement MRI. *Curr. Cardiol. Rev.* **2013**, *9*, 185–190. [[CrossRef](#)] [[PubMed](#)]
23. Lehrke, S.; Lossnitzer, D.; Schob, M.; Steen, H.; Merten, C.; Kemmling, H.; Pribe, R.; Ehlermann, P.; Zugck, C.; Korosoglou, G.; et al. Use of Cardiovascular Magnetic Resonance for Risk Stratification in Chronic Heart Failure: Prognostic Value of Late Gadolinium Enhancement in Patients with Non-Ischaemic Dilated Cardiomyopathy. *Heart* **2011**, *97*, 727–732. [[CrossRef](#)]
24. Sree Raman, K.; Nucifora, G.; Leong, D.P.; Marx, C.; Shah, R.; Woodman, R.J.; Molaee, P.; Shirazi, M.G.; McGavigan, A.D.; De Pasquale, C.G.; et al. Long Term Prognostic Importance of Late Gadolinium Enhancement in First-Presentation Non-Ischaemic Dilated Cardiomyopathy. *Int. J. Cardiol.* **2019**, *280*, 124–129. [[CrossRef](#)] [[PubMed](#)]
25. Halliday, B.P.; Baksi, A.J.; Gulati, A.; Ali, A.; Newsome, S.; Izgi, C.; Arzanauskaite, M.; Lota, A.; Tayal, U.; Vassiliou, V.S.; et al. Outcome in Dilated Cardiomyopathy Related to the Extent, Location, and Pattern of Late Gadolinium Enhancement. *JACC Cardiovasc. Imaging* **2019**, *12*, 1645–1655. [[CrossRef](#)] [[PubMed](#)]
26. Becker, M.A.J.; Cornel, J.H.; van de Ven, P.M.; van Rossum, A.C.; Allaart, C.P.; Germans, T. The Prognostic Value of Late Gadolinium-Enhanced Cardiac Magnetic Resonance Imaging in Nonischemic Dilated Cardiomyopathy. *JACC Cardiovasc. Imaging* **2018**, *11*, 1274–1284. [[CrossRef](#)] [[PubMed](#)]
27. Stolfo, D.; Merlo, M.; Pinamonti, B.; Barbati, G.; Di Lenarda, A.; Sinagra, G. Evolution of Left Ventricular Sphericity Index in Idiopathic Dilated Cardiomyopathy: Clinical and Prognostic Implications. *Eur. Heart J.* **2013**, *34* (Suppl. 1), P1196. [[CrossRef](#)]
28. Marchal, P.; Lairez, O.; Cognet, T.; Chabbert, V.; Barrier, P.; Berry, M.; Mejean, S.; Roncalli, J.; Rousseau, H.; Carrie, D.; et al. Relationship between Left Ventricular Sphericity and Trabeculation Indexes in Patients with Dilated Cardiomyopathy: A Cardiac Magnetic Resonance Study. *Eur. Heart J. Cardiovasc. Imaging* **2013**, *14*, 914–920. [[CrossRef](#)]
29. Ben Halima, A.; Zidi, A. The Cardiac Magnetic Resonance Sphericity Index in the Dilated Cardiomyopathy: New Diagnostic and Prognostic Marker. *Arch. Cardiovasc. Dis. Suppl.* **2018**, *10*, 42. [[CrossRef](#)]
30. Ambale-Venkatesh, B.; Yoneyama, K.; Sharma, R.K.; Ohyama, Y.; Wu, C.O.; Burke, G.L.; Shea, S.; Gomes, A.S.; Young, A.A.; Bluemke, D.A.; et al. Left Ventricular Shape Predicts Different Types of Cardiovascular Events in the General Population. *Heart* **2017**, *103*, 499–507. [[CrossRef](#)]
31. Nakamori, S.; Ismail, H.; Ngo, L.H.; Manning, W.J.; Nezafat, R. Left Ventricular Geometry Predicts Ventricular Tachyarrhythmia in Patients with Left Ventricular Systolic Dysfunction: A Comprehensive Cardiovascular Magnetic Resonance Study. *J. Cardiovasc. Magn. Reson.* **2017**, *19*, 79. [[CrossRef](#)] [[PubMed](#)]
32. Gjesdal, O.; Almeida, A.L.C.; Hopp, E.; Beitnes, J.O.; Lunde, K.; Smith, H.-J.; Lima, J.A.C.; Edvardsen, T. Long Axis Strain by MRI and Echocardiography in a Postmyocardial Infarct Population. *J. Magn. Reson. Imaging* **2014**, *40*, 1247–1251. [[CrossRef](#)] [[PubMed](#)]

33. Schuster, A.; Backhaus, S.J.; Stiermaier, T.; Kowallick, J.T.; Stulle, A.; Koschalka, A.; Lotz, J.; Kutty, S.; Bigalke, B.; Gutberlet, M.; et al. Fast Manual Long-Axis Strain Assessment Provides Optimized Cardiovascular Event Prediction Following Myocardial Infarction. *Eur. Heart J. Cardiovasc. Imaging* **2019**, *20*, 1262–1270. [[CrossRef](#)] [[PubMed](#)]
34. Gjesdal, O.; Yoneyama, K.; Mewton, N.; Wu, C.; Gomes, A.S.; Hundley, G.; Prince, M.; Shea, S.; Liu, K.; Bluemke, D.A.; et al. Reduced Long Axis Strain Is Associated with Heart Failure and Cardiovascular Events in the Multi-Ethnic Study of Atherosclerosis. *J. Magn. Reson. Imaging* **2016**, *44*, 178–185. [[CrossRef](#)]
35. Agoston-Coldea, L.; Bheecarry, K.; Cionca, C.; Petra, C.; Strimbu, L.; Ober, C.; Lupu, S.; Fodor, D.; Mocan, T. Incremental Predictive Value of Longitudinal Axis Strain and Late Gadolinium Enhancement Using Standard CMR Imaging in Patients with Aortic Stenosis. *J. Clin. Med.* **2019**, *8*, 165. [[CrossRef](#)]
36. Riffel, J.H.; Keller, M.G.P.; Rost, F.; Arenja, N.; Andre, F.; aus dem Siepen, F.; Fritz, T.; Ehlermann, P.; Taeger, T.; Frankenstein, L.; et al. Left Ventricular Long Axis Strain: A New Prognosticator in Non-Ischemic Dilated Cardiomyopathy? *J. Cardiovasc. Magn. Reson.* **2016**, *18*, 36. [[CrossRef](#)]
37. Kano, N.; Okumura, T.; Hiraiwa, H.; Watanabe, N.; Kondo, T.; Fukaya, K.; Sawamura, A.; Morimoto, R.; Bando, Y.; Murohara, T. Prognostic Impact of Combination of Sphericity Index and Late Gadolinium Enhancement on Cardiac Magnetic Resonance in Patients with Dilated Cardiomyopathy. *J. Card. Fail.* **2016**, *22*, S177. [[CrossRef](#)]



© 2020 by the authors. Licensee MDPI, Basel, Switzerland. This article is an open access article distributed under the terms and conditions of the Creative Commons Attribution (CC BY) license (<http://creativecommons.org/licenses/by/4.0/>).



Article

Desminopathy: Novel Desmin Variants, a New Cardiac Phenotype, and Further Evidence for Secondary Mitochondrial Dysfunction

Miloš Kubánek ^{1,*}, Tereza Schimerová ^{1,2}, Lenka Piherová ³, Andreas Brodehl ⁴, Alice Krebsová ¹, Sandra Ratnavadivel ⁴, Caroline Stanasiuk ⁴, Hana Hansíková ⁵, Jiří Zeman ⁵, Tomáš Paleček ⁶, Josef Houštěk ⁷, Zdeněk Drahoř ⁷, Hana Nůsková ⁷, Jana Mikešová ⁷, Josef Zámečník ⁸, Milan Macek Jr. ⁹, Petr Ridzoň ¹⁰, Jana Malusková ¹¹, Viktor Stránecký ³, Vojtěch Melenovský ¹, Hendrik Milting ⁴ and Stanislav Kmoch ³

¹ Department of Cardiology, Institute for Clinical and Experimental Medicine, 14021 Prague, Czech Republic; nedt@ikem.cz (T.S.); krea@ikem.cz (A.K.); vome@ikem.cz (V.M.)

² Institute of Physiology, First Faculty of Medicine, Charles University, 11636 Prague, Czech Republic

³ Research Unit for Rare Diseases, Department of Pediatrics and Adolescent Medicine, First Faculty of Medicine, Charles University, 11636 Prague, Czech Republic; Lenka.Piherova@lf1.cuni.cz (L.P.); Viktor.Stranecky@lf1.cuni.cz (V.S.); skmoch@lf1.cuni.cz (S.K.)

⁴ Erich and Hanna Klessmann Institute, Heart and Diabetes Center NRW, University Hospital of the Ruhr-University Bochum, 32545 Bad Oeynhausen, Germany; ABrodehl@hdz-nrw.de (A.B.); SRatnavadivel@hdz-nrw.de (S.R.); CStanasiuk@hdz-nrw.de (C.S.); HMilting@hdz-nrw.de (H.M.)

⁵ Department of Pediatrics and Adolescent Medicine, First Faculty of Medicine, Charles University and General University Hospital in Prague, 12108 Prague, Czech Republic; Hana.Hansikova@lf1.cuni.cz (H.H.); jzem@lf1.cuni.cz (J.Z.)

⁶ 2nd Department of Medicine—Department of Cardiovascular Medicine, First Faculty of Medicine, Charles University and General University Hospital in Prague, 12108 Prague, Czech Republic; Tomas.Palecek@lf1.cuni.cz

⁷ Institute of Physiology, Czech Academy of Sciences, 11720 Prague, Czech Republic; josef.houstek@fgu.cas.cz (J.H.); zdenek.drahoř@fgu.cas.cz (Z.D.); h.nuskova@dkfz-heidelberg.de (H.N.); jana.mikesova@uochb.cas.cz (J.M.)

⁸ Department of Pathology and Molecular Medicine, Second Faculty of Medicine, Charles University, 11636 Prague, Czech Republic; josef.zamecnik@lfmotol.cuni.cz

⁹ Department of Biology and Medical Genetics, Second Faculty of Medicine, Charles University, 11636 Prague, Czech Republic; milan.macek.jr@lfmotol.cuni.cz

¹⁰ Department of Neurology, Thomayer's Hospital, 14059 Prague, Czech Republic; petr.ridzon@ftn.cz

¹¹ Department of Pathology, Institute for Clinical and Experimental Medicine, 14021 Prague, Czech Republic; Institute for Clinical and Experimental Medicine, 14021 Prague, Czech Republic; jana.maluszkova@ikem.cz

* Correspondence: milos.kubaneck@ikem.cz; Tel.: +42-0236-055-047; Fax: +42-0236-052-989

Received: 13 February 2020; Accepted: 24 March 2020; Published: 29 March 2020

Abstract: Background: The pleomorphic clinical presentation makes the diagnosis of desminopathy difficult. We aimed to describe the prevalence, phenotypic expression, and mitochondrial function of individuals with putative disease-causing desmin (DES) variants identified in patients with an unexplained etiology of cardiomyopathy. **Methods:** A total of 327 Czech patients underwent whole exome sequencing and detailed phenotyping in probands harboring DES variants. **Results:** Rare, conserved, and possibly pathogenic DES variants were identified in six (1.8%) probands. Two DES variants previously classified as variants of uncertain significance (p.(K43E), p.(S57L)), one novel DES variant (p.(A210D)), and two known pathogenic DES variants (p.(R406W), p.(R454W)) were associated with characteristic desmin-immunoreactive aggregates in myocardial and/or skeletal biopsy samples. The individual with the novel DES variant p.(Q364H) had a decreased myocardial expression of desmin with absent desmin aggregates in myocardial/skeletal muscle biopsy and presented with familial left ventricular non-compaction cardiomyopathy (LVNC), a relatively novel

phenotype associated with desminopathy. An assessment of the mitochondrial function in four probands heterozygous for a disease-causing *DES* variant confirmed a decreased metabolic capacity of mitochondrial respiratory chain complexes in myocardial/skeletal muscle specimens, which was in case of myocardial succinate respiration more profound than in other cardiomyopathies. **Conclusions:** The presence of desminopathy should also be considered in individuals with LVNC, and in the differential diagnosis of mitochondrial diseases.

Keywords: desmin; dilated cardiomyopathy; mitochondrial dysfunction; myopathy; non-ischemic cardiomyopathy; whole exome sequencing

1. Introduction

Desminopathy (OMIM # 601409) represents a group of autosomal inherited disorders caused by pathogenic variants in the disease-causing desmin (*DES*) gene, encoding the major muscle specific intermediate filament protein desmin (OMIM: #125660) [1]. Desmin is the major component of intermediate filaments in cardiac, skeletal, and smooth muscle cells, with a particularly high content in Purkinje fibers and diaphragmatic muscle cells [1]. Consequently, cardiomyopathy, cardiac conduction disease, and progressive skeletal myopathy are the most common clinical presentations of desminopathy. It may occur as an isolated cardiac disease or in variable combinations and with different onsets. As summarized in a meta-analysis [1], 49%, 60%, and 74% of individuals harboring a pathogenic *DES* variant develop cardiomyopathy, cardiac conduction disease, and skeletal myopathy, respectively. The most common form of myocardial involvement is dilated cardiomyopathy (DCM) [1–3], followed by restrictive (RCM) [4–7], arrhythmogenic (ACM) and hypertrophic cardiomyopathy (HCM), and arrhythmogenic cardiomyopathy pattern [8–11]. On the other hand, there is low evidence regarding an association between desminopathy and left ventricular noncompaction cardiomyopathy (LVNC). Importantly, intermediate filaments are essential not only for cellular integrity, organization, and differentiation, but also for a signal transduction and adequate mitochondrial function [12]. Accordingly, several experimental [12–14] and clinical [15,16] studies have proven a secondary mitochondrial dysfunction in desminopathy, which in one case even mimicked mitochondrial disease [16].

The pleomorphic clinical presentation makes the diagnosis of desminopathy challenging. Fortunately, massively parallel sequencing (MPS) utilizing either cardiomyopathy panels and/or even whole exome sequencing (WES) aid in the diagnosis of desminopathy regardless of its clinical presentation. Hereby, we aimed to describe the prevalence of desminopathy and their phenotypes in a large representative cohort of patients with cardiomyopathy of unexplained etiology using WES.

2. Materials and Methods

A representative cohort of 327 Czech patients with an unexplained etiology of cardiomyopathy underwent WES between September 2015 and June 2017. The cohort consisted mainly of cases with familial and sporadic DCM (81%), LVNC (13%), and less frequently of RCM (6%) or ACM (6%). Rare and possibly pathogenic missense *DES* variants were identified in 6 (1.8%) index patients from 6 different families (Figure 1).

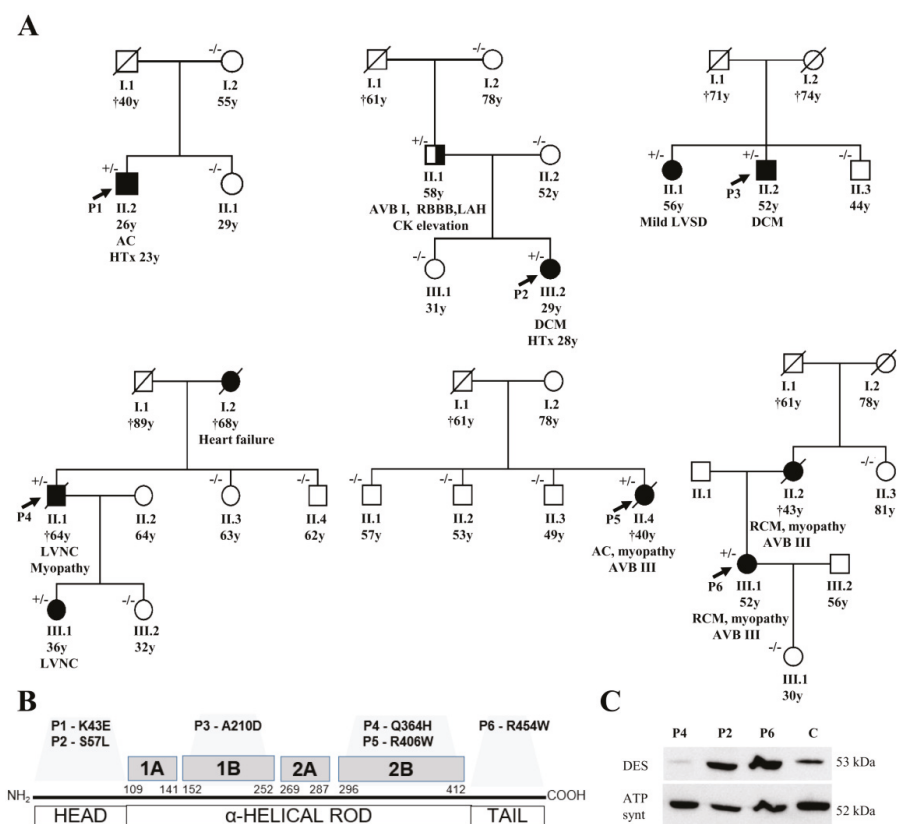


Figure 1. (A) shows pedigrees of the affected families and segregation of desmin variants (+/- heterozygous status, -/- wild type). In the fourth family (with P4) we also assessed a segregation of the rare variant of *MYH7* (NM_000257.3), c.4679G > C, p.(Arg1560Pro), which was present just in P4 (II/1) and absent in II/3, II/4, III/1, and III/2. (B) summarizes the structure of the desmin gene with localization of the detected variants. (C) illustrates the detection of desmin by western blot in myocardial samples (P2, P4, P6, control sample; 30ug protein aliquots) with an obvious reduction of signal in P4 with left ventricular non-compaction cardiomyopathy (*DES*-p.(Q364H)). Abbreviations: AC = arrhythmogenic cardiomyopathy, AVB = atrioventricular block, DCM = dilated cardiomyopathy, DES = desmin, HTx = heart transplantation, LAH = left anterior hemiblock, LVNC = left ventricular non-compaction cardiomyopathy, LVSD = left ventricular systolic dysfunction, RBBB = right bundle branch block, and RCM = restrictive cardiomyopathy.

2.1. Clinical Description of Studied Patients and of Their Families

Comprehensive clinical, laboratory, and electrophysiological data of all index cases were collected. Two probands of them (P2, P4) also underwent cardiovascular magnetic resonance imaging (Siemens Trio scanner, Siemens Medical Solutions, Erlangen, Germany) as described previously [17]. All available relatives undertook cardiologic screening, which included physical examination, electrocardiography, and echocardiography as well as a collection of blood samples for genetic analysis. Patients with suspected disease-causing *DES* variants were subjected to a detailed neurologic assessment, measurement of serum creatine phosphokinase, nerve conductance, and electromyography of two muscles (left vastus medialis and left deltoid muscle), as reported previously [17].

The study was approved by the Institutional Review Board's representing all clinical collaborators (Institute for Clinical and Experimental Medicine and Thomayer's Hospital; 1st Faculty of Medicine of the Charles University and General Faculty Hospital; both Prague) and was conducted in accordance with the principles of the Declaration of Helsinki. Written informed consent was obtained from all probands.

2.2. Genetic Analysis and Detection of Variants

To detect causal genetic variants, WES was performed according to internationally accepted guidelines [18]. Full technical details are provided in the Supplementary Materials. The criteria for classifying variants as putative disease-causing variants included their rare occurrence ($\leq 0.05\%$ among control samples), changes in predicted amino acid sequences, conservation across different species (<http://www.ncbi.nlm.nih.gov/BLAST/>), segregation within the family, and previously reported pathogenicity in databases.

Exons with identified variants of the *DES* gene were PCR amplified (Table S1) from genomic DNA of all available individuals from the analyzed families and sequenced using the version 3.1 Dye Terminator cycle sequencing kit with electrophoresis on an ABI 3500XL Avant Genetic Analyzer (both ThermoFisher Scientific; Waltham, MA, USA). Data were analyzed using Sequencing Analysis software version 6.0 (both ThermoFisher Scientific; USA) and the segregation of the candidate *DES* variants with the phenotype was evaluated.

2.3. In Vitro Analysis of DES Variants

As many but not all pathogenic *DES* variants cause an abnormal cytoplasmic desmin aggregation, we constructed for the identified *DES* variants expression plasmids by site-directed mutagenesis (Agilent Technologies, Santa Clara, CA, USA) according to the manufacturer's instructions. Desmin encoding parts of all plasmids were verified by Sanger sequencing (Macrogen, Amsterdam, Netherlands). The plasmid pmRuby-N1-DES and pmRuby-N1-DES-p.(Y122C) have been previously described [19,20]. Previously reported variant DES-p.(Y122C) was used as a positive control forming abnormal cytoplasmic aggregates [20]. HT1080 cells, which do not express endogenous desmin and cardiomyocytes derived from human induced pluripotent stem cells (iPSC) (NP00040-8) were transfected using Lipofectamin 3000 (ThermoFisher Scientific) or nucleofection using the 4D Nucleofector (Lonza, Cologne, Germany) in combination with the P3 Primary Cell 4D Nucleofector Kit according to the manufacturer's instructions. The differentiation of hiPSCs has been previously described [21]. Transfected HT1080 cells were fixed using 4% paraformaldehyde, permeabilized using 0.05% Triton X100, and stained with phalloidin conjugated with Alexa-488. Transfected hiPSC-derived cardiomyocytes were stained with primary antibodies against the Z-band protein α -actinin as a cardiomyocytes specific marker (Sigma-Aldrich, Missouri, MO, USA, #A7732) in combination with secondary antibodies conjugated to Alexa-488 (ThermoFisher). Confocal microscopy was performed as previously described [22].

2.4. Statistical Analysis of Aggregate Formation

A total of 3 to 4 independent transfection experiments were analyzed by counting the number of aggregate forming cells. Non-parametric Kruskal–Wallis for multiple comparison was performed using GraphPad Prism version 8.3.0 for Windows (GraphPad Software, San Diego, CA, USA). *p*-values < 0.05 were considered as significant.

2.5. Histopathology, Immunohistochemistry, Desmin Western Blot, and Electron Microscopy

In 5 probands (P1–P4, P6), formalin-fixed paraffin-embedded samples of myocardium were available either from endomyocardial biopsy (P2, P3) and/or from hearts explanted during transplantation (P1, P2, P6) or post-mortem (P4). The samples were snap frozen in liquid nitrogen and stored at $-70\text{ }^{\circ}\text{C}$. Resin-embedded myocardial samples for electron microscopy were analyzed in 4 patients (P1, P2, P4, and P6). A biopsy of skeletal muscle was performed in 3 individuals with

clinical signs of myopathy (P4 and P5: Soleus-, P6: Deltoid muscle). In P4, also we obtained samples of intercostal muscles post-mortem. The excisions from the skeletal muscle (approx. 10 × 5 × 5 mm in size) were snap frozen in isopentane (2-methylbutane; Merck, Kenilworth, NJ, USA) and cooled in liquid nitrogen. Cryosections were examined by routine hematoxylin–eosin staining and a conventional spectrum of histochemical reactions, including myofibrillary ATPase, nicotinamide adenine dinucleotide-tetrazolium reductase (NADH-TR), succinate dehydrogenase (SDH), and cytochrome c oxidase (COX), as described elsewhere [23].

Desmin immunohistochemistry and electron microscopy were performed on both skeletal muscle and myocardium samples according to standard protocols (Supplementary Materials).

2.6. Analysis of Mitochondrial Function in Biopsies

Skeletal muscle homogenate (5%, w/v) was prepared from fresh tissue by using a glass-Teflon homogenizer in a medium containing 150 mM KCl, 50 mM Tris-HCl, 2 mM EDTA, pH 7.4, and 0.2 µg/mL Aprotinin at 4 °C. Mitochondria were isolated from the homogenate by differential centrifugation as described elsewhere [24]. Heart tissue homogenates (7%, w/v) were prepared from –80 °C stored frozen samples of left and right heart ventricles in 0.32 M sucrose, 10 mM Tris-HCl, 1 mM EDTA, pH 7.4, and 1 µg/mL PIC (protease inhibitor mixture Sigma P8340) using glass-Teflon and glass-glass Dounce homogenizers. The subsequent methods are described in detail in Supplementary Materials. A western blot analysis of mitochondrial proteins, measurement of mitochondrial DNA content, measurement of activities of respiratory chain complexes and citrate synthase [25], high resolution oxygraphy, and measurement of the content of total coenzyme Q10 were described previously in details and in the Supplementary Materials.

3. Results

3.1. Description of DES Variants and Their Segregation in Families

Probably disease-causing *DES* variants in heterozygous constitution were identified in six index cases (1.8%). Two missense variants were identified within the non-helical head (amino-terminal) domain of desmin, i.e., in P1 with biventricular form of ACM (NM_001927.3: c.127A > G; NP_001918.3: p.(K43E)) and in P2 with DCM (NM_001927.3: c.170C > T; NP_001918.3: p.(S57L)) (Figure 1, Tables S2 and S3). Both of them were previously reported in Clinvar database as variants of uncertain significance. In addition, we analyzed the desmin filament formation in transfected HT1080 and in iPSC-derived cardiomyocytes, revealing an abnormal cytoplasmic aggregation in the DES-p.(K43E) variant and known pathogenic DES-p.(R406W) variant (Figure 2). Two novel variants were found in the highly conserved central α -helical rod domain, i.e., in P3 with familial DCM located in the 1B helical domain (NM_001927.3:c.629C > A; NP_001918.3: p.(A210D)) and in P4 with familial LVNC in combination with skeletal myopathy located in the 2B helical domain (NM_001927.3: c.1092G>T; NP_001918.3: p.(Q364H)) (Figure 1, Tables S2 and S3). The findings in the biopsies are described below. The remaining two probands had the following known *DES* pathogenic variants: P5 with ACM and skeletal myopathy in the 2B helical domain (NM_001927.3: c.1216C>T; NP_001918.3: p.(R406W); HGMD database (<http://www.hgmd.cf.ac.uk/ac/index.php>) CM000368) [6] and P6 with RCM and skeletal myopathy within the non-helical tail (carboxy-terminal) domain (NM_001927.3: c.1360C > T; NP_001918.3: p.(R454W); HGMD CM071700) [26] (Figure 1, Tables S2 and S3). Table S4 contains lists of rare genetic variants of further cardiomyopathy associated genes in all probands (frequency in Exac database less than 0.00001). Just the variant of *MYH7* (NM_000257.3) c.4679G > C, p.(Arg1560Pro) in proband 4 could be relevant in a patient with LVNC. However, it was not present in other members of the family tested (II 1, 3, 4; III 1, 2) (Figure 1) and did not co-segregate with the phenotype of LVNC. Importantly, any pathogenic variants in mitochondrial proteins coded by nuclear DNA or mitochondrial DNA were not found in these six probands.

Figure 1 illustrates the segregation of *DES* variants in families. Family history or clinical screening revealed a similar cardiac disease in a first-degree relative in P3, P4, and P6 segregating with occurrence of *DES* variants (Figure 1, Table S2). In the father of P2, heterozygous for *DES* p.(S57L) variant, we observed an incomplete penetrance of the disease with atrioventricular block grade I, right bundle branch block, left anterior hemiblock, normal echocardiography, and a mild elevation of creatinine phosphokinase of 6.1 μ kat/l (upper limit of normal 2.3 μ kat/L) without clinical signs of myopathy. Cases P1 and P5 seemed to be sporadic (segregation assessed in mother and sister of P1, and three siblings of P5).

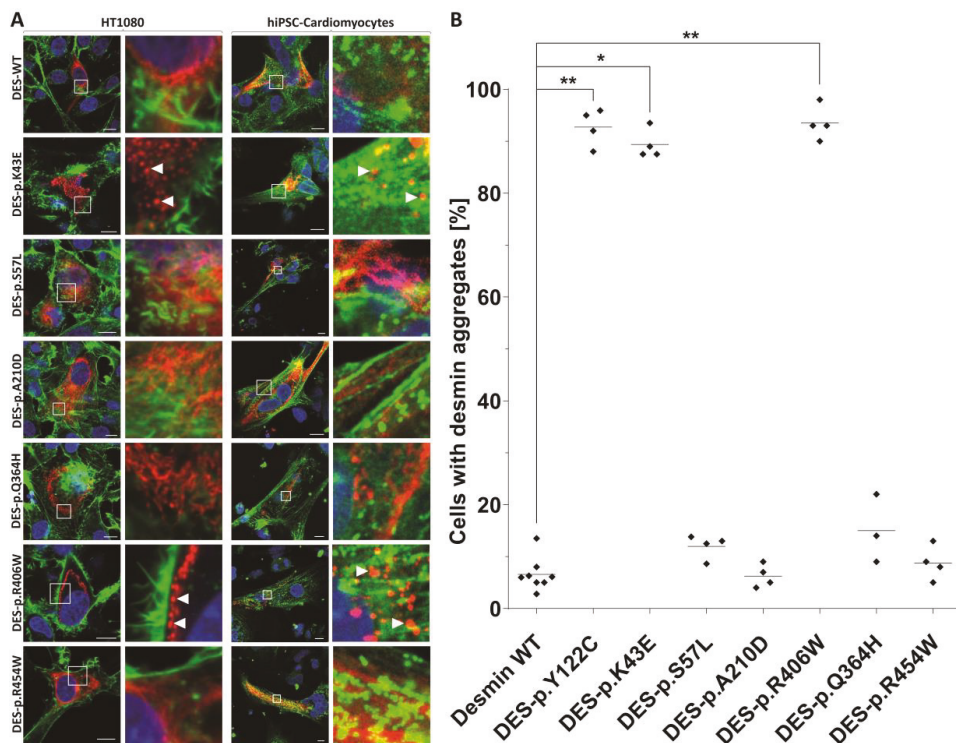


Figure 2. Cell transfection experiments of transfected HT1080 cells and iPSC-derived cardiomyocytes. Mutant and wild-type desmin was expressed with the red fluorescent protein-tag mRuby at the C-terminus (shown in red). Representative confocal images are shown (A). In case of HT1080 cells, F-actin was stained using phalloidin-Alexa488 (shown in green) and the nuclei were stained using 4',6-diamidin-2-phenylindole (shown in blue). In case of iPSC-cardiomyocytes, the cardiomyocyte marker α -actinin was stained using antibodies (shown in green) and the nuclei were stained with DAPI (shown in blue). Scale bars represent 10 μ m. (B) Quantification of aggregate formation was performed in three to four independent transfection experiments of HT1080 cells. * $p < 0.05$ and ** $p < 0.01$. The variant DES-p.(Y122C) was used as a positive control forming abnormal cytoplasmic aggregates [20].

3.2. Phenotypes of Desminopathy

The initial clinical presentation included cardiac arrest due to ventricular tachycardia in the 2nd decennium (P1), complete atrioventricular blockade in the 3rd decennium (P5, P6), and heart failure in the 3rd to 5th decennium (P2, P3, and P4). Skeletal myopathy and dysfunction of bulbar muscles became apparent during the 4th to 6th decennium in cases 4–6 (Table S2 and S3). An unusual clinical presentation had proband 2. A young female presented with acute heart failure, a severe

systolic dysfunction of mildly dilated left ventricle, persistent elevation of troponin T (> 10 times the upper limit of normal) (Table S3), and an extensive mid-wall late gadolinium enhancement of the septum and anterior wall of the left ventricle (Figure 3). These findings mimicked inflammatory cardiomyopathy however, there was no sign of inflammation as assessed by endomyocardial biopsy. Inflammation was absent also in her heart explanted during transplantation three years later. The arrhythmogenic left ventricular cardiomyopathy was considered as an alternative diagnosis in P2. However, her electrocardiogram was unremarkable and ventricular extrasystoles were infrequent. Proband 4 presented with a unique phenotype of LVNC. Magnetic resonance imaging (Figure 3) confirmed the diagnosis of LVNC with a percentage of non-compaction within the total left ventricular mass of 43%. Proband 6 was incorrectly diagnosed with mitochondrial disease based on skeletal muscle biopsy performed several years ago. This diagnosis was reclassified to desminopathy after the identification of known pathogenic desmin mutation (p.(R454W)) and morphological analysis of myocardial samples from the explanted heart. Table S3 illustrates additional clinical and laboratory data of the study group including echocardiography. During a median follow-up of 56 months (31–182), five probands (83%) developed end-stage heart failure.

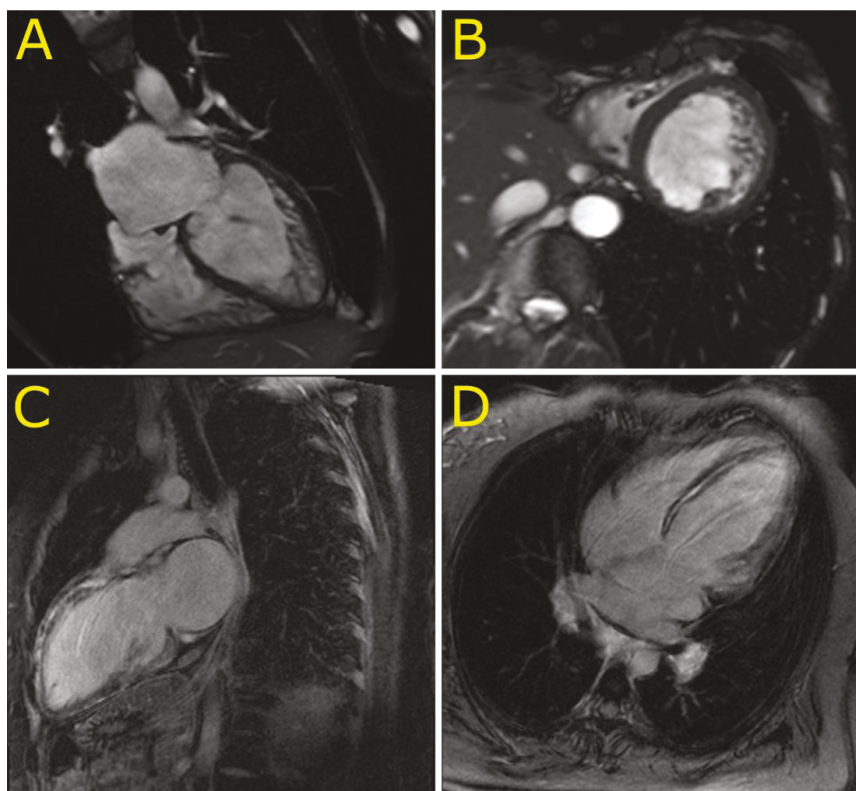


Figure 3. Cardiovascular magnetic resonance imaging in patients with left ventricular non-compaction cardiomyopathy (P4) and dilated cardiomyopathy with an extensive late gadolinium enhancement (P2). (A,B): Four chamber and short axis views of left ventricular non-compaction cardiomyopathy in P4. (C,D): Two chamber long axis and four chamber views of an extensive late gadolinium enhancement in the ventricular septum and left ventricular anterior wall mimicking inflammatory cardiomyopathy in P2.

3.3. Morphology of Desminopathy in Myocardial and Skeletal Muscle Samples

An immunohistochemical examination of myocardial samples in P1–P3 and P6 showed a diffuse alteration of desmin distribution in cardiomyocytes with a formation of desmin aggregates revealing strong immunoreactivity in the cytoplasm (shown in P1, P3; Figure 4A,E). Electron microscopy of cardiomyocytes in P1, P2, and P6 revealed myofibrillar disruption, streaming Z bands, and deposits of dense, amorphous granulofilamentous material of variable size and shape (shown in P1, P2; Figure 4B,C). In addition, we constructed a set of expression plasmids for the six *DES* missense variants and transfected HT1080 as a cell model without endogenous desmin expression and iPSC-derived cardiomyocytes. These experiments revealed a severe intermediate filament formation defect for *DES*-p.(K43E) and *DES*-p.(R406W) underlining their pathogenicity. Furthermore, electron microscopy of cardiac tissue demonstrated in P2, P4, and P6 focally increased the number of mitochondria, often in clusters, with loss of mitochondrial spatial organization (P2; Figure 4D). Importantly, desmin aggregates were absent in myocardial samples of P4 both at immunohistochemical and ultrastructural analysis. An expression of desmin in myocardium (P2, P4, and P6) was also assessed by Western blot analysis. There was an obvious reduction of the signal in P4 (Figure 1B).

Samples of the skeletal muscle (P4–P5 m. soleus, P4 intercostal muscle, P6 m. deltoideus) showed different findings in P4 and P6 as compared with P5. The morphological analysis in P4 and P6 detected only mild myopathic changes. The light microscopy with hematoxylin-eosin staining showed a marked variability in fiber size and increased number of internal nuclei (P4; Figure 4F). No inclusions were observed by light microscopy. Similarly, desmin immunohistochemistry did not reveal any protein aggregates in the sarcoplasm of P4 and P6 (P4; Figure 4G). In the NADH and SDH reactions, many fibers did not possess the characteristic checkerboard pattern, and in a proportion of fibers there was increased oxidative activity at the periphery of the muscle fibers, indicating the pathological accumulation of mitochondria (P4; Figure 4H). However, no typical ragged red fibers were observed. The distribution of COX reactivity was altered similarly to a NADH/SDH pattern with very few COX-negative fibers present (P4; Figure 4I). On the other hand, the muscle biopsy in P5 showed severe myopathic changes with a large amount of fibro-fatty tissue in the interstitium of the muscle. Desmin immunohistochemistry confirmed in P5 a diffuse alteration of desmin distribution with a formation of desmin aggregates in the cytoplasm of muscle fibers.

An ultrastructural analysis of skeletal muscle biopsies revealed a focally increased number of mitochondria, often in clusters, with an altered distribution in P4 and P6 (P4; Figure 4J) however, no ultrastructural abnormality in mitochondria morphology was observed. Typical deposits of dense granulofilamentous material were absent in P4 and were not observed in P6 at the first reading. Thus the first description of the skeletal muscle biopsy in P6 led to the diagnosis of mitochondrial myopathy. Nevertheless, the second reading of the skeletal muscle biopsy performed with the knowledge of the results of genetic tests and abnormal immunostaining of desmin in myocardium discovered a focus of dense amorphous material in a single fiber at electron microscopy (not shown).

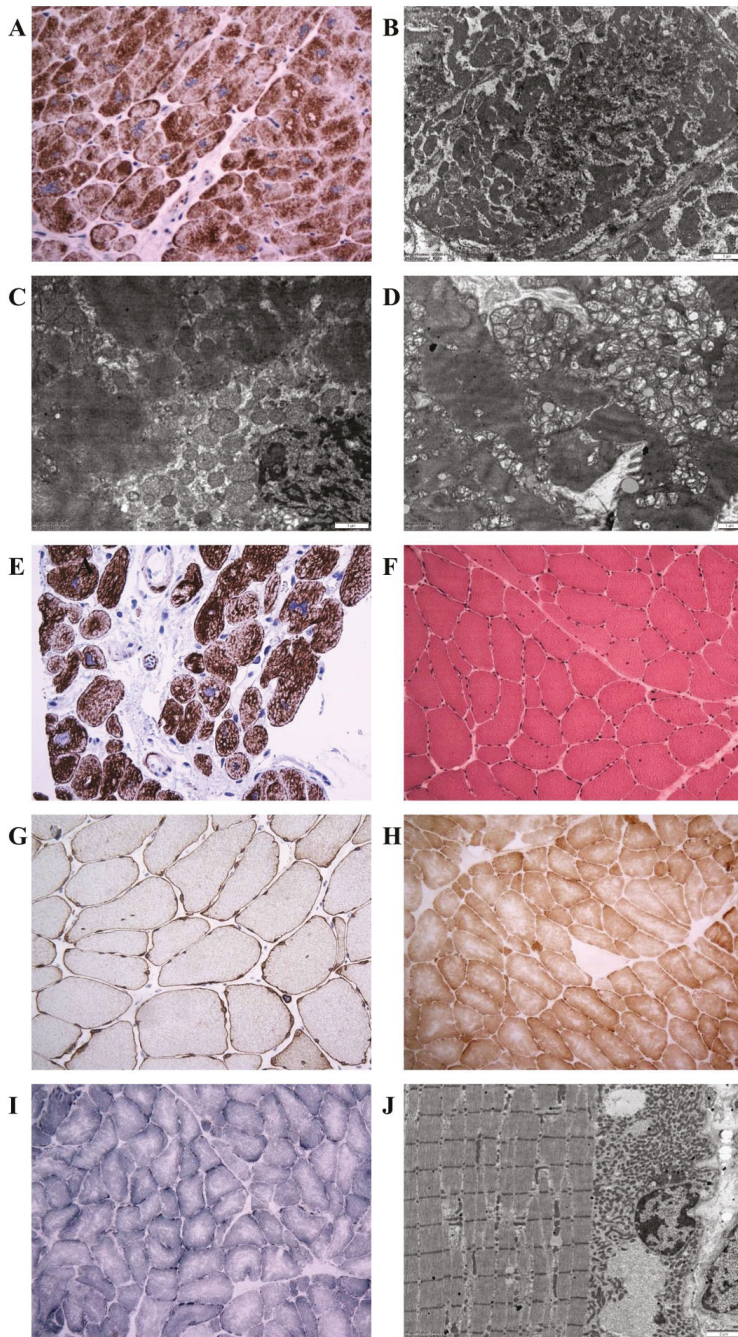


Figure 4. Illustration of histopathology, immunohistochemistry, and electron microscopy in individuals with the novel desmin variants. (A): Desmin immunohistochemistry (left ventricular myocardium, explanted heart, P1) documenting a diffuse alteration of desmin distribution with a formation of desmin aggregates revealing strong immunoreactivity in the cytoplasm. Original magnification $\times 400$. (B): Electron

microscopy (left ventricular myocardium, explanted heart, P1) detects amorphous granulofilamentous material in the cytoplasm of cardiomyocytes compatible with desmin aggregates. Original magnification $\times 10,000$. (C,D): Electron microscopy (left ventricular myocardium, explanted heart, P2). (C): Pathological dense granulofilamentous inclusions in the cytoplasm of cardiomyocyte. Original magnification $\times 12,000$. (D): Increased number of mitochondria in cardiomyocyte, often in clusters, with altered distribution. Original magnification $\times 8000$. (E): Desmin immunohistochemistry (right ventricular myocardium, endomyocardial biopsy, P3) revealed an abnormal staining of cardiomyocytes with a formation of desmin positive aggregates. Original magnification $\times 400$. (F–J) Diagnostic skeletal muscle biopsy specimens, Soleus muscle, P4, original magnification $\times 400$. (F): By light microscopy with hematoxylin–eosin, there was a marked variability in fiber size, absent inclusions, and increased number of internal nuclei. (G): Desmin immunohistochemistry did not reveal any protein aggregates in the sarcoplasm. (H): Nicotinamide adenine dinucleotide (NADH) and succinate dehydrogenase (SDH) immunohistochemistry identified few muscle fibers with increased oxidative activity at their periphery, indicating the pathological accumulation of mitochondria. However, no typical ragged red fibers were observed. (I): Very few COX-negative fibers were also present. (J): Electron-microscopic analysis revealed increased number of mitochondria, often in clusters, with altered distribution. No accumulation of intermediate filaments was observed. Original magnification $\times 6000$.

3.4. Indications for the Pathogenicity of the Novel Desmin Variants

A typical myocardial histopathology and ultrastructure with pathological desmin-immunoreactive aggregates strongly supported the pathogenicity of desmin variants p.(K43E), p.(S57L), and p.(A210D). In addition, the desmin filament formation experiments in transfected HT1080 and in iPSC-derived cardiomyocytes revealed an abnormal cytoplasmic aggregation of DES-p.(K43E). On the other hand, the pathogenicity of the novel desmin variant p.(Q364H) is supported mainly by decreased myocardial desmin expression and co-segregation of the above desmin variant in the family in the absence of other segregating cardiomyopathy-related genes as assessed by WES in the proband.

3.5. Mitochondrial Function and Content in Skeletal Muscle and Heart

An analysis of mitochondrial respiratory enzymes in skeletal muscle homogenates (Table 1) revealed a decreased activity of citrate synthase in P5, the activity of respiratory chain complex IV, and the quantity of mitochondrial respiratory chain proteins were decreased (Figure 5A). An oxygraphy analysis of P6 skeletal muscle fibers further showed a decrease in coupled (state 3-ADP) oxidation of NADH-dependent substrates (pyruvate + malate) to 35% of the mean of the controls (Table 1). More consistent data were provided by the analysis of isolated mitochondria from skeletal muscles of P4–P6. Specific activities of respiratory chain complexes I + III (NADH: Cytochrome c reductase), complex IV (cytochrome c oxidase), and citrate synthase were decreased to 30%–50% of the mean of the controls. Both P5 and P6 had a decreased content of coenzyme Q (Table 1). A low specific content of respiratory chain enzymes, citrate synthase, and porin was further apparent in isolated muscle mitochondria of P4–P6, with the most pronounced decrease observed in P5 (Figure 5A).

Table 1. Activities of respiratory chain enzymes in skeletal muscle homogenates (A), muscle fibers (B), and isolated mitochondria (C) of proband P4–P6. For analysis samples of m. tibialis (P4, P5) or m. deltoideus sin. (P6) were used. Enzyme activities and Coenzyme Q10 content are expressed per mg protein.

(A)				
Enzyme Activity of Muscle Homogenates (nmol/min/mg protein)	P4	P5	P6	Controls <i>n</i> = 30
Complex IV	130.1	38.1	81.8	68–213
Citrate synthase (CS)	109.5	41.4	97.8	48–128
Complex IV/CS	1.19	0.92	0.84	080–160
Coenzyme Q10 content (pmol/mg)	282.9	140.5	112.5	180–460
(B)				
Respiratory Activity of Permeabilized Muscle Fibers (pmol O ₂ /s/mg protein)				Controls <i>n</i> = 9
ADP-stimulated oxidation of NADH-dependent substrates	P6			16–26
ADP-stimulated oxidation of succinate				9–18
Cytochrome <i>c</i> oxidase respiration				43–83
(C)				
Enzyme Activity of Isolated Mitochondria (nmol/min/mg protein)	P4	P5	P6	Controls <i>n</i> = 30
Complex I	328.5	230.8	131.2	110–290
Complex I+III	94.1	18.7	53.2	126–316
Complex II	69.7	50.5	49.5	21–93
Complex II+III	174.2	92.9	146.7	82–251
Complex III	303.0	342.7	535.0	200–600
Complex IV	578.4	311.6	236.6	658–1552
Citrate synthase	372.5	240.4	384.2	435–1234
Complex I/CS	0.88	0.96	0.34	0.17–0.41
Complex I+III/CS	0.25	0.07	0.13	0.07–0.27
Complex II/CS	0.19	0.21	0.13	0.04–0.12
Complex II+III/CS	0.47	0.39	0.38	0.35–0.36
Complex III/CS	0.81	1.43	1.39	0.56–1.46
Complex IV/CS	1.55	1.30	0.62	0.82–1.88

Abbreviations: ADP–adenosine diphosphate, ATP–adenosine triphosphate, and NADH–reduced form of nicotinamide adenine dinucleotide.

Myocardium of two patients with desminopathy (P2, P6) (Table 2) revealed a general decrease in respiratory chain enzyme activities. An oxidation of NADH and succinate and cytochrome *c* oxidase respiration decreased to 20%–55% of the controls and activities of respiratory complexes I+III, II+III, and IV decreased to 15%–81%, respectively, indicating more extensive impairment in P2 heart ventricles (Table 2). The impairment of succinate respiration was the most profound with a mean of 277 pmol O₂/s/mg. This was much lower than in our historical controls from donor hearts unsuitable for transplantation (653 ± 244 pmol O₂/s/mg, *n* = 38) and even myocardium explanted during heart transplantation or ventricular assist device implantation (508 ± 211 pmol O₂/s/mg, *n* = 91) [25]. Western blot quantification of mitochondrial proteins showed a decrease in specific content of respiratory chain complexes, also more pronounced in P2, where a very low content of complexes IV and I was associated with the upregulation of complex II (Figure 5B). Other mitochondrial proteins, as porin

(shown in Figure 5A) and adenine nucleotide translocator (not shown) were less affected. Analysis of native forms of respiratory chain complexes by BlueNative electrophoresis (Figure 5C) confirmed a marked reduction of complexes I and IV in P2 heart and further showed that it led to a pronounced decrease of high molecular weight respiratory supercomplexes consisting of complexes I, III, and IV. Similar, yet a smaller decrease of supercomplexes was observed in soleus of R349P desmin knock-in mouse [15] or heart of desmin knockout mouse [27]. The content of mitochondrial DNA (relative to nuclear DNA, D-loop/GAPDH, and 16S RNA/GAPDH) was slightly decreased in P6 heart ventricles (60%–90% of the average value of the controls) but was unchanged in P2 heart. These data indicate mild to pronounced attenuation of the energetic function of mitochondria due to a decreased content and activity of respiratory complexes and supercomplexes in failing hearts of patients with desminopathy.

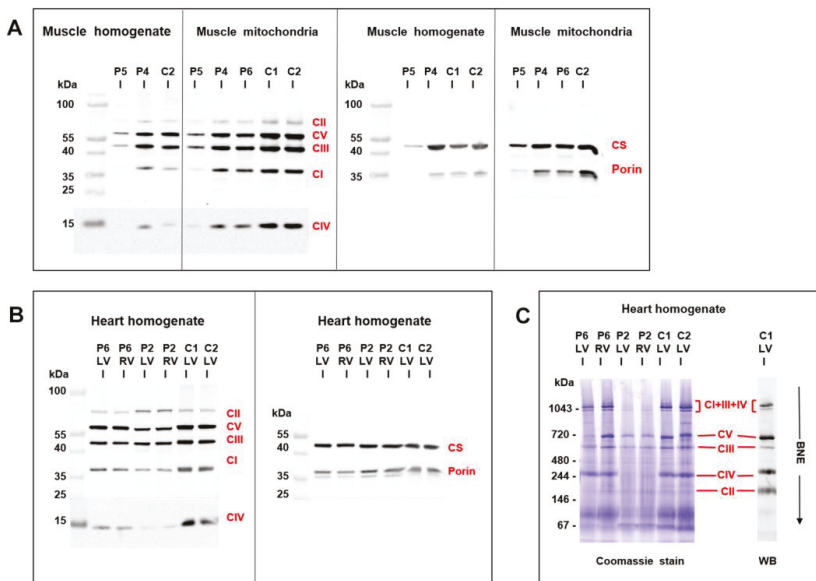


Figure 5. Western blot detection of mitochondrial proteins in skeletal muscle and heart. Analysis of SDS-PAGE resolved proteins from (A) muscle homogenates (6 µg protein aliquots) and isolated muscle mitochondria (2 µg protein aliquots) demonstrated a pronounced decrease of respiratory chain complexes (CI–CV), citrate synthase (CS), and porin in skeletal muscle of P5 compared to controls (C), P4 and P6 were less affected. Analysis of (B) heart homogenates (4 µg protein aliquots) from left and right heart ventricles (LV, RV) demonstrated a marked decrease of respiratory chain enzymes in P2 and a mild decrease in P6 compared to controls (C). CS and porin were less affected. BlueNative electrophoresis (C) further showed a marked decrease of native respiratory supercomplexes consisting of CI + CIII + CIV in P2 heart ventricles (12 µg protein aliquots).

Table 2. Activities of respiratory chain enzymes and mtDNA content in hearts of proband 2 and 6.

Respiratory/Enzyme Activity	P2 Left Ventricle	P2 Right Ventricle	P6 Left Ventricle	P6 Right Ventricle	Controls n = 38
(pmol O ₂ /s/mg)					
NADH respiration	245	203	448	229	235–2356
Succinate respiration	295	242	254	319	365–1529
Cytochrome c oxidase respiration	766	991	1003	1047	561–4120
(nmol/min/mg)					
Complex I+III	26.1	30.3	145.1	83.9	44–386
Complex II+III	88.0	71.3	59.5	56.7	27–195
Complex IV	262.6	432.4	430.5	276.8	389–1989
Citrate synthase (CS)	915.9	975.2	562.2	483.6	446–1207
(activity ratio)					
Complex I+III/CS	0.03	0.03	0.26	0.17	0.09–0.63
Complex II+III/CS	0.10	0.07	0.11	0.12	0.04–0.37
Complex IV/CS	0.29	0.44	0.77	0.57	0.54–2.60
mtDNA content (2 ^{-ΔCt})					
D-loop/GAPDH	4980	5499	2863	3592	2052–10519
16S RNA/GAPDH	11629	10914	8017	7299	3715–15843

Enzyme activities are expressed per mg protein, mtDNA content is expressed as 2^{-ΔCt} value indicating the number of mtDNA copies per a haploid genome. Abbreviation: GAPDH–glyceraldehyde 3-phosphate dehydrogenase.

As changes in mitochondria energetic function can affect a generation of reactive oxygen species, the content of antioxidative enzymes was analyzed by Western blot analysis in skeletal muscle and heart samples from patients with desminopathy (Figure 6). Both P4 and P5 muscle homogenates revealed highly increased glutathione reductase (GR) and superoxide dismutase 1 (SOD1) as well as a variable increase of catalase (CAT) and superoxide dismutase 2 (SOD2). Higher CAT was found in P5 isolated mitochondria, while the most increased SOD1 was of extra-mitochondrial origin (also apparent from the SOD1/SOD2 ratio). An increased content of GR and SOD1 was also found in heart ventricles of P6.

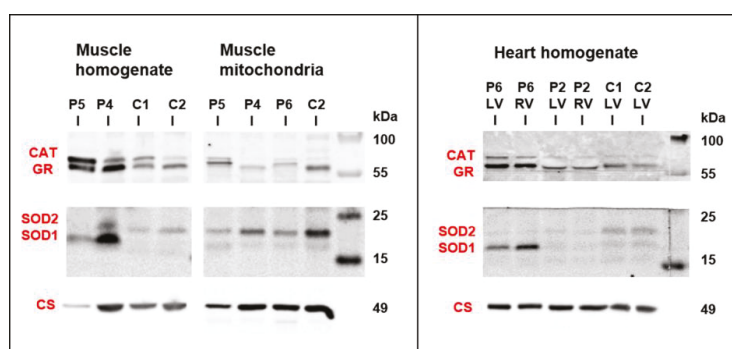


Figure 6. Western blot detection of antioxidative enzymes in skeletal muscle and heart. Both P4 and P5 muscle homogenates revealed variable increase in antioxidative enzymes glutathione reductase (GR), catalase (CAT), and superoxide dismutases 1 and 2 (SOD1, SOD2). Increased content of CAT, GR, and SOD1 was also found in heart ventricles of P6. Protein aliquots—muscle homogenate 30 μg, muscle mitochondria 15 μg, and heart homogenate 20 μg. For comparison, citrate synthase signal (CS) from Figure 5 is shown.

4. Discussion

Firstly, the prevalence of desminopathy in a large cohort of patients with an unexplained etiology of cardiomyopathy assessed with WES was 1.8%. Secondly, the presence of pathological desmin aggregates in myocardial/skeletal muscle samples of P1–P3 and decreased myocardial desmin expression in P4 suggested a pathogenicity of two novel *DES* variants and two *DES* variants previously classified as of uncertain significance. Thirdly, a pathogenicity of one variant of uncertain significance (*DES*-p.(K43E)) was supported also by abnormal desmin filament formation and its cytoplasmic aggregation in transfected HT1080 cells and in iPSC-derived cardiomyocytes. Fourthly, we provided further evidence for LVNC as a novel phenotype of desminopathy. Fifthly, we described secondary mitochondrial dysfunction in skeletal muscle and in myocardium, which was in case of myocardial succinate respiration more profound than in end-stage heart failure of other etiology. To the best of our knowledge, this seems to be the first comprehensive description of mitochondrial dysfunction in human myocardium affected by desminopathy. Finally, secondary mitochondrial dysfunction and/or an extensive left ventricular late gadolinium enhancement in desminopathy may imitate a primary mitochondrial disease or an inflammatory cardiomyopathy.

4.1. Clinical and Histopathological Correlates of Desminopathy

The majority of 68 pathogenic desmin variants that were reported so far are missense or small in-frame deletion variants localized in the helical rod domain [26,28]. A phenotype-genotype correlation meta-analyses revealed that pathogenic variants in the rod 2B domain of *DES* are common among patients with both skeletal and cardiac muscle phenotype, whereas head and tail domain pathogenic variants result mainly in clinically isolated cardiac phenotype [1,29,30]. In agreement with these findings, we found that two *DES* variants in head region (p.(K43E), p.(S57L)) and one novel *DES* variant (p.(A210D)) in the 1B helical domain had in probands isolated cardiac involvement. On the other hand, the novel *DES* mutation located in the 2B helical domain (p.(Q364H)) and two known *DES* variants (p.(R406W), p.(R454W)) affected both the cardiac and skeletal muscle.

Immunohistochemistry revealed pathological desmin aggregates in skeletal or cardiac myocytes in five probands from our study group. Importantly, desmin aggregates were absent in the deltoid muscle of proband 6 (*DES*-p.(R454W)), but present in her myocardial samples. Desmin aggregates were completely absent in proband 4 (*DES*-p.(Q364H)). Immunohistochemistry and electron microscopy of diagnostic muscle soleus biopsy and post-mortem myocardial and intercostal muscle samples failed to detect any pathological protein aggregates. Interestingly, Western blot analysis of the myocardial sample showed a decreased expression of desmin suggesting decreased protein synthesis. This is in agreement with the experience of pathologists that myopathological findings in genetically proven desminopathies may range from no overt pathology over subtle myopathic changes with sporadic protein aggregates to the picture of a vacuolar myopathy [31]. An absence of desmin aggregates has been recently documented both in autosomal dominant [32] and autosomal recessive [33] desminopathy.

4.2. Novel Cardiac Phenotypes of Desminopathy

In addition to known cardiac phenotypes of desminopathy like DCM, RCM HCM, and ACM [1,28,29], we observed LVNC as a relatively novel phenotype. So far, *DES* variants have been associated with LVNC just in a few individuals [34–37]. The first report from Arbustini et al. [34] described a family with a segregation of *DES* variant p.(G84S) with non-obstructive hypertrophic cardiomyopathy and one case of LVNC. Another group [35] reported one sporadic case of LVNC in a child with a *DES* variant p.(L398P). An occurrence of two cases of LVNC in one family has been recently associated with an in-frame mutation of desmin p.(Q113_L115del) affecting the α -helical rod domain [36] with a formation of typical desmin-immunoreactive aggregates. We expanded the available evidence by a description of another familial occurrence of two cases of LVNC associated

with the desmin variant p.(Q364H) with a decreased myocardial expression of desmin and absent desmin aggregates in myocardial/skeletal biopsy.

Recently, a novel phenotype of desminopathy describing left ventricular arrhythmogenic cardiomyopathy was reported to have a significant amount of subepicardial fibrosis [32]. A similar phenotype had our P2, which mimicked inflammatory cardiomyopathy by an extensive late gadolinium enhancement in the left ventricle and persistent elevation of cardiac troponins. However, ventricular ectopy and an inversion of T waves in inferior and precordial leads were absent. Taken together, the presence of desminopathy should be considered also in unexplained cases of LVNC and non-ischemic left ventricular systolic dysfunction with an extensive subepicardial or intramural fibrosis.

4.3. Mitochondrial Dysfunction in Desminopathy

Desminopathy may also imitate a mitochondrial disease, as was shown by Mc Cormic et al. [16]. The presence of SDH positive/COX negative muscle fibers, decreased activities of mitochondrial respiratory chain enzymes, and reduced mitochondrial DNA content in skeletal muscle biopsy lead to the suspicion of mitochondrial disease. We observed similar findings in our patient (P6) with an absence of desmin aggregates and signs of mitochondrial dysfunction in deltoid muscle biopsy. The correct diagnosis in our case provided genetic testing and immunostaining of myocardial samples.

Studies in desmin null mice and patients with recessive desmin-null muscular dystrophy revealed abnormalities in nuclear and mitochondrial localization and morphology, as well as impaired mitochondrial respiratory capacity [13,14]. Secondary mitochondrial dysfunction was also confirmed by Schröder et al. [38] and Vincent et al. [39] in skeletal muscle biopsies of heterozygous patients with desminopathy. Furthermore, Vincent et al. [39] reported a deficiency of respiratory chain complex I and IV compared to age matched controls and a low mitochondrial mass compared to controls. Our morphological and functional data from skeletal muscle samples are in agreement with the above mentioned studies and further evidence [40,41]. We observed a variable mitochondrial dysfunction characterized by a decreased expression of mitochondrial respiratory chain components and other mitochondrial proteins, as well as decreased enzyme activities, suggesting secondary changes in mitochondrial energetic function. The upregulation of several anti-oxidative enzymes, in particular that of superoxide dismutase 1 in homogenates, but not in isolated mitochondria, indicated increased antioxidative defense outside mitochondria.

Novel findings provided our analysis of myocardial energetic function in the explanted failing hearts of two probands with desminopathy. In one case harboring p.(R454W) desmin tail mutation we found a mild decrease in the content and activities of respiratory chain complexes while in the other case with p.(S57L) mutation in the desmin head region was present a very pronounced decrease in mitochondria proteins and an alteration of the bioenergetics function. Interestingly, changes in respiratory chain enzymes thus also caused a downregulation of respiratory supercomplexes that are expected to modulate the catalytic function as well as reactive oxygen species production by the respiratory chain [42]. This was associated with a decrease in several marker proteins of different mitochondrial compartments suggesting a complex mitochondrial dysfunction. The most pronounced was the impairment of myocardial succinate respiration, which was in our patients with desminopathy more profound than in end-stage heart failure of other etiologies.

4.4. Study Limitations

There are several limitations to our study. First, the small study group size reflects the rare occurrence of desminopathy and may limit the general applicability of the study results. Secondly, the small size of affected families limited the segregation studies. However, WES enabled us to exclude the presence of other pathogenic variants in cardiomyopathy- and skeletal myopathy-related genes, including genes coding mitochondrial proteins. Thirdly, an assessment of the mitochondrial function in tissues was possible only in a subgroup of patients with a clinical indication to biopsy or undergoing cardiac surgery. Finally, decreased desmin expression in P4 with a missense variant of *DES* might be

related to replacement fibrosis of the myocardium or epigenetic factors. Unfortunately, we cannot provide data supporting any of these hypotheses.

5. Conclusions

Desminopathy is a rare cause of cardiomyopathy and/or skeletal muscle myopathy with a pleomorphic clinical presentation and poor prognosis. This diagnosis should also be considered in individuals with LVNC. Differential diagnosis also includes mitochondrial and inflammatory myocardial diseases.

Supplementary Materials: The following are available online at <http://www.mdpi.com/2077-0383/9/4/937/s1>, Table S1 Primers for PCR Amplification of DES for segregation analysis in families, Table S2 Main clinical characteristics of probands, Table S3 Additional clinical, electrocardiographic, laboratory and echocardiographic data of probands, Table S4 Rare variants of non-desmin genes in probands, frequency in Exac database less than 0.00001.

Author Contributions: Conceptualization, M.K., T.S., L.P., A.K., V.M., and S.K.; Methodology, M.K., T.S., L.P., V.M., H.M., and S.K.; Validation, M.K. and S.K.; Formal Analysis, M.K., T.S., L.P., and S.K.; Investigation, clinical assessment M.K., A.K., T.P., and P.R.; Molecular-genetic analysis T.S., L.P., M.M., and V.S.; iPSC differentiation, cloning, transfection, confocal microscopy A.B.; Quantitative analysis of aggregate formation S.R.; site directed mutagenesis C.S.; analysis of mitochondrial function H.H., J.Z., J.H., Z.D., H.N., and J.M. (Jana Mikešová); histopathology and electron microscopy J.Z. and J.M. (Malusková); Resources, H.M., S.K.; Data Curation, M.K., T.S., and L.P.; Writing—Original Draft Preparation, M.K., T.S., L.P., and J.H.; Writing—Review & Editing, M.K., A.B., J.H., M.M., and S.K.; Visualization, T.S., L.P., and A.B.; Supervision, M.K., J.H., V.M., H.M., and S.K.; Project Administration, M.K. and T.S.; Funding Acquisition, H.M., M.K., and S.K. All authors have read and agreed to the published version of the manuscript.

Acknowledgments: M.K., T.S., and L.P. contributed equally to the manuscript. This study was supported by the research grant of the Ministry of Health, Czech Republic [MZ AZV 15-27682A], [NV19-08-00122], [MZ AZV 17-28784A], Ministry of Health, Czech Republic - conceptual development of research organization („Institute for Clinical and Experimental Medicine – IKEM, IN 00023001“) and by institutional support from the Ministry of Health (RVO-VFN64165) and Czech Academy of Sciences (RVO:67985823). We thank the National Center for Medical Genomics (LM2015091) for exome sequencing and providing ethnically matched population frequency data (project CZ.02.1.01/0.0/0.0/16_013/0001634). A.B. and H.M. are thankful for financial support by Deutsche Stiftung für Herzforschung (DSHF, F07/17) and by Deutsche Forschungsgesellschaft (DFG, MI-1146/2–2).

Conflicts of Interest: The authors have no conflicts of interest.

Abbreviations and Acronyms

ACM	arrhythmogenic cardiomyopathy
CAT	catalase
COX	cytochrome c oxidase
DCM	dilated cardiomyopathy
DES	desmin gene
GADPH	glyceraldehyde 3-phosphate dehydrogenase
GR	glutathione reductase
HCM	hypertrophic cardiomyopathy
LVNC	left ventricular non-compaction cardiomyopathy
NADH	reduced form of nicotinamide adenine dinucleotide
MPS	massively parallel sequencing
RCM	restrictive cardiomyopathy
SDH	succinate dehydrogenase
SOD	superoxide dismutase
WES	whole exome sequencing

References

1. van Spaendonck-Zwarts, K.Y.; van Hessem, L.; Jongbloed, J.D.; de Walle, H.E.; Capetanaki, Y.; van der Kooi, A.J.; van Langen, I.M.; van den Berg, M.P.; van Tintelen, J.P. Desmin-related myopathy. *Clin. Genet.* **2011**, *80*, 354–366. [[CrossRef](#)]

2. Li, D.; Tapscoft, T.; Gonzalez, O.; Burch, P.E.; Quiñones, M.A.; Zoghbi, W.A.; Hill, R.; Bachinski, L.L.; Mann, D.L.; Roberts, R. Desmin mutation responsible for idiopathic dilated cardiomyopathy. *Circulation* **1999**, *100*, 461–464. [[CrossRef](#)]
3. Taylor, M.R.; Slavov, D.; Ku, L.; Di Lenarda, A.; Sinagra, G.; Carniel, E.; Haubold, K.; Boucek, M.M.; Ferguson, D.; Graw, S.L.; et al. Prevalence of desmin mutations in dilated cardiomyopathy. *Circulation* **2007**, *115*, 1244–1251. [[CrossRef](#)]
4. Goldfarb, L.G.; Park, K.Y.; Cervenakova, L.; Gorokhova, S.; Lee, H.S.; Vasconcelos, O.; Nagle, J.W.; Semino-Mora, C.; Sivakumar, K.; Dalakas, M.C. Missense mutations in desmin associated with familial cardiac and skeletal myopathy. *Nat. Genet.* **1998**, *19*, 402–403. [[CrossRef](#)]
5. Arbustini, E.; Morbini, P.; Grasso, M.; Fasani, R.; Verga, L.; Bellini, O.; Dal Bello, B.; Campana, C.; Piccolo, G.; Febo, O.; et al. Restrictive cardiomyopathy, atrioventricular block and mild to subclinical myopathy in patients with desmin-immunoreactive material deposits. *J. Am. Coll. Cardiol.* **1998**, *31*, 645–653. [[CrossRef](#)]
6. Park, K.Y.; Dalakas, M.C.; Semino-Mora, C.; Lee, H.S.; Litvak, S.; Takeda, K.; Ferrans, V.J.; Goldfarb, L.G. Desmin myopathy, a skeletal myopathy with cardiomyopathy caused by mutations in the desmin gene. *N. Engl. J. Med.* **2000**, *342*, 770–780. [[CrossRef](#)]
7. Pruszczyk, P.; Kostera-Pruszczyk, A.; Shatunov, A.; Goudeau, B.; Dрамиńska, A.; Takeda, K.; Sambuughin, N.; Vicart, P.; Strelkov, S.V.; Goldfarb, L.G.; et al. Restrictive cardiomyopathy with atrioventricular conduction block resulting from a desmin mutation. *Int. J. Cardiol.* **2007**, *117*, 244–253. [[CrossRef](#)] [[PubMed](#)]
8. Olive, M.; Armstrong, J.; Miralles, F.; Pou, A.; Fardeau, M.; Gonzalez, L.; Martínez, F.; Fischer, D.; Martínez Matos, J.A.; Shatunov, A.; et al. Phenotypic patterns of desminopathy associated with three novel mutations in the desmin gene. *Neuromuscul. Disord.* **2007**, *17*, 443–450. [[CrossRef](#)] [[PubMed](#)]
9. Otten, E.; Asimaki, A.; Maass, A.; van Langen, I.M.; van der Wal, A.; de Jonge, N.; van den Berg, M.P.; Saffitz, J.E.; Wilde, A.A.; Jongbloed, J.D.; et al. Desmin mutations as a cause of right ventricular heart failure affect the intercalated disks. *Heart Rhythm* **2010**, *7*, 1058–1064. [[CrossRef](#)] [[PubMed](#)]
10. Klauke, B.; Kossmann, S.; Gaertner, A.; Brand, K.; Stork, I.; Brodehl, A.; Dieding, M.; Walhorn, V.; Anselmetti, D.; Gerdes, D.; et al. De novo desmin mutation N116S is associated with arrhythmogenic right ventricular cardiomyopathy. *Hum. Mol. Genet.* **2010**, *19*, 4595–4607. [[CrossRef](#)]
11. Lorenzon, A.; Beffagna, G.; Bauce, B.; De Bortoli, M.; Li Mura, I.E.A.; Calore, M.; Dazzo, E.; Basso, C.; Nava, A.; Thiene, G.; et al. Desmin mutations and arrhythmogenic right ventricular cardiomyopathy. *Am. J. Cardiol.* **2013**, *111*, 400–405. [[CrossRef](#)] [[PubMed](#)]
12. Capetanaki, Y.; Bloch, R.J.; Kouloumenta, A.; Mavroidis, M.; Psarras, S. Muscle intermediate filaments and their links to membranes and membranous organelles. *Exp. Cell. Res.* **2007**, *313*, 2063–2076. [[CrossRef](#)] [[PubMed](#)]
13. Milner, D.J.; Mavroidis, M.; Weisleder, N.; Capetanaki, Y. Desmin cytoskeleton linked to muscle mitochondrial distribution and respiratory function. *J. Cell. Biol.* **2000**, *150*, 1283–1298. [[CrossRef](#)] [[PubMed](#)]
14. Henderson, M.; Waele, L.D.; Hudson, J.; Eagle, M.; Sewry, C.; Marsh, J.; Charlton, R.; He, L.; Blakely, E.L.; Horrocks, I.; et al. Recessive desmin-null muscular dystrophy with central nuclei and mitochondrial abnormalities. *Acta Neuropathol. (Berl.)* **2013**, *125*, 917–919. [[CrossRef](#)] [[PubMed](#)]
15. Winter, L.; Wittig, I.; Peeva, V.; Eggers, B.; Heidler, J.; Chevessier, F.; Kley, R.A.; Barkovits, K.; Strecker, V.; Berwanger, C.; et al. Mutant desmin substantially perturbs mitochondrial morphology, function and maintenance in skeletal muscle tissue. *Acta Neuropathol.* **2016**, *132*, 453–473. [[CrossRef](#)]
16. McCormick, E.M.; Kenyon, L.; Falk, M.J. Desmin common mutation is associated with multi-systemic disease manifestations and depletion of mitochondria and mitochondrial DNA. *Front. Genet.* **2015**, *6*, 199. [[CrossRef](#)]
17. Hartmannova, H.; Kubanek, M.; Sramko, M.; Piherova, L.; Noskova, L.; Hodanova, K.; Stranecky, V.; Pristoupilova, A.; Sovova, J.; Marek, T.; et al. Isolated X-linked hypertrophic cardiomyopathy caused by a novel mutation of the Four-and-a-half LIM domain 1 gene. *Circ. Cardiovasc. Genet.* **2013**, *6*, 543–551. [[CrossRef](#)]
18. Kalia, S.S.; Adelman, K.; Bale, S.J.; Chung, W.K.; Eng, C.; Evans, J.P.; Herman, G.E.; Hufnagel, S.B.; Klein, T.E.; Korf, B.R.; et al. Recommendations for reporting of secondary findings in clinical exome and genome sequencing, 2016 update (ACMG SF v2.0): A policy statement of the American College of Medical Genetics and Genomics. *Genet. Med.* **2017**, *19*, 249–255. [[CrossRef](#)]

19. Brodehl, A.; Dieding, M.; Biere, N.; Unger, A.; Klauke, B.; Walhorn, V.; Gummert, J.; Schulz, U.; Linke, W.A.; Gerull, B.; et al. Functional characterization of the novel DES mutation p.L136P associated with dilated cardiomyopathy reveals a dominant filament assembly defect. *J. Mol. Cell. Cardiol.* **2016**, *91*, 207–214. [[CrossRef](#)]
20. Brodehl, A.; Pour Hakimi, S.A.; Stanasiuk, C.; Ratnavadivel, S.; Hendig, D.; Gaertner, A.; Gerull, B.; Gummert, J.; Paluszkiwicz, L.; Milting, H. Restrictive Cardiomyopathy is Caused by a Novel Homozygous Desmin (DES) Mutation p.Y122H Leading to a Severe Filament Assembly Defect. *Genes (Basel)* **2019**, *11*, 918. [[CrossRef](#)]
21. Debus, J.D.; Milting, H.; Brodehl, A.; Kassner, A.; Anselmetti, D.; Gummert, J.; Gaertner-Rommel, A. In vitro analysis of arrhythmic cardiomyopathy associated desmoglein-2 (DSG2) mutations reveals diverse glycosylation patterns. *J. Mol. Cell. Cardiol.* **2019**, *129*, 303–313. [[CrossRef](#)] [[PubMed](#)]
22. Brodehl, A.; Gaertner-Rommel, A.; Klauke, B.; Grewe, S.A.; Schirmer, I.; Peterschröder, A.; Faber, L.; Vorgerd, M.; Gummert, J.; Anselmetti, D.; et al. The novel α B-crystallin (CRYAB) mutation p.D109G causes restrictive cardiomyopathy. *Hum. Mutat.* **2017**, *38*, 947–952. [[CrossRef](#)] [[PubMed](#)]
23. Sheehan, D.C.; Hrapchak, B.B. *Theory and Practice of Histotechnology*, 2nd ed.; Mosby: Columbus, OH, USA, 1987.
24. Makinen, M.W.; Lee, C.P. Biochemical studies of skeletal muscle mitochondria. I. Microanalysis of cytochrome content, oxidative and phosphorylative activities of mammalian skeletal muscle mitochondria. *Arch. Biochem. Biophys.* **1968**, *126*, 75–82. [[CrossRef](#)]
25. Melenovsky, M.; Petrak, J.; Mracek, T.; Benes, J.; Borlaug, B.A.; Nuskova, H.; Pluhacek, T.; Spatenka, J.; Kovalcikova, J.; Drahota, Z.; et al. Myocardial Iron Content and Mitochondrial Function in Heart Failure: Direct Tissue Analysis. *Eur. J. Heart Fail.* **2017**, *19*, 522–530. [[CrossRef](#)]
26. Brodehl, A.; Gaertner-Rommel, A.; Milting, H. Molecular insights into cardiomyopathies associated with desmin (DES) mutations. *Biophys. Rev.* **2018**, *10*, 983–1006. [[CrossRef](#)]
27. Diokmetzidou, A.; Soumaka, E.; Kloukina, I.; Tsikitis, M.; Makridakis, M.; Varela, A.; Davos, C.H.; Georgopoulos, S.; Anesti, A.; Vlachou, A.; et al. Desmin and α B-Crystallin Interplay in Maintenance of Mitochondrial Homeostasis and Cardiomyocyte Survival. *J. Cell Sci.* **2016**, *129*, 3705–3720. [[CrossRef](#)]
28. Bär, H.; Goudeau, B.; Wälde, S.; Casteras-Simon, M.; Mücke, N.; Shatunov, A.; Goldberg, Y.P.; Clarke, C.; Holton, J.L.; Eymard, B.; et al. Conspicuous involvement of desmin tail mutations in diverse cardiac and skeletal myopathies. *Hum. Mutat.* **2007**, *28*, 374–386. [[CrossRef](#)]
29. Capetanaki, Y.; Papatheanasiou, S.; Diokmetzidou, A.; Vatsellas, G.; Tsikitis, M. Desmin related disease: A matter of cell survival failure. *Curr. Opin. Cell Biol.* **2015**, *32*, 113–120. [[CrossRef](#)]
30. Kostera-Pruszczyk, A.; Pruszczyk, P.; Kamińska, A.; Lee, H.S.; Goldfarb, L.G. Diversity of cardiomyopathy phenotypes caused by mutations in desmin. *Int. J. Cardiol.* **2008**, *131*, 146–147. [[CrossRef](#)]
31. Clemen, C.S.; Herrmann, H.; Strelkov, S.V.; Schröder, R. Desminopathies: Pathology and mechanisms. *Acta Neuropathol.* **2013**, *125*, 47–75. [[CrossRef](#)]
32. Bermúdez-Jiménez, F.J.; Carriel, V.; Brodehl, A.; Alaminos, M.; Campos, A.; Schirmer, I.; Milting, H.; Abril, B.Á.; Álvarez, M.; López-Fernández, S.; et al. The Novel Desmin Mutation p.Glu401Asp Impairs Filament Formation, Disrupts Cell Membrane Integrity and Causes Severe Arrhythmic Left Ventricular Cardiomyopathy/Dysplasia. *Circulation* **2018**, *137*, 1595–1610. [[CrossRef](#)] [[PubMed](#)]
33. Cetin, N.; Balci-Hayta, B.; Gundesli, H.; Korkusuz, P.; Purali, N.; Talim, B.; Tan, E.; Selcen, D.; Erdem-Ozdamar, S.; Dincer, P. A novel desmin mutation leading to autosomal recessive limb-girdle muscular dystrophy: Distinct histopathological outcomes compared with desminopathies. *J. Med. Genet.* **2013**, *50*, 437–443. [[CrossRef](#)] [[PubMed](#)]
34. Arbustini, E.; Favalli, V.; Narula, N.; Serio, A.; Grasso, M. Left Ventricular Noncompaction: A Distinct Genetic Cardiomyopathy? *J. Am. Coll. Cardiol.* **2016**, *68*, 949–966. [[CrossRef](#)] [[PubMed](#)]
35. van Wanang, J.I.; Caliskan, K.; Hoedemaekers, Y.M.; van Spaendonck-Zwarts, K.Y.; Baas, A.F.; Boekholdt, S.M.; van Melle, J.P.; Teske, A.J.; Asselbergs, F.W.; Backx, A.P.C.M.; et al. Genetics, Clinical Features, and Long-Term Outcome of Noncompaction Cardiomyopathy. *J. Am. Coll. Cardiol.* **2018**, *71*, 711–722. [[CrossRef](#)]
36. Marakhonov, A.V.; Brodehl, A.; Myasnikov, R.P.; Sparber, P.A.; Kiseleva, A.V.; Kulikova, O.V.; Meshkov, A.N.; Zharikova, A.A.; Koretsky, S.N.; Kharlap, M.S.; et al. Noncompaction cardiomyopathy is caused by a novel in-frame desmin (DES) deletion mutation within the 1A coiled-coil rod segment leading to a severe filament assembly defect. *Hum. Mutat.* **2019**, *40*, 734–741. [[CrossRef](#)]

37. Miszalski-Jamka, K.; Jefferies, J.L.; Mazur, W.; Głowacki, J.; Hu, J.; Lazar, M.; Gibbs, R.A.; Liczko, J.; Kłyś, J.; Venner, E.; et al. Novel Genetic Triggers and Genotype-Phenotype Correlations in Patients with Left Ventricular. *Noncompact. Circ. Cardiovasc. Genet.* **2017**, *10*, e001763. [[CrossRef](#)]
38. Schröder, R.; Goudeau, B.; Simon, M.C.; Fischer, D.; Eggermann, T.; Clemen, C.S.; Li, Z.; Reimann, J.; Xue, Z.; Rudnik-Schöneborn, S.; et al. On noxious desmin: Functional effects of a novel heterozygous desmin insertion mutation on the extrasarcomeric desmin cytoskeleton and mitochondria. *Hum. Mol. Genet.* **2003**, *12*, 657–669. [[CrossRef](#)]
39. Vincent, A.E.; Grady, J.P.; Rocha, M.C.; Alston, C.L.; Rygiel, K.A.; Barresi, R.; Taylor, R.W.; Turnbull, D.M. Mitochondrial dysfunction in myofibrillar myopathy. *Neuromuscul. Disord.* **2016**, *26*, 691–701. [[CrossRef](#)]
40. Galata, Z.; Kloukina, I.; Kostavasil, I.; Varela, A.; Davos, C.H.; Makridakis, M.; Bonne, G.; Capetanaki, Y. Amelioration of desmin network defects by α B-crystallin overexpression confers cardioprotection in a mouse model of dilated cardiomyopathy caused by LMNA gene mutation. *J. Mol. Cell. Cardiol.* **2018**, *125*, 73–86. [[CrossRef](#)]
41. Tsikitis, M.; Galata, Z.; Mavroidis, M.; Psarras, S.; Capetanaki, Y. Intermediate filaments in cardiomyopathy. *Bioph. Rev.* **2018**, *10*, 1007–1031. [[CrossRef](#)]
42. Milenkovic, D.; Blaza, J.N.; Larsson, N.G.; Hirst, J. The Enigma of the Respiratory Chain Supercomplex. *Cell Metab.* **2017**, *25*, 765–776. [[CrossRef](#)] [[PubMed](#)]



© 2020 by the authors. Licensee MDPI, Basel, Switzerland. This article is an open access article distributed under the terms and conditions of the Creative Commons Attribution (CC BY) license (<http://creativecommons.org/licenses/by/4.0/>).



Article

Epigenetic Regulation of Alternative mRNA Splicing in Dilated Cardiomyopathy

Weng-Tein Gi^{1,2,3}, Jan Haas^{1,2,3}, Farbod Sedaghat-Hamedani^{1,2,3}, Elham Kayvanpour^{1,2,3},
Rewati Tappu^{1,2,3}, David Hermann Lehmann^{1,3}, Omid Shirvani Samani^{1,2,3},
Michael Wisdom^{1,2,3}, Andreas Keller⁴, Hugo A. Katus^{1,2,3} and Benjamin Meder^{1,2,3,5,*}

- ¹ Institute for Cardiomyopathies Heidelberg (ICH), Heart Center Heidelberg, University of Heidelberg, 69121 Heidelberg, Germany; Weng-Tein.Gi@med.uni-heidelberg.de (W.-T.G.); jan.haas@med.uni-heidelberg.de (J.H.); Farbod.Sedaghat-Hamedani@med.uni-heidelberg.de (F.S.-H.); Elham.Kayvanpour@med.uni-heidelberg.de (E.K.); Rewati.Tappu@med.uni-heidelberg.de (R.T.); DavidHermann.Lehmann@med.uni-heidelberg.de (D.H.L.); Omid.ShirvaniSamani@med.uni-heidelberg.de (O.S.S.); Michael.Wisdom@med.uni-heidelberg.de (M.W.); hugo.katus@med.uni-heidelberg.de (H.A.K.)
- ² DZHK (German Center for Cardiovascular Research), 69121 Heidelberg, Germany
- ³ Department of Medicine III, University of Heidelberg, INF 410, 69120 Heidelberg, Germany
- ⁴ Department of Clinical Bioinformatics, Medical Faculty, Saarland University, 66123 Saarbrücken, Germany; Andreas.Keller@ccb.uni-saarland.de
- ⁵ Department of Genetics, Stanford University School of Medicine, Stanford, CA 94305, USA
- * Correspondence: Benjamin.Meder@med.uni-heidelberg.de

Received: 10 March 2020; Accepted: 12 May 2020; Published: 16 May 2020

Abstract: In recent years, the genetic architecture of dilated cardiomyopathy (DCM) has been more thoroughly elucidated. However, there is still insufficient knowledge on the modifiers and regulatory principles that lead to the failure of myocardial function. The current study investigates the association of epigenome-wide DNA methylation and alternative splicing, both of which are important regulatory principles in DCM. We analyzed screening and replication cohorts of cases and controls and identified distinct transcriptomic patterns in the myocardium that differ significantly, and we identified a strong association of intronic DNA methylation and flanking exons usage ($p < 2 \times 10^{-16}$). By combining differential exon usage (DEU) and differential methylation regions (DMR), we found a significant change of regulation in important sarcomeric and other DCM-associated pathways. Interestingly, inverse regulation of Titin antisense non-coding RNA transcript splicing and DNA methylation of a locus reciprocal to *TTN* substantiate these findings and indicate an additional role for non-protein-coding transcripts. In summary, this study highlights for the first time the close interrelationship between genetic imprinting by DNA methylation and the transport of this epigenetic information towards the dynamic mRNA splicing landscape. This expands our knowledge of the genome–environment interaction in DCM besides simple gene expression regulation.

Keywords: dilated cardiomyopathy; DNA methylation; alternative splicing; epigenetics

1. Introduction

Dilated cardiomyopathy (DCM) is the predominant heart muscle disease, characterized by a dilated left ventricle (LV) and reduced contractility. It is associated with high hospitalization rates, sudden cardiac death risk, and substantial demand for heart failure therapies. The prevalence of all forms of DCM is estimated to be as high as 1:250 [1]. In the patients with DCM, approximately 30%–50% are assumed to have familial predisposition of the disease [2], and 40% of the familial DCM patients possess currently identifiable genetic variations [3], with most of them having an autosomal-dominant

transmission pattern [4]. On the other side, some sporadic DCM patients have de novo genetic mutations. As the technology of next generation sequencing grows expeditiously, causative genetic variants of DCM have been detected in over 30 genes, with a great number of them encoding sarcomere proteins, such as *TTN*, *MYH6*, *MYH7*, and *TNNT2*, and others encoding proteins constituting calcium or potassium channels, such as *SCN5A*, proteins essential in the nuclear membrane, such as *LMNA*, as well as others such as *BAG3* or *TAZ* (G 4.5) [1,5]. Truncating variants in *TTN* (TTNtv) account for 15%–25% of familial DCM and 10%–18% of sporadic DCM [6]. Otherwise, most DCM-related genetic variants are reported to be nonsynonymous missense, while other types of mutations, such as frameshifts, insertions, deletions, and splice-site-mutations, were also detected [1].

Recently, a drastically increased number of disease-causing variants have been pinpointed with the help of genome-wide association studies. In the era of precision medicine, an in-depth understanding of the disease-causing mechanism of these detected variants has proved to be challenging, but it is the key to the development of novel personalized therapies [7]. Aside from traditional single-point gene variants, new evidence suggests a possible role of genetic–environmental interactions in human cardiomyopathies, for example, through alterations of DNA methylation [8,9] and through changes of histone modifications [10]. In a recent study by us on human DCM, the DNA methylation level within the promoter region was found to correlate negatively with gene expression. It was observed that the pattern of DNA methylation in promoter regions is significantly changed when comparing DCM patients with healthy controls. Numerous hot spots with statistically significant phenotype–epigenotype correlations were identified in the genome of DCM patients [8].

On the other side, post-transcriptional modifications of sarcomeric proteins were also reported to play a critical role in the pathogenesis of DCM. Aberrantly spliced sarcomere proteins, including titin, troponin T, tropomyosin, and LDB3 protein, were detected in patients with DCM, generating abnormal protein products predisposing people to heart failure. *TTN*, encoding titin, is the most commonly mutated gene in DCM. An RNA-binding splicing factor *RBM20* can bind directly to the intronic parts of titin and affect its splicing. Genetic variations in *RBM20* in 3%–5% of genetic DCM cases cause the expression of a dysregulated isoform of titin, N2BA-G, generating reduced passive tension of the muscle fiber in DCM [11–13].

We sought here to identify a role of DNA methylation changes in the somatic tissue of DCM patients and the impact of such alterations on mRNA splicing. By using an epigenome-wide and whole transcriptome approach, we found a strong association of intragenic DNA methylation and exon usage. Particularly interesting are changes of the Titin locus, where we found reciprocal alterations in an encoded Titin-antisense non-coding RNA in DCM compared to control.

2. Materials and Methods

2.1. Patient Enrollment and Phenotyping

In the present study, we used data generated in the Care4DCM multi-omics project [8,14]. The diagnosis of DCM was established by impaired heart systolic function, after ruling out coronary artery disease through coronary angiography. Notably, aside from DCM patients with advanced heart failure, patients in early stages of the disease, i.e., left ventricular ejection function > 45% and < 55%, were also included in the present study. Patients with concomitant valvular heart disease, myocarditis, and inflammatory DCM were excluded from the study after being screened with echocardiography and cardiac magnetic resonance imaging (CMR), and after the myocardial biopsy of the patients were examined histopathologically. Other exclusion criteria included previous cardiotoxic chemotherapy, alcoholism, illicit substance abuse, and untreated arterial hypertension. For control subjects, after written informed consent, we collected 31 specimens of left ventricle biopsy from asymptomatic patients after heart transplantation at least 6 months ago. All patient recruitment was authorized by the ethics committee. An independent replication cohort comprised 18 explanted DCM hearts and 8 healthy hearts from traffic accident victims. The following library preparation and analytic

procedures were identical in both the screening and replication cohorts. Further information regarding patient enrollment and phenotyping can be found in our previously published study [8].

2.2. Library Preparation and Next Generation Sequencing

In the Care4DCM cohort, the biopsies were retrieved from the LV apex during heart catheterization [8]. The specimen of each patient was immediately washed and preserved in liquid nitrogen according to standardized protocols. After the histopathological work-up, DNA and RNA were extracted from the leftover cardiac tissues using Allprep Kits (Qiagen, Düsseldorf, Germany). In the replication cohort, the DCM hearts were immediately transported and stored after explantation, and the hearts of healthy traffic accident victims were flash-frozen less than three hours after death. Before starting sequencing, a Bioanalyzer 2100 (Agilent Technologies, Santa Clara, CA, USA) and a eukaryote total RNA pico assay (Agilent Technologies, Santa Clara, CA, USA) were utilized to examine the purity and concentration of RNA. The sequencing of DNA methylation profiling was carried out using the Infinium HumanMethylation 450K BeadChip kit (Illumina, San Diego, CA, USA). The RNA sequencing was performed with the TrueSeq RNA Sample Prep Kit (Illumina, San Diego, CA, USA) to paired-end reads, unstrandedly in the screening cohort and strandedly in the replication cohort.

2.3. Quality Control of Sequencing Data

All obtained RNA sequences and DNA methylation profiling went through diverse quality checks. The number of reads with assigned feature was calculated with *samtools* in the Unix environment [15]. Samples with less than 1,000,000 assigned reads were not included in the further downstream analysis. Finally, 55 samples from the screening cohort passed the RNA quality control, of them, 34 were DCM patients and 21 were controls; 16 samples from the replication cohort passed the RNA quality filter, of them, 11 were DCM patients and 5 were healthy controls. The overall sequencing depth of the samples in the final cohorts is visualized in the histograms (Figure S5A,B). In addition, the probed methylation sites in that Infinium HumanMethylation 450 K BeadChip kit, known to be possibly influenced by genetic variants, were removed from the following downstream analysis, because the influence of genetic variation on methylation profiling was not in the lens of the present study. In addition, probed methylation sites on X and Y chromosomes and those known to cross-hybridize with non-targeted DNA were dropped. Subsequently, 394,247 qualified probed loci with methylation measurements were included in further analysis.

2.4. Data Normalization and Batch Effect Correction

Principal component analysis (PCA) was done using package *factoextra* in R programming [16]. When analyzing the data characteristics of RNA sequences from both cohorts together, a batch effect could be delineated in the principal component analysis derived from the normalized count matrix. In the PCA plot, samples from both cohorts clustered independently from each other, because the first principal component, responsible for up to 40% of the data variances (Figure S2A), significantly represented the distance between the two cohorts, as could be visualized in the PCA plot (Figure S2B). However, since the relative distribution of the DCM samples and controls samples were consistent in both screening and replication cohorts, and no statistical test of samples across different cohorts were planned to be made, we did not use a cross-cohort batch correction. When performing the statistical tests for differential exon use (DEU) between DCM patients and controls, a normalization of the read count for each gene and each exonic part defined by hg19/GrCh37 was performed. Likewise, all methylation measurements were normalized. The batch effects from different sequencing dates and flow cells were removed.

2.5. Bioinformatic Computation and Analysis

The RNA sequences were mapped to hg19/GrCh37 using *HISAT2* in the Unix environment [17], and the annotated bam files were generated. The genome-wide statistical tests for differential gene

expression (DGE) between DCM patients and controls were performed using the *DESeq2* package in R programming [18]. The genome-wide statistical tests for differential exon use (DEU) between DCM patients and controls were performed using the *DEXSeq* package in R programming [19]. Features (exonic bins) with a total read count of all samples less than six were filtered out, in order to reduce false positives. The PSI score for each annotated exonic region defined by reference genome GRCh37/hg19 was computed [20]. Moreover, the methylation measurement of each probed site was also mapped to the reference genome hg19/GrCh37 through the *GenomicRanges* package in R programming [21]. Statistical tests of differential methylated regions of the 394,247 qualified probed methylation sites across the whole genome were performed with the *limma* package in R programming [22]. The M-values of DNA methylation were used. With *limma*, linear models of methylation values were defined with the following parameters: condition (DCM or control), sex, age, use of tacrolimus, use of mycophenolate, use of steroid, use of everolimus, use of ciclosporin, principal component 1, and principal component 2. Parameters sex and age were defined as categorical variables; parameters tacrolimus, mycophenolat, steroid, everolimus, and ciclosporin were binary variables, meaning intake of the specific immunosuppressive drug. Parameters principal component 1 and principal component 2 were continuous variables, which were the top two principal components of the methylation data, representing the potential substratefications of the DNA methylation data. A moderated t-statistic was applied for each probe, *p* values and adjusted *p* values in the setting of multiple testing were calculated using the Benjamini–Hochberg method. The results were mapped to the reference genome GRCh37/hg19 using the *GenomicRanges* package in R programming.

2.6. Genome-Wide Analysis of Neighboring Intron and Exon

The inclusion of a specific exon and the methylation status of its flanking intron were analyzed across the whole genome in order to investigate the potential local effects of intronic DNA methylation on the inclusion of alternative exons. We determined the bordering exon and intron pairs using the *GenomicRanges* package in R programming, and implemented a logistic regression analysis in quasi-Poisson distribution, with the independent variable as the intronic DNA methylation levels and the dependent variable as the exon usage. The logistic regression model was carried out in both DCM patients and controls, respectively, and both in intron-exon and exon-intron pairs, respectively. The regression model was adjusted by the distance between intron and exon in the pair. Additionally, we identified the regions with concomitant DEU and DMR (*p* value <0.05, respectively). The distinguished regions underwent gene ontology analysis using *GeneTrail2* (version 1.6) website [23,24].

2.7. Methylome-Transcriptome Correlation

To further investigate the methylome–transcriptome correlation in DCM, we accomplished an epigenome-wide association analysis, modified from a genome-wide association study (GWAS), between the DNA methylation measurement (beta value) and PSI score. The correlational analyses were done both in DCM patients and in control subjects. The advantage of this approach was that not only local but also remote regulation of intronic DNA methylation on the exon inclusion within the same gene could be thoroughly explored. The single locus analysis was used. Logistic regression was applied as it permits adjustment with additional parameters and provides odds ratios as effect sizes [25]. An odds ratio and a *p* value were calculated for each generated regression model. The first two principal components were integrated in the regression model as covariates in order to account for possible population stratification and to minimize the inflation. The robustness of this genome-wide association approach was evaluated and subsequently optimized following the criteria suggested commonly [26]. In addition to the above-mentioned procedure, we carried out genome-wide statistical tests of significance for the difference between correlation coefficients in DCM patients and in controls. The aim of this approach was to identify genomic regions with significantly divergent methylome–transcriptome relationship between DCM patients and controls. The statistical tests were performed using Fischer’s *z* test with the help of the *cocor* package in R programming [27].

The significance threshold was determined to be FDR < 0.05 by Benjamini–Hochberg in the screening cohort and a raw *p* value < 0.05 in the replication cohort.

3. Results

3.1. DCM-Related Reconnection of mRNA Expression

We first normalized the read counts of RNA-Seq of each gene in each sample. In the sample–sample distance plot of the screening cohort, clustering of the majority of DCM samples could be seen (Figure 1B), while only a few DCM samples were close to the cluster of control samples. This was an expected picture confirming the known heterogenous transcriptomic profile of DCM patients having disease states ranging from mild to severe. In the corresponding principal component analysis, a similar distribution pattern was detected (Figure 1C). In the sample–sample distance plot of the replication cohort, only one sample in each group were outliers (Figure S1A), and the same effect can be seen in the PCA plot (Figure S1B). Overall, the existence of outliers in the data might render further analysis more challenging; however, since our attempt was to pinpoint only the most robust associations, we set to work with all samples.

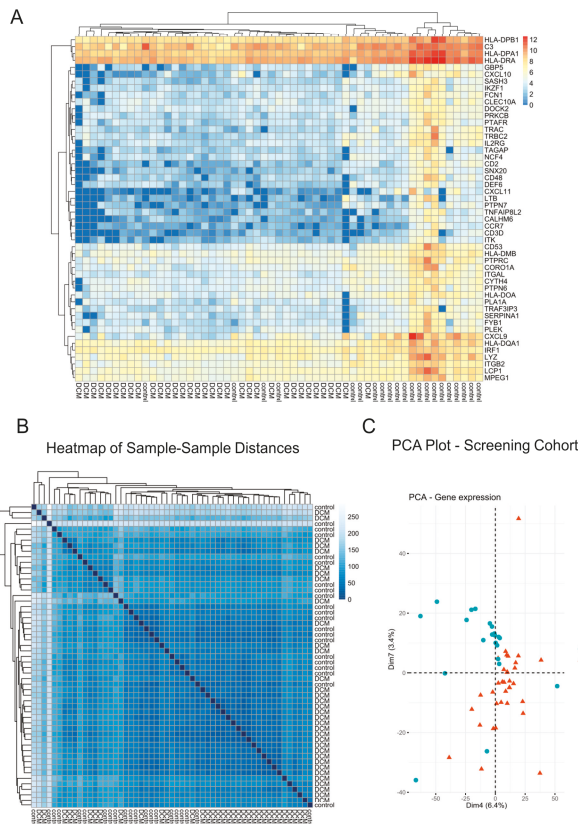


Figure 1. RNA sequences in the screening cohort. (A) Heatmap of the normalized gene counts of the fifty most significantly differentially expressed genes between dilated cardiomyopathy (DCM) and control samples, as an example to demonstrate a distinct pattern of gene expression in DCM and control subjects. (B) Heatmap of sample–sample-distances of the gene expression. (C) Principal component analysis (PCA) plot of the gene expression.

In the analysis for differential gene expression, 1330 genes were found to be significantly differentially expressed between DCM and control samples with a significance threshold of $FDR < 0.05$ (Supplemental File 1). Of these, 259 genes were upregulated and 1071 genes were downregulated (Supplemental File 2). These findings indicate that, on the transcriptomic level, orchestrated changes of gene expression govern the disease state (Figure 1A). The FPKM (fragments per kilobase per million) scatter presents the relative expression between the DCM and control (Figure 2B). The MA plot visualized the relationship between the mean of normalized count and the log fold change in the analyzed samples (Figure 2A). As examples of the upregulated genes in DCM, we demonstrated the gene browser tracks of genes *NPPA* and *NPPB* (Figure 2C). *NPPA* and *NPPB* genes encode natriuretic peptides, ANP and BNP, respectively, which are commonly used as biomarkers in diagnostics and monitoring of DCM since they are strongly associated with the disease.

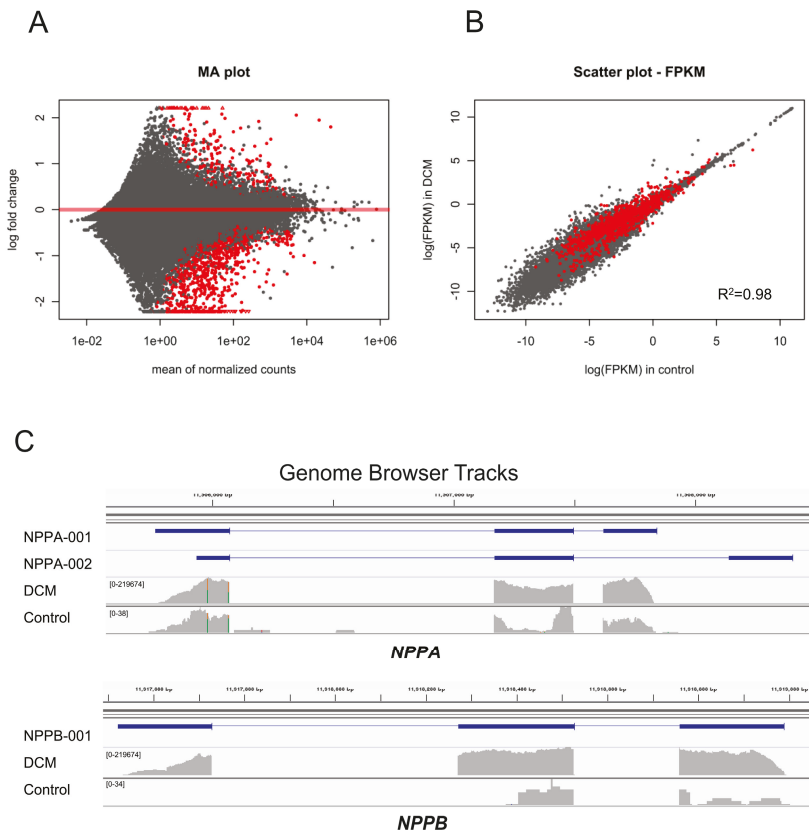


Figure 2. (A) MA plot for the analysis of differential gene expression. The significant candidates ($FDR < 0.05$) are marked in red. (B) FPKM scatter plot of the gene expression in DCM and control samples. The significantly differentially expressed genes ($FDR < 0.05$) are marked in red. FPKM: fragments per kilobase per million. (C) Gene browser tracks for *NPPA* and *NPPB* as examples for differential gene expression. The track(s) on top represent(s) common transcripts of the genes. RNA-Seq coverage of only one selected DCM sample and one selected control sample is shown below. It appears that both genes may have a different abundance of transcripts. However, when pooling all samples of the same condition together and using robust statistic testing, isoform differences could not be shown.

In the gene ontology analysis for cellular components (Supplemental File 3), the upregulated genes were found to be enriched for several neural system components, extracellular matrix components, ion channel complexes, as well as contractile fibers and sarcolemma (FDR < 0.05). The down-regulated genes were enriched for several immunological complexes, ribosomal subunits, and numerous cellular membranous components, including reticulum membrane (FDR < 0.05). These are typical findings of DCM pathogenesis. In summary, the data on whole-transcriptomes from patients and controls accentuates the distinct expression landscape of mRNA transcripts. This raised the question of whether the individual transcripts are also differentially composed, e.g., by alternative splicing.

3.2. Epigenome-Wide Linkage of DNA Methylation and Inclusion of Exon

In the data exploration of 394,247 qualified methylation probes in the screening cohort, two principal components could well separate the samples of DCM patients from samples of control subjects, and the two clusters had an overlapping area in the middle (Figure S3A). In the replication cohort, the clustering of DCM patients and control subjects was more delineated in the PCA plot (Figure S3B), as only one outlier of the DCM sample stood out in the top right quadrant.

Of all probed sites of the Infinium HumanMethylation 450 K BeadChip, 88,699 probes were found to locate in intronic regions, comprising approximately 20% of all probes. Further, we identified around 33% of all exons to have accessible methylation measurements in their neighboring introns (either upstream, downstream, or both-sides). Subsequently, these identified exonic regions and their flanking introns with available methylation measurements were analyzed as pairs together in order to inspect the possible regional effects of intronic methylation on the inclusion of alternative exons. The analyzable pairs included 41,158 intron-exon-pairs and 41,253 exon-intron pairs across the whole genome (Figure 3). The association between intronic DNA methylation and the calculated exon usage was modeled with logistic regression, which consequently showed a robust positive correlation between intronic DNA methylation and exon usage (up- and downstream, p value < 2×10^{-16} and p value < 2×10^{-16} , respectively), even after adjustment for intron-exon distance (Table 1).

Intron-exon and exon-intron pairs for epigenome-wide analysis

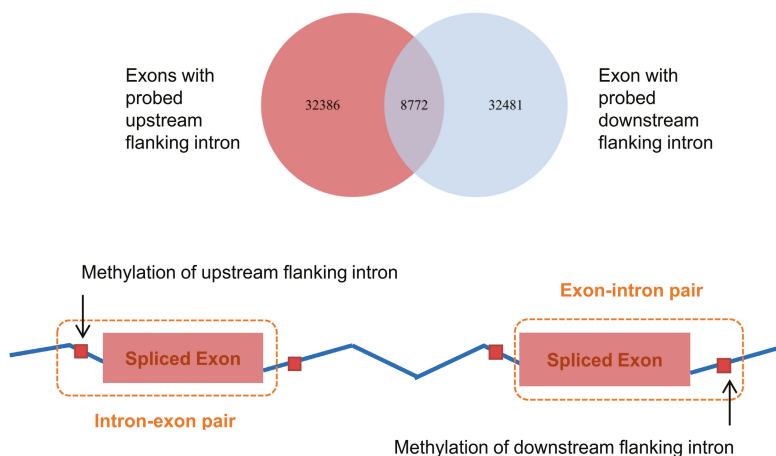


Figure 3. Scheme presenting the included intron-exon and exon-intron pairs in the epigenome-wide analysis between DNA methylation and inclusion of exon.

Table 1. Correlation between exon usage and DNA methylation in flanking intron *.

	Variables	Group	Coefficient	p Values
Without adjustment	Methylation level in upstream flanking intron ^{&}	DCM	0.310220	$<2 \times 10^{-16}$
		Control	0.319190	$<2 \times 10^{-16}$
	Methylation level in downstream flanking intron [§]	DCM	0.333570	$<2 \times 10^{-16}$
		Control	0.361230	$<2 \times 10^{-16}$
Adjusted by distance between exon and intron [#]	Methylation level in upstream flanking intron ^{&}	DCM	0.315900	$<2 \times 10^{-16}$
		Control	0.325100	$<2 \times 10^{-16}$
	Methylation level in downstream flanking intron [§]	DCM	0.336900	$<2 \times 10^{-16}$
		Control	0.365900	$<2 \times 10^{-16}$

* Generalized regression analysis using quasi-Poisson distribution. # Median distance between exon and intron = 1741 bp. [&]*n* = 41,158 intron-exon pairs. [§]*n* = 41,253 exon-intron pairs.

3.3. Co-Occurrence of Differential Exon Usage and Differential DNA Methylation between DCM and Control

We attempted to define regions with differential DNA methylation levels and associated differential exon usage between DCM patients and controls. This approach was set to provide important mechanistic insights into repatterning of epigenetic regulation during cardiac disease. We carried out statistical tests for differential exon use (DEU) of all exons in all gene transcripts, as well as differential methylated regions (DMR) of all probes across the whole epigenome between DCM patients and healthy controls. As mentioned in the Methods section, the *DEXSeq* package was used to perform statistical tests for differential exon use. During the process, we estimated the variability of RNA sequences data in each exonic part of each gene in each sample (Figure S4A) to effectively distinguish between actual effects across different conditions (DCM vs. control) and noises caused by biological or technical variations. Further, dispersion per exon was evaluated (black dots) and a mean relative to it was determined (rot dots) based on the estimated dispersion. Finally, the dispersion could be shrunk (blue dots) and utilized as an effective reference to examine differential exon usage. Next, statistical testing was carried out for all annotated exonic bins to determine if the fraction of the reads aligned to specific exons was different between DCM and control samples. We were able to identify 22,871 out of in total 644,354 (4%) exonic regions to be differentially used with a *p* value less than 5%. The MA plot (Figure S4B) visualized the differential exon usage based on the number of the reads mapped to each exonic region. These exonic regions were located in 8631 of the total 60,153 coding and non-coding genes (14%) annotated in hg19/GrCh37.

As mentioned in the Methods, we used the *limma* package to implement epigenome-wide statistical tests of differential methylated regions (DMR) between DCM patients and controls. As a result, we detected 13,223 of the total 394,247 (3%) probes to be significantly differentially methylated (*p* value <0.05). When overlaying the hits of DEU and DMR on the reference genome, we found 706 intron-exon pairs from 630 genes as well as 650 exon-intron pairs from 564 genes with concomitant DEU and DMR (Figure 4A). As an example of these identified candidate regions, we generated gene browser tracks for *LDB3* (Figure 5). In the gene ontology analysis, these detected genes were enriched for critical cellular components in the sarcomere, such as myofibril, contractile fibers, and actomyosin (FDR < 0.05), which are highly relevant in DCM. The relevant results of gene ontology analysis are depicted in Figure 4B, and detailed information can be found in Supplemental File 4.

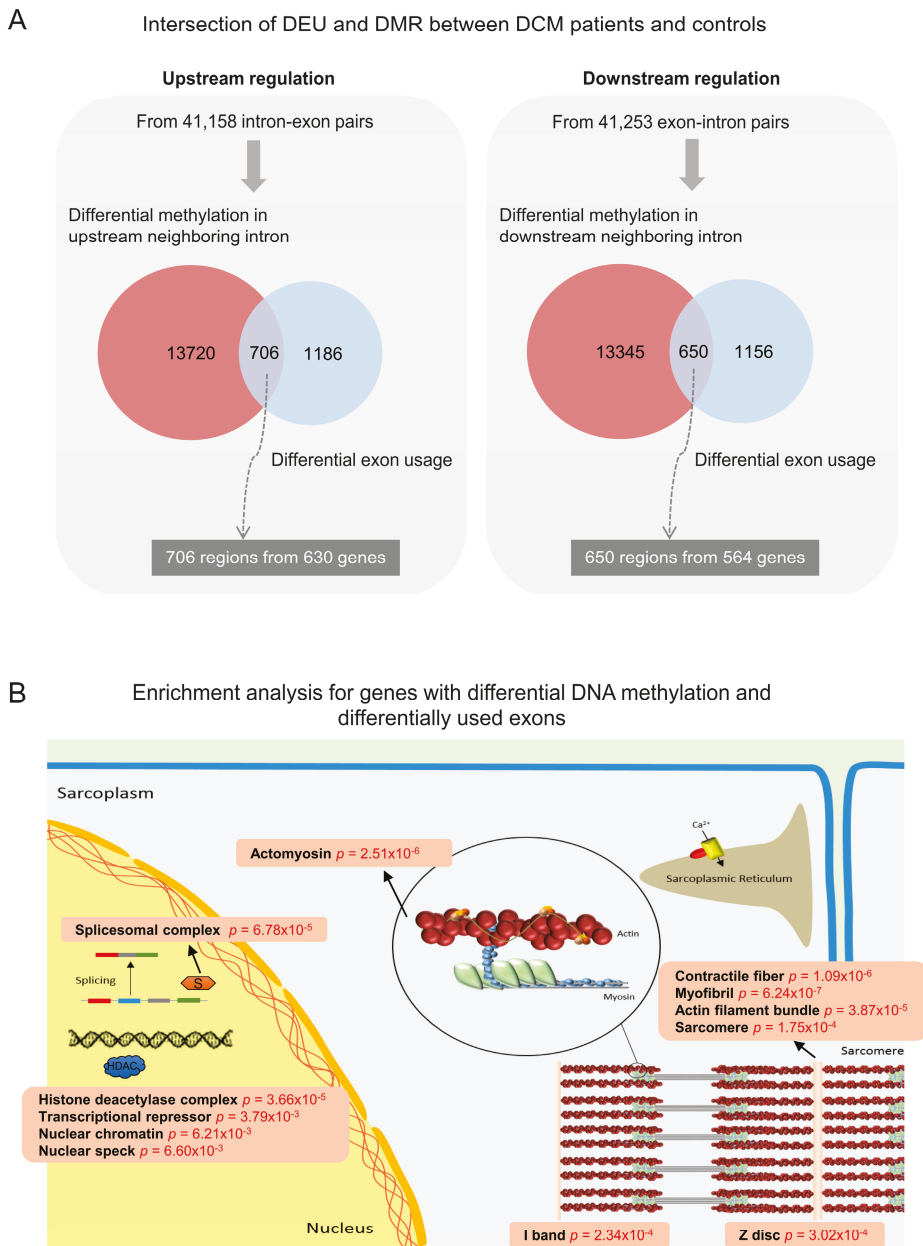


Figure 4. Identification of genomic regions with concurrent differential exon usage (DEU) and differential methylation regions (DMR). (A) Intersection of DEU and DMR between DCM patients and controls. (B) Enrichment analysis for genes containing genomic regions with concomitant DEU and DMR.

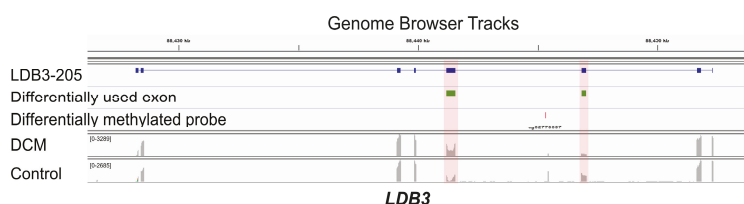


Figure 5. Genome browser tracks demonstrating the co-occurrence of differentially used exons and the differentially methylated locus in *LDB3*. The first track represents a reference transcript, LDB3-205. The second track shows the differentially used exonic parts (green). The third track points out the position of the differentially methylated locus (red). The last two tracks are RNA-Seq coverage tracks of DCM and control.

3.4. Epigenome-Wide Association of Intronic DNA Methylation and Splicing in DCM vs. Control

We first performed a genome-wide analysis of variance (ANOVA) and discovered that, on average, 2.71% (95%CI: 2.70–2.72, $n = 2,684,933$ tests) of the variance of PSI scores could be explained by the intronic DNA methylation on the same gene, which is sizable at the genomic scale. Thereafter, we carried out an epigenome-wide association study between methylation measurements and PSI scores of exons within the very same gene. Correlation coefficient, odds ratio, and p value of each association test were determined. Moreover, we compared the correlation coefficients between DCM and control samples, that is, we carried out statistical tests of significance for the difference between correlation coefficients in DCM patients and those in controls. As shown in the Manhattan plot for genome-wide statistical tests (Figure 6A), several loci with significantly different (FDR <0.05) correlation coefficients between DCM patients and controls were detected in the screening cohort, signifying a disease-dependent differential impact of DNA methylation on alternative splicing.

In the replication cohort, five exonic regions in *TTN-AS1* as well as one exonic region in *DCTN1* were validated with statistical significance ($p < 0.05$). However, only the five verified exonic regions in *TTN-AS1* could also be “directionally replicated” in the replication cohort (Figure 6B), with a positive correlation between PSI scores and methylation values in DCM patients, as well as a negative correlation between PSI scores and methylation values in healthy controls, as shown in Figure 7. Tables 2 and 3 list the odds ratios per 0.01 increments of DNA methylation (beta value) and p values derived from logistic regression models of both cohorts. The values in the parentheses indicate the 95% confidence interval. In all identified candidates, the odds ratios in DCM were less than one, indicating a negative association, that is, if there is an increase of DNA methylation in DCM patients, a decrease of PSI value is expected, and vice versa. On the other hand, in all identified candidates, the odds ratios in control samples were greater than one, suggesting a positive correlation. In terms of significance level, the positive association between DNA methylation and PSI value in control samples reached statistical significance both in screening and replication cohorts. However, the positive correlation between DNA methylation and PSI values in the DCM samples reached statistical significance only in the replication cohort, which could be due to less noise in the replication cohort owing to the stranded RNA-Seq, providing more of an advantage for antisense analysis.

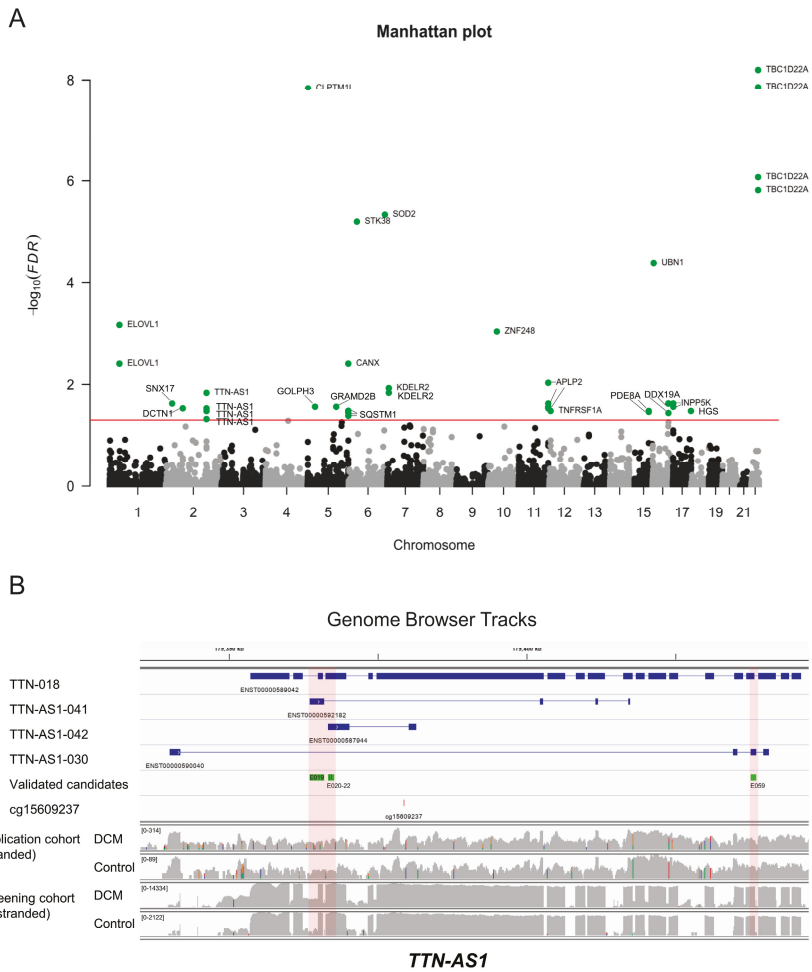


Figure 6. (A) Manhattan plot summarizing genome-wide statistical tests of significance for the difference of correlation coefficients between DCM and control samples in the screening cohort. The red horizontal line represents the FDR of 0.05. (B) Genomic browser tracks showing the relative positions of the validated candidates from the epigenome-wide association study in *TTN-AS1*. The PSI scores of the validated exonic regions (green) in *TTN-AS1* were significantly associated with the methylation level of the highlighted locus (red). The first track is a reference transcript of *TTN*, the following three tracks are transcripts of *TTN-AS1*. The last four tracks were added to visualize the log-scaled RNA-Seq coverage in DCM and control, in both screening and replication cohorts. It should be noted that the RNA-Seq of the replication cohort was stranded, while the RNA-Seq of the screening cohort was unstranded. Hence, coverage in the screening cohort is noisier than in the replication cohort. Nevertheless, the candidates in *TTN-AS1* could be replicated in the replication cohort with statistical significance.

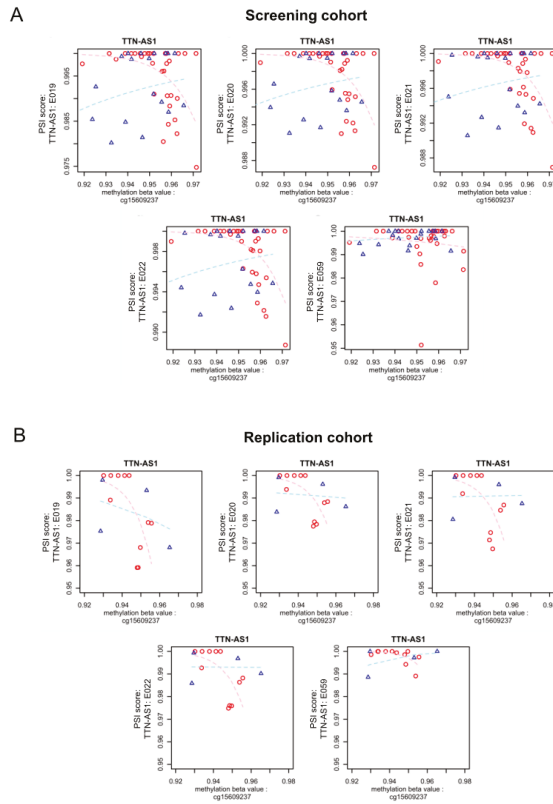


Figure 7. Visualization of DNA methylation measurements and PSI scores of validated genomic regions in *TTN-AS1*. For each validated candidate, all study subjects of the screening cohort were plotted by their methylation measurements (X-axis) and PSI scores (Y-axis). The conditions of the samples are color-coded (red: DCM, blue: Control). The depicted regression lines were computed using logistic regression and are also color coded (pink: DCM, light blue: Control). The same visualization for the replication cohort is presented below, showing the conserved principle. (A) Screening cohort; (B) Replication cohort.

Table 2. Odds ratios of the replicated candidates in the screening cohort.

Variables	Odds Ratio		<i>p</i> Value	
	DCM	Control	DCM	Control
cg15609237 vs. TTN-AS1:E019	0.71 (0.08–3.02)	1.18 (1.11–1.25)	0.71	0.000018
cg15609237 vs. TTN-AS1:E020	0.73 (0.06–3.46)	1.17 (1.11–1.24)	0.76	0.000017
cg15609237 vs. TTN-AS1:E021	0.72 (0.07–3.17)	1.18 (1.11–1.25)	0.73	0.000024
cg15609237 vs. TTN-AS1:E022	0.72 (0.07–3.12)	1.18 (1.11–1.25)	0.71	0.000013
cg15609237 vs. TTN-AS1:E059	0.78 (0.14–2.53)	1.18 (1.12–1.24)	0.74	0.000006

Table 3. Odds ratios of the replicated candidates in the replication cohort.

Variables	Odds Ratio		<i>p</i> Value	
	DCM	Control	DCM	Control
cg15609237 vs. TTN-AS1:E019	0.34 (0.13–0.77)	4.75 (0.62–Inf)	0.01	0.011
cg15609237 vs. TTN-AS1:E020	0.35 (0.13–0.75)	5.34 (0.85–Inf)	0.01	0.003
cg15609237 vs. TTN-AS1:E021	0.35 (0.13–0.78)	5.07 (1.01–Inf)	0.01	0.007
cg15609237 vs. TTN-AS1:E022	0.36 (0.14–0.78)	5.84 (0.92–73.01)	0.01	0.007
cg15609237 vs. TTN-AS1:E059	0.78 (0.14–2.53)	7.83 (3.37–73.01)	0.25	0.112

4. Discussion

The present study utilized an epigenome-wide association approach to examine the interaction between DNA methylome and splicing of the transcriptome in the heart, as both biological processes were only recently shown to play an essential regulatory role in DCM. A significant positive correlation between intronic DNA methylation and usage of adjacent exons was detected. Moreover, we pinpointed and stringently validated several regions in *TTN-AS1* with a disease-dependent differential regulation of DNA methylation on alternative splicing. This is the first study to investigate in the full epigenome the complex yet highly ordered orchestration of methylome and transcriptome in the healthy human heart as well as in DCM.

In the past few years, GWAS have helped to identify several novel genomic regions associated with cardiac phenotypes. As a result, there has been a rapid progress in functional genetics to assist in the exploration of biological meaning of disease-associated genomic regions. Although genome studies massively advanced our knowledge of DCM, plenty of biological mechanisms of disease still need to be deciphered, and investigations on epigenetic–genetic and epigenetic–transcriptomic levels have been proposed to provide yet another crucial piece in disease etiology [28]. As an example, Wang et al. implemented the GWAS approach on an epigenomic dataset to identify signatures related to clinical parameters, such as from electrocardiograms (ECG). Eventually, they were able to experimentally validate the findings in iPSC cardiomyocytes [29]. The present study relied on human cardiac tissue as disease-relevant processes are often tissue- and species-specific [30]. While other studies attempted to investigate DNA methylation and alternative splicing in cell cultures, our approach is the first to inspect the relationship between DNA methylation and alternative splicing in heart muscle disorders using human cardiac tissues [31].

We discovered a positive correlation between DNA methylation of the flanking introns and the inclusion of the bordering exon across the whole genome. This relationship exists both in DCM and control subjects. There are three potential mechanisms underlying these findings. First, as early as in 1988, it was identified that splicing occurs during transcription [32]. Hence, it is possible that the detected association is mediated by some specific DNA-binding proteins, such as CTCF and MeCP2. These proteins can change their binding affinity to DNA by apprehending methylation signatures of DNA. When they are bound to DNA, they can impact the elongation rate of RNA polymerase II, influence the time for the splicing machinery to recognize weak splice-sites, and subsequently affect the inclusion of alternative exons [33–35]. Aside from the known proteins, other DNA-binding proteins with similar functions could still exist and be undiscovered so far. Second, it is also possible that DNA methylation-dependent recruitment of splicing factors takes place. For example, it has been reported that the adaptor protein HP1 can recruit splicing factors if bound to methylated DNA [36]. Interestingly, it has been suggested that histone modifications could facilitate the splicing factors to bind

to pre-mRNA [37], while there is literature reporting the strong link between histone modifications and DNA methylation [38–40], which is in line with our theory. Third, based on the evidence demonstrating DNA methylation's correlation with nucleosome occupancy as well as the regulatory role of DNA methylation on the modification of histones [41–46], it is reasonable to speculate that DNA methylation influences splicing through regulating the orchestration of chromatin remodeling and nucleosome positioning, especially the nucleosome positioning relative to the splice sites of interest [47], while more in-depth understanding of the interaction between DNA methylation and nucleosome occupancy is still needed.

In the present study, we identified numerous regions on *TTN-AS1* with a DCM-dependent differential regulation of DNA methylation on alternative splicing, while *TTN-AS1* is practically an inverse counterpart to *TTN*. *TTN-AS1* encodes Titin antisense 1, which is a long noncoding RNA (lncRNA) that produces an estimate of 80 different transcripts. In the literature, lncRNAs were reported to play a role in cardiac development and regeneration, in the pathogenesis of cardiovascular diseases, as well as in the doxorubicin-induced cardiac toxicity, which predisposes people to DCM [48–50]. Furthermore, disrupted splicing of lncRNAs were found to cause dysregulation of important cardiac proteins in mice, such as potassium voltage-gated channel proteins encoded by *Kcna1* and *Kcna2* [51–53]. In addition, a cluster of antisense lncRNAs in the MYH7 locus was noticed to be essential in early development of cardiomyopathy under pressure-overload [54]. Interestingly, in recent studies, Titin antisense 1 was shown to act as a competing endogenous RNA (ceRNA) to sequester diverse microRNAs (miRNAs) and transcription factors, thus, consequently facilitating tumor aggressiveness in several cancers, including lung cancer [55], cervical cancer [56], esophageal cancer [57], gastric cancer [58], papillary thyroid cancer [59], colorectal cancer [60], and prostate cancer [61]. However, although *TTN-AS1* is highly expressed in the heart, there is minimal understanding of its cardiac role in the literature, and more investigations are required. The validated regions were found to locate at the counterpart locus of the genomic region encoding the A-band of titin. This finding is intriguing, because genetic variations in titin A-band are the leading cause of DCM [62,63]. Hence, based on our finding, it is not unreasonable to speculate that dysregulated splicing of Titin antisense 1 might be able to induce deleterious exon-skipping in the A-band of titin, which may mimic the pathologies seen in TTNtv, and that modification of this region might even be a therapeutic principle [64,65]. Hence, the current study provides new understanding of the regulation of this important gene locus.

A potential limitation of the here conducted epigenome-wide approach is the sparse preexisting data on false-positive and false-negative discovery rates and adequate power calculations of epigenome-wide association analysis and in particular the here conducted multi-omics type of analysis [29]. Our approach, although explorative in the screening stage, used an independent validation step. Since cardiac tissue is highly limited for research studies, the sizes of both cohorts were still relatively small compared to traditional GWAS. However, the combination of information from *a priori* connected biological processes and coordinated molecular layers is able to reduce false-positive discoveries and add statistical power [8].

In conclusion, this study emphasizes the intricate interplay between the DNA methylation landscape and the mRNA splicing machinery. With a state-of-the-art epigenome-wide approach and utilization of human cardiac tissue as study material, a new understanding of the genome–epigenome relationship in DCM was presented. We showed that dysregulated methylation of the gene encoding Titin antisense 1 is associated with its splicing, which could induce pathological exon-skipping during the transcription of *TTN*.

Supplementary Materials: The supplementary materials are available online at <http://www.mdpi.com/2077-0383/9/5/1499/s1>. Figure S1: RNA-Seq in the replication cohort. Figure S2: PCA of RNA-Seq in both cohorts. Figure S3: PCA of DNA methylation measurement in both cohorts. Figure S4: Dispersion plot and MA plot of differential exon usage analysis in the screening cohort. Figure S5: Histograms showing the sequencing depth of both cohorts. File S1: Results of differential gene expression analysis. File Table S2: List of up- and down-regulated genes. File Table S3: Gene ontology analysis of up- and down-regulated genes. File S4: Gene ontology analysis of regions with concurrent DEU and DMR.

Author Contributions: Conceptualization, B.M., J.H. and W.-T.G.; methodology, B.M. and W.-T.G.; software, W.-T.G., R.T., D.H.L., J.H.; validation, W.-T.G. and A.K.; formal analysis, W.-T.G.; investigation, B.M. and W.-T.G.; resources, H.A.K. and B.M.; data curation, J.H., F.S.-H., E.K. and O.S.S.; writing—original draft preparation, W.-T.G.; writing—review and editing, W.-T.G., B.M. and M.W.; visualization, W.-T.G.; supervision, B.M.; project administration, J.H., F.S.-H., E.K.; funding acquisition, B.M. and H.A.K. All authors have read and agreed to the published version of the manuscript.

Funding: This work was supported by grants from the Deutsches Zentrum für Herz-Kreislauf-Forschung (German Center for Cardiovascular Research, DZHK), the German Ministry of Education and Research (CaRNAtion, FKZ 031L0075B), Informatics for Life (Klaus Tschira Foundation), the Faculty of Medicine of the Leipzig University (to M.M.-W.), the European Union (Detectin-HF), and the Deutsche Forschungsgemeinschaft (DFG). B.M. was supported by an excellence fellowship of the Else Kröner Fresenius Foundation.

Acknowledgments: We thank Sabine Herch, Anne Marie Müller, Antje Weber, and Rouven Nietsch for excellent technical support.

Conflicts of Interest: All authors declare no conflicts of interest.

References

1. Hershberger, R.E.; Hedges, D.J.; Morales, A. Dilated cardiomyopathy: The complexity of a diverse genetic architecture. *Nat. Rev. Cardiol.* **2013**, *10*, 531–547. [[CrossRef](#)] [[PubMed](#)]
2. McNally, E.M.; Mestroni, L. Dilated Cardiomyopathy: Genetic Determinants and Mechanisms. *Circ. Res.* **2017**, *121*, 731–748. [[CrossRef](#)] [[PubMed](#)]
3. Ganesh, S.K.; Arnett, D.K.; Assimes, T.L.; Basson, C.T.; Chakravarti, A.; Ellinor, P.T.; Engler, M.B.; Goldmuntz, E.; Herrington, D.M.; Hershberger, R.E.; et al. Genetics and genomics for the prevention and treatment of cardiovascular disease: Update: A scientific statement from the American Heart Association. *Circulation* **2013**, *128*, 2813–2851. [[CrossRef](#)] [[PubMed](#)]
4. Towbin, J.A.; Bowles, N.E. The failing heart. *Nature* **2002**, *415*, 227–233. [[CrossRef](#)]
5. Kayvanpour, E.; Sedaghat-Hamedani, F.; Amr, A.; Lai, A.; Haas, J.; Holzer, D.B.; Frese, K.S.; Keller, A.; Jensen, K.; Katus, H.A.; et al. Genotype-phenotype associations in dilated cardiomyopathy: Meta-analysis on more than 8000 individuals. *Clin. Res. Cardiol.* **2017**, *106*, 127–139. [[CrossRef](#)]
6. Herman, D.S.; Lam, L.; Taylor, M.R.; Wang, L.; Teekakirikul, P.; Christodoulou, D.; Conner, L.; DePalma, S.R.; McDonough, B.; Sparks, E.; et al. Truncations of titin causing dilated cardiomyopathy. *N. Engl. J. Med.* **2012**, *366*, 619–628. [[CrossRef](#)]
7. Paldino, A.; De Angelis, G.; Merlo, M.; Gigli, M.; Dal Ferro, M.; Severini, G.M.; Mestroni, L.; Sinagra, G. Genetics of Dilated Cardiomyopathy: Clinical Implications. *Curr. Cardiol. Rep.* **2018**, *20*, 83. [[CrossRef](#)]
8. Meder, B.; Haas, J.; Sedaghat-Hamedani, F.; Kayvanpour, E.; Frese, K.; Lai, A.; Nietsch, R.; Scheiner, C.; Mester, S.; Bordalo, D.M.; et al. Epigenome-Wide Association Study Identifies Cardiac Gene Patterning and a Novel Class of Biomarkers for Heart Failure. *Circulation* **2017**, *136*, 1528–1544. [[CrossRef](#)]
9. Pepin, M.E.; Drakos, S.; Ha, C.M.; Tristani-Firouzi, M.; Selzman, C.H.; Fang, J.C.; Wende, A.R.; Wever-Pinzon, O. DNA methylation reprograms cardiac metabolic gene expression in end-stage human heart failure. *Am. J. Physiol. Heart Circ. Physiol.* **2019**, *317*, H674–H684. [[CrossRef](#)]
10. Ito, E.; Miyagawa, S.; Fukushima, S.; Yoshikawa, Y.; Saito, S.; Saito, T.; Harada, A.; Takeda, M.; Kashiyama, N.; Nakamura, Y.; et al. Histone modification is correlated with reverse left ventricular remodeling in nonischemic dilated cardiomyopathy. *Ann. Thorac. Surg.* **2017**, *104*, 1531–1539. [[CrossRef](#)]
11. Deo, R.C. Alternative Splicing, Internal Promoter, Nonsense-Mediated Decay, or All Three: Explaining the Distribution of Truncation Variants in Titin. *Circ. Cardiovasc. Genet.* **2016**, *9*, 419–425. [[CrossRef](#)] [[PubMed](#)]
12. Sedaghat-Hamedani, F.; Haas, J.; Zhu, F.; Geier, C.; Kayvanpour, E.; Liss, M.; Lai, A.; Frese, K.; Pribe-Wolferts, R.; Amr, A.; et al. Clinical genetics and outcome of left ventricular non-compaction cardiomyopathy. *Eur. Heart J.* **2017**, *38*, 3449–3460. [[CrossRef](#)] [[PubMed](#)]
13. Beqqali, A.; Bollen, I.A.; Rasmussen, T.B.; van den Hoogenhof, M.M.; van Deutekom, H.W.; Schafer, S.; Haas, J.; Meder, B.; Sørensen, K.E.; van Oort, R.J.; et al. A mutation in the glutamate-rich region of RNA-binding motif protein 20 causes dilated cardiomyopathy through missplicing of titin and impaired Frank-Starling mechanism. *Cardiovasc. Res.* **2016**, *112*, 452–463. [[CrossRef](#)] [[PubMed](#)]

14. Haas, J.; Mester, S.; Lai, A.; Frese, K.S.; Sedaghat-Hamedani, F.; Kayvanpour, E.; Rausch, T.; Nietsch, R.; Boeckel, J.N.; Carstensen, A.; et al. Genomic structural variations lead to dysregulation of important coding and non-coding RNA species in dilated cardiomyopathy. *EMBO Mol. Med.* **2018**, *10*, 107–120. [CrossRef] [PubMed]
15. Li, H.; Handsaker, B.; Wysoker, A.; Fennell, T.; Ruan, J.; Homer, N.; Marth, G.; Abecasis, G.; Durbin, R. The sequence alignment/map format and SAMtools. *Bioinformatics* **2009**, *25*, 2078–2079. [CrossRef] [PubMed]
16. Factoextra: Extract and Visualize the Results of Multivariate Data Analyses. Available online: <https://rpkg.sdatanovia.com/factoextra/index.html> (accessed on 1 March 2020).
17. Siren, J.; Valimaki, N.; Mäkinen, V. Indexing Graphs for Path Queries with Applications in Genome Research. *IEEE ACM Trans. Comput. Biol. Bioinform.* **2014**, *11*, 375–388. [CrossRef] [PubMed]
18. Love, M.I.; Huber, W.; Anders, S. Moderated estimation of fold change and dispersion for RNA-seq data with DESeq2. *Genome Biol.* **2014**, *15*, 550. [CrossRef]
19. Anders, S.; Reyes, A.; Huber, W. Detecting differential usage of exons from RNA-seq data. *Genome Res.* **2012**, *22*, 2008–2017. [CrossRef]
20. Schafer, S.; Miao, K.; Benson, C.C.; Heinig, M.; Cook, S.A.; Hubner, N. Alternative Splicing Signatures in RNA-seq Data: Percent Spliced in (PSI). *Curr. Protoc. Hum. Genet.* **2015**, *87*, 11–16. [CrossRef]
21. Lawrence, M.; Huber, W.; Pagès, H.; Aboyoun, P.; Carlson, M.; Gentleman, R.; Morgan, M.; Carey, V. Software for Computing and Annotating Genomic Ranges. *PLoS Computat. Biol.* **2013**, *9*, e1003118. [CrossRef]
22. Ritchie, M.E.; Phipson, B.; Wu, D.; Hu, Y.; Law, C.W.; Shi, W.; Smyth, G.K. limma powers differential expression analyses for RNA-sequencing and microarray studies. *Nucleic Acids Res.* **2015**, *43*, e47. [CrossRef] [PubMed]
23. GeneTrail2 v1.6 Statistica analysis and molecular signatures. Available online: <https://genetrail2.bioinf.uni-sb.de/> (accessed on 23 May 2018).
24. Daniel, S.; Tim, K.; Patrick, T.; Lara, S.; Christina, B.; Nicole, L.; Andreas, G.; Michael, K.; Manfred, G.; Norbert, G.; et al. Multi-omics Enrichment Analysis using the GeneTrail2 Web Service. *Bioinformatics* **2016**, *32*, 1502–1508.
25. Bush, W.S.; Moore, J.H. Chapter 11: Genome-wide association studies. *PLoS Comput. Biol.* **2012**, *8*, e1002822. [CrossRef]
26. Chanoock, S.J.; Manolio, T.; Boehnke, M.; Boerwinkle, E.; Hunter, D.J.; Thomas, G.; Hirschhorn, J.N.; Abecasis, G.; Altshuler, D.; Bailey-Wilson, J.E.; et al. Replicating genotype-phenotype associations. *Nature* **2007**, *447*, 655–660.
27. Diedenhofen, B.; Musch, J. cocor: A comprehensive solution for the statistical comparison of correlations. *PLoS ONE* **2015**, *10*, e0121945. [CrossRef]
28. Do, C.; Shearer, A.; Suzuki, M.; Terry, M.B.; Gelernter, J.; Grealley, J.M.; Tycko, B. Genetic-epigenetic interactions in cis: A major focus in the post-GWAS era. *Genome Biol.* **2017**, *18*, 120. [CrossRef]
29. Wang, X.; Tucker, N.R.; Rizki, G.; Mills, R.; Krijger, P.H.; de Wit, E.; Subramanian, V.; Bartell, E.; Nguyen, X.X.; Ye, J.; et al. Discovery and validation of sub-threshold genome-wide association study loci using epigenomic signatures. *Elife* **2016**, *5*, e10557. [CrossRef]
30. Pastinen, T.; Hudson, T.J. Cis-acting regulatory variation in the human genome. *Science* **2004**, *306*, 647–650. [CrossRef]
31. Wan, J.; Oliver, V.F.; Zhu, H.; Zack, D.J.; Qian, J.; Merbs, S.L. Integrative analysis of tissue-specific methylation and alternative splicing identifies conserved transcription factor binding motifs. *Nucleic Acids Res.* **2013**, *41*, 8503–8514. [CrossRef]
32. Beyer, A.L.; Osheim, Y.N. Splice site selection, rate of splicing, and alternative splicing on nascent transcripts. *Genes Dev.* **1988**, *2*, 754–765. [CrossRef]
33. Shukla, S.; Kavak, E.; Gregory, M.; Imashimizu, M.; Shutinoski, B.; Kashlev, M.; Oberdoerffer, P.; Sandberg, R.; Oberdoerffer, S. CTCF-promoted RNA polymerase II pausing links DNA methylation to splicing. *Nature* **2011**, *479*, 74–79. [CrossRef]
34. Maunakea, A.K.; Chepelev, I.; Cui, K.; Zhao, K. Intragenic DNA methylation modulates alternative splicing by recruiting MeCP2 to promote exon recognition. *Cell Res.* **2013**, *23*, 1256–1269. [CrossRef]
35. Lev Maor, G.; Yearim, A.; Ast, G. The alternative role of DNA methylation in splicing regulation. *Trends Genet.* **2015**, *31*, 274–280. [CrossRef]
36. Yearim, A.; Gelfman, S.; Shayevitch, R.; Melcer, S.; Glaich, O.; Mallm, J.P.; Nissim-Rafinia, M.; Cohen, A.H.S.; Rippe, K.; Meshorer, E.; et al. HP1 is involved in regulating the global impact of DNA methylation on alternative splicing. *Cell Rep.* **2015**, *10*, 1122–1134. [CrossRef]

37. Luco, R.F.; Allo, M.; Schor, I.E.; Kornblihtt, A.R.; Misteli, T. Epigenetics in alternative pre-mRNA splicing. *Cell* **2011**, *144*, 16–26. [[CrossRef](#)]
38. Vire, E.; Brenner, C.; Deplus, R.; Blanchon, L.; Fraga, M.; Didelot, C.; Morey, L.; Van Eynde, A.; Bernard, D.; Vanderwinden, J.M.; et al. The Polycomb group protein EZH2 directly controls DNA methylation. *Nature* **2006**, *439*, 871–874. [[CrossRef](#)]
39. Schlesinger, Y.; Straussman, R.; Keshet, I.; Farkash, S.; Hecht, M.; Zimmerman, J.; Eden, E.; Yakhini, Z.; Ben-Shushan, E.; Reubinoff, B.E.; et al. Polycomb-mediated methylation on Lys27 of histone H3 pre-marks genes for de novo methylation in cancer. *Nat. Genet.* **2007**, *39*, 232–236. [[CrossRef](#)]
40. Bird, A. Molecular biology. Methylation talk between histones and DNA. *Science* **2001**, *294*, 2113–2115. [[CrossRef](#)]
41. Kelly, T.K.; Liu, Y.; Lay, F.D.; Liang, G.; Berman, B.P.; Jones, P.A. Genome-wide mapping of nucleosome positioning and DNA methylation within individual DNA molecules. *Genome Res.* **2012**, *22*, 2497–2506. [[CrossRef](#)]
42. Chodavarapu, R.K.; Feng, S.; Bernatavichute, Y.V.; Chen, P.Y.; Stroud, H.; Yu, Y.; Hetzel, J.A.; Kuo, F.; Kim, J.; Cokus, S.J.; et al. Relationship between nucleosome positioning and DNA methylation. *Nature* **2010**, *466*, 388–392. [[CrossRef](#)]
43. Hashimshony, T.; Zhang, J.; Keshet, I.; Bustin, M.; Cedar, H. The role of DNA methylation in setting up chromatin structure during development. *Nat. Genet.* **2003**, *34*, 187–192. [[CrossRef](#)] [[PubMed](#)]
44. Bernstein, B.E.; Meissner, A.; Lander, E.S. The mammalian epigenome. *Cell* **2007**, *128*, 669–681. [[CrossRef](#)] [[PubMed](#)]
45. Fan, S.; Zhang, M.Q.; Zhang, X. Histone methylation marks play important roles in predicting the methylation status of CpG islands. *Biochem. Biophys. Res. Commun.* **2008**, *374*, 559–564. [[CrossRef](#)] [[PubMed](#)]
46. Cedar, H.; Bergman, Y. Linking DNA methylation and histone modification: Patterns and paradigms. *Nat. Rev. Genet.* **2009**, *10*, 295–304. [[CrossRef](#)]
47. Gelfman, S.; Ast, G. When epigenetics meets alternative splicing: The roles of DNA methylation and GC architecture. *Epigenomics* **2013**, *5*, 351–353. [[CrossRef](#)]
48. Ounzain, S.; Crippa, S.; Pedrazzini, T. Small and long non-coding RNAs in cardiac homeostasis and regeneration. *Biochim. Biophys. Acta* **2013**, *1833*, 923–933. [[CrossRef](#)]
49. Calore, M.; De Windt, L.J.; Rampazzo, A. Genetics meets epigenetics: Genetic variants that modulate noncoding RNA in cardiovascular diseases. *J. Mol. Cell. Cardiol.* **2015**, *89*, 27–34. [[CrossRef](#)]
50. Xie, Z.; Xia, W.; Hou, M. Long intergenic noncoding RNAp21 mediates cardiac senescence via the Wnt/betacatenin signaling pathway in doxorubicin-induced cardiotoxicity. *Mol. Med. Rep.* **2018**, *17*, 2695–2704.
51. Thum, T.; Condorelli, G. Long noncoding RNAs and microRNAs in cardiovascular pathophysiology. *Circ. Res.* **2015**, *116*, 751–762. [[CrossRef](#)]
52. Korostowski, L.; Sedlak, N.; Engel, N. The Kcnq1ot1 long non-coding RNA affects chromatin conformation and expression of Kcnq1, but does not regulate its imprinting in the developing heart. *PLoS Genet.* **2012**, *8*, e1002956. [[CrossRef](#)]
53. Long, Q.Q.; Wang, H.; Gao, W.; Fan, Y.; Li, Y.F.; Ma, Y.; Yang, Y.; Shi, H.J.; Chen, B.R.; Meng, H.Y.; et al. Long Noncoding RNA Kcna2 Antisense RNA Contributes to Ventricular Arrhythmias via Silencing Kcna2 in Rats with Congestive Heart Failure. *J. Am. Heart Assoc.* **2017**, *6*, e005965. [[CrossRef](#)] [[PubMed](#)]
54. Han, P.; Li, W.; Lin, C.H.; Yang, J.; Shang, C.; Nurnberg, S.T.; Jin, K.K.; Xu, W.; Lin, C.Y.; Lin, C.J.; et al. A long noncoding RNA protects the heart from pathological hypertrophy. *Nature* **2014**, *514*, 102–106. [[CrossRef](#)] [[PubMed](#)]
55. Jia, Y.; Duan, Y.; Liu, T.; Wang, X.; Lv, W.; Wang, M.; Wang, J.; Liu, L. LncRNA TTN-AS1 promotes migration, invasion, and epithelial mesenchymal transition of lung adenocarcinoma via sponging miR-142-5p to regulate CDK5. *Cell Death Dis.* **2019**, *10*, 573. [[CrossRef](#)] [[PubMed](#)]
56. Chen, P.; Wang, R.; Yue, Q.; Hao, M. Long non-coding RNA TTN-AS1 promotes cell growth and metastasis in cervical cancer via miR-573/E2F3. *Biochem. Biophys. Res. Commun.* **2018**, *503*, 2956–2962. [[CrossRef](#)] [[PubMed](#)]
57. Lin, C.; Zhang, S.; Wang, Y.; Wang, Y.; Nice, E.; Guo, C.; Zhang, E.; Yu, L.; Li, M.; Liu, C.; et al. Functional Role of a Novel Long Noncoding RNA TTN-AS1 in Esophageal Squamous Cell Carcinoma Progression and Metastasis. *Clin. Cancer Res.* **2018**, *24*, 486–498. [[CrossRef](#)]

58. Dong, M.M.; Peng, S.J.; Yuan, Y.N.; Luo, H.P. LncRNA TTN-AS1 contributes to gastric cancer progression by acting as a competing endogenous RNA of miR-376b-3p. *Neoplasma* **2019**, *66*, 564–575. [[CrossRef](#)]
59. Cui, Z.; Luo, Z.; Lin, Z.; Shi, L.; Hong, Y.; Yan, C. Long non-coding RNA TTN-AS1 facilitates tumorigenesis of papillary thyroid cancer through modulating the miR-153-3p/ZNF2 axis. *J. Gene Med.* **2019**, *21*, e3083. [[CrossRef](#)]
60. Wang, Y.; Jiang, F.; Xiong, Y.; Cheng, X.; Qiu, Z.; Song, R. LncRNA TTN-AS1 sponges miR-376a-3p to promote colorectal cancer progression via upregulating KLF15. *Life Sci.* **2020**, *244*, 116936. [[CrossRef](#)]
61. Zhu, Y.; Yang, Z.; Luo, X.H.; Xu, P. Long noncoding RNA TTN-AS1 promotes the proliferation and migration of prostate cancer by inhibiting miR-1271 level. *Eur. Rev. Med. Pharmacol. Sci.* **2019**, *23*, 10678–10684.
62. Roberts, A.M.; Ware, J.S.; Herman, D.S.; Schafer, S.; Baksi, J.; Bick, A.G.; Buchan, R.J.; Walsh, R.; John, S.; Wilkinson, S.; et al. Integrated allelic, transcriptional, and phenomic dissection of the cardiac effects of titin truncations in health and disease. *Sci. Transl. Med.* **2015**, *7*, 270ra6. [[CrossRef](#)]
63. Schafer, S.; de Marvao, A.; Adami, E.; Fiedler, L.R.; Ng, B.; Khin, E.; Rackham, O.J.; Van Heesch, S.; Pua, C.J.; Kui, M.; et al. Titin-truncating variants affect heart function in disease cohorts and the general population. *Nat. Genet.* **2017**, *49*, 46–53. [[CrossRef](#)] [[PubMed](#)]
64. Gramlich, M.; Pane, L.S.; Zhou, Q.; Chen, Z.; Murgia, M.; Schötterl, S.; Goedel, A.; Metzger, K.; Brade, T.; Parrotta, E.; et al. Antisense-mediated exon skipping: A therapeutic strategy for titin-based dilated cardiomyopathy. *EMBO Mol. Med.* **2015**, *7*, 562–576. [[CrossRef](#)] [[PubMed](#)]
65. Hahn, J.K.; Neupane, B.; Pradhan, K.; Zhou, Q.; Testa, L.; Pelzl, L.; Maleck, C.; Gawaz, M.; Gramlich, M. The assembly and evaluation of antisense oligonucleotides applied in exon skipping for titin-based mutations in dilated cardiomyopathy. *J. Mol. Cell. Cardiol.* **2019**, *131*, 12–19. [[CrossRef](#)] [[PubMed](#)]



© 2020 by the authors. Licensee MDPI, Basel, Switzerland. This article is an open access article distributed under the terms and conditions of the Creative Commons Attribution (CC BY) license (<http://creativecommons.org/licenses/by/4.0/>).



Article

Can Circulating Cardiac Biomarkers Be Helpful in the Assessment of *LMNA* Mutation Carriers?

Przemyslaw Chmielewski ¹, Ewa Michalak ¹, Ilona Kowalik ², Maria Franaszczyk ³, Malgorzata Sobieszczanska-Malek ⁴, Grazyna Truszkowska ³, Malgorzata Stepien-Wojno ¹, Elzbieta Katarzyna Biernacka ⁵, Bogna Foss-Nieradko ¹, Michal Lewandowski ⁶, Artur Oreziak ⁷, Maria Bilinska ⁷, Mariusz Kusmierczyk ⁸, Frédérique Tesson ⁹, Jacek Grzybowski ¹⁰, Tomasz Zielinski ⁴, Rafal Ploski ¹¹ and Zofia T. Bilinska ^{1,*}

¹ Unit for Screening Studies in Inherited Cardiovascular Diseases, National Institute of Cardiology, 04-628 Warsaw, Poland; pchmielewski@ikard.pl (P.C.); emichalak@ikard.pl (E.M.); mstepien@ikard.pl (M.S.-W.); bfn@ikard.pl (B.F.-N.)

² Department of Coronary Artery Disease and Cardiac Rehabilitation, National Institute of Cardiology, 04-628 Warsaw, Poland; ikowalik@ikard.pl

³ Molecular Biology Laboratory, Department of Medical Biology, National Institute of Cardiology, 04-628 Warsaw, Poland; m.fran@wp.pl (M.F.); gtruszkowska@ikard.pl (G.T.)

⁴ Department of Heart Failure and Transplantology, National Institute of Cardiology, 04-628 Warsaw, Poland; m.sobieszczanska@ikard.pl (M.S.-M.); tzielin@ikard.pl (T.Z.)

⁵ Department of Congenital Heart Diseases, National Institute of Cardiology, 04-628 Warsaw, Poland; e.biernacka@ikard.pl

⁶ 2nd Department of Arrhythmia, National Institute of Cardiology, 04-628 Warsaw, Poland; mlewan@ikard.pl

⁷ 1st Department of Arrhythmia, National Institute of Cardiology, 04-628 Warsaw, Poland; aoreziak@ikard.pl (A.O.); mbilinska@ikard.pl (M.B.)

⁸ Department of Cardiac Surgery and Transplantology, National Institute of Cardiology, 04-628 Warsaw, Poland; m.kusmierczyk@ikard.pl

⁹ Interdisciplinary School of Health Sciences, Faculty of Health Sciences, University of Ottawa, Ottawa, ON K1N 6N5, Canada; ftesson@uOttawa.ca

¹⁰ Department of Cardiomyopathy, National Institute of Cardiology, 04-628 Warsaw, Poland; j.grzybowski@ikard.pl

¹¹ Department of Medical Genetics, Medical University of Warsaw, 02-106 Warsaw, Poland; rploski@wp.pl

* Correspondence: zbilinska@ikard.pl; Tel.: +48-223434711

Received: 1 April 2020; Accepted: 8 May 2020; Published: 12 May 2020

Abstract: Mutations in the lamin A/C gene are variably phenotypically expressed; however, it is unclear whether circulating cardiac biomarkers are helpful in the detection and risk assessment of cardiomyopathies. We sought to assess (1) clinical characteristics including serum biomarkers: high sensitivity troponin T (hsTnT) and N-terminal prohormone brain natriuretic peptide (NT-proBNP) in clinically stable cardiomyopathy patients, and (2) outcome among pathogenic/likely pathogenic lamin A/C gene (*LMNA*) mutation carriers. Our single-centre cohort included 53 patients from 21 families. Clinical, laboratory, follow-up data were analysed. Median follow-up was 1522 days. The earliest abnormality, emerging in the second and third decades of life, was elevated hsTnT (in 12% and in 27% of patients, respectively), followed by the presence of atrioventricular block, heart failure, and malignant ventricular arrhythmia (MVA). In patients with missense vs. other mutations, we found no difference in MVA occurrence and, surprisingly, worse transplant-free survival. Increased levels of both hsTnT and NT-proBNP were strongly associated with MVA occurrence (HR > 13, $p \leq 0.02$ in both) in univariable analysis. In multivariable analysis, NT-proBNP level > 150 pg/mL was the only independent indicator of MVA. We conclude that assessment of circulating cardiac biomarkers may help in the detection and risk assessment of cardiomyopathies.

Keywords: laminopathy; *LMNA*; biomarkers; troponin T; NT-proBNP; malignant ventricular arrhythmia; arrhythmic risk stratification

1. Introduction

Dilated cardiomyopathy (DCM) is a major cause of heart failure (HF) and has a genetic basis in 40–50% of cases [1]. There is growing evidence of distinct arrhythmogenic phenotype in DCM related to *LMNA*, *SCN5A*, *PLN*, *RBM20*, *FLNC*, and *DSP* mutations [2–6]. Of these, cardiolaminopathies have been studied most extensively and are phenotypically quite well characterized [7–13]. Nevertheless, none of the studies involved baseline characteristics including circulating cardiac biomarkers. In 2005, a Canadian–Irish–Polish joint study showed the presence of *LMNA* mutations in 4.4% of consecutive DCM cases [14]. In a further study, we found that 7.6% of 66 heart transplant (HTX) recipients and 9.1% of consecutive DCM patients referred for familial evaluation carry *LMNA* mutations [15]. Since then, we have identified subsequent 28 *LMNA* mutation carriers in the National Institute of Cardiology, Warsaw.

In this study, we sought to assess the clinical characteristics including serum biomarkers, penetrance of abnormal clinical findings, and prognostic risk factors in all identified *LMNA* mutation carriers.

2. Materials and Methods

All carriers signed a written informed consent form for the genotyping and consented to the publishing of all data generated. This study was funded by external grant 0010/P05B/98/14 from the Polish Committee for Scientific Research, statutory grants from the National Institute of Cardiology (Warsaw, Poland) no 2.57/VII/03, 2.18/II/08, 2.10/II/10, and 2.56/II/14; external grant from National Science Centre Poland 2011/01/B/NZ4/03455 RP; and the recent NCBiR ERA-CVD DETECTIN-HF/2/2017 IB.4/II/17 grant. The study received the approval of the Bioethics Committee of the National Institute of Cardiology.

Data from all persons (proband and relatives) with *LMNA* mutations and cardiac involvement in the care of the National Institute of Cardiology, Warsaw, were retrospectively collected. All mutations were identified between 2000 and 2018 and were considered to be pathogenic/likely pathogenic according to The American College of Medical Genetics and Genomics (ACMG) criteria [16]. On a prospective basis, genetic testing was offered to all probands and all agreed to participate in the study. Cascade screening was offered to all probands' families. Baseline clinical information from the first documented visit to the Institute and follow-up data were recorded. In particular, data were obtained for all major cardiovascular events. The probands as well as their informed and consenting relatives underwent a clinical examination, 12-lead electrocardiography, two-dimensional Doppler echocardiography, 24-h Holter ECG monitoring, and blood sampling for genetic testing. In all probands, coronary angiography or, more recently, coronary computed tomography angiography was performed. In addition, whenever available, we quantified the serum biomarkers—high sensitivity troponin T (hsTnT) and N-terminal prohormone brain natriuretic peptide (NT-proBNP)—at baseline and during ambulatory visits in patients without worsening of HF for 3 months.

In patients with no history of sudden cardiac arrest (SCA) or sustained ventricular tachycardia (sVT), we evaluated the prognostic value of circulating cardiac biomarker concentrations, assessed during initial visit or in the time window \pm 6 months with regard to occurrence of malignant ventricular arrhythmia (MVA) during the follow-up, and compared it with other established risk factors. We also sought to examine the influence of such factors as proband status, sex, and type of mutation on life-time prognosis with regard to occurrence of end-stage HF and MVA.

2.1. Definitions

Left ventricular enlargement (LVE) was ascertained when the left ventricular end diastolic diameter (LVEDD) exceeded 112% of the predicted value, corrected for age and body surface area according to Henry's formula, while left ventricular dysfunction (LVD) was ascertained when left

ventricular ejection fraction (LVEF) was <50%. The diagnosis of DCM was made when both criteria were met. When no LVE but more distinct LVD was present (LVEF < 45%), hypokinetic non-dilated cardiomyopathy (HNDC) was diagnosed [17]. In the presence of other relevant abnormalities, such as LVE > 117%, cardiac conduction defect (CCD), or atrial or ventricular arrhythmias unexplained by other conditions, we used the term indeterminate cardiomyopathy (indeterminate CM).

CCD included atrioventricular block (AVB) and left bundle branch block (LBBB). First-degree AVB was defined by a PR interval >200 ms on standard 12-lead ECG. High-degree AVB included type II second degree or third degree AVB. Atrial arrhythmias included atrial fibrillation, flutter, and paroxysmal tachycardia lasting \geq 30 s. Non-sustained ventricular tachycardia (nsVT) was defined as \geq 3 consecutive ventricular beats at >120 bpm and a duration for <30 s on 24-h Holter electrocardiographic monitoring. If the VT lasted over 30 s, it was considered sustained (sVT). Ventricular arrhythmias included sVT, nsVT, and frequent ventricular extrasystoles (>500/24 h).

HF was recognized in the presence of typical symptoms (e.g., breathlessness or fatigue), accompanied by structural and/or functional cardiac abnormalities, resulting in a reduced cardiac output and/or elevated intracardiac pressures. End-stage HF was defined as HTX, implantation of left ventricular assist device, or death caused by HF.

MVA was defined as sudden cardiac death (SCD), cardiopulmonary resuscitation (CPR), or appropriate implantable cardioverter defibrillator (ICD) shock (an ICD discharge for termination of ventricular fibrillation/VT). Death was classified as sudden if it occurred within 1 h of the onset of cardiac manifestations, during sleep (in the absence of previous hemodynamic deterioration), or within 24 h after the patient was last seen apparently stable clinically. Sudden cardiac arrest (SCA) was defined as occurring within 1 h of the onset of acute symptoms and was reversed by CPR. Relatives included all probands' family members with *LMNA* gene mutation confirmed as a result of cascade screening, irrespective of degree of kinship. A family history of SCD was considered positive if \geq 1 first degree relative had died suddenly before the age of 60 years.

2.2. Biomarkers' Measurements

The plasma levels of NT-proBNP were measured by the electrochemiluminescent immunoassays Elecsys 2010 (Roche, Mannheim, Germany). Two cutoff points of NT-proBNP were used: 125 pg/mL, upper limit of normal values in the assay defined by the manufacturer, and 150 pg/mL after analysis of a receiver-operating characteristic curve (ROC), identifying the criterion of maximum sensitivity and specificity for MVA occurrence. The plasma levels of cardiac troponin T were measured by the troponin T hs-STAT (Roche, Mannheim, Germany). Again, two cutoff points for hsTnT were used: 14 ng/L, upper limit of normal values in the assay defined by the manufacturer, and 20 ng/L, after the ROC analysis which fulfils the criterion of maximum sensitivity and specificity for MVA occurrence. All measurements were performed in the National Institute of Cardiology laboratory.

2.3. Mutation Screening

DNA was obtained from the peripheral blood by phenol extraction or the salting-out method. Direct Sanger sequencing of twelve *LMNA* exons (canonical transcript NM_170707.4) including flanking intronic regions was performed in 16 probands as described previously [15]. In one case, it was followed by multiplex ligation-dependent probe amplification (MRC Holland, Amsterdam, Netherlands) [18]. In 5 probands, next generation sequencing (NGS) was performed. Libraries were prepared using an Illumina: TruSeq Exome Enrichment Kit for whole exome sequencing (WES) in 1 proband, Nextera Rapid Capture Exome Library Kit with different enrichment probes for TruSight One (TSO) gene panels in 2 probands and TruSight Cardio (TSC) Sequencing Kit in 2 probands (Illumina, San Diego, CA, USA). WES and TSO libraries were sequenced on Illumina HiSeq1500 and TSC on Illumina MiSeq. Library preparation, sequencing, and data analysis were performed as described previously [19]. Variants identified in probands were followed up by Sanger sequencing of relatives' DNA using BigDye Terminator v3.1/v1.1 Cycle Sequencing Kit (Life Technologies) according to the

manufacturer’s instructions and the 3500xL/3130xL Genetic Analyzer (Life Technologies, Carlsbad, CA, USA). The results were analysed with Variant Reporter 1.1 Software (Life Technologies). Non-missense mutations included insertions, deletions, nonsense mutations, or mutations affecting splicing.

2.4. Statistical Analysis

All results for categorical variables were presented as numbers and percentages and, for continuous variables, as mean and standard deviation (SD) or median and quartiles (Q1:25th–Q2:75th percentiles). The Fisher exact test was used for comparison of categorical variables. The differences between continuous variables were tested by Student’s t-test (for two independent samples and for paired observation, normally distributed data) or, in the case of irregular distribution, nonparametric Mann–Whitney and paired signed rank tests. A receiver-operating characteristic curve (ROC) analysis was used to assess the cutoff point of the markers for the prediction of events (supplementary Figure S1). The optimal cutoff was defined as the value with the maximal sum of sensitivity and specificity. Event analysis over time was made by using the univariable and multiple Cox proportional-hazards regression model. In order to indicate independent predictors of events, the stepwise variable selection procedure was used. Risk was quantified as a hazard ratio with 95% confidence interval (CI). Survival curves were constructed by the Kaplan–Meier method and compared by the log-rank test. We used two different start points for the time-to-event analysis: from the first cardiologic assessment in our centre and from date of birth to assess life-time risk. In subjects without an event, the follow-up period extended to the most recent evaluation or the date of July 31st, 2019. All hypotheses were two-tailed with a 0.05 type I error. All statistical analyses were performed using SAS statistical software, version 9.4 (SAS Institute, Cary, NC, USA) and Statistica v16.

3. Results

3.1. Molecular Findings in the Study Cohort

We identified 18 different *LMNA* variants (three identified twice) in 21 probands (Table 1). Of the 18 variants, 14 were described before [13–15,18,20–28] and four were novel. The identified variants were pathogenic ($n = 12$) or likely pathogenic ($n = 6$) according to ACMG criteria. Figure 1 shows the distribution of *LMNA* variants found in this study in the topology of the *LMNA* gene. Eight (38.1%) of 21 probands carried *LMNA* missense variants. Of the 13 probands with non-missense variants, seven had nonsense variants, four had frameshift variants, one had a large deletion, and one was splice variant. Non-missense variants were expected to result in truncation of the protein or, in one case (c.640-10A>G), in aberrant splicing resulting in a three amino acid insertion [29]. In five probands which had NGS performed, no additional likely pathogenic/pathogenic rare variants according to ACMG criteria in coding/splicing regions of genes causing DCM were found.

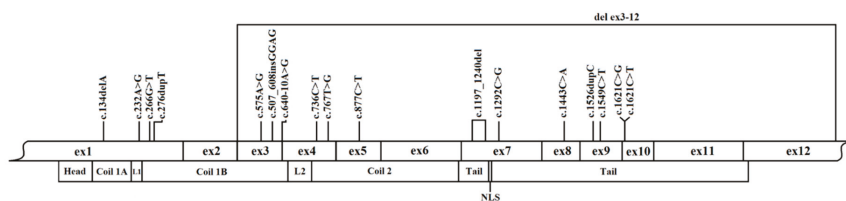


Figure 1. Distribution of *LMNA* variants in our study cohort. Legend: NLS, nuclear localization signal.

Table 1. Genotyping results and clinical phenotypes in probands.

LMNA Gene Mutation	Protein Mutation	Type	Exon (NLS Class)	ACMG Classification	No. of Probands/Relatives	Proband Phenotype	References
c.134delA	p.Tyr45Ser fsTer51	truncation	1 (1)	pathogenic	1/1	HNDC, AVB, AF, nsVT, HTX	novel
c.232A>G	p.Lys78Glu	missense	1 (1)	likely pathogenic	1/1	DCM, SCA, AVB, HTX	Koungiannidis et al. [20]
c.266G>T	p.Arg89Leu	missense	1 (1)	likely pathogenic	1/0	DCM, AVB, AF, HTX	Pasotti et al. [21], Taylor et al. [13], Saj et al. [15]
c.276dupT	p.Asp93Ter	truncation	1 (1)	pathogenic	1/3	DCM, AF, nsVT	novel
del_ex3-12	n/a	truncation	2/3 (1)	pathogenic	1/0	DCM, AVB, AF, nsVT, ICD shocks, HTX	Gupta et al. [18], Saj et al. [15]
c.575A>G	p.Asp192Gly	missense	3 (1)	likely pathogenic	2/1	DCM, AVB, AF, nsVT, HTX/HF death	Sylvius et al. [14], Saj et al. [15], Fidzianska et al. [28]
c.607_608 insGCAG	p.Glu219ClyfsTer12	truncation	3 (1)	pathogenic	1/4	DCM, AVB, sVT, HTX	novel
c.640-10A>G	n/a	inframe insertion	3/4 (1)	likely pathogenic	1/2	DCM, sVT	Otomo et al. [29], Ito et al. [27]
c.736C>T	p.Gln246Ter	truncation	4 (1)	pathogenic	1/0	DCM, AVB, AF, nsVT, HF death	Pasotti et al. [21], Saj et al. [15]
c.767T>G	p.Val256Gly	missense	4 (1)	likely pathogenic	1/0	DCM, AF, AVB, nsVT, HF death	Saj et al. [15]
c.877C>T	p.Gln293Ter	truncation	5 (1)	pathogenic	1/0	LVE, AVB, AF, nsVT	novel
c.1197_1240del	p.Gly400Arg fsTer11	truncation	7 (1)	pathogenic	1/2	DCM, SCA, ICD shocks, AVB, AF	Saj et al. [15]
c.1292C>G	p.Ser431Ter	truncation	7 (2)	pathogenic	1/5	DCM, AVB, nsVT, HTX	Saj et al. [15]
c.1443C>A	p.Tyr481Ter	truncation	8 (2)	pathogenic	1/3	DCM, AVB, AF, nsVT, HTX	Sylvius et al. [14]
c.1526dupC	p.Thr510Tyr fsTer42	truncation	9 (2)	pathogenic	1/4	DCM, AVB, AF, nsVT, HTX	Saj et al. [15], Pugh et al. [26]
c.1549C>T	p.Gln517Ter	truncation	9 (2)	pathogenic	2/3	DCM, SCA, AVB, AF, nsVT	Stallmeyer et al. [23]
c.1621C>G	p.Arg541Gly	missense	10 (2)	likely pathogenic	1/2	DCM, nsVT	Malek et al. [22], Saj et al. [15]
c.1621C>T	p.Arg541Cys	missense	10 (2)	likely pathogenic	2/1	DCM, AVB, SCA, HTX	Forissier et al. [24], Hrookana et al. [25], Saj et al. [15], Pugh et al. [26]

Legend: ACMG: American College of Medical Genetics and Genomics; AF: atrial fibrillation; AVB: atrioventricular block; DCM: dilated cardiomyopathy; HF: heart failure; HNDC: hypokinetic non-dilated cardiomyopathy; HTX: heart transplantation; ICD: implantable cardioverter-defibrillator; LVE: left ventricular enlargement; n/a: not applicable; NLS: nuclear localization signal; nsVT: non-sustained ventricular tachycardia; sVT: sustained ventricular tachycardia.

3.2. Study Population and Clinical Characteristics

Figure 2 shows the diagnoses of the probands and relatives at baseline and at last follow-up. At baseline, the majority of probands had DCM ($n = 17.81\%$), one (5%) HNDC, and three (14%) indeterminate CM, while among relatives, four (13%) had DCM, 18 (56%) had indeterminate CM, and ten (31%) had no signs of cardiomyopathy.

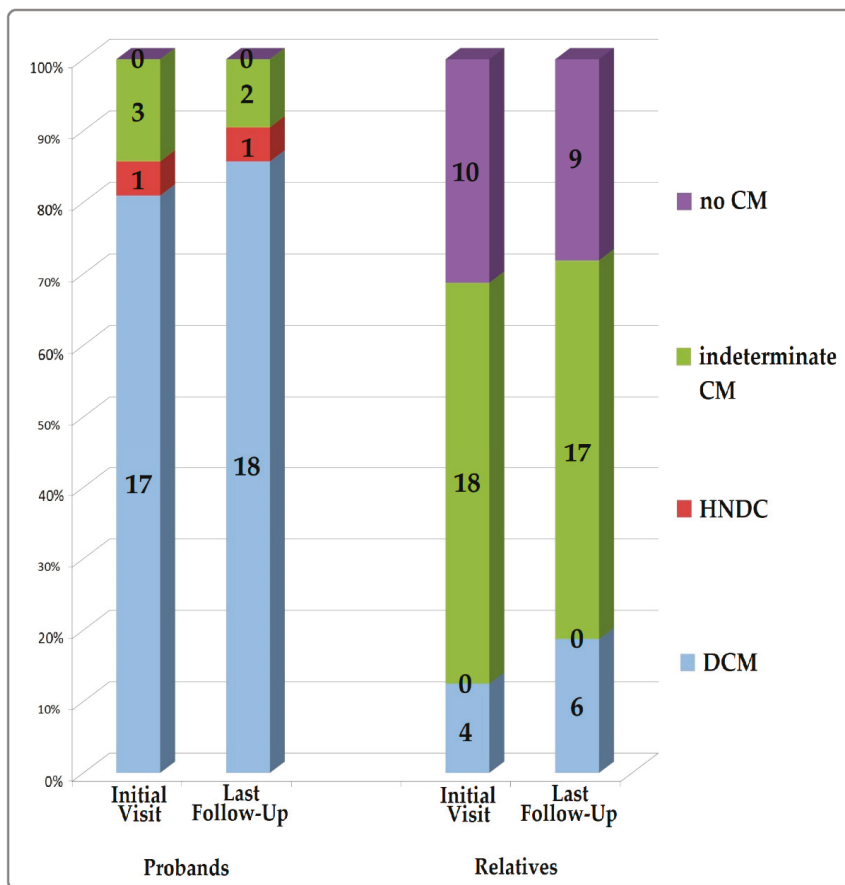


Figure 2. Diagnoses of probands and relatives at initial visit and last follow-up. Legend: CM: cardiomyopathy; DCM: dilated cardiomyopathy; HNDC: hypokinetic non-dilated cardiomyopathy.

Table 2 shows baseline clinical characteristics of 21 probands and 32 relatives. In the study group, relatives were a decade younger than probands ($p = 0.002$), allowing us to better understand the early phase of the disease. As expected, HF symptoms with advancement of left ventricular dysfunction were more frequent in probands as well as arrhythmias and ICD requirements. Of interest, while AVB was present in nearly half of the relatives (43.7%), LBBB was found in probands only. In line with the previous findings, the presence of elevated NT-proBNP was significantly more common in probands than in relatives ($p = 0.003$); however, the presence of elevated levels of hsTnT merely tended to be more common in probands versus relatives ($p = 0.065$), indicating that elevated hsTnT might be a useful biomarker of the onset of the disease. Of note, elevated hsTnT level tended to be more common than elevated creatine phosphokinase (CK) activity, a widely accepted marker of syndromic form of cardiomyopathy (48% vs. 28% of *LMNA* mutation carriers respectively, $p = 0.06$).

Table 2. Baseline clinical characteristics of LMNA variant carriers at initial visit.

	Total n = 53	Probands n = 21 (39.6%)	Relatives n = 32 (60.4%)	p
Age (years)	33.2 ± 12.4	39.6 ± 10.0	29.0 ± 12.2	0.002
Men, n (%)	31 (58.5%)	14 (66.7%)	17 (53.1%)	0.328
LMNA missense variants, n (%)	13 (24.5%)	8 (38.1%)	5 (15.6%)	0.063
Symptoms				
Syncope, n (%) (n = 49)	12 (24.5%)	8 (42.1%)	4 (13.3%)	0.039
Family history of SCD <60 years, n (%) (n = 50)	25 (50%)	8 (44.4%)	17 (53.1%)	0.556
Heart failure, n (%)	19 (35.9%)	15 (71.4%)	4 (12.5%)	<0.0001
NYHA class ≥ 3, n (%)	7 (13.2%)	6 (28.6%)	1 (3.1%)	0.012
Arrhythmias				
Atrial arrhythmias, n (%) (n = 52)	19 (36.5%)	13 (61.9%)	6 (19.4%)	0.002
nsVT, n (%) (n = 50)	30 (60%)	19 (100%)	11 (35.5%)	<0.0001
SCA/sVT, n (%) (n = 50)	9 (18.0%)	7 (36.8%)	2 (6.4%)	0.018
CCD				
LBBB, n (%) (n = 47)	8 (17.0%)	8 (50.0%)	0 (0%)	<0.0001
AV block (≥1), n (%) (n = 52)	31 (59.6%)	17 (85.0%)	14 (43.7%)	0.003
Cardiomyopathies				
LVEF < 50%, n (%)	19 (35.8%)	15 (71.4%)	4 (12.5%)	<0.0001
LVEF (%)	50.5 ± 16.2	36.9 ± 15.7	59.4 ± 8.9	<0.0001
LVE > 112%, n (%)	28 (52.8%)	18 (85.7%)	10 (31.3%)	0.0001
LVEDD (mm)	53.7 ± 8.7	59.1 ± 8.2	50.2 ± 7.2	0.0001
Biomarkers				
CK (IU/l) (n = 46)	162.5 (93–291)	121 (83–253)	178 (93–458)	0.157
elevated CK, n (%) (n = 46)	13 (28.3%)	2 (10.5%)	11 (40.7%)	0.025
hs Troponin T (ng/L) (n = 42)	13.6 (7.0–23.9)	19.2 (13.4–28.9)	11.9 (5.7–19.9)	0.018
elevated hs Troponin T, n (%) (n = 42)	20 (47.6%)	10 (66.7%)	10 (37.0%)	0.065
NT-proBNP (pg/mL) (n = 42)	161.0 (72.7–683.7)	683.7 (224–1211)	84.9 (52.4–183.0)	<0.001
elevated NT-proBNP, n (%) (n = 42)	23 (54.8%)	14 (82.3%)	9 (36.0%)	0.003
Comorbidities				
Coronary artery disease, n (%)	2 (3.8%)	1 (4.8%)	1 (3.1%)	1.000
Hypertension, n (%)	6 (11.3)	1 (4.8%)	5 (15.6%)	0.384
Implantable devices				
ICD in primary PPX, n (%)	8 (15.1%)	5 (23.8%)	3 (9.4%)	0.204
ICD in secondary PPX, n (%)	8 (15.1%)	6 (28.6%)	2 (6.3%)	0.047
ICD/CRT-D implantation, n (%)	16 (30.2%)	11 (52.4%)	5 (15.6%)	0.004
Medication				
β-Blocker, n (%)	25 (47.2%)	16 (76.2%)	9 (28.1%)	<0.001
ACE-I or ARB, n (%)	21 (39.6%)	17 (81.0%)	4 (12.5%)	<0.0001
MRA, n (%)	6 (11.3%)	6 (28.6%)	0 (0%)	0.002

Legend: Number of subjects is expressed as n (%). Continuous variables are shown as mean ± SD or median and quartiles (Q1:25th–Q2:75th percentiles). ACE-I: angiotensin converting enzyme inhibitor; ARB: angiotensin receptor blocker; AV block: atrioventricular block; CCD: cardiac conduction defect; CK: creatine phosphokinase; CRT-D: cardiac resynchronization therapy defibrillator; hs: high sensitive; ICD: implantable cardioverter defibrillator; LBBB: left bundle branch block; LVE: left ventricular enlargement; LVEDD: left ventricular end-diastolic dimension; LVEF: left ventricular ejection fraction; MRA: mineralocorticoid receptor antagonist; nsVT: non-sustained ventricular tachycardia; NT-proBNP: N-terminal pro-brain natriuretic peptide; NYHA class: New York Heart Association functional class; PPX: prophylaxis; SCA: sudden cardiac arrest; SCD: sudden cardiac death; sVT: sustained ventricular tachycardia.

3.3. Penetrance of Cardiolaminopathy Indicators

Penetrance of cardiac disorders along with abnormal levels of cardiac biomarkers was age dependent (Figure 3). During lifespan, the earliest abnormality, emerging in the second decade of life in 12% of LMNA variant carriers and in the third decade in 27%, was hsTnT level >14 ng/L, followed by the presence of AVB and HF (each 5% in the 2nd and 15% in the 3rd decade of life) and MVA (2% and 13%, respectively). Penetrance of cardiolaminopathy indicators was nearly complete in the 7th

decade of life with 98% of patients presenting with AVB, 100% with SVA, 90% with HF, 92% with serum biomarker hsTnT >14 ng/L, and 100% with NT-proBNP >125 pg/mL.

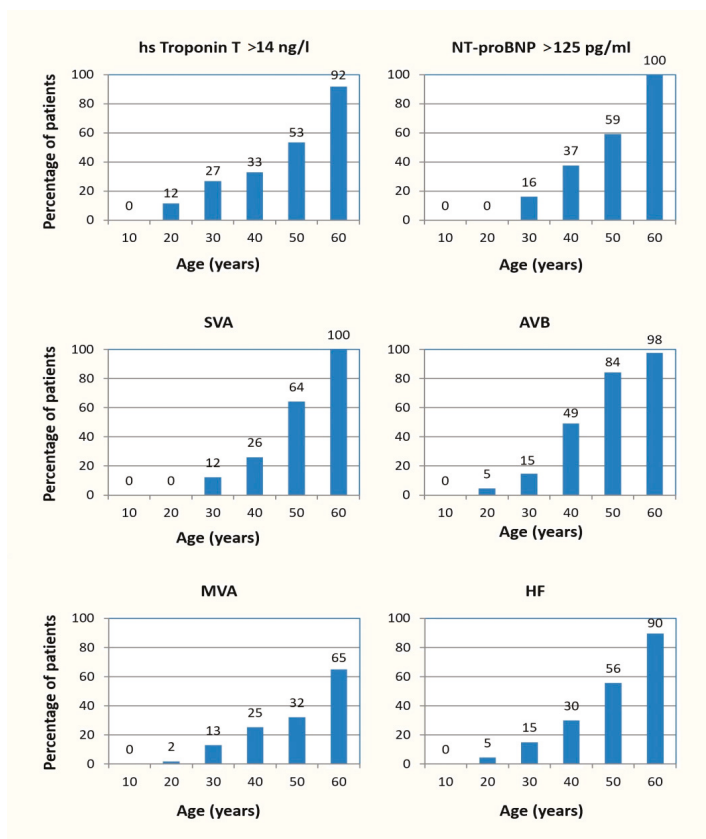


Figure 3. Penetrance of cardiolaminopathy indicators. Legend: AVB: atrioventricular block; HF: heart failure; hs: highly sensitive; MVA: malignant ventricular arrhythmia; NT-proBNP: N-terminal pro-brain natriuretic peptide; SVA: supraventricular arrhythmia.

During the follow-up, there was a modest but significant increase in the hsTnT level (Table 3), possibly reflecting progressive myocardial damage. The change in NT-proBNP level was much more noticeable, reflecting that HF was more common and advanced at the end of the follow-up period. Changes in cardiac biomarkers' concentrations measured during the initial and subsequent visits in patients with two or more measurements are shown in Figures S2 and S3.

Table 3. Change in circulating biomarkers' levels between baseline and last measurement.

Biomarker	Baseline	Last Measurement	Relative Change	p
hs Troponin T (ng/L) n = 32	15.1 (7.6–24.7)	17.4 (9.6–30.6)	+15.2%	0.002
NT-proBNP (pg/mL) n = 27	223.8 (72.7–683.7)	478.3 (86.3–1353)	+114%	0.0003

The results are shown as median and quartiles (Q1:25th–Q2:75th percentiles). Legend: hs Troponin T: highly sensitive troponin T; NT-proBNP: N-terminal prohormone brain natriuretic peptide.

3.4. Phenotypic Differences in Missense versus Non-Missense LMNA Variant Carriers

We assessed clinical differences among non-missense and missense variant carriers at last follow-up. Of interest, missense variant carriers had LBBB more frequently (54.5% vs. 14.3%, $p = 0.017$) and more advanced cardiomyopathy with regard to left ventricular size and function (Table 4). Of note, all subjects with elevated CK activity were found among non-missense variant carriers (supplementary Table S4). Other variables were comparable; in particular, we found no significant differences with regard to cardiac biomarkers' concentrations.

Table 4. Clinical Characteristics of LMNA variant carriers at last follow-up.

	Total n = 53	Non-Missense n = 40	Missense n = 13	p
Age (years)	38.6 ± 12.5	39.6 ± 13.3	35.5 ± 9.6	0.318
Men, n (%)	31 (58.5%)	24 (60.0%)	7 (53.8%)	0.696
Probands, n (%)	21 (39.6%)	13 (32.5%)	8 (61.5%)	0.063
Symptoms				
Heart failure, n (%)	27 (50.9%)	18 (45.0%)	9 (69.2%)	0.129
NYHA class ≥ 3, n (%)	17 (32.1%)	11 (27.5%)	6 (46.2%)	0.306
Arrhythmias				
Atrial arrhythmias, n (%) (n = 52)	24 (46.2%)	20 (51.3%)	4 (30.8%)	0.199
nsVT, n (%) (n = 51)	35 (68.6%)	27 (69.2%)	8 (66.7%)	1.000
CCD				
LBBB, n (%) (n = 39)	10 (25.6%)	4 (14.3%)	6 (54.5%)	0.017
AV block (≥1), n (%)	36 (67.9%)	29 (72.5%)	7 (53.8%)	0.306
Cardiomyopathies				
LVEF < 50%, n (%)	22 (41.5%)	13 (32.5%)	9 (69.2%)	0.019
LVEF (%)	46.9 ± 17.4	51.9 ± 15.3	38.0 ± 17.9	0.012
LVE > 112%, n (%)	29 (54.7%)	19 (47.5%)	10 (76.9%)	0.064
LVEDD (mm)	54.8 ± 9.1	51.0 ± 10.5	60.1 ± 12.2	0.016
Biomarkers				
hs Troponin T (ng/L) (n = 42)	16.1 (9.9–29.8)	16.2 (9.9–31.5)	13.9 (10.4–17.1)	0.520
elevated hs Troponin T, n (%) (n = 42)	24 (57.1%)	20 (60.6%)	4 (44.4%)	0.462
NT-proBNP (pg/mL) (n = 41)	397.2 (85–1037)	359.3 (84–1012)	722.0 (86–2245)	0.324
elevated NT-proBNP, n (%) (n = 41)	26 (63.4%)	18 (60%)	8 (72.7%)	0.716
Implantable devices				
ICD in primary PPX, n (%)	26 (49.1%)	20 (50.0%)	6 (46.2%)	0.810
ICD in secondary PPX, n (%)	8 (15.1%)	5 (12.5%)	3 (23.1%)	0.389
ICD/CRT-D implantation, n (%)	34 (64.2%)	25 (62.5%)	9 (69.2%)	0.749
Events during follow-up				
Malignant ventricular arrhythmia, n (%)	13 (24.5%)	9 (22.5%)	4 (30.8%)	0.712
Appropriate ICD shock, n (%)	11 (31.4%)	7 (26.9%)	4 (44.4%)	0.416
RF ablation for VA, n (%)	7 (13.2%)	4 (10%)	3 (23.1%)	0.343
Cardiopulmonary resuscitation, n (%)	1 (1.9%)	1 (2.5%)	0 (0%)	1.000
Sudden cardiac death, n (%)	1 (1.9%)	1 (2.5%)	0 (0%)	1.000
End-stage heart failure, n (%)	14 (26.4%)	9 (22.5%)	5 (38.5%)	0.292
Heart transplantation, n (%)	11 (20.8%)	8 (20.0%)	3 (23.1%)	1.000
HF death, n (%)	3 (5.7%)	1 (2.5%)	2 (15.4%)	0.145

Legend: Number of subjects is expressed as n (%). Continuous variables are shown as mean ± SD or median and quartiles (Q1:25th–Q2:75th percentiles). RF ablation: radiofrequency ablation; VA: ventricular arrhythmia.

3.5. Follow-Up and Risk Stratification Including Biomarkers

Mean follow-up was 1769 days, median 1522 (Q1: 771–Q3: 2564). During the follow-up period, 14/53 (26.4%) patients developed end-stage HF: three (5.6%) of them died, and eleven (20.8%) were transplanted. There was one SCD, while another patient had SCA with successful resuscitation.

At the end of follow-up only 19/53 (36%) patients remained free of ICD (including a patient who refused to have an ICD implanted and died suddenly). Of the 34/53 (64%) patients with ICD, 10/34 (29%) experienced adequate ICD discharge.

The disease progressed to end-stage HF only in patients with DCM/HNDC. MVA occurred in 41% of them and in 19% of patients with indeterminate status (supplementary Table S5).

The comparison of clinical data of probands and relatives between the initial and last follow-up visits confirmed progressive character of LMNA-related disease both with regard to HF and to arrhythmia (Table 2 and supplementary Table S6).

The influence of prespecified risk factors on the risk of MVA assessed from the date of the initial evaluation in the subgroup of 44 patients with no history of SCA or sVT and, on the risk of end-stage HF and MVA during lifespan in the whole cohort of 53 patients, is summarized in the Table 5.

Table 5. Potential risk factors affecting MVA-free and HTX-free survival.

	Cumulate Incidence	p-Value Log-Rank	Univariable		Multivariable	
			HR (95% CI)	p-Value Wald	HR (95% CI)	p-Value Wald
MVA, from date of first visit						
at 8 years of follow-up (n = 44)						
Sex: Male vs. Female	24 vs. 20	0.929	1.07 (0.24–4.79)	0.929	-	-
Mutation type: Missense vs. Other	25 vs. 22	0.727	0.69 (0.08–5.73)	0.729	-	-
AV block: yes vs. no	42 vs. 0	0.007	NA	-	-	-
nsVT: yes vs. no	37 vs. 9	0.031	7.38 (0.88–61.7)	0.064	-	-
LVEF: <45% vs. ≥45%	48 vs. 16	0.100	3.32 (0.73–15.04)	0.120	-	-
LVEF: <55% vs. ≥55%	42 vs. 11	0.026	5.54 (1.02–27.78)	0.047	-	-
NT-proBNP: ≥150 vs. <150 pg/mL	67 vs. 6	0.002	13.40 (1.6–112.7)	0.017	10.4 (1.21–89.79)	0.010
hsTn T: ≥20 vs. <20 ng/L	66 vs. 6	0.003	13.16 (1.49–115.8)	0.020	-	-
MVA, from date of birth						
at 60 years (n = 53)						
Status: Proband vs. Relative	65 vs. 62	0.746	1.18 (0.43; 3.29)	0.746	-	-
Sex: Male vs. Female	100 vs. 41	0.087	2.61 (0.84; 8.05)	0.096	-	-
Mutation type: Missense vs. Other	58 vs. 64	0.095	2.52 (0.82–7.72)	0.106	-	-
End-stage HF, from date of birth						
at 60 years (n = 53)						
Status: Proband vs. Relative	83 vs. 41	0.034	3.71 (1.02; 13.47)	0.046	-	-
Sex: Male vs. Female	84 vs. 50	0.004	5.55 (1.52; 20.27)	0.009	6.18 (1.66–23.0)	0.007
Mutation type: Missense vs. other	100 vs. 63	0.041	3.18 (0.99; 10.25)	0.052	3.83 (1.14–12.85)	0.029

Legend: AV block: atrioventricular block; CI: confidence interval; HF: heart failure; hsTnT: high-sensitive Troponin T; HTX: heart transplantation; LVEF: left ventricular ejection fraction; MVA: malignant ventricular arrhythmia; NA: not applicable; nsVT: non-sustained ventricular tachycardia; NT-proBNP: N-terminal prohormone brain natriuretic peptide.

3.5.1. Arrhythmic Risk Stratification During the Follow-Up

The univariable analysis of MVA events during follow-up showed no impact of sex and type of mutation on MVA occurrence and confirmed the involvement of established risk factors, such as the presence of AVB, nsVT, or reduced LVEF (with cutoff value at 55%).

The analysis of the influence of circulating biomarker concentrations on MVA occurrence suggested that circulating biomarker concentrations could be more potent risk factors than established risk factors: hazard ratio for hsTnT with a cutoff value at 20 ng/L was 13.2 (95% CI: 1.5–115.8, $p = 0.020$) and, for NT-proBNP with a cutoff value at 150 pg/mL, was 13.4 (95% CI: 1.6–112.7, $p = 0.017$).

In fact, in multivariable analysis, elevated NT-proBNP level was the only indicator of the occurrence of MVA at 8 years of follow-up (HR: 10.4, 95% CI: 1.21–89.79, $p = 0.010$).

The Kaplan–Meier curves showing MVA-free survival during the follow-up period according to respective risk factors are available online at Figure S7.

3.5.2. Factors Affecting Lifelong Prognosis in Cardiomyopathies

Kaplan–Meier analysis from the date of birth in the whole cohort showed a worse transplant-free survival among probands versus relatives ($p = 0.0339$) (supplementary Figure S8), male vs. female

patients ($p = 0.0041$), and surprisingly in patients with missense vs. other mutations ($p = 0.0412$) (Figure 4). Analogous analysis with respect to MVA events (Figure 5 and supplementary Figure S9) showed trends toward more common MVA among males vs. females ($p = 0.0872$) and patients with missense vs. other variants ($p = 0.0948$) and no impact of the proband status ($p = 0.7469$).

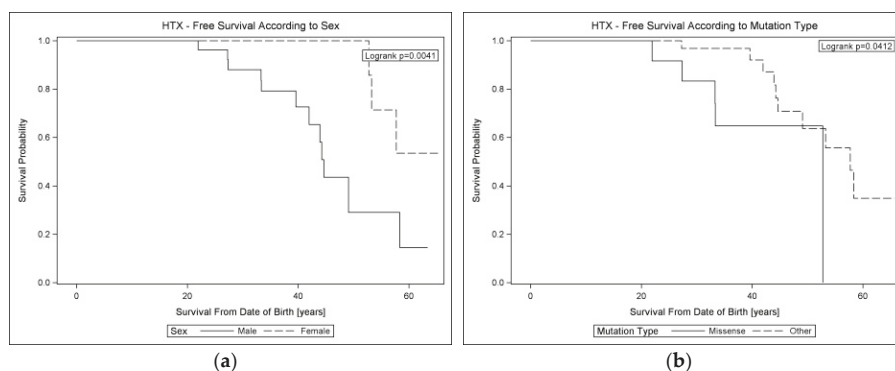


Figure 4. Kaplan–Meier lifelong HTX-free survival curves in cardiomyopathy according to (a) sex and (b) mutation type. Legend: HTX: heart transplantation.

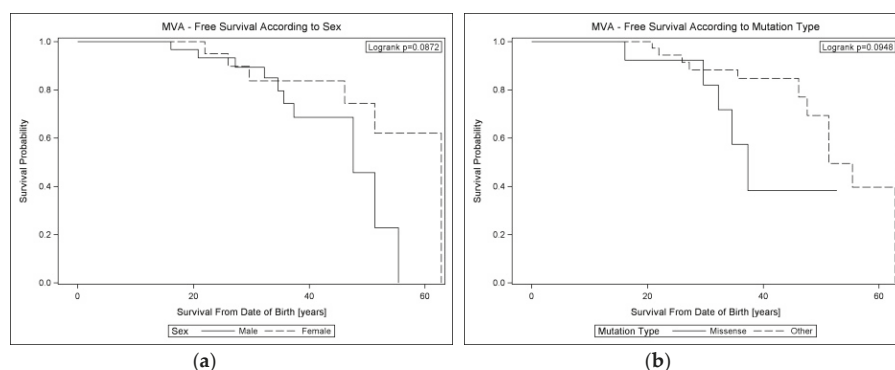


Figure 5. Kaplan–Meier lifelong MVA-free survival curves in cardiomyopathy according to (a) sex and (b) mutation type. Legend: MVA: malignant ventricular arrhythmia.

In multivariable Cox regression analysis (Table 5), we found that male sex (HR: 6.18, 95% CI: 1.66–23.0, $p = 0.007$) and missense variants (HR: 3.83, 95% CI: 1.14–12.85, $p = 0.029$) were independently related with the occurrence of end-stage HF at 60 years.

4. Discussion

4.1. Penetrance of Cardiomyopathy Indicators

A major finding of the study is that the earliest marker of the carrier status in *LMNA*-related cardiomyopathy is elevated hsTnT level, followed by widely recognized features, such as AVB, HF, and MVA [9,10,30]. In 2013, Rapezzi et al. [31] proposed a framework for the clinical approach to diagnosis in cardiomyopathies based on the recognition of diagnostic “red flags” that can be used to guide rational selection of specialized tests. Our study shows that elevated hsTnT level > 14 ng/L was present in two thirds of probands and in more than one third of relatives, indicating that it might be a “red flag” to introduce at least lifestyle modifications in asymptomatic or mildly symptomatic carriers.

To the best of our knowledge, circulating cardiac biomarkers in relation to the disease penetrance or prognosis have not been reported in cardiomyopathies. The role of circulating cardiac biomarkers in the detection of HF has been established [32]. Little is known about the significance of circulating biomarkers in early stage of DCM in humans [33], while routinely used biomarkers (NT-proBNP and hsTnT) are widely accepted in the diagnosis of occult DCM in Doberman Pinschers [34].

In the study, similarly to others, we found high and age-dependent penetrance of cardiac manifestations in *LMNA* mutation carriers [10,21,30]. Despite the fact that our study group was young (mean age at baseline was 33.2 years for all carriers and 29.0 years for the relatives), the majority of relatives (56%) had indeterminate CM and phenotypic expression was absent in only 31% of them. In the study by Kumar et al. [10], 18/35 (51.4%) relatives were phenotypically normal while the study cohort was older than the one we studied (mean age of 41 years). In the study by Pasotti et al. [21], 29/67 (43%) relatives had no signs of cardiomyopathy. This discrepancy may be related to adopted definitions of early stage disease but may also underscore the need of diagnostic vigilance (e.g., repeated 24-h ECG examinations). Of note, the Cardiomyopathy Registry of the EURObservational Research Programme of the European Society of Cardiology [35] showed that Holter monitoring was performed only in 37% of DCM patients. In the setting of cardiomyopathies, it is of crucial importance to monitor asymptomatic carriers with Holter monitoring; however, the appearance of elevated hsTnT concentrations precedes the appearance of arrhythmia, as shown in our study.

4.2. Phenotypic Differences in Missense versus Non-Missense *LMNA* Variants

No significant differences were found with regard to cardiac biomarkers' levels between missense and non-missense *LMNA* variant carriers. A novel finding in this study is the higher frequency of LBBB (54.5% vs. 14.3%, $p = 0.017$) among missense versus non-missense *LMNA* carriers. It cannot however be excluded that the observed difference is dependent on the degree of left ventricular impairment rather than on the mutation type. More advanced heart failure among missense variant carriers may in turn result from the fact that probands constituted almost two thirds of this group but only one third of non-missense variant carriers ($p = 0.063$). In the study by Nishiuchi et al. [36], prevalence of low LVEF and degree of left ventricular dilation was similar in the truncation mutation vs. missense mutation group. There are scarce data on the relationship between the level of conduction defects and type of *LMNA* mutations. Nishiuchi et al. [36] showed that AVB was more common among patients with non-missense variants. In our study, the frequencies of LBBB, right bundle branch block (RBBB), and AVB at baseline were 17%, 0%, and 60%, respectively, while in the recent and largest study to date by Wahbi et al., it was lower with regard to LBBB and AVB (4.6% and 34.7%, respectively), whereas 6% of patients had RBBB. This underlines the differences in the studied populations.

4.3. Arrhythmic Risk Stratification Including Biomarkers

Another interesting finding of our study was the strong, independent association between NT-proBNP level > 150 pg/mL and the occurrence of MVA among *LMNA* mutation carriers.

Recently, several studies defining prognostic markers of SCD in arrhythmogenic DCM and cardiomyopathies have been published [2,7,36,37], with European Society of Cardiology (ESC) guidelines [38] adopting the results of an earlier study by van Rijsingen et al. [7]. Based on retrospective eight-centre analysis, the authors proved that non-missense variants were independently associated with MVA. Similarly, based on retrospective 5-centre analysis, Kumar et al. [10] showed the independent association of non-missense variants with sustained ventricular arrhythmia and death. Wahbi et al. [37] presented an MVA risk prediction model for *LMNA* variant carriers and further stressed the role of non-missense variants as one of significant risk factors along with male sex, nsVT, AVB of 1st and higher degree, and reduced LVEF. In contrast, Pasotti et al. [21] did not show any association between non-missense *LMNA* variants and a worse prognosis, similarly to Captur et al. [39], who recently performed hierarchical cluster analysis of the published literature. In our cohort, we also could not confirm worse MVA-free survival in relation to *LMNA* non-missense variants either during the

follow-up period or from the date of birth, and surprisingly, they were characterized by more favourable prognosis with regard to end-stage HF during lifespan. Further studies are warranted to explain the differences and to better assess the impact of the type of *LMNA* mutations.

The excellent prognostic role of NT-proBNP in patients with HF is widely recognized [40]. The association of raised levels of NT-proBNP and MVA in HF patients was shown previously [41,42]. Nevertheless, it has neither been included in currently used risk models nor has it been evaluated in *LMNA*-related cardiac disorder.

The utility of cardiac troponins in determining prognosis in HF and DCM was shown, primarily in patients with acute HF admitted to hospitals but also in ambulatory care [40,43]. To our knowledge, however, their usefulness has been investigated with regard to HF end-points, such as HF deaths and hospitalizations [43], and not as a predictor of arrhythmic risk. In our study, elevated hsTnT > 20 ng/L was associated with increased MVA occurrence only in univariable analysis; thus, its role as an independent risk factor needs further evaluation. Also, due to recent advances in cardiac biomarker sensing technologies [44], point-of-care (POC) applications can be hopefully used in the management of cardiomyopathies in the foreseeable future.

4.4. Molecular Findings in the Study Cohort

In our study, *LMNA* non-missense mutation carriers constituted nearly two thirds (62%) of the cohort. For comparison, in the study by Nishiuchi et al. [36], they constituted 75% of patients, whereas in the cohorts by Kumar et al. [10] and van Rijnsingen et al. [7], they represented 42% and 45%, respectively. In the study by Wahbi et al. [37], carriers of non-missense variants were less common in the derivation sample (29%) but better represented in the smaller validation sample (46%).

4.5. Study Limitations

The major limitation of the study is small sample size due to its single-centre character and, hence, small number of major cardiovascular events, precluding the use of multivariate analysis models. The retrospective observational design of the study may include confounders. This study comes from a tertiary referral centre, one of two leading cardiological centres in Poland performing HTX. Therefore, patients referred to this tertiary referral centre may present with more severe disease than patients usually admitted in other hospitals.

5. Conclusions

LMNA mutation-related cardiac disorders are associated with high and age-dependent penetrance of cardiac manifestations, rapid progression to end-stage HF, and high incidence of life-threatening arrhythmic events. Elevated hsTnT level seems the earliest abnormality emerging in the course of cardiomyopathies and may facilitate early detection of the *LMNA* carrier status. Circulating cardiac biomarkers, especially increased NT-proBNP level, may be helpful in arrhythmic risk stratification.

Supplementary Materials: The following are available online at <http://www.mdpi.com/2077-0383/9/5/1443/s1>. Figure S1. Receiver-operating characteristic curves used to assess the cutoff points of the biomarkers for prediction of MVA. Figure S2. Highly sensitive troponin T level profiles at baseline and during follow-up visits on a logarithmic scale. Figure S3. N-terminal pro-brain natriuretic peptide level profiles at baseline and during follow-up visits. Table S4. Baseline clinical characteristics of *LMNA* variant carriers at initial visit according to mutation type. Table S5. Comparison of outcome according to diagnosis at initial visit. Table S6. Clinical characteristics of *LMNA* variant carriers at last follow-up according to proband status. Figure S7. Kaplan–Meier MVA-free survival curves during follow-up in patients with cardiomyopathy and no prior history of sudden cardiac arrest or sustained ventricular tachycardia. Figure S8. Kaplan–Meier lifelong HTX-free survival curves in cardiomyopathy according to proband status. Figure S9. Kaplan–Meier lifelong MVA-free survival curves in cardiomyopathy according to proband status.

Author Contributions: Conceptualization, P.C. and Z.T.B.; data curation, P.C., E.M., M.F., G.T., M.S.-W., and B.F.-N.; formal analysis, P.C., and I.K.; investigation, P.C., E.M., M.F., M.S.-M., G.T., M.S.-W., E.K.B., B.F.-N., M.L., A.O., M.B., M.K., F.T., J.G., T.Z., R.P., and Z.T.B.; methodology, P.C., E.M., I.K., R.P., and Z.T.B.; project administration, Z.T.B.; supervision, R.P. and Z.T.B.; visualization, P.C., I.K., and G.T.; writing—original draft, P.C., I.K., G.T.,

and Z.T.B.; writing—review and editing, P.C., E.M., I.K., M.F., M.S.-M., G.T., M.S.-W., E.K.B., B.F.-N., M.L., A.O., M.B., M.K., F.T., J.G., T.Z., R.P., and Z.T.B.. All authors have read and agreed to the published version of the manuscript.

Funding: The work of P.C., G.T., and Z.T.-B. was supported by NCBiR ERA-CVD DETECTIN-HF/2017 IB.4/II/17 grant.

Conflicts of Interest: The authors declare no conflict of interest. The funders had no role in the design of the study; in the collection, analyses, or interpretation of data; in the writing of the manuscript, or in the decision to publish the results.

References

1. Hershberger, R.E.; Morales, A. *Dilated Cardiomyopathy Overview*; Adam, M.P., Ardinger, H.H., Pagon, R.A., Wallace, S.E., Bean, L.J.H., Stephens, K., Amemiya, A., Eds.; GeneReviews(R): Seattle, WA, USA, 1993.
2. Spezzacatene, A.; Sinagra, G.; Merlo, M.; Barbatì, G.; Graw, S.L.; Brun, F.; Slavov, D.; Di Lenarda, A.; Salcedo, E.E.; Towbin, J.A.; et al. Arrhythmogenic Phenotype in Dilated Cardiomyopathy: Natural History and Predictors of Life-Threatening Arrhythmias. *J. Am. Heart Assoc.* **2015**, *4*, e002149. [[CrossRef](#)] [[PubMed](#)]
3. Peters, S.; Kumar, S.; Elliott, P.; Kalman, J.M.; Fatkin, D. Arrhythmic Genotypes in Familial Dilated Cardiomyopathy: Implications for Genetic Testing and Clinical Management. *Heart Lung Circ.* **2019**, *28*, 31–38. [[CrossRef](#)] [[PubMed](#)]
4. Begay, R.L.; Graw, S.L.; Sinagra, G.; Asimaki, A.; Rowland, T.J.; Slavov, D.B.; Gowan, K.; Jones, K.L.; Brun, F.; Merlo, M.; et al. Filamin C Truncation Mutations Are Associated With Arrhythmogenic Dilated Cardiomyopathy and Changes in the Cell-Cell Adhesion Structures. *JACC Clin. Electrophysiol.* **2018**, *4*, 504–514. [[CrossRef](#)] [[PubMed](#)]
5. Ortiz-Genga, M.; Cuenca, S.; Ferro, M.D.; Zorio, E.; Aranda, R.S.; Climent, V.; Padron-Barthe, L.; Duro-Aguado, I.; Jiménez-Jáimez, J.; Hidalgo-Olivares, V.M.; et al. Truncating FLNC Mutations Are Associated With High-Risk Dilated and Arrhythmogenic Cardiomyopathies. *J. Am. Coll. Cardiol.* **2016**, *68*, 2440–2451. [[CrossRef](#)]
6. Augusto, J.; Eiros, R.; Nakou, E.; Moura-Ferreira, S.; A Treibel, T.; Captur, G.; Akhtar, M.M.; Protonotarios, A.; Gossios, T.D.; Savvatis, K.; et al. Dilated cardiomyopathy and arrhythmogenic left ventricular cardiomyopathy: A comprehensive genotype-imaging phenotype study. *Eur. Heart J. Cardiovasc. Imaging* **2019**. [[CrossRef](#)]
7. Van Rijsingen, I.A.; Arbustini, E.; Elliott, P.M.; Mogensen, J.; Hermans-van Ast, J.F.; van der Kooij, A.J.; van Tintelen, J.P.; van den Berg, M.P.; Pilotto, A.; Pasotti, M.; et al. Risk factors for malignant ventricular arrhythmias in lamin a/c mutation carriers a European cohort study. *J. Am. Coll. Cardiol.* **2012**, *59*, 493–500. [[CrossRef](#)]
8. Captur, G.; Bilińska, Z.; Arbustini, E. Lamin missense mutations—the spectrum of phenotype variability is increasing. *Eur. J. Heart Fail.* **2018**, *20*, 1413–1416. [[CrossRef](#)]
9. Arbustini, E.; Pilotto, A.; Repetto, A.; Grasso, M.; Negri, A.; Diegoli, M.; Campana, C.; Scelsi, L.; Baldini, E.; Gavazzi, A.; et al. Autosomal dominant dilated cardiomyopathy with atrioventricular block: A lamin A/C defect-related disease. *J. Am. Coll. Cardiol.* **2002**, *39*, 981–990. [[CrossRef](#)]
10. Kumar, S.; Baldinger, S.H.; Gandjbakhch, E.; Maury, P.; Sellal, J.M.; Androulakis, A.F.; Waintraub, X.; Charron, P.; Rollin, A.; Richard, P.; et al. Long-Term Arrhythmic and Nonarrhythmic Outcomes of Lamin A/C Mutation Carriers. *J. Am. Coll. Cardiol.* **2016**, *68*, 2299–2307. [[CrossRef](#)]
11. Ollila, L.; Nikus, K.; Holmström, M.; Jalanko, M.; Jurkko, R.; Kaartinen, M.; Koskenvuo, J.; Kuusisto, J.; Kärkkäinen, S.; Palojoki, E.; et al. Clinical disease presentation and ECG characteristics of LMNA mutation carriers. *Open Heart* **2017**, *4*, e000474. [[CrossRef](#)]
12. Fatkin, D.; Macrae, C.; Sasaki, T.; Wolff, M.R.; Porcu, M.; Frenneaux, M.; Atherton, J.; Vidaillet, H.J.; Spudich, S.; De Girolami, U.; et al. Missense Mutations in the Rod Domain of the Lamin A/C Gene as Causes of Dilated Cardiomyopathy and Conduction-System Disease. *N. Engl. J. Med.* **1999**, *341*, 1715–1724. [[CrossRef](#)] [[PubMed](#)]
13. Taylor, M.R.G.; Fain, P.R.; Sinagra, G.; Robinson, M.L.; Robertson, A.D.; Carniel, E.; Di Lenarda, A.; Bohlmeier, T.J.; A Ferguson, D.; Brodsky, G.L.; et al. Natural history of dilated cardiomyopathy due to lamin A/C gene mutations. *J. Am. Coll. Cardiol.* **2003**, *41*, 771–780. [[CrossRef](#)]

14. Sylvius, N.; Bilinska, Z.T.; Veinot, J.P.; Fidzianska, A.; Bolongo, P.M.; Poon, S.; McKeown, P.; Davies, R.; Chan, K.-L.; Tang, A.S.L.; et al. In vivo and in vitro examination of the functional significances of novel lamin gene mutations in heart failure patients. *J. Med. Genet.* **2005**, *42*, 639–647. [[CrossRef](#)]
15. Saj, M.; Bilinska, Z.T.; Tarnowska, A.; Sioma, A.; Bolongo, P.; Sobieszczńska-Malek, M.; Michalak, E.; Golen, D.; Mazurkiewicz, L.; Malek, L.A.; et al. LMNA mutations in Polish patients with dilated cardiomyopathy: Prevalence, clinical characteristics, and in vitro studies. *BMC Med Genet.* **2013**, *14*, 55. [[CrossRef](#)]
16. Richards, S.; Aziz, N.; Bale, S.; Bick, D.; Das, S.; Gastier-Foster, J.; Grody, W.W.; Hegde, M.; Lyon, E.; Spector, E.; et al. Standards and guidelines for the interpretation of sequence variants: A joint consensus recommendation of the American College of Medical Genetics and Genomics and the Association for Molecular Pathology. *Genet. Med.* **2015**, *17*, 405–423. [[CrossRef](#)]
17. Pinto, Y.M.; Elliott, P.; Arbustini, E.; Adler, Y.; Anastasakis, A.; Böhm, M.; Duboc, D.; Gimeno, J.; De Groote, P.; Imazio, M.; et al. Proposal for a revised definition of dilated cardiomyopathy, hypokinetic non-dilated cardiomyopathy, and its implications for clinical practice: A position statement of the ESC working group on myocardial and pericardial diseases. *Eur. Heart J.* **2016**, *37*, 1850–1858. [[CrossRef](#)] [[PubMed](#)]
18. Gupta, P.; Bilinska, Z.T.; Sylvius, N.; Boudreau, E.; Veinot, J.P.; Labib, S.; Bolongo, P.M.; Hamza, A.; Jackson, T.; Płoski, R.; et al. Genetic and ultrastructural studies in dilated cardiomyopathy patients: A large deletion in the lamin A/C gene is associated with cardiomyocyte nuclear envelope disruption. *Basic Res. Cardiol.* **2010**, *105*, 365–377. [[CrossRef](#)]
19. Płoski, R.; Pollak, A.; Müller, S.; Franaszczyk, M.; Michalak, E.; Kosińska, J.; Stawinski, P.; Spiewak, M.; Seggewiss, H.; Bilinska, Z.T. Does p.Q247X in TRIM63 cause human hypertrophic cardiomyopathy? *Circ. Res.* **2014**, *114*, 2–5. [[CrossRef](#)]
20. Kourgiannidis, G.; Anastasakis, A.; Lampropoulos, K.; Iliopoulos, T. A patient with ventricular tachycardia due to a novel mutation of the lamin A/C gene: Case presentation and mini review. *Hellenic. J. Cardiol.* **2013**, *54*, 326–330.
21. Pasotti, M.; Klersy, C.; Pilotto, A.; Marziliano, N.; Rapezzi, C.; Serio, A.; Mannarino, S.; Gambarin, F.I.; Favalli, V.; Grasso, M.; et al. Long-Term Outcome and Risk Stratification in Dilated Cardiomyopathies. *J. Am. Coll. Cardiol.* **2008**, *52*, 1250–1260. [[CrossRef](#)]
22. Malek, L.A.; Labib, S.; Mazurkiewicz, L.; Saj, M.; Płoski, R.; Tesson, F.; Bilinska, Z.T. A new c.1621 C>G, p.R541G lamin A/C mutation in a family with DCM and regional wall motion abnormalities (akinesia/dyskinesia): Genotype–phenotype correlation. *J. Hum. Genet.* **2010**, *56*, 83–86. [[CrossRef](#)]
23. Stallmeyer, B.; Koopmann, M.; Schulze-Bahr, E. Identification of Novel Mutations in LMNA Associated with Familial Forms of Dilated Cardiomyopathy. *Genet. Test. Mol. Biomarkers* **2012**, *16*, 543–549. [[CrossRef](#)] [[PubMed](#)]
24. Forissier, J.F.; Bonne, G.; Bouchier, C.; Duboscq-Bidot, L.; Richard, P.; Wisniewski, C.; Briault, S.; Moraine, C.; Dubourg, O.; Schwartz, K.; et al. Apical left ventricular aneurysm without atrio-ventricular block due to a lamin A/C gene mutation. *Eur. J. Heart Fail. J. Work. Group Heart Fail. Eur. Soc. Cardiol.* **2003**, *5*, 821–825.
25. Hookana, E.; Junntila, M.J.; Särkioja, T.; Sormunen, R.; Niemelä, M.; Raatikainen, M.P.; Uusimaa, P.; Lizotte, E.; Peuhkurinen, K.; Brugada, R.; et al. Cardiac Arrest and Left Ventricular Fibrosis in a Finnish Family with the Lamin A/C Mutation. *J. Cardiovasc. Electrophysiol.* **2008**, *19*, 743–747. [[CrossRef](#)]
26. Pugh, T.J.; Kelly, M.A.; Gowrisankar, S.; Hynes, E.D.; Seidman, M.; Baxter, S.; Bowser, M.; Harrison, B.; Aaron, D.; Mahanta, L.M.; et al. The landscape of genetic variation in dilated cardiomyopathy as surveyed by clinical DNA sequencing. *Genet. Med.* **2014**, *16*, 601–608. [[CrossRef](#)]
27. Ito, K.; Patel, P.N.; Gorham, J.M.; McDonough, B.; DePalma, S.R.; Adler, E.E.; Lam, L.; MacRae, C.A.; Mohiuddin, S.M.; Fatkin, D.; et al. Identification of pathogenic gene mutations in LMNA and MYBPC3 that alter RNA splicing. *Proc. Natl. Acad. Sci. USA* **2017**, *114*, 7689–7694. [[CrossRef](#)]
28. Fidzianska, A.; Bilinska, Z.T.; Tesson, F.; Wagner, T.; Walski, M.; Grzybowski, J.; Ruzyło, W.; Hausmanowa-Petrusewicz, I. Obliteration of cardiomyocyte nuclear architecture in a patient with LMNA gene mutation. *J. Neurol. Sci.* **2008**, *271*, 91–96. [[CrossRef](#)]
29. Otomo, J.; Kure, S.; Shiba, T.; Karibe, A.; Shinozaki, T.; Yagi, T.; Naganuma, H.; Tezuka, F.; Miura, M.; Ito, M.; et al. Electrophysiological and Histopathological Characteristics of Progressive Atrioventricular Block Accompanied by Familial Dilated Cardiomyopathy Caused by a Novel Mutation of Lamin A/C Gene. *J. Cardiovasc. Electrophysiol.* **2005**, *16*, 137–145. [[CrossRef](#)]
30. Nakajima, K.; Aiba, T.; Makiyama, T.; Nishiuchi, S.; Ohno, S.; Kato, K.; Yamamoto, Y.; Doi, T.; Shizuta, S.; Onoue, K.; et al. Clinical Manifestations and Long-Term Mortality in Lamin A/C Mutation Carriers From a Japanese Multicenter Registry. *Circ. J.* **2018**, *82*, 2707–2714. [[CrossRef](#)] [[PubMed](#)]

31. Rapezzi, C.; Arbustini, E.; Caforio, A.L.P.; Charron, P.; Blanes, J.G.; Heliö, T.; Linhart, A.; Mogensen, J.; Pinto, Y.; Ristic, A.; et al. Diagnostic work-up in cardiomyopathies: Bridging the gap between clinical phenotypes and final diagnosis. A position statement from the ESC Working Group on Myocardial and Pericardial Diseases. *Eur. Heart J.* **2012**, *34*, 1448–1458. [[CrossRef](#)]
32. McKie, P.M.; AbouEzzeddine, O.F.; Scott, C.G.; Mehta, R.; Rodeheffer, R.J.; Redfield, M.M.; Burnett, J.C.; Jaffe, A.S. High-Sensitivity Troponin I and Amino-Terminal Pro-B-Type Natriuretic Peptide Predict Heart Failure and Mortality in the General Population. *Clin. Chem.* **2014**, *60*, 1225–1233. [[CrossRef](#)] [[PubMed](#)]
33. Grzybowski, J.; Bilinska, Z.T.; Janas, J.; Michalak, E.; Ruzylo, W. Plasma concentrations of N-terminal atrial natriuretic peptide are raised in asymptomatic relatives of dilated cardiomyopathy patients with left ventricular enlargement. *Heart* **2002**, *88*, 191–192. [[CrossRef](#)] [[PubMed](#)]
34. Wess, G.; Domenech, O.; Dukes-McEwan, J.; Häggström, J.; Gordon, S. European Society of Veterinary Cardiology screening guidelines for dilated cardiomyopathy in Doberman Pinschers. *J. Veter. Cardiol.* **2017**, *19*, 405–415. [[CrossRef](#)] [[PubMed](#)]
35. Charron, P.; Elliott, P.; Gimeno, J.R.; Caforio, A.L.P.; Kaski, J.P.; Tavazzi, L.; Tendera, M.; Maupain, C.; Laroche, C.; Rubis, P.; et al. The Cardiomyopathy Registry of the EURObservational Research Programme of the European Society of Cardiology: Baseline data and contemporary management of adult patients with cardiomyopathies. *Eur. Heart J.* **2018**, *39*, 1784–1793. [[CrossRef](#)] [[PubMed](#)]
36. Nishiuchi, S.; Makiyama, T.; Aiba, T.; Nakajima, K.; Hirose, S.; Kohjitani, H.; Yamamoto, Y.; Harita, T.; Hayano, M.; Wuriyanghai, Y.; et al. Gene-Based Risk Stratification for Cardiac Disorders in LMNA Mutation Carriers. *Circ. Cardiovasc. Genet.* **2017**, *10*, e001603. [[CrossRef](#)]
37. Wahbi, K.; Ben Yaou, R.; Gandjbakhch, E.; Anselme, F.; Gossios, T.; Lakdawala, N.K.; Stalens, C.; Sacher, F.; Babuty, M.; Trochu, J.-N.; et al. Development and Validation of a New Risk Prediction Score for Life-Threatening Ventricular Tachyarrhythmias in Laminopathies. *Circulation* **2019**, *140*, 293–302. [[CrossRef](#)]
38. Priori, S.G.; Blomström-Lundqvist, C.; Mazzanti, A.; Blom, N.; Borggrefe, M.; Camm, J.; Elliott, P.M.; Fitzsimons, D.; Hatala, R.; Hindricks, G.; et al. 2015 ESC Guidelines for the management of patients with ventricular arrhythmias and the prevention of sudden cardiac death: The Task Force for the Management of Patients with Ventricular Arrhythmias and the Prevention of Sudden Cardiac Death of the European Society of Cardiology (ESC). Endorsed by: Association for European Paediatric and Congenital Cardiology (AEPC). *Eur. Heart J.* **2016**, *17*, 2793–2867.
39. Captur, G.; Arbustini, E.; Syrris, P.; Radenkovic, D.; O'Brien, B.; McKenna, W.J.; Moon, J.C. Lamin mutation location predicts cardiac phenotype severity: Combined analysis of the published literature. *Open Heart* **2018**, *5*, e000915. [[CrossRef](#)]
40. Ponikowski, P.; Voors, A.A.; Anker, S.D.; Bueno, H.; Cleland, J.G.F.; Coats, A.J.S.; Falk, V.; González-Juanatey, J.R.; Harjola, V.P.; Jankowska, E.A.; et al. 2016 ESC Guidelines for the diagnosis and treatment of acute and chronic heart failure: The Task Force for the diagnosis and treatment of acute and chronic heart failure of the European Society of Cardiology (ESC) Developed with the special contribution of the Heart Failure Association (HFA) of the ESC. *Eur. Heart J.* **2016**, *37*, 2129–2200.
41. Özmen, Ç.; Deniz, A.; Deveci, O.S.; Cagliyan, C.E.; Celik, A.I.; Yildiz, I.; Yildiz, P.Ö.; Demir, M.; Kanadaşı, M. Association among tenascin-C and NT-proBNP levels and arrhythmia prevalence in heart failure. *Clin. Investig. Med.* **2017**, *40*, 219. [[CrossRef](#)]
42. Medina, A.; Moss, A.J.; McNitt, S.; Zareba, W.; Wang, P.J.; Goldenberg, I. Brain natriuretic peptide and the risk of ventricular tachyarrhythmias in mildly symptomatic heart failure patients enrolled in MADIT-CRT. *Heart Rhythm.* **2016**, *13*, 852–859. [[CrossRef](#)] [[PubMed](#)]
43. Aimo, A.; Januzzi, J.L.; Vergaro, G.; Ripoli, A.; Latini, R.; Masson, S.; Magnoli, M.; Anand, I.S.; Cohn, J.N.; Tavazzi, L.; et al. Prognostic Value of High-Sensitivity Troponin T in Chronic Heart Failure. *Circulation* **2018**, *137*, 286–297. [[CrossRef](#)] [[PubMed](#)]
44. Alawieh, H.; Chemaly, T.; Alam, S.; Khraiche, M. Towards Point-of-Care Heart Failure Diagnostic Platforms: BNP and NT-proBNP Biosensors. *Sensors* **2019**, *19*, 5003. [[CrossRef](#)] [[PubMed](#)]



Article

Characterization of Left Ventricular Non-Compaction Cardiomyopathy

Rebeca Lorca ^{1,2}, María Martín ^{1,2}, Isaac Pascual ^{1,2,3,*}, Aurora Astudillo ^{3,4},
Beatriz Díaz Molina ^{1,2}, Helena Cigarrán ⁵, Elías Cuesta-Llavona ^{1,2}, Pablo Avanzas ^{1,2,3},
José Julián Rodríguez Reguero ^{1,2}, Eliecer Coto ^{1,2,3}, César Morís ^{1,2,3} and Juan Gómez ^{1,2}

¹ Unidad de Referencia de Cardiopatías Familiares-HUCA, Área del Corazón y Departamento de Genética Molecular, Hospital Universitario Central Asturias, 33014 Oviedo, Spain; lorcarebeca@gmail.com (R.L.); mmartinf7@hotmail.com (M.M.); beadimo@gmail.com (B.D.M.); eliascllavona@gmail.com (E.C.-L.); avanzas@gmail.com (P.A.); josejucasa@yahoo.es (J.J.R.R.); eliecer.coto@sarpa.es (E.C.); cesarmoris@gmail.com (C.M.); uo167835@uniovi.es (J.G.)

² Instituto de Investigación Sanitaria del Principado de Asturias, ISPA, 33014 Oviedo, Spain

³ Faculty of Medicine, University of Oviedo, 33014 Oviedo, Spain; aurostudillo@gmail.com

⁴ Anatomía Patológica, Hospital Universitario Central Asturias, 33014 Oviedo, Spain

⁵ Servicio de Radiodiagnóstico, Hospital Universitario Central Asturias, 33014 Oviedo, Spain; hcigarran@icloud.com

* Correspondence: ipascua@live.com; Tel.: +34-985-108-000; Fax: +34-985-274-688

Received: 15 June 2020; Accepted: 3 August 2020; Published: 5 August 2020

Abstract: Left ventricle non-compaction cardiomyopathy (LVNC) has gained great interest in recent years, being one of the most controversial cardiomyopathies. There are several open debates, not only about its genetic heterogeneity, or about the possibility to be an acquired cardiomyopathy, but also about its possible overdiagnosis based on imaging techniques. In order to better understand this entity, we identified 38 LVNC patients diagnosed by cardiac MRI (CMRI) or anatomopathological study that could undergo NGS-sequencing and clinical study. Anatomopathological exam was performed in eight available LVNC hearts. The genetic yield was 34.2%. Patients with negative genetic testing had better left ventricular ejection fraction (LVEF) or it showed a tendency to improve in follow-up, and a possible trigger factor for LVNC was identified in 1/3 of them. Nonetheless, cerebrovascular accidents occurred in similar proportions in both groups. We conclude that in LVNC there seem to be different ways to achieve the same final phenotype. Genetic testing has a good genetic yield and provides valuable information. LVNC without an underlying genetic cause may have a better prognosis in terms of LVEF evolution. However, anticoagulation to prevent cerebrovascular accident (CVA) should be carefully evaluated in all patients. Larger series with pathologic examination are needed to help better understand this entity.

Keywords: left ventricle non-compaction cardiomyopathy; non-ischemic cardiomyopathy; genetics; cardiac magnetic resonance

1. Introduction

Left ventricular (LV) non-compaction (LVNC) is characterized by prominent myocardial trabeculations in a thick, non-compacted layer adjacent to a thin compacted layer. LVNC is the most recently categorized cardiomyopathy, and probably the most controversial one, without available clinical guidelines. The American Heart Association classified LVNC as a distinct primary cardiomyopathy with a genetic aetiology [1]. However, it is considered an unclassified cardiomyopathy according to the European Society of Cardiology (ESC) [2] or the World Health Organization [3].

LVNC had historically been categorized as congenital condition, secondary to a failure of the compaction process during embryonic cardiac development [4–8]. However, recent data proposed

additional etiopathogenic mechanisms, including acquired forms of LVNC secondary to overloading conditions [4,9–11]. Therefore, there has been a classical division between isolated LVNC [12,13] and LVNC associated with significant congenital heart defects (CHD) [14–16]. In fact, according to Jenni et al. [17], the absence of coexisting cardiac anomalies was mandatory to diagnose LVNC [17]. Nevertheless, it was also suggested that both could actually be co-occurring [18].

Agreement between the three most commonly cited transthoracic echocardiogram (TTE) diagnostic criteria, described by Chin et al. [19], Jenni et al. [17], and Stöllberger et al. [20] is known to be poor [21]. Moreover, there is a raising concern about sensitivity and specificity of TTE criteria, and whether, in fact, LVNC may be overdiagnosed [22,23]. In this scenario, cardiac MRI (CMRI) offers a high spatial resolution, and is becoming more and more used in LVNC evaluation, displacing TTE [24]. However, CMRI also raises concerns about overdiagnosis [25–27]. According to diagnostic criteria by Petersen et al., LVNC can be diagnosed if the ratio of non-compacted to compacted myocardium is >2.3 at end-diastole. [28]. Thus, LVNC is commonly associated with other overlapping cardiomyopathies phenotypes. In fact, intrafamilial phenotypic variability, including LVNC, hypertrophic cardiomyopathy (HCM), and dilated cardiomyopathy (DCM), may suggest that these cardiomyopathies could be part of a broader cardiomyopathy spectrum [29–31]. In this context, genetics play an important role. From 17% to up to a 50% of patients with LVNC have a relative with another primary cardiomyopathy [32–34]. However, due to all the controversy around LVNC and the limitations in assigning its clinical diagnosis based on imaging criteria, strong genetic causal relationships have been harder to establish compared to those in HCM [31,35]. Nowadays, achieving a reliable genetic variants interpretation remains a real challenge and it is likely that some previously interpreted as pathogenic variants [36] in LVNC would need to be reclassified, based on current evidence and new criteria [18,37–39].

Moreover, the yield of genetic testing in LVNC varies from 9% to 41%, depending on patient selection and the number of genes screened [18,29,40,41]. Due to small cohort sizes, little is known about LVNC genotype-phenotype correlations. What is more, contrary to HCM guidelines [42], some authors did not support general genetic screening in all patients with LVNC [35].

On the other hand, although a gold-standard diagnostic technique for LVNC is missing [43], anatomopathological examination (APE) could be considered as such. In fact, only three APE cases were enough to support Chin TTE diagnostic criteria [19] and seven for Jenni's criteria [17]. However, again contrary to HCM, LVNC histopathological characteristics are poorly known. Burke et al. [4,44] established the anatomopathological LVNC criteria based on 14 cases, and only a few more case-series have been published ever since, mostly focusing on compaction/non-compaction ratio and not going deeper into histopathological features.

The aim of the current investigation was to provide a comprehensive clinical view of LVNC based on genetic and anatomopathological information.

2. Methods

2.1. Study Population

Adult patients (>21 years old) with LVNC diagnosis were recruited consecutively from a tertiary hospital from Spain, referral for cardiogenetics. Due to the controversy about the diagnostic criteria of LVNC, only patients diagnosed with LVNC, either by Petersen CMRI criteria, or Burke APE criteria, were included. Reports from 824 CMRI (from 2007 to 2015) and 89 transplanted hearts (from 2009 to 2015) were reviewed. At this step, LVNC was considered irrespective of its co-occurrence with other primary cardiomyopathies.

According to these criteria, 43 consecutive patients with LVNC diagnosis, either from CMRI criteria (from 2007 to 2015), or from APE criteria (from 2009 to 2015) were identified. Next-generation sequencing was performed in all patients who met the inclusion criteria (excluding significant CHD) and were still alive at the time this study was performed. Three patients could not be included in the clinical study due to decease without genetic testing available. Two patients with LVNC associated

with significant CHD (that could induce significant hemodynamic changes) were excluded. Therefore, clinical and genetic study was available for the remaining 38 alive patients with LVNC.

Apart from that, histopathological exam was performed in all available LVNC hearts, including those patients who had died without the possibility of a genetic test.

2.2. Clinical Evaluation

A retrospective medical record review of the recruited individuals evaluated was performed. Proband and available family members studied were evaluated by history taking, physical examination, 12-lead electrocardiography, 24-h Holter monitoring, TTE and CMRI or APE. Left ventricular ejection fraction (LVEF) evolution will be categorized into normal, slightly depressed (LVEF <55%), moderately (LVEF 45–35%) depressed, or severely depressed (LVEF <35%).

Possible trigger factors for LVNC (overloading conditions like pregnancy, anaemia or fistula as well as high intensity sport activity) were specifically investigated. Available relatives were screened with the same protocol.

2.3. Genetic Testing

Genetic screening was carried out with DNA samples from the 38 LVNC recruited patients. All of them were NGS sequenced for a gene panel including *MYBPC3*, *MYH7*, *TNNI3*, *TNNT2*, *TPM1*, *TNNC*, *MYL1*, *MYL2*, *ACTC1*, *FLNC*, *MIB1*, *TAZ*, *LDB3*, *DTNA*, *HNC4*, *RYR2*, *LMNA*, *NKX2-5*, *MYH6*, *PRDM16*, *ACTN2*, *DMD*, *DNAJC19*, *FHL1*, *PLN*, and *TTN* genes by Ion Torrent semiconductor chip technology in a Ion GeneStudio S5 Sequencer (Thermo Fisher Scientific, Waltham, MA, USA), according to previously described protocols [45,46]. Overall coverage of the gene panel was >95% (Supplementary Table S1). Variant Caller v5 software was used to variant identification (Thermo Fisher Scientific, Waltham, MA, USA). Ion Reporter (Thermo Fisher Scientific, Waltham, MA, USA) and HD Genome One (DREAMgenics S.L., Oviedo, Spain) software were used for variant annotation, including population, functional, disease-related, and in silico predictive algorithms databases.

Data acquisition and analysis was performed in compliance with protocols evaluated by the Ethical Local Committee of the Hospital Universitario Central de Asturias (No. 2020.224). Written informed consent was obtained from all 38 participants, prior to genetic study.

Interpretation of all gene variants with an allele frequency <0.01 was based the American College of Medical Genetics and Genomics (ACMG-AMP) 2015 Standards and Guidelines [37,47,48]. All genetic variants identified in this cohort were reviewed by two biologists and two cardiologists trained in cardiogenetics. Results provided will be divided in 3 groups: (1) pathogenic (P) or likely pathogenic (LP) variants carriers; (2) negative genetic result (benign or likely benign variants); (3) carriers of variants of uncertain significance (VUS). If a P or LP variant was identified direct Sanger sequencing was performed for family screening.

2.4. Anatomopathological Exam

All 89 available hearts between 2009 and 2015 from our tertiary referral hospital with a heart transplant program were evaluated. Moreover, a patient diagnosed of LVNC by CMR was also transplanted. APE found eight hearts that fulfilled APE criteria for LVNC: six patients with isolated LVNC, one with congenital heart disease associated and one with concomitant three vessels ischemic disease.

The examination was performed by an experienced pathologist expert in the field, based on the LVNC anatomopathological criteria from Burke et al. [4,44]. Firstly, a macroscopic examination was performed. All hearts were systematically inspected, measured, weighted, and coronary sections were performed. They were examined for pathological changes in the four chambers, septum, pericardium, endocardium, and coronary arteries. Multiple samples were obtained, fixed in formaldehyde, paraffin embedded and stained with haematoxylin/eosin. Macroscopic findings were confirmed in microscopic sections. A minimum of three thin sections from each ventricle and two additionally from

the septal area were obtained from paraffin blocks. The macroscopic thickness was measured on the coronary sections of explanted hearts. We selected for microscopy the same area where the macroscopic measurement was performed, and then confirmed the measurements. Compaction and non-compaction wall thickness was measured in coronal macroscopic cuts and ratios were calculated and confirmed in haematoxylin/eosin samples. Histopathological exam was performed, studying fibrosis, inflammation, and cardiomyocytes' hypertrophy. All sections were stained with Haematoxylin-eosin, Masson trichrome, and Periodic Acid-Schiff (PAS) reaction. Fibre diameter measurements were performed only where the section produced a longitudinal view of cardiomyocytes. The measurement of each diameter was made at the nucleus height, and on a minimum of 50 fibres randomly selected. The nuclear size was measured systematically on longitudinal thinnest axis of nuclei, and over a minimum of 50, randomly selected. We used a Nikon microscope (Tokyo, Japan) with digital camera DS-FI2, and software—Nikon NIS D Elements (Tokyo, Japan), where annotations and measurements were registered. We performed all measurements with the same Nikon planacromatic objective size, using a scale provided from the software programme for each size of lens. The quantification was repeated twice in different journeys and performed by a pathologist and a technician. All the observations and results were reviewed by two professional cardiologists and pathologists.

2.5. Statistical Analysis

Statistical analyses were performed with SPSS v.19 (SPSS Inc., Chicago, IL, USA). Descriptive data for continuous variables are presented as mean + SD and as frequencies or percentages for categorical variables. The Chi-square test or Fisher exact test were used to compare frequencies, whereas differences in continuous variables were evaluated with either the Student *t* test or Mann–Whitney *U* test. $p < 0.05$ was considered to be significant.

3. Results

3.1. Study Population with Genetic and Clinical Evaluation

A total of 38 isolated LVNC patients diagnosed by CMRI, APE, or both (Figure 1), were evaluated. Results of genetic evaluation are presented in Table 1.

Table 1. Remarkable identified genetic variants: Pathogenic (P), likely pathogenic (LP) variants, or variants of uncertain significance (VUS), classified according to American College of Medical Genetics and Genomics (ACMG) [37], in our LVNC cohort.

Patient	GENE	hg38	NM	PROTEIN	cDNA	FUNCTION	GnomAD Exomes Frequency	HCMG-AMP
1	LMNA	chr1:156134508	NM_170707	p.Gln207ArgfsTer273	c.619delC	Truncating	-	P
2	LMNA	chr1:156134457	NM_170707	p.Arg190Ttp	c.568C > T	missense	-	LP
3	MYBPC3	chr11:47347891	NM_000256	p.Gly263Ter	c.787G > T	Truncating	-	P
4	MYBPC3	chr11:47347891	NM_000256	p.Gly263Ter	c.787G > T	Truncating	-	P
5	MYH7	chr14:23427614	NM_000257	p.Leu620Pro	c.1859T > C	missense	-	LP
6	MYH7	chr14:23427614	NM_000257	p.Leu620Pro	c.1859T > C	missense	-	LP
7	FLNC	chr7:128848595	NM_01458	p.Ala1539Thr	c.4615G > A	missense	-	LP
8	MYH7	chr14:23427597	NM_000257	p.Gly626Ttp	c.1876G > T	missense	-	LP
9	TTN	chr2:178553135	NM_003319	p.Lys20857ValfsTer7	c.62569_62570delAA	Truncating	-	LP
9	FLNC	chr7:28844249	NM_01458	p.Pro1059Ser	c.3175C > T	missense	-	VUS
10	MYH7	chr14:23430954	NM_000257	p.Arg281Lys	c.842G > C	missense	-	LP
11	TTN	chr2:78557876	NM_003319	p.Glu20095Ter	c.60283G > T	Truncating	-	LP
12	TTN	chr2:178546323	NM_003319	p.Arg22605Ter	c.67813C > T	Truncating	0.00000402	LP
13	TTN	chr2:178563588	NM_003319	p.Arg18450SerfsTer28	c.55346_55349dupTTAG	Truncating	-	LP
13	ACTN2	chr1:236717925	NM_011103	p.Asp65Ala	c.194A > C	missense	-	VUS
14	MYH6	chr14:23862208	NM_002471.3	p.Arg1055Gln	c.3164G > A	missense	0.000123	VUS
15	MYH7	chr14:23424965	NM_000257	p.Pro828Leu	c.2483C > T	missense	-	VUS
16	RBM20	chr10:110780815	NM_001134363	p.Leu69Pro	c.206T > C	missense	-	VUS
17	TTN	chr2:178775139	NM_003319	p.Met2145GlyfsTer4	c.6433_6434delAT	Truncating	-	VUS

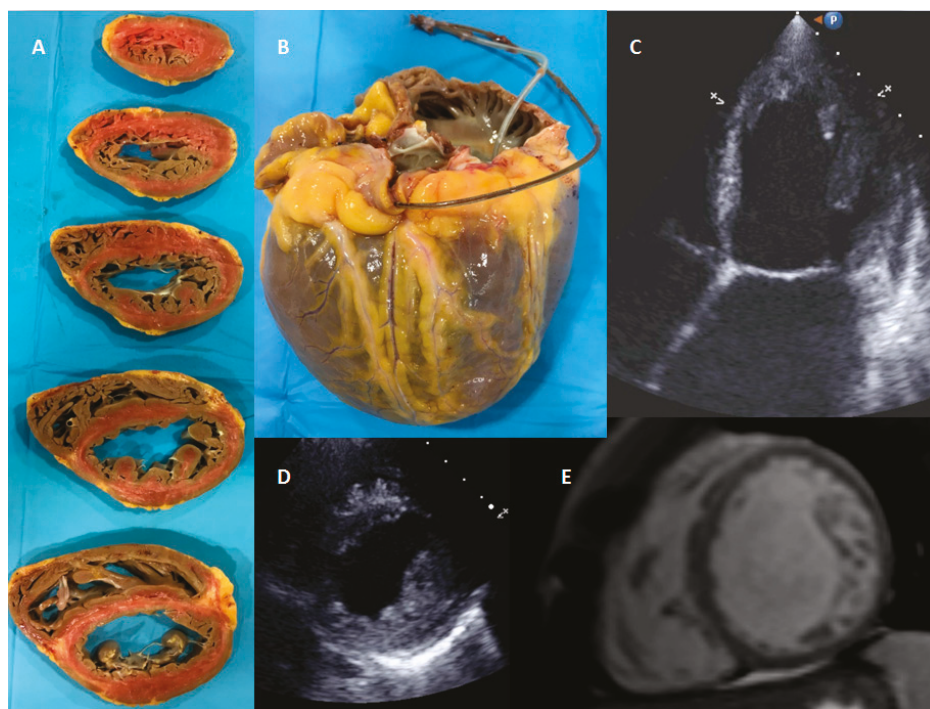


Figure 1. Transplanted patient with isolated left ventricle non-compaction cardiomyopathy diagnosed by CMRI and confirmed by anatomopathological examination. Panel (A) Transversal slides of the explanted heart. (B) Spheroidal shape of the transplanted heart. (C) Apical 4 chamber view in TTE. (D) Parasternal short axis in TTE. (E) LVNC in CMRI.

A P/LP variant was found in 13 patients (patients 1–13, group 1), meaning a genetic yield of 34.2%. Genetic testing was negative (no relevant genetic variants were identified) in patients 18 to 38 (group 2). Another five patients were carriers of VUS and, therefore, considered separately (patients 14–17, group 3). Family screening was performed in all available relatives, supporting variants segregation criteria in P/LP variants (Figure 2).

Principal clinical characteristics of patients with isolated LVNC are summarized in Table 2. Mean age was 49.4 ± 13.9 SD and 65% of patients were men. Median follow-up of patients was 9.5 ± 5 SD. Most patients were referred to cardiology due to symptoms, especially due to dyspnoea or other heart failure secondary symptoms. If left ventricular dysfunction was present, optimal medical treatment was given in all patients. LVNC was correctly suspected in first echocardiogram only in 55% of patients. A cerebrovascular accident (CVA) occurred in 18.4% of patients. In fact, neurological study was the reason for referral in four patients (10.8%). Atrial fibrillation (AF) was identified in only four of the seven patients with ACV. Two patients had suffered CVA with a normal LVEF and without documented AF. What is more, one of them had a recurrent CVA despite and international normalized ratio (INR) of 2.7. Possible trigger factors were identified in 18.4% of patients, most of them due to high intensity sport activity and one of them due to a high flow arteriovenous fistula. Family history of cardiomyopathy was present in 31.5% and 13.15% of patients required heart transplantation.

Table 2. Clinical characteristics of LVNC patients. CVA, cerebrovascular accident, EKG, electrocardiography; TTE, transthoracic echocardiogram; Tx, transplanted; FH, family history; LVEF, left ventricular ejection fraction (0, normal; 1, mild depressed, 2; moderate; 3, severely depressed).

Patient	Gender	Genetics	LVNC Suspicion in TTE	Reason for Referral	CVA	Tx	FH	Trigger Factors	LVEF Evolution
1	Male	P/LP	Yes	Dyspnoea/arrhythmia	no	yes	yes	no	2-3
2	Male	P/LP	No	EKG	no	yes	yes	no	2-3
3	Female	P/LP	No	CVA	Yes	no	yes	no	0-2
4	Male	P/LP	Yes	Heart murmur	Yes	no	yes	no	0-3
5	Male	P/LP	No	Syncope	no	no	yes	no	0-1-0
6	Female	P/LP	Yes	Family screening	no	no	yes	no	0
7	Female	P/LP	Yes	Dyspnoea/palpitations	no	yes	yes	no	0-3
8	Male	P/LP	Yes	Heart failure	no	no	yes	no	3-2
9	Male	P/LP	No	unknown	no	yes	no	no	3-2-3
10	Female	P/LP	No	Cardiogenic Shock	Yes	no	no	no	0
11	Male	P/LP	Yes	Cardiogenic Shock	no	no	no	no	3-1-3
12	Male	P/LP	Yes	unknown	no	no	no	no	3-2
13	Female	P/LP	No	Dyspnoea	no	no	no	no	0
14	Female	VUS	No	Dyspnoea	no	Yes	yes	no	2-3
15	Female	VUS	Yes	Palpitations/Syncope	no	no	no	no	0
16	Male	VUS	No	EKG	no	no	no	no	2-3
17	Male	VUS	No	Ischemic heart disease	no	no	no	no	0-3-1
18	Female	Negative	No	Dyspnoea	no	no	no	yes	1-0
19	Female	Negative	Yes	Vagal syncope	no	no	yes	yes	0
20	Male	Negative	No	Dyspnoea	no	no	no	no	3-1
21	Male	Negative	Yes	Family screening	no	no	yes	no	3-1
22	Male	Negative	No	Neurological study	Yes	no	no	no	3-0
23	Female	Negative	Yes	Dyspnoea	Yes	no	no	no	2-0
24	Male	Negative	Yes	Heart failure	no	no	no	no	3-0
25	Female	Negative	No	Heart failure	no	no	no	no	3-0
26	Male	Negative	Yes	Heart failure	no	no	no	no	3-2
27	Male	Negative	No	EKG	no	no	no	no	1-2-1
28	Male	Negative	No	EKG	no	no	no	yes	0
29	Male	Negative	Yes	Palpitations	no	no	no	yes	0
30	Male	Negative	No	EKG	no	no	yes	yes	0-1
31	Female	Negative	Yes	CVA	Yes	no	no	no	0
32	Male	Negative	Yes	Heart murmur	no	no	no	no	0
33	Male	Negative	Yes	CVA	Yes	no	no	no	0
34	Male	Negative	Yes	EKG	no	no	no	no	0
35	Male	Negative	Yes	Syncope	no	no	no	no	0
36	Male	Negative	Yes	unknown	no	no	no	yes	0
37	Female	Negative	Yes	Palpitations	no	no	no	no	0
38	Male	Negative	No	EKG	no	no	no	yes	0

With genetic screening, up to 22 relatives with P/LP variant carriers and 27 non-carriers relatives were identified. Intrafamilial phenotypic variability was frequently found. As expected, in LMNA families, DCM phenotype was present and HCM in those with sarcomeric pathogenic variants (Figure 2). Moreover, a fluctuant LVEF was found in a relative with previous history of a TTN LP variant carrier (Fam. 8, Figure 2). Clinical and genetic screening for suspicious VUS variants was also performed. However, information obtained was not considered strong enough yet to classify these variants as LP or likely benign variants.

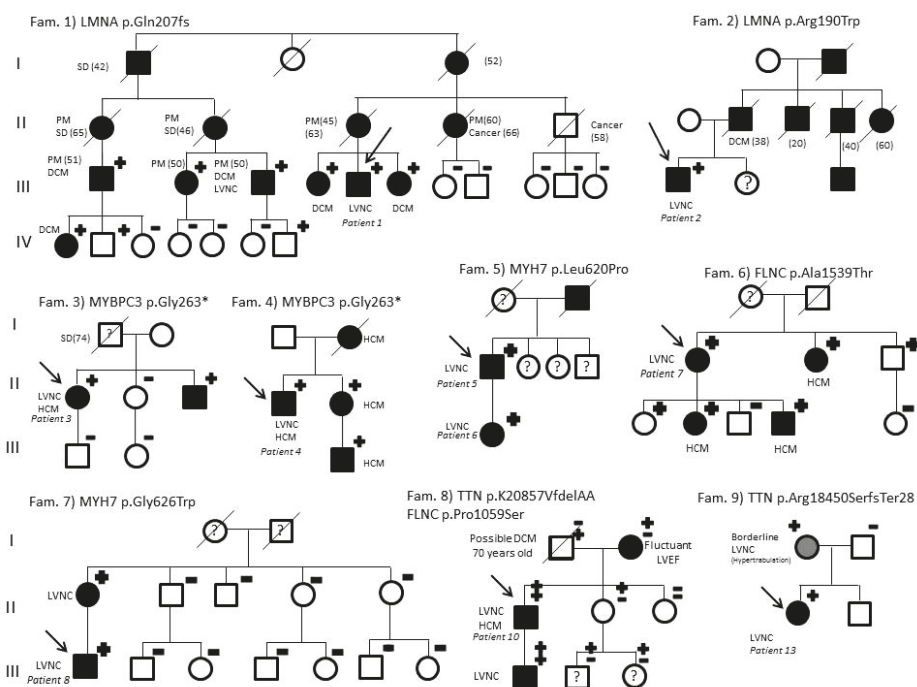


Figure 2. Pedigree of families with LVNC. Fam., family; SD, sudden death; PM, pacemaker; LVNC, left ventricular non-compaction; DCM, dilated cardiomyopathy; HCM, hypertrophic cardiomyopathy. Symbols denote sex and disease status: +, carriers; −, non-carriers; without sign, not studied; box, male; circle, female; darkened, phenotype of hypertrophic cardiomyopathy; symbol clear, unaffected; ?, unknown phenotype; slashed, deceased; without sign, not genetically studied; arrow, proband. Age of deceased or PM implantation in brackets.

Main clinical differences between patients with P/LP variants (group 1) and those with negative genetic result, carriers of benign or likely benign variants (group 2) are shown in Table 3. Most patients from group 1 had a known family history of cardiomyopathy. Conversely to group 1, in group 2, a possible trigger factor for LVNC was found in 1/3 of them. Besides, the evolution of LVEF in time showed different patterns between these groups (Figure 3). Initial LVEF in group 2 was better and those impaired a tendency to improve under optimal medical therapy. At baseline, only 57% of them had normal LVEF and 28.6% had a moderate or severe dysfunction. During follow-up, 76.2% of them reached a normal LVEF, being only slightly reduced in 19%. No patients underwent cardiac transplantation or presented severe cardiac dysfunction in follow-up. However, during follow-up, most patients from group 1 (69.2%) presented moderate-severe LV dysfunction and 30.8% underwent heart transplantation.

Table 3. Clinical characteristics of carriers of P/LP variants (group 1) and patients with negative genetic result, carriers of benign or likely benign variants (group 2).

	Group 1	Group 2
% Men	61.5%	75%
Possible trigger factors for LVNC	0%	33.3%
Family history of cardiomyopathy	61.5%	15%
LVEF evolution	Tendency to worsen	Normal/Tendency to improve
Heart transplantation	30%	0%

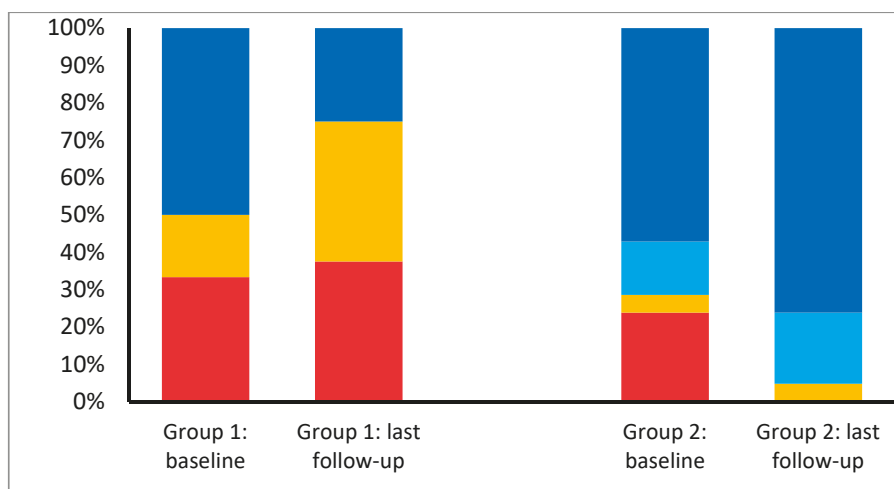


Figure 3. Left ventricle systolic function evolution in follow-up. Group 1, LVNC with pathogenic or likely pathogenic variants; Group 2, LVNC with benign or likely benign variants. Red colour, severely depressed LVEF; yellow, moderately depressed LVEF, bright blue, slightly depressed LVEF; dark blue, normal LVEF.

An internal cardiac defibrillator (ICD) was implanted in 12 patients. Almost half of patients from group 1 had an ICD (46.1%), 50% with at least one appropriate therapy during follow-up. Conversely, only three patients from group 2 (14.3%) received an ICD. What is more, in all three LVEF improved during follow-up and even normalized in two of them.

Apart from that, despite these differences in LVEF, patients suffered cerebrovascular accidents in similar proportions in both groups (23% group 1 vs. 19% group 2, $p = 0.4$). Atrial fibrillation or flutter had been detected in six patients from group 1 and 4 from group 2. However, in both groups, a patient suffered a cerebrovascular accident without previous known arrhythmias.

3.2. Anatomopathological Evaluation

Eight LVNC cases that fulfilled APE criteria were evaluated (Figure 1). All patients had been transplanted in final stages of heart failure. Only one patient presented LVNC associated with CHD (heart 6, coarctation of the aorta with severely dilated aortic root and severe aortic insufficiency), and another one presented concomitant ischemic heart disease.

In macroscopic examination, all of them presented a non-compacted layer with prominent myocardial trabeculations, adjacent to a thin compacted layer and prominent myocardial trabeculations. Thickness of both layers was quantified in macroscopy slides and confirmed in haematoxylin/eosin samples, where the measurements were performed. Cellular hypertrophy was evaluated in both layers, and also the presence of fibrosis (Table 4).

Table 4. Histopathological characteristics of hearts with LVNC diagnosis. NC, non-compaction; C, compaction; LV, left ventricle. Cellular hypertrophy: 0 = none; 1 = mild; 2 = moderate; 3 = severe.

Heart	NC Thickness	C Thickness	LV wall Thickness	NC/C	Fibrosis	NC Cellular Hypertrophy	C Cellular Hypertrophy	Genetic Variants
1	16	8	23	2	yes	3	3	LMNA p.Gln207fs
2	16	5	21	3.2	no	3	2	LMNA p.Arg190Trp
3	16	7	23	2.3	yes	Not valuable	1	FLNC p.Ala1539Thr
4	11	4	15	2.7	no	3	2	TTN p.K20857VfsdelAA FLNC p.Pro1059Ser
5	17	5	22	3.4	no	3	2	MYH6 R1055Q
6	20	5	25	4	no	3	2	Negative
7	14	3	17	4.6	no	3	2	unavailable
8	17	7	24	2.4	yes	2	2	unavailable

Cardiomyocytes description deserved special attention. In all analysed cases, their nucleus were enlarged, hyperchromatic and presented irregular striking shapes (Figure 4). Nevertheless, no remarkable abnormal nucleoli were found. Chromatin was, in general soft and without much heterochromatin volume. Cardiomyocyte diameter was enlarged in some of the layers, especially in non-compacted area. In seven cases, neither inflammatory infiltrate, necrosis nor other signs of histological malignancy were found. However, necrosis was identified in one heart, fibrosis in 3 of them, and some areas of slight fat infiltration and some of myocardiosclerosis.

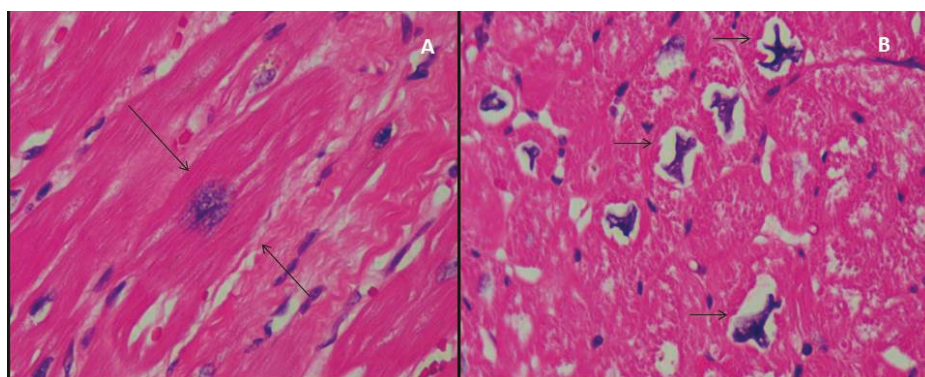


Figure 4. Microscopic haematoxylin/eosin samples (×40) from LVNC explanted hearts. Panel (A) myocyte cellular hypertrophy (delimited by arrows); (B) deformed nuclear cardiomyocyte shapes.

Two patients died after heart transplant, without genetic testing. Out of the six available patients for genetic testing, LP/P variants were found in four of them, a VUS in the fourth one, and only B/LB variants in the other one, with concomitant CHD (heart six, excluded for clinical study). The genetic yield of this small but severely affected cohort of isolated LVNC is 80%.

4. Discussion

Over the past few decades, technological advances in genetic sequencing have allowed to perform genetic testing worldwide. The number of genetic variants to analyse has increased massively [49] and so has the complexity of its interpretation. Achieving a reliable classification is crucial [36], especially in controversial entities like LVNC. LVNC is the most recently described cardiomyopathy and broadening the knowledge of its genetics field is an absolute necessity. Genetic yield is really variable depending on the reported series and very few papers have tried to compare LVNC phenotype with or without an identifiable genetic cause. Moreover, genetic variants classification performed before ACMG-AMP

criteria [37] should be interpreted with caution. In addition, most studies included LVNC patients diagnosed only based on TTE criteria.

A study performed about 10 years ago, found a genetic “mutation” in 17.5% of their TTE-based cohort [40]. The generic yield improved to 29% in a study of 63 isolated LVNC diagnosed by TTE [50] and to 41% in another TTE based study [29]. However, no differences in clinical phenotypes between positive and negative pathogenic variants’ carriers were found in either of these two studies.

In 2017, an interesting study in children classified variants according to ACMG [37] with a genetic yield of only 9% and, unfortunately, no comparison between carriers and non-carriers were done [18]. Wang et al. also analysed a childhood cohort with a higher genetic yield [38%] describing a poorer prognosis in pathogenic variants carriers (earlier age of onset and lower LVEF) than those without pathogenic variants [41]. Another German study of 68 index LVNC patients diagnosed by TTE reported a 38% genetic yield and described worse clinical outcomes in patients with pathogenic variants in LMNA and RBM20. In their cohort, TTN variants were the most frequent cause for LVNC and they associated TTN truncating variants with LVNC phenotype [51].

In our study, genetic testing identified a genetic cause in up to 34.2% of patients, a percentage within the expected ranges according to previously reported series. However, better understanding of VUS may improve this yield. Thanks to genetic screening not only 22 relatives at risk were identified, but also 27 relatives could be discharged. LVNC have been accepted to be a possible inherited condition. Therefore, we believe that genetic screening should be strongly recommended, like in any other kind inherited cardiomyopathy. Moreover, in this entity, genetic testing may be useful not only for family screening, but also to help in differential diagnosis with hypertrabeculation mimicking LVNC. In fact, if genetic testing had only been performed in those with moderate to severe LV dysfunction in follow-up, genetic yield would have improved to 75% (9/12).

The strength of our cohort relies not only in the genetic variants’ classification based on ACMG-AMP guidelines [37], but also on the patient’s selection to achieve a LVNC cohort with a solid diagnosis. Carriers of VUS (group 3) were not included in any comparison group, as its classification may easily change into LP or LB as genetic knowledge improves. However, interesting differences between carriers of P/LP variants (group 1) and non-carriers (group 2) were found. Family history of cardiomyopathies is mainly found in group 1, and possible trigger factors were only identified in group 2. In fact, trigger factors may explain the hypertrabeculation in one in every three patients from group 2. However, the most stunning finding was the LVEF evolution in follow-up (Figure 3). LVEF showed a tendency to improve in time in group 2, contrary to the tendency to worsen in group 1. Although these results should be interpreted with caution, genetic results could represent a predictor factor for LVEF evolution, especially if a trigger factor had been identified. In our cohort, this information could have been useful, for example, to delay the ICD implant decision in patients from group 2, whose LVEF improved with optimal medical therapy. Besides, all carries of TTN variants presented a fluctuant LVEF. On the other hand, CVAs are present in the same proportion in both groups, highlighting the importance of emboli risk assessment in all LVNC phenotypes.

We believe that our data reinforce the hypothesis that there are different ways to reach the same final phenotype, whether as congenital heart defect or as an inherited cardiomyopathy or as an acquired one. Although in this study we included LVNC patients based on the same criteria, they had different etiologies. It seems obvious that patients from group 1 have an inherited kind of cardiomyopathy. However, the presence of trigger factors in 1/3 of patients from group 2 support the hypothesis that LVNC phenotype could also be an acquired cardiomyopathy [4,9–11]. On the basis of an apparently normal heart with an underlying predisposition, the developing of hypertrabeculation leading to LVNC phenotype may (or may not) start to manifest at a certain age. Although prognostic differences in these different scenarios may be found (highlighting the role of genetic testing and LVEF evolution), clinicians should be aware of possible related complications like CVA in all LVNC phenotypes.

In addition, our data also supports the theory that LVNC could actually been underdiagnosed previously, even in autopsies [13,21,44,52]. In our series, TTE misdiagnosed LVNC in the first place in

up to 45% of LVNC cohort. No wonder why the diagnostic based on imaging criteria is still a real challenge and an ongoing debate.

Furthermore, APE has played a critical role in helping to describe and classify LVNC as a novel cardiomyopathy and to settle its diagnostic criteria [17,19]. Nevertheless, contrary to HCM, there are no large case series available [44,53] and deep histopathological characterization is missing. HCM is known for its disarray, hypertrophy of myocytes and possible fibrosis [54]. This hypertrophy of myocytes is maximal at subendocardium [55,56] and nuclei can be enlarged, presenting nuclear pleomorphism and hyperchromasia [54]. In LVNC, APE data have been focused in compaction/non-compaction layers description and quantification [4,44], neglecting meticulous histopathological description [4,57]. Fibrosis areas considered secondary to ischemia due to microvascular dysfunction are described in some studies [58–60]. Burke et al. [4,44] did not find any difference between isolated LVNC and associated with CHD. Although Jenni et al. [17] claimed that no disarray was present, a recent transplantation series found it in one LVNC patient [59]. Proper myocyte description beyond isolated cases is also missing [59,61,62], and no genetic data are reported in any series. For this reason, the APE description of our sample, although small, is important. According to previous data, fibrosis and one case of necrosis were identified, but no inflammatory pattern. However, the most important finding was the cellular hypertrophy of myocytes, present in all the studied hearts. Moreover, its distribution is not uniform, being more pronounced in the non-compacted layer. However, the most striking feature was the irregular nuclear shape (Figure 4). In addition, the available genetic data, with a good yield in these patients with severe phenotype of LVNC, are really interesting. Although the described histopathological findings are present in the eight hearts, two of them intriguingly present a LP variant in a gene that encodes a component of the nuclear lamina, which determines nuclear shape and size.

5. Limitations

Family screening was not available for all relatives. All genetic variants identified in this cohort were reviewed by two biologists and two cardiologists trained in cardiogenetics, according to current published guidelines and available data [37]. Despite these efforts, some variants may be reclassified as additional data become available. Family screening for TTN variants from patients 11 and 12 are still pending due to the COVID-19 pandemic. The genetic testing yield may also improve as gene panels continue to expand and better classification of VUS is achieved. Further investigation in genetics and histopathological exam, expanding the series number, is definitely necessary to draw further conclusions.

6. Conclusions

There seem to be different ways to achieve the same final phenotype: LVNC. As genetic testing in LVNC has a good genetic yield and provides valuable information, it should be recommended for all LVNC patients. LVNC without an underlying genetic cause may have a better prognosis in terms of LVEF evolution in time. However, anticoagulation to prevent CVA should be carefully evaluated in all patients. Larger series with pathologic examination are needed to help better understand this entity.

Supplementary Materials: The following are available online at <http://www.mdpi.com/2077-0383/9/8/2524/s1>, Table S1: Overall coverage of the gene panel.

Author Contributions: Conceptualization, R.L., I.P., and J.J.R.R.; Data curation, M.M., E.C.-L., and J.G.; Formal analysis, R.L., H.C., and E.C.-L.; Funding acquisition, I.P.; Investigation, R.L., A.A., B.D.M., E.C., and J.G.; Methodology, M.M., I.P., A.A., and P.A.; Resources, C.M.; Software, H.C.; Supervision, M.M., I.P., J.J.R.R. and C.M.; Validation, A.A., B.D.M., E.C., and J.G.; Writing—original draft, R.L.; Writing—review & editing, R.L., M.M., P.A., J.J.R.R., and J.G. All authors have read and agreed to the published version of the manuscript.

Funding: This research received no external funding.

Conflicts of Interest: The authors declare no conflict of interest.

References

1. Maron, B.J.; Towbin, J.A.; Thiene, G.; Antzelevitch, C.; Corrado, D.; Arnett, D.; Moss, A.J.; Seidman, C.E.; Young, J.B. Contemporary definitions and classification of the cardiomyopathies: An American Heart Association Scientific Statement from the Council on Clinical Cardiology, Heart Failure and Transplantation Committee; Quality of Care and Outcomes Research and Functional Genomics and Translational Biology Interdisciplinary Working Groups; and Council on Epidemiology and Prevention. *Circulation* **2006**, *113*, 1807–1816.
2. Elliott, P.; Andersson, B.; Arbustini, E.; Bilinska, Z.; Cecchi, F.; Charron, P.; Dubourg, O.; Kühl, U.; Maisch, B.; McKenna, W.J.; et al. Classification of the cardiomyopathies: A position statement from the European Society Of Cardiology Working Group on Myocardial and Pericardial Diseases. *Eur. Heart J.* **2008**, *29*, 270–276. [[CrossRef](#)]
3. Richardson, P.; McKenna, W.; Bristow, M.; Maisch, B.; Mautner, B.; O'Connell, J.; Olsen, E.; Thiene, G.; Goodwin, J.; Gyarfás, I.; et al. Report of the 1995 World Health Organization/International Society and Federation of Cardiology Task Force on the Definition and Classification of cardiomyopathies. *Circulation* **1996**, *93*, 841–842.
4. Arbustini, E.; Weidemann, F.; Hall, J.L. Left ventricular noncompaction: A distinct cardiomyopathy or a trait shared by different cardiac diseases? *J. Am. Coll. Cardiol.* **2014**, *64*, 1840–1850. [[CrossRef](#)]
5. Liu, J.; Bressan, M.; Hassel, D.; Huisken, J.; Staudt, D.; Kikuchi, K.; Poss, K.D.; Mikawa, T.; Stainier, D.Y. A dual role for ErbB2 signaling in cardiac trabeculation. *Development* **2010**, *137*, 3867–3875. [[CrossRef](#)]
6. Gupta, V.; Poss, K.D. Clonally dominant cardiomyocytes direct heart morphogenesis. *Nature* **2012**, *484*, 479–484. [[CrossRef](#)]
7. Risebro, C.A.; Riley, P.R. Formation of the ventricles. *Sci. World J.* **2006**, *6*, 1862–1880. [[CrossRef](#)]
8. Sedmera, D.; Thompson, R.P. Myocyte proliferation in the developing heart. *Dev. Dyn.* **2011**, *240*, 1322–1334. [[CrossRef](#)]
9. Gati, S.; Papadakis, M.; Van Niekerk, N.; Reed, M.; Yeghen, T.; Sharma, S. Increased left ventricular trabeculation in individuals with sickle cell anaemia: Physiology or pathology? *Int. J. Cardiol.* **2013**, *168*, 1658–1660. [[CrossRef](#)]
10. Gati, S.; Papadakis, M.; Papamichael, N.D.; Zaidi, A.; Sheikh, N.; Reed, M.; Sharma, R.; Thilaganathan, B.; Sharma, S. Reversible de novo left ventricular trabeculations in pregnant women: Implications for the diagnosis of left ventricular noncompaction in low-risk populations. *Circulation* **2014**, *130*, 475–483. [[CrossRef](#)]
11. Gati, S.; Chandra, N.; Bennett, R.L.; Reed, M.; Kervio, G.; Panoulas, V.F.; Ghani, S.; Sheikh, N.; Zaidi, A.; Wilson, M.; et al. Increased left ventricular trabeculation in highly trained athletes: Do we need more stringent criteria for the diagnosis of left ventricular non-compaction in athletes? *Heart* **2013**, *99*, 401–408. [[CrossRef](#)] [[PubMed](#)]
12. Engberding, R.; Bender, F. Identification of a rare congenital anomaly of the myocardium by two-dimensional echocardiography: Persistence of isolated myocardial sinusoids. *Am. J. Cardiol.* **1984**, *53*, 1733–1734. [[CrossRef](#)]
13. Ritter, M.; Oechslin, E.; Sutsch, G.; Attenhofer, C.; Schneider, J.; Jenni, R. Isolated noncompaction of the myocardium in adults. *Mayo Clin. Proc.* **1997**, *72*, 26–31. [[CrossRef](#)]
14. Grant, T. An unusual anomaly of the coronary vessels in the malformed heart of a child. *Heart* **1926**, *13*, 273–283.
15. Pignatelli, R.H.; McMahon, C.J.; Dreyer, W.J.; Denfield, S.W.; Price, J.; Belmont, J.W.; Craigen, W.J.; Wu, J.; El Said, H.; Bezold, L.I.; et al. Clinical characterization of left ventricular noncompaction in children: A relatively common form of cardiomyopathy. *Circulation* **2003**, *108*, 2672–2678. [[CrossRef](#)]
16. Jenni, R.; Rojas, J.; Oechslin, E. Isolated noncompaction of the myocardium. *N. Engl. J. Med.* **1999**, *340*, 966–967. [[CrossRef](#)]
17. Jenni, R.; Oechslin, E.; Schneider, J.; Attenhofer Jost, C.; Kaufmann, P.A. Echocardiographic and pathoanatomical characteristics of isolated left ventricular non-compaction: A step towards classification as a distinct cardiomyopathy. *Heart* **2001**, *86*, 666–671. [[CrossRef](#)]
18. Miller, E.M.; Hinton, R.B.; Czossek, R.; Lorts, A.; Parrott, A.; Shikany, A.R.; Ittenbach, R.F.; Ware, S.M. Genetic testing in pediatric left ventricular noncompaction. *Circ. Cardiovasc. Genet.* **2017**, *10*, e001735. [[CrossRef](#)]

19. Chin, T.K.; Perloff, J.K.; Williams, R.G.; Jue, K.; Mohrmann, R. Isolated noncompaction of left ventricular myocardium. A study of eight cases. *Circulation* **1990**, *82*, 507–513. [[CrossRef](#)]
20. Stollberger, C.; Gerecke, B.; Finsterer, J.; Engberding, R. Refinement of echocardiographic criteria for left ventricular noncompaction. *Int. J. Cardiol.* **2013**, *165*, 463–467. [[CrossRef](#)]
21. Kohli, S.K.; Pantazis, A.A.; Shah, J.S.; Adeyemi, B.; Jackson, G.; McKenna, W.J.; Sharma, S.; Elliott, P.M. Diagnosis of left-ventricular non-compaction in patients with left-ventricular systolic dysfunction: Time for a reappraisal of diagnostic criteria? *Eur. Heart J.* **2008**, *29*, 89–95. [[CrossRef](#)] [[PubMed](#)]
22. Habib, G.; Charron, P.; Eicher, J.C.; Giorgi, R.; Donal, E.; Laperche, T.; Boulmier, D.; Pascal, C.; Logeart, D.; Jondeau, G.; et al. Isolated left ventricular non-compaction in adults: Clinical and echocardiographic features in 105 patients. Results from a French registry. *Eur. J. Heart Fail.* **2011**, *13*, 177–185. [[CrossRef](#)] [[PubMed](#)]
23. Niemann, M.; Stork, S.; Weidemann, F. Left ventricular noncompaction cardiomyopathy: An overdiagnosed disease. *Circulation* **2012**, *126*, 240–243. [[CrossRef](#)] [[PubMed](#)]
24. Yoon, Y.E.; Hong, Y.J.; Kim, H.K.; Kim, J.A.; Na, J.O.; Yang, D.H.; Kim, Y.J.; Choi, E.Y. The Korean Society of Cardiology and the Korean Society of Radiology. 2014 Korean guidelines for appropriate utilization of cardiovascular magnetic resonance imaging: A joint report of the Korean Society of Cardiology and the Korean Society of Radiology. *Korean J. Radiol.* **2014**, *15*, 659–688. [[CrossRef](#)] [[PubMed](#)]
25. Ross, S.B.; Jones, K.; Blanch, B.; Puranik, R.; McGeechan, K.; Barratt, A.; Semsarian, C. A systematic review and meta-analysis of the prevalence of left ventricular non-compaction in adults. *Eur. Heart J.* **2020**, *41*, 1428–1436. [[CrossRef](#)]
26. Ross, S.B.; McGeechan, K.; Barratt, A.; Semsarian, C. Overdiagnosis of left ventricular non-compaction in adults: The data tells the story. *Eur. Heart J.* **2019**, *40*, 3206. [[CrossRef](#)]
27. Protonotarios, A.; Elliott, P.M. Left ventricular non-compaction: Have we reached the limits of conventional imaging? *Eur. Heart J.* **2019**, *41*, 1437–1438. [[CrossRef](#)]
28. Petersen, S.E.; Selvanayagam, J.B.; Wiesmann, F.; Robson, M.D.; Francis, J.M.; Anderson, R.H.; Watkins, H.; Neubauer, S. Left ventricular non-compaction: Insights from cardiovascular magnetic resonance imaging. *J. Am. Coll. Cardiol.* **2005**, *46*, 101–105. [[CrossRef](#)]
29. Hoedemaekers, Y.M.; Caliskan, K.; Michels, M.; Frohn-Mulder, I.; van der Smagt, J.J.; Phefferkorn, J.E.; Wessels, M.W.; ten Cate, F.J.; Sijbrands, E.J.; Dooijes, D.; et al. The importance of genetic counseling, DNA diagnostics, and cardiologic family screening in left ventricular noncompaction cardiomyopathy. *Circ. Cardiovasc. Genet.* **2010**, *3*, 232–329. [[CrossRef](#)]
30. Lorca, R.; Martín, M.; Gómez, J.; Santamarta, E.; Moris, C.; Reguero, J.J.; Coto, E. Hypertrophic cardiomyopathy and left ventricular non-compaction: Different manifestations of the same cardiomyopathy spectrum? *Int. J. Cardiol.* **2015**, *190*, 26–28. [[CrossRef](#)]
31. Van Waning, J.L.; Caliskan, K.; Hoedemaekers, Y.M.; van Spaendonck-Zwarts, K.Y.; Baas, A.F.; Boekholdt, S.M.; van Melle, J.P.; Teske, A.J.; Asselbergs, F.W.; Backx, A.; et al. Genetics, clinical features, and long-term outcome of noncompaction cardiomyopathy. *J. Am. Coll. Cardiol.* **2018**, *71*, 711–722. [[CrossRef](#)] [[PubMed](#)]
32. Oechslin, E.N.; Attenhofer Jost, C.H.; Rojas, J.R.; Kaufmann, P.A.; Jenni, R. Long-term follow-up of 34 adults with isolated left ventricular noncompaction: A distinct cardiomyopathy with poor prognosis. *J. Am. Coll. Cardiol.* **2000**, *36*, 493–500. [[CrossRef](#)]
33. Weiford, B.C.; Subbarao, V.D.; Mulhern, K.M. Noncompaction of the ventricular myocardium. *Circulation* **2004**, *109*, 2965–2971. [[CrossRef](#)] [[PubMed](#)]
34. Ichida, F.; Hamamichi, Y.; Miyawaki, T.; Ono, Y.; Kamiya, T.; Akagi, T.; Hamada, H.; Hirose, O.; Isobe, T.; Yamada, K.; et al. Clinical features of isolated noncompaction of the ventricular myocardium: Long-term clinical course, hemodynamic properties, and genetic background. *J. Am. Coll. Cardiol.* **1999**, *34*, 233–240. [[CrossRef](#)]
35. Finsterer, J.; Stollberger, C.; Towbin, J.A. Left ventricular noncompaction cardiomyopathy: Cardiac, neuromuscular, and genetic factors. *Nat. Rev. Cardiol.* **2017**, *14*, 224–237. [[CrossRef](#)]
36. Walsh, R.; Thomson, K.L.; Ware, J.S.; Funke, B.H.; Woodley, J.; McGuire, K.J.; Mazarrotto, F.; Blair, E.; Seller, A.; Taylor, J.; et al. Reassessment of Mendelian gene pathogenicity using 7,855 cardiomyopathy cases and 60,706 reference samples. *Genet. Med.* **2017**, *19*, 192–203. [[CrossRef](#)]

37. Richards, S.; Aziz, N.; Bale, S.; Bick, D.; Das, S.; Gastier-Foster, J.; Grody, W.W.; Hegde, M.; Lyon, E.; Spector, E.; et al. Standards and guidelines for the interpretation of sequence variants: A joint consensus recommendation of the American College of Medical Genetics and Genomics and the Association for Molecular Pathology. *Genet. Med.* **2015**, *17*, 405–424. [[CrossRef](#)]
38. Finsterer, J.; Stollberger, C. Are RYR2 exon-3 deletions truly causative for non-compaction? *Europace* **2014**, *16*, 1864. [[CrossRef](#)]
39. Finsterer, J.; Zarrouk-Mahjoub, S. Lamin A/C mutations do not cause left ventricular hypertrabeculation/noncompaction. *Tex. Heart Inst. J.* **2015**, *42*, 301–302. [[CrossRef](#)]
40. Klaassen, S.; Probst, S.; Oechslin, E.; Gerull, B.; Krings, G.; Schuler, P.; Greutmann, M.; Hürlimann, D.; Yegitbasi, M.; Pons, L.; et al. Mutations in sarcomere protein genes in left ventricular noncompaction. *Circulation* **2008**, *117*, 2893–2901. [[CrossRef](#)]
41. Wang, C.; Hata, Y.; Hirono, K.; Takasaki, A.; Ozawa, S.W.; Nakaoka, H.; Saito, K.; Miyao, N.; Okabe, M.; Ibuki, K.; et al. A wide and specific spectrum of genetic variants and genotype-phenotype correlations revealed by next-generation sequencing in patients with left ventricular noncompaction. *J. Am. Heart Assoc.* **2017**, *6*, e006210. [[CrossRef](#)] [[PubMed](#)]
42. Task Force Members; Elliott, P.M.; Anastasakis, A.; Borger, M.A.; Borggrefe, M.; Cecchi, F.; Charron, P.; Hagege, A.A.; Lafont, A.; Limongelli, G.; et al. 2014 ESC Guidelines on diagnosis and management of hypertrophic cardiomyopathy: The Task Force for the Diagnosis and Management of Hypertrophic Cardiomyopathy of the European Society of Cardiology (ESC). *Eur. Heart J.* **2014**, *35*, 2733–2779.
43. Yin, L. Non-compact cardiomyopathy or ventricular non-compact syndrome? *J. Cardiovasc. Ultrasound.* **2014**, *22*, 165–172. [[CrossRef](#)] [[PubMed](#)]
44. Burke, A.; Mont, E.; Kutys, R.; Virmani, R. Left ventricular noncompaction: A pathological study of 14 cases. *Hum. Pathol.* **2005**, *36*, 403–411. [[CrossRef](#)]
45. Gómez, J.; Reguero, J.R.; Moris, C.; Martín, M.; Alvarez, V.; Alonso, B.; Iglesias, S.; Coto, E. Mutation analysis of the main hypertrophic cardiomyopathy genes using multiplex amplification and semiconductor next-generation sequencing. *Circ. J.* **2014**, *78*, 2963–2971. [[CrossRef](#)]
46. Gómez, J.; Lorca, R.; Reguero, J.R.; Moris, C.; Martín, M.; Tranche, S.; Alonso, B.; Iglesias, S.; Alvarez, V.; Díaz-Molina, B.; et al. Screening of the filamin C gene in a large cohort of hypertrophic cardiomyopathy patients. *Circ. Cardiovasc. Genet.* **2017**, *10*, e001584. [[CrossRef](#)]
47. Telenti, A.; Pierce, L.C.; Biggs, W.H.; di Iulio, J.; Wong, E.H.; Fabani, M.M.; Kirkness, E.F.; Moustafa, A.; Shah, N.; Xie, C.; et al. Deep sequencing of 10,000 human genomes. *Proc. Natl. Acad. Sci. USA* **2016**, *113*, 11901–11906. [[CrossRef](#)]
48. Jagadeesh, K.A.; Wenger, A.M.; Berger, M.J.; Guturu, H.; Stenson, P.D.; Cooper, D.N.; Bernstein, J.A.; Bejerano, G. M-CAP eliminates a majority of variants of uncertain significance in clinical exomes at high sensitivity. *Nat. Genet.* **2016**, *48*, 1581–1586. [[CrossRef](#)]
49. Sen-Chowdhry, S.; Jacoby, D.; Moon, J.C.; McKenna, W.J. Update on hypertrophic cardiomyopathy and a guide to the guidelines. *Nat. Rev. Cardiol.* **2016**, *13*, 651–675. [[CrossRef](#)]
50. Probst, S.; Oechslin, E.; Schuler, P.; Greutmann, M.; Boyé, P.; Knirsch, W.; Berger, F.; Thierfelder, L.; Jenni, R.; Klaassen, S. Sarcomere gene mutations in isolated left ventricular noncompaction cardiomyopathy do not predict clinical phenotype. *Circ. Cardiovasc. Genet.* **2011**, *4*, 367–374. [[CrossRef](#)]
51. Sedaghat-Hamedani, F.; Haas, J.; Zhu, F.; Geier, C.; Kayvanpour, E.; Liss, M.; Lai, A.; Frese, K.; Pribe-Wolferts, R.; Amr, A.; et al. Clinical genetics and outcome of left ventricular non-compaction cardiomyopathy. *Eur. Heart J.* **2017**, *38*, 3449–3460. [[CrossRef](#)] [[PubMed](#)]
52. Rigopoulos, A.; Rizos, I.K.; Aggeli, C.; Kloufetos, P.; Papacharalampous, X.; Stefanadis, C.; Toutouzas, P. Isolated left ventricular noncompaction: An unclassified cardiomyopathy with severe prognosis in adults. *Cardiology* **2002**, *98*, 25–32. [[CrossRef](#)] [[PubMed](#)]
53. Val-Bernal, J.F.; Garijo, M.F.; Rodriguez-Villar, D.; Val, D. Non-compaction of the ventricular myocardium: A cardiomyopathy in search of a pathoanatomical definition. *Histol. Histopathol.* **2010**, *25*, 495–503. [[PubMed](#)]
54. Hughes, S.E. The pathology of hypertrophic cardiomyopathy. *Histopathology* **2004**, *44*, 412–427. [[CrossRef](#)] [[PubMed](#)]
55. Unverferth, D.V.; Baker, P.B.; Pearce, L.I.; Lautman, J.; Roberts, W.C. Regional myocyte hypertrophy and increased interstitial myocardial fibrosis in hypertrophic cardiomyopathy. *Am. J. Cardiol.* **1987**, *59*, 932–936. [[CrossRef](#)]

56. Varnava, A.M.; Elliott, P.M.; Sharma, S.; McKenna, W.J.; Davies, M.J. Hypertrophic cardiomyopathy: The interrelation of disarray, fibrosis, and small vessel disease. *Heart* **2000**, *84*, 476–482. [[CrossRef](#)]
57. Gerger, D.; Stöllberger, C.; Grassberger, M.; Gerecke, B.; Andresen, H.; Engberding, R.; Finsterer, J. Pathomorphologic findings in left ventricular hypertrabeculation/noncompaction of adults in relation to neuromuscular disorders. *Int. J. Cardiol.* **2013**, *169*, 249–253. [[CrossRef](#)]
58. Finsterer, J.; Stollberger, C.; Feichtinger, H. Histological appearance of left ventricular hypertrabeculation/noncompaction. *Cardiology* **2002**, *98*, 162–164. [[CrossRef](#)]
59. Ottaviani, G.; Segura, A.M.; Rajapreyar, I.N.; Zhao, B.; Radovancevic, R.; Loyalka, P.; Kar, B.; Gregoric, I.; Buja, L.M. Left ventricular noncompaction cardiomyopathy in end-stage heart failure patients undergoing orthotopic heart transplantation. *Cardiovasc. Pathol.* **2016**, *25*, 293–299. [[CrossRef](#)]
60. Jenni, R.; Wyss, C.A.; Oechslin, E.N.; Kaufmann, P.A. Isolated ventricular noncompaction is associated with coronary microcirculatory dysfunction. *J. Am. Coll. Cardiol.* **2002**, *39*, 450–454. [[CrossRef](#)]
61. Bleyl, S.B.; Mumford, B.R.; Brown-Harrison, M.C.; Pagotto, L.T.; Carey, J.C.; Pysher, T.J.; Ward, K.; Chin, T.K. Xq28-linked noncompaction of the left ventricular myocardium: Prenatal diagnosis and pathologic analysis of affected individuals. *Am. J. Med. Genet.* **1997**, *72*, 257–265. [[CrossRef](#)]
62. Ivan, D.; Flamm, S.D.; Abrams, J.; Kindo, M.; Heck, K.; Frazier, O.H. Isolated ventricular non-compaction in adults with idiopathic cardiomyopathy: Cardiac magnetic resonance and pathologic characterization of the anomaly. *J. Heart Lung Transplant.* **2005**, *24*, 781–786. [[CrossRef](#)] [[PubMed](#)]



© 2020 by the authors. Licensee MDPI, Basel, Switzerland. This article is an open access article distributed under the terms and conditions of the Creative Commons Attribution (CC BY) license (<http://creativecommons.org/licenses/by/4.0/>).

Article

Left Ventricular Noncompaction and Congenital Heart Disease Increases the Risk of Congestive Heart Failure

Keiichi Hirono ^{1,*}, Yukiko Hata ², Nariaki Miyao ¹, Mako Okabe ¹, Shinya Takarada ¹, Hideyuki Nakaoka ¹, Keijiro Ibuki ¹, Sayaka Ozawa ¹, Naoki Yoshimura ³, Naoki Nishida ², Fukiko Ichida ⁴ and LVNC study collaborators

¹ Department of Pediatrics, Graduate School of Medicine, University of Toyama, Toyama 930-0194, Japan; nijjiroongakutai@yahoo.co.jp (N.M.); macoron.coron@gmail.com (M.O.); toyamadaikensyu2013@gmail.com (S.T.); kmc.ash7-oe.iaa03@maroon.plala.or.jp (H.N.); kibk9925@gmail.com (K.I.); sozawa34@med.u-toyama.ac.jp (S.O.)

² Legal Medicine, Graduate School of Medicine, University of Toyama, Toyama 930-0194, Japan; yhatalm@med.u-toyama.ac.jp (Y.H.); nishida0717@yahoo.co.jp (N.N.)

³ First Department of Surgery, Graduate School of Medicine, University of Toyama, Toyama 930-0194, Japan; ynaoki@med.u-toyama.ac.jp

⁴ Department of Pediatrics, International University of Health and Welfare, Tokyo 107-0052, Japan; fkichida@iuhw.ac.jp

* Correspondence: khirono1973@gmail.com; Tel.: +81-76-434-7313; Fax: +81-76-434-5029

Received: 12 February 2020; Accepted: 9 March 2020; Published: 13 March 2020

Abstract: Background: Left ventricular noncompaction (LVNC) is a hereditary cardiomyopathy that is associated with high morbidity and mortality rates. Recently, LVNC was classified into several phenotypes including congenital heart disease (CHD). However, although LVNC and CHD are frequently observed, the role and clinical significance of genetics in these cardiomyopathies has not been fully evaluated. Therefore, we aimed to evaluate the impact on the perioperative outcomes of children with concomitant LVNC and CHD using next-generation sequencing (NGS). Methods: From May 2000 to August 2018, 53 Japanese probands with LVNC (25 males and 28 females) were enrolled and we screened 182 cardiomyopathy-associated genes in these patients using NGS. Results: The age at diagnosis of the enrolled patients ranged from 0 to 14 years (median: 0.3 months). A total of 23 patients (43.4%) were diagnosed with heart failure, 14 with heart murmur (26.4%), and 6 with cyanosis (11.3%). During the observation period, 31 patients (58.5%) experienced heart failure and 13 (24.5%) developed arrhythmias such as ventricular tachycardia, supraventricular tachycardia, and atrioventricular block. Moreover, 29 patients (54.7%) had ventricular septal defects (VSDs), 17 (32.1%) had atrial septal defects, 10 had patent ductus arteriosus (PDA), and 7 (13.2%) had Ebstein's anomaly and double outlet right ventricle. Among the included patients, 30 underwent surgery, 19 underwent biventricular repair, and 2 underwent pulmonary artery banding, bilateral pulmonary artery banding, and PDA ligation. Overall, 30 genetic variants were identified in 28 patients with LVNC and CHD. Eight variants were detected in *MYH7* and two in *TPM1*. Echocardiography showed lower ejection fractions and more thickened trabeculations in the left ventricle in patients with LVNC and CHD than in age-matched patients with VSDs. During follow-up, 4 patients died and the condition of 8 worsened postoperatively. The multivariable proportional hazards model showed that heart failure, LV ejection fraction of < 24%, LV end-diastolic diameter z-score of > 8.56, and noncompacted-to-compacted ratio of the left ventricular apex of > 8.33 at the last visit were risk factors for survival. Conclusions: LVNC and CHD are frequently associated with genetic abnormalities. Knowledge of the association between CHD and LVNC is important for the awareness of clinical implications during the preoperative and postoperative periods to identify the populations who are at an increased risk of additional morbidity.

Keywords: left ventricular noncompaction; congenital heart disease; congestive heart failure; non-ischemic cardiomyopathy; genetics

1. Introduction

Left ventricular noncompaction (LVNC) is the most recently classified cardiomyopathy. First described in 1990, it is characterized by a pattern of thickened trabeculations and deep intertrabecular fossa communicating with the left ventricular (LV) cavity [1]. LVNC has a wide spectrum, ranging from asymptomatic to severe congestive heart failure (CHF) with concomitant risks of arrhythmia, systemic thromboembolization, and sudden cardiac death. Although its diagnosis has primarily focused on the identification of trabeculation, other features are important to classify the specific subtypes of LVNC [2]. The specific phenotype of LVNC has the risk of adverse clinical outcomes in children and may occasionally be seen in association with congenital heart disease (CHD) [3].

The etiology of LVNC in patients with CHD has been unknown [4]. Previously, LVNC occurs most frequently in patients with Ebstein's anomaly, following with septal defects, LV outflow tract obstructive lesions, hypoplastic left heart syndrome, and other right heart lesions [3–5]. However, the natural history of patients with LVNC and CHD has not been fully elucidated. In addition, it is considered difficult to estimate prognosis and to identify the surgical indications in children with LVNC because they have highly variable clinical presentations. Therefore, the aim of our study was to evaluate the impact on the perioperative outcomes of patients with concomitant LVNC and CHD.

2. Methods

2.1. Subjects

From May 2000 to August 2018, 53 Japanese probands with LVNC and CHD were referred to our institution for genetic testing from several institutions in Japan. Patients aged < 18 years diagnosed as LVNC at the participating institutions were eligible for this study. Patients with secondary etiologies of cardiomyopathy (e.g., endocrine, rheumatic, pulmonary, and immunologic diseases; systemic hypertension; and cardiotoxic exposures), those with a pacemaker because of rhythm disturbance, and those with non-follow-up records were excluded. Clinical data were retrospectively retrieved from the patients' medical records according to the following time course: initial visit, preoperation, postoperation, and last visit. Cardiac death, LV assist device implantation, heart transplant (HT), and implantable cardioverter-defibrillator (ICD) shock were classified as major adverse cardiac events (MACEs).

Age matched patients with ventricular septal defects (VSDs) were selected from the Toyama University Hospital Database for comparison. All these patients underwent a surgery during the same period to endorse similarity of medical management.

Informed consent was gained from all patients or their guardians according to the institutional guidelines. The study protocol conformed to the ethical guidelines of the 1975 Declaration of Helsinki as reflected in the *a priori* approval of the Research Ethics Committee of the University of Toyama, Japan.

2.2. Endpoint Assessment

Primary outcome was the time to the combined endpoint of MACEs, whereas secondary outcomes were arrhythmia, thromboembolic events, echocardiographic parameters, and genetic status.

2.3. Electrocardiogram Collection

All electrocardiograms were assessed independently by two well-trained investigators (K.H. and N.M.) who were blinded to the clinical data. The two investigators judged more than 95% consistency. The final judgment was made by a third experienced investigator (electrophysiologist) in

cases of disagreement. The criteria for J wave and fragmented QRS were based on the description by Antzelevitch, Yan, and Das [6,7].

2.4. Echocardiographic Data Collection

Echocardiography (two-dimensional, color Doppler, and M-mode) was performed to assess cardiac structure, ventricular size and function (fractional shortening and ejection fraction (EF)), and valvular regurgitation. The diagnosis of congestive heart failure (CHF) was defined by clinical findings of tachypnea, feeding difficulty, and cyanosis; cardiomegaly on chest radiography; and decreased LVEF on echocardiography. Cardiomegaly was defined as a cardiothoracic ratio of ≥ 0.55 (≥ 0.60 for patients aged less than 1 year) on chest radiography or LV end-diastolic diameter (LVDD) of $\geq 120\%$ of the normal value on echocardiography.

Patients were diagnosed with LVNC based on the following criteria defined by Ichida et al.: (1) two-layered myocardium with a noncompacted-to-compacted (N/C) ratio of more than 2.0 at end diastole, (2) prominent endomyocardial trabeculations that are distributed in more than one LV wall segment, and (3) deep fossas filled with blood from the ventricular cavity on color Doppler imaging [8]. All echocardiographic records were analyzed by two reviewers (K.H. and S.O.).

The thickness of the LV wall and N/C ratio (N; the depth of trabecular recesses. C; compacted wall thickness) were measured according to previously reported methods to quantify the extent of the trabecular meshwork [9,10]. The thickness of the compacted layer in the LV posterior wall (LVPWC) and LVDD are represented as z-scores based on the body surface area [11].

N/C ratios of 5 LV wall segments at end diastole; the anterior, lateral, and posterior walls; and interventricular septum at the level of the papillary muscles in the short-axis view and the apex in the long-axis view were measured [12–14].

2.5. Variant Screening

After obtaining informed consent from the patients or their parents, DNA was isolated from a whole-blood or heart tissue sample from each patient. Next-generation sequencing (NGS) was performed with 182 cardiac disorder-related genes (Table S1) using the Ion PGM System (Life Technologies, Carlsbad, CA, USA).

After all candidate pathogenic variants passed the selection criteria, to validate the result of NGS, Sanger sequencing was conducted.

2.6. Data Analysis and Variant Classification

The gnomAD database and Human Genetic Variation Database (HGVD), which contain data from 1208 Japanese individuals, was used to determine the allelic frequency of all detected variants. All variants were filtered with a minor allele frequency (MAF) of ≥ 0.0005 among the gnomAD and HGVD population. To evaluate the pathogenicity of the variants, seven different *in silico* predictive algorithms were used (Table S2). The pathogenicity of an identified variant was evaluated by the guidelines of the American College of Medical Genetics and Genomics [15].

2.7. Gene-Based Collapsing Test

A genic collapsing test was performed to confer risk genes of LVNC [16,17]. Fisher's exact test was conducted for each gene in collapsing analysis with a nominal significance level of $< 2.74 \times 10^{-4}$ for the number of assessable genes according to Bonferroni's correction.

2.8. Statistical Analysis

Continuous variables are presented as mean \pm standard deviation, and medians and ranges as appropriate. Categorical variables are given as frequencies and percentages. Statistical analyses were conducted with the use of the JMP software (version 13; SAS Institute, Cary, NC, USA). Receiver

operating characteristic curve analysis was performed to determine the optimum cutoff levels of the number of derivations obtained from electrocardiogram and echocardiographic data to predict MACES. A *p*-value of <0.05 was considered statistically significant.

3. Results

3.1. Clinical and Cardiological Characteristics

Patient demographics and outcomes are shown in Table 1 and Figure 1. Overall, 53 patients (25 males and 28 females) were enrolled in this study. Their age at diagnosis ranged from 0 to 14 years (median: 0.3 months). The median follow-up period was 3.0 years (0.5–17.0 years). A total of 11 patients (20.8%) reported a family history of cardiomyopathy; 23 (43.4%) were diagnosed with CHF, 14 with heart murmur (26.4%), and 6 with cyanosis (11.3%). During the observation period, 31 patients (58.5%) experienced CHF and 13 (24.5%) developed arrhythmias such as ventricular tachycardia, supraventricular tachycardia, and atrioventricular block. No patient had a history of thrombosis. Other systemic malformations were observed in 10 patients (18.9%; Table S3).

Table 1. Comparison of physical findings of patients with LVNC and VSD.

	LVNC with CHD (<i>n</i> = 53)	LVNC with VSD (<i>n</i> = 25)	VSD (<i>n</i> = 57)	<i>p</i> Value
Demographic data				
Male	25 (47.1%)	15 (60%)	29 (50.9%)	0.4724
Age at diagnosis (m, median)	0.27 (0–168)	0.4 (0–60)	0.10 (0–3)	0.3659
Duration of follow up (year)	3.0 (0.5–17)	3.0 (1.0–17)	3.9 (0.5–12.2)	0.6803
Family history of CM	11 (20.8%)			
Symptoms at diagnosis				
Heart failure	23 (43.4%)	11 (44.0%)	4 (7.0%)	0.0002
Heart murmur	14 (26.4%)	8 (32.0%)	50 (87.7%)	<0.0001
Cyanosis	6 (11.3%)	1 (4.0%)	0 (0%)	0.3086
Fetal screening	5 (9.4%)	3 (12.0%)	1 (1.8%)	0.0822
Neonatal screening	4 (7.5%)	1 (4.0%)	2 (3.5%)	0.6696
Arrhythmia	1 (1.9%)	1 (4.0%)	0 (0%)	0.3049
Current clinical presentation				
Heart failure	31 (58.5%)			
Embolism	0 (0%)			
Arrhythmia	13 (24.5%)			
VT	5 (9.4%)			
SVT	2 (3.8%)			
CAVB	4 (7.5%)			
AFL	2 (3.8%)			
Extracardiac abnormalities	10 (18.9%)			
HF requiring hospitalization	44 (83.0%)			
Age at surgery	11.15 ± 14.78			
Death	4 (7.5%)	1 (4.0%)	0 (0%)	0.2963
Type of CHD				
VSD	29 (54.7%)	25 (100%)	57 (100%)	<0.0001
ASD	17 (32.1%)			
PDA	10 (18.9%)			
Ebstein’s disease				
DORV	7 (13.2%)			
CoA	4 (7.5%)			
PS	4 (7.5%)			
AS	2 (3.8%)			
hypo RV	2 (3.8%)			
absent PV	1 (1.9%)			
IAA	1 (1.9%)			

Table 1. Cont.

	LVNC with CHD (n = 53)	LVNC with VSD (n = 25)	VSD (n = 57)	p Value
Heterotaxy syndrome	1 (1.9%)			
MA	1 (1.9%)			
PA	1 (1.9%)			
TA	1 (1.9%)			
TGA	1 (1.9%)			
TOF	1 (1.9%)			
TS	1 (1.9%)			
Type of surgery				
BVR	19 (35.8%)			
PAB	2 (3.8%)			
bil PAB	2 (3.8%)			
PDA ligation	2 (3.8%)			
PTPV	2 (3.8%)			
PTAV	1 (1.9%)			
PA debanding + PA plasty	1 (1.9%)			
Electrocardiography				
ST-segment depression	3 (7.5%)			
T-wave abnormality	8 (20.0%)			
Pathologic Q-wave	7 (17.5%)			
LBBB	3 (7.5%)			
RBBB	10 (25.0%)			
fragmented QRS	16 (40.0%)			
J wave	7 (17.5%)			
LQT	5 (12.5%)			
WPW syndrome	1 (2.5%)			

LVNC-CHD; left ventricular noncompaction with congenital heart disease, VSD; ventricular septal defect, CM; cardiomyopathy, VT; ventricular tachycardia, SVT; supra ventricular tachycardia, CAVB; complete AV block, AFL; atrial flutter, HF; heart failure, ASD; atrial septal defect, PDA; patent ductus arteriosus, Ebstein; Ebstein's anomaly, DORV; double outlet of right ventricle, CoA; coarctation of aorta, PS; pulmonary valve stenosis, AS; aortic valve stenosis, hypo RV; hypoplastic right ventricle, PV; pulmonary valve, IAA; interruption of aortic arch, MA; mitral valve atresia, PA; pulmonary valve atresia, TA; tricuspid valve atresia, TGA; transposition of the great arteries, TOF; tetralogy of Fallot, TS; tricuspid valve stenosis, BVR; biventricular repair, PAB; pulmonary artery banding, bil PAB; bilateral pulmonary artery banding, PTPV; percutaneous transvenous pulmonary valvuloplasty, PTAV; percutaneous transvenous artery valvuloplasty, LBBB; left bundle branch block, RBBB; right bundle branch block, LQT; long QT. Continuous variables between the group of LVNC with VSD and the group of VSD were compared using the unpaired t-test, non-parametric Mann-Whitney test, or one-way analysis of variance, and categorical variables were compared using χ^2 statistics or Fisher's exact test, as appropriate.

According to the type of CHD, 29 patients (54.7%) had VSDs, 17 (32.1%) had atrial septal defects, 10 had patent ductus arteriosus (PDA), and 7 (13.2%) had Ebstein's anomaly and double outlet right ventricle.

A total of 30 patients underwent surgery at, on average, 11.2 months of age; 19 underwent biventricular repair (BVR); and 2 underwent pulmonary artery banding (PAB), bilateral PAB, and PDA ligation. Moreover, 13 patients (43.3%) were diagnosed with LVNC postoperatively (Figure 1).

Upon electrography, fragmented QRS was frequently observed in 16 patients (40.0%), followed by right bundle branch block (25.0%), T-wave abnormality (20.0%), Q wave (17.5%), J wave (17.5%), ST-segment depression (12.3%), and long QT syndrome (12.5%).

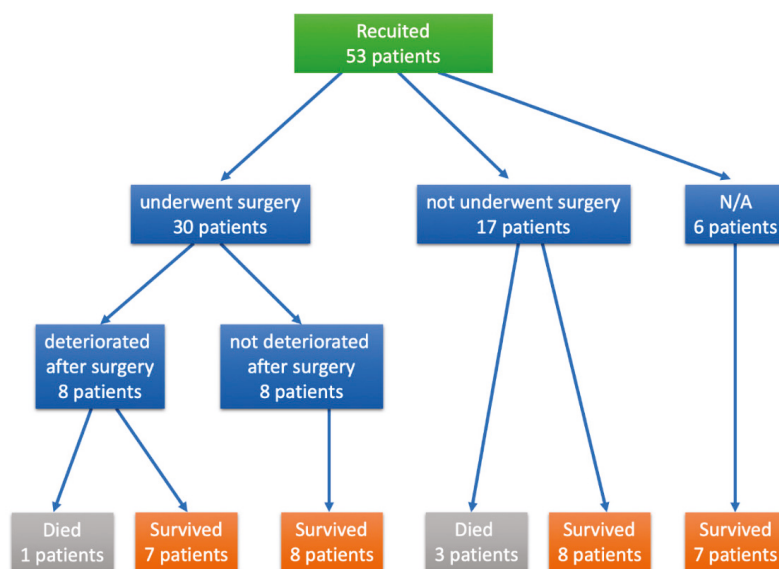


Figure 1. Flowchart of included and excluded patients. Thirty patients underwent surgery and the condition of 8 worsened postoperatively. Adverse events were noted in 4 patients.

3.2. Genetic Analysis

After excluding common polymorphisms on the basis of variant frequencies reported in gnomAD and HGVD and *in silico* analysis predictions, we identified 30 rare exonic (25 missense and 2 frameshift indel) and 3 splice site variants classified as pathogenic or likely pathogenic (Table 2) in 28 patients with LVNC and CHD. Eight variants were detected in *MYH7*, two in *TPM1*, and one in *ACTC1*, *ANK2*, *COL4A1*, *DAAM1*, *DSG2*, *DSP*, *FGF16*, *FGFR2*, *HCN4*, *JUP*, *MYBPC3*, *MYH6*, *MYL2*, *PKP2*, *PRDM16*, *RYR2*, and *TAZ* each. Sarcomere gene variants accounted for 50.0%. All variants affected conserved amino acid residues. In addition, the genetic collapsing test showed that variants in *MYH7* ($p = 2.104 \times 10^{-16}$, ranked first) and *TPM1* ($p = 1.356 \times 10^{-4}$, ranked second) reached significance (adjusted alpha = $p < 2.74 \times 10^{-4}$), which strongly suggested that variants in both genes increase the risk of LVNC (Table S4).

Table 2. Variants identified in patients with LVNC.

Patient Number	Gene	Protein	Coding	dbSNP	gnomAD (EA)	gnomAD	Sift	Fathmm	Polyphen2	GVGD	Mutation Taster	Provean	CADD	Clin Var
1	LDB3	p.Thr282Met	c.845C > T	n/a	0.00001088	0.00001991	0	n/a	1	C0	1	-0.28	-4.91	uncertain significance
2	DSP	p.Arg907Cys	c.Z719C > T	n/a	0	0.000003185	0	-3.43	0.999	C0	1	1.96	-3.58	uncertain significance
2	PKF2	p.Thr50fs	c.148_151delACAG	rs397517067	n/a	n/a	n/a	-4.54	n/a	n/a	n/a	n/a	n/a	n/a
6	LJP	p.Arg233Pro	c.698G > C	n/a	n/a	n/a	0.03	-4.39	0.999	C0	1	1.03	-4.36	n/a
9	MYL2	p.Glu88Lys	c.262C > A	rs753032598	n/a	n/a	0.017	-0.23	0.996	C15	1	-1.15	-3.62	n/a
11	MYH7	p.Arg712His	c.2135G > A	rs719947346	n/a	n/a	0	-5.47	0.988	C25	1	-4.54	-6.25	n/a
16	MYH7	p.Met362Arg	c.1085T > G	rs199473346	n/a	n/a	0	-5.47	0.001	0	1	-3.64	-5.15	n/a
18	MYH7	p.Met362Arg	c.1085T > G	rs199473346	n/a	n/a	0	-5.47	0.001	0	1	-3.64	-5.15	n/a
20	MYBPC3	p.Arg891Trp	c.2671C > T	rs200229074	0.0000271	0.00001996	0.001	-1.83	1	C65	1	0.37	-6.52	uncertain significance
21	TPM1	p.Arg238Gln	c.713C > A	n/a	n/a	n/a	0.001	-3.32	0.999	C35	1	-6.36	-3.22	n/a
23	MYH7	—	c.896-1C > T	n/a	n/a	n/a	n/a	-4.49	n/a	n/a	n/a	n/a	n/a	n/a
24	MYH7	p.Phe230Ser	c.689T > C	n/a	n/a	n/a	0	5.9	0.984	0	1	-4.96	-6.07	n/a
25	DAAMI	p.Ala187fs	c.557_558msA	n/a	n/a	n/a	n/a	n/a	n/a	n/a	n/a	—	—	n/a
27	MYH7	p.Leu693Arg	c.2078T > G	rs749051278	n/a	n/a	0	1.96	0.997	C65	1	-4.85	-5.29	n/a
28	MYH7	p.Leu620Pro	c.1859T > C	n/a	0.000003977	0	7	n/a	0.969	C65	1	-4.06	-6.25	n/a
30	MYH7	p.Arg237Trp	c.67C > T	rs749297714	0.00002475	0	0.002	3.31	0.997	0	1	-2.08	-4.22	uncertain significance
31	PRDM16	p.Ser723fs	c.2168delC	n/a	n/a	0.00001071	n/a	-2.31	n/a	n/a	n/a	n/a	n/a	n/a
33	TPM1	p.Arg238Gln	c.713C > A	n/a	n/a	n/a	0.001	n/a	0.999	C35	1	-6.36	-3.22	n/a
34	FGF16	—	c.105 + 4AG > GT	n/a	n/a	n/a	n/a	n/a	n/a	n/a	n/a	n/a	n/a	n/a
34	FGFR2	—	c.939 + 40T > C	n/a	0.0000533	0.0004516	n/a	n/a	n/a	n/a	n/a	n/a	n/a	n/a
35	COL4A1	p.Pro108Ser	c.322C > T	rs769020772	n/a	n/a	0	n/a	0.999	C65	1	5.9	-5.28	n/a
36	RYR2	p.Leu459Ser	c.13790T > C	n/a	n/a	n/a	0	n/a	0.999	C0	1	-5.09	-4.614	n/a
37	ACTC1	p.Arg212His	c.635C > A	rs121908411	n/a	n/a	0	-7.52	0.887	C25	1	-4.54	-3.896	uncertain significance
38	TNNI2	p.Lys298Thr	c.893A > C	rs121908411	n/a	n/a	0	-7.52	0.998	C0	1	2.19	-3.071	n/a
43	ANK2	p.Arg895Gln	c.2684G > A	rs146581757	0.00004773	0.0002719	0.05	-0.23	0.998	C0	1	-0.3	-3.277	n/a
45	TAZ	p.Gly216Arg	c.646G > A	n/a	n/a	n/a	0.05	1.03	1	C0	1	-3.5	-6.733	n/a
46	MYH6	p.Glu1713Lys	c.5157G > A	rs121908441	0.00003197	0.00005013	0	-2.4	1	C55	1	-1.84	-2.522	uncertain significance
47	DSG2	p.Tyr235His	c.703T > C	rs199472921	n/a	n/a	0	-4.93	1	C65	1	-0.41	-4.678	n/a
48	COL4A1	p.Gln462Arg	c.1385A > G	rs147445322	0.00001991	0.0002718	0.04	-6.37	0.491	C0	1	-3.19	-1.633	n/a
50	HCN4	p.Asp432His	c.1294G > C	rs147445322	n/a	n/a	0.12	-2.61	1	C0	1	-4.92	-5.923	n/a

3.3. Cardiological Characteristics

Echocardiography showed lower EFs and more thickened trabeculations in LV in children with LVNC and CHD than in those with VSDs (Table 3 and Figure 2). The average LV posterior wall (LVPW) z-score at the last visit was significantly higher than that at the initial visit ($p = 0.0482$). The average z-score of LVPWC thickness at the last visit was significantly lower than that of the initial visit ($p = 0.0061$).

Table 3. Comparison of physical findings of patients with LVNC and VSD between the initial and last visit.

	LVNC with VSD (<i>n</i> = 21)			VSD (<i>n</i> = 57)		
	Initial	Last	<i>p</i> Value	Initial	Last	<i>p</i> Value
Age	5.43 ± 13.24	56.25 ± 76.97	0.2768	19.05 ± 28.26	33.39 ± 28.32	<0.0001
Cardiac function at diagnosis						
LVEF (%)	59.00 ± 12.97	57.85 ± 14.73	0.7192	70.09 ± 8.29	68.47 ± 5.35	0.1363
LVDD Z-score	1.323 ± 3.16	1.14 ± 2.31	0.9576	2.02 ± 1.74	0.19 ± 1.00	<0.0001
LVPW Z-score	6.13 ± 1.57	4.72 ± 1.84	0.0482	2.73 ± 1.78	2.13 ± 1.53	0.0814
LVPWC Z-score	-3.13 ± 2.22	-5.48 ± 2.11	0.0061	-2.67 ± 2.07	-2.78 ± 1.89	0.5709
N/C ratio						
Anterior wall	-3.13 ± 2.22	-5.48 ± 2.11	0.5370	0.50 ± 0.31	0.38 ± 0.18	0.0632
Septal wall	-3.13 ± 2.22	-5.48 ± 2.11	0.1723	0.41 ± 0.20	0.29 ± 0.11	0.0015
Lateral wall	-3.13 ± 2.22	-5.48 ± 2.11	0.9385	0.73 ± 0.44	0.72 ± 0.37	0.8735
Posterior wall	3.21 ± 1.45	3.81 ± 1.50	0.2028	1.30 ± 0.50	1.14 ± 0.49	0.0846
Apex	3.45 ± 1.72	3.97 ± 1.62	0.1913	1.52 ± 0.88	4.22 ± 1.62	<0.0001
Mean 5 segments	2.13 ± 0.84	2.19 ± 0.61	0.4897	0.89 ± 0.24	1.35 ± 0.38	<0.0001

LVNC-CHD; left ventricular noncompaction with congenital heart disease, VSD; ventricular septal defect, LVEF; left ventricular ejection fraction, LVDD; left ventricular diastolic dimension, LVPW; left ventricular posterior wall, LVPWC; compacted layer of left ventricular posterior wall, N/C; ratio of noncompacted/compacted layer.

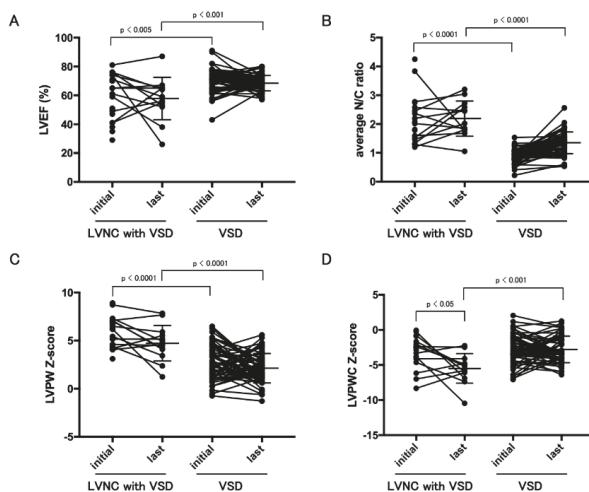


Figure 2. Longitudinal data of echocardiographic data between LVNC with CHD and VSD groups. LVEF (A), average N/C ratio (B), LVPW z-score (C), and LVPWC z-score (D) between the initial and last visits. LVNC; left ventricular noncompaction, VSD; ventricular septal defect, LVEF; left ventricular ejection fraction, N/C; ratio of noncompacted/compacted layer, LVPW; left ventricular posterior wall, LVPWC; compacted layer of left ventricular posterior wall.

3.4. Characteristics of Patients with Adverse Events

Adverse events were observed in 4 patients, and 4 patients died (Table 4 and Figure 1). Although cardiac death, LV assist device implantation, HT, and ICD shock were classified as MACEs in this study, none of the patients underwent HT or LV assist device implantation or experienced ICD shock. Aside from 1 patient, 3 died at early infancy and never underwent surgery.

The condition of 8 patients worsened postoperatively (Table 5 and Figure 1), all patients had VSDs, 3 had variants in *MYH7*, 6 underwent BVR, and long-term medical therapy were required in all patients for myocardial dysfunction after their latest surgeries.

The analysis of the multivariable proportional hazards model revealed that CHF during follow-up, LVEF of < 24%, LVDD z-score of > 8.56, and N/C ratio of the LV apex of > 8.33 at the last visit were risk factors for survival without MACE occurrence (Table 6). Patients with LVNC and CHD had a worse prognosis than those with VSDs (Figure 3).

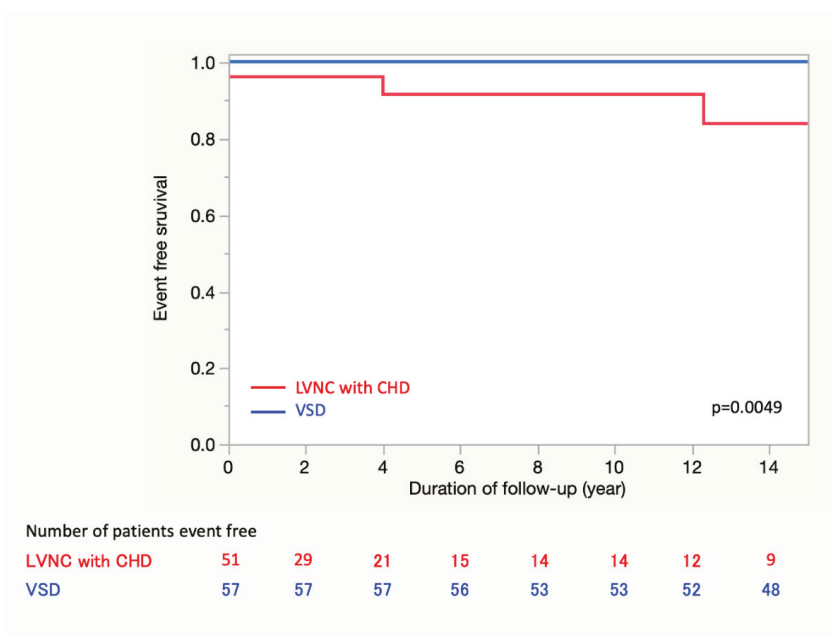


Figure 3. Event-free survival to the endpoint of major adverse cardiac events in LVNC with CHD and VSD groups. LVNC; left ventricular noncompaction, VSD; ventricular septal defect.

Table 4. Summary of death cases.

ID	Sex	Age at Diagnosis	Symptoms at Diagnosis	CHD	Variants	FH of CM	Extracardiac Abnormalities	Current Clinical Presentation	Age at Death	Cause of Death
13	F	1 d	bradycardia	VSD	-	yes	no	CHF	1d	shock
43	M	0 d	CHF	DORV, TGA, VSD	ANK2	no	no	CHF	12y	CHF
45	M	0 d	CHF	ASD, PDA	TAZ	no	no	CHF	2m	shock
52	M	fetus	CHF	Ebstein	-	no	no	CHF	0d	shock

CHD; congenital heart disease, FH; family history, CM; cardiomyopathy, VSD; ventricular septal defect, DORV; double outlet of right ventricle, Ebstein; Ebstein's anomaly, ASD; atrial septal disease, TVD; tricuspid valve dysplasia. BVR; biventricular repair, CHF; congestive heart failure.

Table 5. Summary of deteriorated cases postoperatively.

ID	Sex	Age at Diagnosis	Symptoms at Diagnosis	CHD	Variants	FH of CM	Extracardiac Abnormalities	Type of Surgery	Age at Surgery	Current Clinical Presentation	Outcome
5	M	1 d	cyanosis	DORV, VSD, IAA	-	no	no	BVR	5	CHF	alive
16	F	fetus	cyanosis	Ebstein, VSD, CoA	MYH7	yes	no	BVR	1	CHF	alive
17	F	1 y	CHF	VSD	-	no	no	BVR	16	CHF	alive
18	F	4 d	heart murmur	Ebstein, VSD, CoA	MYH7	yes	no	BVR	0	CHF	alive
23	F	fetus	CHF	DORV, VSD, IAA	MYH7	yes	no	bilPAB	0	CHF	alive
43	M	0 d	cyanosis	TGA, DORV, VSD	ANK2	no	no	BVR	17	CHF	death
47	F	12 d	heart murmur	ASD, VSD, PDA	DSG2	no	chromosome 12 abnormality	PA debanding + PA plasty	34	CHF	alive
53	M	1 m	CHF	VSD	-	no	no	BVR	1	no	alive

CHD; congenital heart disease, FH; family history, CM; cardiomyopathy, DORV; double outlet of right ventricle, VSD; ventricular septal defect, IAA; interruption of aortic arch, Ebstein; Ebstein's anomaly, CoA; coarctation of aorta, TGA; transposition of the great arteries, ASD; atrial septal disease, PDA; patent ductus arteriosus, BVR; biventricular repair, PAB; pulmonary artery banding, bil PAB; bilateral pulmonary artery banding.

Table 6. Univariate analysis of risk factors for death in the patients with LVNC.

Variable	Univariable Survival Analysis	
	Odds Ratio (95% CI)	p Value
Male	3.54 (0.42–74.51)	0.2536
Family history	4.33 (0.47–40.33)	0.1809
Heart failure at diagnosis	4.39×10^7 (0.62–)	0.1049
Heart failure	8.06×10^6 (1.13–)	0.0404
Extracardiac abnormalities	4.75 (0.51–44.78)	0.1586
Gene variants	0.85 (0.96–7.52)	0.8726
Double variants	2.87×10^{-6} (-5.89×10^{-121})	0.5676
UCG parameters at first visit		
LVEF < 50%	0.89 (0.098–8.13)	0.9160
UCG parameters at last visit		
LVEF < 24%	1.84×10^{15} (0.0051–10.55)	0.0051
LVDD Z score > 8.56	1.84×10^{15} (0.0054–9.95)	0.0054
N/C ratio of apex > 8.33	1.84×10^{15} (0.0051–10.55)	0.0051

CI, confidence interval, UCG; cardiac ultrasound, LVEF; left ventricular ejection fraction, LVDD; left ventricular diastolic dimension, N/C; ratio of noncompacted/compacted layer.

4. Discussion

LVNC is associated with CHD, ranging from PDA or atrial septal defects/VSDs to more severe diseases such as Ebstein's anomaly [4]. Our study demonstrated three features: (1) pathogenic variants were identified in more than half of the patients; (2) patients with LVNC had lower EFs than those with VSDs throughout the study period; and (3) postoperative deterioration was observed in several patients.

A variety of genetic disorders are associated with LVNC, including Z-disk and sarcomere gene variants, mitochondrial disorders, and ion channel gene variants [18–22]. Thus, structural congenital malformations and impaired LV myocardial differentiation may be caused by genetic abnormalities. Additionally, for the development of LVNC in a patient with genetic variants, remarkable change of hemodynamic circulation in the fetus may be a cofactor [23]. In our results, variants in *MYH7* were most commonly identified and the variants significantly increase the risk of LVNC by rare variant collapsing analysis. The mechanisms by which variants in the *MYH7* gene induce LVNC remain unclear. Analyzing the positions of these variants against their amino acid location showed several hotspots wherein variants are more popular, which seemed to tend to be in key functional locations. We observed that all variants in *MYH7* associated with LVNC were found in the segment 1 domain. Moreover, enrichment of pathogenic variants was observed in the crucial functional domains of the ATP-binding domain [24–26]. It suggested that the majority of the identified variants affect the force output by affecting either regulation of the ATPase cycle, movement of the lever, or interaction between myosin and actin. Remarkably, the location of variants in *MYH7* in LVNC was different from that in hypertrophic cardiomyopathy (HCM) patients. Hotspots of HCM were mostly located in the surface spanning the converter domain and the myosin mesa; the flat surface of the myosin catalytic domain [27]. It is important to distinguish variant types and assess them in light of well-known disease mechanisms. Therefore, to understand the pathophysiology and development of LVNC, it is critically notable for the patients with LVNC and CHD to characterize genetic variants and phenotypic abnormalities.

Children with LVNC and CHD have a higher incidence of CHF than patients with VSDs. Additionally, our results showed that the condition of 8 of the 30 patients (26.7%) worsened postoperatively, whether palliative or radical. The underlying pathophysiologic mechanisms of CHF remain unclarified. Systolic dysfunction in LVNC is believed to be due to subendocardial hypoperfusion [1,28]. It is also believed that diastolic dysfunction occurs by a restrictive filling pattern and abnormal relaxation because of the presence of LV hypertrabeculation [29]. These speculations are based on the evidence that the noncompacted layer has typically low perfusion, which has been

demonstrated on multiple modalities [30]. Functionally, LV torsion is more common in patients with LVNC [31]. LV twist is generated by the movement of two orthogonally oriented muscular bands of a helical myocardial structure concomitant with a clockwise rotation of the base and counterclockwise rotation of the apex in LV [32]. Van Dalen et al. used two-dimensional speckle tracking echocardiography and demonstrated that LV basal and apical rotation are in the same direction, resulting in a lack of LV twist in patients with LVNC [33]. Bellavia et al. reported that in adults, the value of LV rotation/torsion excessively decreased in patients with LVNC, whereas normal EF were retained when compared with those in controls [31]. Nawaytow et al. reported that almost half of the children with LVNC exhibit reverse apical rotation, resulting in decreased LV torsion and untwist rate, which are associated with the degree of LVNC [34]. These previous studies might support that the deterioration of LV function occurs during the perioperative period, although LV systolic function was preserved preoperatively because of its unique structure.

In our study, 13 patients were diagnosed with LVNC postoperatively. The existence of additional triggers such as dynamic hemodynamic changes during the perioperative period were suggested. Indeed, the etiology of LVNC remains unknown. One possibility is that primary abnormality in early myocardial morphogenesis may cause LVNC. Another possibility is that prenatal or postnatal additional triggers such as pressure overload on the LV may cause LVNC. LVNC in the setting of CHD may be one of the models where both hemodynamic and genetic factors interact with each other, resulting in abnormal LV differentiation. Thus, additional stress to the myocardium may trigger the worsening of systolic function in patients with LVNC and CHD because LVNC is more frequently associated with systolic dysfunction than that of CHD without LVNC.

There were no predictors of postoperative CHF in this study. Preoperative preserved systolic function did not predict the outcome of patients with LVNC and CHD. In fact, not all patients with LVNC had systolic dysfunction during the preoperative evaluation. Most patients with LVNC and CHD had mildly depressed systolic function preoperatively. These facts may complicate the establishment of medical treatment during the operative period and optimal timing of surgery.

In our study, patients with LVNC and CHD were observed to have a higher frequency of arrhythmias (24.5%). Recently, it was demonstrated in pediatric patients that LVNC with associated CHD confers additional risk [35]. Although there were no data relationships between mortality and the prevalence of arrhythmias in patients with LVNC and CHD, our data suggest that more attention should be paid to the occurrence of arrhythmia and CHF because of the higher prevalence of these symptoms.

Limitations

The number of patients in our study was small. We were not able to track patients for a long period of time, particularly those who were referred from external facilities, because this was a retrospective study. This study included data from over approximately 15 years. During this period, the development of disease-modifying treatments was improved, which may have altered study outcomes. The small number of patients with genetic variants also has a limitation regarding the significance of the association with variants and prognosis. To clarify the effect of variants on clinical manifestations and prognosis, further analyses of larger numbers of patients are required. Additionally, functional analyses are also required to clarify the significance of the identified variants which contribute to the etiology of LVNC.

5. Conclusions

To the best of our knowledge, this is the first large cohort study to reveal the etiology and genetic background of LVNC and CHD. Recognition of the association between LVNC and CHD is crucial considering the increased risk of CHF as demonstrated in our results. Moreover, our data suggest that concomitant LVNC with CHD is a surgical risk factor, so additional perioperative planning such as CHF treatment may be beneficial if identified preoperatively. Therefore, elucidation of genotype-phenotype

correlation in patients with LVNC and CHD may be important to understand the pathophysiology and development of LVNC in patients with CHD. Further studies will continue to determine long-term and genotype–phenotype correlations.

Supplementary Materials: The following are available online at <http://www.mdpi.com/2077-0383/9/3/785/s1>, Table S1: List of 182 analyzed genes of NGS, Table S2: Silico predictive algorithms used in the study, Table S3: List of patients with extracardiac anomaly, and Table S4: Gene collapsing test of rare variants.

Author Contributions: Conceptualization, K.H.; methodology, Y.H.; validation, N.N. and N.Y.; formal analysis, Y.H.; investigation, S.T. and H.N. and K.I. and S.O.; data curation, M.O.; writing—original draft preparation, K.H.; writing—review and editing, K.H.; visualization, N.M.; supervision, F.I.; project administration, K.H.; All authors have read and agreed to the published version of the manuscript.

Funding: This research received no external funding.

Acknowledgments: The authors wish to acknowledge Masaya Aoki, Teruhiko Higashida, Daisuke Torizuka, Hitoshi Moriuchi, Haruna Hirai, and Eriko Masuda for their expert technical assistance.

Conflicts of Interest: The authors declare no conflict of interest.

Abbreviations

LVNC	left ventricular noncompaction
LV	left ventricle
CHD	congenital heart disease
CHF	congestive heart failure

References

1. Chin, T.K.; Perloff, J.K.; Williams, R.G.; Jue, K.; Mohrmann, R. Isolated noncompaction of left ventricular myocardium. A study of eight cases. *Circulation* **1990**, *82*, 507–513. [[CrossRef](#)] [[PubMed](#)]
2. Jefferies, J.L.; Wilkinson, J.D.; Sleeper, L.A.; Colan, S.D.; Lu, M.; Pahl, E.; Kantor, P.F.; Everitt, M.D.; Webber, S.A.; Kaufman, B.D.; et al. Cardiomyopathy Phenotypes and Outcomes for Children With Left Ventricular Myocardial Noncompaction: Results From the Pediatric Cardiomyopathy Registry. *J. Card. Fail.* **2015**, *21*, 877–884. [[CrossRef](#)] [[PubMed](#)]
3. Towbin, J.A.; Jefferies, J.L. Cardiomyopathies Due to Left Ventricular Noncompaction, Mitochondrial and Storage Diseases, and Inborn Errors of Metabolism. *Circ. Res.* **2017**, *121*, 838–854. [[CrossRef](#)]
4. Stahl, B.E.; Gebhard, C.; Biaggi, P.; Klaassen, S.; Valsangiacomo Buechel, E.; Attenhofer Jost, C.H.; Jenni, R.; Tanner, F.C.; Greutmann, M. Left ventricular non-compaction: Prevalence in congenital heart disease. *Int. J. Cardiol.* **2013**, *167*, 2477–2481. [[CrossRef](#)] [[PubMed](#)]
5. Attenhofer Jost, C.H.; Connolly, H.M. Left ventricular non-compaction: Dreaming of the perfect diagnostic tool. *Eur. J. Heart Fail.* **2012**, *14*, 113–114. [[CrossRef](#)] [[PubMed](#)]
6. Antzelevitch, C.; Yan, G.X. J wave syndromes. *Heart Rhythm* **2010**, *7*, 549–558. [[CrossRef](#)] [[PubMed](#)]
7. Das, M.K.; Saha, C.; El Masry, H.; Peng, J.; Dandamudi, G.; Mahenthiran, J.; McHenry, P.; Zipes, D.P. Fragmented QRS on a 12-lead ECG: A predictor of mortality and cardiac events in patients with coronary artery disease. *Heart Rhythm* **2007**, *4*, 1385–1392. [[CrossRef](#)]
8. Ichida, F. Left ventricular noncompaction—Risk stratification and genetic consideration. *J. Cardiol.* **2019**. [[CrossRef](#)]
9. Jenni, R.; Rojas, J.; Oechslin, E. Isolated noncompaction of the myocardium. *N. Engl. J. Med.* **1999**, *340*, 966–967. [[CrossRef](#)]
10. Wald, R.; Veldtman, G.; Golding, F.; Kirsh, J.; McCrindle, B.; Benson, L. Determinants of outcome in isolated ventricular noncompaction in childhood. *Am. J. Cardiol.* **2004**, *94*, 1581–1584. [[CrossRef](#)]
11. Kampmann, C.; Wiethoff, C.M.; Wenzel, A.; Stolz, G.; Betancor, M.; Wippermann, C.F.; Huth, R.G.; Habermehl, P.; Knuf, M.; Emschermann, T.; et al. Normal values of M mode echocardiographic measurements of more than 2000 healthy infants and children in central Europe. *Heart* **2000**, *83*, 667–672. [[CrossRef](#)] [[PubMed](#)]

12. Pignatelli, R.H.; McMahon, C.J.; Dreyer, W.J.; Denfield, S.W.; Price, J.; Belmont, J.W.; Craigen, W.J.; Wu, J.; El Said, H.; Bezold, L.L.; et al. Clinical characterization of left ventricular noncompaction in children: A relatively common form of cardiomyopathy. *Circulation* **2003**, *108*, 2672–2678. [[CrossRef](#)] [[PubMed](#)]
13. Oechslin, E.N.; Attenhofer Jost, C.H.; Rojas, J.R.; Kaufmann, P.A.; Jenni, R. Long-term follow-up of 34 adults with isolated left ventricular noncompaction: A distinct cardiomyopathy with poor prognosis. *J. Am. Coll. Cardiol.* **2000**, *36*, 493–500. [[CrossRef](#)]
14. Wang, C.; Takasaki, A.; Watanabe Ozawa, S.; Nakaoka, H.; Okabe, M.; Miyao, N.; Saito, K.; Ibuki, K.; Hirono, K.; Yoshimura, N.; et al. Long-Term Prognosis of Patients With Left Ventricular Noncompaction-Comparison Between Infantile and Juvenile Types. *Circ. J.* **2017**, *81*, 694–700. [[CrossRef](#)] [[PubMed](#)]
15. Richards, S.; Aziz, N.; Bale, S.; Bick, D.; Das, S.; Gastier-Foster, J.; Grody, W.W.; Hegde, M.; Lyon, E.; Spector, E.; et al. Standards and guidelines for the interpretation of sequence variants: A joint consensus recommendation of the American College of Medical Genetics and Genomics and the Association for Molecular Pathology. *Genet. Med.* **2015**, *17*, 405–424. [[CrossRef](#)]
16. Cirulli, E.T.; Lasseigne, B.N.; Petrovski, S.; Sapp, P.C.; Dion, P.A.; Leblond, C.S.; Couthouis, J.; Lu, Y.F.; Wang, Q.; Krueger, B.J.; et al. Exome sequencing in amyotrophic lateral sclerosis identifies risk genes and pathways. *Science* **2015**, *347*, 1436–1441. [[CrossRef](#)]
17. Bagnall, R.D.; Crompton, D.E.; Petrovski, S.; Lam, L.; Cutmore, C.; Garry, S.I.; Sadleir, L.G.; Dibbens, L.M.; Cairns, A.; Kivity, S.; et al. Exome-based analysis of cardiac arrhythmia, respiratory control, and epilepsy genes in sudden unexpected death in epilepsy. *Ann. Neurol.* **2016**, *79*, 522–534. [[CrossRef](#)]
18. Stollberger, C.; Wegner, C.; Benatar, A.; Chin, T.K.; Dangel, J.; Majoor-Krakauer, D.; Mondal, T.K.; Sivanandam, S.; Silverman, N.H.; van Waning, J.; et al. Postnatal Outcome of Fetal Left Ventricular Hypertrabeculation/Noncompaction. *Pediatr. Cardiol.* **2016**, *37*, 919–924. [[CrossRef](#)]
19. Arbustini, E.; Weidemann, F.; Hall, J.L. Left ventricular noncompaction: A distinct cardiomyopathy or a trait shared by different cardiac diseases? *J. Am. Coll. Cardiol.* **2014**, *64*, 1840–1850. [[CrossRef](#)]
20. Hoedemaekers, Y.M.; Caliskan, K.; Michels, M.; Frohn-Mulder, I.; van der Smagt, J.J.; Phefferkorn, J.E.; Wessels, M.W.; ten Cate, F.J.; Sijbrands, E.J.; Dooijes, D.; et al. The importance of genetic counseling, DNA diagnostics, and cardiologic family screening in left ventricular noncompaction cardiomyopathy. *Circ. Cardiovasc. Genet.* **2010**, *3*, 232–239. [[CrossRef](#)]
21. Dellefave, L.M.; Pytel, P.; Mewborn, S.; Mora, B.; Guris, D.L.; Fedson, S.; Waggoner, D.; Moskowitz, I.; McNally, E.M. Sarcomere mutations in cardiomyopathy with left ventricular hypertrabeculation. *Circ. Cardiovasc. Genet.* **2009**, *2*, 442–449. [[CrossRef](#)]
22. Wang, C.; Hata, Y.; Hirono, K.; Takasaki, A.; Ozawa, S.W.; Nakaoka, H.; Saito, K.; Miyao, N.; Okabe, M.; Ibuki, K.; et al. A Wide and Specific Spectrum of Genetic Variants and Genotype-Phenotype Correlations Revealed by Next-Generation Sequencing in Patients with Left Ventricular Noncompaction. *J. Am. Heart Assoc.* **2017**, *6*. [[CrossRef](#)]
23. Sedmera, D.; Pexieder, T.; Vuillemin, M.; Thompson, R.P.; Anderson, R.H. Developmental patterning of the myocardium. *Anat. Rec.* **2000**, *258*, 319–337. [[CrossRef](#)]
24. Moore, J.R.; Leinwand, L.; Warshaw, D.M. Understanding cardiomyopathy phenotypes based on the functional impact of mutations in the myosin motor. *Circ. Res.* **2012**, *111*, 375–385. [[CrossRef](#)] [[PubMed](#)]
25. Buvoli, M.; Hamady, M.; Leinwand, L.A.; Knight, R. Bioinformatics assessment of beta-myosin mutations reveals myosin's high sensitivity to mutations. *Trends Cardiovasc. Med.* **2008**, *18*, 141–149. [[CrossRef](#)] [[PubMed](#)]
26. Rayment, I.; Holden, H.M.; Sellers, J.R.; Fananapazir, L.; Epstein, N.D. Structural interpretation of the mutations in the beta-cardiac myosin that have been implicated in familial hypertrophic cardiomyopathy. *Proc. Natl. Acad. Sci. USA* **1995**, *92*, 3864–3868. [[CrossRef](#)] [[PubMed](#)]
27. Spudich, J.A. The myosin mesa and a possible unifying hypothesis for the molecular basis of human hypertrophic cardiomyopathy. *Biochem. Soc. Trans.* **2015**, *43*, 64–72. [[CrossRef](#)] [[PubMed](#)]
28. Weiford, B.C.; Subbarao, V.D.; Mulhern, K.M. Noncompaction of the ventricular myocardium. *Circulation* **2004**, *109*, 2965–2971. [[CrossRef](#)] [[PubMed](#)]
29. Agmon, Y.; Connolly, H.M.; Olson, L.J.; Khandheria, B.K.; Seward, J.B. Noncompaction of the ventricular myocardium. *J. Am. Soc. Echocardiogr.* **1999**, *12*, 859–863. [[CrossRef](#)]
30. Soler, R.; Rodriguez, E.; Monserrat, L.; Alvarez, N. MRI of subendocardial perfusion deficits in isolated left ventricular noncompaction. *J. Comput. Assist. Tomogr.* **2002**, *26*, 373–375. [[CrossRef](#)]

31. Bellavia, D.; Michelena, H.I.; Martinez, M.; Pellikka, P.A.; Bruce, C.J.; Connolly, H.M.; Villarraga, H.R.; Veress, G.; Oh, J.K.; Miller, F.A. Speckle myocardial imaging modalities for early detection of myocardial impairment in isolated left ventricular non-compaction. *Heart* **2010**, *96*, 440–447. [[CrossRef](#)] [[PubMed](#)]
32. Kocica, M.J.; Corno, A.F.; Carreras-Costa, F.; Ballester-Rodes, M.; Moghbel, M.C.; Cueva, C.N.; Lackovic, V.; Kanjuh, V.I.; Torrent-Guasp, F. The helical ventricular myocardial band: Global, three-dimensional, functional architecture of the ventricular myocardium. *Eur. J. Cardiothorac. Surg.* **2006**, *29*, S21–S40. [[CrossRef](#)]
33. van Dalen, B.M.; Caliskan, K.; Soliman, O.I.; Nemes, A.; Vletter, W.B.; Ten Cate, F.J.; Geleijnse, M.L. Left ventricular solid body rotation in non-compaction cardiomyopathy: A potential new objective and quantitative functional diagnostic criterion? *Eur. J. Heart Fail.* **2008**, *10*, 1088–1093. [[CrossRef](#)] [[PubMed](#)]
34. Nawaytou, H.M.; Montero, A.E.; Yubbu, P.; Calderon-Anyosa, R.J.C.; Sato, T.; O'Connor, M.J.; Miller, K.D.; Ursell, P.C.; Hoffman, J.I.E.; Banerjee, A. A Preliminary Study of Left Ventricular Rotational Mechanics in Children with Noncompaction Cardiomyopathy: Do They Influence Ventricular Function? *J. Am. Soc. Echocardiogr.* **2018**, *31*, 951–961. [[CrossRef](#)] [[PubMed](#)]
35. Punn, R.; Silverman, N.H. Cardiac segmental analysis in left ventricular noncompaction: Experience in a pediatric population. *J. Am. Soc. Echocardiogr.* **2010**, *23*, 46–53. [[CrossRef](#)] [[PubMed](#)]



© 2020 by the authors. Licensee MDPI, Basel, Switzerland. This article is an open access article distributed under the terms and conditions of the Creative Commons Attribution (CC BY) license (<http://creativecommons.org/licenses/by/4.0/>).

Review

Improved Left Atrial Function in CRT Responders: A Systematic Review and Meta-Analysis

Ibadete Bytyçi^{1,2}, Gani Bajraktari^{1,2}, Per Lindqvist^{1,3} and Michael Y. Henein^{1,4,*}

¹ Institute of Public Health and Clinical Medicine, Umeå University, 90187 Umeå, Sweden; i.bytyci@hotmail.com (I.B.); gani.bajraktari@umu.se (G.B.); per.lindqvist@umu.se (P.L.)

² Clinic of Cardiology, University Clinical Centre of Kosovo, 10000 Prishtina, Kosovo

³ Faculty of Medicine, Department of Surgical and Perioperative Sciences, Clinical Physiology, Umeå University, 90187 Umeå, Sweden

⁴ Molecular and Clinic Research Institute, St George University, London SW17 0QT, UK

* Correspondence: michael.henein@umu.se; Tel.: +46-90-785-14-31

Received: 19 December 2019; Accepted: 15 January 2020; Published: 21 January 2020

Abstract: Cardiac resynchronization therapy (CRT) is associated with reverse left atrial (LA) remodeling. The aim of this meta-analysis was to assess the relationship between clinical response to CRT and LA function changes. We conducted a systematic search of all electronic databases up to September 2019 which identified 488 patients from seven studies. At (mean) 6 months follow-up, LA systolic strain and emptying fraction (EF) were increased in CRT responders, with a -5.70% weighted mean difference (WMD) [95% confidence interval (CI) -8.37 to -3.04 , $p < 0.001$ and a WMD of -8.98% [CI -15.1 to -2.84 , $p = 0.004$], compared to non-responders. The increase in LA strain was associated with a fall in left ventricle (LV) end-systolic volume (LVESV) $r = -0.56$ (CI -0.68 to -0.40 , $p < 0.001$) and an increase in the LV ejection fraction (LVEF) $r = 0.58$ (CI 0.42 to 0.69 , $p < 0.001$). The increase in LA EF correlated with the fall in LVESV $r = -0.51$ (CI -0.63 to -0.36 , $p < 0.001$) and the increase in the LVEF $r = 0.48$ (CI 0.33 to 0.61 , $p = 0.002$). The increase in LA strain correlated with the increase in the LA EF, $r = 0.57$ (CI 0.43 to 0.70 , $p < 0.001$). Thus, the improvement of LA function in CRT responders reflects LA reverse remodeling and is related to its ventricular counterpart.

Keywords: left atrial strain; cardiac resynchronization therapy; heart failure

1. Introduction

Heart failure (HF) is a clinical syndrome that is becoming a major public health problem worldwide because of its increasing incidence and prevalence as well as its related morbidity and mortality [1]. Despite its failure in about one-third of treated patients, cardiac resynchronization therapy (CRT) still remains the best treatment for symptomatic HF patients on full medical therapy [2,3].

Responders to CRT have shown clear evidence for improved cardiac performance, left ventricular (LV) function, and the reverse remodeling of the left atrium (LA) [4,5]. LA function can be assessed by various echocardiographic techniques, among which myocardial deformation has recently shown significant accuracy. Despite this, the relationship between CRT-related LA and ventricular function changes remains poorly established, irrespective of the fact that CRT is associated with both cavity reverse remodeling and reduced atrial arrhythmia [6–8].

The aim of this meta-analysis was to assess the relationship between clinical response to CRT, LA function improvement, and LV function improvement.

2. Methods

The research methodology used in this study followed the Meta-analysis of Observational Studies in Epidemiology (MOOSE) statement for reporting systematic reviews and meta-analyses of

observational studies [9]. Due to the study design (meta-analysis), neither Institutional Review Board (IRB) approval nor informed consent was needed [10].

2.1. Search Strategy

We systematically searched PubMed–Medline, EMBASE, Scopus, Google Scholar, the Cochrane Central Registry of Controlled Trials, and ClinicalTrial.gov, up to September 2019, with the following key words: “Cardiac resynchronization therapy” OR “CRT” AND “Left atrial function” OR “LA function” OR “Left atrial strain” OR “LA strain” OR “LA emptying fraction” OR “LA ejection fraction (EF)” AND “Outcome” OR “CRT responders” OR “CRT non-responders” AND “Follow-up”.

Additional searches for potential trials included the references of review articles on the subject and the abstracts presented at the scientific sessions of the European Society of Cardiology (ESC), the American Heart Association (AHA), American College of Cardiology (ACC), and European Association of Cardiovascular Imaging (EACVI). The wild-card term “*” was used to enhance the sensitivity of the search strategy. The literature search was limited to articles published in English and to studies of humans.

Two reviewers (I.B and G.B) independently evaluated each article. No filters were applied. The remaining articles were obtained in full-text and assessed, again by the same two researchers who separately evaluated each article and carried out data extraction and quality assessment. Disagreements between the reviewers were resolved by discussion with a third party (M.Y.H.).

2.2. Study Selection

The criteria for inclusion in the meta-analysis were: (i) studies investigating patients undergoing cardiac resynchronization therapy; (ii) reporting left atrial predictors of CRT responders and non-responders; (iii) over three months of completed follow-up; and (iv) an enrolled population of adults aged ≥ 18 years.

Exclusion criteria were: (i) insufficient statistical data to compare two groups; (ii) less than three months follow-up period; (iii) non-human subjects; and (iv) articles not published in English.

2.3. Outcome Variables

The key clinical end-points were the relationships between clinical response to CRT and LA function changes. The main outcome measures were LA function, peak atrial longitudinal strain (PALS), and the total EF.

2.4. Data Extraction

Eligible studies were reviewed, and the following data were abstracted: (1) first author’s name; (2) year of publication; (3) study design; (4) data on two arms: CRT responders and non-responders; (5) LA strain measured by echocardiography; (6) baseline characteristics of the patients; (7) baseline LA strain; (8) mean follow-up period; (9) age and gender of study participants; and (10) follow-up LA function.

Peak atrial longitudinal strain (PALS) was measured as the first peak between the QRS complex and the T wave during LV systole, guided by the superimposed electrocardiogram (ECG). When P–P gating was used, and the strain curve was taken as the negative deflection (that represents the peak LA contraction strain) followed by a positive deflection. The sum of the two parts of the curve (negative + positive) represented the peak LA wall strain (Figure 1) [11]. The two types of gating were extracted from the papers’ available text or images.

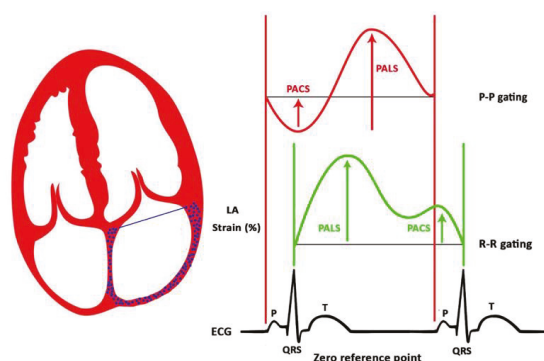


Figure 1. Two types of gating, based on zero reference point (P-P and R-R gating).

2.5. Quality Assessment

The assessment of risk of bias and applicability concerns in the included studies was evaluated by the same investigators by using the quality assessment of diagnostic accuracy studies questionnaire (QUADAS-2), which was optimized for these study questions (Table S1: Supplement 1) [12]. The QUADAS-2 tool has 4 domains for risk of bias-patient selection, index test, reference test, and flow and timing-and three domains for applicability-patient selection, index, and reference test domains.

2.6. Statistical Analysis

The meta-analysis was conducted with statistical analysis that was performed with the RevMan software (Review Manager Version 5.1, The Cochrane Collaboration, Copenhagen, Denmark), with two-tailed $p < 0.05$ considered as significant. Weighted mean differences (WMD) and a 95% confidence interval (CI) were calculated for each study. The baseline characteristics are reported as the median and range. Mean and standard deviation (SD) values were estimated by using the method described by Hozo et al. [13].

To test the potential associations between LA function and CRT response, we used the MedCalc program (Version 19.0, Medcalc Software, Ostend, Belgium) and applied the Hedges–Olkin (1985) method for calculating the weighted summary correlation coefficient under the fixed/random effects model by using a fisher Z transformation of the correlation coefficients. The heterogeneity statistics were incorporated to calculate the summary correlation coefficient under the random effects model (DerSimonian and Laird, 1986).

The meta-analysis is presented in forest plots and was performed with a fixed-effects model. The heterogeneity between studies was assessed with Cochran’s Q test and the I^2 index. As a guide, $I^2 < 25\%$ indicated a low heterogeneity, 25–50% indicated a moderate heterogeneity, and $>50\%$ indicated high heterogeneity [14]. To assess the additive (between-study) component of variance, the reduced maximum likelihood method (τ^2) incorporated the occurrence of residual heterogeneity into the analysis [15]. Publication bias was assessed via visual inspections of funnel plots and Egger’s test.

3. Results

3.1. Search Results and Trial Flow

Of 2819 articles identified in the initial search, 201 were screened as potentially relevant. After excluding 201 studies, 20 full articles were assessed according to the inclusion and exclusion criteria. After careful assessment of these 20 articles, 13 were excluded, and only seven articles were included in the final analysis [16–22] (Figure S1: Supplement 2). In all LA function studies, two dimensional (2D)

LA strain (PALS) was measured based on R–R gating, and the sonographers were blinded to pressure measurements. (Table S2: Supplement 3).

3.2. Characteristics of Included Studies

A total of 488 patients from the seven observational studies were included (Table 1). CRT responders were 181 and CRT non-responders were 118, with mean follow-up period of six months for both groups. The mean age of patients was 62.1 ± 10.2 years, and 68.3% were males. The mean QRS duration was 156 ± 38 , and ischemic etiology for heart failure was found in 33.4% of patients. Between the two groups of patients, CRT responders and non-responders had no difference in age (61.9 ± 7.3 vs. 62.4 ± 10 years, $p = 0.67$, respectively), male gender (69% vs. 66%, $p = 0.19$), ischemic etiology (34% vs. 31.8%, $p = 0.58$) or QRS duration (155.2 ± 31 vs. 156.3 ± 34 ms, $p = 0.42$, Table 2).

Table 1. Main characteristics of studies included in the study.

Study, Year	Study Design	Type of Intervention	Inclusion Criteria	Exclusion Criteria	Key Endpoints	Echo-Cardiography	Criteria for CRT Respond	Follow Up
Yo et al. 2007	Prospective observational	CRT	LV < 40% QRS ≥ 120 ms NYHA-III-IV	Patients with AF	LA predictors	2DE	LVESV ≥ 15%	3 mo
Marsan et al. 2008	Prospective observational	CRT-D	LV ≤ 35% QRS ≥ 120 ms NYHA-III-IV	Patients with AF	LA and LV predictors	3DE	LVESV ≥ 15%	6 mo
Donal et al. 2009	Prospective observational	CRT	HFrEF LV ≤ 35% QRS ≥ 120 ms	Patients with AF Fibrillation; MR (EROA > 20 mm ²)	LA predictors	2DE	LVESV ≥ 15%	6 mo
Feneon et al. 2015	Prospective observational	CRT	LV ≤ 35% QRS ≥ 120 ms NYHA-II-IV NYHA-III-IV	Patients with AF	LA predictors	2DE	LVESV ≥ 15%	6 mo
Valzania et al. 2016	Prospective observational	CRT	HFrEF LV ≤ 35% QRS ≥ 120 ms	Patients with AF	LA predictors	2DE	LVESV ≥ 15%	12 mo
Badran et al. 2017	Prospective observational	CRT	LV ≤ 35% QRS ≥ 120 ms NYHA-II-IV	Patients with AF	LA predictors	2DE	LVESV ≥ 15%	3 mo
Hansen et al. 2017	Clinical trial	CRT	LV ≤ 35% QRS ≥ 120 ms NYHA-II-IV	Recently MI CRF, contrast allergy	LA predictors	2DE	LVESV ≥ 15%	6 mo

HF (heart failure), HFrEF (heart failure with reduced ejection fraction), CRT (cardiac resynchronization therapy), LV (left ventricle), EF (ejection fraction), AF (atrial fibrillation), CRF (chronic renal failure), MR (mitral regurgitation), 2DE (two dimensional echocardiography), LVESV (left ventricle end-systolic volume) and mo (months).

Table 2. Main characteristics of patients among trials included in the study.

Study, Year	Arms	No.	Age		Male (%)	QRS Duration (ms)	NYHA Functional Class	Ischemic Etiology (%)	Mean Change of LA Strain %	Mean Change of LA EF %
			Year	Year						
Yo et al. 2007	R	62	66 ± 11 *	75 *	75 *	142 ± 28	3.0 ± 0.5	NR	-5.1	-14
	Non-R	45				154 ± 31	3.0 ± 0.4	NR	-2.7	-5.2
Marsan et al. 2008	R	34	65 ± 7	78	78	142 ± 28	3.0 ± 0.5	NR	-6	-5.0
	Non-R	17	67 ± 10	70	70	154 ± 31	3.0 ± 0.4	NR	0	0
Donal et al. 2009	R	23	67 ± 10.4 *	76 *	76 *	NR	3.2 ± 0.6 *	NR	-12.1	NR
	Non-R	23							1.4	NR
Feneon et al. 2015	R	54	62.3 ± 10	63	63	163 ± 27	N-II = 24%	18.6	NR	NR
	Non-R	25	66.5 ± 10	80	80	158 ± 30	N-II = 22%	60	NR	NR
Valzania et al. 2016	R	18	61 ± 13	63	63	160 ± 24	2.9 ± 0.2	20	-5.5	-72
	Non-R	12	67 ± 8	50	50	159 ± 23	3.1 ± 0.3	50	4.5	NR
Badran et al. 2017	R	24	56 ± 9.8	71	71	NR	N-IV = 33%	29	-4.2	-35.2
	Non-R	13	53 ± 9.5	69	69	NR	N-IV = 46%	23	2.87	-0.3
Hansen et al. 2017	R	114	69.4 ± 9 *	80 *	80 *	166.2 ± 23.0 *	N-IV = 3% *	50 *	-4.4	-5.0
	Non-R	24							-2	NR

R (respond), Non-R (non-respond), LVESV (left ventricle end-systolic volume), LVEF (left ventricle ejection fraction), NR (non-reported) and * only whole group represented. Mean change of LVESV. LVEF was represented only in CRT responders.

3.3. LA Function in CRT Responders Versus CRT Non-Responders

The pooled analysis showed that CRT responders had no baseline difference in LA strain compared to non-responders, with a WMD of 1.46% [95% CI from -1.58 to 4.50, $p = 0.35$], whereas the LA EF was higher with a WMD of 4.25% [95% CI from 0.42 to 8.08, $p = 0.03$; Figure 2a,b] in responders.

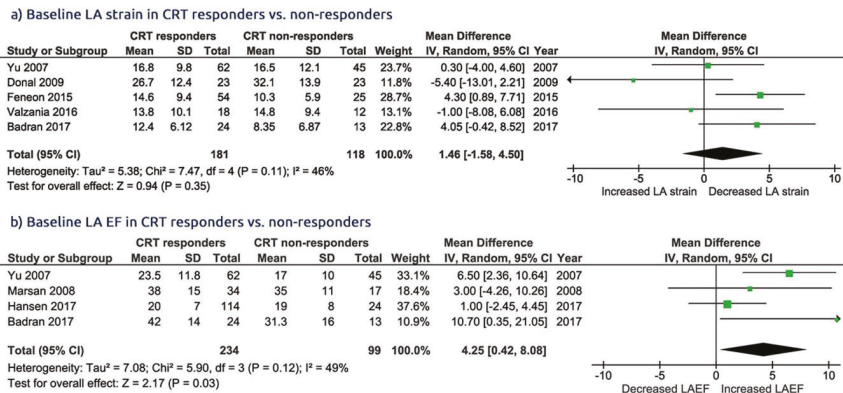


Figure 2. Baseline comparison of LA (left atrial), CRT (function in group of patients with cardiac resynchronization therapy), responders vs. CRT non responders. (a) LA strain; (b) LA ejection fraction (EF).

At follow-up, LA strain increased significantly in CRT responders with a WMD of -5.70% [95% CI from -8.37 to -3.04, $p < 0.001$] compared to non-responders, in whom it remained unchanged, with a WMD of 1.29% [95% CI from -2.08 to 4.67, $p = 0.45$; Figure 3a,b]. Likewise, the LA EF increased in CRT responders: WMD = -8.98% [95% CI from -15.1 to -2.84, $p = 0.004$] vs. WMD = -0.50% [95% CI from -13.3 to 12.3, $p = 0.10$] in non-responders (Figure 4). Heterogeneity across the included studies was not encountered at follow-up in either CRT responders or non-responders ($\text{Chi}^2 = 4.05$, $I^2 = 26$ df = 3, and $p = 0.60$ vs. $\text{Chi}^2 = 4.78$, $I^2 = 37$, df = 3, $p = 0.37$, respectively) except for the moderate heterogeneity detected at the baseline LA strain between the two groups, as tested by the random-effect analysis ($\text{Chi}^2 = 7.47$, $I^2 = 46$, df = 4, $p = 0.11$).

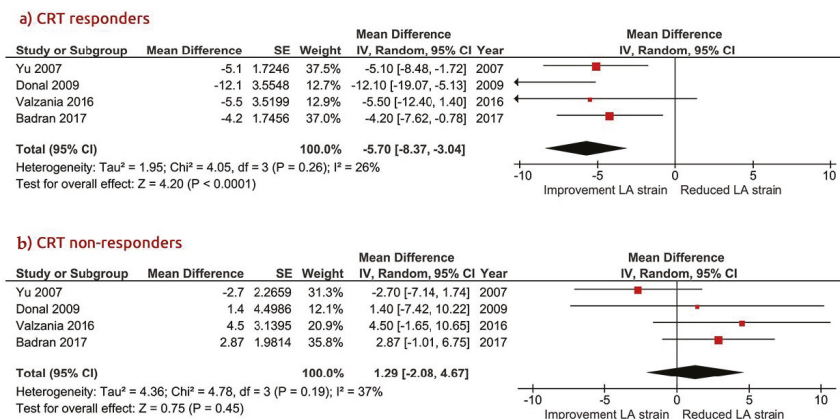
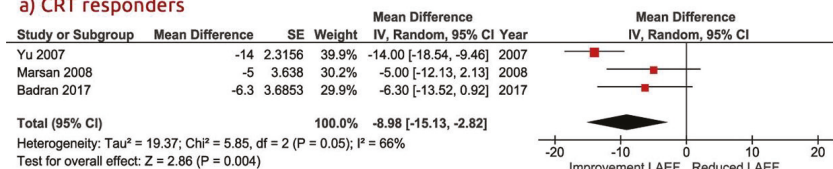


Figure 3. Mean changed LA (left atrial) strain in patients with CRT (cardiac resynchronization therapy). (a) CRT responders; (b) CRT non responders.

a) CRT responders



b) CRT non-responders

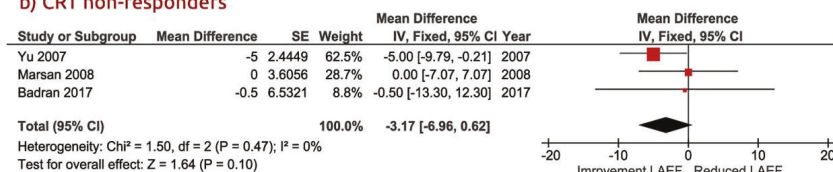


Figure 4. Mean changed LA (left atrial) EF (ejection fraction) in patients with CRT (cardiac resynchronization therapy). (a) CRT responders; (b) CRT non-responders.

3.4. LV Dimension and Function in CRT Responders Versus CRT Non-Responders

There was no difference in baseline LV dimensions, systolic function, and QRS duration between CRT responders and the CRT non-responders: WMD = -2.18% [95% CI from -24.01 to 19.6, *p* < 0.85]; baseline left ventricle end-systolic volume (LVESV): WMD = -4.22% [95% CI from -22.1 to 13.6, *p* = 0.64]; baseline left ventricular end-diastolic dimension - LVEDd: WMD = -1.74% [95% CI from -4.76 to 1.27, *p* = 0.26]; baseline left ventricle ejection fraction (LVEF): WMD = 0.76% [95% CI from -3.34 to 4.86, *p* = 0.72] (Figure S2: Supplement 4); and baseline QRS duration; WMD = -2.60% [95% CI from -10.9 to 5.79, *p* = 0.54] (Figure S3: Supplement 5). Similarly, no difference was found in the LA dimension, which had a WMD of -2.17% [95% CI from -7.1 to 2.67, *p* = 0.38], between the two groups.

3.5. The Relationship between LA and LV Function in CRT Responders

To test for potential associates with CRT response, we calculated the weighted summary correlation coefficient between the LA function and LV parameters of CRT responders. This analysis showed that the increase in LA strain was associated with a fall in left ventricular end-systolic volume - LVESV's weighted summary correlation (*r*) [*r* = -0.56 (CI from -0.68 to -0.40, *p* < 0.001) Q² = 0.06, df = 0.2, I² = 0.0%, *p* = 0.86] and an increase in the LVEF [*r* = 0.58 (CI from 0.42 to 0.69, *p* < 0.001) Q² = 0.72, df = 2, I² = 0.0%, *p* = 0.69; Figure 5,b]. Similarly, although with a less significance, the increase in the LA EF correlated with the fall in LVESV [*r* = -0.51 (CI from -0.63 to -0.36, *p* < 0.001) Q² = 0.92, df = 0.2, I² = 0.0%, *p* = 0.86] and with the increase in the LVEF [*r* = 0.48 (CI from 0.33 to 0.61, *p* = 0.002) Q² = 0.36, df = 0.2, I² = 0.0%, *p* = 0.83; Figure 5c,d]. The increase in LA strain correlated with the increase in the LA EF (*r* = 0.57 (CI from 0.43 to 0.70, *p* < 0.001) Q² = 0.16, df = 1, I² = 0.0%, *p* = 0.64; Figure S4: Supplement 6).

Meta-analysis: correlation

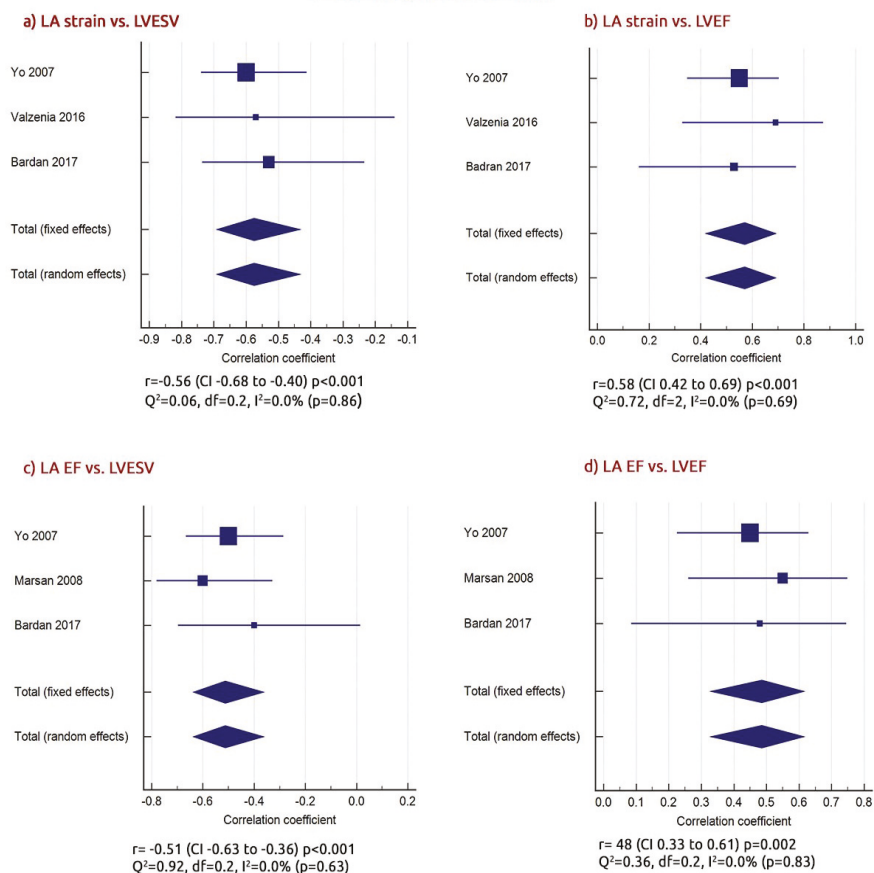


Figure 5. Weighted summary correlation between (a) LA (left atrial) (strain vs. left ventricle end-systolic volume (LVESV); (b) LA strain vs. left ventricle ejection fraction (LVEF); (c) LA EF (ejection fraction) (vs. LVESV; and (d) LA EF vs. LVEF (left ventricle ejection fraction).

3.6. Relationship between LA Strain Change and Baseline Age and Male Gender

The % mean change of LA strain was not related to baseline mean age or male gender ($\beta = -0.20$ (from 0.159 to -0.516), $p = 0.20$, $\text{Tau} = 0.00\%$, $I^2 = 0.00\%$, $Q = 0.19$, $d = 4$) or age ($\beta = -0.24$ (from 0.22 to -0.69), $p = 0.27$, $\text{Tau} = 0.00\%$, $I^2 = 0.00\%$, $Q = 1.20$, $d = 4$) (Figure S5: Supplement 7). There was no heterogeneity across the included studies.

3.7. Risk of Bias Assessment

Based on quality assessment of diagnostic accuracy studies questionnaire (QUADAS-2), four domains of criteria for risk of bias and three for applicability were analyzed, and the risk of bias was assessed as “low risk”, “high risk”, or “unclear risk” (Table S1: Supplement 1) [10]. Most studies had a low or moderate risk of bias and clearly defined their objectives and the main outcomes (Table S3, Figure S6, Supplement 8, 9). The QUADAS-2 analysis for bias evaluation showed all domains to have had low risk of bias ($\leq 40\%$). Additionally, there was no evidence for publication bias, as evaluated by Egger’s test for our findings.

4. Discussion

Despite its failure in about one-third of treated patients, cardiac resynchronization therapy (CRT) still remains the best treatment for symptomatic heart failure patients on full medical therapy, as stated in the European and American guidelines [23,24]. One of the known causes of symptoms in such patients is atrial arrhythmia, which is known to be related to LA cavity enlargement and disturbed function, both of which may improve in CRT responders [16,18]. The regression of atrial arrhythmia with CRT treatment has been reported and interpreted on the basis of reversed LA cavity remodeling [25,26]. Despite these suggestions, the exact contribution of LA function in cardiac reverse remodeling related to CRT remains poorly established [27]. This meta-analysis evaluated the relationship between LA function in patients who received CRT for heart failure.

Findings: Our analysis shows that CRT responders had no baseline difference in LA strain compared CRT non-responders, but the LA EF was higher in responders. At follow-up, both LA strain and the LA EF only significantly increased in responders. The increase in LA strain was associated with a fall in LVESV and a rise in the LVEF. Similarly, although with a less significance, the increase in the LA EF correlated with the fall in LVESV and the increase in the LVEF. Finally, the increase in LA strain correlated with the increase in the LA EF.

Data Interpretation: LA function is an integral part of cardiac function, and its pump function normally contributes by at least one third to overall LV filling, which increases with age [28]. In heart failure, responders to CRT are mainly those with worse LV dyssynchrony, which itself compromises LA emptying and consequently stroke volume. Additionally, reduced LA emptying results in raised LA pressure and, consequently, myocardial stretch, which then leads to cavity function instability and arrhythmia. Studies have shown that an increase in LA volume is the most accurate predictor of atrial arrhythmia [29,30].

With an optimum response to CRT, LV systolic function improves and the ejection fraction increases, and ESV falls as stroke volume increases. These changes have been shown to have significant hemodynamic effects on overall cardiac performance and symptoms [30]. Furthermore, an improved LV pump function results in better LA emptying as a further contribution to stroke volume. The other side of the benefit from CRT lies at the LA myocardial function level; as has been shown by our results, LA strain increases parallel to the increased cavity emptying fraction, thus providing further evidence for the improvement in LA integral function in the form of myocardial intrinsic function and overall pump performance. It is of interest that these aspects of improvements of LA function did not happen independently of the LV, but they were associated, although modestly, with the fall in LVESV and the increase in ejection fraction [31–33]. Such a relationship is of clinical and academic interest, since the described fall in LVESV, usually referred to as a sign of LV reverse remodeling, seems to happen also in a similar way in the left atrium, with an increase in emptying fraction [20,34]. Thus, although the term reverse remodeling might sound non-specific, our results shed light on some of its ingredients in the setting of LV and LA structure and function changes in response to CRT [15–21]. Finally, our results highlight the fact that the LA is not only a conduit chamber but also a more complex anatomical and function structure, both in and of itself and in its relationship with the LV [35,36]. Our recently published meta-analysis [5] showed a concordant relationship between LA indexed volume and LV volume and function with CRT. The documented improvement of LA myocardial intrinsic function and emptying function is expected to be associated with a fall in cavity pressure with its direct implications on the frequency of atrial arrhythmias known in patients with significant heart failure [11].

Limitations: The analysis of LA function and LVESV and/or LVES was based on a small number of studies, so its results should be seen as having modest accuracy until proven in a larger number of studies. The data included in the meta-analysis were collected from the published papers, on whose quality we did not have control; we had to trust the academic merit of the investigators. We were unable to comment on the relevance of our findings in controlling atrial arrhythmia in the analyzed studies because of the limited available data. Likewise, we had hoped to provide evidence for long term benefits from CRT, but, again, such information was not available in the analyzed studies. Finally, we sought to assess the relationship between the individual and combined LA and LV function changes

with CRT against symptoms in more detail, but the available data on LA function parameters that could be used in such analysis were very limited. It would have been of great interest to analyze subgroups of patients according to the concordant/discordant relationships between improvements of LA and LV functions, but, again, such data were not uniformly available in the small studies we analyzed.

Clinical Implications: The left atrium is an integral component of the overall cardiac structure and function, and it should be seen more than just a conduit. Based on the anatomical myocardial fiber architecture, the association between the left atrial and left ventricular function changes further strengthen such relationship, particularly in the setting of HF with a reduced EF and increased diastolic pressures. Our findings may assist in explaining the well documented lack of symptomatic improvement with CRT in patients with atrial fibrillation, since significant components of the mechanisms of LA emptying and myocardial contraction that contribute to the overall cavity strain does not exist [37].

5. Conclusions

Clinical response to CRT is associated with an improvement of LA function, reflecting cavity reverse remodeling. These changes are related to their ventricular counterparts, thus supporting the importance of assessing LA function in patients treated by CRT for heart failure. Future studies should focus on concordant changes in LA and LV function that contribute to clinical improvement of patients receiving CRT for heart failure.

Supplementary Materials: The following are available online at <http://www.mdpi.com/2077-0383/9/2/298/s1>, Figure S1: Flow chart of study section, Figure S2: Comparison of baseline LVEDV, LVESV, LVEDd and EF in group of patients with CRT responders vs. CRT non responders, Figure S3: Comparison of baseline QRS duration and LA dimension in group of patients with CRT responders vs. CRT non responders, Figure S4: Weighted summary correlation between LA strain and LA EF, Figure S5: Relationship between LA strain change and (a) male gender; (b) age, Figure S6: Summary of QUADAS-2 Assessment of Selected Studies, Table S1: Summary of quality assessment analysis (Quality Assessment of Diagnostic Accuracy Studies-QUADAS 2), Table S2: Echocardiographic characteristics of LA functional measurements, Echocardiographic characteristics of LA functional measurements, Table S3: Summary of QUADAS-2 Assessment of Selected Studies.

Author Contributions: I.B. and M.Y.H., designed and drafted the article; I.B. and G.B. performed the literature search, study selection and data extraction. I.B. and M.Y.H., analyzed and interpreted the data; M.Y.H., G.B. and P.L. critically revised the article. All authors have read and agreed to the published version of the manuscript.

Funding: This research received no external funding.

Conflicts of Interest: The authors declare no conflict of interest.

Abbreviations

CRT	Cardiac Resynchronization Therapy
LA	Left atrium/atrial
LA function	Left atrial function
LA EF	Left atrial emptying fraction
LA strain	Left atrial strain
LV	Left ventricle/ventricular
EF	Ejection fraction
ESV	End systolic volume
EDV	End diastolic volume
EDD	End diastolic dimension
ESD	End systolic dimension
NYHA class	New York Heart Association class
2D	Two dimensional
2D STE	Two-dimensional speckle-tracking echocardiography
PALS	Peak atrial longitudinal strain (peak atrial longitudinal strain during LV systole)
HF	Heart failure
FFrEF	Heart failure with reduced ejection fraction
CI	Confidence interval
WMD	Weighted mean difference
SE	Standard error
WMD	Weighted mean difference

References

1. Chioncel, O.; Lainscak, M.; Seferovic, P.M.; Anker, S.D.; Crespo-Leiro, M.G.; Harjola, V.P.; Parissis, J.; Laroche, C.; Piepoli, M.F.; Fonseca, C.; et al. Epidemiology and one-year outcomes in patients with chronic heart failure and preserved, mid-range and reduced ejection fraction: An analysis of the ESC Heart Failure Long-Term Registry. *Eur. J. Heart Fail.* **2017**, *19*, 1574–1585. [[CrossRef](#)]
2. Daubert, C.; Behar, N.; Martins, R.P.; Mabo, P.; Leclercq, C. Avoiding non-responders to cardiac resynchronization therapy: A practical guide. *Eur. Heart J.* **2017**, *38*, 1463–1472. [[CrossRef](#)]
3. Engels, E.B.; Vis, A.; van Rees, B.D.; Marcantoni, L.; Zanon, F.; Vernoooy, K.; Prinzen, F.W. Improved acute haemodynamic response to cardiac resynchronization therapy using multipoint pacing cannot solely be explained by better resynchronization. *J. Electrocardiol.* **2018**, *51*, S61–S66. [[CrossRef](#)] [[PubMed](#)]
4. Gasparini, M.; Leclercq, C.; Lunati, M.; Landolina, M.; Auricchio, A.; Santini, M.; Boriani, G.; Lamp, B.; Proclemer, A.; Curnis, A.; et al. Cardiac resynchronization therapy in patients with atrial fibrillation: The CERTIFY study (Cardiac Resynchronization Therapy in Atrial Fibrillation Patients Multinational Registry). *JACC Heart Fail.* **2013**, *1*, 500–507. [[CrossRef](#)] [[PubMed](#)]
5. Bytyçi, I.; Bajraktari, G.; Henein, M.Y. The relationship between left atrial volume indexed and cardiac resynchronization therapy: A systematic review and meta-analysis. *Arch. Med. Sci.* **2019**, *15*, 845–856.
6. Sarvari, S.I.; Haugaa, K.H.; Stokke, T.M.; Ansari, H.Z.; Leren, I.S.; Hegbom, F.; Smiseth, O.A.; Edvardsen, T. Strain echocardiographic assessment of left atrial function predicts recurrence of atrial fibrillation. *Eur. Heart J. Cardiovasc. Imaging* **2016**, *17*, 660–667. [[CrossRef](#)]
7. Ziaeeian, B.; Zhang, Y.; Albert, N.M.; Curtis, A.B.; Gheorghiadu, M.; Heywood, J.T.; Mehra, M.R.; O'Connor, C.M.; Reynolds, D.; Walsh, M.N.; et al. Clinical effectiveness of CRT and ICD therapy in heart failure patients by racial/ethnic classification: Insights from the IMPROVE HF registry. *J. Am. Coll. Cardiol.* **2014**, *64*, 797–807. [[CrossRef](#)]
8. Kosztin, A.; Boros, A.M.; Geller, L.; Merkely, B. Cardiac resynchronization therapy: Current benefits and pitfalls. *Kardiol Pol.* **2018**, *76*, 1420–1425. [[CrossRef](#)]
9. Stroup, D.F.; Berlin, J.A.; Morton, S.C.; Olkin, I.; Williamson, G.D.; Rennie, D.; Moher, D.; Becker, B.J.; Sipe, T.A.; Thacker, S.B.; et al. Meta-analysis of observational studies in epidemiology: A proposal for reporting. Meta-analysis Of Observational Studies in Epidemiology (MOOSE) group. *JAMA* **2000**, *283*, 2008–2012. [[CrossRef](#)]
10. Higgins, J.P.T.; Green, S. *Cochrane Handbook for Systematic Reviews of Interventions*, version 5.0.2; The Cochrane Collaboration: Charity, UK, 2009.
11. Bytyçi, I.; Bajraktari, G.; Lindqvist, P.; Henein, M.Y. Compromised left atrial function and increased size predict raised cavity pressure: A systematic review and meta-analysis. *Clin. Physiol. Funct. Imaging* **2019**, *39*, 297–307. [[CrossRef](#)]
12. Whiting, P.F.; Rutjes, A.W.S.; Westwood, M.E.; Mallett, S.; Deeks, J.J.; Reitsma, J.B.; Leeflang, M.M.; Sterne, J.A.; Bossuyt, P.M.; QUADAS-2 Group. QUADAS-2: A revised tool for the quality assessment of diagnostic accuracy studies. *Ann. Intern. Med.* **2011**, *155*, 529–536. [[CrossRef](#)] [[PubMed](#)]
13. Hozo, S.P.; Djulbegovic, B.; Hozo, I. Estimating the mean and variance from the median, range, and the size of a sample. *BMC Med. Res. Methodol.* **2005**, *5*, 13. [[CrossRef](#)] [[PubMed](#)]
14. Morton, S.C.; Adams, J.L.; Suttrop, M.J.; Shekelle, P.G. *Meta-Regression Approaches: What, Why, When, and How?* Report No.: 04-0033; Agency for Healthcare Research and Quality: Rockville, MD, USA, 2004.
15. Higgins, J.P.; Thompson, S.G.; Deeks, J.J.; Altman, D.G. Measuring inconsistency in meta analyses. *BMJ* **2003**, *327*, 557–560. [[CrossRef](#)] [[PubMed](#)]
16. Yu, C.M.; Fang, F.; Zhang, Q.; Yip, G.W.; Li, C.M.; Chan, J.Y.; Wu, L.; Fung, J.W. Improvement of atrial function and atrial reverse remodeling after cardiac resynchronization therapy for heart failure. *J. Am. Coll. Cardiol.* **2007**, *50*, 778–785. [[CrossRef](#)] [[PubMed](#)]
17. Marsan, N.A.; Bleeker, G.B.; Ypenburg, C.; Van Bommel, R.J.; Ghio, S.; Van de Veire, N.R.; Delgado, V.; Holman, E.R.; van der Wall, E.E.; Schalij, M.J.; et al. Real-time three-dimensional echocardiography as a novel approach to assess left ventricular and left atrium reverse remodeling and to predict response to cardiac resynchronization therapy. *Heart Rhythm.* **2008**, *5*, 1257–1264. [[CrossRef](#)] [[PubMed](#)]

18. Donal, E.; Tan, K.; Leclercq, C.; Ollivier, R.; Derumeaux, G.; Bernard, M.; de Place, C.; Mabo, P.; Daubert, J.C. Left atrial reverse remodeling and cardiac resynchronization therapy for chronic heart failure patients in sinus rhythm. *J. Am. Soc. Echocardiogr.* **2009**, *22*, 1152–1158. [[CrossRef](#)]
19. Feneon, D.; Behaghel, A.; Bernard, A.; Fournet, M.; Mabo, P.; Daubert, J.C.; Leclercq, C.; Donal, E. Left atrial function, a new predictor of response to cardiac resynchronization therapy? *Heart Rhythm.* **2015**, *12*, 1800–1806. [[CrossRef](#)]
20. Valzania, C.; Gadler, F.; Boriani, G.; Rapezzi, C.; Eriksson, M.J. Effect of Cardiac Resynchronization Therapy on Left Atrial Size and Function as Expressed by Speckle Tracking 2-Dimensional Strain. *Am. J. Cardiol.* **2016**, *118*, 237–243. [[CrossRef](#)]
21. Badran, H.A.; Abdelhamid, M.A.; Ibrahim, M.T.; Abdelmoteleb, A.M.; Zarif, J.K. Left atrium in cardiac resynchronization therapy: Active participant or innocent bystander. *J. Saudi Heart Assoc.* **2017**, *29*, 259–269. [[CrossRef](#)]
22. Hansen, P.B.; Sommer, A.; Nørgaard, B.L.; Kronborg, M.B.; Nielsen, J.C. Left atrial size and function as assessed by computed tomography in cardiac resynchronization therapy: Association to echocardiographic and clinical outcome. *Int. J. Cardiovasc. Imaging* **2017**, *33*, 917–925. [[CrossRef](#)]
23. Brignole, M.; Auricchio, A.; Baron-Esquivias, G.; Bordachar, P.; Boriani, G.; Breithardt, O.A.; Cleland, J.; Deharo, J.C.; Delgado, V.; Elliott, P.M.; et al. 2013 ESC Guidelines on cardiac pacing and cardiac resynchronization therapy: The Task Force on cardiac pacing and resynchronization therapy of the European Society of Cardiology (ESC). Developed in collaboration with the European Heart Rhythm Association (EHRA). *Eur. Heart J.* **2013**, *34*, 2281–2329. [[PubMed](#)]
24. Al-Khatib, S.M.; Stevenson, W.G.; Ackerman, M.J.; Bryant, W.J.; Callans, D.J.; Curtis, A.B.; Deal, B.J.; Dickfeld, T.; Field, M.E.; Fonarow, G.C.; et al. 2017 AHA/ACC/HRS Guideline for Management of Patients With Ventricular Arrhythmias and the Prevention of Sudden Cardiac Death: Executive Summary: A Report of the American College of Cardiology/American Heart Association Task Force on Clinical Practice Guidelines and the Heart Rhythm Society. *Heart Rhythm.* **2018**, *15*, e190–e252. [[PubMed](#)]
25. Leon, A.R.; Greenberg, J.M.; Kanuru, N.; Baker, C.M.; Mera, F.V.; Smith, A.L.; Langberg, J.J.; DeLurgio, D.B. Cardiac resynchronization in patients with congestive heart failure and chronic atrial fibrillation: Effect of upgrading to biventricular pacing after chronic right ventricular pacing. *J. Am. Coll. Cardiol.* **2002**, *39*, 1258–1263. [[CrossRef](#)]
26. Upadhyay, G.A.; Choudhry, N.K.; Auricchio, A.; Ruskin, J.; Singh, J.P. Cardiac resynchronization in patients with atrial fibrillation: A meta-analysis of prospective cohort studies. *J. Am. Coll. Cardiol.* **2008**, *52*, 1239–1246. [[CrossRef](#)] [[PubMed](#)]
27. D’Andrea, A.; Caso, P.; Romano, S.; Scarafilo, R.; Riegler, L.; Salerno, G.; Limongelli, G.; Di Salvo, G.; Calabrò, P.; Del Viscovo, L.; et al. Different effects of cardiac resynchronization therapy on left atrial function in patients with either idiopathic or ischaemic dilated cardiomyopathy: A two-dimensional speckle strain study. *Eur. Heart J.* **2007**, *28*, 2738–2748. [[CrossRef](#)] [[PubMed](#)]
28. Stefanadis, C.; Dernellis, J.; Toutouzas, P. A clinical appraisal of left atrial function. *Eur. Heart J.* **2001**, *22*, 22–36. [[CrossRef](#)] [[PubMed](#)]
29. Moreno-Ruiz, L.A.; Madrid-Miller, A.; Martínez-Flores, J.E.; González-Hermosillo, J.A.; Arenas-Fonseca, J. Left atrial longitudinal strain by speckle tracking as independent predictor of recurrence after electrical cardioversion in persistent and long standing persistent non-valvular atrial fibrillation. *Int. J. Cardiovasc. Imaging* **2019**, *35*, 1587–1596. [[CrossRef](#)]
30. Jones, S.; Lumens, J.; Sohaib, S.M.A.; Finegold, J.A.; Kanagaratnam, P.; Tanner, M.; Duncan, E.; Moore, P.; Leyva, F.; Frenneaux, M.; et al. Cardiac resynchronization therapy: Mechanisms of action and scope for further improvement in cardiac function. *Europace* **2017**, *19*, 1178–1186. [[CrossRef](#)]
31. Lupu, S.; Mitre, A.; Sus, I.; Rudzik, R.; Beke, I.; Dobreanu, D. Changes in left atrial size and function early after cardiac resynchronization therapy as assessed by conventional two-dimensional echocardiography. *Med. Ultrason.* **2018**, *20*, 362–370. [[CrossRef](#)]
32. Bytyçi, I.; Bajraktari, G.; Ibrahim, P.; Berisha, G.; Rexhepaj, N.; Henein, M.Y. Left atrial emptying fraction predicts limited exercise performance in heart failure patients. *Int. J. Cardiol. Heart Vessel.* **2014**, *4*, 203–207. [[CrossRef](#)]

33. Sade, L.E.; Atar, I.; Özin, B.; Yüce, D.; Müderrisoğlu, H. Determinants of New-Onset Atrial Fibrillation in Patients Receiving CRT: Mechanistic Insights From Speckle Tracking Imaging. *JACC Cardiovasc. Imaging* **2016**, *9*, 99–111. [[CrossRef](#)] [[PubMed](#)]
34. Malagoli, A.; Rossi, L.; Franchi, F.; Piepoli, M.F.; Malavasi, V.; Casali, E.; Modena, M.G.; Villani, G.Q. Effect of cardiac resynchronization therapy on left atrial reverse remodeling: Role of echocardiographic AV delay optimization. *Int. J. Cardiol.* **2013**, *167*, 1456–1460. [[CrossRef](#)]
35. Blume, G.G.; Mcleod, C.J.; Barnes, M.E.; Seward, J.B.; Pellikka, P.A.; Bastiansen, P.M.; Tsang, T.S. Left atrial function: Physiology, assessment, and clinical implications. *Eur. J. Echocardiogr.* **2011**, *12*, 421–430. [[CrossRef](#)] [[PubMed](#)]
36. Sengupta, P.P.; Korinek, J.; Belohlavek, M.; Narula, J.; Vannan, M.A.; Jahangir, A.; Khandheria, B.K. Left ventricular structure and function: Basic science for cardiac imaging. *J. Am. Coll. Cardiol.* **2006**, *48*, 1988–2001. [[CrossRef](#)] [[PubMed](#)]
37. Chen, A.; Landman, S.R.; Stadler, R.W. Reasons for Loss of Cardiac Resynchronization Therapy Pacing. *Circ. Arrhythmia Electrophysiol.* **2012**, *5*, 884–888. [[CrossRef](#)] [[PubMed](#)]



© 2020 by the authors. Licensee MDPI, Basel, Switzerland. This article is an open access article distributed under the terms and conditions of the Creative Commons Attribution (CC BY) license (<http://creativecommons.org/licenses/by/4.0/>).

Review

Modifications of Titin Contribute to the Progression of Cardiomyopathy and Represent a Therapeutic Target for Treatment of Heart Failure

Charles Tharp, Luisa Mestroni and Matthew Taylor *

Adult Medical Genetics Program, Cardiovascular Institute, University of Colorado Anschutz Medical Campus, CO 80045, USA; charles.tharp@cuanschutz.edu (C.T.); luisa.mestroni@cuanschutz.edu (L.M.)

* Correspondence: matthew.taylor@cuanschutz.edu; Tel.: +1-303-724-1400

Received: 22 July 2020; Accepted: 24 August 2020; Published: 26 August 2020

Abstract: Titin is the largest human protein and an essential component of the cardiac sarcomere. With multiple immunoglobulin(Ig)-like domains that serve as molecular springs, titin contributes significantly to the passive tension, systolic function, and diastolic function of the heart. Mutations leading to early termination of titin are the most common genetic cause of dilated cardiomyopathy. Modifications of titin, which change protein length, and relative stiffness affect resting tension of the ventricle and are associated with acquired forms of heart failure. Transcriptional and post-translational changes that increase titin's length and extensibility, making the sarcomere longer and softer, are associated with systolic dysfunction and left ventricular dilation. Modifications of titin that decrease its length and extensibility, making the sarcomere shorter and stiffer, are associated with diastolic dysfunction in animal models. There has been significant progress in understanding the mechanisms by which titin is modified. As molecular pathways that modify titin's mechanical properties are elucidated, they represent therapeutic targets for treatment of both systolic and diastolic dysfunction. In this article, we review titin's contribution to normal cardiac physiology, the pathophysiology of titin truncation variations leading to dilated cardiomyopathy, and transcriptional and post-translational modifications of titin. Emphasis is on how modification of titin can be utilized as a therapeutic target for treatment of heart failure.

Keywords: titin; RNA binding motif protein 20 (RBM20); sarcomere; systolic dysfunction; diastolic dysfunction; dilated cardiomyopathy; phosphorylation; non-sense mRNA decay; mammalian target of rapamycin (mTOR) complex-1

1. Titin Is an Essential Molecule within the Sarcomere Where It Contributes to Cardiac Function

1.1. Titin Contains Four Structural Domains That Impart Important Molecular Properties to the Sarcomere during Cardiac Function

The essential function of the heart is generation of circulatory blood flow to organs and tissues. This circulatory flow or cardiac output is created by coordinated contraction and relaxation of the heart muscle, termed systole and diastole, respectively. During systole, the heart muscle contracts and ejects blood from the heart delivering oxygen and vital nutrients to the body. During diastole, the heart muscle relaxes allowing blood to fill the ventricles in preparation for systole. Dysfunction of systole and diastole can lead to the development of heart failure. Heart failure is a clinical syndrome where dysfunction affecting systole, diastole or both leads to significant symptoms and mortality. Heart failure is one of the most morbid health conditions affecting an estimated 5.1 million people in the United States and 23 million people worldwide [1,2]. As a basic principle, heart failure results from dysfunction of the cardiomyocyte and sarcomeric structures. Cardiomyocytes are specialized muscle cells that contain

sarcomeres which are the fundamental sub-cellular structure that convert chemical energy to muscular contraction. The sarcomere is a complex protein structure with rigid vertical M-lines and Z-lines that anchor overlapping longitudinal filaments. During cardiac contraction, the myosin heads pull actin filaments in one direction bringing the vertical M-line and Z-lines together resulting in contraction and mechanical force generation [3].

One of the most important proteins that compose the sarcomere is titin. Titin is a filamentous protein anchored in the Z-line and extending to the M-line thereby providing structural support to the sarcomere [4,5]. Titin is the largest known protein with a measured length of up to 1.2 μM and comprised of 27,000–33,000 amino acids with a molecular mass of 3800 kDa [6,7]. Titin is encoded by the titin gene *TTN*, which is 294 kb and contains 364 exons [8]. Although titin has many complex molecular properties, its mechanical role supporting the sarcomere and providing passive tension and force modulation during contraction and relaxation has been the most well described and are the focus of this paper [5,9]. The molecular properties of titin as it contributes to normal function are imparted by the four structural domains (Figure 1). The N-terminal domain embeds and anchors it to the Z-disk, while the C-terminal domain similarly anchors titin to the M-band [4,5,10]. Titin filaments in the Z-disk and M-line are embedded to domains of adjacent titin proteins from the opposing sarcomere to form overlapping connections that create a continuous filamentous connection spanning the myofibril [11]. The I-band is adjacent to the Z-disk and is composed of repetitive immunoglobulin-like domains, a region rich in proline (P), glutamate (E), valine (V), and lysine (K) termed the PEVK region, as well as the N2B element [5,11]. The I-band is highly elastic and provides a spring-like function that imparts passive tension during relaxation, elongates during contraction, and returns the sarcomere to its previous length after contraction [12,13]. The A-band serves as a rigid region that binds to the thick filament and interacts with myosin to translate force during contraction to the sarcomere [14].

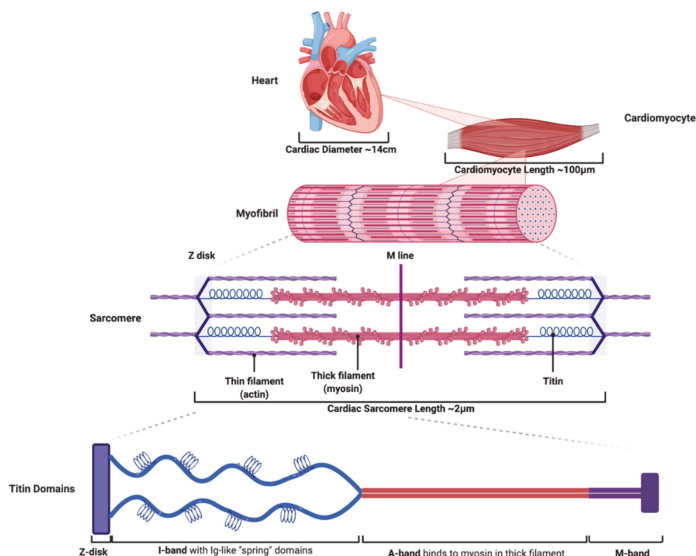


Figure 1. Titin structural domains serve essential functional roles as part of the sarcomere, myofibril, and cardiomyocyte. Cardiac tissue is composed of cardiomyocytes that impart contractile function. The contractile subunit of the cardiomyocyte is the myofibril, which is made of sarcomeres. Titin is an essential component of the sarcomere composed of four domains. The N-terminal domain embeds titin to the Z-disk. The I-band contains immunoglobulin-like (Ig) domains that impart extensibility and provide titin “spring-like” characteristics. The A-band binds to myosin and serves as a rigid region during contraction. The C-terminal domains embeds titin to the M-band.

1.2. Titin's Structure Is Essential to Normal Cardiac Function, Passive Tension, and Length Dependent Activation

The structure of titin domains provides essential functions to the cardiomyocyte and overall physiology of the heart. The elasticity of titin that is derived from the spring-like I-band is a major contributor to the length dependent activation described in the Frank-Starling effect. In normal cardiac function, increased blood volume in the ventricle during diastole (measured by left ventricular end diastolic pressure) leads to increased force of contraction during systole (measured by stroke volume; see Figure 2). The Frank-Starling effect is an essential principal of cardiac function that allows the heart to compensate for physiological changes and increased demands for cardiac output [15]. While there are many factors that influence the relationship between diastolic filling and stroke volume, titin's ability to stretch is an essential contributor. As the sarcomere expands in diastole, the springy Ig-like domains of titin's I-band elongate, thereby increasing tension that is released as restorative force during systole. This increased diastolic tension also modulates actomyosin interactions to increase the force of contraction during systole [16,17]. Because titin spans the entirety of the sarcomere, its length and elasticity are major contributors to the passive tension of the ventricle including diastolic tension and diastolic volume [18]. In addition to the mechanical support titin provides to the sarcomere, stretching of titin leads to cellular signaling activation that promotes myocyte growth and contributes to chronic changes of the myocardium [15].

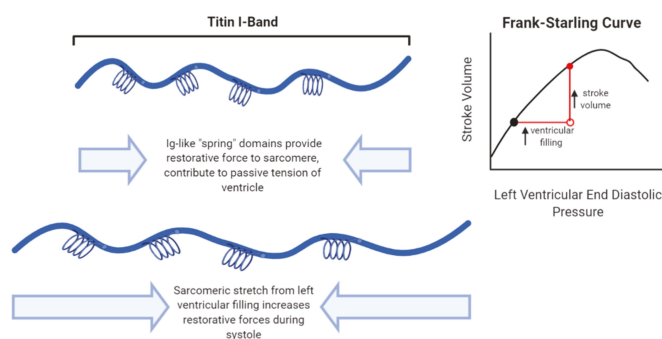


Figure 2. Titin's I-band serves as a molecular spring that contributes to passive tension of the heart. The I-band is extensible due to Ig-like domains that serve as molecular springs. Because titin spans the sarcomere, the extensibility of the I-band imparts much of the resting tension of the cardiomyocyte. In addition, the I-band provides increased restorative forces when the ventricle and sarcomeres are stretched and contributes to the length dependent activation described in the Frank-Starling Curve.

1.3. Abnormalities in Titin Contribute to Systolic and Diastolic Heart Failure

The essential function of titin in the sarcomere and cardiac function is illustrated by the significant cardiac phenotypes in patients who have *TTN* mutations. In addition, patients who develop heart failure related to other causes have significant changes to titin at the transcriptional and post translational level. Cardiomyopathy and heart failure are categorized clinically into systolic dysfunction and diastolic dysfunction. In systolic dysfunction, there is decreased contraction of the heart leading to decreased stroke volume and elevated cardiac pressures. Systolic dysfunction is categorized into dilated cardiomyopathy and hypertrophic cardiomyopathy. In dilated cardiomyopathy, dysfunction of the cardiomyocytes during contraction leads to remodeling of the myocardium in an eccentric pattern which causes dilation of the ventricle. In hypertrophic cardiomyopathy, changes in myocardial function result in concentric hypertrophy and thickening of the ventricle. Restrictive cardiomyopathy is caused by progression of diastolic dysfunction where the contractile force of the heart is preserved; however, due to abnormal relaxation of the heart during diastole, the ventricle cannot fill appropriately resulting in decreased cardiac function. In both systolic and diastolic dysfunction, there are elevated cardiac

filling pressures leading to the clinical presentation of heart failure with development of peripheral and pulmonary edema, dyspnea, and fatigue.

We will review how mutations in *TTN* contribute to cardiomyopathy. We will discuss how transcriptional changes and regulation of titin affect cardiac physiology. We will describe post-translational modifications of titin that occur with heart failure. In covering these topics, there will be a translational focus on associating molecular pathways with clinical phenotypes and how these pathways may lead to novel therapeutic targets for treatment of cardiomyopathy.

2. Truncation Mutations in *TTN* Cause Dilated Cardiomyopathy (DCM)

2.1. *TTN* Truncation Variations in Highly Constitutively Expressed Exons Cause DCM

TTN mutations are the most common cause of genetic DCM due in part to *TTN*'s large gene size as well as its essential role in the sarcomere and cardiomyocyte function. There are numerous point mutations of *TTN* leading to missense changes in single amino acids that are associated with diverse phenotypes including several types of cardiomyopathies [19,20]. However, pathogenic *TTN* mutations most commonly result from nonsense mutations leading to frameshifts and incorporation of early stop codons predicting a truncated, shortened titin protein, termed titin truncation variations (TTNtv) [21]. Interestingly, TTNtv, mostly restricted to the I-band, are found in 2–3% of the general population [13,22,23] and there is substantial interest in determining the associated impact of TTNtvs in ostensibly healthy persons. While phenotypes of TTNtvs can be diverse and may present with restrictive cardiomyopathy, they are mostly associated with DCM that presents later in life [24,25]. There is a relationship between mutation location and pathogenicity of TTNtv phenotype. Given the size of *TTN*, there are many alternative splicing events during transcription and hundreds of unique isoforms expressed in cardiac tissue. The key predictor of pathogenicity of TTNtv is whether the mutated exon is expressed in a high proportion of the total cardiac-expressed isoforms. In a population-based study with genome sequencing, RNA sequencing, and cardiac phenotyping, pathogenicity of a given TTNtv was correlated with how frequently the mutated exon is expressed. This was assigned a value, proportion spliced in (PSI) from 0 to 1, with a PSI > 0.9 imparting a 93% probability of pathogenicity [23]. The association of PSI and phenotype is further supported by pathogenicity data from the Clinvar (<https://www.ncbi.nlm.nih.gov/clinvar/>) database where exon locations of high PSI mutations are correlated with known pathogenic mutations [17]. This is an essential finding because *TTN* mutations are common, therefore predicting whether a given cardiac phenotype is attributable to a TTNtv mutation or an alternative cause is helpful for clinical prognostication. The PSI score as a predictor of pathogenicity fits with previous observations that A-band mutations are more pathogenic, as A-band exons are more constitutively expressed. As a corollary, Z-disk mutations are less pathogenic, likely to be due to lower constitutive expression of Z-disk exons. In addition, there is a common *TTN* isoform, *TTN1*, that has an alternative downstream translational start site that can compensate for upstream truncation mutations [26]. Recently there have been examples of TTNtv with high PSI without cardiac phenotypes. There is evidence that in these circumstances, exons with TTNtv can be translated either through utilization of internal ribosomal entry site or stop codon suppression [27].

2.2. *TTNtv* Cause DCM through Haploinsufficiency, Increased Metabolic Stress, and Activation of the mTOR Signalling Cascade

The exact mechanism for how TTNtv lead to a cardiac phenotype has not been clearly demonstrated. There are studies that suggest specific mutations cause direct damage to the sarcomere and cardiomyocyte. This was observed in a cell culture experiment using human induced pluripotent stem-cell derived cardiomyocytes (hiPSC-CM) isolated from a symptomatic patient with an A-band TTNtv. In the derived cardiomyocytes, a shortened titin protein was isolated and associated with disorganized sarcomere formation and impaired contractility [28]. Similarly, hiPSC-CM derived from a patient with unique A-band TTNtv demonstrated abnormal sarcomerogenesis and cardiomyocyte force generation due to loss of a β -cardiac myosin binding site on the mutated titin protein [29]. Despite these findings

in cell culture experiments, abnormal titin proteins leading to direct sarcomere damage in a “poison peptide” model have not been shown in human studies. Biopsied cardiomyocytes from symptomatic patients with TTNtv did not demonstrate similar alterations in maximum force in myofibril contraction studies [30].

An alternative to the dominant negative model of TTNtv is a model of haploinsufficiency. In this more likely explanation for pathogenicity, TTNtv do not directly damage the sarcomere but instead lead to increased metabolic stress that has chronic effects on cardiomyocyte and cardiac function. Metabolic stress is generated by abnormal mRNA transcripts from the truncation variant leading to increased non-sense mRNA decay (NMD). This leads to long term compensatory changes and development of a common DCM phenotype that is independent of TTN mutation location [31–33] (Figure 3). Rat models with A-band and I-band TTNtv do not alter the amount of TTN expressed, but there is increased NMD and a shift in cardiac metabolism to preference branched chain amino acids and glycolytic intermediates instead of fatty acids that are typically utilized in healthy cardiomyocytes [34,35]. Increased metabolic stress associated with NMD activates mammalian target of rapamycin (mTOR) complex-1 signaling resulting in pathologic protein synthesis and autophagy leading to cardiac phenotypes [31,36]. This was demonstrated in a rat model with TTNtv where there was elevated mTOR complex activation and decreased antiphagocytic degradation in cells. This led to increased reactive oxygen species and mitochondrial dysfunction. Interestingly, treatment of rats with the mTOR inhibitor, rapamycin, rescued the cardiac phenotype [31]. Activation of the mTOR complex appears to be a common downstream pathway of heart failure as its activation is associated with other causes of DCM [37,38]. Further elucidation of these pathways is required to better understand how TTNtv lead to DCM phenotypes which will provide additional opportunities to develop therapies. Animal models are essential for understanding molecular pathways, and several have been utilized to study TTNtv including a mouse model with an A-band truncation mutation, and zebrafish models that have several different truncation variations [39–42]. A review of these important models has been recently carried out [43].

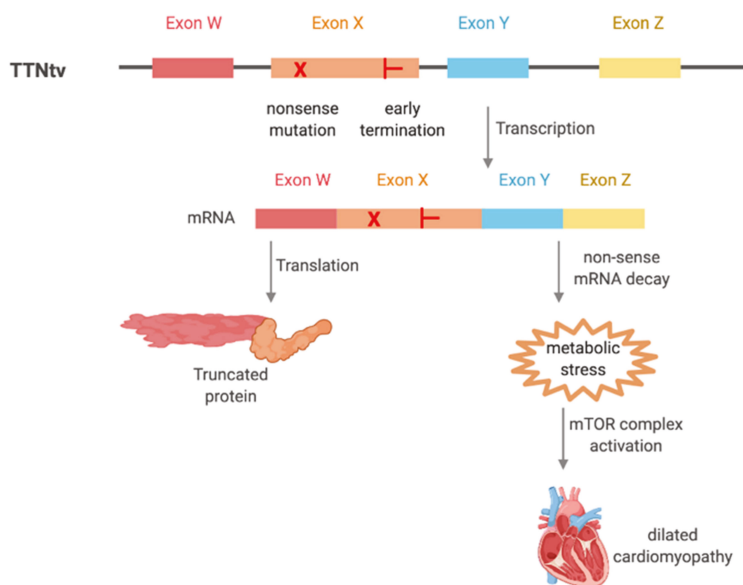


Figure 3. Titin truncation variations (TTNtv) lead to dilated cardiomyopathy related to haploinsufficiency and increased metabolic stress. TTNtv is likely to lead to dilated cardiomyopathy phenotype due to increased non-sense mRNA decay leading to increased metabolic stress and activation of the mammalian target of rapamycin (mTOR) complex signaling pathway. mTOR complex activation is associated with development of dilated cardiomyopathy as a downstream signaling cascade.

2.3. *TTNtv Are Associated with Late Presentation Of DCM, Are More Pathogenic in European Ancestry, and Are Associated with Early Atrial Arrhythmias*

The mechanism of haploinsufficiency leading to abnormal metabolism and increased stress is in keeping with the described human cardiac phenotypes of TTNtv. Mutations of *TTN* are the most common cause of genetic cardiomyopathy and account for 20–25% of genetic DCM [11]. TTNtv are associated with a later presentation (47.9 years) and greater longevity (70.4 years) compared to other genetic and non-genetic causes of cardiomyopathy [24,44]. While patients with TTNtv often present later in life, there is evidence that carriers have pre-symptomatic cardiac dysfunction with eccentric cardiac remodeling as detected by MRI [35]. In a study of 71,000 patients who have been genotyped and undergone cardiac phenotyping, pathogenic TTNtv defined as PSI > 0.9 imparted an increased risk of reduced systolic function regardless of symptoms. In addition, patients with pathologic TTNtv had high risk of developing DCM compared to controls. Interestingly, risk of developing DCM with pathologic TTNtv was associated with ethnicity. Patients with European ancestry and TTNtv had increased odds of developing DCM compared to healthy controls (odds ratio 18.7). Patients with African ancestry and TTNtv had odds of developing DCM that were nearer to the general population (odds ratio 1.8) [45]. While TTNtv have not been closely associated with life threatening ventricular arrhythmias, they are associated with development of atrial arrhythmias including atrial fibrillation. In a case control study of a cohort of 2781 who developed atrial fibrillation before age 66, TTNtv were found in 2.1% of patients compared to 1.1% of controls (odds ratio 1.76). In patients who develop very early atrial fibrillation before age 30, TTNtv were found in 6.5% of patients (odds ratio 5.94) suggesting TTNtv impart increased risk of developing very early atrial fibrillation [46].

2.4. *TTNtv Are Associated with Worse Outcomes When Combined with Additional Cardiac Risk Factors*

Although TTNtv are associated with late development of DCM, when combined with additional risk factors for cardiomyopathy they are associated with earlier presentations and worse outcomes. This suggests a two hit hypothesis for development of TTNtv cardiomyopathy where *TTN* haploinsufficiency increases metabolic stress and when combined with additional risks such as age, toxins, pregnancy or acquired disease can lead to development of DCM [47]. In recent case reports of patients who developed anthracycline associated chemotherapy-induced cardiomyopathy (CCM) and underwent genetic studies, TTNtv were discovered [48]. In a larger study of 213 patients with CCM, TTNtv were present in 7.5% of patients compared to 1.1% of controls. In addition, patients with CCM and TTNtv had more severe cardiac dysfunction and increased risk of atrial fibrillation compared to patients with CCM without a TTNtv [49]. These data suggest that TTNtv when combined with exposure to cardiotoxic chemotherapy increases risk for development of cardiomyopathy. Similar evidence is seen in alcohol cardiomyopathy (ACM), which is a toxic cardiomyopathy related to excessive alcohol consumption. In 141 patient with ACM screened for genetic causes, TTNtv were present in 9.9% of ACM patients compared to 0.7% in controls [50]. Using a multivariate analysis comparing patients with TTNtv versus patients without TTNtv who consume excessive alcohol but do not have clinical ACM, patients with TTNtv had an 8.7% reduction in left ventricular ejection fraction compared to patients without TTNtv [50]. In addition, TTNtv have been associated with increased risk of peripartum cardiomyopathy. In 172 women with peripartum cardiomyopathy, TTNtv were discovered in 65% of patients compared to 4.7% in healthy controls [51]. These results suggest that genetic testing to identify TTNtv in patients with cardiomyopathies of alternative etiologies may be beneficial for prognostication and family screening.

2.5. *Inhibition of the mTOR Pathway and Antisense Oligo Nucleotide Mediated Exon Skipping Are Potential Therapies for TTNtv Related DCM*

Identification of TTNtv in DCM is helpful for prognosis; however, as targeted therapies for TTNtv become available, this may also change clinical management (Table 1). Given the association of TTNtv inducing upregulation of the mTOR complex, mTOR inhibitors such as rapamycin may be reasonable to consider for therapeutic trials of TTNtv DCM [52]. There have also been promising results in correcting

the frameshift and early termination in TTNtv using antisense oligonucleotide (AON) mediated exon skipping. In this strategy, single stranded oligonucleotides are designed to bind pre mRNA either at the intron-exon border of the mutated exon, or to block exon splicing motifs. The goal is to skip the mutated exon that contains the frameshift mutation via alternative splicing and prevent early termination of titin during translation. This strategy has been successfully utilized in other genetic conditions such as Duchenne Muscular dystrophy with FDA approval of an AON molecule [53]. The advantage of this approach is that separate AONs can be designed for each exon containing a TTNtv allowing a targeted approach to therapy. Feasibility of this approach has been demonstrated in a mouse model with a TTNtv where AON exon skipping resulted in rescue of the DCM phenotype [54]. AON mediated exon skipping has also been tested in hiPSC-CMs derived from a patient with TTNtv, where treatment of cardiomyocytes with AON rescued defective myofibril assembly [55]. AON mediated exon skipping represents a viable treatment strategy for patients with TTNtv with DCM that is actively being pursued.

Table 1. Proposed Therapies For Treatment Of Heart Failure That Modify Titin.

Proposed Titin Modifying Therapy	Mechanism of Action	Effect on Cardiac Function
mTOR inhibitor: rapamycin	Decrease mTOR complex signaling that is activated Titin truncation variations (TTNtv) mediated mRNA decay	Improve DCM phenotype for patients with TTNtv
Antisense oligonucleotide mediated exon skipping	Bind mRNA during transcription to skip exon containing missense mutation and prevent early termination	Improve DCM phenotype for patients with TTNtv
T3 hormone, insulin	Increase RBM20 expression to transcriptionally select shorter, stiffer N2B TTN isoform	Increase passive tension to treat DCM
Cardenolides: digoxin and digitoxin	Decrease RBM20 expression to transcriptionally select longer, softer N2BA TTN isoform	Decrease passive tension to treat diastolic dysfunction
Metformin, insulin	Increase ERK2 mediated phosphorylation of N2Bus element	Decrease passive tension to treat diastolic dysfunction
Neuregulin-1 (NRG-1)	Increase ERK2 mediated phosphorylation of N2Bus element, inhibit PKC α phosphorylation of PEVK element	Decrease passive tension to treat diastolic dysfunction
cGMP agonists: sildenafil, vericiguat	Increases cGMP activity to increase PKG mediated phosphorylation of N2Bus element	Decrease passive tension to treat diastolic dysfunction

3. Titin Transcriptional Modifications Are Associated with Development of Cardiomyopathy and Represent a Therapeutic Target for Inherited and Acquired Heart Failure

3.1. Transcriptional Changes of Titin Isoforms Alter Passive Tension and Myocardial Stiffness in Heart Failure

Due to the critical role of titin in the sarcomere and cardiomyocyte, modifications and changes to titin are seen in many forms of heart failure regardless of the etiology. Specifically, transcriptional regulation of *TTN* and selection of isoforms contribute to adaptation to cardiac changes as well as maladaptation and cardiac dysfunction. Understanding and altering transcriptional regulation of titin represents a therapeutic target for treating systolic and diastolic heart failure. Titin has six named major transcriptional isoforms that impart different structural properties based on their size and extensibility [56]. Several of these isoforms are expressed only in neonatal tissue or in skeletal muscle. The two predominant isoforms in adult cardiac tissue are N2B and N2BA [57]. These isoforms differ in the I-band domain where the N2B isoform contains a short PEVK region and few Ig domains, making

it relatively short and stiff. The N2BA isoform has a longer PEVK region and more spring-like Ig domains making it relatively long and soft [56] (Figure 4). The ratio of titin isoform expression in cardiac tissue is correlated with morphology and global cardiac function. In normal hearts, the ratio of N2BA:N2B is typically 70:30 [58]. In heart tissue from patients with end stage DCM, the predominant titin isoform is the longer, softer N2BA. This correlated with decreased passive tension measured on left ventricular muscle strips and in cardio-myofibrils with estimated decreased stiffness of 10% [18,58]. The predominance of the N2BA isoform in patients with DCM also correlated with echocardiographic findings with increased end diastolic volume: pressure ratio suggesting lower global myocardial stiffness [18]. These results suggest that as heart failure progresses there is a maladaptive response leading to selection of the longer, softer N2BA isoform that decreases sarcomere passive stiffness leading to increased end diastolic volume that correlates with ventricular dilation (Figure 4).

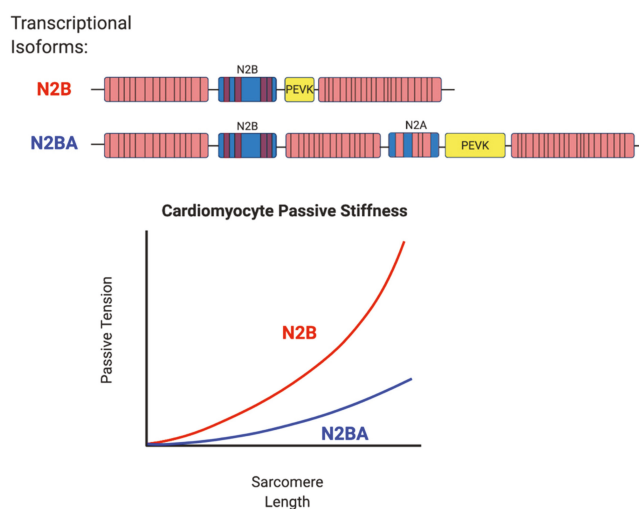


Figure 4. Transcriptional selection of titin isoforms affects cardiomyocyte passive stiffness. There are two major transcriptional isoforms of titin that are expressed in adult cardiac tissue. The N2B isoform has a shorter PEVK domain and has fewer Ig-like domains making it a shorter and stiffer protein. The N2BA isoform has a larger PEVK domain with more Ig-like domains and an N2A element making it a longer and softer protein. The increased size and extensibility of the N2BA isoform decreases cardiomyocyte passive stiffness and is correlated with dilated cardiomyopathy. Modified from [59].

3.2. RBM20 Is a Key Regulator of Titin Isoform Preference

Selecting isoform expression of titin in cardiac tissue represents a potential therapeutic target in treating both systolic and diastolic dysfunction. In systolic dysfunction including DCM, transcriptionally favoring the shorter, stiffer N2B isoform may increase resting tension, decrease end diastolic volume and improve systolic function. Conversely for diastolic dysfunction where there is impaired cardiac relaxation, favoring the longer, softer N2BA isoform may decrease passive tension and improve diastolic filling. One key regulator of transcriptional selection of titin isoforms is RNA binding motif protein 20 (RBM20) [60]. RBM20 is an RNA splicing factor that participates in the spliceosome during maturation of mRNA [57,61]. RBM20 binds introns near splice sites and adjacent to U1 and U2 small nuclear ribonucleoprotein (snRNP) binding sites to regulate transcription [62]. The exact mechanism by which RBM20 regulates titin isoform selection has not been demonstrated; however, RBM20 clearly plays an essential role. Patients with RBM20 mutations develop severe DCM and are at risk of sudden cardiac death [61,63–65]. Sudden cardiac death associated with RBM20 mutations are related to increased arrhythmias with this mutation that are likely caused by abnormal calcium handling and increased

calcium release from the sarcoplasmic reticulum [66]. In addition, RBM20 mutations have been associated with left ventricular non-compaction [67]. Humans with RBM20 mutations have a marked increase in the N2BA isoform [60]. This is also demonstrated in animal models including a rat knockout of RBM20 [60]. Further animal models for RBM20 and its targets have been described but are not as well characterized [43]. The preference for the longer, softer N2BA isoform in RBM20 mutants results in decreased active and passive tension of cardiomyocytes contributing to dilation of the ventricle [68]. Upregulation of RBM20 to preference the shorter, stiffer N2B isoform may be appealing as a treatment for patients with DCM or systolic dysfunction. To date there has been no clear mechanism or small molecule that will increase RBM20 activity. Recent studies in rats have shown that RBM20 can be upregulated by thyroid hormone-triiodothyronine (T3) resulting in preference of the N2B isoform suggesting that modification of the thyroid pathway may be beneficial in treatment of systolic heart failure [69]. Additionally, in cultured rat cells, administration of insulin activates the mTOR kinase axis and RBM20 to preference the N2B isoform [70]. Further understanding of the thyroid and insulin pathways and how they specifically affect RBM20 and titin isoform selection is needed to identify novel therapeutics for systolic dysfunction and DCM.

3.3. *Modifications of Titin Isoforms Represent a Therapeutic Target for Treatment of Heart Failure*

Downregulation of RBM20 favors the longer, softer N2BA isoform which could improve diastolic dysfunction and serve as a therapy for heart failure with preserved ejection fraction (HFpEF). In animal models, reduction of RBM20 improved diastolic dysfunction as measured by left ventricular wall thickness, echocardiographic markers, and hemodynamic markers including end diastolic pressure [71,72]. A novel approach has been developed to complete high throughput screening of small molecules to identify compounds that decrease RBM20 levels. The initial trial identified cardenolides, which include digoxin and digitoxin, as small molecules that can effectively reduce RBM20 levels and preference N2BA isoform expression [73]. Further studies in animal models are needed to determine if cardenolides represent plausible therapies for HFpEF via reduction of RBM20 and preference for the longer softer N2BA isoform. In addition to RBM20, other molecules are likely to be capable of regulating titin isoform expression and may represent alternative therapeutic targets. Another molecule that can modify titin transcriptionally is RNA binding motif protein 24 (RBM24). RBM24 is expressed in mammalian hearts and when knocked out in mice causes DCM. In one study, RBM24 knockout mice had a disorganized sarcomere and altered titin isoform expression: however, N2BA:N2B isoform expression was not determined [74]. Further studies of RBM24 are necessary including determination of how specifically titin isoform expression is altered by RBM24. In addition to proteins involved directly in transcription, micro RNAs are capable of transcriptional regulation by binding to mRNA and targeting it for degradation. In a mouse model carrying a TTNtv that develops DCM, it was demonstrated that the micro mRNA miR-208b is significantly over-expressed. Over-expression of miR-208b was also found in patients with DCM not related to TTNtv. When miR-208b was inhibited, mice did not develop a DCM phenotype suggesting that miR-208b plays a role in development of DCM possibly through transcriptional regulation of titin, although the exact mechanism for miR-208b has not been demonstrated [75].

4. **Post-Translational Modifications of Titin Affect Myocardial Physiology and Can Be Modified to Treat Heart Failure**

4.1. *Phosphorylation of the PEVK Element of Titin Increases Cardiomyocyte Passive Tension*

In addition to genetic and transcriptional modifications, post-translational modifications of titin also play an important role in cardiac physiology and changes associated with heart failure. The most well described post-translational modification of titin is phosphorylation and dephosphorylation [76]. Based on proteomic analysis, there are hundreds of predicted phosphorylation sites on titin [77–79]. Only a few of these potential phosphosites have been studied and demonstrated to impart functional

changes on titin with a majority of the studied sites located in the spring-like I-band domain [17]. Phosphorylation within different regions of the I-band have different effects on the functional properties of titin. The PEVK element has a predominantly negative charge, therefore phosphorylation of this element with a positively charged phosphate group increases electrostatic attraction making the extensible region more rigid [76]. Treatment of human cardiomyocytes with the protein kinase C alpha (PKC α) has been shown to cause phosphorylation of the PEVK element and increase passive tension [80]. In a study of cardiomyocytes isolated by biopsy from patients with mixed systolic and diastolic heart failure, there was greater activation of PKC α within the cardiomyocytes compared to control samples. This increase in PKC α activity also correlated with increased passive tension studied on skinned myocardial fibers [81]. PKC α is activated by excess catecholamines or hypertrophic signaling cascades and may represent a terminal pathway in heart failure that leads to increased myofilament stiffness. Activation of PKC α and the resultant increase in passive tension of cardiomyocytes may be a compensatory change to increase passive stiffness in patients with DCM in order to improve cardiac function. PKC α mediated increased passive stiffness may also represent a dysregulated pathway that leads to pathologic passive tension and may result in diastolic dysfunction [82,83]. Additional studies comparing PKC α activation and passive tension between cardiomyocytes isolated from patients with DCM and patients with diastolic dysfunction may be helpful to better understand the molecular pathways involving PKC α and heart failure. It should be considered that modification of this pathway represents a viable therapeutic target for treatment of heart failure when it is more clearly understood.

4.2. Phosphorylation of the N2B Unique Sequence (N2Bus) Element of Titin Decreases Cardiomyocyte Passive Tension

Functionally significant phosphosites have also been discovered within the I-band in the N2Bus. This is a positively charged region, therefore phosphorylation increases repulsion forces leading to elongation and softening of titin [84]. Kinases capable of phosphorylating this element include protein kinase A (PKA), extracellular signal-regulated kinase 2 (ERK2), protein kinase G (PKG), and calcium/calmodulin-dependent protein kinase II delta (CaMKII δ) [17]. Dephosphorylation of the N2Bus has been demonstrated by protein phosphatase 5 (PP5) [85].

4.3. Diabetes Contributes to Diastolic Dysfunction via Abnormal Phosphorylation of Titin, Which Can Be Reversed by Treatment with Metformin, and Neuregulin-1 (NRG-1)

Modification of titin's stiffness via phosphorylation and dephosphorylation represents a way to modify global cardiac function. There has been clinical association between development of diastolic dysfunction and diabetes. The exact mechanism for how diabetes contributes to diastolic dysfunction is not known, but there are data suggesting that it is related to abnormal protein phosphorylation. One common therapy for diabetes that has been associated with improvement in diastolic dysfunction is metformin. It was demonstrated in a mouse model of diastolic dysfunction that metformin increases activation of PKG leading to phosphorylation of the N2Bus element and reduced passive stiffness of the sarcomere resulting in improvement of diastolic dysfunction [86]. In another study, cardiomyocytes isolated from patients with diabetes who also had diastolic dysfunction demonstrated increased passive tension compared to controls. Concurrent with the mechanical changes, the cardiomyocytes from patients with diastolic dysfunction also showed changes to the phosphorylation of titin. This included increased activation of PKC α and phosphorylation in the PEVK element, as well as reduced activation of PKG and decreased phosphorylation of the N2Bus element. These changes in phosphorylation are both predicted to increase passive tension as was observed [87]. When metformin or insulin were applied to the cells in culture, there was increased activity of ERK2 leading to increased phosphorylation of the N2Bus element which reduces passive tension; however, this was partially counteracted by increased phosphorylation of the PEVK element by PKC α . Similar abnormalities in phosphorylation were seen in a diastolic dysfunction mouse model, and the abnormal phosphorylation was reversed by treating the animals with neuregulin-1 (NRG-1). NRG-1 increased phosphorylation of the N2Bus

element via ERK2 and decreased phosphorylation of the PEVK element via PKC α . The animals showed improvement in their diastolic dysfunction as measured by reduced end-diastolic pressure [87]. This study suggests that NRG-1 can reduce passive stiffness of cardiomyocytes by specifically altering phosphorylation of titin and can improve diastolic dysfunction.

4.4. Activation of Cyclic Guanosine Monophosphate (cGMP) and PKG Decreases Titin Passive Tension and Represents a Viable Therapy for Treatment of Heart Failure

In addition to metformin and NRG-1, sildenafil has been proposed as a therapy for diastolic dysfunction due to its effects on phosphorylation of titin. Sildenafil inhibits phosphodiesterase-5 leading to increased nitric oxide (NO) and increased cGMP signaling. cGMP is known to activate PKG, which phosphorylates the N2Bus element of titin resulting in softening of titin and decreased myocardial stiffness [88]. In a dog model of diastolic dysfunction, treatment with sildenafil increased phosphorylation of the N2Bus element via increased activation of cGMP resulting in improved diastolic function compared to untreated controls [89]. Based on these results, sildenafil was studied in patients with diastolic dysfunction to determine whether cGMP dependent PKG phosphorylation of titin can improve clinical outcomes. Unfortunately, in this placebo controlled, randomized trial, treatment with sildenafil did not significantly improve clinical, laboratory, or echocardiographic outcomes in patients [90]. Interestingly patients who received sildenafil showed no significant increase in plasma cGMP levels suggesting that the medication did not have the desired therapeutic effect on altering PKG dependent phosphorylation. Activating cGMP to improve heart failure has been pursued further with novel therapies including vericiguat which is an oral soluble guanylate cyclase stimulator that generates cGMP. This compound was studied in patients with systolic dysfunction in a high quality randomized clinical trial. Compared to placebo, treatment with vericiguat reduced hospitalizations and cardiovascular death among patients with systolic dysfunction [91]. This represents a significant breakthrough for clinical management of heart failure with a medication that utilizes a novel mechanism of action. Although increasing levels of cGMP is likely to have many effects for improving heart failure, the effects on phosphorylation of the titin N2Bus element is likely to be significant. Further study is warranted to determine mechanistically how vericiguat alters cardiomyocytes and how it affects titin. Based on the mechanism of action, vericiguat is an appealing medication to treat diastolic dysfunction due to activation of PKG, phosphorylation of the TTN N2Bus element and softening of the titin protein. Given the clinical burden of diastolic dysfunction, and the lack of effective therapeutic medications, vericiguat should be studied in patients with diastolic dysfunction. Indeed, there are at least two clinical trials of vericiguat ongoing in patients with diastolic dysfunction [92,93].

Post-translational modifications of titin including phosphorylation and dephosphorylation of specific elements contribute to development of heart failure and represent targets for therapies to treat heart failure. Further study of post-translational modifications is needed to better understand and treat heart failure. In addition to phosphorylation, there are likely to be many other post-translational modifications of titin that exist and should be studied.

5. Conclusions

Heart failure is a common clinical syndrome often caused by abnormalities within sarcomeric proteins including the giant, spring like protein titin. The structure of titin, specifically Ig-like domains, impart important physiologic characteristics to cardiac tissues including length dependent activation and passive tension of the ventricle. Truncation mutations of titin are the most common genetic causes of dilated cardiomyopathy and often lead to a phenotype that presents later in life and is associated with atrial arrhythmias. The pathophysiology of TTNtv leading to DCM is likely related to increased intracellular stress associated with increased nonsense mRNA decay leading to activation of the mTOR signaling cascade which results in abnormalities in cellular metabolism and ultimate dysfunction of the cardiomyocyte. This increased metabolic stress is likely to predispose patients with TTNtv to development of DCM when combined with other cardiac risk factors such as age, chemotherapy, alcohol

use, and pregnancy. There are promising therapies for treating TTNtv including mTOR inhibitors and oligonucleotides that lead to alternative splicing that exclude mutated exons (Table 1).

Transcriptional modifications of titin are associated with both systolic and diastolic dysfunction and therefore titin represents a viable therapeutic target for treatment of cardiomyopathy. Patients with systolic heart failure have increased expression of the N2BA titin transcriptional variant that encodes a longer and softer titin protein, which correlates with decreased passive tension and increased left ventricular end diastolic volume. Therefore, transcriptional modification of titin to preference the shorter, stiffer N2B isoform may improve systolic heart failure. Conversely, in patients with abnormal ventricular relaxation, favoring the longer, softer titin isoform may improve diastolic filling and treat diastolic dysfunction. Although we do not yet have therapies to modulate transcription of titin, RBM20 is a key transcriptional regulator and therapeutic target (Figure 5).

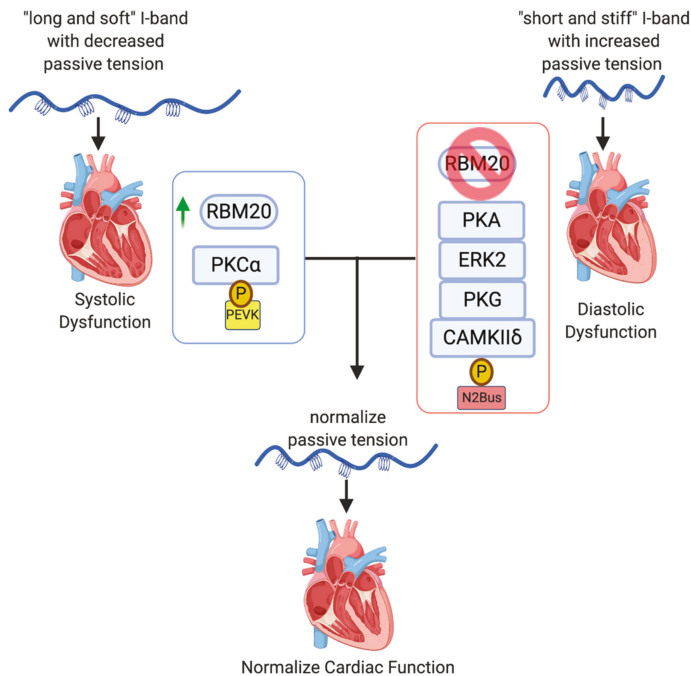


Figure 5. Transcriptional and post-translational modifications of titin alter passive tension and serve as therapeutic targets for treatment of heart failure. Patients with systolic dysfunction have decreased passive stiffness of the ventricle. Modifications of titin by upregulation of RNA binding motif protein 20 (RBM20) and preferring the N2B isoform, or phosphorylation of the PEVK element can increase passive tension of the I-band and may improve cardiac function. Conversely, patients with diastolic dysfunction have increased passive tension of the ventricle. Decreased expression of RBM20 leading to increased expression of the N2BA isoform, or phosphorylation of the N2Bus element may decrease passive tension and improve cardiac function.

Post-translational modifications of titin by phosphorylation of the spring-like I-band are capable of changing the length and stiffness of titin and are correlated with cardiomyopathy. Increased phosphorylation of the PEVK element increases titin passive tension, whereas phosphorylation of the N2Bus element decreases passive tension. Many molecules and signaling pathways affect phosphorylation of these regions and further understanding of their control may provide an opportunity to selectively modify titin and improve both systolic and diastolic heart failure (Table 1, Figure 5).

Author Contributions: Conceptualization, C.T., M.T. and L.M.; resources, C.T.; writing—original draft preparation, C.T.; writing—review and editing, C.T., M.T. and L.M.; funding acquisition, M.T. and L.M. All authors have read and agreed to the published version of the manuscript.

Funding: This work was supported in part by NIH grants R01 HL69071, R01 HL116906, R01 HL147064, NCATS/CTSA UL1 TR001082 and AHA17GRNT33670495 (L.M.); NIH 1K23HI067915 and R01HL109209 (M.T.). This work was also supported in part by the Trans-Atlantic Network of Excellence grants from the Foundation Leducq (14-CVD 03) (M.T., and L.M.).

Acknowledgments: Figures were created with [Biorender.com](https://www.biorender.com).

Conflicts of Interest: The authors declare no conflict of interest.

References

1. Go, A.S.; Mozaffarian, D.; Roger, V.L.; Benjamin, E.J.; Berry, J.D.; Borden, W.B.; Bravata, D.M.; Dai, S.; Ford, E.S.; Fox, C.S.; et al. Heart disease and stroke statistics—2013 update: A report from the American Heart Association. *Circulation* **2013**, *127*, e6–e245. [[CrossRef](#)] [[PubMed](#)]
2. McMurray, J.J.; Petrie, M.C.; Murdoch, D.R.; Davie, A.P. Clinical epidemiology of heart failure: Public and private health burden. *Eur. Heart J.* **1998**, *19* (Suppl. P), P9–P16.
3. Zipes, D.P.; Braunwald, E. *Braunwald's Heart Disease: A Textbook of Cardiovascular Medicine*, 7th ed.; W.B. Saunders: Philadelphia, PA, USA, 2005; Volume xxi, 2183p, p. 75.
4. Furst, D.O.; Osborn, M.; Nave, R.; Weber, K. The organization of titin filaments in the half-sarcomere revealed by monoclonal antibodies in immunoelectron microscopy: A map of ten nonrepetitive epitopes starting at the Z line extends close to the M line. *J. Cell Biol.* **1988**, *106*, 1563–1572. [[CrossRef](#)] [[PubMed](#)]
5. Labeit, S.; Kolmerer, B. Titins: Giant proteins in charge of muscle ultrastructure and elasticity. *Science* **1995**, *270*, 293–296. [[CrossRef](#)] [[PubMed](#)]
6. Whiting, A.; Wardale, J.; Trinick, J. Does titin regulate the length of muscle thick filaments? *J. Mol. Biol.* **1989**, *205*, 263–268. [[CrossRef](#)]
7. Maruyama, K.; Kimura, S.; Yoshidomi, H.; Sawada, H.; Kikuchi, M. Molecular size and shape of beta-connectin, an elastic protein of striated muscle. *J. Biochem.* **1984**, *95*, 1423–1433. [[CrossRef](#)] [[PubMed](#)]
8. Bang, M.L.; Centner, T.; Fornoff, F.; Geach, A.J.; Gotthardt, M.; McNabb, M.; Witt, C.C.; Labeit, D.; Gregorio, C.C.; Granzier, H.; et al. The complete gene sequence of titin, expression of an unusual approximately 700-kDa titin isoform, and its interaction with obscurin identify a novel Z-line to I-band linking system. *Circ. Res.* **2001**, *89*, 1065–1072. [[CrossRef](#)]
9. LeWinter, M.M.; Wu, Y.; Labeit, S.; Granzier, H. Cardiac titin: Structure, functions and role in disease. *Clin. Chim. Acta* **2007**, *375*, 1–9. [[CrossRef](#)]
10. Gotthardt, M.; Hammer, R.E.; Hubner, N.; Monti, J.; Witt, C.C.; McNabb, M.; Richardson, J.A.; Granzier, H.; Labeit, S.; Herz, J. Conditional expression of mutant M-line titins results in cardiomyopathy with altered sarcomere structure. *J. Biol. Chem.* **2003**, *278*, 6059–6065. [[CrossRef](#)]
11. LeWinter, M.M.; Granzier, H. Cardiac titin: A multifunctional giant. *Circulation* **2010**, *121*, 2137–2145. [[CrossRef](#)]
12. Linke, W.A.; Granzier, H. A spring tale: New facts on titin elasticity. *Biophys. J.* **1998**, *75*, 2613–2614. [[CrossRef](#)]
13. Yotti, R.; Seidman, C.E.; Seidman, J.G. Advances in the Genetic Basis and Pathogenesis of Sarcomere Cardiomyopathies. *Annu. Rev. Genom. Hum. Genet.* **2019**, *20*, 129–153. [[CrossRef](#)] [[PubMed](#)]
14. Labeit, S.; Barlow, D.P.; Gautel, M.; Gibson, T.; Holt, J.; Hsieh, C.L.; Francke, U.; Leonard, K.; Wardale, J.; Whiting, A.; et al. A regular pattern of two types of 100-residue motif in the sequence of titin. *Nature* **1990**, *345*, 273–276. [[CrossRef](#)] [[PubMed](#)]
15. Braunwald, E.; Bonow, R.O. *Braunwald's Heart Disease: A Textbook of Cardiovascular Medicine*, 9th ed.; Saunders: Philadelphia, PA, USA, 2012; Volume xxiv, 1961p.
16. Fukuda, N.; Granzier, H.L. Titin/connectin-based modulation of the Frank-Starling mechanism of the heart. *J. Muscle Res. Cell Motil.* **2005**, *26*, 319–323. [[CrossRef](#)] [[PubMed](#)]
17. Tharp, C.A.; Haywood, M.E.; Sbaizero, O.; Taylor, M.R.G.; Mestroni, L. The Giant Protein Titin's Role in Cardiomyopathy: Genetic, Transcriptional, and Post-translational Modifications of TTN and Their Contribution to Cardiac Disease. *Front. Physiol.* **2019**, *10*, 1436. [[CrossRef](#)] [[PubMed](#)]
18. Nagueh, S.F.; Shah, G.; Wu, Y.; Torre-Amione, G.; King, N.M.; Lahmers, S.; Witt, C.C.; Becker, K.; Labeit, S.; Granzier, H.L. Altered titin expression, myocardial stiffness, and left ventricular function in patients with dilated cardiomyopathy. *Circulation* **2004**, *110*, 155–162. [[CrossRef](#)] [[PubMed](#)]

19. Peled, Y.; Gramlich, M.; Yoskovitz, G.; Feinberg, M.S.; Afek, A.; Polak-Charcon, S.; Pras, E.; Sela, B.A.; Konen, E.; Weissbrod, O.; et al. Titin mutation in familial restrictive cardiomyopathy. *Int. J. Cardiol.* **2014**, *171*, 24–30. [[CrossRef](#)]
20. Herman, D.S.; Lam, L.; Taylor, M.R.; Wang, L.; Teekakirikul, P.; Christodoulou, D.; Conner, L.; DePalma, S.R.; McDonough, B.; Sparks, E.; et al. Truncations of titin causing dilated cardiomyopathy. *N. Engl. J. Med.* **2012**, *366*, 619–628. [[CrossRef](#)]
21. Gerull, B.; Gramlich, M.; Atherton, J.; McNabb, M.; Trombitas, K.; Sasse-Klaassen, S.; Seidman, J.G.; Seidman, C.; Granzier, H.; Labeit, S.; et al. Mutations of TTN, encoding the giant muscle filament titin, cause familial dilated cardiomyopathy. *Nat. Genet.* **2002**, *30*, 201–204. [[CrossRef](#)]
22. Golbus, J.R.; Puckelwartz, M.J.; Fahrenbach, J.P.; Dellefave-Castillo, L.M.; Wolfgeher, D.; McNally, E.M. Population-based variation in cardiomyopathy genes. *Circ. Cardiovasc. Genet.* **2012**, *5*, 391–399. [[CrossRef](#)]
23. Roberts, A.M.; Ware, J.S.; Herman, D.S.; Schafer, S.; Baksi, J.; Bick, A.G.; Buchan, R.J.; Walsh, R.; John, S.; Wilkinson, S.; et al. Integrated allelic, transcriptional, and phenomic dissection of the cardiac effects of titin truncations in health and disease. *Sci. Transl. Med.* **2015**, *7*, 270ra276. [[CrossRef](#)] [[PubMed](#)]
24. Gigli, M.; Merlo, M.; Graw, S.L.; Barbati, G.; Rowland, T.J.; Slavov, D.B.; Stolfo, D.; Haywood, M.E.; Dal Ferro, M.; Altinier, A.; et al. Genetic Risk of Arrhythmic Phenotypes in Patients With Dilated Cardiomyopathy. *J. Am. Coll. Cardiol.* **2019**, *74*, 1480–1490. [[CrossRef](#)] [[PubMed](#)]
25. Jansweijer, J.A.; Nieuwhof, K.; Russo, F.; Hoortjje, E.T.; Jongbloed, J.D.; Lekanne Deprez, R.H.; Postma, A.V.; Bronk, M.; van Rijsingen, I.A.; de Haij, S.; et al. Truncating titin mutations are associated with a mild and treatable form of dilated cardiomyopathy. *Eur. J. Heart Fail.* **2017**, *19*, 512–521. [[CrossRef](#)] [[PubMed](#)]
26. Zaunbrecher, R.J.; Abel, A.N.; Beussman, K.; Leonard, A.; von Frieling-Salewsky, M.; Fields, P.A.; Pabon, L.; Reinecke, H.; Yang, X.; Macadangang, J.; et al. Cronos Titin Is Expressed in Human Cardiomyocytes and Necessary for Normal Sarcomere Function. *Circulation* **2019**, *140*, 1647–1660. [[CrossRef](#)]
27. Van Heesch, S.; Witte, F.; Schneider-Lunitz, V.; Schulz, J.F.; Adami, E.; Faber, A.B.; Kirchner, M.; Maatz, H.; Blachut, S.; Sandmann, C.L.; et al. The Translational Landscape of the Human Heart. *Cell* **2019**, *178*, 242–260.e29. [[CrossRef](#)]
28. Hinson, J.T.; Chopra, A.; Nafissi, N.; Polacheck, W.J.; Benson, C.C.; Swist, S.; Gorham, J.; Yang, L.; Schafer, S.; Sheng, C.C.; et al. HEART DISEASE. Titin mutations in iPSC cells define sarcomere insufficiency as a cause of dilated cardiomyopathy. *Science* **2015**, *349*, 982–986. [[CrossRef](#)]
29. Chopra, A.; Kutys, M.L.; Zhang, K.; Polacheck, W.J.; Sheng, C.C.; Luu, R.J.; Eyckmans, J.; Hinson, J.T.; Seidman, J.G.; Seidman, C.E.; et al. Force Generation via beta-Cardiac Myosin, Titin, and alpha-Actinin Drives Cardiac Sarcomere Assembly from Cell-Matrix Adhesions. *Dev. Cell* **2018**, *44*, 87–96.e5. [[CrossRef](#)]
30. Vikhorev, P.G.; Smoktunowicz, N.; Munster, A.B.; Copeland, O.; Kostin, S.; Montgiraud, C.; Messer, A.E.; Toliat, M.R.; Li, A.; Dos Remedios, C.G.; et al. Abnormal contractility in human heart myofibrils from patients with dilated cardiomyopathy due to mutations in TTN and contractile protein genes. *Sci. Rep.* **2017**, *7*, 14829. [[CrossRef](#)]
31. Zhou, Q.; Kesteven, S.; Wu, J.; Aidery, P.; Gawaz, M.; Gramlich, M.; Feneley, M.P.; Harvey, R.P. Pressure Overload by Transverse Aortic Constriction Induces Maladaptive Hypertrophy in a Titin-Truncated Mouse Model. *Biomed Res. Int.* **2015**, *2015*, 163564. [[CrossRef](#)]
32. Ware, J.S.; Cook, S.A. Role of titin in cardiomyopathy: From DNA variants to patient stratification. *Nat. Rev. Cardiol.* **2018**, *15*, 241–252. [[CrossRef](#)]
33. Tabish, A.M.; Azzimato, V.; Alexiadis, A.; Buyandelger, B.; Knoll, R. Genetic epidemiology of titin-truncating variants in the etiology of dilated cardiomyopathy. *Biophys. Rev.* **2017**, *9*, 207–223. [[CrossRef](#)] [[PubMed](#)]
34. Shibayama, J.; Yuzyuk, T.N.; Cox, J.; Makaju, A.; Miller, M.; Lichter, J.; Li, H.; Leavy, J.D.; Franklin, S.; Zaitsev, A.V. Metabolic remodeling in moderate synchronous versus dyssynchronous pacing-induced heart failure: Integrated metabolomics and proteomics study. *PLoS ONE* **2015**, *10*, e0118974. [[CrossRef](#)] [[PubMed](#)]
35. Schafer, S.; de Marvao, A.; Adami, E.; Fiedler, L.R.; Ng, B.; Khin, E.; Rackham, O.J.; van Heesch, S.; Pua, C.J.; Kui, M.; et al. Titin-truncating variants affect heart function in disease cohorts and the general population. *Nat. Genet.* **2017**, *49*, 46–53. [[CrossRef](#)] [[PubMed](#)]
36. Neishabouri, S.H.; Hutson, S.M.; Davoodi, J. Chronic activation of mTOR complex 1 by branched chain amino acids and organ hypertrophy. *Amino Acids* **2015**, *47*, 1167–1182. [[CrossRef](#)] [[PubMed](#)]
37. Yano, T.; Shimoshige, S.; Miki, T.; Tanno, M.; Mochizuki, A.; Fujito, T.; Yuda, S.; Muranaka, A.; Ogasawara, M.; Hashimoto, A.; et al. Clinical impact of myocardial mTORC1 activation in nonischemic dilated cardiomyopathy. *J. Mol. Cell. Cardiol.* **2016**, *91*, 6–9. [[CrossRef](#)]

38. Sweet, M.E.; Cocciolo, A.; Slavov, D.; Jones, K.L.; Sweet, J.R.; Graw, S.L.; Reece, T.B.; Ambardekar, A.V.; Bristow, M.R.; Mestroni, L.; et al. Transcriptome analysis of human heart failure reveals dysregulated cell adhesion in dilated cardiomyopathy and activated immune pathways in ischemic heart failure. *BMC Genom.* **2018**, *19*, 812. [[CrossRef](#)]
39. Gramlich, M.; Michely, B.; Krohne, C.; Heuser, A.; Erdmann, B.; Klaassen, S.; Hudson, B.; Magarin, M.; Kirchner, F.; Todiras, M.; et al. Stress-induced dilated cardiomyopathy in a knock-in mouse model mimicking human titin-based disease. *J. Mol. Cell. Cardiol.* **2009**, *47*, 352–358. [[CrossRef](#)]
40. Zou, J.; Tran, D.; Baalbaki, M.; Tang, L.F.; Poon, A.; Pelonero, A.; Titus, E.W.; Yuan, C.; Shi, C.; Patchava, S.; et al. An internal promoter underlies the difference in disease severity between N- and C-terminal truncation mutations of Titin in zebrafish. *Elife* **2015**, *4*, e09406. [[CrossRef](#)]
41. Shih, Y.H.; Dvornikov, A.V.; Zhu, P.; Ma, X.; Kim, M.; Ding, Y.; Xu, X. Exon- and contraction-dependent functions of titin in sarcomere assembly. *Development* **2016**, *143*, 4713–4722. [[CrossRef](#)]
42. Huttner, I.G.; Wang, L.W.; Santiago, C.F.; Horvat, C.; Johnson, R.; Cheng, D.; von Frieling-Salewsky, M.; Hillcoat, K.; Bemand, T.J.; Trivedi, G.; et al. A-Band Titin Truncation in Zebrafish Causes Dilated Cardiomyopathy and Hemodynamic Stress Intolerance. *Circ. Genom. Precis. Med.* **2018**, *11*, e002135. [[CrossRef](#)]
43. Gerull, B.; Brodehl, A. Genetic Animal Models for Arrhythmogenic Cardiomyopathy. *Front. Physiol.* **2020**, *11*, 624. [[CrossRef](#)] [[PubMed](#)]
44. Fang, H.J.; Liu, B.P. Prevalence of TTN mutations in patients with dilated cardiomyopathy: A meta-analysis. *Herz* **2019**. [[CrossRef](#)] [[PubMed](#)]
45. Haggerty, C.M.; Damrauer, S.M.; Levin, M.G.; Birtwell, D.; Carey, D.J.; Golden, A.M.; Hartzel, D.N.; Hu, Y.; Judy, R.; Kelly, M.A.; et al. Genomics-First Evaluation of Heart Disease Associated With Titin-Truncating Variants. *Circulation* **2019**, *140*, 42–54. [[CrossRef](#)] [[PubMed](#)]
46. Choi, S.H.; Weng, L.C.; Roselli, C.; Lin, H.; Haggerty, C.M.; Shoemaker, M.B.; Barnard, J.; Arking, D.E.; Chasman, D.I.; Albert, C.M.; et al. Association Between Titin Loss-of-Function Variants and Early-Onset Atrial Fibrillation. *JAMA* **2018**, *320*, 2354–2364. [[CrossRef](#)] [[PubMed](#)]
47. Bondue, A.; Arbustini, E.; Bianco, A.; Ciccarelli, M.; Dawson, D.; De Rosa, M.; Hamdani, N.; Hilfiker-Kleiner, D.; Meder, B.; Leite-Moreira, A.F.; et al. Complex roads from genotype to phenotype in dilated cardiomyopathy: Scientific update from the Working Group of Myocardial Function of the European Society of Cardiology. *Cardiovasc. Res.* **2018**, *114*, 1287–1303. [[CrossRef](#)]
48. Linschoten, M.; Teske, A.J.; Baas, A.F.; Vink, A.; Dooijes, D.; Baars, H.F.; Asselbergs, F.W. Truncating Titin (TTN) Variants in Chemotherapy-Induced Cardiomyopathy. *J. Card. Fail.* **2017**, *23*, 476–479. [[CrossRef](#)]
49. Garcia-Pavia, P.; Kim, Y.; Restrepo-Cordoba, M.A.; Lunde, I.G.; Wakimoto, H.; Smith, A.M.; Toepfer, C.N.; Getz, K.; Gorham, J.; Patel, P.; et al. Genetic Variants Associated With Cancer Therapy-Induced Cardiomyopathy. *Circulation* **2019**, *140*, 31–41. [[CrossRef](#)]
50. Ware, J.S.; Amor-Salamanca, A.; Tayal, U.; Govind, R.; Serrano, I.; Salazar-Mendiguchia, J.; Garcia-Pinilla, J.M.; Pascual-Figal, D.A.; Nunez, J.; Guzzo-Merello, G.; et al. Genetic Etiology for Alcohol-Induced Cardiac Toxicity. *J. Am. Coll. Cardiol.* **2018**, *71*, 2293–2302. [[CrossRef](#)]
51. Ware, J.S.; Li, J.; Mazaika, E.; Yasso, C.M.; DeSouza, T.; Cappola, T.P.; Tsai, E.J.; Hilfiker-Kleiner, D.; Kamiya, C.A.; Mazzarotto, F.; et al. Shared Genetic Predisposition in Peripartum and Dilated Cardiomyopathies. *N. Engl. J. Med.* **2016**, *374*, 233–241. [[CrossRef](#)]
52. Zhou, J.; Ng, B.; Ko, N.S.J.; Fiedler, L.R.; Khin, E.; Lim, A.; Sahib, N.E.; Wu, Y.; Chothani, S.P.; Schafer, S.; et al. Titin truncations lead to impaired cardiomyocyte autophagy and mitochondrial function in vivo. *Hum. Mol. Genet.* **2019**, *28*, 1971–1981. [[CrossRef](#)]
53. Syed, Y.Y. Eteplirsen: First Global Approval. *Drugs* **2016**, *76*, 1699–1704. [[CrossRef](#)] [[PubMed](#)]
54. Gramlich, M.; Pane, L.S.; Zhou, Q.; Chen, Z.; Murgia, M.; Schotterl, S.; Goedel, A.; Metzger, K.; Brade, T.; Parrotta, E.; et al. Antisense-mediated exon skipping: A therapeutic strategy for titin-based dilated cardiomyopathy. *Embo Mol. Med.* **2015**, *7*, 562–576. [[CrossRef](#)] [[PubMed](#)]
55. Hahn, J.K.; Neupane, B.; Pradhan, K.; Zhou, Q.; Testa, L.; Pelzl, L.; Maleck, C.; Gawaz, M.; Gramlich, M. The assembly and evaluation of antisense oligonucleotides applied in exon skipping for titin-based mutations in dilated cardiomyopathy. *J. Mol. Cell. Cardiol.* **2019**, *131*, 12–19. [[CrossRef](#)] [[PubMed](#)]
56. Guo, W.; Bharmal, S.J.; Esbona, K.; Greaser, M.L. Titin diversity—alternative splicing gone wild. *J. Biomed. Biotechnol.* **2010**, *2010*, 753675. [[CrossRef](#)]
57. Guo, W.; Sun, M. RBM20, a potential target for treatment of cardiomyopathy via titin isoform switching. *Biophys. Rev.* **2018**, *10*, 15–25. [[CrossRef](#)]

58. Makarenko, I.; Opitz, C.A.; Leake, M.C.; Neagoe, C.; Kulke, M.; Gwathmey, J.K.; del Monte, F.; Hajjar, R.J.; Linke, W.A. Passive stiffness changes caused by upregulation of compliant titin isoforms in human dilated cardiomyopathy hearts. *Circ. Res.* **2004**, *95*, 708–716. [[CrossRef](#)]
59. Gigli, M.; Begay, R.L.; Morea, G.; Graw, S.L.; Sinagra, G.; Taylor, M.R.; Granzier, H.; Mestroni, L. A Review of the Giant Protein Titin in Clinical Molecular Diagnostics of Cardiomyopathies. *Front. Cardiovasc. Med.* **2016**, *3*, 21. [[CrossRef](#)]
60. Guo, W.; Schafer, S.; Greaser, M.L.; Radke, M.H.; Liss, M.; Govindarajan, T.; Maatz, H.; Schulz, H.; Li, S.; Parrish, A.M.; et al. RBM20, a gene for hereditary cardiomyopathy, regulates titin splicing. *Nat. Med.* **2012**, *18*, 766–773. [[CrossRef](#)]
61. Brauch, K.M.; Karst, M.L.; Herron, K.J.; de Andrade, M.; Pellikka, P.A.; Rodeheffer, R.J.; Michels, V.V.; Olson, T.M. Mutations in ribonucleic acid binding protein gene cause familial dilated cardiomyopathy. *J. Am. Coll. Cardiol.* **2009**, *54*, 930–941. [[CrossRef](#)]
62. Maatz, H.; Jens, M.; Liss, M.; Schafer, S.; Heinig, M.; Kirchner, M.; Adami, E.; Rintisch, C.; Dauksaite, V.; Radke, M.H.; et al. RNA-binding protein RBM20 represses splicing to orchestrate cardiac pre-mRNA processing. *J. Clin. Investig.* **2014**, *124*, 3419–3430. [[CrossRef](#)]
63. Li, D.; Morales, A.; Gonzalez-Quintana, J.; Norton, N.; Siegfried, J.D.; Hofmeyer, M.; Hershberger, R.E. Identification of novel mutations in RBM20 in patients with dilated cardiomyopathy. *Clin. Transl. Sci.* **2010**, *3*, 90–97. [[CrossRef](#)] [[PubMed](#)]
64. Refaat, M.M.; Lubitz, S.A.; Makino, S.; Islam, Z.; Frangiskakis, J.M.; Mehdi, H.; Gutmann, R.; Zhang, M.L.; Bloom, H.L.; MacRae, C.A.; et al. Genetic variation in the alternative splicing regulator RBM20 is associated with dilated cardiomyopathy. *Heart Rhythm* **2012**, *9*, 390–396. [[CrossRef](#)] [[PubMed](#)]
65. Hey, T.M.; Rasmussen, T.B.; Madsen, T.; Aagaard, M.M.; Harbo, M.; Molgaard, H.; Moller, J.E.; Eiskjaer, H.; Mogensen, J. Pathogenic RBM20-Variants Are Associated With a Severe Disease Expression in Male Patients With Dilated Cardiomyopathy. *Circ. Heart Fail.* **2019**, *12*, e005700. [[CrossRef](#)] [[PubMed](#)]
66. Van den Hoogenhof, M.M.G.; Beqqali, A.; Amin, A.S.; van der Made, I.; Aufiero, S.; Khan, M.A.F.; Schumacher, C.A.; Jansweijer, J.A.; van Spaendonck-Zwarts, K.Y.; Remme, C.A.; et al. RBM20 Mutations Induce an Arrhythmogenic Dilated Cardiomyopathy Related to Disturbed Calcium Handling. *Circulation* **2018**, *138*, 1330–1342. [[CrossRef](#)]
67. Sedaghat-Hamedani, F.; Haas, J.; Zhu, F.; Geier, C.; Kayvanpour, E.; Liss, M.; Lai, A.; Frese, K.; Pribe-Wolferts, R.; Amr, A.; et al. Clinical genetics and outcome of left ventricular non-compaction cardiomyopathy. *Eur. Heart J.* **2017**, *38*, 3449–3460. [[CrossRef](#)]
68. Streckfuss-Bomeke, K.; Tiburcy, M.; Fomin, A.; Luo, X.; Li, W.; Fischer, C.; Ozcelik, C.; Perrot, A.; Sossalla, S.; Haas, J.; et al. Severe DCM phenotype of patient harboring RBM20 mutation S635A can be modeled by patient-specific induced pluripotent stem cell-derived cardiomyocytes. *J. Mol. Cell. Cardiol.* **2017**, *113*, 9–21. [[CrossRef](#)]
69. Zhu, C.; Yin, Z.; Ren, J.; McCormick, R.J.; Ford, S.P.; Guo, W. RBM20 is an essential factor for thyroid hormone-regulated titin isoform transition. *J. Mol. Cell. Biol.* **2015**, *7*, 88–90. [[CrossRef](#)]
70. Zhu, C.; Yin, Z.; Tan, B.; Guo, W. Insulin regulates titin pre-mRNA splicing through the PI3K-Akt-mTOR kinase axis in a RBM20-dependent manner. *Biochim. Biophys. Acta Mol. Basis Dis.* **2017**, *1863*, 2363–2371. [[CrossRef](#)]
71. Hinze, F.; Dieterich, C.; Radke, M.H.; Granzier, H.; Gotthardt, M. Reducing RBM20 activity improves diastolic dysfunction and cardiac atrophy. *J. Mol. Med. (Berl.)* **2016**, *94*, 1349–1358. [[CrossRef](#)]
72. Methawasin, M.; Strom, J.G.; Slater, R.E.; Fernandez, V.; Saripalli, C.; Granzier, H. Experimentally Increasing the Compliance of Titin Through RNA Binding Motif-20 (RBM20) Inhibition Improves Diastolic Function In a Mouse Model of Heart Failure With Preserved Ejection Fraction. *Circulation* **2016**, *134*, 1085–1099. [[CrossRef](#)]
73. Liss, M.; Radke, M.H.; Eckhard, J.; Neuenschwander, M.; Dauksaite, V.; von Kries, J.P.; Gotthardt, M. Drug discovery with an RBM20 dependent titin splice reporter identifies cardenolides as lead structures to improve cardiac filling. *PLoS ONE* **2018**, *13*, e0198492. [[CrossRef](#)] [[PubMed](#)]
74. Liu, J.; Kong, X.; Zhang, M.; Yang, X.; Xu, X. RNA binding protein 24 deletion disrupts global alternative splicing and causes dilated cardiomyopathy. *Protein. Cell* **2019**, *10*, 405–416. [[CrossRef](#)] [[PubMed](#)]
75. Zhou, Q.; Schotterl, S.; Backes, D.; Brunner, E.; Hahn, J.K.; Ionesi, E.; Aidery, P.; Sticht, C.; Labeit, S.; Kandolf, R.; et al. Inhibition of miR-208b improves cardiac function in titin-based dilated cardiomyopathy. *Int. J. Cardiol.* **2017**, *230*, 634–641. [[CrossRef](#)] [[PubMed](#)]
76. Hamdani, N.; Herwig, M.; Linke, W.A. Tampering with springs: Phosphorylation of titin affecting the mechanical function of cardiomyocytes. *Biophys. Rev.* **2017**, *9*, 225–237. [[CrossRef](#)]

77. Huttlin, E.L.; Jedrychowski, M.P.; Elias, J.E.; Goswami, T.; Rad, R.; Beausoleil, S.A.; Villen, J.; Haas, W.; Sowa, M.E.; Gygi, S.P. A tissue-specific atlas of mouse protein phosphorylation and expression. *Cell* **2010**, *143*, 1174–1189. [[CrossRef](#)]
78. Lundby, A.; Secher, A.; Lage, K.; Nordsborg, N.B.; Dmytriiev, A.; Lundby, C.; Olsen, J.V. Quantitative maps of protein phosphorylation sites across 14 different rat organs and tissues. *Nat. Commun.* **2012**, *3*, 876. [[CrossRef](#)]
79. Hornbeck, P.V.; Zhang, B.; Murray, B.; Kornhauser, J.M.; Latham, V.; Skrzypek, E. PhosphoSitePlus, 2014: Mutations, PTMs and recalibrations. *Nucleic Acids Res.* **2015**, *43*, D512–D520. [[CrossRef](#)]
80. Rain, S.; Bos Dda, S.; Handoko, M.L.; Westerhof, N.; Stienen, G.; Ottenheijm, C.; Goebel, M.; Dorfmuller, P.; Guignabert, C.; Humbert, M.; et al. Protein changes contributing to right ventricular cardiomyocyte diastolic dysfunction in pulmonary arterial hypertension. *J. Am. Heart Assoc.* **2014**, *3*, e000716. [[CrossRef](#)]
81. Kotter, S.; Gout, L.; Von Frieling-Salewsky, M.; Muller, A.E.; Helling, S.; Marcus, K.; Dos Remedios, C.; Linke, W.A.; Kruger, M. Differential changes in titin domain phosphorylation increase myofilament stiffness in failing human hearts. *Cardiovasc. Res.* **2013**, *99*, 648–656. [[CrossRef](#)]
82. Belin, R.J.; Sumandea, M.P.; Allen, E.J.; Schoenfelt, K.; Wang, H.; Solaro, R.J.; de Tombe, P.P. Augmented protein kinase C-alpha-induced myofilament protein phosphorylation contributes to myofilament dysfunction in experimental congestive heart failure. *Circ. Res.* **2007**, *101*, 195–204. [[CrossRef](#)]
83. Solaro, R.J. Multiplex kinase signaling modifies cardiac function at the level of sarcomeric proteins. *J. Biol. Chem.* **2008**, *283*, 26829–26833. [[CrossRef](#)] [[PubMed](#)]
84. Hidalgo, C.; Granzier, H. Tuning the molecular giant titin through phosphorylation: Role in health and disease. *Trends Cardiovasc. Med.* **2013**, *23*, 165–171. [[CrossRef](#)] [[PubMed](#)]
85. Krysiak, J.; Unger, A.; Beckendorf, L.; Hamdani, N.; von Frieling-Salewsky, M.; Redfield, M.M.; Dos Remedios, C.G.; Sheikh, F.; Gergs, U.; Boknik, P.; et al. Protein phosphatase 5 regulates titin phosphorylation and function at a sarcomere-associated mechanosensor complex in cardiomyocytes. *Nat. Commun.* **2018**, *9*, 262. [[CrossRef](#)] [[PubMed](#)]
86. Slater, R.E.; Strom, J.G.; Methawasin, M.; Liss, M.; Gotthardt, M.; Sweitzer, N.; Granzier, H.L. Metformin improves diastolic function in an HFpEF-like mouse model by increasing titin compliance. *J. Gen. Physiol.* **2019**, *151*, 42–52. [[CrossRef](#)] [[PubMed](#)]
87. Hopf, A.E.; Andresen, C.; Kotter, S.; Isic, M.; Ulrich, K.; Sahin, S.; Bongardt, S.; Roll, W.; Drove, F.; Scheerer, N.; et al. Diabetes-Induced Cardiomyocyte Passive Stiffening Is Caused by Impaired Insulin-Dependent Titin Modification and Can Be Modulated by Neuregulin-1. *Circ. Res.* **2018**, *123*, 342–355. [[CrossRef](#)]
88. Kruger, M.; Kotter, S.; Grutzner, A.; Lang, P.; Andresen, C.; Redfield, M.M.; Butt, E.; dos Remedios, C.G.; Linke, W.A. Protein kinase G modulates human myocardial passive stiffness by phosphorylation of the titin springs. *Circ. Res.* **2009**, *104*, 87–94. [[CrossRef](#)]
89. Bishu, K.; Hamdani, N.; Mohammed, S.F.; Kruger, M.; Ohtani, T.; Ogut, O.; Brozovich, F.V.; Burnett, J.C., Jr.; Linke, W.A.; Redfield, M.M. Sildenafil and B-type natriuretic peptide acutely phosphorylate titin and improve diastolic distensibility in vivo. *Circulation* **2011**, *124*, 2882–2891. [[CrossRef](#)]
90. Redfield, M.M.; Chen, H.H.; Borlaug, B.A.; Semigran, M.J.; Lee, K.L.; Lewis, G.; LeWinter, M.M.; Rouleau, J.L.; Bull, D.A.; Mann, D.L.; et al. Effect of phosphodiesterase-5 inhibition on exercise capacity and clinical status in heart failure with preserved ejection fraction: A randomized clinical trial. *JAMA* **2013**, *309*, 1268–1277. [[CrossRef](#)]
91. Armstrong, P.W.; Pieske, B.; Anstrom, K.J.; Ezekowitz, J.; Hernandez, A.F.; Butler, J.; Lam, C.S.P.; Ponikowski, P.; Voors, A.A.; Jia, G.; et al. Vericiguat in Patients with Heart Failure and Reduced Ejection Fraction. *N. Engl. J. Med.* **2020**, *382*, 1883–1893. [[CrossRef](#)]
92. Butler, J.; Lam, C.S.P.; Anstrom, K.J.; Ezekowitz, J.; Hernandez, A.F.; O'Connor, C.M.; Pieske, B.; Ponikowski, P.; Shah, S.J.; Solomon, S.D.; et al. Rationale and Design of the VITALITY-HFpEF Trial. *Circ. Heart Fail.* **2019**, *12*, e005998. [[CrossRef](#)]
93. Filippatos, G.; Maggioni, A.P.; Lam, C.S.P.; Pieske-Kraigher, E.; Butler, J.; Spertus, J.; Ponikowski, P.; Shah, S.J.; Solomon, S.D.; Scalise, A.V.; et al. Patient-reported outcomes in the SOLuble guanylate Cyclase stimulator in heArT failurE patientS with PRESERVED ejection fraction (SOCRATES-PRESERVED) study. *Eur. J. Heart Fail.* **2017**, *19*, 782–791. [[CrossRef](#)] [[PubMed](#)]



Review

Dysregulation of Calcium Handling in Duchenne Muscular Dystrophy-Associated Dilated Cardiomyopathy: Mechanisms and Experimental Therapeutic Strategies

Michelle L. Law¹, Houda Cohen², Ashley A. Martin², Addeli Bez Batti Angulski²
and Joseph M. Metzger^{2,*}

¹ Department of Family and Consumer Sciences, Robbins College of Health and Human Sciences, Baylor University, Waco, TX 76706, USA; Michelle_L_Law@baylor.edu

² Department of Integrative Biology and Physiology, University of Minnesota Medical School, Minneapolis, MN 55455, USA; cohen461@umn.edu (H.C.); aamartin@umn.edu (A.A.M.); abezbatt@umn.edu (A.B.B.A.)

* Correspondence: metzgerj@umn.edu; Tel.: +1-612-625-5902; Fax: +1-612-625-5149

Received: 29 January 2020; Accepted: 6 February 2020; Published: 14 February 2020

Abstract: Duchenne muscular dystrophy (DMD) is an X-linked recessive disease resulting in the loss of dystrophin, a key cytoskeletal protein in the dystrophin-glycoprotein complex. Dystrophin connects the extracellular matrix with the cytoskeleton and stabilizes the sarcolemma. Cardiomyopathy is prominent in adolescents and young adults with DMD, manifesting as dilated cardiomyopathy (DCM) in the later stages of disease. Sarcolemmal instability, leading to calcium mishandling and overload in the cardiac myocyte, is a key mechanistic contributor to muscle cell death, fibrosis, and diminished cardiac contractile function in DMD patients. Current therapies for DMD cardiomyopathy can slow disease progression, but they do not directly target aberrant calcium handling and calcium overload. Experimental therapeutic targets that address calcium mishandling and overload include membrane stabilization, inhibition of stretch-activated channels, ryanodine receptor stabilization, and augmentation of calcium cycling via modulation of the Serca2a/phospholamban (PLN) complex or cytosolic calcium buffering. This paper addresses what is known about the mechanistic basis of calcium mishandling in DCM, with a focus on DMD cardiomyopathy. Additionally, we discuss currently utilized therapies for DMD cardiomyopathy, and review experimental therapeutic strategies targeting the calcium handling defects in DCM and DMD cardiomyopathy.

Keywords: dilated cardiomyopathy; muscular dystrophy; calcium; heart; gene therapy; phospholamban; Serca2a; *mdx*; oxidative stress; membrane stabilization

1. Introduction

1.1. Dilated Cardiomyopathy: Prevalence, Causes, and Clinical Manifestations

Cardiovascular diseases (CVD) contribute to approximately 30% of global morbidity and mortality, representing a major public health concern [1]. Among the several types of CVD, dilated cardiomyopathies (DCM) are an important cause of congestive heart failure and cardiac disease requiring heart transplantation [2]. DCM is a disease of the heart muscle characterized by increased ventricle chamber volume and impaired systolic function involving the left or both ventricles. DCM can develop at any age, is a common form of cardiomyopathy in the pediatric population, and can lead to sudden cardiac death in adolescents and young adults [2,3]. Although the etiology of DCM remains unknown in 66% of cases, myocarditis and neuromuscular diseases are the most commonly

recognized causes of DCM. In 20–48% of cases, the disease is inherited and is referred to as familial dilated cardiomyopathy [2,3].

DCM is commonly underdiagnosed because most individuals are asymptomatic in the early stages of the disease. Typically, DCM is diagnosed during screening for cardiac dysfunction in individuals considered at risk, such as in family members of DCM patients. Early symptoms are nonspecific and include easy fatigability, decreased appetite, effort-induced shortness of breath, intermittent chest pain, fainting, syncope, and/or palpitations [3]. Undiagnosed, patients will later present with symptoms of end organ dysfunction due to systolic defects and peripheral hypoperfusion [3]. Physical examination can reveal sinusoidal tachycardia, gallop rhythm, a heart murmur, jugular-venous distention, pallor, cool hands and feet, and hepatomegaly at more advanced stages. Patients with severe DCM demonstrate symptoms and complications of congestive heart failure, such as dyspnea with exertion or at rest, chest pain, abdominal pain, and peripheral edema. Arrhythmias, thromboembolism, and sudden death are also common in DCM and may occur at any stage [3,4].

1.2. Dilated Cardiomyopathy in Muscular Dystrophy: Prevalence, Clinical Manifestations

Duchenne muscular dystrophy (DMD) is the most common and a severe form of muscular dystrophy. It affects approximately 1 in 5000 males [5]. DMD is an X-linked myopathy caused by a mutation in the dystrophin gene resulting in a complete loss of dystrophin protein in striated muscles. Absence of dystrophin leads to disruption of the dystrophin-associated glycoprotein complex (DGC), which connects the cytoskeleton to the extracellular matrix and contributes to force transmission. Dystrophin is essential for stabilization of the sarcolemma. In DMD, loss of dystrophin leads to a fragile sarcolemma susceptible to stress-induced damage, resulting in myocyte death and progressive muscle wasting [6]. Early signs of muscle weakness in children affected with DMD generally occur between the ages of three and five. Muscle weakness initially involves the proximal muscles (Gowers' sign), followed by distal skeletal muscle groups (limbs and trunk). DMD is progressive, and in the absence of appropriate treatment and care, affected individuals typically lose ambulation by age 10–12 [7].

Until more recently, early loss of mobility and respiratory complications in DMD patients obscured symptoms of cardiac involvement. Over the past two decades, clinical advancements in respiratory assistance [8,9], implementation of anti-inflammatory drugs, and emerging muscle-targeted therapies led to improvement of activity levels, extended ambulation, and increased longevity in the DMD population. This, in turn, revealed cardiomyopathy as a major cause of morbidity and mortality in DMD patients [10–12]. It is estimated that 25% of boys have cardiomyopathy at 6 years of age and 59% by 10 years of age [13]. Cardiac involvement becomes highly prominent as DMD boys advance in age, with more than 90% of young men over 18 years of age having evidence of significant cardiac dysfunction [13].

The development of dilated cardiomyopathy in DMD is a consequence of multiple mechanisms, and a complete understanding of the pathophysiology has not been elucidated. The elevation of plasma creatine kinase (CK) is a hallmark of DMD, indicating that there is increased permeability of the plasma membrane, allowing soluble enzymes to leak out of the muscle cell [14–16]. The absence of dystrophin disrupts force transmission and causes contraction-induced sarcolemma damage and membrane permeability that allows an influx of calcium, triggering death of the myocyte [14–16]. The mechanisms that lead to increased permeability of the plasma membrane are not fully understood; however, it is widely acknowledged that increased calcium influx and calcium overload contribute to the molecular progression of the disease [17–20]. In the earlier stages of disease, compensatory mechanisms have been noted. In particular, an increase in calcium transient amplitude, increased sarcoplasmic reticulum calcium load and leak, and a reduced cardiac reserve are reported in animal models [21,22]. In the later decompensated stage, DMD cardiomyopathy presents as DCM, characterized by enlarged ventricles, reduced systolic function, decreased calcium transients, reduced cardiac wall thickness, and cardiac arrhythmias [3,23].

1.3. Objective of This Review

Understanding in greater detail the underlying mechanisms of DCM pathogenesis in DMD is critical to the development of targeted therapies for this disease. Current advancements in the treatment of skeletal muscle pathology may not benefit dystrophic cardiac muscle in the same way due to key differences in the function and calcium handling of these two striated muscle lineages [24]. Further, treatment of skeletal muscle without regard to the heart may exacerbate cardiac dysfunction [25], as can be seen in patients with X-linked dilated cardiomyopathy. These patients exhibit normal dystrophin expression in skeletal muscle and the absence of dystrophin in the heart [26,27]. Indeed, improved treatment options focused on ameliorating the skeletal muscle pathology of DMD have uncovered a previously underappreciated cardiac involvement, with an estimated 20–30% of deaths now resulting from cardiac failure in this population [28]. The purpose of this paper is to (1) discuss the role of calcium mishandling in DCM development and progression with a focus on DMD cardiomyopathy, (2) detail currently utilized therapies for DMD cardiomyopathy, and (3) evaluate experimental therapeutic strategies for correcting calcium mishandling and calcium overload in DCM and DMD cardiomyopathy.

2. Molecular Mechanisms of Dilated Cardiomyopathy

2.1. Genetic and Acquired Causes of DCM

There are a multitude of genetic and acquired causes of DCM, making the pathology of the disease highly diverse and clinically vexing [23]. Many known genetic and novel mutations leading to DCM are contained within the sarcomere or cytoskeleton. Therefore, these structures will be the main focus here. A schematic outlining common causes of DCM is shown in Figure 1.

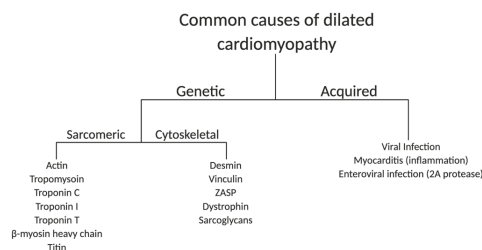


Figure 1. Common genetic and acquired causes of dilated cardiomyopathy in humans. ZASP: z-band alternatively spliced PDZ-motif.

2.1.1. Sarcomere

The cardiac sarcomere consists of a repeating pattern of contractile and regulatory proteins organized into thick and thin myofilaments [29]. The sarcomere is the basic contractile unit of cardiac muscle. Therefore, mutations impacting sarcomeric protein function can have a severe effect on heart performance. Approximately 5–10% of DCM diagnoses are due to mutations in sarcomeric proteins [30]. Thin filament proteins, including actin, tropomyosin (Tm), and the three protein subunits that make up the troponin complex, are common targets of DCM-causing mutations [31]. Mutations in the troponin complex typically cause a reduction in myofilament calcium sensitivity and force production [32]. There is evidence however, that in end stage heart failure, there is an increase in myofilament calcium sensitivity [33,34]. This increase is thought to be due to changes in phosphorylation levels of myofilament proteins such as troponin I (TnI), possibly through protein kinase A (PKA) [35–37]. Another site of DCM mutations is within thick filament proteins, including the MYH7 gene (variant pAsn1918Lys), which encodes β-myosin heavy chain, the primary mechano-motor protein of the adult human heart [38]. These mutations are thought to disrupt the ability of myosin to interact with actin, leading to a contractility defect [30]. Finally, a sarcomeric protein that has recently

been identified as a target of DCM mutations is the giant protein titin [39]. Titin is a multifaceted protein that plays a key role in sarcomere assembly and helps maintain passive tension in muscles [40]. Mutations leading to the truncation of the titin protein account for 1–3% of DCM diagnoses, with disease characterized by significant diastolic dysfunction, highlighting the complex role of titin in regulating contraction of the sarcomere [23].

2.1.2. Cytoskeleton

Mutations in genes encoding cytoskeletal proteins in cardiac muscle are also highly associated with DCM. The loss of dystrophin results in DCM [41], including X-linked DCM where heart dysfunction and failure can be highly pronounced [27]. Mutations in proteins that interact with dystrophin, such as the sarcoglycans, can also represent causal genetic loci for DCM [42]. Although these proteins are found in both skeletal and cardiac muscle, mutations in some of these proteins can cause heart disease without significant skeletal muscle deficits [43]. Other commonly targeted proteins include desmin, vinculin, and z-band alternatively spliced PDZ-motif (ZASP) [44,45]. These proteins are integral for maintaining the connection between muscle fibers, the sarcolemma, and the extracellular matrix. Mutations in cytoskeletal proteins generally inhibit myocyte force transmission and increase muscle membrane instability and permeability. The compromised sarcolemma leaves the muscle cell susceptible to increases in intracellular calcium, which can result in calcium overload and myocyte death [41,46].

2.1.3. Acquired Causes of DCM

DCM can also be acquired through mechanisms unrelated to genetic factors. Causes of DCM outside of familial inheritance include infection or ischemia, which can lead to myocarditis [47]. Viral infection can cause both damaging immune and inflammatory responses and direct viral toxicity, resulting in cardiac myocyte necrosis, fibrotic development, and ventricular dilation [48]. Enterovirus infection can also cause cardiomyopathy, and in its most severe form, sudden death. The mechanism of disease is thought to be through the virus-encoded 2A protease, which cleaves the dystrophin protein. The resulting dystrophin fragment increases risk for fibrosis and ischemic injury *in vivo* [49]. Reductions in myocardial perfusion, a known deficit caused by ischemic heart disease, is also observed in DCM patients [50]. Defects in myocardial blood flow can lead to chronic ischemic events and thus contribute to the progression of DCM [51].

2.2. The Role of Calcium Cycling in DCM Pathogenesis

2.2.1. Calcium Cycling in Healthy Cardiac Myocytes

During contraction in healthy cardiac myocytes, electrical stimulation of the muscle leads to an increase in intracellular calcium, first as a small amount which enters through L-type voltage-gated calcium channels (dihydropyridine receptors (DHPR)) in the sarcolemma. The initial calcium influx then triggers a larger calcium release from the sarcoplasmic reticulum (SR) through ryanodine receptor 2 (RyR2), located in the SR membrane. Together, this process is referred to as calcium-induced calcium release (CICR) [52]. Calcium rises in the cytoplasm and binds to troponin C (TnC), causing the protein to undergo a conformational change, which is facilitated by the binding of troponin I (TnI). As TnI switches binding from actin to TnC, tropomyosin (Tm) is then free to move, exposing myosin-binding sites on the actin filaments [29]. Troponin T (TnT)-Tm binding allows for the cooperative transmission of these conformational changes along the length of the thin filament in a complex series of protein-protein interactions, and cross-bridge binding of myosin to actin stabilizes Tm positioning [29]. Through these interactions the myofilament becomes activated and force can be generated [52] (Figure 2).

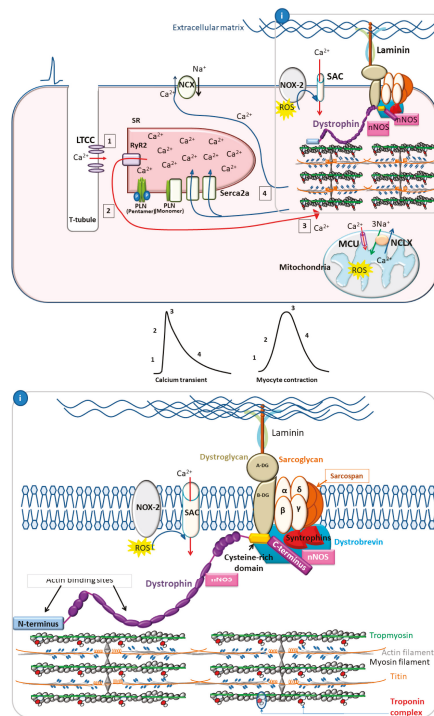


Figure 2. Normal excitation-contraction coupling in cardiac myocytes. Membrane depolarization leads to a small influx of calcium through the L-type calcium channel (LTCC/DHPR) (1), which triggers a larger release of calcium from the sarcoplasmic reticulum (SR) through ryanodine receptor 2 (RyR2) (2). Calcium then binds to the myofilaments, triggering myocyte contraction (3). During the relaxation phase, calcium reuptake occurs by pumping calcium out of the cytoplasm back into the SR via Serca2a or through the $\text{Na}^+/\text{Ca}^{2+}$ exchanger (NCX) (4). Phospholamban negatively regulates Serca2a activity. β -adrenergic signaling leads to phospholamban (PLN) phosphorylation and dissociation from Serca2a, increasing the rate of calcium reuptake into the SR. Normal physiological stretch leads to NADPH oxidase 2 (NOX-2) production of reactive oxygen species (ROS), which increases calcium entry through stretch-activated channels (SACs). Dystrophin serves to stabilize the sarcolemma during the repeated stress of myocyte contraction and relaxation. Inset shows increased detail of the dystrophin glycoprotein complex (DGC) and myofilament proteins. NOS: nitric oxide synthase; MCU: mitochondrial calcium uniporter; NCLX: mitochondrial sodium calcium exchanger.

During relaxation, SR-associated proteins, notably sarco(endo)plasmic reticulum Ca^{2+} -ATPase (SERCA2a) and phospholamban (PLN), are essential to the removal of calcium from the cytoplasm back into the SR [53]. The Serca2a/PLN complex is the major regulator of calcium cycling in cardiac muscle [54]. Serca2a is an ATP-dependent calcium pump localized within the longitudinal membrane of the sarcoplasmic reticulum [55]. Serca2a has a key role in regulating both the rate of calcium reuptake and subsequent myocyte relaxation in diastole, as well as SR calcium load, which affects calcium transient peak height and contractility in systole [54,56]. PLN is a negative regulator of Serca2a function [54]. The monomeric, dephosphorylated form of PLN interacts with Serca2a and decreases its affinity for calcium, thus decreasing SR calcium reuptake velocity. Phosphorylation of PLN at Ser 16 or Thr 17 inhibits its interaction with Serca2a and increases oligomerization of PLN into its pentameric form, thereby relieving Serca2a inhibition [54,56]. The resulting increase in Serca2a function increases

the rate of calcium reuptake in diastole and also increases SR calcium load, resulting in increased contraction amplitude and hastened relaxation (Figure 2).

The phosphorylation status of PLN is what determines its ability to alter Serca2a function. PLN phosphorylation is regulated in large part through β -adrenergic signaling. Stimulation of the sympathetic nervous system leads to increased activation and signaling through β -adrenergic receptors. The subsequent Protein Kinase A (PKA) activation leads to phosphorylation of PLN at Ser 16, relieving its inhibition on Serca2a and increasing SR calcium reuptake [54,56]. Phosphorylation at Thr 17 also relieves inhibition on Serca2a and is accomplished via Ca^{2+} /CaM Kinase in response to physiological stressors including ischemic injury, pacing stress or increased calcium concentration [54,56]. Multiple accessory proteins, including HS-1 associated protein X-1 (HAX-1), Protein-Phosphatase 1 (PP1), endogenous inhibitors of PP1 (I-1 and I-2), Heat Shock Protein 20 (HSP20), and S100A1 proteins, are also associated with the Serca2a/PLN complex and serve to modulate PLN inhibition of Serca2a under various physiological conditions [54].

2.2.2. Calcium Cycling Defects in DCM

DCM-causing mutations affect multiple aspects of calcium handling within the myocyte, from altering calcium sensitivity of the myofilament seen with sarcomeric mutations, to mislocalization and altered expression or function of calcium handling proteins seen with cytoskeletal mutations. In DCM, there is a decrease in peak height of the calcium transient in systole and a decreased rate of calcium reuptake in diastole [57]. Increased calcium leak from RyR2 can be a contributing factor, particularly in DMD cardiomyopathy [58]. The resulting decrease in SR calcium load decreases contractile function in systole [59]. Decreased calcium cycling and decreased SR calcium load can also occur via a decrease in the expression and/or activity of Serca2a [59–61]. PLN expression is not decreased to the same extent in DCM, thus increasing the ratio of PLN to Serca2a [60,61], which results in increased PLN inhibition of Serca2a. Additionally, β -adrenergic desensitization results in reduced PLN phosphorylation, which further increases its inhibition of Serca2a [54,60] (Figure 3).

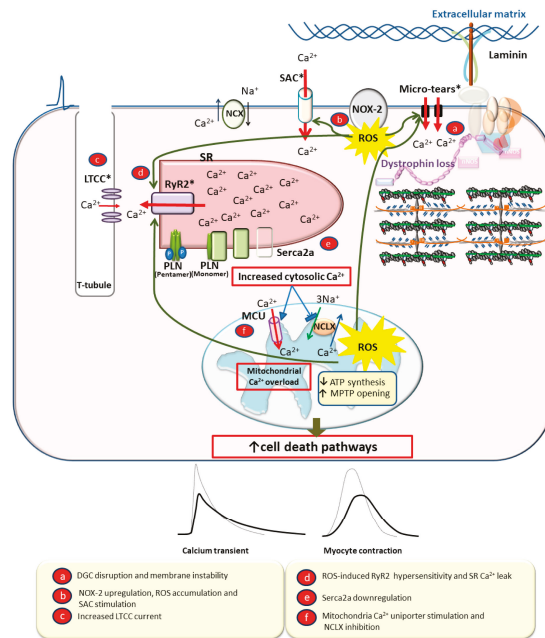


Figure 3. Mechanisms of calcium overload in dystrophin-deficient cardiac myocytes. The absence of dystrophin destabilizes the sarcolemma and leads to stress-induced membrane damage/micro-tears and calcium influx (a). Excessive reactive oxygen species (ROS) production in cardiac myocytes leads to further membrane damage and increased calcium influx via stretch-activated channels (SACs) and ryanodine receptor 2 (RyR2) (b). Increased L-type calcium channel (LTCC/DHPR) current also contributes to increased intracellular calcium (c). Calcium leak from RyR2 (d), decreased Serca2a expression (e) and increased phospholamban (PLN) inhibition of Serca2a decrease sarcoplasmic reticulum (SR) calcium load, subsequently decreasing calcium transient peak height and decay rate and inhibiting contractile function in later stages of Duchenne muscular dystrophy (DMD) cardiomyopathy (dark lines in transients). Increased cytosolic calcium leads to mitochondrial cell death pathways (f). * Indicates points of abnormal calcium entry into the myocyte. NCX: Sodium calcium exchanger; NOX-2: NADPH oxidase 2; NOS: Nitric oxide synthase; MCU: Mitochondrial calcium uniporter; NCLX: Mitochondrial sodium calcium exchanger.

3. Molecular Mechanisms of DMD Cardiomyopathy

The lack of dystrophin in cardiac myocytes leads to instability of the sarcolemma, resulting in calcium overload and oxidative stress. Over time, excess calcium and reactive oxygen species (ROS) activate cell death pathways, fibrosis, and dilation [12]. How dystrophin functions to stabilize the cell membrane is not fully understood, but two prevailing ideas are supported by the literature. First, dystrophin, as part of the DGC, connects the extracellular matrix and the intracellular cytoskeleton and acts as a “shock absorber” for the sarcolemma during the repeated stress of contraction and relaxation [62–64]. Sarcolemmal stress in the absence of dystrophin leads to muscle membrane damage or micro-tears, causing extracellular calcium influx and calcium overload [20,62,63] (Figure 3). Secondly, dystrophin acts as a scaffolding protein to localize and normalize function of proteins involved in intracellular calcium and redox homeostasis. Lack of dystrophin can cause mislocalization and abnormal expression/activity of these proteins, leading to calcium mishandling and oxidative stress [65]. Oxidative stress damages the sarcolemma and increases intracellular calcium entry through stretch-activated channels (SACs) in the sarcolemma [20] and RyR2 in the SR [65,66]. (Figure 3).

3.1. Dystrophin as a Membrane Stabilizer

When dystrophin is absent, as in DMD, the sarcolemma of cardiac myocytes is less compliant, which is revealed during passive length distension [41]. This leads to increased sarcolemma damage evidenced by lactate dehydrogenase (LDH) release under normal preload and afterload conditions in isolated working hearts [67]. This damage is even more pronounced under stress with isoproterenol or partial aortic constriction [67]. Damage is thought to occur via small membrane disruptions (micro-tears) that can lead to transient extracellular calcium influx [62] (Figure 3). Extracellular calcium influx raises intracellular calcium concentration, subsequently activating calcium release from the SR and increasing calcium concentration even further. Calcium overload ultimately results in myocyte hypercontracture and cell death [41,68].

Evidence for membrane destabilization as a primary cause of calcium overload and cell death in DMD comes from studies employing membrane stabilizers in the context of dystrophin deficiency. Membrane stabilizers, most notably the tri-block copolymer P188, have shown efficacy in reducing stress-induced calcium overload, hypercontracture, and cell death in animal models of DMD [41,68]. Membrane stabilizer studies provide evidence that dystrophin confers protection against stress-induced mechanical damage to the sarcolemma, and stabilizing damaged portions of membranes can prevent calcium overload and myocyte death.

3.2. Dystrophin as a Scaffold Protein

In addition to its function as a membrane stabilizer, accumulating evidence suggests a role for dystrophin in regulating ROS production and calcium handling within the myocyte. Dystrophin serves as a scaffold, helping to localize multiple proteins involved in calcium and oxidative homeostasis within the cell [65]. This allows for spatiotemporal control of ROS production and downstream signaling [66]. ROS products are important signaling molecules within the myocyte that regulate calcium cycling during physiological changes in cardiac load [69] (Figure 2). Abnormal or excessive ROS signaling in the absence of dystrophin [70] may contribute to cardiac pathology through aberrant calcium handling [70] (Figure 3).

Increased ROS production in DMD contributes to calcium overload from intracellular sources, namely the SR [66]. Indeed, ROS was found to underlie the hypersensitivity of RyR2 to increasing intracellular calcium concentrations in *mdx* cardiac myocytes, a mouse model of DMD [71]. Physiological stretch of isolated cardiac myocytes was found to induce a localized, rapid and transient increase in RyR2 calcium spark production, and this effect was amplified in *mdx* cardiac myocytes, leading to calcium waves [72]. Antioxidant treatment, microtubule depolymerization, and inhibition of reduced nicotinamide adenine dinucleotide phosphate (NADPH) oxidase 2 (NOX2) all abrogated this effect. It was concluded from this study that myocyte stretch caused microtubule activation of NOX-2, which increased NOX-2 ROS production, sensitized RyR2 and subsequently increased calcium spark frequency [72]. This is a physiologically important mechanism to increase calcium release during increased cardiac load. However, in the context of the dystrophin-deficient myocyte, this effect is amplified [72] and may be a contributing factor to increased diastolic calcium concentration [18] (Figure 3). *Mdx* mice have increased expression and density of microtubules [73], increased expression and activity of NOX-2 [72], and a compromised endogenous reducing system [66], all of which may lead to enhanced production of ROS and increased RyR2 calcium leak. Taken together, these studies reveal an important role for dystrophin in proper function and activity of proteins involved in both ROS and calcium handling within the myocyte.

3.3. Calcium Overload Leading to Myocyte Death, Fibrosis, and Dilatation

Increased intracellular calcium in the context of dystrophin deficiency is a key mediator in myocyte death and fibrotic development [12]. As discussed above, excess calcium originates from both intracellular stores through hypersensitivity of RyR2 and from extracellular influx via sarcolemmal

micro-tears and increased SAC activity [20]. Additionally, there is evidence for increased L-type calcium channel (LTCC) activity, which increases calcium cycling to compensate for myocyte loss and decreased β -adrenergic activity in young *mdx* mice [22]. This is an additional avenue for intracellular calcium overload and a potential cause of arrhythmias in DMD [74]. Increased calcium concentration in the cytosol leads to activation of calcium-dependent proteases and protein degradation [12,75] (Figure 3).

Increased intracellular calcium also causes an increase in mitochondrial uptake of calcium. Increased mitochondrial calcium concentration occurs via the mitochondrial uniporter (MCU) as a consequence of RyR2 calcium leak [76] or increased LTCC calcium current [77]. Additionally, high cytosolic calcium can inhibit mitochondrial calcium extrusion via the mitochondrial sodium-calcium exchanger (NCLX) [78]. Increased mitochondrial calcium leads to enhanced mitochondrial ROS production, depolarization of the mitochondrial membrane, opening of the mitochondrial permeability transition pore (MPTP) [79,80] and decreased ATP production. Additionally, it was found that impaired communication between the LTCC and mitochondria in the absence of dystrophin decreases mitochondrial membrane potential and energy production [81]. The end result of these processes is cell death via necrosis and apoptosis [12,75,79,80] (Figure 3). Mitochondrial-mediated cell death was found to be an important contributor to disease progression and fibrosis development in multiple animal models of muscular dystrophy [82]. Deletion or chemical inhibition of cyclophilin-D, an enzyme that regulates mitochondrial-mediated necrosis resulting from excess calcium [83], improved the dystrophic phenotype and decreased the replacement of healthy myocytes with fibrotic tissue [82].

Myocyte death, as a result of calcium overload, leads to the release of intracellular components and enzymes that initiate an inflammatory response. Clinically, DMD myocardium displays alternating areas of myocyte hypertrophy, atrophy/necrosis and fibrosis with replacement of heart muscle by connective tissue and fat [84–86]. DCM progression in DMD is characterized by a distinctive pattern of fibrosis, initially affecting the posterobasal myocardium of the left ventricular free wall, progressing to the ventricular septum, and extending transmurally to affect the outer half of the ventricular wall [87]. There is likely a long subclinical phase of progressive fibrosis that starts early in the course of the disease [88–90]. The development of progressive fibrosis will eventually lead to overt cardiac disease, dilation, and decreased pump function.

4. Model Systems to Study DCM and DMD Cardiomyopathy

To clarify the mechanisms responsible for the physiologic features of DCM and DMD cardiomyopathy, and to establish novel, preventative, and innovative therapies, several experimental animal and cell models of DCM and DMD cardiomyopathy have been developed and investigated. Most models recapitulate several clinical features of DCM in humans, typically exhibiting dilation of the left or both ventricles, severe impairment of systolic and diastolic left ventricle function, and thinning of the left ventricle wall [91]. This section will highlight both animal and cell models that have been developed to study DCM as an independent disease and models that study it as a pathology of DMD. An overview of this section is summarized in Table 1.

Table 1. Summary of model systems to study dilated cardiomyopathy (DCM) and Duchenne muscular dystrophy (DMD)-cardiomyopathy.

Model System	Strategy	Cardiac Phenotype
Rodent		
Muscle LIM protein (MLP) null mice [92]	Deletion of MLP (actin-associated cytoskeletal protein)	Anatomical and physiological hallmarks of human DCM
Desmin-deficient mice [91,93]	Desmin knockout mice	Severe loss of overall myocardial architecture by degeneration and calcification

Table 1. Cont.

Model System	Strategy	Cardiac Phenotype
Surgical interruptions of coronary arteries [94,95]	Produce myocardial infarction through permanent coronary ligation or re-perfused infarction	DCM phenotype progressively develops post-infarction
Doxorubicin or isoproterenol [96–99]	Toxic drug-mediated cardiomyopathy	Dose-dependent dilated phenotype and overt heart failure over time owing to severe myocardial injury and cell death
<i>mdx</i> mice [100,101]	Nonsense point mutation in exon 23 preventing dystrophin expression	Moderate DCM and functional cardiac impairment, progressive with age
Utrophin knockout <i>mdx</i> mice [102,103]	Crossing <i>mdx</i> mice to the utrophin-null background	Severe cardiomyopathy. Displays physiological indicators of end-stage heart failure
Large animals		
Dogs, pigs and sheep [104–108]	Myocardial infarction, coronary micro-embolization, pacing-induced tachycardia, and toxic injury	DCM phenotype progressively develops post-infarction
Golden retriever muscular dystrophy (GRMD) animal model of DMD [68,109,110]	Spontaneous splice site mutation in the <i>DMD</i> gene. Single nucleotide change that leads to exon skipping and an out-of-frame <i>DMD</i> transcript.	Prominent cardiac lesions present as early as 6 months of age, with ECG abnormalities present at 1 year and profound myocardial contractile abnormalities by 20 months
Human iPSCs		
iPSCs-CMs [111]	iPSCs-CMs derived from a member of a family with DCM carrying a heterozygous mutation in cardiac troponin T	iPSC-derived cardiomyocytes from DCM patients recapitulated to some extent the morphological and functional phenotypes of familial DCM with inherited mutation in troponin T
iPSCs-CMs [112]	Patient-specific DCM iPSC generated from a single member of a family with an autosomal dominant nonsense mutation (p.R225X) in exon 4 of the lamin A/C (LMNA) gene	iPSC-CMs showed morphologic changes, including a higher prevalence of nuclear bleb formation, micronucleation, as well as nuclear senescence and cellular apoptosis
iPSC-CMs [113]	iPSC-CMs derived from a patient with dilated cardiomyopathy with a novel heterozygous mutation of p.A285V codon conversion on exon 4 of the desmin gene	iPSC-CMs provided histologic and functional confirmation that the candidate gene variant detected by whole exome sequencing was responsible for the disease
iPSCs-CMs [114]	iPSC-CMs from DMD patients and healthy control	<i>In vitro</i> model that manifests the major phenotypes of DCM in DMD patients

MLP: muscle LIM-protein; ECG: electrocardiogram; iPSCs-CMs: human induced pluripotent stem cells-derived cardiac myocytes.

4.1. Rodents

Rodent models are commonly used in cardiovascular research as they are easier to handle and house (leading to manageable costs), and have a relatively short life span, allowing the researcher to follow the natural history of the disease. Additionally, of great impact is the capacity to leverage mouse genetic manipulation for both gain/loss of function of specific genes. This includes capacity for temporal control of tissue-specific genetic constructs [115].

To evaluate the development, progression, and potential for regression of DCM, multiple genetically engineered rodent models have been developed. These models include constitutive and inducible transgenic overexpression and/or gene knockout that exhibit a DCM phenotype [116,117]. One of the first DCM mouse models to be described was the muscle *Lin11*, *Isi1* & *Mec-3* (LIM) protein (MLP)-null mouse. Deletion of MLP, an actin-associated cytoskeletal protein, leads to cardiac myocyte architectural disorganization through irregularities in the actin-based cytoskeletal structure. Mice deficient for MLP show many of the anatomical and physiological hallmarks of human DCM [92]. Desmin-deficient models are also commonly used, which exhibit severe loss of myocardial architecture

by degeneration and calcification [93]. Additionally, models with mutations in mitochondria can develop DCM with atrioventricular block due to deficient oxidative phosphorylation [91].

Several non-genetic methods, including drug and surgical techniques, are also used to induce the development of DCM in rodents. Surgical techniques include interruption of coronary arteries to produce myocardial infarction through permanent coronary ligation [94] or re-perfused infarction [95]. After an infarction, the DCM phenotype progressively develops in mice. Chronic doxorubicin [96,97] or isoproterenol [98,99] administration can lead to a dose-dependent dilated phenotype and overt heart failure over time owing to severe myocardial injury and cell death. Toxic drug-mediated cardiomyopathy is characterized by myocyte apoptosis and oxidative stress being highly specific forms of injury, which may also be useful in assessing cardiac responses to stress. It should be noted, however, that although these non-genetic models recapitulate many aspects of a DCM phenotype, DMD-associated DCM has noted differences in pathophysiology compared to these models.

Mdx mice that lack dystrophin are the most commonly used mouse model to study DMD. However, compared to patients with DMD, they exhibit a relatively minor cardiac phenotype [100,101]. Under baseline conditions, *mdx* mice do not demonstrate physiological indicators of heart failure early in life. However, disease can be readily unmasked by cardiac stressors. In efforts to make the baseline *mdx* cardiac phenotype more similar to that of patients, *mdx* mice have been crossed with utrophin knockout (KO) mice, which exhibit a more severe cardiomyopathy [102,103] and display the physiological indicators of end-stage heart failure, including a negative force-frequency relationship and a reduction in force development and impairment of relaxation [101]. Other symptomatic double knock-out strains have been generated by mutating genes involved in: (1) the DGC complex, including δ - sarcoglycan and dystrobrevin [118,119]; (2) muscle repair, such as dysferlin [120,121]; and (3) cytoskeleton-ECM interactions, including desmin and laminin [122,123]. A thorough characterization of the cardiomyopathy in these models will increase the usefulness of these animal models for research into treatments and diagnostics for DMD cardiomyopathy.

4.2. Large Mammals

Although rodent animal models are commonly used in cardiovascular research and may display some of the characteristics of human cardiac disease, they typically do not recapitulate all aspects of DCM found in humans [124,125]. Preclinical validation of therapeutic approaches can be advanced in large animal models due to their proximity to human cardiac physiology and structure [126]. Canines, swine, sheep, and non-human primates have been the most frequently used large animal models for cardiovascular research [104]. Taking into account the similarities in coronary anatomy, organ size, immunology, and physiology compared to humans, swine are considered the most attractive model for pre-clinical studies [105]. DCM can be induced in large animals by myocardial infarction, coronary micro-embolization, pacing-induced tachycardia, and toxic injury. Infarction models, including both re-perfused and non-re-perfused approaches in dogs [106], pigs [107], and sheep [108], are used to evaluate the pathophysiological mechanisms of post-infarction remodeling as well as DCM development, progression, and therapeutic response.

The availability of large animal models of DMD has been instrumental in gaining insights into the cardiomyopathy and progression to heart failure associated with DMD. The golden retriever muscular dystrophy (GRMD) canine model of DMD has been indispensable, not only for the development of therapeutic approaches, but also for the study of the pathobiology of dystrophin deficiency in the heart [68,109,110]. Muscular dystrophy in GRMD animals closely recapitulates the timing and severity of disease progression observed in DMD patients. In addition to the severe skeletal muscle pathology, GRMD animals have prominent cardiac lesions present as early as 6 months of age [127], with ECG abnormalities present at 1 year [128] and profound myocardial contractile abnormalities by 20 months [129].

4.3. Human iPSCs

The contribution of animal models to our overall understanding of DCM has been indispensable. However, many important differences exist between animal models and humans. Additionally, cardiac tissues from DCM patients are difficult to obtain and exhibit a low survival rate in long-term culture. The emergence of induced pluripotent stem cells (iPSCs) [130], and the rapidly advancing technology associated with them have made it possible to obtain functional cardiac myocytes through the differentiation of human iPSCs derived from DCM patients [113,114]. Stem cell-derived cardiac myocytes from cells isolated directly from patients with cardiomyopathies recapitulate certain aspects of human cardiovascular disease and represent a powerful new model system to study the basic mechanisms of inherited cardiomyopathies. Thus, human induced pluripotent stem cell-derived cardiac myocytes (hiPSC-CMs) are an important complement to experimental animal models to study the cellular, molecular, and physiological mechanisms associated with the pathogenesis of DCM, as well as to establish high-throughput platforms for drug screening in human cells.

DCM was first modeled by Sun and coworkers using iPSCs-CMs derived from a member of a family with DCM carrying a heterozygous R173W mutation in cardiac troponin T (TNNT2) [111]. iPSC-derived cardiac myocytes from this patient recapitulated some of the morphological and functional phenotypes of familial DCM with inherited mutations in troponin T. This study describes the first successful modeling of dilated cardiomyopathy in hiPSC-CMs. Another patient-specific DCM iPSC line was generated from a single member of a family with an autosomal dominant nonsense mutation (p.R225X) in exon 4 of the lamin A/C (LMNA) gene. hiPSC-CMs from this patient showed morphologic changes, including a higher prevalence of nuclear bleb formation, micronucleation, as well as nuclear senescence and cellular apoptosis [112]. Additionally, Tse and colleagues generated hiPSC-CMs derived from a DCM patient with a novel heterozygous mutation of p.A285V codon conversion on exon 4 of the desmin (DES) gene [113]. In this study, hiPSC-CMs were able to provide histologic and functional confirmation that the candidate gene variant detected by whole exome sequencing was responsible for the disease.

To study the molecular mechanisms underlying DCM in DMD, Lin and co-workers generated cardiac myocytes (CMs) from DMD patients and healthy control induced pluripotent stem cells (iPSCs). Using DMD patient-derived iPSC-CMs, they have established an *in vitro* model that manifests the major phenotypes of DCM in DMD patients, and uncovered a potential new disease mechanism [114]. In this regard, Lin and co-workers examined a collection of muscular dystrophies (including DMD and Becker Muscular Dystrophy) and healthy hiPSC-derived cardiac myocytes. This included demonstration that loading of the treated DMD hiPSC-derived cardiac myocytes with the calcium sensitive dye, Rhod-2AM, revealed increased cytosolic calcium concentration. The use of calcium assays in hiPSC derived cardiac myocytes is becoming commonplace due to the ease and availability of high speed/resolution optical imaging techniques. Typically, this uses voltage-sensitive dyes or genetically-encoded voltage indicators to measure action potentials and calcium wave propagation. Indeed, Guan and coworkers showed a two-fold increase in T50 (duration of recovery) of calcium transients in hiPSC-derived cardiac myocytes from DMD patients compared to healthy hiPSC derived cardiac myocytes [131]. In addition, Tsurumi et al. reported that the measurement of the fluorescent ratio (410/490 nm) of indo-1 demonstrated that the intracellular calcium concentration was much higher in cardiac myocytes differentiated from DMD-hiPSCs than in those differentiated from control-hiPSCs [132].

HiPSC-CMs represent a unique platform to study basic mechanisms of cardiomyopathies using a human cell-based system. The literature published in the past decade demonstrates the utility of patient-specific iPSCs in disease modeling of cardiomyopathy, and has provided unique insights into disease mechanisms. However, the hiPSC-CMs that are available today still largely represent an immature version of the adult cardiac myocyte, and thus have inherent limitations in the study of cardiovascular disease. Systems to induce greater maturation in hiPSC-CMs are being developed, but considerable work remains to be done to further advance this model system.

5. Currently Utilized Therapies for DMD Cardiomyopathy

5.1. Gene Therapy

Gene addition or gene correction therapies for DMD have gained considerable traction over the past few years. Multiple gene addition clinical trials for DMD are ongoing. These developments have been recently reviewed [133].

5.2. Drugs and Small Molecules

There is currently no cure for DMD, and established small molecule therapy is limited to reducing the symptoms and hindering the mechanisms of disease progression in the heart. One of the predominant small molecules that has been used as a treatment for DMD patients are corticosteroids. Corticosteroids ameliorate the skeletal muscle phenotype with marked improvement in muscle strength and function [134]. Other studies have demonstrated that the use of corticosteroids leads to the stabilization of pulmonary function, prolonged ambulation, and reduced prevalence of scoliosis [135]. Although corticosteroids exhibit more potent effects in skeletal muscle than cardiac muscle, studies show steroids to be protective in the dystrophic heart, with possible benefits including preserved ventricular function, reduction in fibrosis, and improved survival [136–139]. In addition, corticosteroids have been associated with delaying the onset of cardiomyopathy by 4% for each year of treatment [139]. As a result of these documented benefits to skeletal muscle, pulmonary, and cardiac function, a daily regimen with corticosteroids such as deflazacort and prednisone is currently the earliest and most widely used DMD therapy [140]. However, the prolonged use of this drug is not without controversy, with the primary side-effects including reduced bone density, increased adiposity, and increased muscle catabolism [141]. In addition, some concerns stem from preclinical studies providing evidence that steroids may worsen the progression of DMD in the mouse heart [142,143]. Nevertheless, DMD clinical studies are largely in agreement that steroids are likely to be protective in the dystrophic heart, with possible benefits including improved survival, preserved ventricular function, and reductions in fibrosis.

Angiotensin receptor blockers (ARBs) and angiotensin converting enzyme inhibitors (ACEIs) constitute another class of small molecules that have been used as a treatment for DMD patients [144]. Angiotensin II (AngII) and the AngII type 1 receptor (AT1R) exhibit many fundamental effects on the heart, including promoting fibrosis, ROS production, remodeling, and cardiomyocyte death [145–147]. ACE inhibitors are generally implemented when LV systolic dysfunction declines. These inhibitors prevent the conversion of angiotensin-I to angiotensin-II (Ang-II), thereby reducing circulating levels of Ang-II. When angiotensin-II is activated, it stimulates the adrenal cortex to secrete aldosterone, promoting fluid and sodium retention. Both angiotensin-II and aldosterone contribute to the formation of fibrosis and overgrowth of connective tissue in the heart and further complicate the myocardial fibrosis resulting from dystrophin deficiency in DMD patients [148]. Therefore, the use of ACE inhibitors, aldosterone antagonists, and angiotensin receptor blockers (ARBs) has become a significant therapeutic approach for dystrophic cardiomyopathy. ACE inhibitors are a drug class that is often used as the first line of therapy for general heart failure, and was the first drug to be used in trials to demonstrate improved cardiac function and survival among DMD patients [149]. ARBs are equally effective when compared directly to ACEIs and better tolerated by patients, but they are usually utilized as an alternative in cases of poor ACEI tolerance [150].

Beta-blockers are another class of small molecules that are regularly used for the treatment of acquired heart failure, where they are often combined with ACEIs to improve survival and reduce hospitalization rates [151]. Beta-blockers have been considered a candidate for cardiac-directed therapy in DMD aiming to limit β -AR effects. Beta-blockers act by interfering with beta-receptor binding by catecholamines, which leads to a reduction of sympathetic nervous system activity. They are therefore prescribed for arrhythmic patients and those with symptomatic but stable systolic dysfunction. It is

known that combination therapy with ACE and β -adrenergic blocker agents improves the survival of patients with left ventricular dysfunction [152].

A retrospective study demonstrated that DMD patients have improvement in echocardiographic parameters, such as fractional shortening, sphericity index, and left ventricular ejection, after the administration of either ACE inhibitors alone or the combination of both ACE inhibitors and beta-blockers [153]. In a study conducted by Kajimoto and coworkers, patients with different types of muscular dystrophies were assigned to receive either an ACE inhibitor plus a beta-blocker (carvedilol) for at least 2 years or an ACE inhibitor alone (cilazapril or enalapril) for at least 3 years. They observed that the ACE inhibitor treatment alone maintained fractional shortening whereas the combination therapy provided a significant improvement in left ventricular fractional shortening [154]. Studies have also demonstrated that the use of ACE inhibitors in combination with beta-blockers in DMD patients reversed congestive heart failure signs and symptoms, delayed the progression of left ventricular dysfunction, and also improved systolic function [144]. Although some DMD patient studies indicate that beta-blockers have additive effects on cardiac function and survival compared with ACEIs alone, some studies using beta-blockers in DMD cardiomyopathy have shown little effect, making it unclear as to whether these drugs deliver a significant benefit [155,156].

Mineralocorticoid receptor antagonists, such as eplerenone and spironolactone are another class of small molecules that have been used for managing heart failure with low ejection fraction, and are often incorporated into treatment for DMD cardiomyopathy [111]. In a pre-clinical study of DMD cardiomyopathy, the combination of spironolactone and ACEI therapy showed protective effects in both skeletal and cardiac muscle [143]. A recent clinical trial demonstrated that DMD patients with preserved ejection fraction already receiving treatment with an ACEI or ARB showed modest but significant improvements in myocardial strain, ejection fraction, and chamber dilation with eplerenone treatment, compared to those without eplerenone [157].

6. Experimental Therapeutic Strategies to Improve Calcium Handling and Decrease Calcium Overload in DCM and DMD Cardiomyopathy

Although the mechanisms of cardiac dysfunction in DMD are complex and multifactorial, impaired calcium handling and calcium overload are key contributors to both early and late stage pathogenesis, as previously described. Currently utilized clinical therapies for DMD cardiomyopathy do not directly target calcium handling defects. Therefore, development of novel therapeutic strategies should focus on targeting various aspects of these pathways. Upstream targets include repair of the damaged sarcolemma and restoration of hyperactive stretch-activated channel (SAC) activity and RyR2 function. These targets will mitigate calcium overload from both the extracellular space and intracellular stores. Downstream targets include normalization of Serca2a/PLN activity and calcium cycling. These targets will mitigate the contraction and relaxation deficits characteristic of the dilated phenotype in late stage DMD cardiomyopathy. A summary of studies that specifically target various aspects of calcium mishandling and overload in cardiac tissue of muscular dystrophy models is shown in Table 2.

Table 2. Summary of research investigating experimental therapeutic strategies for calcium mishandling and overload in muscular dystrophy cardiomyopathy.

Target	Therapy	Model	Major Findings
Sarcolemma [41,68,158,159]	Copolymer -based membrane stabilizers	<i>mdx</i> mice dysferlin KO mice GRMD canine	↓ Myocyte Ca ²⁺ influx/hypercontracture ↓ Stress-induced functional deficits (acute and chronic) ↓ Fibrosis, serum cTnI, LV remodeling ↓ <i>Ex vivo</i> ischemia/reperfusion injury
Stretch-Activated Channels [160]	GsMTX-4	<i>mdx</i> mice	↓ Myocyte resting Ca ²⁺ concentration

Table 2. Cont.

Target	Therapy	Model	Major Findings
Ryanodine Receptor [161]	N-acetyl cysteine Rycal S107	<i>mdx</i> mice	↓ Myocyte resting Ca ²⁺ concentration ↓ Myocyte RyR2 Ca ²⁺ leak ↓ Arrhythmias
Serca2a [162]	AAV-9 Serca2a	<i>mdx</i> mice	Normalized ECG measurements
Phospholamban [19,163–165]	AAV S16E-PLN Adenovirus anti-PLN antibody Adenovirus inhibitor-2 PLN-KO	BIO14.6 hamster <i>mdx</i> mice	PLN inhibition in BIO14.6 hamsters <ul style="list-style-type: none"> • ↑ Ca²⁺ reuptake in SR vesicles • ↑ Myocyte contractility and Ca²⁺ handling • ↑ LV systolic and diastolic function <ul style="list-style-type: none"> • ↓ Fibrosis • ↑ Survival PLN ablation in <i>mdx</i> mice <ul style="list-style-type: none"> • ↑ Myocyte contractility and Ca²⁺ handling • ↓ LV systolic and diastolic function <ul style="list-style-type: none"> • ↑ EBD uptake • ↑ Fibrosis

KO: knockout; cTnI: cardiac troponin I; LV: left ventricle; RyR2: ryanodine receptor 2; AAV: adeno-associated virus; ECG: electrocardiogram; PLN: phospholamban; EBD: Evan's Blue Dye.

6.1. Membrane Stabilization

Membrane stabilization has been extensively studied as a therapeutic strategy for DMD cardiomyopathy in both small and large animal models [41,68] to mitigate sarcolemmal damage and calcium overload occurring from mechanical stress in the absence of dystrophin. Triblock copolymers, of which Poloxamer 188 (P188) has been most widely studied, consist of a hydrophobic polypropylene oxide (PPO) core, flanked by two hydrophilic polyethylene oxide (PEO) chains [63]. P188 is thought to insert into damaged membranes to provide stability until intrinsic repair mechanisms are able to restore integrity of the membrane [63]. P188 treatment of isolated dystrophic cardiac myocytes improved membrane compliance and decreased calcium influx and hypercontracture during passive physiological stretch [41]. *Ex vivo mdx* heart function was also improved after ischemia reperfusion injury with P188 treatment [159]. Finally, P188-treated *mdx* mice undergoing chronic isoproterenol stress had some improvements in *in vivo* cardiac function after two and four weeks [158], and a large animal model of DMD showed significant improvement in *in vivo* cardiac function after chronic P188 therapy [68]. The reader is referred to excellent recent reviews for more details on this topic [63,166].

Repairing damaged membranes using muscle-specific TRIM (tripartite motif) protein mitsugumin 53 (MG53) provides an additional avenue for targeting membrane instability in DMD. Recombinant MG53 administration to *mdx* mice improved skeletal muscle pathology and decreased damage after downhill treadmill running [167].

6.2. Stretch-Activated Channel Inhibition

In addition to micro-tears in the sarcolemma, increased expression and activity of stretch-activated non-selective ion channels (SACnsc) have been implicated in calcium influx and overload in muscular dystrophy. In skeletal muscle, the transient receptor potential channel (TRPC) family was identified as a therapeutic target for decreasing extracellular calcium entry in DMD. Inhibition of TRPC1 and TRPC4 expression with antisense oligonucleotides decreased calcium entry measured by patch-clamping in myofibers from *mdx* mice [168]. Further, transgenic expression of a dominant negative form of TRPC3 in *mdx* and *Scgd*^{-/-} mice decreased the dystrophic phenotype in skeletal muscle, including decreased fibrosis, serum CK, and occurrence of central nuclei [16]. In the heart, increased expression of TRPC1 has been implicated in the increased slow force response in *mdx* mice, caused by slow calcium influx leading to increased force production over several minutes of myocyte stretch [160]. Blockage of this channel with stretch-activated channel blocker GsMTx-4 decreased resting calcium concentration [160].

Further research is needed to explore whether decreased SAC activity or expression in the heart can delay or inhibit the dilated phenotype of DMD cardiomyopathy.

6.3. RyR2 Stabilization

RyR2 hypersensitivity has been implicated in calcium overload within the dystrophic cardiac myocyte [71]. Calstabin2 is a subunit of RyR2, which stabilizes the closed state of this channel [169]. Phosphorylation [169] or oxidative stress leading to nitrosylation [161] inhibits the association of calstabin2 with RyR2, increasing SR calcium leak. Treatment with N-acetyl cysteine to prevent nitrosylation or RyR2 stabilizer Rycal S107 prevented depletion of calstabin2 and decreased production of calcium sparks and depolarization in *mdx* cardiac myocytes [161]. Treatment of *mdx* mice with Rycal S107 also significantly reduced arrhythmias [161]. Similar studies in skeletal muscle found RyR1 stabilization to improve muscle strength, exercise tolerance, and muscle histopathology [58,170]. Whether long-term treatment to stabilize RyR2 in the heart can lead to improved cardiac outcomes in DMD requires further investigation.

6.4. Modulation of Serca2a/PLN

As a result of the central role of Serca2a and PLN in cardiac calcium cycling, their necessity in the maintenance of low diastolic calcium concentration, and the changes associated with their expression and activity in DCM, this complex has become an important experimental therapeutic target in both DCM and DMD-cardiomyopathy.

6.4.1. Serca2a as a Target for DCM Therapy

Serca2a gene therapy has been studied extensively in a variety of heart failure models. Adenoviral gene transfer of Serca2a in isolated cardiac myocytes from failing human hearts improved peak height of contraction and relaxation rate, which could be explained by increased calcium peak height and decay rate [171]. Multiple small animal models of heart failure have also been used to study the effectiveness of Serca2a gene therapy. Aortic-banded rats with adenoviral gene delivery of Serca2a had improved systolic and diastolic function measured by *in vivo* hemodynamics [172], increased survival rate [173], normalized energetics (PCr:ATP), and more efficient oxygen utilization compared to aortic-banded rats without Serca2a treatment [173,174]. Lentiviral-mediated Serca2a gene delivery after myocardial infarction in rats led to improvement in left ventricular systolic and diastolic dimensions and fractional shortening measured by echocardiography, improved hemodynamic measurements of systolic and diastolic function, and increased survival rate [175]. Two large animal models have also been used to study the effectiveness of Serca2a gene delivery via adeno-associated viral (AAV) gene transfer. In a swine model of mitral regurgitation, AAV delivery of Serca2a led to improved LV systolic and diastolic dimensions, left ventricular ejection fraction, and +dP/dt two months after gene delivery. AAV2/1-Serca2a in sheep with rapid pacing-induced heart failure also had improvements in LV dimensions, as well as increased systolic function and improvements in the pressure-volume relationship [176,177].

As a result of its therapeutic benefit in pre-clinical models of heart failure, Serca2a gene therapy has been tested in two randomized, placebo-controlled clinical trials using intracoronary delivery of AAV1 in advanced heart failure patients. In the first trial, patients that received the highest dose of Serca2a (1×10^{13} DNase resistant particles) showed improvement in pre-defined clinical endpoints including symptomatic, functional, biomarker, and LV function and remodeling abnormalities after six months [178]. The high-dose group also had an 82% decrease in recurrent cardiovascular events after three years of follow-up [179]. This study was followed by a larger multi-center trial of 250 heart failure patients using the high dose of Serca2a. Unlike the initial trial, there was no difference between treatment and control groups in either recurrent or terminal clinical events [180]. The basis for the discrepancy in results between the two studies is uncertain. A small number of heart tissue samples

revealed low vector DNA copy number. Additionally, there were differences between the two trials in the number of total viral particles (including empty capsids) delivered [180].

6.4.2. PLN as a Target for DCM Therapy

As the major regulator of Serca2a, PLN has also been studied for its potential role to mitigate the calcium cycling deficits contributing to DCM. Early studies found PLN overexpression or deficiency decreased or increased calcium cycling and Serca2a calcium sensitivity, respectively, and β -adrenergic signaling was important in determining the level of PLN inhibition of Serca2a [181,182]. Increasing the ratio of PLN to Serca2a in a transgenic mouse model with 2-fold overexpression of PLN decreased peak height of contraction as well as slowed relaxation rate. This was accompanied by similar decreases in calcium transient peak height and decay rate. Depressed *in vivo* function measured by echocardiography was also present, and this was alleviated by isoproterenol treatment [181]. Contrary to PLN overexpression, PLN deficiency increases calcium cycling and cardiac function. Working heart preparations from PLN-deficient mice exhibited both increased systolic and diastolic function, which was not further enhanced by beta-adrenergic stimulation [182]. Increased calcium cycling and subsequent increases in contraction and relaxation function with PLN depletion are dose dependent, with PLN (+/-) mice exhibiting cardiac function at levels between WT and PLN (-/-) animals [183].

These early studies solidifying the inhibitory role of PLN on calcium cycling led to the hypothesis that PLN inhibition may ameliorate the depressed calcium cycling characteristic of DCM. This hypothesis has been tested in multiple models of DCM. In the MLP-deficient mouse [92], PLN deficiency decreased dilation and ultrastructural abnormalities and increased heart function measured by *in vivo* hemodynamics and echocardiography. These improvements could be explained by increased calcium cycling measured in isolated cardiac myocytes [184]. A pseudo-phosphorylated mutant of PLN (S16E) mimics the conformational change occurring in PLN after PKA phosphorylation at serine-16, decreasing interaction with Serca2a. *In vivo* rAAV gene transfer of S16E-PLN improved multiple measures of heart function in a post-myocardial infarction rat model, including dilation, heart size, ejection fraction and E/A ratio measured by echocardiography at 2 and 6 months post-MI. Additionally, multiple hemodynamic measurements were improved compared to infarcted rats without AAV treatment [185]. Similar improvements in heart function were observed in a large animal model of heart failure with S16E-PLN gene transfer. Sheep undergoing four weeks of pacing stress, followed by *in vivo* percutaneous cardiac recirculation-mediated gene delivery of S16E-PLN recovered hemodynamic function after two weeks, whereas control animals continued to have worsening heart failure [186]. Another approach to inhibition of PLN is to inhibit Phosphatase-1 (PP1), which dephosphorylates PLN and causes it to bind and inhibit Serca2a. Using AAV-9 gene delivery of a short-hairpin RNA against PP1beta with a B-type natriuretic peptide (BNP)-promoter created a heart-failure inducible expression system which was tested in the MLP-deficient mouse. This system increased PLN phosphorylation, which was accompanied by decreased cardiac remodeling and improved fractional shortening and hemodynamic function three months after gene transfer [187].

6.4.3. Serca2a and PLN in Muscular Dystrophy-Associated Cardiomyopathy

Although most research has focused on the role of Serca2a/PLN in DCM in general, a number of studies have looked specifically at the cardiomyopathy occurring in models of muscular dystrophy. Serca2a gene expression is decreased in mice with DMD cardiomyopathy [188], suggesting the Serca2a/PLN complex may also be an important therapeutic target for DCM occurring in DMD.

Two studies examined the effect of Serca1 overexpression in skeletal muscle, and one study looked at Serca2a overexpression in the heart of different mouse models of muscular dystrophy. Crossing Serca1 transgenic mice with *mdx*, *mdx:utr^{-/-}*, and *Sgcd^{-/-}* mice, resulting in a 1.5–4-fold overexpression of Serca1, decreased CK release [189,190], reduced Evan's Blue Dye (EBD) uptake [189] and decreased fibrosis [189], suggesting decreased muscle damage. This was attributed to the ability of Serca1 overexpression to improve calcium handling in isolated myocytes [189]. The result of Serca1

overexpression led to restored treadmill running capability [189] and decreased percent torque loss after eccentric contraction-induced injury [190]. Serca2a overexpression in the aged *mdx* heart was examined using AAV-9 gene delivery. In this study, Serca2a was unable to reverse fibrosis, but did result in some improvement in electrocardiographic abnormalities [162].

PLN inhibition has also been tested in the context of muscular-dystrophy associated cardiomyopathy. The BIO14.6 hamster is a model of limb-girdle muscular dystrophy and exhibits a progressive cardiomyopathy phenotype beginning by about 5 weeks of age [191]. Recombinant AAV gene delivery of S16E-PLN in 5-6 week old BIO14.6 hamsters improved calcium cycling in isolated SR vesicles. This resulted in increased fractional shortening and improved maximum and minimum LV dP/dt at both 5 and 28 weeks post-gene transfer compared to BIO14.6 hamsters without AAV treatment [163]. Another study in the BIO14.6 hamster model used adenoviral gene delivery of an antibody targeted against PLN. Just over 50% of myocytes were infected with the virus, which led to short-term improvement in both echocardiographic and hemodynamic markers of systolic and diastolic function. This was accompanied by improved contractility and calcium handling in isolated myocytes, and increased SR calcium reuptake in whole heart homogenates [164]. Additionally, inhibition of PP1 via gene delivery of Inhibitor-2 in the BIO14.6 hamster resulted in beneficial effects on cardiac dimensions and fractional shortening, as well as improved hemodynamic measurements, decreased fibrosis, and improved survival [165].

Similar to PLN, sarcolipin (SLN) is an inhibitor of Serca. SLN expression is increased in heart muscle of *mdx:utr^{-/-}* mice, dystrophic dogs and human patients with DMD. Deletion of either one or both alleles of SLN in *mdx:utr^{-/-}* mice extended the lifespan of these animals, as well as improved heart function (ejection fraction and fractional shortening). Improved function was attributed to decreased left ventricular internal diameter in diastole (LVIDd) and decreased fibrotic and necrotic tissue. Although calcium handling was not measured in heart tissue in this study, skeletal muscle calcium reuptake was increased as a result of reduced SLN expression [192].

As a result of the extensive pre-clinical literature showing beneficial effects of Serca2a overexpression or PLN inhibition on calcium handling and heart failure outcomes in multiple models of heart failure, including muscular dystrophy-associated cardiomyopathy, our laboratory hypothesized that PLN ablation would improve calcium handling and subsequently improve cardiac function in the *mdx* mouse. Isolated cardiac myocytes from these mice did indeed show enhanced contractility and faster relaxation, which was accompanied by increased calcium transient peak height and decay rate. However, *in vivo* echocardiography revealed severe dilation and decreased systolic and diastolic function. Histological analysis revealed significantly more fibrotic development and EBD uptake, indicating sarcolemma integrity was more severely compromised with PLN ablation [19]. It was concluded that, although PLN ablation improved calcium cycling in isolated myocytes, which could potentially decrease the risk of calcium overload, increased contractile function likely placed additional stress on an already compromised sarcolemma. This likely led to even more extensive membrane damage than occurs with dystrophin deficiency alone [19] (Figure 4).

The results of this study are in contrast to others discussed above [162–165]. One potential contributor to these differences is the level of PLN inhibition. In the context of muscular dystrophy models, one study overexpressed Serca2a [162], and others have inhibited PLN to varying degrees through delivery of a pseudophosphorylated PLN [163], an antibody against PLN [164], or inhibitor-2 [165]. Although complete ablation of PLN improved cardiomyopathy in a DCM model [184], this was not the case in *mdx* mice, highlighting key differences mechanistically between the pathophysiology of muscular dystrophy-associated DCM and other causes of DCM. PLN knockout mice have significantly increased calcium cycling leading to increased contractile function [182,183], which likely increased sarcolemmal stress. Additionally, PLN knockout mice are not responsive to β -adrenergic signaling [182] and therefore have very little cardiac reserve. PLN knockout mice also have an increased ATP utilization and oxygen consumption [193], potentially increasing oxidative stress and potentiating membrane damage in the context of muscular dystrophy, which exhibits

decreased endogenous reducing capability [66]. Finally, gene deletion or transgenic expression of genes may have unknown compensatory effects on development which cannot be controlled for. Whether small increases in Serca2a expression or partial inhibition of PLN in *mdx* mice would yield different results needs to be the focus of future studies.

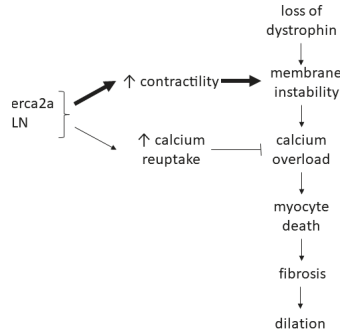


Figure 4. Effects of increased calcium cycling on cardiac myocytes with dystrophin deficiency. Loss of dystrophin destabilizes the sarcolemma and leads to calcium mishandling and overload. Increasing calcium cycling via modulation of Serca2a/PLN function increases calcium uptake into the SR, which could decrease cytosolic calcium concentration. However, increased calcium cycling also increases contractility, which could subsequently cause increased membrane damage and exacerbate calcium overload. In the context of dystrophin deficiency, phospholamban (PLN) ablation led to increased membrane damage and worsened cardiomyopathy [19].

6.4.4. Caution with Serca2a/PLN Therapy for Cardiomyopathy

Although many pre-clinical models of heart failure, including those of muscular dystrophy-associated cardiomyopathy, show significant improvement in cardiac morphology, calcium handling, contractile function, and survival with decreased PLN inhibition of Serca2a, caution should be taken when translating this to human disease. Two mutations leading to loss of PLN function have been identified in humans. A point mutation (T116G) resulting in a premature stop codon and a nonfunctional PLN protein (Leu39-stop) leads to severe DCM requiring transplantation at a young age [194]. Co-expression of Leu39-stop PLN and Serca2a in HEK293 cells revealed this truncated PLN protein was unable to decrease Serca2a affinity for calcium, and gene transfer of Leu39-stop PLN in isolated cardiac myocytes had no effects on calcium cycling or contraction/relaxation kinetics [194]. A C→T missense mutation at nucleotide 25 of the PLN gene encodes an Arg→Cys substitution (R9C) in the cytosolic domain, which also results in DCM and early death [195]. Similar to the Leu39-stop mutation, R9C did not inhibit calcium uptake in HEK293 cells [195]. Further study of this mutation revealed that R9C stabilizes the pentamer conformation of the protein, making it unavailable to inhibit Serca2a [196]. Indeed, acute expression of R9C via adenoviral gene transfer in rabbit cardiac myocytes revealed an increase in contractility and relaxation kinetics, with a concomitant increase in calcium peak height and decay rate [197]. Additionally, R9C transfected cardiac myocytes showed decreased responsiveness to beta-adrenergic stimulation [197]. Finally, patients with specific polymorphisms in alpha2c and beta1 adrenergic receptors, which leads to increased release and sensitivity to norepinephrine, have an odds ratio of 10.11 of developing heart failure compared to patients without these polymorphisms [198]. Chronically increased adrenergic stimulation increases load on the heart and decreases cardiac reserve, both of which also occur with PLN inhibition.

Key differences in cardiac physiology and calcium handling exist between mice and humans, which could account for the divergent outcomes. Approximately 90% of calcium reuptake in mice occurs via Serca2a and only 10% occurs via the sarcolemmal $\text{Na}^+/\text{Ca}^{2+}$ exchanger. In contrast, approximately one-third of calcium is exported from the cytosol via the $\text{Na}^+/\text{Ca}^{2+}$ exchanger in humans. Additionally,

resting heart rate is approximately 10-fold lower in humans compared to mice, and the human heart has a greater variability in heart rate response to physiological stress. Finally, humans have a higher cardiac reserve allowing for increased SR calcium uptake and calcium load during physiological stress. Reducing cardiac reserve in humans by inhibiting PLN or increasing Serca2a may therefore have a much different outcome compared with a similar inhibition in rodents [56,199]. This was demonstrated in the CUPID 2 trial, where Serca2a gene delivery was not successful in meeting beneficial clinical outcomes in heart failure patients [180].

6.5. Calcium Buffering

An alternative and energetically neutral approach to improving calcium reuptake and relaxation rate is to introduce expression of *de novo* calcium buffers into cardiac myocytes. The most well-studied calcium buffer in this context is parvalbumin. Parvalbumin (Parv) is ~12 kDa EF-hand calcium/magnesium binding protein naturally expressed in fast-twitch muscle in order to aid in fast relaxation by buffering calcium away from myofilaments [200,201]. Parvalbumin proteins contain two 12 amino acid EF-hand cation binding loops with binding affinities ranging from $K_{Ca^{2+}} = 10^7-10^9 M^{-1}$ and $K_{Mg^{2+}} = 10^3-10^5 M^{-1}$, for calcium and magnesium, respectively [202,203]. In a resting myocyte, magnesium concentration is ~1 mM and calcium concentration is 10–100 nM, resulting in magnesium occupancy of the EF-hand loops. During contraction, calcium concentration increases, which causes calcium to displace magnesium in the binding loops. Calcium binding to Parv buffers calcium away from myofilaments to aid in rapid relaxation. As calcium is taken back up into the SR during relaxation, cytosolic calcium concentration falls, resulting in magnesium reoccupying the EF-hand cation binding loops. The ability of Parv to bind both magnesium and calcium is important in its function as a delayed calcium buffer. Calcium concentration must be sufficiently increased to induce magnesium dissociation from the EF-hand binding loops. This delay in calcium binding enables calcium to first bind to myofilaments and facilitate contraction of the myocyte before binding to Parv [203].

The ability of Parv to facilitate fast relaxation in the heart has been tested in numerous cell and animal models of diastolic dysfunction. Adenoviral gene transfer of Parv into isolated cardiac myocytes from hypothyroid rats [204], senescent rats [205], and Dahl salt-sensitive rats [206] hastened relaxation by increasing the rate of calcium decay. *In vivo* studies revealed gene delivery of Ad-Parv improved short-term hemodynamic measurements of relaxation, including $-dp/dt$ and time to 50% and 90% pressure decay in hypothyroid rats [207], and decreased tau, a load independent measure of diastolic dysfunction, in senescent rats [208,209]. One advantage to a calcium buffering approach for improved relaxation over increasing Serca2a activity is the energetic efficiency. Mathematical modeling studies indicate Serca2a overexpression leads to a higher peak and total ATP consumption compared to *de novo* Parv expression, which results in a more even distribution of ATP consumption over the course of the contractile cycle [210]. Additionally, Parv expression in cardiac myocytes preserves beta-adrenergic function, which is blunted with increased Serca2a function [211] or PLN inhibition [182].

One drawback to using wild-type Parv for improved relaxation in the heart is the calcium/magnesium binding affinities are not optimized for the relatively slow contractile cycle of the heart. Although Parv is a delayed calcium buffer, requiring magnesium removal from the EF-hand cation binding sites before calcium can bind, the kinetics are optimized for fast-twitch muscle. This results in WT-Parv binding calcium too early in the contractile cycle of cardiac myocytes and inhibiting maximal contractility [206,212]. This is contraindicated in the context of dilated cardiomyopathy, which is characterized by both decreased contractile function and slowed relaxation. A potential solution to this problem with WT-Parv is to genetically modify the EF-hand cation binding site to have optimal binding affinities for the kinetics of the human heart. It was hypothesized and confirmed with mathematical modeling that increasing magnesium affinity and slowing magnesium off-rate even further than WT-Parv would restrict the buffering of calcium to diastole and prevent premature truncation of contraction [210].

To test this hypothesis in myocytes, two genetically modified parvalbumin proteins have been developed. Both involve substitutions of the highly conserved glutamate at residue 12 of the EF-hand cation binding site, one with glutamine (E101Q) [213] and one with aspartate (E101D) [214]. These substitutions eliminate the 7th coordinating oxygen preferred by calcium, resulting in both an increase in magnesium affinity and a decrease in calcium affinity, further delaying the buffering of calcium compared to WT-Parv. Adenoviral gene transfer of these modified parvalbumins increased relaxation rate and unexpectedly also increased contraction amplitude in isolated myocytes from rat (E101Q and E101D), rabbit (E101Q) and canine (E101Q). Additionally, ParvE101Q improved contractility and relaxation in multiple models of heart failure, including thapsigargin-treated rabbit myocytes, failing myocytes from dogs, and *in vivo* hemodynamic function of inducible Serca2a knock-out mice [213,214].

As a result of its primary role in increasing relaxation, most studies with Parv have been done using models of diastolic dysfunction. This is because, as a calcium buffer, the main contribution of Parv in the context of the failing heart has been thought to be sequestration of calcium to enhance relaxation in diastole. In particular, the decreased contractility characteristic of WT-Parv-treated myocytes would be contraindicated for the already compromised contractility in DCM. Whether or not modified parvalbumins could serve to both improve relaxation and increase contractility in models of DCM is unknown and warrants further investigation, particularly because Parv both preserves beta-adrenergic function and is an energetically neutral approach to improving function in the energetically compromised failing heart [215]. Calcium buffering may potentially have a beneficial role in the cardiomyopathy of DMD. Increased diastolic calcium resulting from calcium influx through SACs, sarcolemmal micro-tears, and increased RyR2 leak could theoretically be mitigated through introduction of a calcium buffering system. The localization of these buffers within the myocyte, as well as the buffering capacity and calcium binding kinetics are all factors that need to be optimized and tested when considering this approach in the context of DMD cardiomyopathy.

7. Conclusions

Cardiomyopathy is a significant clinical feature of DMD, with nearly all patients exhibiting cardiac dysfunction by their teens [13]. Improved clinical management of musculoskeletal and respiratory issues in DMD patients has uncovered cardiomyopathy as a significant contributor to morbidity and mortality [13]. The underlying pathology is complex, owing to the multiple functions of dystrophin in the cardiac myocyte, but calcium overload and mishandling due to membrane instability is a key mechanistic contributor to disease onset and progression. Currently utilized clinical therapies for DMD cardiomyopathy do not specifically target calcium handling defects and come with significant side effects. Gene therapeutic strategies to correct calcium handling defects show some promise in experimental models of DCM, but more work must be done to understand the potential benefits and risks of these strategies in models specific to DMD-related cardiomyopathy. Of note, increasing calcium cycling in the context of the membrane instability characteristic of DMD may exacerbate disease progression [19]. Continued work to understand the mechanistic underpinnings of DMD cardiomyopathy, specifically related to calcium handling, will enable a more targeted approach to therapeutic development for this disease.

Author Contributions: Conceptualization: M.L.L. and J.M.M.; literature review and original draft preparation: M.L.L., H.C., A.A.M., A.B.B.A.; revisions and editing: M.L.L., H.C., A.A.M., A.B.B.A., J.M.M.; figure and table preparation: M.L.L., H.C., A.A.M., A.B.B.A.; final manuscript approval: M.L.L., H.C., A.A.M., A.B.B.A., J.M.M.; acquisition of funding: J.M.M. All authors have read and agreed to the published version of the manuscript.

Funding: This work was funded by National Institutes of Health (AR071349, HL138490, HL122323, HL132874) and Muscular Dystrophy Association (513474).

Conflicts of Interest: The authors do not declare any conflict of interest.

References

1. World Health Organization. *World Health Statistics 2017: Monitoring Health for the SDGs, Sustainable Development Goals*; World Health Organization: Geneva, Switzerland, 2017.
2. Benjamin, E.J.; Muntner, P.; Alonso, A.; Bittencourt, M.S.; Callaway, C.W.; Carson, A.P.; Chamberlain, A.M.; Chang, A.R.; Cheng, S.; Das, S.R.; et al. Heart Disease and Stroke Statistics-2019 Update: A Report From the American Heart Association. *Circulation* **2019**, *139*, e56–e528. [[CrossRef](#)] [[PubMed](#)]
3. Jefferies, J.L.; Towbin, J.A. Dilated cardiomyopathy. *Lancet* **2010**, *375*, 752–762. [[CrossRef](#)]
4. Towbin, J.A. Inherited cardiomyopathies. *Circ. J.* **2014**, *78*, 2347–2356. [[CrossRef](#)] [[PubMed](#)]
5. Romitti, P.A.; Zhu, Y.; Puzhankara, S.; James, K.A.; Nabukera, S.K.; Zamba, G.K.D.; Ciafaloni, E.; Cunniff, C.; Druschel, C.M.; Mathews, K.D.; et al. Prevalence of duchenne and becker muscular dystrophies in the United States. *Pediatrics* **2015**, *135*, 513–521. [[CrossRef](#)]
6. Gao, X.; Shen, X.; Dong, X.; Ran, N.; Han, G.; Cao, L.; Gu, B.; Yin, H.F. Peptide nucleic acid promotes systemic dystrophin expression and functional rescue in dystrophin-deficient mdx mice. *Mol. Ther. Nucleic Acids* **2015**, *4*, e255. [[CrossRef](#)]
7. Emery, A.E.H. The muscular dystrophies. *Lancet* **2002**, *359*, 687–695. [[CrossRef](#)]
8. Simonds, A.K.; Muntoni, F.; Heather, S.; Fielding, S. Impact of nasal ventilation on survival in hypercapnic Duchenne muscular dystrophy. *Thorax* **1998**, *53*, 949–952. [[CrossRef](#)]
9. Porte, P. Clinical indications for noninvasive positive pressure ventilation in chronic respiratory failure due to restrictive lung disease, COPD, and nocturnal hypoventilation—A consensus conference report. *Chest* **1999**, *116*, 521–534.
10. Eagle, M.; Baudouin, S.V.; Chandler, C.; Giddings, D.R.; Bullock, R.; Bushby, K. Survival in Duchenne muscular dystrophy: Improvements in life expectancy since 1967 and the impact of home nocturnal ventilation. *Neuromuscul. Disord.* **2002**, *12*, 926–929. [[CrossRef](#)]
11. Kamdar, F.; Garry, D.J. Dystrophin-Deficient Cardiomyopathy. *J. Am. Coll. Cardiol.* **2016**, *67*, 2533–2546. [[CrossRef](#)]
12. Shirokova, N.; Niggli, E. Cardiac phenotype of Duchenne Muscular Dystrophy: Insights from cellular studies. *J. Mol. Cell. Cardiol.* **2013**, *58*, 217–224. [[CrossRef](#)] [[PubMed](#)]
13. Nigro, G.; Comi, L.I.; Politano, L.; Bain, R.J.I. The incidence and evolution of cardiomyopathy in Duchenne muscular dystrophy. *Int. J. Cardiol.* **1990**, *26*, 271–277. [[CrossRef](#)]
14. Petrof, B.J.; Shrager, J.B.; Stedman, H.H.; Kelly, A.M.; Sweeney, H.L. Dystrophin protects the sarcolemma from stresses developed during muscle contraction. *Proc. Natl. Acad. Sci. USA* **1993**, *90*, 3710–3714. [[CrossRef](#)] [[PubMed](#)]
15. Sandri, M.; Podhorska-Okolow, M.; Geromel, V.; Rizzi, C.; Arslan, P.; Franceschi, C.; Carraro, U. Exercise Induces Myonuclear Ubiquitination and Apoptosis in Dystrophin-deficient Muscles of Mice. *J. Neuropathol. Exp. Neurol.* **1997**, *56*, 45–57. [[CrossRef](#)] [[PubMed](#)]
16. Millay, D.P.; Goonasekera, S.A.; Sargent, M.A.; Maillet, M.; Aronow, B.J.; Molkentin, J.D. Calcium influx is sufficient to induce muscular dystrophy through a TRPC-dependent mechanism. *Proc. Natl. Acad. Sci. USA* **2009**, *106*, 19023–19028. [[CrossRef](#)] [[PubMed](#)]
17. Peterson, J.M.; Wang, D.J.; Shettigar, V.; Roof, S.R.; Canan, B.D.; Bakkar, N.; Shintaku, J.; Gu, J.M.; Little, S.C.; Ratnam, N.M.; et al. NF- κ B inhibition rescues cardiac function by remodeling calcium genes in a Duchenne muscular dystrophy model. *Nat. Commun.* **2018**, *9*, 1–14. [[CrossRef](#)]
18. Williams, I.A.; Allen, D.G. Intracellular calcium handling in ventricular myocytes from mdx mice. *Am. J. Physiol. Heart Circ. Physiol.* **2007**, *292*, H846–H855. [[CrossRef](#)]
19. Law, M.L.; Prins, K.W.; Olander, M.E.; Metzger, J.M. Exacerbation of dystrophic cardiomyopathy by phospholamban deficiency mediated chronically increased cardiac Ca²⁺ cycling in vivo. *Am. J. Physiol. Heart Circ. Physiol.* **2018**, *315*, H1544–H1552. [[CrossRef](#)]
20. Fanchaouy, M.; Polakova, E.; Jung, C.; Ogrodnik, J.; Shirokova, N.; Niggli, E. Pathways of abnormal stress-induced Ca²⁺ influx into dystrophic mdx cardiomyocytes. *Cell Calcium* **2009**, *46*, 114–121. [[CrossRef](#)]
21. Li, Z.; Li, Y.; Zhang, L.; Zhang, X.; Sullivan, R.; Ai, X.; Szeto, C.; Cai, A.; Liu, L.; Xiao, W.; et al. Reduced Myocardial Reserve in Young X-Linked Muscular Dystrophy Mice Diagnosed by Two-Dimensional Strain Analysis Combined with Stress Echocardiography. *J. Am. Soc. Echocardiogr.* **2017**, *30*, 815–827. [[CrossRef](#)]

22. Li, Y.; Zhang, S.; Zhang, X.; Li, J.; Ai, X.; Zhang, L.; Yu, D.; Ge, S.; Peng, Y.; Chen, X. Blunted cardiac beta-adrenergic response as an early indication of cardiac dysfunction in Duchenne muscular dystrophy. *Cardiovasc. Res.* **2014**, *103*, 60–71. [[CrossRef](#)] [[PubMed](#)]
23. McNally, E.M.; Mestroni, L. Dilated cardiomyopathy: Genetic determinants and mechanisms. *Circ. Res.* **2017**, *121*, 731–748. [[CrossRef](#)]
24. Bers, D.M. Cardiac excitation-contraction coupling. *Nature* **2002**, *415*, 198–205. [[CrossRef](#)] [[PubMed](#)]
25. Townsend, D.W.; Yasuda, S.; Chamberlain, J.; Metzger, J.M. Cardiac Consequences to Skeletal Muscle-Centric Therapeutics for Duchenne Muscular Dystrophy. *Trends Cardiovasc. Med.* **2009**, *19*, 50–55. [[CrossRef](#)] [[PubMed](#)]
26. Berko, B.A.; Swift, M. X-Linked Dilated Cardiomyopathy. *N. Engl. J. Med.* **1987**, *316*, 1186–1191. [[CrossRef](#)] [[PubMed](#)]
27. Towbin, J.A.; Hejtmancik, J.F.; Brink, P.; Gelb, B.; Zhu, X.M.; Chamberlain, J.S.; McCabe, E.R.B.; Swift, M. X-linked dilated cardiomyopathy: Molecular genetic evidence of linkage to the Duchenne muscular dystrophy (dystrophin) gene at the Xp21 locus. *Circulation* **1993**, *87*, 1854–1865. [[CrossRef](#)] [[PubMed](#)]
28. Eagle, M.; Bourke, J.; Bullock, R.; Gibson, M.; Mehta, J.; Giddings, D.; Straub, V.; Bushby, K. Managing Duchenne muscular dystrophy The additive effect of spinal surgery and home nocturnal ventilation in improving survival. *Neuromuscul. Disord.* **2007**, *17*, 470–475. [[CrossRef](#)] [[PubMed](#)]
29. Gordon, A.M.; Homsher, E.; Regnier, M. Regulation of Contraction in Striated Muscle. *Physiol. Rev.* **2000**, *80*, 853–924. [[CrossRef](#)]
30. Kamisago, M.; Sapna, S.; DePalma, S.; Solomon, S.; Sharma, P.; McDonough, B.; Smoot, L.; Mullen, M.P.; Woolf, P.K.; Wigle, D.; et al. Mutations in sarcomere protein genes as a cause of dilated cardiomyopathy. *N. Engl. J. Med.* **2000**, *343*, 1688–1696. [[CrossRef](#)]
31. McNally, E.M.; Golbus, J.R.; Puckelwartz, M.J. Genetic mutations and mechanisms in dilated cardiomyopathy. *J. Clin. Investig.* **2013**, *123*, 19–26. [[CrossRef](#)]
32. Gomes, A.V.; Potter, J.D. Molecular and Cellular Aspects of Troponin Cardiomyopathies. *Ann. N. Y. Acad. Sci.* **2004**, *1015*, 214–224. [[CrossRef](#)] [[PubMed](#)]
33. Wolff, M.R.; Buck, S.H.; Stoker, S.W.; Greaser, M.L.; Mentzer, R.M. Myofibrillar calcium sensitivity of isometric tension is increased in human dilated cardiomyopathies: Role of altered β -adrenergically mediated protein phosphorylation. *J. Clin. Investig.* **1996**, *98*, 167–176. [[CrossRef](#)] [[PubMed](#)]
34. Nakano, S.J.; Walker, J.S.; Walker, L.A.; Li, X.; Du, Y.; Miyamoto, S.D.; Sucharov, C.C.; Garcia, A.M.; Mitchell, M.B.; Ambardekar, A.V.; et al. Increased myocyte calcium sensitivity in end-stage pediatric dilated cardiomyopathy. *Am. J. Physiol. Heart Circ. Physiol.* **2019**, *317*, H1221–H1230. [[CrossRef](#)] [[PubMed](#)]
35. Van Der Velden, J.; De Jong, J.W.; Owen, V.J.; Burton, P.B.J.; Stienen, G.J.M. Effect of protein kinase A on calcium sensitivity of force and its sarcomere length dependence in human cardiomyocytes. *Cardiovasc. Res.* **2000**, *46*, 487–495. [[CrossRef](#)]
36. Memo, M.; Leung, M.C.; Ward, D.G.; Dos Remedios, C.; Morimoto, S.; Zhang, L.; Ravenscroft, G.; McNamara, E.; Nowak, K.J.; Marston, S.B.; et al. Familial dilated cardiomyopathy mutations uncouple troponin i phosphorylation from changes in myofibrillar Ca^{2+} sensitivity. *Cardiovasc. Res.* **2013**, *99*, 65–73. [[CrossRef](#)] [[PubMed](#)]
37. Messer, A.E.; Marston, S.B. Investigating the role of uncoupling of troponin I phosphorylation from changes in myofibrillar Ca^{2+} -sensitivity in the pathogenesis of cardiomyopathy. *Front. Physiol.* **2014**, *5*, 315. [[CrossRef](#)]
38. Chang, A.N.; Potter, J.D. Sarcomeric protein mutations in dilated cardiomyopathy. *Heart Fail. Rev.* **2005**, *10*, 225–235. [[CrossRef](#)]
39. Mestroni, L.; Brun, F.; Spezzacatene, A.; Sinagra, G.; Taylor, M.R. Genetic Causes of Dilated Cardiomyopathy. *Prog. Pediatr Cardiol* **2014**, *37*, 13–18. [[CrossRef](#)]
40. McNally, E.M. Broken giant linked to heart failure. *Nature* **2012**, *483*, 281–282. [[CrossRef](#)]
41. Yasuda, S.; Townsend, D.W.; Michele, D.E.; Favre, E.G.; Day, S.M.; Metzger, J.M. Dystrophic heart failure blocked by membrane sealant poloxamer. *Nature* **2005**, *436*, 1025–1029. [[CrossRef](#)]
42. Barresi, R.; Di Blasi, C.; Tiziana, N.; Brugnani, R.; Vitali, A.; Felisari, G.; Salandi, A.; Daniel, S.; Cornelio, F.; Morandi, L.; et al. Disruption of heart sarcoglycan complex and severe cardiomyopathy caused by β sarcoglycan mutations. *J. Med. Genet.* **2000**, *37*, 102–107. [[CrossRef](#)] [[PubMed](#)]

43. Tsubata, S.; Bowles, K.R.; Vatta, M.; Zintz, C.; Titus, J.; Muhonen, L.; Bowles, N.E.; Towbin, J.A. Mutations in the human δ -sarcoglycan gene in familial and sporadic dilated cardiomyopathy. *J. Clin. Investig.* **2000**, *106*, 655–662. [[CrossRef](#)] [[PubMed](#)]
44. Shaw, T.; Elliott, P.; McKenna, W.J. Dilated cardiomyopathy: A genetically heterogeneous disease. *Lancet* **2002**, *360*, 654–655. [[CrossRef](#)]
45. Sequeira, V.; Nijenkamp, L.L.A.M.; Regan, J.A.; Van Der Velden, J. The physiological role of cardiac cytoskeleton and its alterations in heart failure. *Biochim. Biophys. Acta Biomembr.* **2014**, *1838*, 700–722. [[CrossRef](#)]
46. Heydemann, A.; McNally, E.M. Consequences of Disrupting the Dystrophin-Sarcoglycan Complex in Cardiac and Skeletal Myopathy. *Trends Cardiovasc. Med.* **2007**, *17*, 55–59. [[CrossRef](#)]
47. Weintraub, R.G.; Semsarian, C.; Macdonald, P. Dilated cardiomyopathy. *Lancet* **2017**, *390*, 400–414. [[CrossRef](#)]
48. Kearney, M.T.; Cotton, J.M.; Richardson, P.J.; Shah, A.M. Viral myocarditis and dilated cardiomyopathy: Mechanisms, manifestations, and management. *Postgrad. Med. J.* **2001**, *77*, 4–10. [[CrossRef](#)]
49. Barnabei, M.S.; Sjaastad, F.V.; Townsend, D.W.; Bedada, F.B.; Metzger, J.M. Severe dystrophic cardiomyopathy caused by the enteroviral protease 2A-mediated C-terminal dystrophin cleavage fragment. *Sci. Transl. Med.* **2015**, *7*, 1–12. [[CrossRef](#)]
50. Parodi, O.; De Maria, R.; Oltrona, L.; Testa, R.; Sambuceti, G.; Roghi, A.; Merli, M.; Belingheri, L.; Accinni, R.; Spinelli, F.; et al. Myocardial blood flow distribution in patients with ischemic heart disease or dilated cardiomyopathy undergoing heart transplantation. *Circulation* **1993**, *88*, 509–522. [[CrossRef](#)]
51. Van Den Heuvel, A.F.M.; Van Veldhuisen, D.J.; Van Der Wall, E.E.; Blanksma, P.K.; Siebelink, H.M.J.; Vaalburg, W.M.; Van Gilst, W.H.; Crijns, H.J.G.M. Regional myocardial blood flow reserve impairment and metabolic changes suggesting myocardial ischemia in patients with idiopathic dilated cardiomyopathy. *J. Am. Coll. Cardiol.* **2000**, *35*, 19–28. [[CrossRef](#)]
52. Eisner, D.A.; Caldwell, J.L.; Kistamás, K.; Trafford, A.W. Calcium and Excitation-Contraction Coupling in the Heart. *Circ. Res.* **2017**, *121*, 181–195. [[CrossRef](#)] [[PubMed](#)]
53. Brittsan, A.G.; Kranias, E.G. Phospholamban and cardiac contractile function. *J. Mol. Cell. Cardiol.* **2000**, *32*, 2131–2139. [[CrossRef](#)] [[PubMed](#)]
54. Kranias, E.G.; Hajjar, R.J. Modulation of cardiac contractility by the phospholamban/SERCA2a regulatome. *Circ. Res.* **2012**, *110*, 1646–1660. [[CrossRef](#)] [[PubMed](#)]
55. MacLennan, D.H.; Abu-Abed, M.; Kang, C.H. Structure-function relationships in Ca^{2+} cycling proteins. *J. Mol. Cell. Cardiol.* **2002**, *34*, 897–918. [[CrossRef](#)]
56. MacLennan, D.H.; Kranias, E.G. Phospholamban: A crucial regulator of cardiac contractility. *Nat. Rev. Mol. Cell Biol.* **2003**, *4*, 566–577. [[CrossRef](#)]
57. Limas, C.J.; Olivari, M.T.; Goldenberg, I.F.; Levine, T.B.; Benditt, D.G.; Simon, A. Calcium uptake by cardiac sarcoplasmic reticulum in human dilated cardiomyopathy. *Cardiovasc. Res.* **1987**, *21*, 601–605. [[CrossRef](#)]
58. Bellinger, A.M.; Reiken, S.; Carlson, C.; Mongillo, M.; Liu, X.; Rothman, L.; Matecki, S.; Lacampagne, A.; Marks, A.R. Hypernitrosylated ryanodine receptor calcium release channels are leaky in dystrophic muscle. *Nat. Med.* **2009**, *15*, 325–330. [[CrossRef](#)]
59. Hasenfuss, G.; Reinecke, H.; Studer, R.; Meyer, M.; Pieske, B.; Holtz, J.; Holubarsch, C.; Posival, H.; Just, H.; Drexler, H. Relation between myocardial function and expression of sarcoplasmic reticulum Ca^{2+} -ATPase in failing and nonfailing human myocardium. *Circ. Res.* **1994**, *75*, 434–442. [[CrossRef](#)]
60. Dash, R.; Frank, K.F.; Carr, A.N.; Moravec, C.S.; Kranias, E.G. Gender influences on sarcoplasmic reticulum Ca^{2+} -handling in failing human myocardium. *J. Mol. Cell. Cardiol.* **2001**, *33*, 1345–1353. [[CrossRef](#)]
61. Meyer, M.; Schillinger, W.; Pieske, B.; Holubarsch, C.; Heilmann, C.; Posival, H.; Kuwajima, G.; Mikoshiba, K.; Just, H.; Hasenfuss, G. Alterations of sarcoplasmic reticulum proteins in failing human dilated cardiomyopathy. *Circulation* **1995**, *92*, 778–784. [[CrossRef](#)]
62. Townsend, D.W.; Yasuda, S.; Metzger, J. Cardiomyopathy of Duchenne muscular dystrophy: Pathogenesis and prospect of membrane sealants as a new therapeutic approach. *Expert Rev. Cardiovasc. Ther.* **2007**, *5*, 99–109. [[CrossRef](#)] [[PubMed](#)]
63. Houang, E.M.; Sham, Y.Y.; Bates, F.S.; Metzger, J.M. Muscle membrane integrity in Duchenne muscular dystrophy: Recent advances in copolymer-based muscle membrane stabilizers. *Skelet. Muscle* **2018**, *8*, 31. [[CrossRef](#)] [[PubMed](#)]

64. Clafin, D.R.; Brooks, S.V. Direct observation of failing fibers in muscles of dystrophic mice provides mechanistic insight into muscular dystrophy. *Am. J. Physiol. Cell Physiol.* **2008**, *294*, C651–C658. [[CrossRef](#)] [[PubMed](#)]
65. Allen, D.G.; Gervasio, O.L.; Yeung, E.W.; Whitehead, N.P. Calcium and the damage pathways in muscular dystrophy. *Can. J. Physiol. Pharmacol.* **2010**, *88*, 83–91. [[CrossRef](#)] [[PubMed](#)]
66. Prosser, B.L.; Khairallah, R.J.; Ziman, A.P.; Ward, C.W.; Lederer, W.J. X-ROS signaling in the heart and skeletal muscle: Stretch-dependent local ROS regulates $[Ca^{2+}]_i$. *J. Mol. Cell. Cardiol.* **2013**, *58*, 172–181. [[CrossRef](#)]
67. Danialou, G.; Comtois, A.S.; Dudley, R.; Karpati, G.; Vincent, G.; Des Rosiers, C.; Petrof, B.J. Dystrophin-deficient cardiomyocytes are abnormally vulnerable to mechanical stress-induced contractile failure and injury. *FASEB J.* **2001**, *15*, 1655–1657. [[CrossRef](#)]
68. Townsend, D.; Turner, I.; Yasuda, S.; Martindale, J.; Davis, J.; Shillingford, M.; Kornegay, J.N.; Metzger, J.M. Chronic administration of membrane sealant prevents severe cardiac injury and ventricular dilatation in dystrophic dogs. *J. Clin. Invest.* **2010**, *120*, 1140–1150. [[CrossRef](#)]
69. Prosser, B.L.; Ward, C.W.; Jonathan Lederer, W. X-ROS signalling is enhanced and graded by cyclic cardiomyocyte stretch. *Cardiovasc. Res.* **2013**, *98*, 307–314. [[CrossRef](#)]
70. Williams, I.A.; Allen, D.G. The role of reactive oxygen species in the hearts of dystrophin-deficient mdx mice. *Am. J. Physiol. Heart Circ. Physiol.* **2007**, *293*, H1969–H1977. [[CrossRef](#)]
71. Ullrich, N.D.; Fanchaouy, M.; Gusev, K.; Shirokova, N.; Niggli, E. Hypersensitivity of excitation-contraction coupling in dystrophic cardiomyocytes. *Am. J. Physiol. Heart Circ. Physiol.* **2009**, *297*, H1992–H2003. [[CrossRef](#)]
72. Prosser, B.L.; Ward, C.W.; Lederer, W.J. X-ROS signaling: Rapid mechano-chemo transduction in heart. *Science* **2011**, *333*, 1440–1445. [[CrossRef](#)] [[PubMed](#)]
73. Prins, K.W.; Asp, M.L.; Zhang, H.; Wang, W.; Metzger, J.M. Microtubule-Mediated Misregulation of Junctophilin-2 Underlies T-Tubule Disruptions and Calcium Mishandling in mdx Mice. *JACC Basic Transl. Sci.* **2016**, *1*, 122–130. [[CrossRef](#)] [[PubMed](#)]
74. Koenig, X.; Rubi, L.; Obermair, G.J.; Cervenka, R.; Dang, X.B.; Lukacs, P.; Kummer, S.; Bittner, R.E.; Kubista, H.; Todt, H.; et al. Enhanced currents through L-type calcium channels in cardiomyocytes disturb the electrophysiology of the dystrophic heart. *Am. J. Physiol. Heart Circ. Physiol.* **2014**, *306*, H564–H573. [[CrossRef](#)] [[PubMed](#)]
75. Valladares, D.; Almarza, G.; Contreras, A.; Pavez, M.; Buvinic, S.; Jaimovich, E.; Casas, M. Electrical stimuli are anti-apoptotic in skeletal muscle via extracellular ATP. Alteration of this signal in Mdx mice is a likely cause of dystrophy. *PLoS ONE* **2013**, *8*, e75340. [[CrossRef](#)] [[PubMed](#)]
76. Seidlmayer, L.K.; Kuhn, J.; Berbner, A.; Arias-Loza, P.A.; Williams, T.; Kaspar, M.; Czolbe, M.; Kwong, J.Q.; Molkenstin, J.D.; Heinze, K.G.; et al. Inositol 1,4,5-Trisphosphate-mediated sarcoplasmic reticulum-mitochondrial crosstalk influences adenosine triphosphate production via mitochondrial Ca^{2+} uptake through the mitochondrial ryanodine receptor in cardiac myocytes. *Cardiovasc. Res.* **2016**, *112*, 491–501. [[CrossRef](#)] [[PubMed](#)]
77. Chen, X.; Zhang, X.; Kubo, H.; Harris, D.M.; Mills, G.D.; Moyer, J.; Berretta, R.; Potts, S.T.; Marsh, J.D.; Houser, S.R. Ca^{2+} influx-induced sarcoplasmic reticulum Ca^{2+} overload causes mitochondrial-dependent apoptosis in ventricular myocytes. *Circ. Res.* **2005**, *97*, 1009–1017. [[CrossRef](#)]
78. Luongo, T.S.; Lambert, J.P.; Gross, P.; Nwokedi, M.; Lombardi, A.A.; Shanmughapriya, S.; Carpenter, A.C.; Kolmetzky, D.; Gao, E.; Van Berlo, J.H.; et al. The mitochondrial Na^+/Ca^{2+} exchanger is essential for Ca^{2+} homeostasis and viability. *Nature* **2017**, *545*, 93–97. [[CrossRef](#)]
79. Jung, C.; Martins, A.S.; Niggli, E.; Shirokova, N. Dystrophic cardiomyopathy: Amplification of cellular damage by Ca^{2+} signalling and reactive oxygen species-generating pathways. *Cardiovasc. Res.* **2008**, *77*, 766–773. [[CrossRef](#)]
80. Kyrychenko, V.; Poláková, E.; Janiček, R.; Shirokova, N. Mitochondrial dysfunctions during progression of dystrophic cardiomyopathy. *Cell Calcium* **2015**, *58*, 186–195. [[CrossRef](#)]
81. Viola, H.M.; Adams, A.M.; Davies, S.M.K.; Fletcher, S.; Filipovska, A.; Hool, L.C. Impaired functional communication between the L-type calcium channel and mitochondria contributes to metabolic inhibition in the mdx heart. *Proc. Natl. Acad. Sci. USA* **2014**, *111*, E2905–E2914. [[CrossRef](#)]

82. Millay, D.P.; Sargent, M.A.; Osinska, H.; Baines, C.P.; Barton, E.R.; Vuagniaux, G.; Sweeney, H.L.; Robbins, J.; Molkentin, J.D. Genetic and pharmacologic inhibition of mitochondrial-dependent necrosis attenuates muscular dystrophy. *Nat. Med.* **2008**, *14*, 442–447. [[CrossRef](#)] [[PubMed](#)]
83. Giorgio, V.; Soriano, M.E.; Basso, E.; Bisetto, E.; Lippe, G.; Forte, M.A.; Bernardi, P. Cyclophilin D in mitochondrial pathophysiology. *Biochim. Biophys. Acta Bioenerg.* **2010**, *1797*, 1113–1118. [[CrossRef](#)] [[PubMed](#)]
84. Finsterer, J.; Stöllberger, C. The heart in human dystrophinopathies. *Cardiology* **2003**, *99*, 1–19. [[CrossRef](#)] [[PubMed](#)]
85. Connuck, D.M.; Sleeper, L.A.; Colan, S.D.; Cox, G.F.; Towbin, J.A.; Lowe, A.M.; Wilkinson, J.D.; Orav, E.J.; Cuniberti, L.; Salbert, B.A.; et al. Characteristics and outcomes of cardiomyopathy in children with Duchenne or Becker muscular dystrophy: A comparative study from the Pediatric Cardiomyopathy Registry. *Am. Heart J.* **2008**, *155*, 998–1005. [[CrossRef](#)]
86. Cox, G.F.; Kunkel, L.M. Dystrophies and heart disease. *Curr. Opin. Cardiol.* **1997**, *12*, 329–343. [[CrossRef](#)]
87. Frankel, K.A.; Rosser, R.J. The pathology of the heart in progressive muscular dystrophy: Epimycocardial fibrosis. *Hum. Pathol.* **1976**, *7*, 375–386. [[CrossRef](#)]
88. Giglio, V.; Pasceri, V.; Messano, L.; Mangiola, F.; Pasquini, L.; Dello Russo, A.; Damiani, A.; Mirabella, M.; Galluzzi, G.; Tonalì, P.; et al. Ultrasound tissue characterization detects preclinical myocardial structural changes in children affected by Duchenne muscular dystrophy. *J. Am. Coll. Cardiol.* **2003**, *42*, 309–316. [[CrossRef](#)]
89. Sasaki, K.; Sakata, K.; Kachi, E.; Hirata, S.; Ishihara, T.; Ishikawa, K. Sequential changes in cardiac structure and function in patients with Duchenne type muscular dystrophy: A two-dimensional echocardiographic study. *Am. Heart J.* **1998**, *135*, 937–944. [[CrossRef](#)]
90. Takenaka, A.; Yokota, M.; Iwase, M.; Miyaguchi, K.; Hayashi, H.; Saito, H. Discrepancy between systolic and diastolic dysfunction of the left ventricle in patients with Duchenne muscular dystrophy. *Eur. Heart J.* **1993**, *14*, 669–676. [[CrossRef](#)]
91. Ikeda, Y.; Ross, J. Models of dilated cardiomyopathy in the mouse and the hamster. *Curr. Opin. Cardiol.* **2000**, *15*, 197–201. [[CrossRef](#)]
92. Arber, S.; Hunter, J.J.; Ross, J.; Hongo, M.; Sansig, G.; Borg, J.; Perriard, J.C.; Chien, K.R.; Caroni, P. MLP-deficient mice exhibit a disruption of cardiac cytoarchitectural organization, dilated cardiomyopathy, and heart failure. *Cell* **1997**, *88*, 393–403. [[CrossRef](#)]
93. Heckmann, M.B.; Bauer, R.; Jungmann, A.; Winter, L.; Rapti, K.; Strucksberg, K.H.; Clemen, C.S.; Li, Z.; Schröder, R.; Katus, H.A.; et al. AAV9-mediated gene transfer of desmin ameliorates cardiomyopathy in desmin-deficient mice. *Gene Ther.* **2016**, *23*, 673–679. [[CrossRef](#)] [[PubMed](#)]
94. Dai, S.; Yuan, F.; Mu, J.; Li, C.; Chen, N.; Guo, S.; Kingery, J.; Prabhu, S.D.; Bolli, R.; Rokosh, G. Chronic AMD3100 antagonism of SDF-1 α -CXCR4 exacerbates cardiac dysfunction and remodeling after myocardial infarction. *J. Mol. Cell. Cardiol.* **2010**, *49*, 587–597. [[CrossRef](#)] [[PubMed](#)]
95. Michael, L.H.; Entman, M.L.; Hartley, C.J.; Youker, K.A.; Zhu, J.; Hall, S.R.; Hawkins, H.K.; Berens, K.; Ballantyne, C.M. Myocardial ischemia and reperfusion: A murine model. *Am. J. Physiol. Heart Circ. Physiol.* **1995**, *269*, H2147–H2154. [[CrossRef](#)] [[PubMed](#)]
96. Weinstein, D.M.; Mihm, M.J.; Bauer, J.A. Cardiac peroxynitrite formation and left ventricular dysfunction following doxorubicin treatment in mice. *J. Pharmacol. Exp. Ther.* **2000**, *294*, 396–401.
97. Robert, J. Long-term and short-term models for studying anthracycline cardiotoxicity and protectors. *Cardiovasc. Toxicol.* **2007**, *7*, 135–139. [[CrossRef](#)]
98. Teerlink, J.R.; Pfeffer, J.M.; Pfeffer, M.A. Progressive ventricular remodeling in response to diffuse isoproterenol-induced myocardial necrosis in rats. *Circ. Res.* **1994**, *75*, 105–113. [[CrossRef](#)]
99. Oudit, G.Y.; Crackower, M.A.; Eriksson, U.; Sarao, R.; Koziaradzki, I.; Sasaki, T.; Irie-Sasaki, J.; Gidrewicz, D.; Rybin, V.O.; Wada, T.; et al. Phosphoinositide 3-Kinase γ -Deficient Mice Are Protected From Isoproterenol-Induced Heart Failure. *Circulation* **2003**, *108*, 2147–2152. [[CrossRef](#)]
100. Hainsey, T.A.; Senapati, S.; Kuhn, D.E.; Rafael, J.A. Cardiomyopathic features associated with muscular dystrophy are independent of dystrophin absence in cardiovascular. *Neuromuscul. Disord.* **2003**, *13*, 294–302. [[CrossRef](#)]
101. Janssen, P.M.L.; Hiranandani, N.; Mays, T.A.; Rafael-Fortney, J.A. Utrrophin deficiency worsens cardiac contractile dysfunction present in dystrophin-deficient mdx mice. *Am. J. Physiol. Heart Circ. Physiol.* **2005**, *289*, 2373–2378. [[CrossRef](#)]

102. Grady, R.M.; Teng, H.; Nichol, M.C.; Cunningham, J.C.; Wilkinson, R.S.; Sanest, J.R. Skeletal and cardiac myopathies in mice lacking utrophin and dystrophin: A model for Duchenne muscular dystrophy. *Cell* **1997**, *90*, 729–738. [[CrossRef](#)]
103. Deconinck, A.E.; Rafael, J.A.; Skinner, J.A.; Brown, S.C.; Potter, A.C.; Metzinger, L.; Watt, D.J.; Dickson, J.G.; Tinsley, J.M.; Davies, K.E. Utrophin-dystrophin-deficient mice as a model for Duchenne muscular dystrophy. *Cell* **1997**, *90*, 717–727. [[CrossRef](#)]
104. Hearse, D.J.; Sutherland, F.J. Experimental Models for the Study of Cardiovascular Function and Disease Defining the Question and Identifying the Model. *Pharmacol. Res.* **2000**, *41*, 597–603. [[CrossRef](#)] [[PubMed](#)]
105. Cui, J.; Li, J.; Mathison, M.; Tondato, F.; Mulkey, S.P.; Micko, C.; Chronos, N.A.F.; Robinson, K.A. A clinically relevant large-animal model for evaluation of tissue-engineered cardiac surgical patch materials. *Cardiovasc. Revasc. Med.* **2005**, *6*, 113–120. [[CrossRef](#)] [[PubMed](#)]
106. Jugdutt, B.I.; Jelani, A.; Palaniyappan, A.; Idikio, H.; Uweira, R.E.; Menon, V.; Jugdutt, C.E. Aging-related early changes in markers of ventricular and matrix remodeling after reperfused st-segment elevation myocardial infarction in the canine model: Effect of early therapy with an angiotensin II type 1 receptor blocker. *Circulation* **2010**, *122*, 341–351. [[CrossRef](#)]
107. Lee, S.T.; White, A.J.; Matsushita, S.; Malliaras, K.; Steenbergen, C.; Zhang, Y.; Li, T.S.; Terrovitis, J.; Yee, K.; Simsir, S.; et al. Intramyocardial injection of autologous cardiospheres or cardiosphere-derived cells preserves function and minimizes adverse ventricular remodeling in pigs with heart failure post-myocardial infarction. *J. Am. Coll. Cardiol.* **2011**, *57*, 455–465. [[CrossRef](#)]
108. Gorman, J.H.; Gorman, R.C.; Plappert, T.; Jackson, B.M.; Hiramatsu, Y.; St. John-Sutton, M.G.; Edmunds, J. Infarct size and location determine development of mitral regurgitation in the sheep model. *J. Thorac. Cardiovasc. Surg.* **1998**, *115*, 615–622. [[CrossRef](#)]
109. Sampaolesi, M.; Blot, S.; D’Antona, G.; Granger, N.; Tonlorenzi, R.; Innocenzi, A.; Mogno, P.; Thibaud, J.L.; Galvez, B.G.; Barthélémy, I.; et al. Mesoangioblast stem cells ameliorate muscle function in dystrophic dogs. *Nature* **2006**, *444*, 574–579. [[CrossRef](#)]
110. Wang, Z.; Kuhr, C.S.; Allen, J.M.; Blankinship, M.; Gregorevic, P.; Chamberlain, J.S.; Tapscott, S.J.; Storb, R. Sustained AAV-mediated dystrophin expression in a canine model of duchenne muscular dystrophy with a brief course of immunosuppression. *Mol. Ther.* **2007**, *15*, 1160–1166. [[CrossRef](#)]
111. Sun, N.; Yazawa, M.; Liu, J.; Han, L.; Sanchez-Freire, V.; Abilez, O.J.; Navarrete, E.G.; Hu, S.; Wang, L.; Lee, A.; et al. Patient-specific induced pluripotent stem cells as a model for familial dilated cardiomyopathy. *Sci. Transl. Med.* **2012**, *4*, 130ra47. [[CrossRef](#)]
112. Siu, C.W.; Lee, Y.K.; Ho, J.C.Y.; Lai, W.H.; Chan, Y.C.; Ng, K.M.; Wong, L.Y.; Au, K.W.; Lau, Y.M.; Zhang, J.; et al. Modeling of lamin A/C mutation premature cardiac aging using patient-specific induced pluripotent stem cells. *Aging Albany NY* **2012**, *4*, 803–822. [[CrossRef](#)] [[PubMed](#)]
113. Tse, H.F.; Ho, J.C.Y.; Choi, S.W.; Lee, Y.K.; Butler, A.W.; Ng, K.M.; Siu, C.W.; Simpson, M.A.; Lai, W.H.; Chan, Y.C.; et al. Patient-specific induced-pluripotent stem cells-derived cardiomyocytes recapitulate the pathogenic phenotypes of dilated cardiomyopathy due to a novel DES mutation identified by whole exome sequencing. *Hum. Mol. Genet.* **2013**, *22*, 1395–1403. [[CrossRef](#)] [[PubMed](#)]
114. Lin, B.; Li, Y.; Han, L.; Kaplan, A.D.; Ao, Y.; Kalra, S.; Bett, G.C.L.; Rasmussen, R.L.; Denning, C.; Yang, L. Modeling and study of the mechanism of dilated cardiomyopathy using induced pluripotent stem cells derived from individuals with duchenne muscular dystrophy. *DMM Dis. Model. Mech.* **2015**, *8*, 457–466. [[CrossRef](#)] [[PubMed](#)]
115. Recchia, F.A.; Lionetti, V. Animal models of dilated cardiomyopathy for translational research. *Vet. Res. Commun.* **2007**, *31*, 35–41. [[CrossRef](#)] [[PubMed](#)]
116. Chu, G.; Haghighi, K.; Kranias, E.G. From mouse to man: Understanding heart failure through genetically altered mouse models. *J. Cardiac Fail.* **2002**, *8*, S432–S449. [[CrossRef](#)] [[PubMed](#)]
117. Wang, Q.D.; Bohlooly, M.; Sjöquist, P.O. Murine models for the study of congestive heart failure: Implications for understanding molecular mechanisms and for drug discovery. *J. Pharmacol. Toxicol. Methods* **2004**, *50*, 163–174. [[CrossRef](#)]
118. Grady, R.M.; Grange, R.W.; Lau, K.S.; Maimone, M.M.; Nichol, M.C.; Stull, J.T.; Sanes, J.R. Role for α -dystrobrevin in the pathogenesis of dystrophin-dependent muscular dystrophies. *Nat. Cell Biol.* **1999**, *1*, 215–220. [[CrossRef](#)]

119. Li, D.; Long, C.; Yue, Y.; Duan, D. Sub-physiological sarcoglycan expression contributes to compensatory muscle protection in mdx mice. *Hum. Mol. Genet.* **2009**, *18*, 1209–1220. [\[CrossRef\]](#)
120. Han, R.; Rader, E.P.; Levy, J.R.; Bansal, D.; Campbell, K.P. Dystrophin deficiency exacerbates skeletal muscle pathology in dysferlin-null mice. *Skelet. Muscle* **2011**, *1*, 35. [\[CrossRef\]](#)
121. Hosur, V.; Kavirayani, A.; Riefler, J.; Carney, L.M.B.; Lyons, B.; Gott, B.; Cox, G.A.; Shultz, L.D. Dystrophin and dysferlin double mutant mice: A novel model for rhabdomyosarcoma. *Cancer Genet.* **2012**, *205*, 232–241. [\[CrossRef\]](#)
122. Banks, G.B.; Combs, A.C.; Odum, G.L.; Bloch, R.J.; Chamberlain, J.S. Muscle Structure Influences Utrophin Expression in mdx Mice. *PLoS Genet.* **2014**, *10*, e1004431. [\[CrossRef\]](#)
123. Gawlik, K.L.; Holmberg, J.; Durbeej, M. Loss of dystrophin and β -sarcoglycan significantly exacerbates the phenotype of laminin α 2 chain-deficient animals. *Am. J. Pathol.* **2014**, *184*, 740–752. [\[CrossRef\]](#)
124. Monnet, E.; Chachques, J.C. Animal models of heart failure: What is new? *Ann. Thorac. Surg.* **2005**, *79*, 1445–1453. [\[CrossRef\]](#)
125. Dixon, J.A.; Spinale, F.G. Large animal models of heart failure; A critical link in the translation of basic science to clinical practice. *Circ. Heart Fail.* **2009**, *2*, 262–271. [\[CrossRef\]](#)
126. Camacho, P.; Fan, H.; Liu, Z.; He, J.Q. Small mammalian animal models of heart disease. *Am. J. Cardiovasc. Dis.* **2016**, *6*, 70–80.
127. Valentine, B.A.; Cummings, J.F.; Cooper, B.J. Development of Duchenne-type cardiomyopathy. Morphologic studies in a canine model. *Am. J. Pathol.* **1989**, *135*, 671–678.
128. Moise, N.S.; Valentine, B.A.; Brown, C.A.; Erb, H.N.; Beck, K.A.; Cooper, B.J.; Gilmour, R.F. Duchenne's cardiomyopathy in a canine model: Electrocardiographic and echocardiographic studies. *J. Am. Coll. Cardiol.* **1991**, *17*, 812–820. [\[CrossRef\]](#)
129. Devaux, J.Y.; Cabane, L.; Esler, M.; Flaouters, H.; Duboc, D. Non-invasive evaluation of the cardiac function in Golden Retriever dogs by radionuclide angiography. *Neuromuscul. Disord.* **1993**, *3*, 429–432. [\[CrossRef\]](#)
130. Takahashi, K.; Tanabe, K.; Ohnuki, M.; Narita, M.; Ichisaka, T.; Tomoda, K.; Yamanaka, S. Induction of Pluripotent Stem Cells from Adult Human Fibroblasts by Defined Factors. *Cell* **2007**, *131*, 861–872. [\[CrossRef\]](#)
131. Guan, X.; Mack, D.L.; Moreno, C.M.; Strande, J.L.; Mathieu, J.; Shi, Y.; Markert, C.D.; Wang, Z.; Liu, G.; Lawlor, M.W.; et al. Dystrophin-deficient cardiomyocytes derived from human urine: New biologic reagents for drug discovery. *Stem Cell Res.* **2014**, *12*, 467–480. [\[CrossRef\]](#)
132. Tsurumi, F.; Baba, S.; Yoshinaga, D.; Umeda, K.; Hirata, T.; Takita, J.; Heike, T. The intracellular Ca^{2+} concentration is elevated in cardiomyocytes differentiated from hiPSCs derived from a Duchenne muscular dystrophy patient. *PLoS ONE* **2019**, *14*, e0213768. [\[CrossRef\]](#)
133. Verhaart, I.E.C.; Aartsma-Rus, A. Therapeutic developments for Duchenne muscular dystrophy. *Nat. Rev. Neurol.* **2019**, *15*, 373–386. [\[CrossRef\]](#)
134. Griggs, R.C.; Moxley, R.T.; Mendell, J.R.; Fenichel, G.M.; Brooke, M.H.; Pestronk, A.; Miller, J.P. Prednisone in Duchenne Dystrophy: A Randomized, Controlled Trial Defining the Time Course and Dose Response. *Arch. Neurol.* **1991**, *48*, 383–388. [\[CrossRef\]](#)
135. Biggar, W.D.; Harris, V.A.; Eliasoph, L.; Alman, B. Long-term benefits of deflazacort treatment for boys with Duchenne muscular dystrophy in their second decade. *Neuromuscul. Disord.* **2006**, *16*, 249–255. [\[CrossRef\]](#)
136. Spurney, C.F. Cardiomyopathy of duchenne muscular dystrophy: Current understanding and future directions. *Muscle Nerve* **2011**, *44*, 8–19. [\[CrossRef\]](#)
137. Schram, G.; Fournier, A.; Leduc, H.; Dahdah, N.; Therien, J.; Vanasse, M.; Khairy, P. All-cause mortality and cardiovascular outcomes with prophylactic steroid therapy in Duchenne muscular dystrophy. *J. Am. Coll. Cardiol.* **2013**, *61*, 948–954. [\[CrossRef\]](#)
138. Raman, S.V.; Cripe, L.H. Glucocorticoid therapy for Duchenne cardiomyopathy: A Hobson's choice? *J. Am. Heart Assoc.* **2015**, *4*, 1–3. [\[CrossRef\]](#)
139. Barber, B.J.; Andrews, J.G.; Lu, Z.; West, N.A.; Meaney, F.J.; Price, E.T.; Gray, A.; Sheehan, D.W.; Pandya, S.; Yang, M.; et al. Oral corticosteroids and onset of cardiomyopathy in Duchenne muscular dystrophy. *J. Pediatr.* **2013**, *163*, 1080–1084. [\[CrossRef\]](#)
140. Griggs, R.C.; Herr, B.E.; Reha, A.; Elfring, G.; Atkinson, L.; Cwik, V.; Mccoll, E.; Tawil, R.; Pandya, S.; Mcdermott, M.P.; et al. Corticosteroids in Duchenne muscular dystrophy: Major variations in practice. *Muscle Nerve* **2013**, *48*, 27–31. [\[CrossRef\]](#)

141. Hoffman, E.P.; Reeves, E.; Damsker, J.; Nagaraju, K.; McCall, J.M.; Connor, E.M.; Bushby, K. Novel Approaches to Corticosteroid Treatment in Duchenne Muscular Dystrophy. *Phys. Med. Rehabil. Clin. N. Am.* **2012**, *23*, 821–828. [[CrossRef](#)]
142. Bauer, R.; Straub, V.; Blain, A.; Bushby, K.; MacGowan, G.A. Contrasting effects of steroids and angiotensin-converting-enzyme inhibitors in a mouse model of dystrophin-deficient cardiomyopathy. *Eur. J. Heart Fail.* **2009**, *11*, 463–471. [[CrossRef](#)]
143. Janssen, P.M.L.; Murray, J.D.; Schill, K.E.; Rastogi, N.; Schultz, E.J.; Tran, T.; Raman, S.V.; Rafael-Fortney, J.A. Prednisolone attenuates improvement of cardiac and skeletal contractile function and histopathology by lisinopril and spironolactone in the mdx mouse model of duchenne muscular dystrophy. *PLoS ONE* **2014**, *9*, e88360. [[CrossRef](#)]
144. Ogata, H.; Ishikawa, Y.; Ishikawa, Y.; Minami, R. Beneficial effects of beta-blockers and angiotensin-converting enzyme inhibitors in Duchenne muscular dystrophy. *J. Cardiol.* **2009**, *53*, 72–78. [[CrossRef](#)]
145. Dikalov, S.I.; Nazarewicz, R.R. Angiotensin II-induced production of mitochondrial reactive oxygen species: Potential mechanisms and relevance for cardiovascular disease. *Antioxid. Redox Signal.* **2013**, *19*, 1085–1094. [[CrossRef](#)]
146. Dasgupta, C.; Zhang, L. Angiotensin II receptors and drug discovery in cardiovascular disease. *Drug Discov. Today* **2011**, *16*, 22–34. [[CrossRef](#)]
147. Kawai, T.; Forrester, S.J.; O'Brian, S.; Baggett, A.; Rizzo, V.; Eguchi, S. AT1 receptor signaling pathways in the cardiovascular system. *Pharmacol. Res.* **2017**, *125*, 4–13. [[CrossRef](#)]
148. Bernal, J.; Pitta, S.R.; Thatai, D. Role of the renin-angiotensin-aldosterone system in diastolic heart failure: Potential for pharmacologic intervention. *Am. J. Cardiovasc. Drugs* **2006**, *6*, 373–381. [[CrossRef](#)]
149. Duboc, D.; Meune, C.; Pierre, B.; Wahbi, K.; Eymard, B.; Toutain, A.; Berard, C.; Vaksman, G.; Weber, S.; Bécane, H.M. Perindopril preventive treatment on mortality in Duchenne muscular dystrophy: 10 years' follow-up. *Am. Heart J.* **2007**, *154*, 596–602. [[CrossRef](#)]
150. Bangalore, S.; Fakheri, R.; Toklu, B.; Ogedegbe, G.; Weintraub, H.; Messerli, F.H. Angiotensin-Converting Enzyme Inhibitors or Angiotensin Receptor Blockers in Patients Without Heart Failure? Insights from 254,301 Patients from Randomized Trials. *Mayo Clin. Proc.* **2016**, *91*, 51–60. [[CrossRef](#)]
151. Triposkiadis, F.; Karayannis, G.; Giamouzis, G.; Skoularigis, J.; Louridas, G.; Butler, J. The Sympathetic Nervous System in Heart Failure. Physiology, Pathophysiology, and Clinical Implications. *J. Am. Coll. Cardiol.* **2009**, *54*, 1747–1762. [[CrossRef](#)]
152. Klapholz, M. B-Blocker Use for the Stages of Heart Failure. *Mayo Clin. Proc.* **2009**, *84*, 718–729. [[CrossRef](#)]
153. Jefferies, J.L.; Eidem, B.W.; Belmont, J.W.; Craigen, W.J.; Ware, S.M.; Fernbach, S.D.; Neish, S.R.; Smith, E.O.B.; Towbin, J.A. Genetic predictors and remodeling of dilated cardiomyopathy in muscular dystrophy. *Circulation* **2005**, *112*, 2799–2804. [[CrossRef](#)]
154. Kajimoto, H.; Ishigaki, K.; Okumura, K.; Tomimatsu, H.; Nakazawa, M.; Saito, K.; Osawa, M.; Nakanishi, T. Beta-blocker therapy for cardiac dysfunction in patients with muscular dystrophy. *Circ. J.* **2006**, *70*, 991–994. [[CrossRef](#)]
155. Matsumura, T.; Tamura, T.; Kuru, S.; Kikuchi, Y.; Kawai, M. Carvedilol can prevent cardiac events in duchenne muscular dystrophy. *Intern. Med.* **2010**, *49*, 1357–1363. [[CrossRef](#)]
156. Viollet, L.; Thrush, P.T.; Flanigan, K.M.; Mendell, J.R.; Allen, H.D. Effects of angiotensin-converting enzyme inhibitors and/or beta blockers on the cardiomyopathy in duchenne muscular dystrophy. *Am. J. Cardiol.* **2012**, *110*, 98–102. [[CrossRef](#)]
157. Raman, S.V.; Hor, K.N.; Mazur, W.; Halnon, N.J.; Kissel, J.T.; He, X.; Tran, T.; Smart, S.; McCarthy, B.; Taylor, M.D.; et al. Eplerenone for early cardiomyopathy in Duchenne muscular dystrophy: A randomised, double-blind, placebo-controlled trial. *Lancet Neurol.* **2015**, *14*, 153–161. [[CrossRef](#)]
158. Spurney, C.F.; Gueron, A.D.; Yu, Q.; Sali, A.; van der Meulen, J.H.; Hoffman, E.P.; Nagaraju, K. Membrane Sealant Poloxamer P188 Protects Against Isoproterenol Induced Cardiomyopathy in Dystrophin Deficient Mice. *BMC Cardiovasc. Disord.* **2011**, *11*, 20–29. [[CrossRef](#)]
159. Martindale, J.J.; Metzger, J.M. Uncoupling of increased cellular oxidative stress and myocardial ischemia reperfusion injury by directed sarcolemma stabilization. *J. Mol. Cell. Cardiol.* **2014**, *67*, 26–37. [[CrossRef](#)]
160. Ward, M.L.; Williams, I.A.; Chu, Y.; Cooper, P.J.; Ju, Y.K.; Allen, D.G. Stretch-activated channels in the heart: Contributions to length-dependence and to cardiomyopathy. *Prog. Biophys. Mol. Biol.* **2008**, *97*, 232–249. [[CrossRef](#)]

161. Fauconnier, J.; Thireau, J.; Reiken, S.; Cassan, C.; Richard, S.; Matecki, S.; Marks, A.R.; Lacampagne, A. Leaky RyR2 trigger ventricular arrhythmias in Duchenne muscular dystrophy. *Proc. Natl. Acad. Sci. USA* **2010**, *107*, 1559–1564. [CrossRef]
162. Shin, J.H.; Bostick, B.; Yue, Y.; Hajjar, R.; Duan, D. SERCA2a gene transfer improves electrocardiographic performance in aged mdx mice. *J. Transl. Med.* **2011**, *9*, 132–138. [CrossRef]
163. Hoshijima, M.; Ikeda, Y.; Iwanaga, Y.; Minamisawa, S.; Date, M.O.; Gu, Y.; Iwatate, M.; Li, M.; Wang, L.; Wilson, J.M.; et al. Chronic suppression of heart-failure progression by a pseudophosphorylated mutant of phospholamban via in vivo cardiac rAAV gene delivery. *Nat. Med.* **2002**, *8*, 864–871. [CrossRef]
164. Dieterle, T.; Meyer, M.; Gu, Y.; Belke, D.D.; Swanson, E.; Iwatate, M.; Hollander, J.; Peterson, K.L.; Ross, J.; Dillmann, W.H. Gene transfer of a phospholamban-targeted antibody improves calcium handling and cardiac function in heart failure. *Cardiovasc. Res.* **2005**, *67*, 678–688. [CrossRef]
165. Yamada, M.; Ikeda, Y.; Yano, M.; Yoshimura, K.; Nishino, S.; Aoyama, H.; Wang, L.; Aoki, H.; Matsuzaki, M. Inhibition of protein phosphatase 1 by inhibitor-2 gene delivery ameliorates heart failure progression in genetic cardiomyopathy. *FASEB J.* **2006**, *20*, 1–22. [CrossRef]
166. Houang, E.M.; Bartos, J.; Hackel, B.J.; Lodge, T.P.; Yannopoulos, D.; Bates, F.S.; Metzger, J.M. Cardiac Muscle Membrane Stabilization in Myocardial Reperfusion Injury. *JACC Basic Transl. Sci.* **2019**, *4*, 275–287. [CrossRef]
167. Weisleder, N.; Takizawa, N.; Lin, P.; Wang, X.; Cao, C.; Zhang, Y.; Tan, T.; Ferrante, C.; Zhu, H.; Chen, P.J.; et al. Recombinant MG53 protein modulates therapeutic cell membrane repair in treatment of muscular dystrophy. *Sci. Transl. Med.* **2012**, *4*, 139ra85. [CrossRef]
168. Vandebrouck, C.; Martin, D.; Van Schoor, M.C.; Debaix, H.; Gailly, P. Involvement of TRPC in the abnormal calcium influx observed in dystrophic (mdx) mouse skeletal muscle fibers. *J. Cell Biol.* **2002**, *158*, 1089–1096. [CrossRef]
169. Huang, F.; Shan, J.; Reiken, S.; Wehrens, X.H.T.; Marks, A.R. Analysis of calstabin2 (FKBP12.6)-ryanodine receptor interactions: Rescue of heart failure by calstabin2 in mice. *Proc. Natl. Acad. Sci. USA* **2006**, *103*, 3456–3461. [CrossRef]
170. Capogrosso, R.F.; Mantuano, P.; Uaesoontrachoon, K.; Cozzoli, A.; Giustino, A.; Dow, T.; Srinivassane, S.; Filipovic, M.; Bell, C.; Vandermeulen, J.; et al. Ryanodine channel complex stabilizer compound S48168/ARM210 as a disease modifier in dystrophin-deficient mdx mice: Proof-of-concept study and independent validation of efficacy. *FASEB J.* **2018**, *32*, 1025–1043. [CrossRef]
171. Del Monte, F.; Harding, S.E.; Schmidt, U.; Matsui, T.; Kang, Z.B.; Dec, G.W.; Gwathmey, J.K.; Rosenzweig, A.; Hajjar, R.J. Restoration of contractile function in isolated cardiomyocytes from failing human hearts by gene transfer of SERCA2a. *Circulation* **1999**, *100*, 2308–2311. [CrossRef]
172. Miyamoto, M.I.; Del Monte, F.; Schmidt, U.; DiSalvo, T.S.; Kang, Z.B.; Matsui, T.; Guerrero, J.L.; Gwathmey, J.K.; Rosenzweig, A.; Hajjar, R.J. Adenoviral gene transfer of SERCA2A improves left-ventricular function in aortic-banded rats in transition to heart failure. *Proc. Natl. Acad. Sci. USA* **2000**, *97*, 793–798. [CrossRef]
173. Del Monte, F.; Williams, E.; Lebeche, D.; Schmidt, U.; Rosenzweig, A.; Gwathmey, J.K.; Lewandowski, E.D.; Hajjar, R.J. Improvement in survival and cardiac metabolism after gene transfer of sarcoplasmic reticulum Ca²⁺-ATPase in a rat model of heart failure. *Circulation* **2001**, *104*, 1424–1429. [CrossRef]
174. Sakata, S.; Lebeche, D.; Sakata, N.; Sakata, Y.; Chemaly, E.R.; Liang, L.F.; Tsuji, T.; Takewa, Y.; del Monte, F.; Peluso, R.; et al. Restoration of mechanical and energetic function in failing aortic-banded rat hearts by gene transfer of calcium cycling proteins. *J. Mol. Cell. Cardiol.* **2007**, *42*, 852–861. [CrossRef]
175. Niwano, K.; Arai, M.; Koitabashi, N.; Watanabe, A.; Ikeda, Y.; Miyoshi, H.; Kurabayashi, M. Lentiviral vector-mediated SERCA2 gene transfer protects against heart failure and left ventricular remodeling after myocardial infarction in rats. *Mol. Ther.* **2008**, *16*, 1026–1032. [CrossRef]
176. Byrne, M.J.; Power, J.M.; Prevolos, A.; Mariani, J.A.; Hajjar, R.J.; Kaye, D.M. Recirculating cardiac delivery of AAV2/1SERCA2a improves myocardial function in an experimental model of heart failure in large animals. *Gene Ther.* **2008**, *15*, 1550–1557. [CrossRef]
177. Mariani, J.A.; Smolic, A.; Prevolos, A.; Byrne, M.J.; Power, J.M.; Kaye, D.M. Augmentation of left ventricular mechanics by recirculation-mediated AAV2/1SERCA2a gene delivery in experimental heart failure. *Eur. J. Heart Fail.* **2011**, *13*, 247–253. [CrossRef]

178. Jessup, M.; Greenberg, B.; Mancini, D.; Cappola, T.; Pauly, D.F.; Jaski, B.; Yaroshinsky, A.; Zsebo, K.M.; Dittrich, H.; Hajjar, R.J. Calcium upregulation by percutaneous administration of gene therapy in cardiac disease (CUPID): A phase 2 trial of intracoronary gene therapy of sarcoplasmic reticulum Ca²⁺-ATPase in patients with advanced heart failure. *Circulation* **2011**, *124*, 304–313. [[CrossRef](#)]
179. Zsebo, K.; Yaroshinsky, A.; Rudy, J.J.; Wagner, K.; Greenberg, B.; Jessup, M.; Hajjar, R.J. Long-term effects of AAV1/SERCA2a gene transfer in patients with severe heart failure: Analysis of recurrent cardiovascular events and mortality. *Circ. Res.* **2014**, *114*, 101–108. [[CrossRef](#)]
180. Greenberg, B.; Butler, J.; Felker, G.M.; Ponikowski, P.; Voors, A.A.; Desai, A.S.; Barnard, D.; Bouchard, A.; Jaski, B.; Lyon, A.R.; et al. Calcium upregulation by percutaneous administration of gene therapy in patients with cardiac disease (CUPID 2): A randomised, multinational, double-blind, placebo-controlled, phase 2b trial. *Lancet* **2016**, *387*, 1178–1186. [[CrossRef](#)]
181. Kadambi, V.J.; Ponniah, S.; Harrer, J.M.; Hoit, B.D.; Dorn, G.W.; Walsh, R.A.; Kranias, E.G. Cardiac-specific overexpression of phospholamban alters calcium kinetics and resultant cardiomyocyte mechanics in transgenic mice. *J. Clin. Investig.* **1996**, *97*, 533–539. [[CrossRef](#)]
182. Luo, W.; Grupp, I.L.; Harrer, J.; Ponniah, S.; Grupp, G.; Duffy, J.J.; Doetschman, T.; Kranias, E.G. Targeted ablation of the phospholamban gene is associated with markedly enhanced myocardial contractility and loss of β -agonist stimulation. *Circ. Res.* **1994**, *75*, 401–409. [[CrossRef](#)] [[PubMed](#)]
183. Luo, W.; Wolska, B.M.; Grupp, I.L.; Harrer, J.M.; Haghghi, K.; Ferguson, D.G.; Slack, J.P.; Grupp, G.; Doetschman, T.; Solaro, R.J.; et al. Phospholamban gene dosage effects in the mammalian heart. *Circ. Res.* **1996**, *78*, 839–847. [[CrossRef](#)] [[PubMed](#)]
184. Minamisawa, S.; Hoshijima, M.; Chu, G.; Ward, C.A.; Frank, K.; Gu, Y.; Martone, M.E.; Wang, Y.; Ross, J.; Kranias, E.G.; et al. Chronic phospholamban-sarcoplasmic reticulum calcium atpase interaction is the critical calcium cycling defect in dilated cardiomyopathy. *Cell* **1999**, *99*, 313–322. [[CrossRef](#)]
185. Iwanaga, Y.; Hoshijima, M.; Gu, Y.; Iwatate, M.; Dieterle, T.; Ikeda, Y.; Date, M.O.; Chrast, J.; Matsuzaki, M.; Peterson, K.L.; et al. Chronic phospholamban inhibition prevents progressive cardiac dysfunction and pathological remodeling after infarction in rats. *J. Clin. Investig.* **2004**, *113*, 727–736. [[CrossRef](#)]
186. Kaye, D.M.; Prevolos, A.; Marshall, T.; Byrne, M.; Hoshijima, M.; Hajjar, R.; Mariani, J.A.; Pepe, S.; Chien, K.R.; Power, J.M. Percutaneous Cardiac Recirculation-Mediated Gene Transfer of an Inhibitory Phospholamban Peptide Reverses Advanced Heart Failure in Large Animals. *J. Am. Coll. Cardiol.* **2007**, *50*, 253–260. [[CrossRef](#)]
187. Miyazaki, Y.; Ikeda, Y.; Shiraishi, K.; Fujimoto, S.N.; Aoyama, H.; Yoshimura, K.; Inui, M.; Hoshijima, M.; Kasahara, H.; Aoki, H.; et al. Heart failure-inducible gene therapy targeting protein phosphatase 1 prevents progressive left ventricular remodeling. *PLoS ONE* **2012**, *7*, 1–13. [[CrossRef](#)]
188. Rohman, M.S.; Emoto, N.; Takeshima, Y.; Yokoyama, M.; Matsuo, M. Decreased mAKAP, ryanodine receptor, and SERCA2a gene expression in mdx hearts. *Biochem. Biophys. Res. Commun.* **2003**, *310*, 228–235. [[CrossRef](#)]
189. Goonasekera, S.A.; Lam, C.K.; Millay, D.P.; Sargent, M.A.; Hajjar, R.J.; Kranias, E.G.; Molkenin, J.D. Mitigation of muscular dystrophy in mice by SERCA overexpression in skeletal muscle. *J. Clin. Investig.* **2011**, *121*, 1044–1052. [[CrossRef](#)]
190. Mázala, D.A.G.; Pratt, S.J.P.; Chen, D.; Molkenin, J.D.; Lovering, R.M.; Chin, E.R. SERCA1 overexpression minimizes skeletal muscle damage in dystrophic mouse models. *Am. J. Physiol. Cell Physiol.* **2015**, *308*, C699–C709. [[CrossRef](#)]
191. Ikeda, Y.; Martone, M.; Gu, Y.; Hoshijima, M.; Thor, A.; Oh, S.S.; Peterson, K.L.; Ross, J. Altered membrane proteins and permeability correlate with cardiac dysfunction in cardiomyopathic hamsters. *Am. J. Physiol. Heart Circ. Physiol.* **2000**, *278*, H1362–H1370. [[CrossRef](#)]
192. Voit, A.; Patel, V.; Pachon, R.; Shah, V.; Bakhutma, M.; Kohlbrenner, E.; McArdle, J.J.; Dell'Italia, L.J.; Mendell, J.R.; Xie, L.H.; et al. Reducing sarcolipin expression mitigates Duchenne muscular dystrophy and associated cardiomyopathy in mice. *Nat. Commun.* **2017**, *8*, 1068. [[CrossRef](#)] [[PubMed](#)]
193. Chu, G.; Luo, W.; Slack, J.P.; Tilgmann, C.; Sweet, W.E.; Spindler, M.; Saupe, K.W.; Boivin, G.P.; Moravec, C.S.; Matlib, M.A.; et al. Compensatory mechanisms associated with the hyperdynamic function of phospholamban-deficient mouse hearts. *Circ. Res.* **1996**, *79*, 1064–1076. [[CrossRef](#)] [[PubMed](#)]
194. Haghghi, K.; Kolokathis, F.; Pater, L.; Lynch, R.A.; Asahi, M.; Gramolini, A.O.; Fan, G.C.; Tsiapras, D.; Hahn, H.S.; Adamopoulos, S.; et al. Human phospholamban null results in lethal dilated cardiomyopathy revealing a critical difference between mouse and human. *J. Clin. Investig.* **2003**, *111*, 869–876. [[CrossRef](#)] [[PubMed](#)]

195. Schmitt, J.P.; Kamisago, M.; Asahi, M.; Hua Li, G.; Ahmad, F.; Mende, U.; Kranias, E.G.; MacLennan, D.H.; Seidman, J.G.; Seidman, C.E. Dilated cardiomyopathy and heart failure caused by a mutation in phospholamban. *Science* **2003**, *299*, 1410–1413. [[CrossRef](#)]
196. Ha, K.N.; Masterson, L.R.; Hou, Z.; Verardi, R.; Walsh, N.; Veglia, G.; Robia, S.L. Lethal Arg9Cys phospholamban mutation hinders Ca²⁺-ATPase regulation and phosphorylation by protein kinase A. *Proc. Natl. Acad. Sci. USA* **2011**, *108*, 2735–2740. [[CrossRef](#)]
197. Abrol, N.; De Tombe, P.P.; Robia, S.L. Acute inotropic and lusitropic effects of cardiomyopathic R9C mutation of phospholamban. *J. Biol. Chem.* **2015**, *290*, 7130–7140. [[CrossRef](#)]
198. Small, K.M.; Wagoner, L.E.; Levin, A.M.; Kardia, S.L.R.; Liggett, S.B. Synergistic polymorphisms of β 1- and α 2C-adrenergic receptors and the risk of congestive heart failure. *N. Engl. J. Med.* **2002**, *347*, 1135–1142. [[CrossRef](#)]
199. Haghghi, K.; Gregory, K.N.; Kranias, E.G. Sarcoplasmic reticulum Ca-ATPase-phospholamban interactions and dilated cardiomyopathy. *Biochem. Biophys. Res. Commun.* **2004**, *322*, 1214–1222. [[CrossRef](#)]
200. Permyakov, E.A. *Parvalbumin*; Uversky, V.N., Ed.; Nova Science Publishers, Inc.: New York, NY, USA, 2007.
201. Hapak, R.C.; Zhao, H.; Boschi, J.M.; Henzl, M.T. Novel avian thymic parvalbumin displays high degree of sequence homology to oncomodulin. *J. Biol. Chem.* **1994**, *269*, 5288–5296.
202. Pauls, T.L.; Cox, J.A.; Berchtold, M.W. The Ca²⁺-binding proteins parvalbumin and oncomodulin and their genes: New structural and functional findings. *Biochim. Biophys. Acta Gene Struct. Expr.* **1996**, *1306*, 39–54. [[CrossRef](#)]
203. Falke, J.J.; Drake, S.K.; Hazard, A.L.; Peersen, O.B. Molecular Tuning of Ion Binding to Calcium Signaling Proteins. *Q. Rev. Biophys.* **1994**, *27*, 219–290. [[CrossRef](#)]
204. Wahr, P.A.; Michele, D.E.; Metzger, J.M. Parvalbumin gene transfer corrects diastolic dysfunction in diseased cardiac myocytes. *Proc. Natl. Acad. Sci. USA* **1999**, *96*, 11982–11985. [[CrossRef](#)]
205. Huq, F.; Lebeche, D.; Iyer, V.; Liao, R.; Hajjar, R.J. Gene transfer of parvalbumin improves diastolic dysfunction in senescent myocytes. *Circulation* **2004**, *109*, 2780–2785. [[CrossRef](#)] [[PubMed](#)]
206. Rodenbaugh, D.W.; Wang, W.; Davis, J.; Edwards, T.; Potter, J.D.; Metzger, J.M. Parvalbumin isoforms differentially accelerate cardiac myocyte relaxation kinetics in an animal model of diastolic dysfunction. *Am. J. Physiol. Heart Circ. Physiol.* **2007**, *293*, H1705–H1713. [[CrossRef](#)] [[PubMed](#)]
207. Szatkowski, M.L.; Westfall, M.V.; Gomez, C.A.; Wahr, P.A.; Michele, D.E.; DelloRusso, C.; Turner, I.I.; Hong, K.E.; Albayya, F.P.; Metzger, J.M. In vivo acceleration of heart relaxation performance by parvalbumin gene delivery. *J. Clin. Investig.* **2001**, *107*, 191–198. [[CrossRef](#)] [[PubMed](#)]
208. Michele, D.E.; Szatkowski, M.L.; Albayya, F.P.; Metzger, J.M. Parvalbumin gene delivery improves diastolic function in the aged myocardium in vivo. *Mol. Ther.* **2004**, *10*, 399–403. [[CrossRef](#)] [[PubMed](#)]
209. Schmidt, U.; Zhu, X.; Lebeche, D.; Huq, F.; Guerrero, J.L.; Hajjar, R.J. In vivo gene transfer of parvalbumin improves diastolic function in aged rat hearts. *Cardiovasc. Res.* **2005**, *66*, 318–323. [[CrossRef](#)]
210. Coutu, P.; Metzger, J.M. Genetic manipulation of calcium-handling proteins in cardiac myocytes. II. Mathematical modeling studies. *Am. J. Physiol. Heart Circ. Physiol.* **2005**, *288*, H613–H631. [[CrossRef](#)]
211. Coutu, P.; Metzger, J.M. Genetic manipulation of calcium-handling proteins in cardiac myocytes. I. Experimental studies. *Am. J. Physiol. Heart Circ. Physiol.* **2005**, *288*, H601–H612. [[CrossRef](#)]
212. Coutu, P.; Metzger, J.M. Optimal range for parvalbumin as relaxing agent in adult cardiac myocytes: Gene transfer and mathematical modeling. *Biophys. J.* **2002**, *82*, 2565–2579. [[CrossRef](#)]
213. Wang, W.; Barnabei, M.S.; Asp, M.L.; Heinis, F.I.; Arden, E.; Davis, J.; Braunlin, E.; Li, Q.; Davis, J.P.; Potter, J.D.; et al. Noncanonical EF-hand motif strategically delays Ca²⁺ buffering to enhance cardiac performance. *Nat. Med.* **2013**, *19*, 305–314. [[CrossRef](#)] [[PubMed](#)]
214. Asp, M.L.; Sjaastad, F.V.; Siddiqui, J.K.; Davis, J.P.; Metzger, J.M. Effects of Modified Parvalbumin EF-Hand Motifs on Cardiac Myocyte Contractile Function. *Biophys. J.* **2016**, *110*, 2094–2105. [[CrossRef](#)] [[PubMed](#)]
215. Liao, R.; Nascimben, L.; Friedrich, J.; Gwathmey, J.K.; Ingwall, J.S. Decreased energy reserve in an animal model of dilated cardiomyopathy: Relationship to contractile performance. *Circ. Res.* **1996**, *78*, 893–902. [[CrossRef](#)] [[PubMed](#)]





Review

Duchenne Dilated Cardiomyopathy: Cardiac Management from Prevention to Advanced Cardiovascular Therapies

Rachele Adorisio ^{1,*}, Erica Mencarelli ¹, Nicoletta Cantarutti ², Camilla Calvieri ², Liliana Amato ¹, Marianna Cicienia ², Massimo Silvetti ², Adele D'Amico ³, Maria Grandinetti ^{1,4}, Fabrizio Drago ² and Antonio Amodeo ¹

¹ Heart Failure Clinic-Heart Failure, Heart Transplant, Mechanical Circulatory Support Unit, Department of Pediatric Cardiology and Cardiac Surgery, Heart and Lung Transplant, Bambino Gesù Children's Hospital, IRCCS, 00165 Rome, Italy; erica.mencarelli@opbg.net (E.M.); liliana.amato@opbg.net (L.A.); marigra525@gmail.com (M.G.); antonio.amodeo@opbg.net (A.A.)

² Pediatric Cardiology and Cardiac Arrhythmias/Syncope Unit, Department of Pediatric Cardiology and Cardiac Surgery, Bambino Gesù Children's Hospital, IRCCS, 00165 Rome, Italy; nicoletta.cantarutti@opbg.net (N.C.); camilla.calvieri@opbg.net (C.C.); marianna.cicienia@opbg.net (M.C.); mstefano.silvetti@opbg.net (M.S.); fabrizio.drago@opbg.net (F.D.)

³ Neuromuscular Disease, Genetic and Rare Disease Research Area, Bambino Gesù Children's Hospital, IRCCS, 00165 Rome, Italy; adele2.damico@opbg.net

⁴ Department of Cardiovascular and Thoracic Sciences, Fondazione Policlinico Universitario A, Gemelli IRCCS, 20097 Rome, Italy

* Correspondence: rachele.adorisio@opbg.net; Tel.: +39-06-6859-2217; Fax: +39-06-6859-2607

Received: 20 August 2020; Accepted: 29 September 2020; Published: 1 October 2020

Abstract: Duchenne muscular dystrophy (DMD) cardiomyopathy (DCM) is characterized by a hypokinetic, dilated phenotype progressively increasing with age. Regular cardiac care is crucial in DMD care. Early recognition and prophylactic use of angiotensin converting enzyme inhibitors (ACEi) are the main stay therapeutic strategy to delay incidence of DMD-DCM. Pharmacological treatment to improve symptoms and left ventricle (LV) systolic function, have been widely implemented in the past years. Because of lack of DMD specific drugs, actual indications for established DCM include current treatment for heart failure (HF). This review focuses on current HF strategies to identify, characterize, and treat DMD-DCM.

Keywords: duchenne muscular dystrophy; dilated cardiomyopathy; heart failure

1. Introduction

Dilated cardiomyopathy (DCM), arrhythmias, and congestive heart failure (HF) represent the most important life-limiting condition in Duchenne muscular dystrophy (DMD) [1–3].

Routinely cardiovascular evaluation including echocardiography is recommended in the current 2018 DMD Care consideration sponsored by Centers of disease control and prevention [4]. Moreover, HF treatments have evolved tremendously since 1980s and the armamentarium of adult HF specialists has been enriched with new drugs and the use of device (i.e., cardiac resynchronization therapy, intracardiac defibrillator, and ventricular assist device) before cardiac transplant. DMD patients are not usually candidate for heart transplantation because of the progressive skeletal myopathy, limited functional capacity [5], and shortage of donor availability.

In this review, we present the cardiologist perspective on current data regarding clinical management of DMD patients.

2. Pathophysiology of DMD-DCM

DMD is an X-linked recessive disorder occurring in one in 3500 male births. It is caused by mutations in the dystrophin gene that result in marked reduction or absence of the sarcolemmal protein dystrophin.

DMD belongs to the group of dystrophinopathies, characterized by different pathogenic conditions and variable degrees of skeletal and cardiac muscle impairment. Typically, DMD is the most severe form while Becker muscular dystrophy (BMD) is the more benign form along with the X-linked DCM (XL-DCM) [6,7] and the cardiomyopathy of DMD/BMD carriers [8].

Several patho-mechanisms are involved in the cellular damage initially caused by the lack of dystrophin, in both skeletal and cardiac muscles. Normally dystrophin provides structural support for the myocyte and sarcolemmal membrane by its linking of actin at the C amino-terminus with the dystrophin-associated protein complex and sarcolemma at the carboxyl-terminus and the extracellular matrix of muscle [9,10]. Dystrophin is also present in T-tubular membranes of cardiac myocytes. Thus, it is involved in the maintenance of membrane stability and in the transduction of mechanical force from the sarcomeres to the extracellular matrix. The absence of the dystrophin leads to an extreme vulnerability of the cellular membranes; cellular stress could be directly mediated by the lack of dystrophin, or indirectly via intracellular Ca^{2+} overload or oxidative stress. The activation of these damaging cellular pathways and Ca^{2+} signaling pathways lead to dystrophic DCM [11]. As muscle disease progresses, skeletal and cardiac myocytes necrotize and mechanisms of repair are not adequate, with consequent progressive replacement by fibrofatty tissue [12].

DMD-DCM is characterized by thinner left ventricle (LV) wall and progressive LV dilatation, reflecting the ongoing myocyte loss [1,5]. In particular the repetitive mechanical stress leads to apoptosis and fibrotic substitution and scarring that proceeds from the epicardium to the endocardium, starting generally at the region behind the posterior and mitral valve apparatus. This scarring spreads downward progressively toward the apex and around the heart, ultimately leading to DCM [13,14].

Clinical Course

Typically, this devastating disease is characterized by progressive skeletal muscle waste, with loss of ambulatory capacity and decline of respiratory and cardiac functions. The onset of muscle weakness is at 7–12 years old and the patient become wheel chair bound at 13 years [15]. The standard use of non-invasive home ventilators and the advance in respiratory care has changed the prognosis and prolonged survival [16]. DCM can occur at any age but often presents around 14–15 years and is very common in patients over 18 years of age [17]. It remains asymptomatic for many years in spite of the progression of cardiac dysfunction, because energy expenditure and oxygen consumption are severely diminished by muscle weakness. The degree of skeletal muscle weakness does not correlate with the severity of cardiomyopathy in patients, individual evaluation is important in order to tailor therapy and clinical assessment. Connuck et al. [5] demonstrated that the mortality rate for DMD patients with cardiomyopathy is significantly worse than that of BMD patients (who often undergo transplant) and similarly aged myocarditis and idiopathic DCM patients. The echocardiographic analysis on clinical course showed that the progression of the cardiomyopathy is slower in DMD when compared to Becker or other forms of cardiomyopathy.

3. Cardiovascular Management

Current 2018 DMD Care Considerations assessed that regular cardiac assessment is essential for DMD care [4]. From the time of DMD diagnosis, every effort should be focused to detect the early onset and the progression of the DCM. Early recognition is also crucial for therapy, conditioning the life expectancy. In non-ambulatory, asymptomatic patient serial evaluation is necessary to assess the progression of the disease. Clinical evaluation remains challenging because most of these patients have often low blood pressure values, cool extremities because of reduced skeletal muscular mass.

Therefore, these clinical features require multiparametric evaluation in order to differentiate whether the cardiac process is ongoing.

4. Cardiovascular Biomarkers

Several biomarkers are currently used in the diagnosis and monitoring of cardiac disease.

Electrocardiogram and cardiac imaging are routinely used to detect the onset of DCM and its progression [5]. These non-invasive tests provide useful information about left and right ventricular function, both systolic and diastolic.

In addition, serum biomarkers provided to be very useful to characterize HF and are currently used to assess the functional status in adult and pediatric patients. In particular, serum levels of cardiac troponin I and T are known to be associated to the extension of myocardial damage, but there are conflicting results about their diagnostic and prognostic implications in the DMD DCM [18–20]. Recently, Voleti et al. [21] demonstrated that troponin I levels were significantly elevated in subjects with mild late gadolinium enhancement (LGE) compared to those without LGE. Interestingly, there was a lack of positive association between troponin levels and moderate-to-severe LGE probably because of a decreased enzyme leak at later stages of the disease, when most of myocardium has already been substituted by fibrofatty tissue. Hence, Troponin I could provide useful information to monitor patients in the clinical practice and further studies are required [21].

Elevation of left atrial pressure as result of left ventricular dysfunction and pulmonary hypertension caused by impairment of the respiratory muscles are considered to be involved in the mechanism of increased values of plasma natriuretic peptide in patients with DMD. A moderate or marked elevation in plasma alpha-ANP levels in patients with terminal DMD were found as a sign of a poor prognosis and may be a useful index for the management of the disease [22]. Villa et al. [23] reported a significant correlation between cystatin C, eGFR with cardiac dysfunction, providing for the first time a novel marker to evidence cardio-renal syndrome in patients with DMD.

5. Imaging

5.1. Transthoracic Echocardiography

Echocardiography plays the main role in identifying LV myocardial dysfunction and serial evaluation is necessary. Regional abnormalities of LV function may be revealed by early other imaging modalities such as speckle tracking echocardiography or cardiac magnetic resonance, before the overt LV dysfunction, assessed by echocardiography [24].

By baseline echocardiography, a dilated LV has been defined in terms of standard deviations, assessed with Z-scores according to the wide variability in the age and body mass index in DMD patients. In particular, LV dysfunction is defined by a LVEF < 55% and a fractional shortening (FS) < 28% [25,26]. Correlation of 2D and 3D echo techniques for LV diastolic (LVEDV) and systolic volumes (LVESV) was significantly positive, although 3D LVEDV and LVESV were lower when compared to 2D results; meanwhile LV ejection fraction estimation resulted similar by the two methods [27]. However, fractional shortening (FS) has been considered the best surrogate of LV systolic function, with respect to LVEF, for its high reproducibility [28]. FS showed a greater intraclass coefficient (ICC) than LV EF, not depending by age and magnitude of measures [28]. Regarding diastolic function, increased mitral A-wave velocities and lower E/A ratio, lower DTI lateral peak E-wave velocities were observed in DMD patients, compared to age-matched controls [28]. Another early marker of cardiac LV dysfunction in DMD patients is the myocardial performance index (MPI) obtained using both pulse-wave Doppler (PWD) and Doppler tissue imaging (DTI). On the basis of intraclass coefficient correlation (ICC), MPI obtained with DTI was more reproducible. Speckle tracking echocardiography is a technique able to evaluate subclinical LV dysfunction before development of overt LVEF reduction and has been increasingly used in DMD patients. Myocardial strain, obtained by 2D speckle tracking echocardiography is abnormal in nearly 50% of DMD patients, showing lower global longitudinal strain (GLS) values compared to healthy children,

despite a normal LVEF [29,30]. Moreover, a decrease of 0.34% per year of GLS in DMD patients according to age has been recently reported [31]. In this prospective multicenter cross-sectional study, a difference in longitudinal, radial, and circumferential strain, respectively of 3.6%, 9%, and 3.8% between DMD children and matched control subjects was observed with significantly lower values in the inferolateral and anterolateral mid-basal segments [31]. Several retrospective studies previously analyzed circumferential and longitudinal strain in DMD patients, using 2D speckle tracking, with a larger magnitude of difference for these indices [25,28]. However, speckle tracking analysis is often limited in DMD because echocardiographic image quality is poor in these patients and declines by 2.5% for each 1-year increase in age [32]. Poor echocardiographic window is due to chest deformities, lung hyperinflation, and limited mobility. A suboptimal echocardiographic quality, defined as more than 30% of segments inadequately visualized, was found in 50% of 13-years-old DMD patients and 78% of 15-years-old patients [32]. Indeed, LV ejection fraction, obtained by echocardiography, has been demonstrated to correlate poorly with cardiac magnetic resonance (CMR) [26], while two-dimensional fractional shortening and 5/6 area length LVEF correlated strongly with CMR LVEF [25]. Echocardiographic reproducibility of FS and 5/6 area length LVEF has been demonstrated in DMD patients, although seemed to underestimate LV function compared to CMR [25].

Right ventricular (RV) function is often preserved in DMD patients, also in presence of LV dysfunction, probably because of the reduced afterload related to respiratory improvements [33]. However, right ventricle is well studied by CMR because of its high spatial resolution and reproducible data on RV myocardial deformation. In detail, Mehmood et al. [33] reported RV normal values in patients with severe LV dysfunction, and only in few cases advanced RV dysfunction.

5.2. Cardiac Magnetic Resonance

Cardiac magnetic resonance is assuming an increasingly important role in DMD DCM, for the ability to identify myocardial fibrosis. Both 2D and 3D LV echocardiographic ejection fractions have a low correlation with CMR LVEF [25], and segmental analysis underestimated wall motion abnormalities detected by CMR. Indeed, CMR, not being limited by body habitus, can provide a complete and more accurate three-dimensional analysis of global and segmental LV function if compared to echocardiography with a better reproducibility. Different clinical settings have recently proved the utility of CMR in DMD patients, such as to stratify severity of myocardial involvement, or to assess the efficacy of anti-remodeling therapy in multicenter trials [34,35] to screen asymptomatic DMD female carriers [36,37], to evaluate perioperative cardiac risk. CMR allows a non-invasive myocardial tissue characterization by LGE and T1 mapping techniques, using non-ionizing radiations. The presence of a transmural LGE pattern, often located at the infero-lateral wall, is an independent predictor of adverse cardiac events in DMD patients, also in those with a preserved LVEF [38]. Furthermore, LGE pattern and distribution, ranging from subepicardial to transmural involvement, stratifies the degree of LV dysfunction severity. The presence of subepicardial LGE in the inferolateral free LV wall is a common finding in CMR of DMD patients [39] (Figure 1). In nearly 45% of DMD female carriers, a similar LGE distribution is observed [36,37,40] and it is also associated with a higher clinical class severity and myocardial enzyme release [41]. CMR is also useful to follow the development of LGE over time in DMD patients and carriers able to predict early LVEF decline, considering the higher LVEF reduction described in DMD patients with LGE, independently from age and steroid therapy [42]. However, LGE can detect focal macroscopic fibrosis, while T1 mapping technique pre- and post-contrast is able to quantify diffuse myocardial fibrosis and extracellular volume expansion (ECV). In DMD patients, T1 mapping has been demonstrated to identify early myocardial fibrosis in absence of LGE [43]. Nevertheless, significant differences in T1 mapping values were observed according to the type of T1 mapping sequence used. Previously, Soslow et al. [44] reported increased ECV values in DMD patients if compared with controls, even in cases of preserved LVEF and in the absence of LGE. Olivieri et al. [43] demonstrated the ability of native T1 mapping, by SASHA and MOLLI sequences, to stratify the presence of fibrosis also in LGE-absence. Thus, T1 mapping in DMD

patients is a surrogate marker of early subclinical involvement detectable before LGE development without the need of contrast. However, T1 mapping has several limitations depending on the type of sequence used, heart rate, different vendors, and inability to discriminate diffuse myocardial fibrosis from inflammation or fat infiltration [45,46]. Finally, myocardial strain analysis may also be obtained by CMR, using feature-tracking technique. Circumferential global myocardial strain has been detected to be more impaired in DMD patients compared to controls, with more pronounced differences in anterolateral, inferolateral, and inferior segments [47]. On the contrary of 2D speckle tracking derived strain, CMR-FT is able to discriminate different values between LGE-positive and LGE-negative areas in DMD patients compared to controls, and also among segments within LGE areas [48].

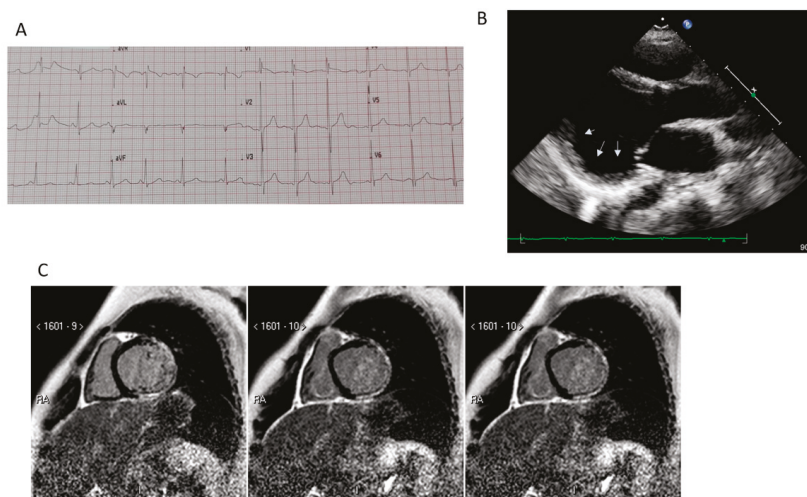


Figure 1. Clinical features of Duchenne muscular dystrophy cardiomyopathy (DMD-DCM). Panel (A): typical EKG with sinus tachycardia and tall R waves. Panel (B): parasternal long axis view of left ventricle (LV). Arrows indicate the presence of posterior wall aneurysm. Panel (C): cardiac magnetic resonance: short axis view of the LV. Presence of a transmurular late gadolinium enhancement pattern located at the infero-lateral wall (Courtesy of Dr. A. Secinaro).

Cardiac magnetic resonance in DMD DCM is important not only to detect early myocardial changes in case of subtle LV dysfunction, but also to evaluate progression of fibrosis in DMD patients on medical treatment [34,35]. However, the high costs, patient's claustrophobia and the length of the CMR study often limit its use in many clinical centers.

6. Therapeutic Strategy for DCM

Usually HF restricts the definition to the manifestation of clinical symptoms. Before clinical symptoms manifest, DCM progresses. Most of the DMD patients are asymptomatic for most of their life, so identifying precursors of the HF is crucial to manage this group. Demonstration of the ventricular dysfunction based on the assessment of ejection fraction help to guide therapy. DMD DCM really comprises a wide range of patients, from those with normal LVEF (typically considered as $\geq 50\%$) to those with reduced LVEF. Patients with an LVEF in the range of 40–49% represent a "grey area," considered as a mid-range of DCM. In the following section, we evaluate all cardiovascular drug therapies according to LVEF [49] (Figure 2).

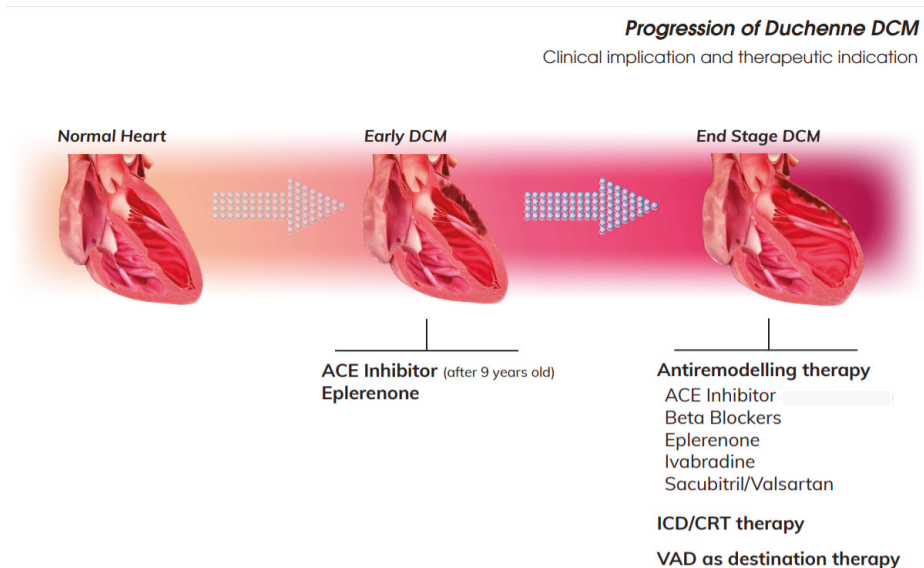


Figure 2. Progression of DMD-DCM. According to clinical stage of the DMD-DCM, different strategy might be considered. ACE: Angiotensin Converting Enzyme; CRT: Cardiac Resynchronization Therapy; ICD: IntraCardiac Defibrillator; VAD: Ventricular Assist Device.

6.1. Early DCM

This group includes all cases in which LVEF is normal or $\geq 50\%$. At this stage of the disease, the aim is to delay the onset of ventricular dysfunction. Because of lack of specific therapy for DMD DCM, 2018 DMD Care Considerations [4] recommend traditional first line HF with ACE-I or angiotensin receptor blockers (ARBs).

In 2005, Duboc [50] for the first time reported a two-phase study conducted over five years for the prophylactic use of perindopril for DMD-DCM. This study was designed to evaluate the effect of perindopril on the development and progression to LV dysfunction. In a multicenter study, 57 children aged 9.5 to 13 years with normal cardiac examination and LVEF of more than 55% at baseline as measured by radionuclide ventriculography, were randomized to perindopril 2–4 mg versus placebo. Chi-squared analysis showed a significant benefit for patients treated in order to prevent the progression of DCM, defined as reduction of LVEF below 45%. After this study, ACEi have been prescribed for prevention.

6.2. DCM with Mid-Range Reduction of LVEF

Few studies have been addressed for DMD patients with mid-range systolic LV dysfunction.

Current indication endorses the use of traditional HF treatment to treat the progression of the disease. In detail, for mid-range ventricular dysfunction, some studies have shown some beneficial effect to preserve ventricular function. Among ACE inhibitors, lisinopril and losartan have been used for comparative analysis in established DCM. Allen 2013 [51] compared the effects of lisinopril (an ACEi) 0.07 mg/kg (5 mg/day) with losartan (an ARB) 0.7 mg/kg (25 mg/day) in a randomized, double-blind, controlled trial of 22 DMD patients. Interestingly, if the LVEF decreased by 5 to 10% the initial dose was doubled. This trial showed no significant difference between lisinopril and losartan in preserving or improving ventricular function.

Cardioprotective effect of adding eplerenone to an ACE inhibitor or ARB was evaluated by MRI after 12 months in 42 DMD patients. This multicenter, randomized, placebo-controlled trial, Raman et al. [35] showed that eplerenone slowed the rate of decline of magnetic resonance (MR)-assessed left ventricular circumferential strain and LVEF at 12 months, when compared to the placebo group.

Raman et al. showed that also spironolactone added to background therapy is noninferior to eplerenone in preserving contractile function. These findings support early mineralocorticoid receptor antagonist therapy as effective and safe in a genetic disease with high cardiomyopathy risk [52].

Therefore, at the early stage of the disease, before any clinical overt DCM, the prophylactic use of perindopril for cardioprotection is entered widely in the clinical practice and endorsed by current indication although biological effects are still unclear. When the DCM is detectable even in case of mild reduction of ejection fraction (>45% LVEF), fosinopril or losartan with the combination of mineralocorticoid receptor antagonists (i.e., eplerenone) might improve ventricular function.

In addition, beta blockers (BB) have been tested. Carvedilol was administered in 22 patients and was progressively uptitrated over 8 weeks. This therapy modestly improved cardiac MRI-derived measured ejection fraction (41% +/- 8.3% to 43% +/- 8%; $p < 0.02$), as well as the mean rate of pressure rise (dp/dt) during isovolumetric contraction (804 +/- 216 to 951 +/- 282 mmHg/s; $p < 0.05$) and the myocardial performance index (0.55 +/- 0.18 to 0.42 +/- 0.15; $p < 0.01$) [53].

6.3. Patients with Severe Ventricular Dysfunction

While in recent years, many studies have focused on the early identification of myocardial damage and the early start of cardiac therapy capable of slowing cardiac remodeling has been emphasized in DMD, the therapeutic strategy for patients with established DCM has been studied less deeply [3,16,54]. Current indication recommends all drugs used for HF treatment.

Although in adult HF, the use of betablockers is mandatory when ventricular function declines, the same evidence in children is lacking. In recent years, some retrospective and non-randomized prospective studies have demonstrated the beneficial effect of BB therapy in patients with DMD/DCM [52,55–58], while in some others this positive effect was not observed [59,60]. Although most of the studies are retrospective including various ages, BB in adjunct to ACEi showed to improve 5-year and 7-year survival rates [58], and also improving ventricular function [56]. These conflicting results have contributed to variable and often delayed initiation of BB use in DMD. However, BBs are usually added to ACEi/ARB when a sufficient improvement in cardiac function is not achieved with the initial therapy.

Furthermore, in DMD DCM, this therapy is often indicated for the presence of autonomic dysfunction and the consequent predisposition to arrhythmias [61].

In the current literature the drugs most frequently used are Carvedilol (0.01–0.02 mg/kg administered twice daily and slowly increased to a dose of 0.5–1 mg/kg) [53,55–57,59], Bisoprolol (3–4 mg per day) [58], and Metoprolol (1 to 2 mg/kg/day) [55,60].

In many studies the combination therapy with ACEi and BBs has been proved to be superior to ACEi alone in the improvement of LV function, [53,56] in the prevention of major cardiac events (death, deterioration of HF, and severe arrhythmias) [57] and in long-term survival [58].

It was noted that in patients treated with BBs the improvement of LVEF was correlated with the reduction of mean heart rate (HR) [57].

6.4. End Stage of DCM DMD

Our group has recently demonstrated the utility of the HR reduction (HRR) strategy obtained with BBs and Ivabradine (2.5 mg twice daily increasing until 15 mg daily every two weeks when HR was still above 70 bpm and LVEF < 40%) in the reduction of the long-term incidence of acute adverse events in DMD patients with advanced cardiac involvement [62]. Previously, ivabradine had been proven to be effective in reducing HR and in improving LVEF in a multicenter, randomized, placebo-controlled trial in children with DCM and symptoms of HF. Unfortunately in this trial DMD patients were excluded and a follow-up of only six months was considered [63].

According to European and American Guidelines for the management of HF in adults, MRAs, spironolactone, and eplerenone, are recommended in all symptomatic patients (despite treatment with an ACEi and BB) with HF and LVEF \leq 35%, to reduce mortality and HF hospitalization [49,64].

In the near future a new MRA called vamorolone, able to mirror the anti-inflammatory effect of glucocorticoids, probably could be a valid alternative to both “old MRAs” and “simple glucocorticoids” in the DMD therapy scenario [65]. To date there are no studies about the use of MRAs in advanced phase of DCM in DMD patients. Despite this, eplerenone or spironolactone are currently used in these patients, at the discretion of the cardiologist, in addition to therapy with ACEi and BB, as long as they do not have renal insufficiency and hyperkalemia.

Sacubitril/valsartan, the first-in-class angiotensin receptor neprilysin inhibitor (ARNI) that in the past decade has changed the treatment of adult HF, has recently been approved by the Food and Drugs Administration (FDA) for the treatment of pediatric patients (aged 1 to 18 years) with symptomatic HF and systemic LV systolic dysfunction. This approval was based on the major reduction in the value of N-terminal pro-B-type natriuretic peptide (NT-proBNP) that was observed in sacubitril/valsartan arm compared to enalapril one after 12 weeks of therapy from the ongoing 52-week PANORAMA-HF trial [66]. Of note, DMD patients are included in the trial.

6.5. Symptomatic Drugs

Furosemide is the most common loop diuretic used to reduce systemic and pulmonary congestion and the correlated symptoms in the advanced stage of disease. For chronic use, 1 to 6 mg/kg of furosemide in partitioned doses are used. The addition of metolazone (0.1 mg/kg dose bis-in-die up to max 20 mg/day) may be useful in patients who are unresponsive to loop diuretic agents alone [67].

It is important to remark that loop diuretics are symptomatic medications and there is no evidence of their effectiveness in improving long-term prognosis [68].

Digoxin has been a pivotal drug in the treatment of HF in children and also reported as standard therapy for treatment of DCM DMD [5]. Today its use has decreased significantly in favor of more effective and safe drugs such ACEi and BBs [67,69].

In patients with severe LV dysfunction an antithrombotic therapy should be considered in the primary prevention of thromboembolic events, although not routinely recommended [70].

7. Advanced Cardiac Therapies

7.1. Heart Transplant and Mechanical Assist Device

A possible treatment for end-stage HF in these patients is the use of left ventricle assist device (LVAD) as a destination therapy (DT) [71,72]. Recently, one patient has been transplanted after 47 months of Heart Ware L-VAD assistance and after accurate respiratory and orthopedic workup. After three months the follow-up was uneventful [73].

LVAD has been currently used in adult and pediatric population with end-stage HF as bridge to heart transplantation or as DT in selected adult patients with medically refractory HF who are not transplant candidates [74–77]. The mechanical assist devices have established their utility in increasing cardiac output and reversing end-organ damage [75–78]. LVAD therapy significantly produced a reverse ventricular remodeling through different mechanisms: reducing ventricular size, LV mass, and at microscopic level myocyte hypertrophy and improving function [79–85].

LVADs have been recently considered as a therapeutic option as destination therapy in DMD with advanced HF [86–88]. The use of mechanical circulatory support in DMD has been described in case reports and small series [86,87,89–93].

Selection of patients is crucial and several aspects should be considered (i.e., kyphoscoliosis, respiratory muscle weakness, and recovery and rehabilitation after surgery). Analysis of costs [94] showed that DT-VAD in DMD exceeds cost-effectiveness thresholds but was similar to cost-effectiveness estimates of DT-VAD in adults who are not transplant candidates.

7.2. Ethical Aspects

Actually, end-of-life management preferences in neuromuscular diseases, including DMD, are a challenging area. Ethical concerns remain open about which patient should be a candidate or excluded. Additionally, The Working Group acknowledged the value of a long-term patient/family/physician relationship before the urgent need for device placement [72]. A multidisciplinary approach with careful evaluation of frailty and co-morbidities is crucial to assess the proper selection of DMD patients. A shared decision process is necessary to obtain a collaborative contact with patient, parents, and caregivers, making this strategy successful [95,96].

8. Arrhythmias in DMD

Arrhythmias occur frequently in cardiomyopathies. They may be also isolated manifestations, mostly in myotonic dystrophies and muscle channelopathies [97]. Potentially fatal arrhythmias are terminal events, and require the implantation of intracardiac defibrillator (ICD). ECG may show right axis deviation, deep and narrow Q waves in inferolateral leads, conduction defects, sinus tachycardia, short PR intervals, and tall R wave in the right precordial leads, right bundle branch block and flat and inverted T waves [98]. In a large multicenter French study, left bundle branch block was present in 13% of patients; 2/3 of them disclosed exonic deletions. Left bundle branch block was significantly associated with cardiac events and mortality [99]. The incidence of supraventricular (6%) and ventricular arrhythmia (VT, 2%) was low in that study, in line with previous data that reported atrial flutter in 5%, sinus pause 5% [100], VT in 7% [101]. Others described that the QRS duration tended to increase progressively with age, irrespective of LV systolic function in patients with DMD [102].

8.1. Electrophysiologic Characteristics

Arrhythmias are observed in a mouse model of DMD after acute β -adrenergic stimulation. In men, a case reported arrhythmic storm after abrupt withdrawal of beta-blocker therapy [103]. Arrhythmia may be linked to aberrant expression and remodeling of the cardiac gap junction protein connexin43 (Cx43). Opening of remodeled Cx43 hemichannels plays a key role in the development of arrhythmias in DMD mice. Then, these channels can be therapeutic targets to prevent fatal arrhythmias in patients with DMD [104].

DMD patients are prone to ventricular arrhythmias, which may be caused by abnormal calcium (Ca^{2+}) homeostasis and elevated reactive oxygen species. In an animal model of DMD, a susceptibility to pacing induced ventricular arrhythmias was demonstrated. Oxidated Ca^{2+} /calmodulin-dependent protein kinase II, Ox-CaMKII, promotes aberrant sarcoplasmic reticulum Ca^{2+} release through RyR2, which leads to delayed afterdepolarizations and triggered ventricular arrhythmias. Genetic inhibition of ox-CaMKII normalized intracellular Ca^{2+} and prevented ventricular arrhythmias in this model [105].

8.2. CRT and Implantable Cardioverter Defibrillator

It is known that DMD patients are at risk of arrhythmias (such as atrial fibrillation, atrial flutter and ventricular tachycardia) but, in the absence of dedicated studies, the DMD Care Considerations Working Group suggests to apply the standard antiarrhythmic medications and device management recommendations. At present, also the indication for the ICD is based on the established adult HF guidelines [49] but should be individualized according to clinical status, nutritional state, and respiratory function.

Cardiac resynchronization therapy (CRT) implantation improved symptoms and heart function in two DMD patients with HF and left bundle branch block. Mortality remains higher in similar DMD patients without CRT [98]. Other authors reported limited benefits with the implantation of ICD and CRT in dystrophinopathic cardiomyopathies, with no increase of EF, no change or worsening of EDV [106]. However, some patients (a quarter) had subjective improvements in their daily activities.

Causes of this poor response in DMD patients could be the normality of QRS complex and the extensive postero-lateral fibrosis [107].

9. DMD Target Therapy

Glucocorticoid treatment has been the standard of care for patients with DMD. Prednisone and deflazacort are the most commonly recommended steroids. The introduction of steroid therapy has changed the natural history of the disease, prolonging the autonomous ambulation period, delaying the cardiorespiratory insufficiency occurrence, and increasing children life-expectancy [4,108].

The understanding of molecular basis and knowledge of DMD has led to the advent of several experimental therapeutic approaches. The therapeutic approaches for DMD have focused on restoring dystrophin expression or mitigating the processes downstream of dystrophin deficiency.

The strategies that have been embraced for dystrophin protein restoration include (1) nonsense readthrough, (2) antisense oligonucleotides for exon skipping, and (3) gene therapy. To mitigate the dystrophic processes the approaches used are (1) inhibiting inflammation, (2) promoting muscle regeneration, (3) reducing fibrosis, and (4) facilitating mitochondrial function.

This translational research has led to the approval of first treatments for DMD and several other agent are under clinical investigation. Ataluren (Translarna™, PTC Therap.) is the first approved drug for DMD in Europe. Ataluren is an oral molecule that binds ribosomal RNA subunits and enables ribosomal readthrough of mRNA containing a premature stop codon. It is indicated for the treatment of DMD resulting from a nonsense mutation in the dystrophin gene.

More recently FDA conditionally approved AONs targeting exon 51 (eteplirsen) and 53 (golodirsen) for the treatment of DMD [61].

10. Female DMD Carriers

DMD is an X-linked condition and it usually affects males, with the majority of females having mutation in a single allele being asymptomatic carriers. About one-third of all DMD cases are caused by de novo mutations, with the other two-thirds due to inheritance from the mother. This means that every mother of an isolated male DMD case has a two-thirds chance of being a carrier. Most females with a pathogenic DMD gene variant present as asymptomatic carriers because of the presence of a second normally functioning allele. However, some female carriers can present symptoms from mild to more severe clinical courses, as muscle weakness, abnormal gait, fatigue, and cardiac involvement [109]. These patients are classified as “manifesting carriers.” The “skewed inactivation of the normal X-chromosome” hypothesis was widely used to explain the mosaic pattern of dystrophin expression in skeletal as well as heart muscle in female DMD carriers. According to this hypothesis, a higher percentage of skewed inactivation of the normal X-chromosome was responsible for the occurrence of cardiomyopathy in some female MD carriers. However, in the study of Brioschi et al. [110], there was no relationship between the dystrophic muscular phenotype and either the X-inactivation pattern or the dystrophin transcriptional behavior, suggesting that the major cause of disease manifestation is simply the total dystrophin protein amount. Each male child of a carrier female has a 50% chance of being clinically affected with DMD. Carrier testing can indicate if a woman is at risk of having affected sons. Although female DMD carriers are mostly free of skeletal muscle symptoms, cardiac symptoms affect about 8% of this population with DCM as a common presentation. They may develop cardiomyopathy ranging from asymptomatic forms with mild abnormalities to progressive HF, even requiring heart transplantation [36]. The onset of clinical manifestations for symptomatic female carriers is variable, ranging from early childhood to late adulthood [111]. The incidence of cardiomyopathy increases with age, even in patients with normal electrocardiograms and no skeletal muscle symptoms. Therefore, in the clinical guidelines in Europe and the United States [15], adult dystrophinopathy carriers are recommended to undergo echocardiography every 5 years. Other cardiac manifestations include conduction defects and arrhythmias, but these could be consequences of long-term DCM. Acute HF and non-sustained ventricular tachycardia have been reported as initial presentations in late adulthood,

although these are not as common. Disease severity is variable and genotype–phenotype correlations are not well established in this group of patients, and cardiac involvement may be present without concomitant skeletal muscle manifestations [111–113]. Cardiac manifestations in female carriers may be subclinical under normal physiological conditions. They can worsen and become symptomatic during major events such as pregnancy. Approximately two-thirds of all patients with limbic-type muscular dystrophy experience muscle weakness during pregnancy and these are probably related with weight gain and diaphragm elevation.

Besides cardiac manifestations, female DMD carriers can present with other systemic features: limb girdle weakness, gait disturbance, exercise intolerance, calf hypertrophy, and scoliosis have all been recognized as skeletal muscle manifestations in these patients. Elevated serum creatinine kinase (CK) is often found in patients with skeletal muscle presentations. Additionally, neurocognitive problems can present as learning disabilities or behavioral problems in this patient population [112,113].

Author Contributions: Conceptualization, R.A. and A.A.; writing—original draft preparation, E.M., N.C., C.C., L.A., M.C., M.S., A.D., M.G.; writing—review and editing, R.A., F.D., A.A.; supervision, R.A., A.A.; project administration, R.A.; funding acquisition, R.A., A.A. All authors have read and agreed to the published version of the manuscript.

Funding: This research was partially funded by Ministry of Health, grant number RRC-2019-2366867.

Conflicts of Interest: The authors declare no conflict of interest.

Abbreviations

ACE:	angiotensin Converting Enzyme
ACE inhibitors:	ACEi
ARNI:	Angiotensin Receptor Neprilysin Inhibitor
ARB:	Angiotensin Receptor Blocker
BB:	Beta Blockers
DCM:	Dilated Cardiomyopathy
DMD:	Duchenne Muscular Dystrophy
DTI:	Doppler Tissue Imaging
EF:	Ejection Fraction
FS:	Fractional Shortening
GLS:	Global Longitudinal Strain
HF:	Heart Failure
ICC:	Intra Class Coefficient
LV:	Left Ventricle
MR:	Magnetic Resonance
MPI:	Mechanical Performance Index
PWD:	Pulse Wave Doppler
RV:	Right Ventricle
TDI:	Tissue Doppler Index

References

1. Kamdar, F.; Garry, D.J. Dystrophin-Deficient Cardiomyopathy. *J. Am. Coll. Cardiol.* **2016**, *67*, 2533–2546. [[CrossRef](#)]
2. McNally, E.M.; Wyatt, E.J. Mutation-Based Therapy for Duchenne Muscular Dystrophy: Antisense Treatment Arrives in the Clinic. *Circulation* **2017**, *136*, 979–981. [[CrossRef](#)]
3. Buddhe, S.; Cripe, L.H.; Friedland-Little, J.; Kertesz, N.; Eghtesady, P.; Finder, J.; Hor, K.N.; Judge, D.P.; Kinnett, K.; McNally, E.M.; et al. Cardiac Management of the Patient With Duchenne Muscular Dystrophy. *Pediatrics* **2018**, *142*, S72–S81. [[CrossRef](#)]
4. Birnkrant, D.J.; Bushby, K.; Bann, C.M.; Alman, B.; Apkon, S.D.; Blackwell, A.; Case, L.; Cripe, L.; Hadjiyannakis, S.; Olson, A.K.; et al. Diagnosis and management of Duchenne muscular dystrophy, part 2: Respiratory, cardiac, bone health, and orthopaedic management. *Lancet Neurol.* **2018**, *17*, 347–361. [[CrossRef](#)]

5. Connuck, D.M.; Sleeper, L.A.; Colan, S.D.; Cox, G.F.; Towbin, J.A.; Lowe, A.M.; Wilkinson, J.D.; Orav, E.J.; Cuniberti, L.; Salbert, B.A.; et al. Characteristics and outcomes of cardiomyopathy in children with Duchenne or Becker muscular dystrophy: A comparative study from the Pediatric Cardiomyopathy Registry. *Am. Heart J.* **2008**, *155*, 998–1005. [\[CrossRef\]](#)
6. Muntoni, F.; Torelli, S.; Ferlini, A. Dystrophin and mutations: One gene, several proteins, multiple phenotypes. *Lancet Neurol.* **2003**, *2*, 731–740. [\[CrossRef\]](#)
7. Nigro, G.; Comi, L.I.; Palladino, A.; Petretta, V.R.; Politano, L. Cardiomyopathies: Diagnosis of types and stages. *Acta Myol.* **2004**, *23*, 97–102. [\[PubMed\]](#)
8. Politano, L.; Nigro, V.; Petretta, V.R.; Passamano, L.; Papparella, S.; Di Somma, S.; Comi, L.I. Development of Cardiomyopathy in Female Carriers of Duchenne and Becker Muscular Dystrophies. *JAMA* **1996**, *275*, 1335. [\[CrossRef\]](#)
9. Hoffman, E.P.; Brown, R.H.; Kunkel, L.M. Dystrophin: The protein product of the duchenne muscular dystrophy locus. *Cell* **1987**, *51*, 919–928. [\[CrossRef\]](#)
10. Campbell, K.P. Three muscular dystrophies: Loss of cytoskeleton-extracellular matrix linkage. *Cell* **1995**, *80*, 675–679. [\[CrossRef\]](#)
11. Shirokova, N.; Niggli, E. Cardiac phenotype of Duchenne Muscular Dystrophy: Insights from cellular studies. *J. Mol. Cell. Cardiol.* **2013**, *58*, 217–224. [\[CrossRef\]](#)
12. Wallace, G.Q.; McNally, E.M. Mechanisms of Muscle Degeneration, Regeneration, and Repair in the Muscular Dystrophies. *Annu. Rev. Physiol.* **2009**, *71*, 37–57. [\[CrossRef\]](#)
13. Yilmaz, A.; Gdynia, H.-J.; Baccouche, H.; Mahrholdt, H.; Meinhardt, G.; Basso, C.; Thiene, G.; Sperfeld, A.-D.; Ludolph, A.C.; Sechtem, U. Cardiac involvement in patients with Becker muscular dystrophy: New diagnostic and pathophysiological insights by a CMR approach. *J. Cardiovasc. Magn. Reson.* **2008**, *10*, 50. [\[CrossRef\]](#)
14. Frankel, K.A.; Rosser, R.J. The pathology of the heart in progressive muscular dystrophy: Epimycocardial fibrosis. *Hum. Pathol.* **1976**, *7*, 375–386. [\[CrossRef\]](#)
15. Bushby, K.; Finkel, R.; Birnkrant, D.J.; Case, L.; Clemens, P.R.; Cripe, L.; Kaul, A.; Kinnett, K.; McDonald, C.M.; Pandya, S.; et al. Diagnosis and management of Duchenne muscular dystrophy, part 2: Implementation of multidisciplinary care. *Lancet Neurol.* **2010**, *9*, 177–189. [\[CrossRef\]](#)
16. Eagle, M.; Baudouin, S.V.; Chandler, C.; Giddings, D.R.; Bullock, R.; Bushby, K. Survival in Duchenne muscular dystrophy: Improvements in life expectancy since 1967 and the impact of home nocturnal ventilation. *Neuromuscul. Disord.* **2002**, *12*, 926–929. [\[CrossRef\]](#)
17. Nigro, G.; Comi, L.; Politano, L.; Bain, R. The incidence and evolution of cardiomyopathy in Duchenne muscular dystrophy. *Int. J. Cardiol.* **1990**, *26*, 271–277. [\[CrossRef\]](#)
18. Hammerer-Lercher, A.; Erlacher, P.; Bittner, R.; Korinthenberg, R.; Skladal, D.; Sorichter, S.; Sperl, W.; Puschendorf, B.; Mair, J. Clinical and Experimental Results on Cardiac Troponin Expression in Duchenne Muscular Dystrophy. *Clin. Chem.* **2001**, *47*, 451–458. [\[CrossRef\]](#)
19. Buyse, G.M.; Goemans, N.; Hauwe, M.V.D.; Thijs, D.; De Groot, I.J.; Schara, U.; Ceulemans, B.; Meier, T.; Mertens, L. Idefenone as a novel, therapeutic approach for Duchenne muscular dystrophy: Results from a 12 month, double-blind, randomized placebo-controlled trial. *Neuromuscul. Disord.* **2011**, *21*, 396–405. [\[CrossRef\]](#)
20. Castro-Gago, M.; Gómez-Lado, C.; Puñal, J.E. Cardiac troponin I for accurate evaluation of cardiac status in myopathic patients. *Brain Dev.* **2009**, *31*, 184. [\[CrossRef\]](#)
21. Voleti, S.; Olivieri, L.; Hamann, K.; Gordish-Dressman, H.; Spurney, C. Troponin I Levels Correlate with Cardiac MR LGE and Native T1 Values in Duchenne Muscular Dystrophy Cardiomyopathy and Identify Early Disease Progression. *Pediatr. Cardiol.* **2020**, 1–7. [\[CrossRef\]](#) [\[PubMed\]](#)
22. Yanagisawa, A.; Yokota, N.; Miyagawa, M.; Kawamura, J.; Ishihara, T.; Aoyagi, T.; Ishikawa, K. Plasma levels of atrial natriuretic peptide in patients with Duchenne's progressive muscular dystrophy. *Am. Heart J.* **1990**, *120*, 1154–1158. [\[CrossRef\]](#)
23. Villa, C.R.; Kaddourah, A.; Mathew, J.; Ryan, T.D.; Wong, B.L.Y.; Goldstein, S.L.; Jefferies, J.L. Identifying evidence of cardio-renal syndrome in patients with Duchenne muscular dystrophy using cystatin C. *Neuromuscul. Disord.* **2016**, *26*, 637–642. [\[CrossRef\]](#) [\[PubMed\]](#)
24. Power, L.C.; O'Grady, G.L.; Hornung, T.S.; Jefferies, C.; Gusso, S.; Hofman, P.L. Imaging the heart to detect cardiomyopathy in Duchenne muscular dystrophy: A review. *Neuromuscul. Disord.* **2018**, *28*, 717–730. [\[CrossRef\]](#) [\[PubMed\]](#)

25. Soslow, J.H.; Xu, M.; Slaughter, J.C.; Stanley, M.; Crum, K.; Markham, L.W.; Parra, D.A. Evaluation of Echocardiographic Measures of Left Ventricular Function in Patients with Duchenne Muscular Dystrophy: Assessment of Reproducibility and Comparison to Cardiac Magnetic Resonance Imaging. *J. Am. Soc. Echocardiogr.* **2016**, *29*, 983–991. [[CrossRef](#)]
26. Buddhe, S.; Lewin, M.; Olson, A.; Ferguson, M.; Soriano, B.D. Comparison of left ventricular function assessment between echocardiography and MRI in Duchenne muscular dystrophy. *Pediatr. Radiol.* **2016**, *46*, 1399–1408. [[CrossRef](#)]
27. Cirino, R.H.D.; Scola, R.H.; Ducci, R.D.-P.; Camarozano, A.C.; Kay, C.S.K.; Lorenzoni, P.J.; Werneck, L.C.; Carmes, E.R.; Da Cunha, C.L.P. Evaluation of Left-Sided Heart Chambers with Novel Echocardiographic Techniques in Men With Duchenne or Becker Muscular Dystrophy. *Am. J. Cardiol.* **2019**, *123*, 972–978. [[CrossRef](#)]
28. Spurney, C.F.; McCaffrey, F.M.; Cnaan, A.; Morgenroth, L.P.; Ghelani, S.J.; Gordish-Dressman, H.; Arrieta, A.; Connolly, A.M.; Lotze, T.E.; McDonald, C.M.; et al. Feasibility and Reproducibility of Echocardiographic Measures in Children with Muscular Dystrophies. *J. Am. Soc. Echocardiogr.* **2015**, *28*, 999–1008. [[CrossRef](#)]
29. Levy, P.T.; Machesky, A.; Sanchez, A.A.; Patel, M.D.; Rogal, S.; Fowler, S.; Yaeger, L.; Hardi, A.; Holland, M.R.; Hamvas, A.; et al. Reference Ranges of Left Ventricular Strain Measures by Two-Dimensional Speckle-Tracking Echocardiography in Children: A Systematic Review and Meta-Analysis. *J. Am. Soc. Echocardiogr.* **2016**, *29*, 209–225.e6. [[CrossRef](#)]
30. Patrianakos, A.P.; Zacharaki, A.; Kalogerakis, A.; Solidakis, G.; Parthenakis, F.; Vardas, P. Two-dimensional global and segmental longitudinal strain: Are the results from software in different high-end ultrasound systems comparable? *Echo Res. Pr.* **2015**, *2*, 29–39. [[CrossRef](#)]
31. Amedro, P.; Vincenti, M.; De La Villeon, G.; Lavastre, K.; Barrea, C.; Guillaumont, S.; Bredy, C.; Gamon, L.; Meli, A.C.; Cazorla, O.; et al. Speckle-Tracking Echocardiography in Children with Duchenne Muscular Dystrophy: A Prospective Multicenter Controlled Cross-Sectional Study. *J. Am. Soc. Echocardiogr.* **2019**, *32*, 412–422. [[CrossRef](#)] [[PubMed](#)]
32. Power, A.; Poonja, S.; Disler, D.; Myers, K.; Patton, D.J.; Mah, J.K.; Fine, N.M.; Greenway, S.C. Echocardiographic Image Quality Deteriorates with Age in Children and Young Adults with Duchenne Muscular Dystrophy. *Front. Cardiovasc. Med.* **2017**, *4*, 82. [[CrossRef](#)] [[PubMed](#)]
33. Mehmood, M.; Hor, K.N.; Al-Khalidi, H.R.; Benson, D.W.; Jefferies, J.L.; Taylor, M.D.; Egnaczyk, G.F.; Raman, S.V.; Basu, S.K.; Cripe, L.H.; et al. Comparison of right and left ventricular function and size in Duchenne muscular dystrophy. *Eur. J. Radiol.* **2015**, *84*, 1938–1942. [[CrossRef](#)] [[PubMed](#)]
34. Silva, M.C.; Magalhães, T.A.; Meira, Z.M.A.; Rassi, C.H.R.E.; Andrade, A.C.D.S.; Gutierrez, P.S.; Azevedo, C.F.; Gurgel-Giannetti, J.; Vainzof, M.; Zatz, M.; et al. Myocardial Fibrosis Progression in Duchenne and Becker Muscular Dystrophy. *JAMA Cardiol.* **2017**, *2*, 190–199. [[CrossRef](#)]
35. Raman, S.V.; Hor, K.N.; Mazur, W.; Halnon, N.J.; Kissel, J.T.; He, X.; Tran, T.; Smart, S.; McCarthy, B.; Taylor, M.D.; et al. Eplerenone for early cardiomyopathy in Duchenne muscular dystrophy: A randomised, double-blind, placebo-controlled trial. *Lancet Neurol.* **2014**, *14*, 153–161. [[CrossRef](#)]
36. Florian, A.-R.; Rösch, S.; Bietenbeck, M.; Engelen, M.; Sechtem, U.; Stypmann, J.; Waltenberger, J.; Yilmaz, A. Cardiac involvement in female Duchenne and Becker muscular dystrophy carriers in comparison to their first-degree male relatives: A comparative cardiovascular magnetic resonance study. *Eur. Heart J. Cardiovasc. Imaging* **2015**, *17*, 326–333. [[CrossRef](#)]
37. Lang, S.M.; Shugh, S.; Mazur, W.; Sticka, J.J.; Rattan, M.S.; Jefferies, J.L.; Taylor, M.D. Myocardial Fibrosis and Left Ventricular Dysfunction in Duchenne Muscular Dystrophy Carriers Using Cardiac Magnetic Resonance Imaging. *Pediatr. Cardiol.* **2015**, *36*, 1495–1501. [[CrossRef](#)]
38. Florian, A.-R.; Ludwig, A.; Engelen, M.; Waltenberger, J.; Rösch, S.; Sechtem, U.; Yilmaz, A. Left ventricular systolic function and the pattern of late-gadolinium-enhancement independently and additively predict adverse cardiac events in muscular dystrophy patients. *J. Cardiovasc. Magn. Reson.* **2014**, *16*, 81. [[CrossRef](#)]
39. Mavrogeni, S.; Markousis-Mavrogenis, G.; Papavasiliou, A.; Kolovou, G. Cardiac involvement in Duchenne and Becker muscular dystrophy. *World J. Cardiol.* **2015**, *7*, 410–414. [[CrossRef](#)]
40. Giglio, V.; Puddu, P.E.; Camastra, G.; Sbarbati, S.; Della Sala, S.W.; Ferlini, A.; Gualandi, F.; Ricci, E.; Sciarra, F.; Ansalone, G.; et al. Patterns of late gadolinium enhancement in Duchenne muscular dystrophy carriers. *J. Cardiovasc. Magn. Reson.* **2014**, *16*, 45. [[CrossRef](#)]

41. Wexberg, P.; Avanzini, M.; Mascherbauer, J.; Pfaffenberger, S.; Freudenthaler, B.; Bittner, R.E.; Bernert, G.; Weidinger, F. Myocardial late gadolinium enhancement is associated with clinical presentation in Duchenne muscular dystrophy carriers. *J. Cardiovasc. Magn. Reson.* **2016**, *18*, 61. [[CrossRef](#)]
42. Tandon, A.; Villa, C.R.; Hor, K.N.; Jefferies, J.L.; Gao, Z.; Towbin, J.A.; Wong, B.L.; Mazur, W.; Fleck, R.J.; Sticka, J.J.; et al. Myocardial Fibrosis Burden Predicts Left Ventricular Ejection Fraction and Is Associated with Age and Steroid Treatment Duration in Duchenne Muscular Dystrophy. *J. Am. Heart Assoc.* **2015**, *4*, e001338. [[CrossRef](#)] [[PubMed](#)]
43. Olivieri, L.J.; Kellman, P.; McCarter, R.J.; Cross, R.R.; Hansen, M.S.; Spurney, C.F. Native T1 values identify myocardial changes and stratify disease severity in patients with Duchenne muscular dystrophy. *J. Cardiovasc. Magn. Reson.* **2016**, *18*, 72. [[CrossRef](#)] [[PubMed](#)]
44. Soslow, J.H.; Damon, S.M.; Crum, K.; Lawson, M.A.; Slaughter, J.C.; Xu, M.; Arai, A.E.; Sawyer, D.B.; Parra, D.A.; Damon, B.M.; et al. Increased myocardial native T1 and extracellular volume in patients with Duchenne muscular dystrophy. *J. Cardiovasc. Magn. Reson.* **2015**, *18*, 5. [[CrossRef](#)] [[PubMed](#)]
45. Roujol, S.; Weingärtner, S.; Foppa, M.; Chow, K.; Kawaji, K.; Ngo, L.H.; Kellman, P.; Manning, W.J.; Thompson, R.; Nezafat, R. Accuracy, precision, and reproducibility of four T1 mapping sequences: A head-to-head comparison of MOLLI, ShMOLLI, SASHA, and SAPPHERE. *Radiology* **2014**, *272*, 683–689. [[CrossRef](#)] [[PubMed](#)]
46. Kellman, P.; Bandettini, W.P.; Mancini, C.; Hammer-Hansen, S.; Hansen, M.S.; Arai, A.E. Characterization of myocardial T1-mapping bias caused by intramyocardial fat in inversion recovery and saturation recovery techniques. *J. Cardiovasc. Magn. Reson.* **2015**, *17*, 1–11. [[CrossRef](#)]
47. Siegel, B.; Olivieri, L.; Gordish-Dressman, H.; Spurney, C. Myocardial Strain Using Cardiac MR Feature Tracking and Speckle Tracking Echocardiography in Duchenne Muscular Dystrophy Patients. *Pediatr. Cardiol.* **2017**, *39*, 478–483. [[CrossRef](#)]
48. Aikawa, T.; Takeda, A.; Oyama-Manabe, N.; Naya, M.; Yamazawa, H.; Koyanagawa, K.; Ito, Y.M.; Anzai, T. Progressive left ventricular dysfunction and myocardial fibrosis in Duchenne and Becker muscular dystrophy: A longitudinal cardiovascular magnetic resonance study. *Pediatr. Cardiol.* **2018**, *40*, 384–392. [[CrossRef](#)]
49. Ponikowski, P.; Voors, A.; Anker, S.D.; Bueno, H.; Cleland, J.G.F.; Coats, A.J.S.; Falk, V.; González-Juanatey, J.R.; Harjola, V.-P.; Jankowska, E.; et al. 2016 ESC Guidelines for the diagnosis and treatment of acute and chronic heart failure. *Eur. Heart J.* **2016**, *37*, 2129–2200. [[CrossRef](#)]
50. Duboc, D.; Meune, C.; Lerebours, G.; Devaux, J.-Y.; Vaksman, G.; Bécane, H.-M. Effect of perindopril on the onset and progression of left ventricular dysfunction in Duchenne muscular dystrophy. *J. Am. Coll. Cardiol.* **2005**, *45*, 855–857. [[CrossRef](#)]
51. Allen, H.D.; Flanigan, K.M.; Thrush, P.T.; Dvorchik, I.; Yin, H.; Canter, C.; Connolly, A.M.; Parrish, M.; McDonald, C.M.; Braunlin, E.; et al. A Randomized, Double-Blind Trial of Lisinopril and Losartan for the Treatment of Cardiomyopathy in Duchenne Muscular Dystrophy. *PLoS Curr.* **2013**, *5*. [[CrossRef](#)] [[PubMed](#)]
52. Raman, S.V.; Hor, K.N.; Mazur, W.; Cardona, A.; He, X.; Halnon, N.; Markham, L.; Soslow, J.H.; Puchalski, M.D.; Auerbach, S.R.; et al. Stabilization of Early Duchenne Cardiomyopathy With Aldosterone Inhibition: Results of the Multicenter AIDMD Trial. *J. Am. Heart Assoc.* **2019**, *8*, e013501. [[CrossRef](#)] [[PubMed](#)]
53. Rhodes, J.; Margossian, R.; Darras, B.T.; Colan, S.D.; Jenkins, K.J.; Geva, T.; Powell, A.J. Safety and Efficacy of Carvedilol Therapy for Patients with Dilated Cardiomyopathy Secondary to Muscular Dystrophy. *Pediatr. Cardiol.* **2007**, *29*, 343–351. [[CrossRef](#)] [[PubMed](#)]
54. Faysoil, A.; Ben Yaou, R.; Ognia, A.; Leturcq, F.; Nardi, O.; Clair, B.; Wahbi, K.; Lofaso, F.; Laforet, P.; Duboc, D.; et al. Clinical profiles and prognosis of acute heart failure in adult patients with dystrophinopathies on home mechanical ventilation. *ESC Heart Fail.* **2017**, *4*, 527–534. [[CrossRef](#)]
55. Jefferies, J.L.; Eidem, B.W.; Belmont, J.W.; Craigen, W.J.; Ware, S.M.; Fernbach, S.D.; Neish, S.R.; Smith, E.O.; Towbin, J. Genetic Predictors and Remodeling of Dilated Cardiomyopathy in Muscular Dystrophy. *Circulation* **2005**, *112*, 2799–2804. [[CrossRef](#)]
56. Kajimoto, H.; Ishigaki, K.; Okumura, K.; Tomimatsu, H.; Nakazawa, M.; Saito, K.; Osawa, M.; Nakanishi, T. Beta-blocker therapy for cardiac dysfunction in patients with muscular dystrophy. *Circ. J.* **2006**, *70*, 991–994. [[CrossRef](#)]
57. Matsumura, T.; Tamura, T.; Kuru, S.; Kikuchi, Y.; Kawai, M. Carvedilol can prevent cardiac events in Duchenne muscular dystrophy. *Intern. Med.* **2010**, *49*, 1357–1363. [[CrossRef](#)]

58. Ogata, H.; Ishikawa, Y.; Ishikawa, Y.; Minami, R. Beneficial effects of beta-blockers and angiotensin-converting enzyme inhibitors in Duchenne muscular dystrophy. *J. Cardiol.* **2009**, *53*, 72–78. [[CrossRef](#)]
59. Saito, T.; Matsumura, T.; Miyai, I.; Nozaki, S.; Shinno, S. Carvedilol effectiveness for left ventricular-insufficient patients with Duchenne muscular dystrophy. *Rinsho Shinkeigaku* **2001**, *41*, 691–694.
60. Viollet, L.; Thrush, P.T.; Flanigan, K.M.; Mendell, J.R.; Allen, H.D. Effects of Angiotensin-Converting Enzyme Inhibitors and/or Beta Blockers on the Cardiomyopathy in Duchenne Muscular Dystrophy. *Am. J. Cardiol.* **2012**, *110*, 98–102. [[CrossRef](#)]
61. Meyers, T.A.; Townsend, D. Cardiac Pathophysiology and the Future of Cardiac Therapies in Duchenne Muscular Dystrophy. *Int. J. Mol. Sci.* **2019**, *20*, 4098. [[CrossRef](#)] [[PubMed](#)]
62. Adorasio, R.; Calvieri, C.; Cantarutti, N.; D'Amico, A.; Catteruccia, M.; Bertini, E.; Baban, A.; Filippelli, S.; Perri, G.; Amodeo, A.; et al. Heart rate reduction strategy using ivabradine in end-stage Duchenne cardiomyopathy. *Int. J. Cardiol.* **2019**, *280*, 99–103. [[CrossRef](#)] [[PubMed](#)]
63. Bonnet, D.; Berger, F.; Jokinen, E.; Kantor, P.F.; Daubeney, P.E. Ivabradine in Children With Dilated Cardiomyopathy and Symptomatic Chronic Heart Failure. *J. Am. Coll. Cardiol.* **2017**, *70*, 1262–1272. [[CrossRef](#)] [[PubMed](#)]
64. Yancy, C.W.; Jessup, M.; Bozkurt, B.; Butler, J.; Casey, D.E., Jr.; Drazner, M.H.; Fonarow, G.C.; Geraci, S.A.; Horwich, T.; Januzzi, J.L.; et al. 2013 ACCF/AHA guideline for the management of heart failure: A report of the American College of Cardiology Foundation/American Heart Association Task Force on Practice Guidelines. *J. Am. Coll. Cardiol.* **2013**, *62*, e147–e239. [[CrossRef](#)]
65. Hoffman, E.P.; Riddle, V.; Siegler, M.A.; Dickerson, D.; Backonja, M.; Kramer, W.G.; Nagaraju, K.; Gordish-Dressman, H.; Damsker, J.M.; McCall, J.M. Phase 1 trial of vamorolone, a first-in-class steroid, shows improvements in side effects via biomarkers bridged to clinical outcomes. *Steroids* **2018**, *134*, 43–52. [[CrossRef](#)]
66. Shaddy, R.E.; Canter, C.; Halnon, N.; Kochilas, L.; Rossano, J.; Bonnet, D.; Bush, C.; Zhao, Z.; Kantor, P.F.; Burch, M.; et al. Design for the sacubitril/valsartan (LCZ696) compared with enalapril study of pediatric patients with heart failure due to systemic left ventricle systolic dysfunction (PANORAMA-HF study). *Am. Heart J.* **2017**, *193*, 23–34. [[CrossRef](#)]
67. Das, B.B. Current State of Pediatric Heart Failure. *Children* **2018**, *5*, 88. [[CrossRef](#)]
68. Mullens, W.; Damman, K.; Harjola, V.-P.; Mebazaa, A.; Rocca, H.-P.B.-L.; Martens, P.; Testani, J.M.; Tang, W.W.; Orso, F.; Rossignol, P.; et al. The use of diuretics in heart failure with congestion—A position statement from the Heart Failure Association of the European Society of Cardiology. *Eur. J. Heart Fail.* **2019**, *21*, 137–155. [[CrossRef](#)]
69. Lewis, A.B.; Chabot, M. The effect of treatment with angiotensin-converting enzyme inhibitors on survival of pediatric patients with dilated cardiomyopathy. *Pediatr. Cardiol.* **1993**, *14*, 9–12.
70. Kirk, R.; Dipchand, A.I.; Rosenthal, D.N.; Addonizio, L.; Burch, M.; Chrisant, M.; Dubin, A.; Everitt, M.; Gajarski, R.; Mertens, L.; et al. The International Society for Heart and Lung Transplantation Guidelines for the management of pediatric heart failure: Executive summary. *J. Heart Lung Transpl.* **2014**, *33*, 888–909. [[CrossRef](#)]
71. D'Amaro, D.; Amodeo, A.; Adorasio, R.; Tiziano, F.D.; Leone, A.M.; Perri, G.; Bruno, P.; Massetti, M.; Ferlini, A.; Pane, M.; et al. A current approach to heart failure in Duchenne muscular dystrophy. *Heart* **2017**, *103*, 1770–1779. [[CrossRef](#)] [[PubMed](#)]
72. McNally, E.M.; Kaltman, J.R.; Benson, D.W.; Canter, C.E.; Cripe, L.H.; Duan, D.; Finder, J.D.; Groh, W.J.; Hoffman, E.P.; Judge, D.P.; et al. Contemporary Cardiac Issues in Duchenne Muscular Dystrophy. *Circulation* **2015**, *131*, 1590–1598. [[CrossRef](#)] [[PubMed](#)]
73. Piperata, A.; Bottio, T.; Toscano, G.; Avesani, M.; Vianello, A.; Gerosa, G. Is heart transplantation a real option in patients with Duchenne syndrome? Inferences from a case report. *ESC Heart Fail.* **2020**. [[CrossRef](#)] [[PubMed](#)]
74. Rose, E.A.; Gelijns, A.C.; Moskowitz, A.J.; Heitjan, D.F.; Stevenson, L.W.; Dembitsky, W.; Long, J.W.; Ascheim, D.D.; Tierney, A.R.; Levitan, R.G.; et al. Long-Term Use of a Left Ventricular Assist Device for End-Stage Heart Failure. *N. Engl. J. Med.* **2001**, *345*, 1435–1443. [[CrossRef](#)] [[PubMed](#)]
75. Starling, R.C.; Naka, Y.; Boyle, A.J.; Gonzalez-Stawinski, G.; John, R.; Jorde, U.; Russell, S.D.; Conte, J.V.; Aaronson, K.D.; McGee, E.C.; et al. Results of the Post-U.S. Food and Drug Administration-Approval

- Study with a Continuous Flow Left Ventricular Assist Device as a Bridge to Heart Transplantation. *J. Am. Coll. Cardiol.* **2011**, *57*, 1890–1898. [[CrossRef](#)]
76. Slaughter, M.S.; Rogers, J.G.; Milano, C.A.; Russell, S.D.; Conte, J.V.; Feldman, D.; Sun, B.; Tatroles, A.J.; Delgado, R.M.; Long, J.W.; et al. Advanced Heart Failure Treated with Continuous-Flow Left Ventricular Assist Device. *N. Engl. J. Med.* **2009**, *361*, 2241–2251. [[CrossRef](#)]
77. Enciso, J.S. Mechanical Circulatory Support: Current Status and Future Directions. *Prog. Cardiovasc. Dis.* **2016**, *58*, 444–454. [[CrossRef](#)]
78. Delgado, R.; Radovancevic, B.; Massin, E.K.; Frazier, O.H.; Benedict, C. Neurohormonal changes after implantation of a left ventricular assist system. *ASAIO J.* **1998**, *44*, 299–302.
79. Barbone, A.; Holmes, J.W.; Heerdt, P.M.; Andrew, H.S.; Naka, Y.; Joshi, N.; Daines, M.; Marks, A.R.; Oz, M.C.; Burkhoff, D. Comparison of Right and Left Ventricular Responses to Left Ventricular Assist Device Support in Patients with Severe Heart Failure. *Circulation* **2001**, *104*, 670–675. [[CrossRef](#)]
80. Madigan, J.D.; Barbone, A.; Choudhri, A.F.; Morales, D.L.; Cai, B.; Oz, M.C.; Burkhoff, D. Time course of reverse remodeling of the left ventricle during support with a left ventricular assist device. *J. Thorac. Cardiovasc. Surg.* **2001**, *121*, 902–908. [[CrossRef](#)]
81. Klotz, S.; Foronjy, R.F.; Dickstein, M.L.; Gu, A.; Garrelts, I.M.; Danser, A.J.; Oz, M.C.; D’Armiento, J.; Burkhoff, D. Mechanical Unloading During Left Ventricular Assist Device Support Increases Left Ventricular Collagen Cross-Linking and Myocardial Stiffness. *Circulation* **2005**, *112*, 364–374. [[CrossRef](#)] [[PubMed](#)]
82. Levin, H.R.; Oz, M.C.; Chen, J.M.; Packer, M.; Rose, E.A.; Burkhoff, D. Reversal of Chronic Ventricular Dilation in Patients With End-Stage Cardiomyopathy by Prolonged Mechanical Unloading. *Circulation* **1995**, *91*, 2717–2720. [[CrossRef](#)] [[PubMed](#)]
83. Zafeiridis, A.; Jeevanandam, V.; Houser, S.R.; Margulies, K.B. Regression of cellular hypertrophy after left ventricular assist device support. *Circulation* **1998**, *98*, 656–662. [[CrossRef](#)] [[PubMed](#)]
84. Altemose, G.T.; Gritsus, V.; Jeevanandam, V.; Goldman, B.; Margulies, K.B. Altered myocardial phenotype after mechanical support in human beings with advanced cardiomyopathy. *J. Heart Lung Transpl.* **1997**, *16*, 765–773.
85. Dipla, K.; Mattiello, J.A.; Jeevanandam, V.; Houser, S.R.; Margulies, K.B. Myocyte recovery after mechanical circulatory support in humans with end-stage heart failure. *Circulation* **1998**, *97*, 2316–2322. [[CrossRef](#)] [[PubMed](#)]
86. Amodeo, A.; Adorisio, R. Left ventricular assist device in Duchenne Cardiomyopathy: Can we change the natural history of cardiac disease? *Int. J. Cardiol.* **2012**, *161*, e43. [[CrossRef](#)]
87. Brancaccio, G.; Filippelli, S.; Michielon, G.; Iacobelli, R.; Alfieri, S.; Gandolfo, F.; Pongiglione, G.; Albanese, S.; Perri, G.; Parisi, F.; et al. Ventricular Assist Devices as a Bridge to Heart Transplantation or as Destination Therapy in Pediatric Patients. *Transpl. Proc.* **2012**, *44*, 2007–2012. [[CrossRef](#)]
88. Kilic, A.; Acker, M.A.; Atluri, P. Dealing with surgical left ventricular assist device complications. *J. Thorac. Dis.* **2015**, *7*, 2158–2164.
89. Ryan, T.D.; Jefferies, J.L.; Sawhani, H.; Wong, B.L.Y.; Gardner, A.; Del Corral, M.; Lorts, A.; Morales, D.L.S. Implantation of the HeartMate II and HeartWare Left Ventricular Assist Devices in Patients With Duchenne Muscular Dystrophy. *ASAIO J.* **2014**, *60*, 246–248. [[CrossRef](#)]
90. Iodice, F.; Testa, G.; Averardi, M.; Brancaccio, G.; Amodeo, A.; Cogo, P. Implantation of a left ventricular assist device as a destination therapy in Duchenne muscular dystrophy patients with end stage cardiac failure: Management and lessons learned. *Neuromuscul. Disord.* **2015**, *25*, 19–23. [[CrossRef](#)]
91. Stoller, U.; Araj, F.; Amin, A.; Fitzsimmons, C.; Morlend, R.; Thibodeau, J.T.; Ramaciotti, C.; Drazner, M.H.; Meyer, D.M.; Mammen, P.P.A. Implantation of a left ventricular assist device to provide long-term support for end-stage Duchenne muscular dystrophy-associated cardiomyopathy. *ESC Heart Fail.* **2017**, *4*, 379–383. [[CrossRef](#)] [[PubMed](#)]
92. Perri, G.; Filippelli, S.; Adorisio, R.; Iacobelli, R.; Iodice, F.; Testa, G.; Paglietti, M.G.; D’Amario, M.; Massetti, M.; Amodeo, A. Left ventricular assist device as destination therapy in cardiac end-stage dystrophinopathies: Midterm results. *J. Thorac. Cardiovasc. Surg.* **2017**, *153*, 669–674. [[CrossRef](#)] [[PubMed](#)]
93. Wittlieb-Weber, C.A.; Villa, C.; Conway, J.; Bock, M.J.; Gambetta, K.E.; Johnson, J.N.; Lal, A.K.; Schumacher, K.R.; Law, S.P.; Deshpande, S.R.; et al. Use of advanced heart failure therapies in Duchenne muscular dystrophy. *Prog. Pediatr. Cardiol.* **2019**, *53*, 11–14. [[CrossRef](#)] [[PubMed](#)]

94. Magnetta, D.A.; Kang, J.; Wearden, P.D.; Smith, K.J.; Feingold, B. Cost-Effectiveness of Ventricular Assist Device Destination Therapy for Advanced Heart Failure in Duchenne Muscular Dystrophy. *Pediatr. Cardiol.* **2018**, *39*, 1242–1248. [[CrossRef](#)]
95. Adorasio, R.; D'Amario, D.; Perri, G.; Amodeo, A. Comment on: 'Implantation of a left ventricular assist device to provide long term support for end-stage Duchenne muscular dystrophy-associated cardiomyopathy. *ESC Heart Fail.* **2018**, *5*, 651–652. [[CrossRef](#)]
96. Feudtner, C. Collaborative Communication in Pediatric Palliative Care: A Foundation for Problem-Solving and Decision-Making. *Pediatr. Clin. N. Am.* **2007**, *54*, 583–607. [[CrossRef](#)]
97. Arbustini, E.; Di Toro, A.; Giuliani, L.; Favalli, V.; Narula, N.; Grasso, M. Cardiac Phenotypes in Hereditary Muscle Disorders. *J. Am. Coll. Cardiol.* **2018**, *72*, 2485–2506. [[CrossRef](#)]
98. Fayssol, A.; Abasse, S.; Silverston, K. Cardiac Involvement Classification and Therapeutic Management in Patients with Duchenne Muscular Dystrophy. *J. Neuromuscul. Dis.* **2017**, *4*, 17–23. [[CrossRef](#)]
99. Fayssol, A.; Ben Yaou, R.; Ogna, A.; Chaffaut, C.; Leturcq, F.; Nardi, O.; Wahbi, K.; Duboc, D.; Lofaso, F.; Prigent, H.; et al. Left bundle branch block in Duchenne muscular dystrophy: Prevalence, genetic relationship and prognosis. *PLoS ONE* **2018**, *13*, e0190518. [[CrossRef](#)]
100. Perloff, J.K. Cardiac rhythm and conduction in Duchenne's muscular dystrophy: A prospective study of 20 patients. *J. Am. Coll. Cardiol.* **1984**, *3*, 1263–1268. [[CrossRef](#)]
101. Corrado, G.; Lissoni, A.; Beretta, S.; Terenghi, L.; Tadeo, G.; Foglia-Manzillo, G.; Tagliagambe, L.M.; Spata, M.; Santarone, M. Prognostic value of electrocardiograms, ventricular late potentials, ventricular arrhythmias, and left ventricular systolic dysfunction in patients with Duchenne muscular dystrophy. *Am. J. Cardiol.* **2002**, *89*, 838–841. [[CrossRef](#)]
102. Segawa, K.; Komaki, H.; Mori-Yoshimura, M.; Oya, Y.; Kimura, K.; Tachimori, H.; Kato, N.; Sasaki, M.; Takahashi, Y. Cardiac conduction disturbances and aging in patients with Duchenne muscular dystrophy. *Medicine (Baltimore)* **2017**, *96*, e8335. [[CrossRef](#)] [[PubMed](#)]
103. Fragakis, N.; Sotiriadou, M.; Krexi, L.; Vassilikos, V. Electrical storm in a patient with Duchenne muscular dystrophy cardiomyopathy triggered by abrupt β -blocker interruption. *Ann. Noninvasive Electrocardiol.* **2017**, *22*, e12477. [[CrossRef](#)] [[PubMed](#)]
104. Lillo, M.A.; Himelman, E.; Shirokova, N.; Xie, L.-H.; Fraidenraich, D.; Contreras, J.E. S-nitrosylation of connexin43 hemichannels elicits cardiac stress-induced arrhythmias in Duchenne muscular dystrophy mice. *JCI Insight* **2019**, *4*, 130091. [[CrossRef](#)] [[PubMed](#)]
105. Wang, Q.; Quick, A.; Cao, S.; Reynolds, J.; Chiang, D.Y.; Beavers, D.; Li, N.; Wang, G.; Rodney, G.G.; Anderson, M.E.; et al. Oxidized CaMKII (Ca²⁺/Calmodulin-Dependent Protein Kinase II) Is Essential for Ventricular Arrhythmia in a Mouse Model of Duchenne Muscular Dystrophy. *Circ. Arrhythmia Electrophysiol.* **2018**, *11*, e005682. [[CrossRef](#)]
106. Palladino, A.; Papa, A.A.; Morra, S.; Russo, V.; Ergoli, M.; Rago, A.; Orsini, C.; Nigro, G.; Politano, L. Are there real benefits to implanting cardiac devices in patients with end-stage dilated dystrophinopathic cardiomyopathy? Review of literature and personal results. *Acta Myol.* **2019**, *38*, 1–7.
107. D'Amario, D.; Gowran, A.; Canonico, F.; Castiglioni, E.; Rovina, D.; Santoro, R.; Spinelli, P.; Adorasio, R.; Amodeo, A.; Perrucci, G.L.; et al. Dystrophin Cardiomyopathies: Clinical Management, Molecular Pathogenesis and Evolution towards Precision Medicine. *J. Clin. Med.* **2018**, *7*, 291. [[CrossRef](#)]
108. Bello, L.; Gordish-Dressman, H.; Morgenroth, L.P.; Henricson, E.K.; Duong, T.; Hoffman, E.P.; Cnaan, A.; McDonald, C.M.; CINRG investigators. Prednisone/prednisolone and deflazacort regimens in the CINRG Duchenne Natural History Study. *Neurology* **2015**, *85*, 1048–1055. [[CrossRef](#)]
109. Lim, K.R.Q.; Sheri, N.; Nguyen, Q.; Yokota, T. Cardiac Involvement in Dystrophin-Deficient Females: Current Understanding and Implications for the Treatment of Dystrophinopathies. *Genes* **2020**, *11*, 765. [[CrossRef](#)]
110. Brioschi, S.; Gualandi, F.; Scotton, C.; Armaroli, A.; Bovolenta, M.; Falzarano, M.S.; Sabatelli, P.; Selvatici, R.; D'Amico, A.; Pane, M.; et al. Genetic characterization in symptomatic female DMD carriers: Lack of relationship between X-inactivation, transcriptional DMD allele balancing and phenotype. *BMC Med. Genet.* **2012**, *13*, 73. [[CrossRef](#)]
111. Finsterer, J.; Stöllberger, C. Muscle, cardiac, and cerebral manifestations in female carriers of dystrophin variants. *J. Neurol. Sci.* **2018**, *388*, 107–108. [[CrossRef](#)] [[PubMed](#)]

112. Ishizaki, M.; Kobayashi, M.; Adachi, K.; Matsumura, T.; Kimura, E. Female dystrophinopathy: Review of current literature. *Neuromuscul. Disord.* **2018**, *28*, 572–581. [[CrossRef](#)] [[PubMed](#)]
113. Kamakura, K. Cardiac involvement of female carrier of Duchenne muscular dystrophy. *Intern. Med.* **2000**, *39*, 2–3. [[CrossRef](#)] [[PubMed](#)]



© 2020 by the authors. Licensee MDPI, Basel, Switzerland. This article is an open access article distributed under the terms and conditions of the Creative Commons Attribution (CC BY) license (<http://creativecommons.org/licenses/by/4.0/>).

Perspective

Cardiac Sodium Channel Dysfunction and Dilated Cardiomyopathy: A Contemporary Reappraisal of Pathophysiological Concepts

Babken Asatryan

Department of Cardiology, Inselspital, Bern University Hospital, Freiburgstrasse 10, 3010 Bern, Switzerland; babken.asatryan@insel.ch; Tel.: +41-31-632-84-37; Fax: +41-31-632-42-11

Received: 29 May 2019; Accepted: 9 July 2019; Published: 12 July 2019

Abstract: A key emerging theme in translational cardiovascular medicine is the need to identify specific causes of arrhythmias and heart failure, defined by phenotype and/or genotype that will respond to a particular intervention. Unlike other genes implicated in hereditary arrhythmias and cardiomyopathies, pathogenic/likely pathogenic variants in the cardiac sodium channel alpha subunit gene (*SCN5A*) produce a remarkably diverse set of electrical and structural phenotypes, one of them being dilated cardiomyopathy. There has been debate about whether left ventricular remodeling is a bona fide phenotypic feature of cardiac sodium channel dysfunction, or a consequence of tachyarrhythmias or conduction disturbances. In light of recent findings, a critical digest of the available experimental and medical literature is necessary. This paper provides a critical appraisal of the evidence linking a dysfunctional cardiac sodium channel to ventricular dysfunction, and discusses the potential mechanisms involved in shaping this phenotype along with implications for precision therapy.

Keywords: *SCN5A*; cardiac sodium channel; cardiac channelopathy; dilated cardiomyopathy; precision medicine

1. Introduction

The alpha subunit of the cardiac voltage-gated sodium channel $Na_v1.5$ (*SCN5A*), which is responsible for the rapid depolarization phase of the cardiac action potential, has been one of the first studied ion channels since the early days of cardiovascular genetic research [1–3]. Unlike other cardiac-relevant genes that are typically implicated in either cardiac channelopathies or cardiomyopathies, rare variants in *SCN5A* have been associated with an incredibly diverse spectrum of frequently overlapping electrical and structural phenotypes. Loss-of-function variants have been linked to Brugada syndrome [4], progressive cardiac conduction disease (PCCD) [5], congenital atrioventricular block [6], sick sinus syndrome [7], idiopathic ventricular fibrillation [3], and atrial standstill [8], while gain-of-function variants have been associated with long QT syndrome type 3 [1], and multifocal ectopic Purkinje-related premature contractions (MEPPC) [9]. Other *SCN5A*-mediated conditions such as familial atrial fibrillation [10], sudden infant death syndrome [11], familial dilated cardiomyopathy (DCM) [8,12], and, rarely, arrhythmogenic right ventricular cardiomyopathy (ARVC) [13], have a more complex pathophysiology with involvement of multiple molecular phenotypes. A great variation of phenotypes has been noted even within the affected families and in individual patients over time, but to date, genotype–phenotype analyses have not been able to explain this variation in a clinical phenotype.

Of more than 450 disease-causing *SCN5A* variants identified, only a handful have been linked to DCM [12]. Pathogenic/likely pathogenic variants in *SCN5A* are associated with a substantially higher burden of atrial and ventricular arrhythmias (in >90% of cases), cardiac conduction disease, and higher risk of sudden cardiac death [12,14–16]. While mechanisms underlying different electrical phenotypes

have been profoundly studied using in vitro and in vivo approaches, little is known about how sodium channel malfunction leads to ventricular dysfunction and dilation. A critical appraisal of the existing scientific evidence might add another missing piece to this puzzle.

2. Clinical Evidence

Early studies reported pathogenic/likely pathogenic *SCN5A* variants in nearly 2% of all DCM cases [14]. Both sporadic cases and familial forms with autosomal dominant inheritance have been reported [12,14]. Variants associated with DCM have been localized to cytoplasmic, extracellular and transmembrane domains (DI-DIV) of $Nav_1.5$ (Figure 1). The main findings that support a potential role in DCM are the familial aggregation of the trait and the segregation of *SCN5A*-variants with clinical phenotype and/or histological characteristics of DCM, with or without associated electrical abnormalities (although with reduced penetrance). A recent study, however, reported no excess variation in *SCN5A* in DCM cases versus an Exome Aggregation Consortium (ExAC) control population, suggesting that most variants in this gene are unlikely to cause DCM [17]. Instead, it has been noted that *SCN5A* is in fact one of the genes with highest background variation. Thus, establishing a causal role of an *SCN5A* variant in DCM requires very strong functional evidence of pathogenicity and/or segregation with phenotype in large pedigrees.

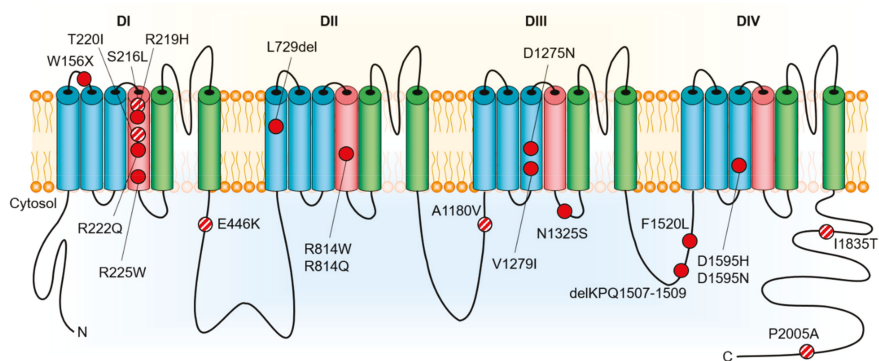


Figure 1. Rare variants in cardiac $Nav_1.5$ voltage-gated sodium channel (*SCN5A*) reported in association with dilated cardiomyopathy. Two additional variants, c.2550-2551insTG and c.3318dupC, causing truncation of the encoded protein in patients with dilated cardiomyopathy, are not shown. Pathogenic/likely pathogenic variants are shown in red, variants with insufficient evidence of pathogenicity in dilated cardiomyopathy are shown in red/white.

3. Experimental Evidence

Most of the reported DCM-associated *SCN5A* variants are missense variants, with a predilection for location in the S3 and S4 transmembrane domains, implicating a disruption of voltage-sensing mechanisms [15]. In vitro studies have shown that these variants commonly have loss-of-function, or infrequently gain-of-function, or rarely combined loss-of-function and gain-of-function effects on $Nav_1.5$ activity [16,18–21]. Additionally, conserved variants R225P and R814W localized at the S4 of DI and DII, respectively, which were associated with an atypical phenotype combining cardiac conduction disturbances, Brugada syndrome or long QT phenotype and DCM, were shown to result in the creation of an alternative permeation pathway through the normally non-conductive voltage sensor domain (gating pore current) [22]. Yet, there is practically no in vivo or in vitro evidence directly linking *SCN5A* defects to DCM. In other words, the existing evidence on biophysical phenotypes of rare *SCN5A* variants demonstrates their potential as a substrate for arrhythmias and conduction disturbances, but does not clearly point to the pathogenesis of DCM. Digging into the thought-provoking hypotheses

regarding how *SCN5A* defects might lead to ventricular dysfunction and heart failure might shed some light on this uncertainty.

4. DCM as a Manifestation of Pure $\text{Na}_V1.5$ Dysfunction

One theory is that DCM represents a direct consequence of $\text{Na}_V1.5$ channel dysfunction, meaning that the structural phenotype is primarily driven by electrical abnormalities [23,24]. Studies have suggested, that a proton leak into the cardiomyocyte through the $\text{Na}_V1.5$ channel, or increased Na^+ influx caused by gain-of-function variants, may lead to compensatory activation of the N^+/H^+ or the $\text{Na}^+/\text{Ca}^{2+}$ exchanger, thus leading to intracellular acidification or Ca^{2+} overload, respectively, and consequent impaired excitation–contraction coupling and/or myocardial damage with subsequent heart failure [22,24]. The first mechanism has been demonstrated for *SCN5A*-R219H [25], while the second was indirectly assumed for the loss-of-function A1180V missense variant [26]. These hypotheses, however, do not explain why the majority of the variants causing significant $\text{Na}_V1.5$ dysfunction do not result in left ventricular (LV) dysfunction. Thus, it is more likely that mechanisms other than direct modulation of $\text{Na}_V1.5$ activity are involved, such as down-regulation of channel expression, or channel mislocalization due to altered cytoskeletal anchoring [14,19]. As such, an increasing body of literature suggests interactions between sodium channel alpha subunits to form dimers [27]. Variants at the interaction sites mediating dimerization and sodium channel macromolecular complex formation might be involved in the DCM pathogenesis.

5. DCM Caused by Disrupted $\text{Na}_V1.5$ Interaction with Partner Proteins

On the other hand, it is possible that the interaction of the defective $\text{Na}_V1.5$ with its partner proteins of the cytoskeleton and intercalated disc, is responsible for the structural phenotype [28]. Interestingly, pathogenic *SCN5A* variants have been described in rare forms of left-ventricular non-compaction with a high arrhythmic burden [29]. Studies on induced pluripotent stem cell-derived cardiomyocytes have shown that the ARVC-associated missense variant *SCN5A*-R1898H leads to a significant reduction in peak I_{Na} current, and of the abundance of $\text{Na}_V1.5$ and N-cadherin clusters at the intercalated disc [13]. Other studies have shown that *SCN5A*-positive Brugada syndrome patients have significant cardiomyopathic changes, primarily in the right ventricular outflow tract, such as fatty wall replacement, fibrosis, and reduced expression of connexin 43 [30–32]. Moreover, missense *PKP2* variants identified in *SCN5A*-negative Brugada syndrome patients were shown to cause a loss of expression of desmosomal protein plakophilin-2, which was associated with decreased I_{Na} , reduced number of $\text{Na}_V1.5$ channels at the intercalated disc, and increased separation of microtubules from the cell end [33]. These interactions between the cardiac sodium channel complex and the intercalated disc likely underline mechanisms relevant to *SCN5A*-mediated ARVC and *PKP2*-mediated Brugada syndrome. Could an abnormal $\text{Na}_V1.5$ channel result in reduced ventricular contractility through disrupting the function of its interacting proteins and/or those already implicated in DCM, such as proteins of the sarcomere, cytoskeleton, or the dystrophin-associated glycoprotein complex?

To date, several proteins interacting with the $\text{Na}_V1.5$ channel have been shown to contribute to the *SCN5A*-mediated phenotypes through their alteration of the sodium channel availability or biophysical properties. $\text{Na}_V1.5$ regulatory proteins caveolin 3 (*CAV3*), alpha 1 syntrophin (*SNTA1*), and cardiac sodium channel beta subunit 4 (*SCN4B*) have been reported in association with rare subtypes of congenital long QT syndrome. Pathogenic variants in cardiac sodium channel beta subunit 3 (*SCN3B*) and glycerol 3 phosphate dehydrogenase 1-like protein have been identified in patients with Brugada syndrome. Interestingly, cardiac sodium channel beta subunit 1 (*SCN1B*) has been linked to Brugada syndrome, atrial fibrillation (also *SCN2B*), and cardiac conduction disease. A number of other proteins have been shown to interact with and regulate the $\text{Na}_V1.5$ channel. These include anchoring adaptor proteins ankyrin-G, syntrophins, MOG1, plakophilin-2, enzymes, such as nedd4-like enzymes, calmodulin kinase II δc , and protein tyrosine phosphatase H1, and other proteins that modulate the channel biophysical properties, such as 14-3-3 η , calmodulin, telethonin, GPD1L, and FHF1B [34].

However, strong associations between pathogenic variants in these protein genes and development of DCM have not been reported.

The sarcolemmal membrane-associated protein (SLMAP) is localized at T-tubules and sarcoplasmic reticulum. Pathogenic variants in *SLMAP* have been shown to cause Brugada syndrome via modulating the intracellular trafficking of the $\text{Na}_v1.5$ channel [35]. A recent report showed that transgenic mice with cardiac-specific expression of the *SLMAP* isoform 3 (*SLMAP3*) develop a significant decrease in fractional shortening and in cardiac output without notable hypertrophy, fibrosis, or fetal gene activation [36]. Electrocardiography identified increased PR interval and a decreased R amplitude. Western blot analysis revealed a decreased protein levels of $\text{Na}_v1.5$ and calcium transport system of the sarcoplasmic reticulum (SERCA2a/PLN), suggesting a selective regulatory role of *SLMAP3* in ion transport proteins at the level of gene expression. It is, however, unclear whether *SLMAP3* is a contributor of DCM phenotype in humans or whether any of the reported DCM-associated *SCN5A* variants disrupts an interacting domain of its partner proteins or other DCM-associated genes/proteins. The list of proteins interacting with $\text{Na}_v1.5$ is also not conclusive, and many aspects require further research. It is expected that these patterns will become clearer with further experimental evidence and with more genotype-phenotype analyses on DCM and related disorders. As a first step, *SCN5A* disruption has been demonstrated to result in TGF- β_1 -mediated fibrosis in a murine model of sinus node dysfunction. It is therefore possible that *SCN5A* variants can influence the pro-fibrotic milieu associated with other protein variants, and thereby contribute to the development of DCM [37].

6. DCM Resulting from Long-Standing and Frequent Arrhythmias

Alternatively, high arrhythmic burden may lead to ventricular dysfunction over time. This theory was primarily based on the finding that in several cases of MEPPC and DCM due to gain-of-function *SCN5A*-R222Q variant, therapy with hydroquinidine, flecainide, or amiodarone (in addition to standard treatment of heart failure) rapidly and effectively reduced the number of multifocal premature ventricular contractions and reversed the LV remodeling [10,16,38]. Following the initial report of R222Q, similar phenotypes have been reported for R222P, I141V, and G213D [39–41]. Nevertheless, whether the recovery of ventricular function relates to the premature ventricular contraction burden reduction or to intracellular mechanisms secondary to pharmacological blockade of the defective sodium channel, remain to be elucidated. Furthermore, some *SCN5A*-DCM patients, such as those carrying the D1275N variant, lack a history of long-lasting ventricular arrhythmias [14], and thus the LV dysfunction in these patients is unlikely to be a consequence of ventricular arrhythmias. It is therefore more likely that this is a contributing mechanism rather than a primary cause.

7. DCM Secondary to Cardiac Conduction Disturbances

DCM might also develop secondary to loss-of-function variants, which leads to reduced sodium conductivity or channel availability. Classical manifestations of loss-of-function *SCN5A* variants are Brugada syndrome and PCCD (Lenège and Lev disease), but development of DCM at late disease stages, often 15 to 20 years after diagnosis, has been described in many cases. In addition, transgenic mice with 90% decreased $\text{Na}_v1.5$ expression [19] and mice with the DCM-associated D1275N variant, have been found to display conduction slowing with progressive age-dependent changes suggestive for DCM [42]. This hypothesis, however, does not explain the development of DCM in rare *SCN5A* variant carriers with unaffected cardiac conduction. The majority of *SCN5A* variants causing cardiac conduction defects are frameshift/truncation variants, which produce a conduction phenotype proportionate to the severity of $\text{Na}_v1.5$ dysfunction, whereas most DCM-related *SCN5A* variants are missense changes.

8. Mechanisms Involving Other Genetic Influences

Genome-wide association studies (GWAS) with case-control design have shown that another *SCN5A*-mediated condition, Brugada syndrome, is more likely to develop in patients who carry multiple common variants with a small effect, referred to as small nucleotide polymorphisms (SNPs).

These SNPs can modulate the expression dosage of $Na_v1.5$ by altering mechanisms such as the dosage of the messenger RNA, the number of channels on the surface of cardiomyocyte, or even by modulating the affinity of a transcription factor for the gene regulatory element. Considering its shared genetic substrate with *SCN5A*-mediated DCM, it is likely that the DCM is also influenced by genetic modifiers, but more GWAS need to be completed before revisiting this hypothesis. Furthermore, measurements of I_{Na} in HEK293 cells expressing DCM-associated variants R222Q and I1835T using whole-cell voltage clamp technique, have revealed that common polymorphisms H558R and Q1077del are relevant for their phenotypic expression and have a large impact on the $Na_v1.5$ biophysical phenotypes [43]. It is therefore more likely that *SCN5A*-mediated phenotypes result from complex oligo-polygenic disease with some effect of post-translational and environmental factors, rather than a strict Mendelian inheritance.

9. Non-Genetic and Epigenetic Influences

The relationship between *SCN5A* variants and the risk of DCM may be influenced by factors other than genotype. Studies of a DCM family carrying the loss-of-function A1180V variant demonstrated that the defective sodium channel reduced the current conduction (manifested as QRS widening) only at high heart rates [26]. These findings speak in favor of the fact that certain *SCN5A* variants might be risk factors of DCM, and that physical activity, lifestyle, and health conditions that increase the heart rate might enhance the phenotype of carriers of certain *SCN5A* variants, such as the A1180V [26]. Alternatively, epigenetic influences on $Na_v1.5$ expression might influence the phenotype development, but this hypothesis requires further investigation.

10. Clinical Implications

Despite the paucity of mechanistic insights into the pathogenesis of *SCN5A*-mediated DCM, one can derive clinical repercussions from the aforementioned theories. In patients with known *SCN5A* variants, a review of the literature for the description of its functional properties is necessary for selection of optimal beta-blockers, since propranolol (but not metoprolol) blocks both the peak and the late (persistent) I_{Na} [44]. This effect might alleviate the ventricular arrhythmias in gain-of-function *SCN5A* variant carriers, but can controversially provoke arrhythmias and cause or worsen cardiac conduction delays at different levels in those with loss-of-function variants. Likewise, the former group might also benefit from treatment with class Ic antiarrhythmic medications that block the sodium channel, such as flecainide, while its use in the latter group might elicit arrhythmias and cardiac conduction delay. These suggestions are however limited to patients with clearly pathogenic and previously studied *SCN5A* variants, and more functional studies are needed to expand our knowledge to more *SCN5A* variants. Perhaps the growing use of the automated patch clamp technique will help advance this process.

11. Conclusions

The aforementioned controversies suggest that neither of the living hypotheses provides an ultimate explanation according to today's knowledge, and that molecular mechanisms responsible for $Na_v1.5/SCN5A$ -related cardiomyopathy are rather multifaceted and yet to be explored. The era of next-generation sequencing gives the advantage of identifying genetic modifiers that may play a role in shaping the DCM phenotype. However, genetic substrates alone in the absence of post-translational and/or environmental influences are unlikely to give full and conclusive explanation for this controversy. Looking ahead, the growing experience with disease modeling based on human induced pluripotent stem cell-derived cardiomyocytes and transgenic animal models, will optimistically pave the way for better characterization of $Na_v1.5$ role in cellular biological processes and help identify mechanisms by which genetic and/or environmental factors affect the ventricular contractility in carriers of *SCN5A* variants. Sound evidence on disease pathogenesis will also guide us on our path for disease modification and show whether gene therapy might be a viable option for treatment of patients with

SCN5A-mediated DCM in the near future. Before that expands our horizon, we need to adhere to the conventional guidelines for management of arrhythmias and heart failure in these patients, and strictly limit our precision therapy with sodium channel blockers only as an alternative therapy to those with known gain-of-function SCN5A variants.

Conflicts of Interest: The authors declare no conflicts of interest.

References

1. Wang, Q.; Shen, J.; Splawski, I.; Atkinson, D.; Li, Z.; Robinson, J.L.; Moss, A.J.; Towbin, J.A.; Keating, M.T. SCN5A mutations associated with an inherited cardiac arrhythmia, long QT syndrome. *Cell* **1995**, *80*, 805–811. [[CrossRef](#)]
2. Schwartz, P.J.; Priori, S.G.; Locati, E.H.; Napolitano, C.; Cantu, F.; Towbin, J.A.; Keating, M.T.; Hammoude, H.; Brown, A.M.; Chen, L.S.; et al. Long QT syndrome patients with mutations of the SCN5A and HERG genes have differential responses to Na⁺ channel blockade and to increases in heart rate. Implications for gene-specific therapy. *Circulation* **1995**, *92*, 3381–3386. [[CrossRef](#)] [[PubMed](#)]
3. Chen, Q.; Kirsch, G.E.; Zhang, D.; Brugada, R.; Brugada, J.; Brugada, P.; Potenza, D.; Moya, A.; Borggrefe, M.; Breithardt, G.; et al. Genetic basis and molecular mechanism for idiopathic ventricular fibrillation. *Nature* **1998**, *392*, 293–296. [[CrossRef](#)] [[PubMed](#)]
4. Rook, M.B.; Bezzina, A.; Alshinawi, C.; Groenewegen, W.A.; van Gelder, I.C.; van Ginneken, A.C.; Jongsma, H.J.; Mannens, M.M.; Wilde, A.A. Human SCN5A gene mutations alter cardiac sodium channel kinetics and are associated with the Brugada syndrome. *Cardiovasc. Res.* **1999**, *44*, 507–517. [[CrossRef](#)]
5. Schott, J.J.; Alshinawi, C.; Kyndt, F.; Probst, V.; Hoorntje, T.M.; Hulsbeek, M.; Wilde, A.A.; Escande, D.; Mannens, M.M.; Le Marec, H. Cardiac conduction defects associate with mutations in SCN5A. *Nat. Genet.* **1999**, *23*, 20–21. [[CrossRef](#)] [[PubMed](#)]
6. Wang, D.W.; Viswanathan, P.C.; Balsler, J.R.; George, A.L., Jr.; Benson, D.W. Clinical, genetic, and biophysical characterization of SCN5A mutations associated with atrioventricular conduction block. *Circulation* **2002**, *105*, 341–346. [[CrossRef](#)] [[PubMed](#)]
7. Benson, D.W.; Wang, D.W.; Dymment, M.; Knilans, T.K.; Fish, F.A.; Strieper, M.J.; Rhodes, T.H.; George, A.L., Jr. Congenital sick sinus syndrome caused by recessive mutations in the cardiac sodium channel gene (SCN5A). *J. Clin. Invest.* **2003**, *112*, 1019–1028. [[CrossRef](#)] [[PubMed](#)]
8. Groenewegen, W.A.; Firouzi, M.; Bezzina, C.R.; Vliex, S.; van Langen, I.M.; Sandkuijl, L.; Smits, J.P.; Hulsbeek, M.; Rook, M.B.; Jongsma, H.J.; et al. A cardiac sodium channel mutation cosegregates with a rare connexin40 genotype in familial atrial standstill. *Circ. Res.* **2003**, *92*, 14–22. [[CrossRef](#)]
9. Laurent, G.; Saal, S.; Amarouch, M.Y.; Beziau, D.M.; Marsman, R.F.; Faivre, L.; Barc, J.; Dina, C.; Bertaux, G.; Barthez, O.; et al. Multifocal ectopic Purkinje-related premature contractions: A new SCN5A-related cardiac channelopathy. *J. Am. Coll. Cardiol.* **2012**, *60*, 144–156. [[CrossRef](#)]
10. Laitinen-Forsblom, P.J.; Makynen, P.; Makynen, H.; Yli-Mayry, S.; Virtanen, V.; Kontula, K.; Aalto-Setälä, K. SCN5A mutation associated with cardiac conduction defect and atrial arrhythmias. *J. Cardiovasc. Electrophysiol.* **2006**, *17*, 480–485. [[CrossRef](#)]
11. Priori, S.G.; Napolitano, C.; Giordano, U.; Collisani, G.; Memmi, M. Brugada syndrome and sudden cardiac death in children. *Lancet* **2000**, *355*, 808–809. [[CrossRef](#)]
12. McNair, W.P.; Ku, L.; Taylor, M.R.; Fain, P.R.; Dao, D.; Wolfel, E.; Mestroni, L.; Familial Cardiomyopathy Registry Research Group. SCN5A mutation associated with dilated cardiomyopathy, conduction disorder, and arrhythmia. *Circulation* **2004**, *110*, 2163–2167. [[CrossRef](#)] [[PubMed](#)]
13. Te Riele, A.S.; Agullo-Pascual, E.; James, C.A.; Leo-Macias, A.; Cerrone, M.; Zhang, M.; Lin, X.; Lin, B.; Sobreira, N.L.; Amat-Alarcon, N.; et al. Multilevel analyses of SCN5A mutations in arrhythmogenic right ventricular dysplasia/cardiomyopathy suggest non-canonical mechanisms for disease pathogenesis. *Cardiovasc. Res.* **2017**, *113*, 102–111. [[CrossRef](#)] [[PubMed](#)]
14. Olson, T.M.; Michels, V.V.; Ballew, J.D.; Reyna, S.P.; Karst, M.L.; Herron, K.J.; Horton, S.C.; Rodeheffer, R.J.; Anderson, J.L. Sodium channel mutations and susceptibility to heart failure and atrial fibrillation. *JAMA* **2005**, *293*, 447–454. [[CrossRef](#)] [[PubMed](#)]

15. McNair, W.P.; Sinagra, G.; Taylor, M.R.; Di Lenarda, A.; Ferguson, D.A.; Salcedo, E.E.; Slavov, D.; Zhu, X.; Caldwell, J.H.; Mestroni, L.; et al. SCN5A mutations associate with arrhythmic dilated cardiomyopathy and commonly localize to the voltage-sensing mechanism. *J. Am. Coll. Cardiol.* **2011**, *57*, 2160–2168. [[CrossRef](#)]
16. Mann, S.A.; Castro, M.L.; Ohanian, M.; Guo, G.; Zodgekar, P.; Sheu, A.; Stockhammer, K.; Thompson, T.; Playford, D.; Subbiah, R.; et al. R222Q SCN5A mutation is associated with reversible ventricular ectopy and dilated cardiomyopathy. *J. Am. Coll. Cardiol.* **2012**, *60*, 1566–1573. [[CrossRef](#)] [[PubMed](#)]
17. Walsh, R.; Thomson, K.L.; Ware, J.S.; Funke, B.H.; Woodley, J.; McGuire, K.J.; Mazzarotto, F.; Blair, E.; Seller, A.; Taylor, J.C.; et al. Reassessment of Mendelian gene pathogenicity using 7,855 cardiomyopathy cases and 60,706 reference samples. *Genet. Med.* **2017**, *19*, 192–203. [[CrossRef](#)]
18. Nikolova, V.; Leimena, C.; McMahon, A.C.; Tan, J.C.; Chandar, S.; Jogia, D.; Kesteven, S.H.; Michalick, J.; Otway, R.; Verheyen, F.; et al. Defects in nuclear structure and function promote dilated cardiomyopathy in lamin A/C-deficient mice. *J. Clin. Invest.* **2004**, *113*, 357–369. [[CrossRef](#)]
19. Hesse, M.; Kondo, C.S.; Clark, R.B.; Su, L.; Allen, F.L.; Geary-Joo, C.T.; Kunnathu, S.; Severson, D.L.; Nygren, A.; Giles, W.R.; et al. Dilated cardiomyopathy is associated with reduced expression of the cardiac sodium channel Scn5a. *Cardiovasc. Res.* **2007**, *75*, 498–509. [[CrossRef](#)]
20. Nguyen, T.P.; Wang, D.W.; Rhodes, T.H.; George, A.L., Jr. Divergent biophysical defects caused by mutant sodium channels in dilated cardiomyopathy with arrhythmia. *Circ. Res.* **2008**, *102*, 364–371. [[CrossRef](#)]
21. Shi, R.; Zhang, Y.; Yang, C.; Huang, C.; Zhou, X.; Qiang, H.; Grace, A.A.; Huang, C.L.; Ma, A. The cardiac sodium channel mutation delQKP 1507-1509 is associated with the expanding phenotypic spectrum of LQT3, conduction disorder, dilated cardiomyopathy, and high incidence of youth sudden death. *Europace* **2008**, *10*, 1329–1335. [[CrossRef](#)] [[PubMed](#)]
22. Moreau, A.; Gosselin-Badaroudine, P.; Boutjdir, M.; Chahine, M. Mutations in the Voltage Sensors of Domains I and II of Nav1.5 that are Associated with Arrhythmias and Dilated Cardiomyopathy Generate Gating Pore Currents. *Front. Pharmacol.* **2015**, *6*, 301. [[CrossRef](#)] [[PubMed](#)]
23. Bezzina, C.R.; Remme, C.A. Dilated cardiomyopathy due to sodium channel dysfunction: What is the connection? *Circ. Arrhythm Electrophysiol.* **2008**, *1*, 80–82. [[CrossRef](#)] [[PubMed](#)]
24. Amin, A.S. SCN5A-related dilated cardiomyopathy: What do we know? *Heart Rhythm.* **2014**, *11*, 1454–1455. [[CrossRef](#)] [[PubMed](#)]
25. Gosselin-Badaroudine, P.; Keller, D.I.; Huang, H.; Pouliot, V.; Chatelier, A.; Osswald, S.; Brink, M.; Chahine, M. A proton leak current through the cardiac sodium channel is linked to mixed arrhythmia and the dilated cardiomyopathy phenotype. *PLoS ONE* **2012**, *7*, e38331. [[CrossRef](#)]
26. Ge, J.; Sun, A.; Paajanen, V.; Wang, S.; Su, C.; Yang, Z.; Li, Y.; Wang, S.; Jia, J.; Wang, K.; et al. Molecular and clinical characterization of a novel SCN5A mutation associated with atrioventricular block and dilated cardiomyopathy. *Circ. Arrhythm Electrophysiol.* **2008**, *1*, 83–92. [[CrossRef](#)] [[PubMed](#)]
27. Clatot, J.; Hoshi, M.; Wan, X.; Liu, H.; Jain, A.; Shinlapawittayatorn, K.; Marionneau, C.; Ficker, E.; Ha, T.; Deschenes, I. Voltage-gated sodium channels assemble and gate as dimers. *Nat. Commun.* **2017**, *8*, 2077. [[CrossRef](#)] [[PubMed](#)]
28. Abriel, H.; Rougier, J.S.; Jalife, J. Ion channel macromolecular complexes in cardiomyocytes: Roles in sudden cardiac death. *Circ. Res.* **2015**, *116*, 1971–1988. [[CrossRef](#)]
29. Shan, L.; Makita, N.; Xing, Y.; Watanabe, S.; Futatani, T.; Ye, F.; Saito, K.; Ibuki, K.; Watanabe, K.; Hirono, K.; et al. SCN5A variants in Japanese patients with left ventricular noncompaction and arrhythmia. *Mol. Genet. Metab.* **2008**, *93*, 468–474. [[CrossRef](#)]
30. Coronel, R.; Casini, S.; Koopmann, T.T.; Wilms-Schopman, F.J.; Verkerk, A.O.; de Groot, J.R.; Bhuiyan, Z.; Bezzina, C.R.; Veldkamp, M.W.; Linnenbank, A.C.; et al. Right ventricular fibrosis and conduction delay in a patient with clinical signs of Brugada syndrome: A combined electrophysiological, genetic, histopathologic, and computational study. *Circulation* **2005**, *112*, 2769–2777. [[CrossRef](#)]
31. Frustaci, A.; Priori, S.G.; Pieroni, M.; Chimenti, C.; Napolitano, C.; Rivolta, I.; Sanna, T.; Bellocci, F.; Russo, M.A. Cardiac histological substrate in patients with clinical phenotype of Brugada syndrome. *Circulation* **2005**, *112*, 3680–3687. [[CrossRef](#)] [[PubMed](#)]
32. Nademane, K.; Raju, H.; de Noronha, S.V.; Papadakis, M.; Robinson, L.; Rothery, S.; Makita, N.; Kowase, S.; Boonmee, N.; Vitayakritsirikul, V.; et al. Fibrosis, Connexin-43, and Conduction Abnormalities in the Brugada Syndrome. *J. Am. Coll. Cardiol.* **2015**, *66*, 1976–1986. [[CrossRef](#)]

33. Cerrone, M.; Lin, X.; Zhang, M.; Agullo-Pascual, E.; Pfenniger, A.; Chkourko Gusky, H.; Novelli, V.; Kim, C.; Tirasawadichai, T.; Judge, D.P.; et al. Missense mutations in plakophilin-2 cause sodium current deficit and associate with a Brugada syndrome phenotype. *Circulation* **2014**, *129*, 1092–1103. [CrossRef] [PubMed]
34. Abriel, H. Cardiac sodium channel Na(v)1.5 and interacting proteins: Physiology and pathophysiology. *J. Mol. Cell Cardiol.* **2010**, *48*, 2–11. [CrossRef] [PubMed]
35. Ishikawa, T.; Sato, A.; Marcou, C.A.; Tester, D.J.; Ackerman, M.J.; Crotti, L.; Schwartz, P.J.; On, Y.K.; Park, J.E.; Nakamura, K.; et al. A novel disease gene for Brugada syndrome: Sarcolemmal membrane-associated protein gene mutations impair intracellular trafficking of hNav1.5. *Circ. Arrhythm Electrophysiol.* **2012**, *5*, 1098–1107. [CrossRef] [PubMed]
36. Mlynarova, J.; Trentin-Sonoda, M.; Gaisler da Silva, F.; Major, J.L.; Salih, M.; Carneiro-Ramos, M.S.; Tuana, B.S. SLMAP3 isoform modulates cardiac gene expression and function. *PLoS ONE* **2019**, *14*, e0214669. [CrossRef]
37. Hao, X.; Zhang, Y.; Zhang, X.; Nirmalan, M.; Davies, L.; Konstantinou, D.; Yin, F.; Dobrzynski, H.; Wang, X.; Grace, A.; et al. TGF-beta1-mediated fibrosis and ion channel remodeling are key mechanisms in producing the sinus node dysfunction associated with SCN5A deficiency and aging. *Circ. Arrhythm Electrophysiol.* **2011**, *4*, 397–406. [CrossRef]
38. Zakrzewska-Koperska, J.; Franaszczyk, M.; Bilinska, Z.; Truszkowska, G.; Karczmarz, M.; Szumowski, L.; Zielinski, T.; Ploski, R.; Bilinska, M. Rapid and effective response of the R222Q SCN5A to quinidine treatment in a patient with Purkinje-related ventricular arrhythmia and familial dilated cardiomyopathy: A case report. *BMC Med. Genet.* **2018**, *19*, 94. [CrossRef]
39. Beckermann, T.M.; McLeod, K.; Murday, V.; Potet, F.; George, A.L., Jr. Novel SCN5A mutation in amiodarone-responsive multifocal ventricular ectopy-associated cardiomyopathy. *Heart Rhythm.* **2014**, *11*, 1446–1453. [CrossRef]
40. Swan, H.; Amarouch, M.Y.; Leinonen, J.; Marjamaa, A.; Kucera, J.P.; Laitinen-Forsblom, P.J.; Lahtinen, A.M.; Palotie, A.; Kontula, K.; Toivonen, L.; et al. Gain-of-function mutation of the SCN5A gene causes exercise-induced polymorphic ventricular arrhythmias. *Circ. Cardiovasc. Genet.* **2014**, *7*, 771–781. [CrossRef]
41. Calloe, K.; Broendberg, A.K.; Christensen, A.H.; Pedersen, L.N.; Olesen, M.S.; de Los Angeles Tejada, M.; Friis, S.; Thomsen, M.B.; Bundgaard, H.; Jensen, H.K. Multifocal atrial and ventricular premature contractions with an increased risk of dilated cardiomyopathy caused by a Nav1.5 gain-of-function mutation (G213D). *Int. J. Cardiol.* **2018**, *257*, 160–167. [CrossRef] [PubMed]
42. Watanabe, H.; Yang, T.; Stroud, D.M.; Lowe, J.S.; Harris, L.; Attack, T.C.; Wang, D.W.; Hipkens, S.B.; Leake, B.; Hall, L.; et al. Striking In vivo phenotype of a disease-associated human SCN5A mutation producing minimal changes in vitro. *Circulation* **2011**, *124*, 1001–1011. [CrossRef] [PubMed]
43. Cheng, J.; Morales, A.; Siegfried, J.D.; Li, D.; Norton, N.; Song, J.; Gonzalez-Quintana, J.; Makielski, J.C.; Hershberger, R.E. SCN5A rare variants in familial dilated cardiomyopathy decrease peak sodium current depending on the common polymorphism H558R and common splice variant Q1077del. *Clin. Transl. Sci.* **2010**, *3*, 287–294. [CrossRef] [PubMed]
44. Wang, D.W.; Mistry, A.M.; Kahlig, K.M.; Kearney, J.A.; Xiang, J.; George, A.L., Jr. Propranolol blocks cardiac and neuronal voltage-gated sodium channels. *Front. Pharmacol.* **2010**, *1*, 144. [CrossRef] [PubMed]



© 2019 by the author. Licensee MDPI, Basel, Switzerland. This article is an open access article distributed under the terms and conditions of the Creative Commons Attribution (CC BY) license (<http://creativecommons.org/licenses/by/4.0/>).

MDPI
St. Alban-Anlage 66
4052 Basel
Switzerland
Tel. +41 61 683 77 34
Fax +41 61 302 89 18
www.mdpi.com

Journal of Clinical Medicine Editorial Office
E-mail: jcm@mdpi.com
www.mdpi.com/journal/jcm



MDPI
St. Alban-Anlage 66
4052 Basel
Switzerland

Tel: +41 61 683 77 34
Fax: +41 61 302 89 18

www.mdpi.com



ISBN 978-3-03943-762-7